WOODHEAD PUBLISHING SERIES IN BIOMATERIALS

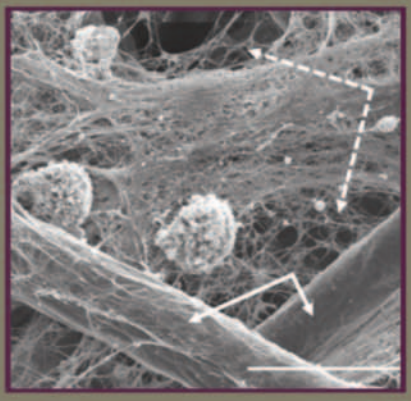

Nanocomposites for Musculoskeletal Tissue Regeneration

Edited by Huinan Liu

WP
WOODHEAD PUBLISHING

Nanocomposites for Musculoskeletal Tissue Regeneration

Related titles

Bioactive Glasses
(ISBN 978-1-84569-768-6)

Bioceramics and Their Clinical Applications
(ISBN 978-1-84569-204-9)

Bone Repair Biomaterials
(ISBN 978-1-84569-385-5)

Woodhead Publishing Series in Biomaterials: Number 109

Nanocomposites for Musculoskeletal Tissue Regeneration

Edited by

Huinan Liu

AMSTERDAM • BOSTON • CAMBRIDGE • HEIDELBERG
LONDON • NEW YORK • OXFORD • PARIS • SAN DIEGO
SAN FRANCISCO • SINGAPORE • SYDNEY • TOKYO
Woodhead Publishing is an imprint of Elsevier

Woodhead Publishing is an imprint of Elsevier
The Officers' Mess Business Centre, Royston Road, Duxford, CB22 4QH, UK
50 Hampshire Street, 5th Floor, Cambridge, MA 02139, USA
The Boulevard, Langford Lane, Kidlington, OX5 1GB, UK

Notices
Knowledge and best practice in this field are constantly changing. As new research and experience broaden our understanding, changes in research methods, professional practices, or medical treatment may become necessary.

Practitioners and researchers must always rely on their own experience and knowledge in evaluating and using any information, methods, compounds, or experiments described herein. In using such information or methods they should be mindful of their own safety and the safety of others, including parties for whom they have a professional responsibility.

To the fullest extent of the law, neither the Publisher nor the authors, contributors, or editors, assume any liability for any injury and/or damage to persons or property as a matter of products liability, negligence or otherwise, or from any use or operation of any methods, products, instructions, or ideas contained in the material herein.

British Library Cataloguing-in-Publication Data
A catalogue record for this book is available from the British Library

Library of Congress Cataloging-in-Publication Data
A catalog record for this book is available from the Library of Congress

ISBN: 978-1-78242-452-9 (print)
ISBN: 978-1-78242-475-8 (online)

Publisher: Matthew Deans
Acquisition Editor: Laura Overend
Editorial Project Manager: Lucy Beg
Production Project Manager: Poulouse Joseph
Designer: Greg Harris

Typeset by TNQ Books and Journals

Contents

This page intentionally left blank

List of contributors

S. Anil King Saud University, Riyadh, Saudi Arabia

J. Buschmann University Hospital Zurich, Zurich, Switzerland

N.J. Castro The George Washington University, Washington, DC, United States

C. Chain Purdue University, West Lafayette, IN, United States

Y.E. Choonara University of the Witwatersrand, Johannesburg, South Africa

M. D'Agati Stony Brook University, Stony Brook, NY, United States

M. Del Ponte Purdue University, West Lafayette, IN, United States

M. Deng Purdue University, West Lafayette, IN, United States

B. Farshid Stony Brook University, Stony Brook, NY, United States

S.A. Guelcher Vanderbilt University, Nashville, TN, United States

A.J. Harmata Vanderbilt University, Nashville, TN, United States

C.B. Horner University of California-Riverside, Riverside, CA, United States

R. Jayakumar Pukyong National University, Busan, South Korea; Amrita Institute of Medical Sciences and Research Centre, Kochi, India

J. Jiang University of Nebraska Medical Center, Omaha, NE, United States

W. Jiang University of California, Riverside, CA, United States

S.-K. Kim Pukyong National University, Busan, South Korea

W.E. Krause North Carolina State University, Raleigh, NC, United States

L. Kuang Purdue University, West Lafayette, IN, United States

P. Kumar University of the Witwatersrand, Johannesburg, South Africa

G. Lalwani Stony Brook University, Stony Brook, NY, United States

H. Liu University of California, Riverside, CA, United States

W. Liu Peking University School and Hospital of Stomatology, Beijing, PR China; Northeastern University, Boston, MA, United States

K. Low University of California-Riverside, Riverside, CA, United States

L.A. Lucia North Carolina State University, Raleigh, NC, United States; Key Laboratory of Pulp & Paper Science and Technology of the Ministry of Education, Jinan, People's Republic of China

A. Martins University of Minho, Barco, Guimarães, Portugal; ICVS/3B's – PT Government Associate Laboratory, Braga/Guimarães, Portugal

G. Modi University of the Witwatersrand, Johannesburg, South Africa

V. Mouriño University of Buenos Aires, Buenos Aires, Argentina; A CONICET, Buenos Aires, Argentina

J. Nam University of California-Riverside, Riverside, CA, United States

A.G. Nandgaonkar North Carolina State University, Raleigh, NC, United States

N. Narayanan Purdue University, West Lafayette, IN, United States

N.M. Neves University of Minho, Barco, Guimarães, Portugal; ICVS/3B's – PT Government Associate Laboratory, Braga/Guimarães, Portugal

P. Palmero Politecnico di Torino, Department of Applied Science and Technology, Corso Duca degli Abruzzi 24, Torino, Italy

V. Pillay University of the Witwatersrand, Johannesburg, South Africa

R.L. Reis University of Minho, Barco, Guimarães, Portugal; ICVS/3B's – PT Government Associate Laboratory, Braga/Guimarães, Portugal

F.D. Shuler Marshall University, Huntington, WV, United States

B. Sitharaman Stony Brook University, Stony Brook, NY, United States

P. Sol University of Minho, Barco, Guimarães, Portugal; ICVS/3B's – PT Government Associate Laboratory, Braga/Guimarães, Portugal

M.J. Teusink University of Nebraska Medical Center, Omaha, NE, United States

J. Venkatesan Pukyong National University, Busan, South Korea

T.J. Webster Northeastern University, Boston, MA, United States; King Abdulaziz University, Jeddah, Saudi Arabia

J. Xie University of Nebraska Medical Center, Omaha, NE, United States

L.G. Zhang The George Washington University, Washington, DC, United States

This page intentionally left blank

Woodhead Publishing Series in Biomaterials

1 **Sterilisation of tissues using ionising radiations**
Edited by J. F. Kennedy, G. O. Phillips and P. A. Williams
2 **Surfaces and interfaces for biomaterials**
Edited by P. Vadgama
3 **Molecular interfacial phenomena of polymers and biopolymers**
Edited by C. Chen
4 **Biomaterials, artificial organs and tissue engineering**
Edited by L. Hench and J. Jones
5 **Medical modelling**
R. Bibb
6 **Artificial cells, cell engineering and therapy**
Edited by S. Prakash
7 **Biomedical polymers**
Edited by M. Jenkins
8 **Tissue engineering using ceramics and polymers**
Edited by A. R. Boccaccini and J. Gough
9 **Bioceramics and their clinical applications**
Edited by T. Kokubo
10 **Dental biomaterials**
Edited by R. V. Curtis and T. F. Watson
11 **Joint replacement technology**
Edited by P. A. Revell
12 **Natural-based polymers for biomedical applications**
Edited by R. L. Reiss et al.
13 **Degradation rate of bioresorbable materials**
Edited by F. J. Buchanan
14 **Orthopaedic bone cements**
Edited by S. Deb
15 **Shape memory alloys for biomedical applications**
Edited by T. Yoneyama and S. Miyazaki
16 **Cellular response to biomaterials**
Edited by L. Di Silvio
17 **Biomaterials for treating skin loss**
Edited by D. P. Orgill and C. Blanco
18 **Biomaterials and tissue engineering in urology**
Edited by J. Denstedt and A. Atala

19 **Materials science for dentistry**
B. W. Darvell
20 **Bone repair biomaterials**
Edited by J. A. Planell, S. M. Best, D. Lacroix and A. Merolli
21 **Biomedical composites**
Edited by L. Ambrosio
22 **Drug–device combination products**
Edited by A. Lewis
23 **Biomaterials and regenerative medicine in ophthalmology**
Edited by T. V. Chirila
24 **Regenerative medicine and biomaterials for the repair of connective tissues**
Edited by C. Archer and J. Ralphs
25 **Metals for biomedical devices**
Edited by M. Niinomi
26 **Biointegration of medical implant materials: Science and design**
Edited by C. P. Sharma
27 **Biomaterials and devices for the circulatory system**
Edited by T. Gourlay and R. Black
28 **Surface modification of biomaterials: Methods analysis and applications**
Edited by R. Williams
29 **Biomaterials for artificial organs**
Edited by M. Lysaght and T. Webster
30 **Injectable biomaterials: Science and applications**
Edited by B. Vernon
31 **Biomedical hydrogels: Biochemistry, manufacture and medical applications**
Edited by S. Rimmer
32 **Preprosthetic and maxillofacial surgery: Biomaterials, bone grafting and tissue engineering**
Edited by J. Ferri and E. Hunziker
33 **Bioactive materials in medicine: Design and applications**
Edited by X. Zhao, J. M. Courtney and H. Qian
34 **Advanced wound repair therapies**
Edited by D. Farrar
35 **Electrospinning for tissue regeneration**
Edited by L. Bosworth and S. Downes
36 **Bioactive glasses: Materials, properties and applications**
Edited by H. O. Ylänen
37 **Coatings for biomedical applications**
Edited by M. Driver
38 **Progenitor and stem cell technologies and therapies**
Edited by A. Atala
39 **Biomaterials for spinal surgery**
Edited by L. Ambrosio and E. Tanner
40 **Minimized cardiopulmonary bypass techniques and technologies**
Edited by T. Gourlay and S. Gunaydin
41 **Wear of orthopaedic implants and artificial joints**
Edited by S. Affatato
42 **Biomaterials in plastic surgery: Breast implants**
Edited by W. Peters, H. Brandon, K. L. Jerina, C. Wolf and V. L. Young

43 **MEMS for biomedical applications**
Edited by S. Bhansali and A. Vasudev
44 **Durability and reliability of medical polymers**
Edited by M. Jenkins and A. Stamboulis
45 **Biosensors for medical applications**
Edited by S. Higson
46 **Sterilisation of biomaterials and medical devices**
Edited by S. Lerouge and A. Simmons
47 **The hip resurfacing handbook: A practical guide to the use and management of modern hip resurfacings**
Edited by K. De Smet, P. Campbell and C. Van Der Straeten
48 **Developments in tissue engineered and regenerative medicine products**
J. Basu and J. W. Ludlow
49 **Nanomedicine: Technologies and applications**
Edited by T. J. Webster
50 **Biocompatibility and performance of medical devices**
Edited by J.-P. Boutrand
51 **Medical robotics: Minimally invasive surgery**
Edited by P. Gomes
52 **Implantable sensor systems for medical applications**
Edited by A. Inmann and D. Hodgins
53 **Non-metallic biomaterials for tooth repair and replacement**
Edited by P. Vallittu
54 **Joining and assembly of medical materials and devices**
Edited by Y. (Norman) Zhou and M. D. Breyen
55 **Diamond-based materials for biomedical applications**
Edited by R. Narayan
56 **Nanomaterials in tissue engineering: Fabrication and applications**
Edited by A. K. Gaharwar, S. Sant, M. J. Hancock and S. A. Hacking
57 **Biomimetic biomaterials: Structure and applications**
Edited by A. J. Ruys
58 **Standardisation in cell and tissue engineering: Methods and protocols**
Edited by V. Salih
59 **Inhaler devices: Fundamentals, design and drug delivery**
Edited by P. Prokopovich
60 **Bio-tribocorrosion in biomaterials and medical implants**
Edited by Y. Yan
61 **Microfluidic devices for biomedical applications**
Edited by X.-J. James Li and Y. Zhou
62 **Decontamination in hospitals and healthcare**
Edited by J. T. Walker
63 **Biomedical imaging: Applications and advances**
Edited by P. Morris
64 **Characterization of biomaterials**
Edited by M. Jaffe, W. Hammond, P. Tolias and T. Arinzeh
65 **Biomaterials and medical tribology**
Edited by J. Paolo Davim
66 **Biomaterials for cancer therapeutics: Diagnosis, prevention and therapy**
Edited by K. Park

67 **New functional biomaterials for medicine and healthcare**
E. P. Ivanova, K. Bazaka and R. J. Crawford
68 **Porous silicon for biomedical applications**
Edited by H. A. Santos
69 **A practical approach to spinal trauma**
Edited by H. N. Bajaj and S. Katoch
70 **Rapid prototyping of biomaterials: Principles and applications**
Edited by R. Narayan
71 **Cardiac regeneration and repair Volume 1: Pathology and therapies**
Edited by R.-K. Li and R. D. Weisel
72 **Cardiac regeneration and repair Volume 2: Biomaterials and tissue engineering**
Edited by R.-K. Li and R. D. Weisel
73 **Semiconducting silicon nanowires for biomedical applications**
Edited by J. L. Coffer
74 **Silk biomaterials for tissue engineering and regenerative medicine**
Edited by S. Kundu
75 **Biomaterials for bone regeneration: Novel techniques and applications**
Edited by P. Dubruel and S. Van Vlierberghe
76 **Biomedical foams for tissue engineering applications**
Edited by P. Netti
77 **Precious metals for biomedical applications**
Edited by N. Baltzer and T. Copponnex
78 **Bone substitute biomaterials**
Edited by K. Mallick
79 **Regulatory affairs for biomaterials and medical devices**
Edited by S. F. Amato and R. Ezzell
80 **Joint replacement technology Second edition**
Edited by P. A. Revell
81 **Computational modelling of biomechanics and biotribology in the musculoskeletal system: Biomaterials and tissues**
Edited by Z. Jin
82 **Biophotonics for medical applications**
Edited by I. Meglinski
83 **Modelling degradation of bioresorbable polymeric medical devices**
Edited by J. Pan
84 **Perspectives in total hip arthroplasty: Advances in biomaterials and their tribological interactions**
S. Affatato
85 **Tissue engineering using ceramics and polymers Second edition**
Edited by A. R. Boccaccini and P. X. Ma
86 **Biomaterials and medical-device associated infections**
Edited by L. Barnes and I. R. Cooper
87 **Surgical techniques in total knee arthroplasty (TKA) and alternative procedures**
Edited by S. Affatato
88 **Lanthanide oxide nanoparticles for molecular imaging and therapeutics**
G. H. Lee
89 **Surface modification of magnesium and its alloys for biomedical applications Volume 1: Biological interactions, mechanical properties and testing**
Edited by T. S. N. Sankara Narayanan, I. S. Park and M. H. Lee

90 **Surface modification of magnesium and its alloys for biomedical applications Volume 2: Modification and coating techniques**
Edited by T. S. N. Sankara Narayanan, I. S. Park and M. H. Lee
91 **Medical modelling: the application of advanced design and rapid prototyping techniques in medicine Second Edition**
Edited by R. Bibb, D. Eggbeer and A. Paterson
92 **Switchable and responsive surfaces and materials for biomedical applications**
Edited by Z. Zhang
93 **Biomedical textiles for orthopaedic and surgical applications: Fundamentals, applications and tissue engineering**
Edited by T. Blair
94 **Surface coating and modification of metallic biomaterials**
Edited by C. Wen
95 **Hydroxyapatite (HAP) for biomedical applications**
Edited by M. Mucalo
96 **Implantable neuroprostheses for restoring function**
Edited by K. Kilgore
97 **Shape memory polymers for biomedical applications**
Edited by L. Yahia
98 **Regenerative engineering of musculoskeletal tissues and interfaces**
Edited by S. P. Nukavarapu, J. W. Freeman and C. T. Laurencin
99 **Advanced cardiac imaging**
Edited by K. Nieman, O. Gaemperli, P. Lancellotti and S. Plein
100 **Functional marine biomaterials: Properties and applications**
Edited by S. K. Kim
101 **Shoulder and elbow trauma and its complications Volume 1: The shoulder**
Edited by R. M. Greiwe
102 **Nanotechnology-enhanced orthopedic materials: Fabrications, applications and future trends**
Edited by L. Yang
103 **Medical devices: Regulations, standards and practices**
Edited by S. Ramakrishna, L. Tian, C. Wang, S. L. and T. Wee Eong
104 **Biomineralisation and biomaterials: Fundamentals and applications**
Edited by C. Aparicio and M. Ginebra
105 **Shoulder and elbow trauma and its complications Volume 2: The elbow**
Edited by R. M. Greiwe
106 **Characterisation and design of tissue scaffolds**
Edited by P. Tomlins
107 **Biosynthetic polymers for medical applications**
Edited by L. Poole-Warren, P. Martens and R.Green
108 **Advances in polyurethane biomaterials**
Edited by S. L. Cooper
109 **Nanocomposites for musculoskeletal tissue regeneration**
Edited by H. Liu
110 **Thin film coatings for biomaterials and biomedical applications**
Edited by H. J. Griesser

This page intentionally left blank

Part One

Designing nanocomposites for musculoskeletal tissue regeneration

This page intentionally left blank

1 Design and fabrication of nanocomposites for musculoskeletal tissue regeneration

N. Narayanan, L. Kuang, M. Del Ponte, C. Chain, M. Deng
Purdue University, West Lafayette, IN, United States

1.1 Introduction

Musculoskeletal tissues comprise bone, muscles, cartilage, ligament, tendons, and other connecting tissues. They contribute to the body movement and provide structural support. There are 206 bones that make up the human adult skeletal system. It can be separated into two parts, the axial skeleton with 74 bones and the appendicular skeleton with 126 bones. The auditory ossicle consists of six bones (Clarke, 2008). The primary function of the skeletal system is to provide rigid structural support for the human body. In combination with other parts of the musculoskeletal system, it provides movement and locomotion. Skeletal muscles are one of the three major muscle types found in the body and are under the influence of the somatic nervous system. Skeletal muscles consist of directional muscle fibers that are formed by fusion of myoblasts. These muscle fibers are connected to the skeletal system by tendons. The junction formed between a muscle and a tendon is called the myotendinous junction (Kannus, 2000). Tendons are rich in collagen and elastin, thereby providing the required mechanical support to bridge the hard bone structure and the soft muscle fibers. Similarly, ligaments are structures that connect one bone to another. Ligaments are fibrous connective tissues composed mainly of collagen. The primary function of ligaments is to provide mechanical support by stabilizing the bone joints (Frank, 2004). Cartilage is a specialized connective tissue present in joints, ears, nose, rib cage, bronchial tubes, and invertebrate discs. The primary components are collagen, proteoglycans, and elastin molecules, therefore providing structural support at the terminal end of long bones. There are three different types of cartilage present in human body: the articular cartilage, elastic cartilage, and fibrocartilage.

Musculoskeletal tissue loss or damage resulting from trauma, surgery, or disease presents a significant medical challenge. More than 34 million musculoskeletal injuries are reported annually in the United States alone (Deng et al., 2012). Current treatment options for patients include organ/tissue transplantation of autografts/allografts, delivery of bioactive agents, and utilization of synthetic replacements composed of metals, polymers, and ceramics. However, each strategy suffers from a number of disadvantages. For example, the commonly used autografts and allografts are often associated with limited availability and risks of immunogenicity (Deng et al., 2012).

Nanocomposites for Musculoskeletal Tissue Regeneration. http://dx.doi.org/10.1016/B978-1-78242-452-9.00001-7

Tissue engineering aims to repair, restore, or regenerate functional tissues using biomaterials, cells, and biological factors alone or in combination (Deng et al., 2012; Laurencin et al., 1999; Langer and Vacanti, 1993). Biomaterials are fabricated into three-dimensional (3D) scaffolds that mimic the natural extracellular matrices (ECMs). The scaffolds can be implanted alone at the site of injury or seeded with cells to regenerate the lost tissue. During the repair/regeneration process, the scaffold provides structural and mechanical restoration of the damaged tissues, gradually degrades into biocompatible products, and presents an interconnected porous structure to accommodate cell infiltration and vascularization and promote ECM synthesis. Additionally, biological factors can be applied to facilitate tissue regeneration. Both natural and synthetic biomaterials including biodegradable polymers and composites have been fabricated into various scaffolds that mimic the structures of native tissues for regenerative applications (Nair and Laurencin, 2007; Kumbar et al., 2014). Biodegradable polymers are attractive scaffold materials owing to flexibility in chemistry and the ability to be excreted or resorbed by the body. The regenerative efficacy of a scaffold is largely dependent on its nature, composition, and structural properties. The following properties of the scaffolds are essential for achieving desirable regenerative efficacy:

- Biocompatibility: The scaffold should not cause any adverse tissue reactions (eg, inflammation or release of any toxic compounds) when implanted inside the body.
- Biodegradation: The scaffold used for tissue regeneration should be biodegradable. In an ideal scenario, the rate of scaffold degradation should match the rate of tissue healing so that the newly formed tissue compensates the mechanical and mass loss of the degraded scaffold.
- Mechanical properties: The mechanical properties of the scaffold should match those of surrounding tissues. This is crucial to restore mechanical function and transmit the mechanical cues across the defect to the regenerative cells.
- Structural properties: The scaffold should have appropriate structures and surfaces (eg, porosity and nanotopography) that support cell function and tissue regeneration. For example, the interconnected scaffold porous structure enables the transport of oxygen and nutrients (Deng et al., 2010c), and the surface nanotopography affects cell adhesion, proliferation, and differentiation (Deng et al., 2012).

It is often difficult for a single class of materials to satisfy all the ideal scaffold requirements. Various polymeric composites have been fabricated to synergistically combine the beneficial properties of the constituents (Roether et al., 2002; Rezwan et al., 2006). Recent advances at the interfaces of cell biology and nanotechnology have demonstrated the importance of nanotopographical cues such as pores, ridges, grooves, and fibers as an important signaling modality in controlling cellular processes for tissue engineering applications (Zhang and Webster, 2009). Therefore, there has been increasing interest in development of nanocomposites for tissue regeneration (Okamoto and John, 2013; Armentano et al., 2010; Deng et al., 2011b). For example, bone is a natural nanocomposite material of collagen and hydroxyapatite ($Ca_{10}(PO_4)_6(OH)_2$, HA) (James et al., 2011a). The collagen fibers present in bone provide the structural frame onto which inorganic HA is embedded thus strengthening the collagen framework. The HA crystal plates are in the dimension of 50×25 nm (length × width).

This chapter presents an overview and recent advances of nanocomposites for scaffold-based musculoskeletal tissue regeneration. Critical design considerations of nanocomposites are discussed with a focus on the efforts to achieve optimal cell–material interactions. It further reviews different fabrication strategies to engineer nanocomposites for musculoskeletal tissue regeneration.

1.2 Design considerations of nanocomposites for musculoskeletal tissue engineering

Nanocomposites are composite materials that have one of their components in nanoscale (Armentano et al., 2010). Choosing appropriate material components is of primary importance for design of nanocomposites with necessary physical, chemical, and biological cues to guide cell functions and tissue regeneration. In the body, cells encounter various topographical features, and a significant interplay exists between cells and nanoscale features (Stevens and George, 2005). It is essential to consider the cell–material interactions when the design components are chosen. The following sections highlight the importance of different biomaterials and cell–biomaterial interactions for the rational design of nanocomposites for musculoskeletal tissue regeneration.

1.2.1 Biomaterials

Both natural and synthetic polymers, as well as bioactive ceramics, have been extensively researched in the field of tissue engineering (Nair and Laurencin, 2007; Kumbar et al., 2014). Natural polymers such as collagen, alginate, chitosan, and cellulose are attractive materials due to their excellent biocompatibility and capacity to structurally mimic native ECM (Cen et al., 2008; Alsberg et al., 2001; Kim et al., 2008; Svensson et al., 2005; Jiang et al., 2014). On the other hand, synthetic polymers including polyesters, polyanhydrides, and polyphosphazenes offer unique advantages such as predictable properties and ease of tailoring for specific applications due to their synthetic flexibility (Chu et al., 1995; Karp et al., 2002; Kweon et al., 2003). Bioactive ceramics such as calcium phosphates, calcium sulfates, and bioactive glass have been extensively investigated for orthopedic applications (Deng et al., 2011b). They are inorganic, nonmetallic materials that are osteointegrative through direct bonding to living bone adjacent to the defect site. The rationale for using these ceramics, especially calcium phosphates, lies in the fact that they are composed of calcium and phosphate ions, the main constituents of bone. In particular, nanosized HA (nHA) particles have been widely investigated for bone regeneration due to biocompatibility, bioactivity, and osteointegration ability (Lewandrowski et al., 2003; Chen et al., 2006; Huang et al., 2007; Zhou and Lee, 2011). These ceramics are typically characterized by high compressive strengths, low ductility, and variable degradation rates (Deng et al., 2011b). Tremendous efforts have been focused on the development of ideal composite biomaterials by using polymers alone or in combination with ceramics (Liao et al., 2005; Dai et al., 2004; Jin et al., 2008; Chen et al., 2000). The following

paragraphs highlight some of the research efforts in developing nanocomposites for musculoskeletal tissue engineering.

1.2.1.1 Collagen

Collagen is one of the major components of the ECM. Collagen forms the connective tissue on which the cells adhere and proliferate. Type I collagen is the most used collagen type for tissue regeneration applications. The removal of telepeptide in collagen has been shown to reduce its antigenicity (Glowacki and Mizuno, 2008). Collagen is the major organic component present in the bone and forms natural nanocomposites with HA. Li and Chang (2008) reported the synthesis of bone-like collagen/nHA crystals. The collagen fibers were phosphorylated to act as nucleation sites for the HA crystal formation when incubated in simulated body fluid (SBF). The fabricated nanocomposites showed bone-like composition and crystal morphology. Pek et al. (2008) fabricated porous scaffolds made of collagen nanocomposites. Synthetic nHA crystals were dispersed in type I collagen solution and freeze-dried to create the nanocomposites. The fabricated nanocomposites showed enhanced osteoconductivity and improved the healing of nonunion fracture in rat femur as well as a critical-sized defect in pig tibia (Fig. 1.1). In another study, Marelli et al. (2011) demonstrated that nanocomposites made of bioglass and collagen supported accelerated mineralization, indicating their potential suitability as osteoinductive cell delivery scaffolds for bone regeneration.

1.2.1.2 Poly(lactic acid) and poly(lactic-co-glycolic acid)

Poly(lactic acid) (PLA) and poly(lactic-co-glycolic acid) (PLGA) are linear aliphatic polyesters. PLA is a homopolymer containing lactide subunits as monomer, whereas

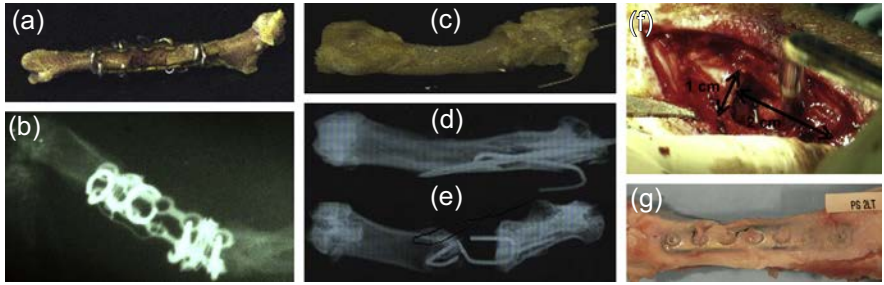

Figure 1.1 In vivo implantation and healing with the collagen–apatite nanocomposite scaffold. Wistar rat femur with 5 mm of the central section removed, and (a–d) replaced with a nanocomposite scaffold of 32.5 wt% of type I collagen and 67.5 wt% of nanocrystalline apatite, or (e) not replaced with any implant. (a, c) Photographs and (b, d, e) X-ray images of the samples (a, b) immediately and (c, d, e) 5 months after the surgery. Yorkshire–Landrace pig tibia with (f) critical-sized segmental bone defect, and (g) 6 months after defect was healed with nanocomposite scaffold.
Reproduced from Pek, Y.S., et al., 2008. Porous collagen-apatite nanocomposite foams as bone regeneration scaffolds. Biomaterials 29 (32), 4300–4305. Available at: http://www.ncbi.nlm.nih.gov/pubmed/18706690 (accessed 10.10.14.).

PLGA has lactide and glycolide as its monomer subunits. They are the most widely used polymers for medical applications due to approval by the Food and Drug Administration (FDA) for a number of clinical applications (Athanasiou et al., 1996). These polymers are usually synthesized via ring-opening polymerization of cyclic lactide and/or glycolide diesters. Their degradation products are lactic acid and glycolic acid, which are natural metabolites present in the body. The degradation properties of these polymers can be fine-tuned by varying the lactide-to-glycolide ratio in the polymer content. The lactide groups are more hydrophobic when compared to the glycolide groups due to the presence of an extra $—CH_3$ (Young et al., 2005).

Lv et al. (2009, 2013) fabricated and optimized nHA/PLGA composite scaffolds for bone regeneration. The incorporation of nHA contributed to the bioactivity of the scaffolds for osteointegration. Under in vitro culture condition, human mesenchymal stem cells (hMSCs) expressed elevated expression of phenotypic markers such as alkaline phosphatase as well as mineral deposition on the composite scaffolds as compared to PLGA scaffolds.

Kim et al. (2005) employed PLA electrospun fibers as a nanocomposite material to investigate their role in bone regeneration. The authors have used HA as nanofiller components to synthesize the nanocomposite scaffolds. The scaffolds supported enhanced attachment and proliferation of osteoblasts. In another study, Jose et al. (2009) employed aligned PLGA nanofibers along with HA to fabricate nanocomposite scaffolds. The authors showed that the nanocomposites enhanced scaffold mechanical properties as compared to the PLGA nanofibers.

1.2.1.3 Polycaprolactone

Polycaprolactone (PCL), a hydrophobic polymer with semicrystalline structure, is made of caprolactone subunits linked together by the process of ring-opening polymerization. These polymers have longer degradation time than PLGA and PLA (Woodruff and Hutmacher, 2010). FDA has approved PCL for sutures with a trade name of Maxon™. PCL is soluble in a wide variety of organic solvents; therefore, it can be blended with other polymers (Sarasam and Madihally, 2005; Marra et al., 1999; Ghasemi-Mobarakeh et al., 2008). Bernstein et al. (2010) developed nanocomposites using PCL and tricalcium phosphates for potential bone tissue regeneration applications. The mixture of the polymer and the ceramic was cold-sintered to obtain the nanocomposites. The fabricated nanocomposites showed the ability to form apatite layer when incubated in SBF. In another study, Lee et al. (2007) synthesized nanocomposite materials by grafting PCL from the surface of functionalized nHA crystals. The authors reported favorable protein adsorption on the surface of the synthesized nanocomposites.

1.2.1.4 Polyphosphazenes

Polyphosphazenes, a unique synthetic polymer class, are inorganic–organic hybrid polymers with a backbone of alternating phosphorus and nitrogen atoms and with each phosphorus atom bearing two organic or organometallic side groups (Deng et al., 2010d). Nitrogen and phosphorus atoms on the polymer backbone are linked

by alternating single and double bonds, whereas each phosphorus atom is substituted with two side groups. The ability to control polymer properties by modulating side-group chemistry has enabled the generation of a library of biomaterials with tunable physical, chemical, and biological properties (Deng et al., 2010d). Biodegradable polyphosphazenes undergo hydrolytic degradation yielding nontoxic and neutral-pH degradation products due to the buffering capacity of phosphates and ammonia that are produced simultaneously during polyphosphazene degradation. A variety of polyphosphazene-based composite structures and matrices has been prepared and investigated for musculoskeletal regeneration (Bhattacharyya et al., 2006, 2009; Brown et al., 2010; Deng et al., 2008, 2010a,b, 2011a; Nukavarapu et al., 2008; Peach et al., 2012a,b). Bhattacharyya et al. (2006, 2009) fabricated poly[bis(ethyl alanato)phosphazene] (PNEA) as well as PNEA/nHA composite nanofibrous scaffolds for bone tissue engineering applications. Such polyphosphazene nanofiber structures closely mimic the ECM architecture, and have shown improved cell performance over the conventional scaffold architectures. Nukavarapu et al. (2008) prepared composite microspheres of poly[bis(ethyl phenylalaninato)phosphazene] (PNEPhA) with 100 nm-sized HA with varying HA compositions between 10% and 30% (w/w). These composite microspheres were sintered into 3D architecture using a solvent/nonsolvent approach. In vitro studies confirmed that the composite scaffolds were able to support good osteoblast adhesion, proliferation, and alkaline phosphatase expression throughout the 21-day culture. Brown et al. (2010) developed a novel structure that combines the robust mechanical aspects of the sintered microsphere scaffold with a highly bioactive nanofiber structure to produce a composite scaffold that demonstrates an ability to mimic the mechanical environment of trabecular bone while also promoting the osteoinduction of osteoblast progenitor cells. Exploiting the chemistry of two biodegradable polymers, a 3D PLA nanofiber mesh was successfully incorporated within the void spaces between sintered PNEPhA microspheres. The nonload-bearing fiber portion of these scaffolds is sufficiently porous to allow cell migration and ECM matrix production throughout the fibrous portion of the scaffold. These composite nanofiber/microsphere scaffolds promote osteoinduction through focal adhesion kinase activity. Ultimately, the focal adhesion kinase activity on the composite nanofiber/microsphere scaffolds demonstrated causality over the production of the mature osteoblast marker, osteocalcin, and the development of a calcified matrix. The phenotype progression of osteoblast progenitor cells on the composite nanofiber/microsphere scaffolds illustrated a stronger and more rapid progression leading to fully matured osteoblasts by 21 days.

1.2.1.5 Other materials

There are other nanocomposite materials apart from the ones mentioned in the previous sections. Table 1.1 lists a few examples of other nanocomposites employed in musculoskeletal tissue engineering. For example, carbon nanotubes have also gained a lot of interest in the fabrication of nanocomposites for musculoskeletal tissue engineering applications due to their unique mechanical and electrical properties (Harrison and Atala, 2007; Ahadian et al., 2014). Sitharaman et al. (2008) fabricated biodegradable

Table 1.1 List of nanocomposites used for musculoskeletal tissue regeneration

Polymer	Nanocomponent	Application	References
Methacrylated gelatin (GelMA)	Carbon nanotubes	Muscle	Ahadian et al. (2014)
Chitosan	Carbon nanotubes	Bone	Venkatesan et al. (2012)
	TiO_2 nanoneedles	Bone	Jayakumar et al. (2011a)
	ZrO_2	Bone	Jayakumar et al. (2011)
	Nano-hydroxyapatite (nHA)	Bone	Tripathi et al. (2012)
	nHA and Cu-Zn alloy nanoparticles (nCu-Zn)	Bone	Tripathi et al. (2012)
	nHA and nano-silver particles (nAg)	Bone	Saravanan et al. (2011)
Chitosan and Alginate	Nano-silica ($nSiO_2$)	Bone	Sowjanya et al. (2013)
PCL	Carbon nanotubes	Bone	Mattioli-Belmonte et al. (2012)
	nHA	Bone	Wang et al. (2010)
Alginate	nHA and nAg	Bone	Marsich et al. (2013)
PLA	Octadecylamine-functionalized nanodiamond (ND-ODA)	Bone	Zhang et al. (2012b)
	nHA	Bone	Wei and Ma (2004)
PNEA	nHA	Bone	Bhattacharyya et al. (2006) and Bhattacharyya et al. (2009)
Polystyrene	Carbon nanotube	Bone	Zhang et al. (2012a)
Poly(propylene fumarate)	Carbon nanotubes Dodecylated US-tube	Bone	Shi et al. (2007)

Table 1.1 Continued

Polymer	Nanocomponent	Application	References
PLGA/Collagen blend	nHA	Bone	Jose et al. (2010)
	Nanobiphasic calcium phosphate (nBCP)	Bone	Ebrahimian-Hosseinabadi et al. (2011)
	Nanostructured titanium	Bone	Smith et al. (2007)
Cross-linked poly(ethylene glycol) (PEG) and Pluronic F-127	calcium phosphate nanocrystals	Cartilage	Schlichting et al. (2011)
PLA	nHA	Cartilage	Spadaccio et al. (2009)
PLA	Poly(1,8-octanediol-co-citrate) (POC), poly(1,10-decanediol-co-citrate) (PDC)	Cartilage, ligament	Webb et al. (2007)
Dissolved cellulose phase	Undissolved cellulose phase	Ligament, tendon	Mathew et al. (2012)
Collagen	Cellulose nanofibers	Ligament, tendon	Mathew et al. (2013)
PLA	Gold nanoparticles	Skeletal muscle	McKeon-Fischer and Freeman (2011)
PCL	Carbon nanotubes	Skeletal muscle	McKeon-Fischer et al. (2011)

nanocomposites comprising poly(propylene fumarate) (PPF) and single-walled carbon nanotubes (SWCNTs) as bone tissue engineering scaffolds. The authors tested the in vivo biocompatibility of the fabricated nanocomposites in a rabbit model. At 12 weeks, an enhanced bone ingrowth was found in femoral bone defects containing the nanocomposites as compared to the control polymer scaffolds.

1.2.2 Cell–material interaction at the nanoscale

The cell–material interaction is a dynamic process which controls the cellular response and function (Rosso et al., 2004; Ruosiahti and Pierschbacher, 1987; Lamers et al., 2012; Lamers et al., 2012). The first phase of the process involves protein adsorption, which occurs on contact with body fluids and is influenced by the physicochemical characteristics of the material and its fabricated form. This is followed by the cell-adhesion phase involving various biological molecules such as ECM, cell membrane, and cytoskeletal protein components. These interactions at the nanoscale modulate cellular responses in terms of migration, cell proliferation, and differentiation. Thus, considerable research efforts have been focused on development of nanomaterials with appropriate properties to enhance cell performance. The material properties in controlling the cell–material interactions can be broadly classified as physical, chemical, and biological cues (von der Mark et al., 2010).

1.2.2.1 Physical cues

Physical cues involve the physical interactions between the cells and the materials. The effect of surface nanotopography on cell behavior and tissue development has gained significant research interest in the field of tissue regeneration. For example, surface nanostructures of a square array of nanoscale pits were able to retain MSC phenotype and multipotency (McMurray et al., 2011), whereas a nanografting surface induced MSC differentiation (Yim et al., 2007). The structure of muscle tissue is composed of oriented muscle fibers that are formed by the fusion of myoblasts (Hawke and Garry, 2001). This orientation in fiber alignment enables an anisotropic organization of muscle tissue ECM for functional contraction. Accordingly, aligned fiber scaffolds have been developed to mimic skeletal muscle orientation and provide the necessary ECM cues to guide cellular organization. Huang et al. (2006) demonstrated that aligned PLA nanofibers promoted cell and cytoskeleton alignment, myoblast proliferation, myotube assembly, and myotube striation. The size of the nanotopography has also been reported to regulate cell–material interactions. Cai et al. (2007) demonstrated that the 20 nm nHA showed enhanced MSC proliferation along with inhibition of the osteosarcoma cells when compared with 40 and 80 nm nHA. Shi et al. (2009) also demonstrated that both cell proliferation and cell apoptosis are related to the size of the HA particles and concluded that nHA may be a better candidate for an apatite substitute of bone than microsized hydroxyapatite (mHA). The nHA also showed better osteoblast adhesion when compared to the mHA (Balasundaram et al., 2006). In addition, the material stiffness is another important factor that affects cell behavior (Reilly and Engler, 2010; Levy-Mishali et al., 2009; Discher et al., 2005).

1.2.2.2 Chemical cues

The presence of chemical functional groups (eg, -CH_3, -OH, -COOH, and -NH_2) on the material surface alters the surface properties of the material and cell–material interactions (Deng et al., 2012). For example, the presence of negatively charged functional groups on biomaterial surfaces is beneficial for the formation of an apatite layer and integration of biomaterials with surrounding bone. Nanocomposites containing —COOH functionalized SWCNTs have shown an enhanced chondrocyte activity (Chahine et al., 2014). In addition, the presence of amino acid groups in HA has been shown to enhance the osteoblast cell proliferation and cell mineralization (Boanini et al., 2006).

1.2.2.3 Biological cues

In addition to physical and chemical cues, the presence of bioactive molecules in a material influences cell adhesion, proliferation, and differentiation. Bioactive molecules can be either attached onto the material surface or incorporated into the material. For example, bone morphogenetic proteins (BMPs) have been used in combination with nanocomposites to enhance bone regeneration due to their osteoinductive capabilities (Chung et al., 2007). Lo et al. (2012) have shown that stimulation of protein kinase A (PKA) signaling pathway by continuous administration of 6-Bnz-cAMP, which is a PKA-specific cyclic adenosine monophosphate (cAMP) analog, promoted in vitro osteogenesis in MC3T3-E1 and hMSCs. A different route to achieve surface functionalization of the polymeric fibers involves the use of Arg-Gly-Asp (RGD) peptide (Paletta et al., 2010). Surface functionalization of PLA nanofibers with RGD was achieved using plasma treatment in combination with 1-ethyl-3-[3-dimethylaminopropyl]carbodiimide (EDC)/*N*-hydroxysulfosuccinimide (Sulfo-NHS) activation. The functionalized nanofibers mediated the expression of osteocalcin by hMSCs.

1.3 Fabrication of nanocomposites for musculoskeletal tissue engineering

The previous sections described the different classes of biomaterials and nanoscale components that have been used to create nanocomposites. This section will elaborate on the different techniques to fabricate nanocomposites.

1.3.1 Electrospinning

Polymeric nanofibers due to their similarity to natural ECM have been actively investigated for musculoskeletal tissue regeneration (Deng et al., 2012). A typical polymeric nanofiber scaffold is composed of ultrathin continuous fibers with high surface-to-volume ratio and porosity. Electrospinning provides a versatile technology platform for the design and fabrication of nanofiber-based matrices from various biodegradable polymers due to the ease of fabrication, efficient control over the process, and easy

scale-up (Huang et al., 2003). In an electrospinning process, polymeric nanofibers are created from a jet of polymer solution under the influence of applied electrical field between an ejecting needle and a collector. Fibers with diameters ranging from few nanometers to several micrometers can be obtained via electrospinning. Several parameters that control the electrospinning process include polymer solution viscosity and flow rate, applied electrical potential, distance between spinneret and collector, motion of the grounded target, and ambient conditions. So far, polymeric materials have been fabricated by electrospinning into various nanofiber structures such as random nanofibers (Kumbar et al., 2008; Li et al., 2001), aligned nanofibers (Shalumon et al., 2012; Xie et al., 2010), and polymer/ceramic nanocomposites (Zhang et al., 2008; Bhattacharyya et al., 2009). Other examples include micro-/nanofiber composites (Shim et al., 2009; Pham et al., 2006), core–shell nanofibers (Jiang et al., 2012; Pakravan et al., 2012), and 3D structures (Wang et al., 2014; Kumbar et al., 2011).

Laurencin and colleagues demonstrated for the first time the potential of electrospun PLGA scaffolds for applications in engineering tissues (Li et al., 2001). A number of tissue-specific electrospun polymeric nanofiber scaffolds have been fabricated from PLGA, polyphosphazenes, and PCL polymer blends or composites for regenerating bone (Bhattacharyya et al., 2006; Deng et al., 2011a), and soft tissues (Kumbar et al., 2008; Taylor, 2010; James et al., 2011b; Peach et al., 2012a). Inspired by the hierarchical structures that enable bone function, Deng et al. (2011a) developed a mechanically competent 3D scaffold mimicking the bone marrow cavity, as well as the lamellar structure of bone by orienting electrospun polyphosphazene–polyester blend nanofibers in a concentric manner with an open central cavity (Fig. 1.2). The 3D biomimetic scaffold exhibited a similar characteristic mechanical behavior to that of native bone. Compressive modulus of the scaffold was found within the range of human trabecular bone. The potential of this scaffold for bone repair was further investigated by monitoring the cellular activity and mechanical performance over time using in vitro culture. These blend nanofiber matrices supported osteoblast adhesion and proliferation and showed an elevated phenotype expression compared to PLGA nanofibers. This biomimetic scaffold supported the robust osteoblast growth throughout the scaffold architecture and maintained osteoblast phenotype expression in vitro, which resulted in a similar cell–matrix organization to that of native bone and maintenance of structure integrity.

Fu et al. (2012) fabricated electrospun nanofibers comprising polycaprolactone–polyethylenegylcol–polycaprolactone (PCEC) containing nHA (Fig. 1.3). The fabricated nanocomposite showed enhanced activity for bone regeneration when compared to the sham control in the in vivo rabbit model study. The electrospinning process has also been combined with other fabrication processes. Zhang et al. (2008) combined coprecipitation with electrospinning to obtain HA/chitosan nanocomposites. The nanocomposites were shown to have improved osteogenic inductivity when compared to the electrospun chitosan polymers. The incorporated HA nanoparticles enhanced the osteoconductivity of the nanocomposite material when compared to the chitosan. Aligned PLGA/HA nanofibers have also been researched for their potential in bone regeneration (Jose et al., 2009). Initial increase in HA content increased storage modulus but further increase in HA reduced the storage modulus. Electrospun PLGA

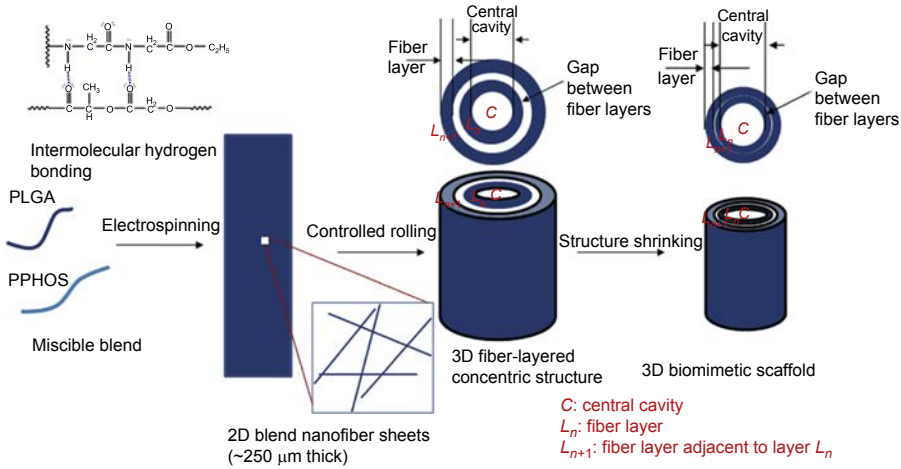

Figure 1.2 Schematics of 3D biomimetic scaffold design and fabrication. Intermolecular hydrogen-bonding interactions between polyphosphazine (PPHOS) and PLGA result in a miscible-blend system. Electrospinning of the polymer-blend solution creates a nonwoven nanofiber mat. Rectangular polymer sheets are then cut from the nanofiber mat (~250 μm thick) and rolled up into a 3D-fiber layered concentric structure in a controlled fashion. Finally, incubation in the cell media drives away the air within the structure and leads to structure shrinkage resulting in the formation of a 3D intact nanostructured scaffold. During shrinkage, the scaffold structure including the gap space between the fiber layers (L_n and L_{n+1}) is significantly reduced. However, the dimensional stability of the open central cavity (C) is maintained to encourage nutrient transport.
Reproduced from Deng, M., Kumbar, S.G., et al., 2011a. Biomimetic structures: biological implications of dipeptide-substituted polyphosphazene-polyester blend nanofiber matrices for load-bearing bone regeneration. Advanced Functional Materials 21 (14), 2641–2651. Available at: http://doi.wiley.com/10.1002/adfm.201100275 (accessed 11.12.14.).

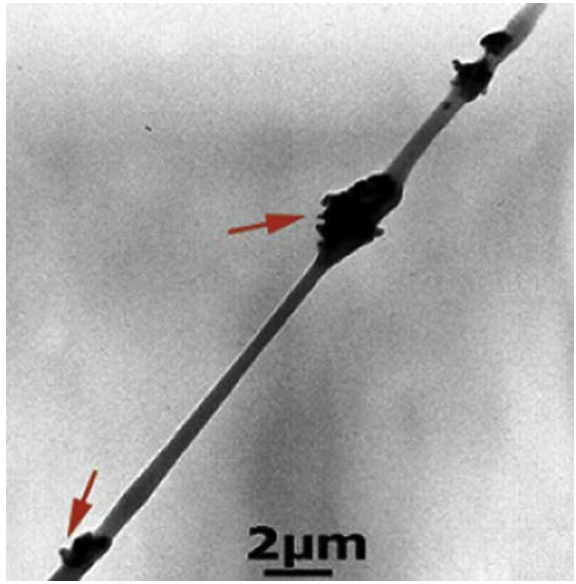

Figure 1.3 TEM photograph of electrospun PCEC/nHA composite fiber. Arrows denote the HA particles.
Reproduced from Fu, S., et al., 2012. In vivo biocompatibility and osteogenesis of electrospun poly(e-caprolactone)-poly(ethylene glycol)-poly(e-caprolactone)/nano-hydroxyapatite composite scaffold. Biomaterials 33 (33), 8363–8371.

nanofibers coated with gradient calcium phosphates have also been researched for their potential in tendon-to-bone mimics (Li et al., 2009).

Electrospun fibers have also been researched for cartilage regeneration procedures. Thorvaldsson et al. (2008) used a combination of micro- and nanofibers to create novel fiber structures. This enhanced the pore structure characteristics of the fabricated scaffold. The synthesized scaffold enhanced the human chondrocyte infiltration. Nanocomposites consisting of multiwalled carbon nanotubes (MWCNTs) and PLA were fabricated using electrospinning. The nanocomposite material displayed enhanced mechanical properties and improved the chondrogenesis of MSCs (Holmes et al., 2013).

In addition, a variety of polymer composites with unique conductive and electric properties have been developed for skeletal muscle regeneration by combining polymers with metal nanoparticles (McKeon-Fischer and Freeman, 2011) and carbon nanotubes (McKeon-Fischer et al., 2014). For example, McKeon-Fischer et al. (2011) has developed an electrospun scaffold through the combination of PCL with MWCNTs and a hydrogel consisting of polyvinyl alcohol and polyacrylic acid as a potential nanoactuator for skeletal muscle engineering.

1.3.2 Lithography

Lithography is a technique that can be employed to fabricate materials with specified dimensions and patterns. Lithography techniques have been widely utilized to create patterned surfaces in microelectromechanical systems (MEMS) and nanoelectromechanical systems (NEMS) (Schulz, 2009). With the recent studies highlighting the importance of patterned surfaces in controlling cellular responses, researchers have gained interest in using lithography for tissue engineering applications (Kai et al., 2011; Shekaran and Garcia, 2011; Stratakis et al., 2011; Kaji et al., 2011).

Two different lithographic techniques have been employed for fabrication of polymer-based nanocomposites:

- **Photolithography:** Photolithographic technique is applied to photosensitive polymers. UV/X-rays can be used as sources of irradiation. The photosensitive polymer precursors polymerize upon the contact with UV radiation. The photoinitiator present in polymer matrix initiates the polymerization reaction (Ingrosso et al., 2010). The regions that have been masked will not undergo polymerization. Therefore, hard polymerized region can be patterned from this technique.
- **Electron beam lithography:** During electron beam lithography (EBL), the incident electron beam is bombarded onto the exposed region of the polymer matrix. The bombarded electron beam generates secondary electrons. These electrons spread and cleave the polymer backbone, thereby obtaining patterned surfaces (Lewis and Piccirillo, 2002). The proximity effects play a major role in developing nanostructures when EBL is used. When nanocomposite materials are employed, the proximity effects are reduced and, therefore, can provide precise patterning of the surfaces (Ishii et al., 1997, 2000; Gonsalves et al., 2001). For example, EBL technique has been used to fabricate ordered arrays of nanodimensions for the examination of cell–nanoenvironment interactions (Dalby et al., 2007; Vieu et al., 2000).

In addition, mask-free methods involving 3D printing have also been employed to fabricate polymer nanocomposites. 3D printed scaffolds have tailored pore structures with high precision. The 3D structural data are converted to 2D data by slicing the 3D structures. 2D structures are printed layer by layer to obtain the final 3D structures. Computer-aided modeling tools are used to process the 3D structural data into 2D structural data (Leukers et al., 2005). For example, nanocomposites consisting of titania nanoparticles and PLGA have been 3D printed (Liu and Webster, 2007). The 3D-printed scaffolds showed enhanced osteoblast adhesion and infiltration.

The patterned surfaces provide guidance for the cells to adhere, proliferate, and elongate.

1.3.3 Layer-by-layer self-assembly

Layer-by-layer (LbL) assembly is a technique used for fabricating multilayered film structures that are composed of polyelectrolyte molecules. Decher et al. (1992) demonstrated the proof of concept for LbL self-assembly by fabricating multilayered films with alternating anionic and cationic polyelectrolytes. The layers are held together on the basis of hydrogen bonding, electrostatic, covalent, hydrophobic, and biological interactions (Shukla and Almeida, 2014). Layers with compliment functionality are deposited one after the other. The thickness of the layers can be modulated by varying the coating time. The adsorption kinetic of the species on the surface plays an important role in growth of the film (Shukla and Almeida, 2014). The ion concentration, pH of the media, and the working medium polarity can also modulate the properties of the species and species interactions (Dubas and Schlenoff, 1999; Bieker and Schönhoff, 2010). LbL assembly can be employed for macroscopic surfaces (Saurer et al., 2009) and nanoscale surfaces (Poon et al., 2011). LbL assembly can be extended to lipids, polypeptides, nucleic acids, proteins, and any charged surfaces (Tang et al., 2006). The LbL assembly can also be used to create polymer nanocomposite structures by adsorbing the nanoparticles on the surface of the polymer layer.

Li et al. employed LbL self-assembly to construct multilayered films on top of nonwoven PCL fibers. The multilayered film consisted of gelatin and polystyrene salt. The top layer was further coated with calcium phosphate. The fabricated scaffold was tested for its potential in bone tissue engineering. Results indicated an enhanced cell proliferation for the LbL-assembled scaffolds (Li et al., 2008). Zhang et al. (2005) employed LbL fabrication technique to form multilayers consisting of type I collagen and hyaluronic acid and were able to generate fibrous multilayered structures that supported the attachment of chondrosarcoma cells.

Crouzier et al. (2011) coated ceramic β-tricalcium phosphate/HA granules with poly-L-lysine/hyaluronic acid. The authors further loaded BMP-2 and cross-linked the polyelectrolyte multilayer films. Controlled release of BMP-2 was achieved by varying the cross-linking ratio. The fabricated porous scaffold showed good osteoconductivity (Crouzier et al., 2011). Because LbL assembly can be performed on any surface, it opens up research avenues of coating metallic implants with polyelectrolyte multilayer films. Guillot et al. introduced polyelectrolyte multilayer coating on titanium implants. The polyelectrolyte coating was embedded with BMP-2. The polyelectrolyte

multilayer coating consisted of cross-linked poly-L-lysine and hyaluronic acid. The BMP-2-loaded titanium implant surface showed enhanced osteoinductive properties. The authors have also tested for the shelf life of the fabricated implant and reported that the implant can be stored at 4°C for at least 6 months (Guillot et al., 2014).

1.3.4 Other fabrication techniques

Apart from the fabrication techniques mentioned in the previous sections, other fabrication techniques such as solvent casting, freeze-drying, and electrodeposition, and hot-melt extrusion have been successfully employed for tissue engineering applications.

Solvent casting involves the dispersion of the nanoscale components into the polymer solution. The solution containing the polymer and the nanoscale components are subsequently casted and dried till the solvent evaporates. A specific-sized porogen agent (such as salt, sugar, or others) is often dispersed in the polymer solution for fabrication of a porous structure. Torabinejad et al. (2014) fabricated nanocomposites comprising nHA and triblock copolymers of L-lactide and ε-caprolactone by solvent casting. The fabricated scaffolds supported osteoblast attachment and mineralization (Fig. 1.4). This technique is simple and involves no complex instrumentation. Scale-up of this technique is highly efficient; therefore, this technique can be used in industries for large-scale production (Tanaka et al., 2008).

Freeze drying has been employed to fabricate nanocomposites by dispersing the nanoscale components in the polymer and freezing them at very low temperatures (−80°C). During the process of cooling, there will be phase separation due to thermodynamic instability (Sun et al., 2011). When they are dried, the solvent phase evaporates, leaving behind the porous nanocomposite materials.

Nanoscale components can be coated on the material surfaces via electrodeposition. He et al. (2010) demonstrated the use of this technique by mineralizing calcium phosphate on PLA nanofibers. The PLA nanofibers were collected on metal electrodes used for the fabrication process of electrodeposition. The calcium phosphate coating was deposited on the electrodes containing the PLA nanofibers. The authors have also varied the topography of the surface by changing the electrodeposition process parameters.

Hot-melt extrusion has also been used to fabricate nanocomposites. Liao et al. (2013) employed a hot-melt extrusion fabrication technique to fabricate polypropylene-based nanocomposites. Polypropylene, MWCNTs, and HA nanorods were added to the twin-screw extruder. The nanocomposites were molded into rectangular shapes. The authors have hypothesized the potential of the fabricated nanocomposite for bone implants.

1.4 Conclusions

Tissue engineering is a multidisciplinary field involving materials science, chemistry, cell biology, bioengineering, and medicine. It aims to develop functional biological tissue substitutes by engineering 3D scaffolds with appropriate physical, chemical,

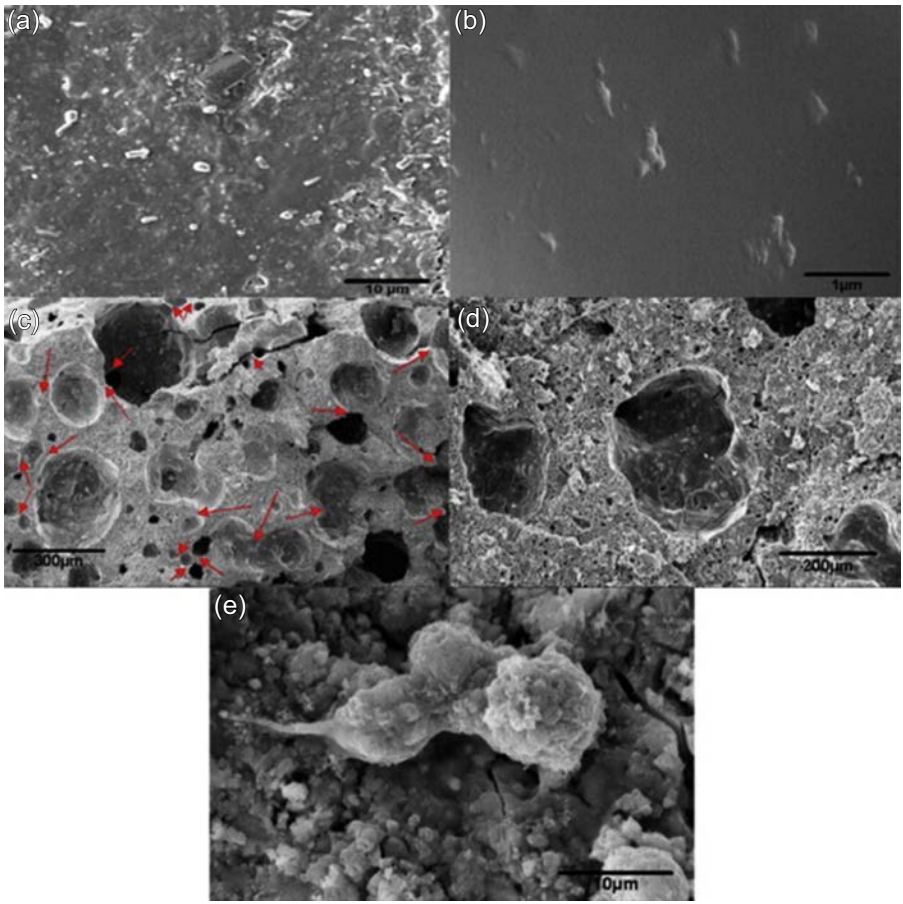

Figure 1.4 SEM images of (a), (b) nanocomposite 30% nHA, scaffold 30% nHA; (c) before cell culture with interconnectivity (pore size 200–300 µm, ~70% porosity); The arrows indicate interconnected pore structures; (d) before cell culture; and (e) after cell culture. Reproduced from Torabinejad, B., et al., 2014. Synthesis and characterization of nanocomposite scaffolds based on triblock copolymer of L-lactide, e-caprolactone and nano-hydroxyapatite for bone tissue engineering. Materials Science & Engineering. C, Materials for Biological Applications 42, 199–210. Available at: http://www.ncbi.nlm.nih.gov/pubmed/25063111 (accessed 25.09.14.).

and biological properties. Nanocomposites have demonstrated great promise for the development of tissue-specific scaffolds that promote regeneration of individual musculoskeletal tissues as evidenced from the studies previously mentioned. However, grand challenges remain in successful regeneration of musculoskeletal tissue interfaces and complex tissue systems possessing tissue-type heterogeneity and anisotropic properties. The integration of physical, chemical, and biological cues built from the nanoscale will be accelerated through a further understanding of cell–material interactions at the nanoscale as well as advances in fabrication technology.

Acknowledgments

Funding support from Showalter Trust, Purdue Research Foundation, and Purdue Start-up Package is greatly appreciated.

References

Ahadian, S., et al., 2014. Hybrid hydrogels containing vertically aligned carbon nanotubes with anisotropic electrical conductivity for muscle myofiber fabrication. Scientific Reports 4, 4271. Available at: http://www.pubmedcentral.nih.gov/articlerender.fcgi?artid=3958721&tool=pmcentrez&rendertype=abstract (accessed 04.04.14.).

Alsberg, E., et al., 2001. Cell-interactive alginate hydrogels for bone tissue engineering. Journal of Dental Research 80 (11), 2025–2029. Available at: http://jdr.sagepub.com/cgi/doi/10.1177/00220345010800111501 (accessed 10.10.14.).

Armentano, I., et al., 2010. Biodegradable polymer matrix nanocomposites for tissue engineering: a review. Polymer Degradation and Stability 95 (11), 2126–2146. Available at: http://linkinghub.elsevier.com/retrieve/pii/S0141391010002430 (accessed 14.07.14.).

Athanasiou, K.A., Niederauer, G.G., Agrawal, C.M., 1996. Biocompatibility and clinical applications of polylactic acid/polyglycolic acid copolymers. Biomaterials 17 (2).

Balasundaram, G., Sato, M., Webster, T.J., 2006. Using hydroxyapatite nanoparticles and decreased crystallinity to promote osteoblast adhesion similar to functionalizing with RGD. Biomaterials 27 (14), 2798–2805. Available at: http://www.ncbi.nlm.nih.gov/pubmed/16430957 (accessed 08.10.14.).

Bernstein, M., et al., 2010. Low temperature fabrication of β-TCP-PCL nanocomposites for bone implants. Advanced Engineering Materials 12 (8), B341–B347. Available at: http://doi.wiley.com/10.1002/adem.201080027 (accessed 10.10.14.).

Bhattacharyya, S., et al., 2006. Electrospinning of poly [bis (ethyl alanato) phosphazene] nanofibers. Journal of Biomedical Nanotechnology 2 (1), 36–45.

Bhattacharyya, S., et al., 2009. Biodegradable polyphosphazene-nanohydroxyapatite composite nanofibers: scaffolds for bone tissue engineering. Journal of Biomedical Nanotechnology 5 (1), 69–75.

Bieker, P., Schönhoff, M., 2010. Linear and exponential growth regimes of multilayers of weak polyelectrolytes in dependence on pH. Macromolecules 43 (11), 5052–5059. Available at: http://pubs.acs.org/doi/abs/10.1021/ma1007489 (accessed 08.10.14.).

Boanini, E., et al., 2006. Nanocomposites of hydroxyapatite with aspartic acid and glutamic acid and their interaction with osteoblast-like cells. Biomaterials 27 (25), 4428–4433. Available at: http://www.ncbi.nlm.nih.gov/pubmed/16682075 (accessed 08.10.14.).

Brown, J.L., et al., 2010. Composite scaffolds: bridging nanofiber and microsphere architectures to improve bioactivity of mechanically competent constructs. Journal of Biomedical Materials Research. Part A 95 (4), 1150–1158. Available at: http://www.ncbi.nlm.nih.gov/pubmed/20878987 (accessed 10.10.14.).

Cai, Y., et al., 2007. Role of hydroxyapatite nanoparticle size in bone cell proliferation. Journal of Materials Chemistry 17 (36), 3780. Available at: http://xlink.rsc.org/?DOI=b705129h (accessed 08.10.14.).

Cen, L., et al., 2008. Collagen tissue engineering: development of novel biomaterials. Pediatric Research 63 (5), 492–496.

Chahine, N.O., et al., 2014. Nanocomposite scaffold for chondrocyte growth and cartilage tissue engineering: effects of carbon nanotube surface functionalization. Tissue Engineering. Part A 20 (17–18), 2305–2315. Available at: http://www.ncbi.nlm.nih.gov/pubmed/24593020 (accessed 08.10.14.).

Chen, G., Ushida, T., Tateishi, T., 2000. Hybrid biomaterials for tissue engineering: a preparative method for PLA or PLGA-collagen hybrid sponges. Advanced Materials 12 (6), 455–457. Available at: http://doi.wiley.com/10.1002/(SICI)1521-4095(200003)12:6<455::AID-ADMA455>3.0.CO;2-C.

Chen, F., et al., 2006. Biocompatibility of electrophoretical deposition of nanostructured hydroxyapatite coating on roughen titanium surface: in vitro evaluation using mesenchymal stem cells. Journal of Biomedical Materials Research Part B 82, 183–191.

Chu, C.R., et al., 1995. Articular cartilage repair using allogeneic perichondrocyte- seeded biodegradable porous polylactic acid (PLA): a tissue-engineering study. Journal of Biomedical Materials Research 29, 1147–1154.

Chung, Y.-I., et al., 2007. Enhanced bone regeneration with BMP-2 loaded functional nanoparticle-hydrogel complex. Journal of Controlled Release : Official Journal of the Controlled Release Society 121 (1–2), 91–99. Available at: http://www.ncbi.nlm.nih.gov/pubmed/17604871 (accessed 19.12.14.).

Clarke, B., 2008. Normal bone anatomy and physiology. Clinical Journal of the American Society of Nephrology : CJASN 3 (Suppl. 3), S131–S139. Available at: http://www.pubmedcentral.nih.gov/articlerender.fcgi?artid=3152283&tool=pmcentrez&rendertype=abstract (accessed 09.07.14.).

Crouzier, T., et al., 2011. The performance of BMP-2 loaded TCP/HAP porous ceramics with a polyelectrolyte multilayer film coating. Biomaterials 32 (30), 7543–7554. Available at: http://www.ncbi.nlm.nih.gov/pubmed/21783243 (accessed 29.09.14.).

Dai, N.-T., et al., 2004. Composite cell support membranes based on collagen and polycaprolactone for tissue engineering of skin. Biomaterials 25 (18), 4263–4271. Available at: http://www.ncbi.nlm.nih.gov/pubmed/15046916 (accessed 10.10.14.).

Dalby, M.J., et al., 2007. The control of human mesenchymal cell differentiation using nanoscale symmetry and disorder. Nature Materials 6 (12), 997–1003. Available at: http://www.nature.com/doifinder/10.1038/nmat2013.

Decher, G., Hong, J.D., Schmitt, J., 1992. Buildup of ultrathin multilayer films by a self-assembly process: III. Consecutively alternating adsorption of anionic and cationic polyelectrolytes on charged surfaces. Thin Solid Films 210–211, 831–835. Available at: http://linkinghub.elsevier.com/retrieve/pii/004060909290417A.

Deng, M., et al., 2008. Miscibility and in vitro osteocompatibility of biodegradable blends of poly[(ethyl alanato) (p-phenyl phenoxy) phosphazene] and poly(lactic acid-glycolic acid). Biomaterials 29 (3), 337–349. Available at: http://www.pubmedcentral.nih.gov/articlerender.fcgi?artid=2129129&tool=pmcentrez&rendertype=abstract.

Deng, M., Nair, L.S., Nukavarapu, S.P., Kumbar, S.G., Brown, J.L., et al., 2010a. Biomimetic, bioactive etheric polyphosphazenepoly(lactide-co-glycolide) blends for bone tissue engineering. Journal of Biomedical Materials Research. Part A 92 (1), 114–125.

Deng, M., Nair, L.S., Nukavarapu, S.P., Jiang, T., et al., 2010b. Dipeptide-based polyphosphazene and polyester blends for bone tissue engineering. Biomaterials 31 (18), 4898–4908. Available at: http://dx.doi.org/10.1016/j.biomaterials.2010.02.058.

Deng, M., Nair, L.S., Nukavarapu, S.P., Kumbar, S.G., Jiang, T., et al., 2010c. In situ porous structures: a unique polymer erosion mechanism in biodegradable dipeptide-based polyphosphazene and polyester blends producing matrices for regenerative engineering. Advanced Functional Materials 20 (17), 2794–2806.

Deng, M., et al., 2010d. Polyphosphazene polymers for tissue engineering: an analysis of material synthesis, characterization and applications. Soft Matter 6, 3119–3132. Available at: <Go to ISI>://000279566800002.

Deng, M., Kumbar, S.G., et al., 2011a. Biomimetic structures: biological implications of dipeptide-substituted polyphosphazene-polyester blend nanofiber matrices for load-bearing bone regeneration. Advanced Functional Materials 21 (14), 2641–2651. Available at: http://doi.wiley.com/10.1002/adfm.201100275 (accessed 11.12.14.).

Deng, M., Kumbar, S.G., et al., 2011b. Novel polymer-ceramics for bone repair and regeneration. Recent Patents on Biomedical Engineering 4 (3), 168–184. Available at: http://www.pubmedcentral.nih.gov/articlerender.fcgi?artid=4030995&tool=pmcentrez&rendertype=abstract.

Deng, M., et al., 2012. Nanostructured polymeric scaffolds for orthopaedic regenerative engineering. IEEE Transactions on Nanobioscience 11 (1), 3–14.

Discher, D.E., Janmey, P., Wang, Y.-L., 2005. Tissue cells feel and respond to the stiffness of their substrate. Science (New York, NY) 310 (5751), 1139–1143. Available at: http://www.ncbi.nlm.nih.gov/pubmed/16293750 (accessed 12.07.14.).

Dubas, S.T., Schlenoff, J.B., 1999. Factors controlling the growth of polyelectrolyte multilayers. Macromolecules 32 (24), 8153–8160. Available at: http://pubs.acs.org/doi/abs/10.1021/ma981927a.

Ebrahimian-Hosseinabadi, M., et al., 2011. Evaluating and modeling the mechanical properties of the prepared PLGA/nano-BCP composite scaffolds for bone tissue engineering. Journal of Materials Science & Technology 27 (12), 1105–1112. Available at: http://linkinghub.elsevier.com/retrieve/pii/S1005030212600048 (accessed 10.10.14.).

Frank, C.B., 2004. Ligament structure, physiology and function. Journal of Musculoskeletal and Neuronal Interactions 4 (2), 199–201.

Fu, S., et al., 2012. In vivo biocompatibility and osteogenesis of electrospun poly(ε-caprolactone)-poly(ethylene glycol)-poly(ε-caprolactone)/nano-hydroxyapatite composite scaffold. Biomaterials 33 (33), 8363–8371.

Ghasemi-Mobarakeh, L., et al., 2008. Electrospun poly(epsilon-caprolactone)/gelatin nanofibrous scaffolds for nerve tissue engineering. Biomaterials 29 (34), 4532–4539. Available at: http://www.ncbi.nlm.nih.gov/pubmed/18757094 (accessed 09.10.14.).

Glowacki, J., Mizuno, S., 2008. Collagen scaffolds for tissue engineering. Biopolymers 89 (5), 338–344. Available at: http://www.ncbi.nlm.nih.gov/pubmed/17941007 (accessed 15.07.14.).

Gonsalves, B.K.E., et al., 2001. Organic – inorganic nanocomposites : unique resists for nanolithography **. Advanced Materials 13 (10), 703–714.

Guillot, R., et al., 2014. Europe PMC funders group the stability of BMP loaded polyelectrolyte multilayer coatings on titanium. Biomaterials 34 (23), 5737–5746.

Harrison, B.S., Atala, A., 2007. Carbon nanotube applications for tissue engineering. Biomaterials 28 (2), 344–353. Available at: http://www.ncbi.nlm.nih.gov/pubmed/16934866 (accessed 17.09.14.).

Hawke, T.J., Garry, D.J., 2001. Myogenic satellite cells physiology to molecular biology. Journal of Applied Physiology 91, 534–551.

He, C., et al., 2010. Electrodeposition on nanofibrous polymer scaffolds: rapid mineralization, tunable calcium phosphate composition and topography. Advanced Functional Matter 20 (20), 3568–3576.

Holmes, B., et al., 2013. Enhanced human bone marrow mesenchymal stem cell functions in novel 3D cartilage scaffolds with hydrogen treated multi-walled carbon nanotubes. Nanotechnology 24 (36), 365102. Available at: http://www.ncbi.nlm.nih.gov/pubmed/23959974 (accessed 08.10.14.).

Huang, Z.-M., et al., 2003. A review on polymer nanofibers by electrospinning and their applications in nanocomposites. Composites Science and Technology 63 (15), 2223–2253. Available at: http://linkinghub.elsevier.com/retrieve/pii/S0266353803001787 (accessed 11.07.14.).

Huang, N.F., et al., 2006. Myotube assembly on nanofibrous and micropatterned polymers. Nano Letters 6 (3), 537–542. Available at: http://www.ncbi.nlm.nih.gov/pubmed/16522058.

Huang, J., et al., 2007. Development of nano-sized hydroxyapatite reinforced composites for tissue engineering scaffolds. Journal of Materials Science. Materials in Medicine 18 (11), 2151–2157. Available at: http://www.ncbi.nlm.nih.gov/pubmed/17891551 (accessed 11.10.14.).

Ingrosso, C., et al., 2010. Colloidal inorganic nanocrystal based nanocomposites: functional materials for micro and nanofabrication. Materials 3 (2), 1316–1352. Available at: http://www.mdpi.com/1996-1944/3/2/1316/ (accessed 02.10.14.).

Ishii, T., Nozawa, H., Tamamura, T., 1997. Nanocomposite resist system. Applied Physics Letters 70 (9), 1110. Available at: http://scitation.aip.org/content/aip/journal/apl/70/9/10.1063/1.118500 (accessed 10.10.14.).

Ishii, T., Takamura, T., Shigehara, K., 2000. Fullerene-derivative nanocomposite resist for nanometer pattern fabrication fullerene-derivative nanocomposite resist for nanometer pattern fabrication. Japan Journal of Applied Physics 39, 1068–1070.

James, R., et al., 2011a. Nanocomposites and bone regeneration. Frontiers of Materials Science 5 (4), 342–357. Available at: http://link.springer.com/article/10.1007%2Fs11706-011-0151-.

James, R., et al., 2011b. Tendon tissue engineering: adipose-derived stem cell and GDF-5 mediated regeneration using electrospun matrix systems. Biomedical Materials (Bristol, England) 6 (2), 025011. Available at: http://www.pubmedcentral.nih.gov/articlerender.fcgi?artid=3206634&tool=pmcentrez&rendertype=abstract.

Jayakumar, R., Ramachandran, R., Divyarani, V.V., et al., 2011a. Fabrication of chitin-chitosan/nano TiO2-composite scaffolds for tissue engineering applications. International Journal of Biological Macromolecules 48 (2), 336–344. Available at: http://www.ncbi.nlm.nih.gov/pubmed/21182857 (accessed 10.10.14.).

Jayakumar, R., Ramachandran, R., Sudheesh Kumar, P.T., et al., 2011b. Fabrication of chitin-chitosan/nano ZrO(2) composite scaffolds for tissue engineering applications. International Journal of Biological Macromolecules 49 (3), 274–280. Available at: http://www.ncbi.nlm.nih.gov/pubmed/21575656 (accessed 10.10.14.).

Jiang, Y.-N., Mo, H.-Y., Yu, D.-G., 2012. Electrospun drug-loaded core-sheath PVP/zein nanofibers for biphasic drug release. International Journal of Pharmaceutics 438 (1–2), 232–239. Available at: http://www.ncbi.nlm.nih.gov/pubmed/22981688 (accessed 04.06.14.).

Jiang, T., et al., 2014. Micro- and nanofabrication of chitosan structures for regenerative engineering. Acta Biomaterialia 10 (4), 1632–1645. Available at: http://linkinghub.elsevier.com/retrieve/pii/S1742706113003425.

Jin, X.B., et al., 2008. Tissue engineered cartilage from hTGF beta2 transduced human adipose derived stem cells seeded in PLGA/alginate compound in vitro and in vivo. Journal of Biomedical Materials Research. Part A 86 (4), 1077–1087. Available at: http://www.ncbi.nlm.nih.gov/pubmed/18080296 (accessed 10.10.14.).

Jose, M.V., et al., 2009. Aligned PLGA/HA nanofibrous nanocomposite scaffolds for bone tissue engineering. Acta Biomaterialia 5 (1), 305–315. Available at: http://www.ncbi.nlm.nih.gov/pubmed/18778977 (accessed 08.10.14.).

Jose, M.V., et al., 2010. Aligned bioactive multi-component nanofibrous nanocomposite scaffolds for bone tissue engineering. Macromolecular Bioscience 10 (4), 433–444. Available at: http://www.ncbi.nlm.nih.gov/pubmed/20112236 (accessed 10.10.14.).

Kai, D., et al., 2011. Guided orientation of cardiomyocytes on electrospun aligned nanofibers for cardiac tissue engineering. Journal of Biomedical Materials Research. Part B, Applied Biomaterials 98 (2), 379–386. Available at: http://www.ncbi.nlm.nih.gov/pubmed/21681953 (accessed 19.12.14.).

Kaji, H., et al., 2011. Engineering systems for the generation of patterned co-cultures for controlling cell-cell interactions. Biochimica Et Biophysica Acta 1810 (3), 239–250. Available at: http://www.pubmedcentral.nih.gov/articlerender.fcgi?artid=3026923&tool=pmcentrez&rendertype=abstract (accessed 19.11.14.).

Kannus, P., 2000. Structure of the tendon connective tissue. Scandinavian Journal of Medicine and Science in Sports 10 (6), 312–320. Available at: http://doi.wiley.com/10.1034/j.1600-0838.2000.010006312.x.

Karp, J.M., Shoichet, M.S., Davies, J.E., 2002. Bone formation on two-dimensional poly (DL-lactide-co-glycolide) (PLGA) films and three-dimensional PLGA tissue engineering scaffolds in vitro. Journal of Biomedical Materials Research 64, 388–396.

Kim, H.-W., Kim, H.-E., Salih, V., 2005. Stimulation of osteoblast responses to biomimetic nanocomposites of gelatin-hydroxyapatite for tissue engineering scaffolds. Biomaterials 26 (25), 5221–5230. Available at: http://www.ncbi.nlm.nih.gov/pubmed/15792549 (accessed 10.10.14.).

Kim, I.-Y., et al., 2008. Chitosan and its derivatives for tissue engineering applications. Biotechnology Advances 26 (1), 1–21. Available at: http://www.ncbi.nlm.nih.gov/pubmed/17884325 (accessed 22.08.14.).

Kumbar, S.G., et al., 2008. Electrospun poly(lactic acid-co-glycolic acid) scaffolds for skin tissue engineering. Biomaterials 29 (30), 4100–4107. Available at: http://www.pubmedcentral.nih.gov/articlerender.fcgi?artid=2605109&tool=pmcentrez&rendertype=abstract (accessed 09.10.14.).

Kumbar, S.G., et al., 2011. Novel mechanically competent polysaccharide scaffolds for bone tissue engineering. Biomedical Materials 6, 065005.

Kumbar, S.G., Laurencin, C.T., Deng, M., 2014. In: Kumbar, S.G., Laurencin, C.T., Deng, M. (Eds.), Natural and Synthetic Biomedical Polymers. Elsevier, Burlington, San Diego.

Kweon, H., et al., 2003. A novel degradable polycaprolactone networks for tissue engineering. Biomaterials 24, 801–808.

Lamers, E., et al., 2012. Dynamic cell adhesion and migration on nanoscale. European Cells and Material 23, 182–194.

Langer, R., Vacanti, J.P., 1993. Tissue engineering. Science 260 (5110), 920–926.

Laurencin, C.T., et al., 1999. Tissue engineering: orthopedic applications. Annual Review of Biomedical Engineering 1, 19–46.

Lee, H.J., et al., 2007. The effect of surface-modified nano-hydroxyapatite on biocompatibility of poly(ε-caprolactone)/hydroxyapatite nanocomposites. European Polymer Journal 43 (5), 1602–1608. Available at: http://linkinghub.elsevier.com/retrieve/pii/S0014305707001309 (accessed 10.10.14.).

Leukers, B., et al., 2005. Hydroxyapatite scaffolds for bone tissue engineering made by 3D printing. Journal of materials science. Materials in Medicine 16 (12), 1121–1124. Available at: http://www.ncbi.nlm.nih.gov/pubmed/16362210.

Levy-mishali, M., et al., 2009. Effect of scaffold stiffness on myoblast differentiation. Tissue Engineering. Part A 15 (4), 23–27.

Lewandrowski, K., et al., 2003. Enhanced bioactivity of a poly (propylene fumarate) bone graft substitute by augmentation with nano-hydroxyapatite. Biomedical Materials and Engineeirng 13, 115–124.

Lewis, S., Piccirillo, L., 2002. Influence of nanocomposite materials for next generation nano lithography. In: Reddy, B. (Ed.), Advances in Diverse Industrial Applications of Nanocomposites. InTech, pp. 475–500.

Li, X., Chang, J., 2008. Preparation of bone-like apatite-collagen nanocomposites by a biomimetic process with phosphorylated collagen. Journal of Biomedical Materials Research. Part A 85 (2), 293–300. Available at: http://www.ncbi.nlm.nih.gov/pubmed/17688292 (accessed 10.10.14.).

Li, W., et al., 2001. Electrospun nanofibrous structure : a novel scaffold for tissue engineering. Journal of Biomedical Materials Research 60, 613–621.

Li, X., et al., 2008. Coating electrospun poly (ε-caprolactone) fibers with gelatin and calcium phosphate and their use as biomimetic scaffolds for bone tissue engineering. Langmuir (4), 14145–14150.

Li, X., et al., 2009. Nanofiber scaffolds with gradations in mineral content for mimicking the tendon-to-bone insertion site. Nano Letters 9 (7), 2763–2768. Available at: http://www.pubmedcentral.nih.gov/articlerender.fcgi?artid=2726708&tool=pmcentrez&rendertype=abstract.

Liao, S., et al., 2005. A three-layered nano-carbonated hydroxyapatite/collagen/PLGA composite membrane for guided tissue regeneration. Biomaterials 26 (36), 7564–7571. Available at: http://www.ncbi.nlm.nih.gov/pubmed/16005963 (accessed 10.10.14.).

Liao, C.Z., et al., 2013. Novel polypropylene biocomposites reinforced with carbon nanotubes and hydroxyapatite nanorods for bone replacements. Materials Science & Engineering. C, Materials for Biological Applications 33 (3), 1380–1388. Available at: http://www.ncbi.nlm.nih.gov/pubmed/23827585 (accessed 08.10.14.).

Liu, H., Webster, T.J., 2007. Ceramic/polymer nanocomposite tissue engineering scaffolds for more effective orthopedic applications: from 2D surfaces to novel 3D architectures. Materials Research Society 950 (i), 1–6.

Lv, Q., Nair, L., Laurencin, C.T., 2009. Fabrication, characterization, and *in vitro* evaluation of poly(lactic acid glycolic acid)/nano-hydroxyapatite composite microsphere-based scaffolds for bone tissue engineering in rotating bioreactors. Journal of Biomedical Materials Research. Part A 91A (3), 679–691. Available at: http://doi.wiley.com/10.1002/jbm.a.32302.

Lv, Q., et al., 2013. Nano-ceramic composite scaffolds for bioreactor-based bone engineering. Clinical Orthopaedics and Related Research® 471 (8), 2422–2433. Available at: http://link.springer.com/10.1007/s11999-013-2859-0.

Marelli, B., et al., 2011. Accelerated mineralization of dense collagen-nano bioactive glass hybrid gels increases scaffold stiffness and regulates osteoblastic function. Biomaterials 32 (34), 8915–8926. Available at: http://www.ncbi.nlm.nih.gov/pubmed/21889796 (accessed 08.10.14.).

von der Mark, K., et al., 2010. Nanoscale engineering of biomimetic surfaces: cues from the extracellular matrix. Cell and Tissue Research 339 (1), 131–153. Available at: http://www.ncbi.nlm.nih.gov/pubmed/19898872 (accessed 14.09.14.).

Marra, K.G., et al., 1999. In vitro analysis of biodegradable polymer blend/hydroxyapatite composites for bone tissue engineering. Journal of Biomedical Materials Research 47 (3), 324–335. Available at: http://www.ncbi.nlm.nih.gov/pubmed/10487883.

Marsich, E., et al., 2013. Nano-composite scaffolds for bone tissue engineering containing silver nanoparticles: preparation, characterization and biological properties. Journal of Materials Science. Materials in Medicine 24 (7), 1799–1807. Available at: http://www.ncbi.nlm.nih.gov/pubmed/23553569 (accessed 10.10.14.).

Mathew, A.P., et al., 2012. Fibrous cellulose nanocomposite scaffolds prepared by partial dissolution for potential use as ligament or tendon substitutes. Carbohydrate Polymers 87 (3), 2291–2298. Available at: http://linkinghub.elsevier.com/retrieve/pii/S0144861711009696 (accessed 01.10.14.).

Mathew, A.P., et al., 2013. Biocompatible fibrous networks of cellulose nanofibres and collagen crosslinked using genipin: potential as artificial ligament/tendons. Macromolecular Bioscience 13 (3), 289–298. Available at: http://www.ncbi.nlm.nih.gov/pubmed/23225770 (accessed 10.10.14.).

Mattioli-Belmonte, M., et al., 2012. Tuning polycaprolactone–carbon nanotube composites for bone tissue engineering scaffolds. Materials Science and Engineering: C 32 (2), 152–159. Available at: http://linkinghub.elsevier.com/retrieve/pii/S0928493111002827 (accessed 23.09.14.).

McKeon-Fischer, K., Freeman, J., 2011. Characterization of electrospun poly (L-lactide) and gold nanoparticle composite scaffolds for skeletal muscle tissue engineering. Journal of Tissue Engineering and Regenerative Medicine 5, 560–568 (December 2010).

McKeon-Fischer, K.D., Flagg, D.H., Freeman, J.W., 2011. Coaxial electrospun poly (ε-caprolactone), multiwalled carbon nanotubes, and polyacrylic acid/polyvinyl alcohol scaffold for skeletal muscle tissue engineering. Journal of Biomedical Materials Research. Part A 99 (3), 493–499. Available at: http://www.ncbi.nlm.nih.gov/pubmed/21913315 (accessed 12.04.14.).

McKeon-Fischer, K.D., et al., 2014. *In vivo* skeletal muscle biocompatibility of composite, coaxial electrospun, and microfibrous scaffolds. Tissue Engineering Part A 20 (13–14), 1961–1970. Available at: http://online.liebertpub.com/doi/abs/10.1089/ten.tea.2013.0283.

McMurray, R.J., et al., 2011. Nanoscale surfaces for the long-term maintenance of mesenchymal stem cell phenotype and multipotency. Nature Materials 10 (8), 637–644. Available at: http://dx.doi.org/10.1038/nmat3058.

Nair, L.S., Laurencin, C.T., 2007. Biodegradable polymers as biomaterials. Progress in Polymer Science (Oxford) 32 (8–9), 762–798.

Nukavarapu, S.P., et al., 2008. Polyphosphazene/nano-hydroxyapatite composite microsphere scaffolds for bone tissue engineering. Biomacromolecules 9 (7), 1818–1825. Available at: http://www.pubmedcentral.nih.gov/articlerender.fcgi?artid=2746952&tool=pmcentrez&rendertype=abstract.

Okamoto, M., John, B., 2013. Synthetic biopolymer nanocomposites for tissue engineering scaffolds. Progress in Polymer Science 38 (10–11), 1487–1503. Available at: http://linkinghub.elsevier.com/retrieve/pii/S0079670013000646 (accessed 06.10.14.).

Pakravan, M., Heuzey, M.C., Ajji, A., 2012. Core-shell structured PEO-chitosan nanofibers by coaxial electrospinning. Biomacromolecules 13 (2), 412–421.

Paletta, J.R.J., et al., 2010. RGD-functionalisation of PLLA nanofibers by surface coupling using plasma treatment: influence on stem cell differentiation. Journal of Materials Science: Materials in Medicine 21 (4), 1363–1369. Available at: http://link.springer.com/10.1007/s10856-009-3947-2.

Peach, M.S., Kumbar, S.G., et al., 2012a. Design and optimization of polyphosphazene functionalized fiber matrices for soft tissue regeneration. Journal of Biomedical Nanotechnology 8 (1), 107–124. Available at: http://apps.webofknowledge.com/full_record.do?product=WOS&search_mode=GeneralSearch&qid=5&SID=X129TD1RqgvO3go4H3c&page=1&doc=2.

Peach, M.S., James, R., et al., 2012b. Polyphosphazene functionalized polyester fiber matrices for tendon tissue engineering: in vitro evaluation with human mesenchymal stem cells. Biomedical Materials (Bristol, England) 7 (4), 045016. Available at: http://www.ncbi.nlm.nih.gov/pubmed/22736077 (accessed 10.10.14.).

Pek, Y.S., et al., 2008. Porous collagen-apatite nanocomposite foams as bone regeneration scaffolds. Biomaterials 29 (32), 4300–4305. Available at: http://www.ncbi.nlm.nih.gov/pubmed/18706690 (accessed 10.10.14.).

Pham, Q.P., Sharma, U., Mikos, A.G., 2006. Electrospun poly (e-caprolactone) microfiber and multilayer nanofiber/microfiber scaffolds : characterization of scaffolds and measurement of cellular infiltration. Biomacromolecules 2796–2805.

Poon, Z., et al., 2011. Layer-by-layer nanoparticles with a pH-sheddable layer for in vivo targeting of tumor hypoxia. ACS Nano (6), 4284–4292.

Reilly, G.C., Engler, A.J., 2010. Intrinsic extracellular matrix properties regulate stem cell differentiation. Journal of Biomechanics 43 (1), 55–62. Available at: http://www.ncbi.nlm.nih.gov/pubmed/19800626 (accessed 09.07.14.).

Rezwan, K., et al., 2006. Biodegradable and bioactive porous polymer/inorganic composite scaffolds for bone tissue engineering. Biomaterials 27 (18), 3413–3431. Available at: http://www.ncbi.nlm.nih.gov/pubmed/16504284 (accessed 09.07.14.).

Roether, J., et al., 2002. Development and in vitro characterisation of novel bioresorbable and bioactive composite materials based on polylactide foams and bioglass® for tissue engineering applications. Biomaterials 23 (18), 3871–3878. Available at: http://linkinghub.elsevier.com/retrieve/pii/S014296120200131X.

Rosso, F., et al., 2004. From cell-ECM interactions to tissue engineering. Journal of Cellular Physiology 199 (2), 174–180. Available at: http://www.ncbi.nlm.nih.gov/pubmed/15039999 (accessed 02.08.14.).

Ruosiahti, E., Pierschbacher, M.D., 1987. New adhesion: perspectives in cell integrins. Science 238 (4826), 491–497.

Sarasam, A., Madihally, S.V., 2005. Characterization of chitosan-polycaprolactone blends for tissue engineering applications. Biomaterials 26 (27), 5500–5508. Available at: http://www.ncbi.nlm.nih.gov/pubmed/15860206 (accessed 09.10.14.).

Saravanan, S., et al., 2011. Preparation, characterization and antimicrobial activity of a bio-composite scaffold containing chitosan/nano-hydroxyapatite/nano-silver for bone tissue engineering. International Journal of Biological Macromolecules 49 (2), 188–193. Available at: http://www.ncbi.nlm.nih.gov/pubmed/21549747 (accessed 10.10.14.).

Saurer, E.M., et al., 2009. Assembly of erodible, DNA-containing thin films on the surfaces of polymer microparticles: toward a layer-by-layer approach to the delivery of DNA to antigen-presenting cells. Acta Biomaterialia 5 (3), 913–924. Available at: http://www.pubmedcentral.nih.gov/articlerender.fcgi?artid=2667125&tool=pmcentrez&rendertype=abstract (accessed 08.10.14.).

Schlichting, K.E., et al., 2011. Synthesis of a novel photopolymerized nanocomposite hydrogel for treatment of acute mechanical damage to cartilage. Acta Biomaterialia 7 (8), 3094–3100. Available at: http://www.ncbi.nlm.nih.gov/pubmed/21530694 (accessed 08.10.14.).

Schulz, M., 2009. Polymer derived ceramics in MEMS/NEMS – a review on production processes and application. Advances in Applied Ceramics 108 (8), 454–460. Available at: http://www.maneyonline.com/doi/abs/10.1179/174367609X422171 (accessed 19.12.14.).

Shalumon, K., et al., 2012. Fabrication of aligned poly (lactic acid)-chitosan nanofibers by novel parallel blade collector method for skin tissue engineering. Journal of Biomedical Nanotechnology 8 (3), 405–416. Available at: http://stacks.iop.org/0295-5075/105/i=1/a=15001.

Shekaran, A., Garcia, A.J., 2011. Nanoscale engineering of extracellular matrix-mimetic bioadhesive surfaces and implants for tissue engineering. Biochimica Et Biophysica Acta 1810 (3), 350–360. Available at: http://www.pubmedcentral.nih.gov/articlerender.fcgi?artid=2924948&tool=pmcentrez&rendertype=abstract (accessed 19.12.14.).

Shi, X., et al., 2007. Fabrication of porous ultra-short single-walled carbon nanotube nanocomposite scaffolds for bone tissue engineering. Biomaterials 28 (28), 4078–4090. Available at: http://www.pubmedcentral.nih.gov/articlerender.fcgi?artid=3163100&tool=pmcentrez&rendertype=abstract (accessed 08.10.14.).

Shi, Z., et al., 2009. Size effect of hydroxyapatite nanoparticles on proliferation and apoptosis of osteoblast-like cells. Acta Biomaterialia 5 (1), 338–345. Available at: http://www.ncbi.nlm.nih.gov/pubmed/18753024 (accessed 08.10.14.).

Shim, I.K., et al., 2009. Chitosan nano-/microfibrous double-layered membrane with rolled-up three-dimensional structures for chondrocyte cultivation. Journal of Biomedical Materials Research. Part A 90 (2), 595–602. Available at: http://www.ncbi.nlm.nih.gov/pubmed/18563820.

Shukla, A., Almeida, B., 2014. Advances in cellular and tissue engineering using layer-by-layer assembly. Wiley Interdisciplinary Reviews. Nanomedicine and Nanobiotechnology 6 (5), 411–421. Available at: http://www.ncbi.nlm.nih.gov/pubmed/24723385 (accessed 06.10.14.).

Sitharaman, B., et al., 2008. In vivo biocompatibility of ultra-short single-walled carbon nanotube/biodegradable polymer nanocomposites for bone tissue engineering. Bone 43 (2), 362–370. Available at: http://www.ncbi.nlm.nih.gov/pubmed/18541467 (accessed 24.09.14.).

Smith, L.J., et al., 2007. Increased osteoblast cell density on nanostructured PLGA-coated nanostructured titanium for orthopedic applications. International Journal of Nanomedicine 2 (3), 493–499.

Sowjanya, J.A., et al., 2013. Biocomposite scaffolds containing chitosan/alginate/nano-silica for bone tissue engineering. Colloids and Surfaces. B, Biointerfaces 109, 294–300. Available at: http://www.ncbi.nlm.nih.gov/pubmed/23668983 (accessed 03.10.14.).

Spadaccio, C., et al., 2009. Poly-L-lactic acid/hydroxyapatite electrospun nanocomposites induce chondrogenic differentiation of human MSC. Annals of Biomedical Engineering 37 (7), 1376–1389. Available at: http://www.ncbi.nlm.nih.gov/pubmed/19418224 (accessed 08.10.14.).

Stevens, M.M., George, J.H., 2005. Exploring and engineering the cell surface interface. Science (New York, NY) 310 (5751), 1135–1138.

Stratakis, E., Ranella, A., Fotakis, C., 2011. Biomimetic micro/nanostructured functional surfaces for microfluidic and tissue engineering applications. Biomicrofluidics 5 (1), 13411. Available at: http://www.pubmedcentral.nih.gov/articlerender.fcgi?artid=3082348&tool=pmcentrez&rendertype=abstract (accessed 19.12.14.).

Sun, F., Zhou, H., Lee, J., 2011. Various preparation methods of highly porous hydroxyapatite/polymer nanoscale biocomposites for bone regeneration. Acta Biomaterialia 7 (11), 3813–3828. Available at: http://www.ncbi.nlm.nih.gov/pubmed/21784182 (accessed 11.09.14.).

Svensson, A., et al., 2005. Bacterial cellulose as a potential scaffold for tissue engineering of cartilage. Biomaterials 26 (4), 419–431. Available at: http://www.ncbi.nlm.nih.gov/pubmed/15275816 (accessed 16.07.14.).

Tanaka, M., et al., 2008. Formation of hydroxyapatite on a self-organized 3D honeycomb-patterned biodegradable polymer film. Colloids and Surfaces A: Physicochemical and Engineering Aspects 313–314, 515–519. Available at: http://linkinghub.elsevier.com/retrieve/pii/S092777570700564X (accessed 08.10.14.).

Tang, Z., et al., 2006. Biomedical applications of layer-by-layer assembly: from biomimetics to tissue engineering. Advanced Materials 18 (24), 3203–3224. Available at: http://doi.wiley.com/10.1002/adma.200600113 (accessed 07.08.14.).

Taylor, E.D., 2010. Novel nanostructured scaffolds as therapeutic replacement options for rotator cuff disease. The Journal of Bone and Joint Surgery (American) 92 (Suppl. 2), 170. Available at: http://jbjs.org/cgi/doi/10.2106/JBJS.J.01112.

Thorvaldsson, A., et al., 2008. Electrospinning of highly porous scaffolds for cartilage regeneration. Biomacromolecules 9 (3), 1044–1049. Available at: http://www.ncbi.nlm.nih.gov/pubmed/18260633.

Torabinejad, B., et al., 2014. Synthesis and characterization of nanocomposite scaffolds based on triblock copolymer of L-lactide, ε-caprolactone and nano-hydroxyapatite for bone tissue engineering. Materials Science & Engineering. C, Materials for Biological Applications 42, 199–210. Available at: http://www.ncbi.nlm.nih.gov/pubmed/25063111 (accessed 25.09.14.).

Tripathi, A., et al., 2012. Bio-composite scaffolds containing chitosan/nano-hydroxyapatite/nano-copper-zinc for bone tissue engineering. International Journal of Biological Macromolecules 50 (1), 294–299. Available at: http://www.ncbi.nlm.nih.gov/pubmed/22123094 (accessed 10.10.14.).

Venkatesan, J., et al., 2012. Preparation and characterization of chitosan-carbon nanotube scaffolds for bone tissue engineering. International Journal of Biological Macromolecules 50 (2), 393–402. Available at: http://www.ncbi.nlm.nih.gov/pubmed/22234296 (accessed 10.10.14.).

Vieu, C., et al., 2000. Electron beam lithography: resolution limits and applications. Applied Surface Science 164 (1), 111–117.

Wang, Y., Liu, L., Guo, S., 2010. Characterization of biodegradable and cytocompatible nano-hydroxyapatite/polycaprolactone porous scaffolds in degradation in vitro. Polymer Degradation and Stability 95 (2), 207–213. Available at: http://linkinghub.elsevier.com/retrieve/pii/S0141391009003735 (accessed 18.09.14.).

Wang, Y., et al., 2014. Electrospun tubular scaffold with circumferentially aligned nano fibers for regulating smooth muscle cell growth. ACS Applied Material and Interfaces 6.

Webb, A.R., Kumar, V.A., Ameer, G.A., 2007. Biodegradable poly(diol citrate) nanocomposite elastomers for soft tissue engineering. Journal of Materials Chemistry 17 (9), 900. Available at: http://xlink.rsc.org/?DOI=b611353b (accessed 08.10.14.).

Wei, G., Ma, P.X., 2004. Structure and properties of nano-hydroxyapatite/polymer composite scaffolds for bone tissue engineering. Biomaterials 25 (19), 4749–4757. Available at: http://www.ncbi.nlm.nih.gov/pubmed/15120521 (accessed 09.07.14.).

Lo, K.W., et al., 2012. The small molecule PKA-specific cyclic AMP analogue as an inducer of osteoblast-like cells differentiation and mineralization. Journal of Tissue Engineering and Regenerative Medicine 6, 408–417.

Woodruff, M.A., Hutmacher, D.W., 2010. The return of a forgotten polymer—polycaprolactone in the 21st century. Progress in Polymer Science 35 (10), 1217–1256. Available at: http://linkinghub.elsevier.com/retrieve/pii/S0079670010000419 (accessed 10.07.14.).

Xie, J., et al., 2010. Radially aligned, electrospun nanofibers and tissue regeneration applications. ACS Nano 4 (9), 5027–5036.

Yim, E.K.F., Pang, S.W., Leong, K.W., 2007. Synthetic nanostructures inducing differentiation of human mesenchymal stem cells into neuronal lineage. Experimental Cell Research 313 (9), 1820–1829. Available at: http://linkinghub.elsevier.com/retrieve/pii/S0014482707000924.

Young, J., et al., 2005. Characterization of degradation behavior for PLGA in various pH condition by simple liquid chromatography method. Bio-medical Materials and Engineering 15, 279–288.

Zhang, L., Webster, T.J., 2009. Nanotechnology and nanomaterials: promises for improved tissue regeneration. Nano Today 4 (1), 66–80. Available at: http://linkinghub.elsevier.com/retrieve/pii/S1748013208000182 (accessed 04.07.14.).

Zhang, J., et al., 2005. Natural polyelectrolyte films based on layer-by-layer deposition of collagen and hyaluronic acid. Biomaterials 26 (16), 3353–3361. Available at: http://www.ncbi.nlm.nih.gov/pubmed/15603831 (accessed 08.10.14.).

Zhang, Y., et al., 2008. Electrospun biomimetic nanocomposite nanofibers of hydroxyapatite/chitosan for bone tissue engineering. Biomaterials 29 (32), 4314–4322. Available at: http://www.ncbi.nlm.nih.gov/pubmed/18715637 (accessed 15.09.14.).

Zhang, K., et al., 2012a. Ultrasonically prepared polystyrene/multi-walled carbon nanotube nanocomposites. Journal of Materials Science 48 (8), 3088–3096. Available at: http://link.springer.com/10.1007/s10853-012-7083-x (accessed 01.10.14.).

Zhang, Q., et al., 2012b. Mechanical properties and biomineralization of multifunctional nanodiamond-PLLA composites for bone tissue engineering. Biomaterials 33 (20), 5067–5075. Available at: http://www.ncbi.nlm.nih.gov/pubmed/22494891 (accessed 10.10.14.).

Zhou, H., Lee, J., 2011. Nanoscale hydroxyapatite particles for bone tissue engineering. Acta Biomaterialia 7 (7), 2769–2781. Available at: http://www.ncbi.nlm.nih.gov/pubmed/21440094 (accessed 17.07.14.).

This page intentionally left blank

Carbon and inorganic nanomaterial-reinforced polymeric nanocomposites for bone tissue engineering

2

G. Lalwani, M. D'Agati, B. Farshid, B. Sitharaman
Stony Brook University, Stony Brook, NY, United States

2.1 Introduction

Bone defects due to incidents such as fractures, diseases (osteoporosis and osteosarcoma), or surgeries (tumor removal) are treated using autografts (tissue from the person's own body), allografts (from a donor of the same species), or xenografts (from a donor of a different species) [1]. Natural bone grafts and implants have several limitations such as disease transfer, limited availability and reproducibility, donor scarcity, alterations in the properties of natural matrices due to sterilization, and immune rejection. Extensive research has been performed to engineer synthetic biocompatible polymers for tissue engineering and regenerative medicine applications [2]. Typically, synthetic biomaterials have several advantages over materials derived from natural sources; for instance, synthetic biomaterials can be produced using well-established protocols, their physical and chemical properties can be tailored depending on the application, and they offer ease of sterilization and mass production.

The porous and nonporous synthetic bone grafts are fabricated using metals, ceramics, polymers, and their combinations (hybrid materials and composites) in various morphologies such as cylinders, screws, pins, plates, and rods, as well as formable pastes and gels. Although rigid synthetic biomaterials require implantation thorough an invasive surgery, amorphous pastes and gels can be injected to bone defect sites and undergo in situ formation. The metallic orthopedic implants used in clinic are bioinert and have higher mechanical properties compared to native bone tissue leading to bone atrophy due to stress shielding [3]. Ceramic bone grafts have been used; however, their application is limited because of their low tensile mechanical properties and brittleness. Furthermore, metallic and ceramic implants are nonbiodegradable and require a secondary surgery for removal post bone healing. In contrast, the structure and composition of polymers can be tailored to impart specific properties, for instance, by manipulating the molecular weight and chemical bonds polymers can be degraded by either hydrolysis upon exposure to an aqueous environment or enzymatically by cells. Polymers can be easily synthesized at large scale using well-established protocols, and their properties can be tailored by molecular design. Therefore, polymeric scaffolds and composites have been extensively investigated for applications in tissue engineering and regenerative medicine.

Nanocomposites for Musculoskeletal Tissue Regeneration. http://dx.doi.org/10.1016/B978-1-78242-452-9.00002-9

Recent advances in nanotechnology have played a significant role in the development of tissue-engineering approaches over the last decade. Nanomaterials can be synthesized from ceramics, metals, organic and inorganic materials, and composites using methods such as chemical vapor deposition [4], self-assembly [5], phase separation [6], chemical etching [7], photolithography [8], electron beam lithography [9], laser ablation [10], chemical oxidation [11], and liquid exfoliation [12] in various morphologies such as tubes, platelets, spheres, ribbons, horns, wires, films, and clusters (Fig. 2.1) [7,11–21]. Nanomaterials are used in various fields of tissue engineering and regenerative medicine for bioimaging [13,22–24], drug and gene delivery [25–28], as substrates for tissue engineering [29–31], as reinforcing agents to improve mechanical properties of polymeric scaffolds [32–35], antimicrobial agents [36,37], and for cellular therapy and diagnoses [38–40]. Furthermore, due to their large surface area and high surface roughness, nanomaterials can be functionalized with various chemical groups (oxy, epoxy, carboxylate, nitrile, phosphate, disulfide, amine, and hydroxyl), drugs (doxorubicin, etc.),

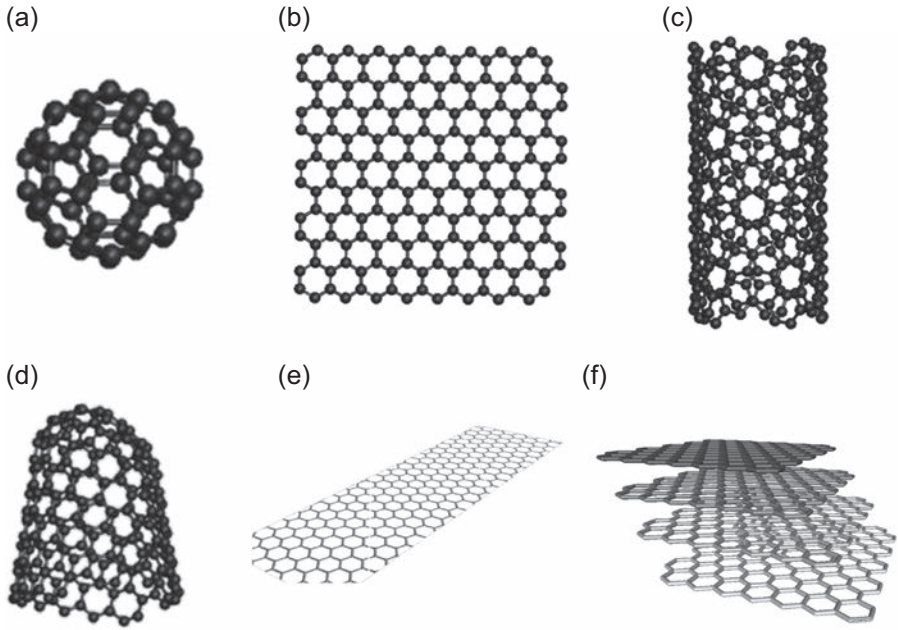

Figure 2.1 Schematic representation of (a) nanospheres (fullerenes), (b) nanosheets (graphene), (c) tubes (carbon nanotube), (d) horn (carbon nanohorn), (e) graphene nanoribbons, (f) graphene nanoplatelets.
(a–d) Adapted from Costa RD, Lodermeyer F, Casillas R, Guldi DM. Recent advances in multifunctional nanocarbons used in dye-sensitized solar cells. Energy Environ Sci 2014;7:1281–96, with permission. Copyright © Royal Society of Chemistry, 2014.
(e) Adapted from Terrones M. Sharpening the chemical scissors to unzip carbon nanotubes: crystalline graphene nanoribbons. ACS Nano 2010;4:1775–81, with permission. Copyright © American Chemical Society, 2010. (f) Adapted from Nanochemistry.it (Enzo Menna).

proteins, and peptides (arginyl-glycyl-aspartic acid [RGD], etc.) to impart novel physiochemical properties and mitigate toxicity.

Biodegradable polymers such as poly(L-lactide acid) (LPLA), poly(glycolide acid) (PGA), poly(D,L-lactide acid) (DLPLA), poly(dioxanone) (PDO), poly(D,L-lactide-co-L-lactide acid) (LDLPLA), poly(D,L-lactide-co-glycolide) (DLPLG), poly(glycolide-co-trimethylene carbonate), poly(L-lactide-co-glycolide) (LPLG), poly(ε-caprolactone) (PCL), poly(ethylene glycol) (PEG), poly(propylene fumarate) (PPF), polyurethane (PU), poly(lactic acid) (PLA), poly(glycolic acid) (PLGA), poly(butylene succinate) (PBSC) have been used to prepare tissue-engineering scaffolds (Fig. 2.2) [41–48]. Porous polymeric scaffolds permit cellular infiltration, which is critical for tissue regeneration. However, porous scaffolds have low mechanical properties, unsuitable for tissue engineering of load-bearing bones. Several approaches have been used to improve the mechanical properties of polymeric scaffolds, for

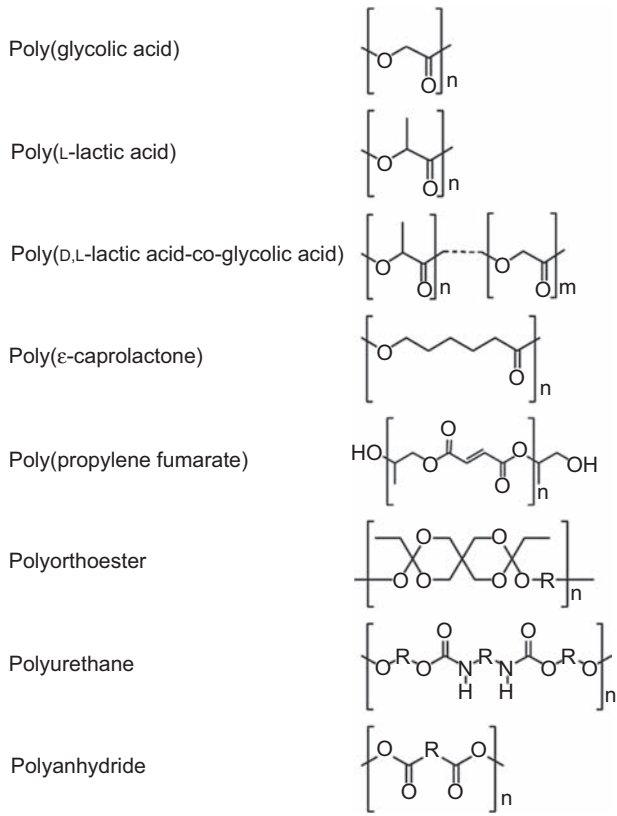

Figure 2.2 Structural representation of various biodegradable polymers for bone-tissue engineering.
Adapted from Kasper FK, Tanahashi K, Fisher JP, Mikos AG. Synthesis of poly (propylene fumarate). Nat Protoc 2009;4:518–25, with permission. Copyright © Macmillan Publishers Limited, 2009.

example, use of polymers with high molecular weight, increasing cross-linking density of polymers, and the fabrication of polymeric composites with reinforcing agents (a second particulate phase that typically has higher mechanical properties than native polymer) [49,50]. The fabrication of nanomaterial-reinforced polymeric nanocomposites for tissue-engineering applications has gained attention over the last decade due to their multifunctional attributes. For instance, dispersion of nanomaterials in the polymeric matrix not only improves the mechanical properties, these nanomaterials can also be loaded with drugs, growth factors, or bioimaging molecules, thereby imparting additional multifunctional properties such as noninvasive in vivo longitudinal imaging of scaffold degradation and tissue regeneration along with the delivery of biotherapeutics and growth factors to guide cellular processes.

Excellent reviews on the use of nanomaterials such as fullerenes, graphene, carbon nanotubes, and gold and ceramic nanoparticles for tissue engineering and regenerative medicine applications have been published [24,51–57]. Other inorganic materials such as alumoxane nanospheres, tungsten nanotubes, and molybdenum nanoplatelets have also been investigated for biomedical applications [32–34,58]. In this chapter, we will review the use of various zero- (fullerenes), one- (carbon and tungsten nanotubes, and alumoxane nanoparticles, etc.), and two-dimensional (graphene and molybdenum nanoplatelets, graphene nanoribbons, etc.) carbon and inorganic nanomaterials as reinforcing agents toward the fabrication of polymeric nanocomposites and scaffolds for bone-tissue engineering applications. We will discuss scaffold design parameters critical for maximum mechanical reinforcement along with various cytotoxicity and biocompatibility issues associated with their use in tissue engineering and regenerative medicine.

2.2 Nanomaterial-reinforced polymeric nanocomposites

Nanomaterials can be classified as zero- (0D), one- (1D) and two-dimensional (2D) materials based on their size. 0D nanomaterials are composed of a limited number of atoms (usually under 100). They are nanomaterials that have all the dimensions (x–y–z) in the nanoscale. 1D nanomaterials have a large aspect ratio and have at least one dimension greater than nanoscale (for instance nanotubes with diameter in nanoscale and length on the micron scale). 2D nanomaterials have at least two dimensions on the micron scale, for instance, nanoplatelets and nanoribbons with length, breadth, or diameter on the micron scale. 2D nanomaterials are generally sheets, ribbons, or platelets with a nanoscale thickness (z).

2.2.1 Mechanical properties of 0D nanomaterial-reinforced polymeric nanocomposites

Table 2.1 lists the mechanical properties of various polymeric nanocomposites. Fullerene (C_{60}) has been used as reinforcing agent to improve the mechanical properties of PPF and polycarbonate (PC) nanocomposites. Saotome et al. have characterized the mechanical properties of PC nanocomposites reinforced with C_{60} and

Table 2.1 Mechanical properties of various polymeric nanocomposites

Nanomaterial	Content (wt%)	Polymer matrix	Mechanical property	Percent increase	References
Fullerenes and single-walled carbon nanotubes and ultrashort carbon nanotubes	0.05–1	Poly(propylene fumarate) (PPF)	Compressive modulus Flexural modulus	70–95% 10–50%	Sitharaman et al. [35]
Fullerenes	1–10	Poly(methyl methacrylate) (PMMA)	Strength breaking strain and Young's modulus,	400% 100%	Ginzburg et al. [60]
Single-walled carbon nanotubes and multiwalled carbon nanotubes	0.05	PPF	Flexural modulus Compressive modulus	69% 74%	Shi et al. [71]
Single-walled carbon nanotubes and multiwalled carbon nanotubes	0.05–2	PPF	Compressive modulus, Compressive yield strength Flexural modulus, Flexural yield strength	15–60%	Lalwani et al. [33]
Multiwalled carbon nanotubes	0.25	Poly(lactic-co-glycolic acid)	Young's modulus Tensile stress Elongation stress	8% 80% 49%	Zhang et al. [72]
Multiwalled carbon nanotubes	0–5	Chitosan	Elastic modulus Compressive modulus	113% 218%	Chen et al. [73]
Tungsten disulfide nanotubes	0.01–0.2	PPF	Compressive modulus Compressive yield strength Flexural modulus Flexural yield strength	61% 55% 29% 191%	Lalwani et al. [34]
Tungsten disulfide nanotubes	2	PMMA	Elastic modulus Tensile strength and toughness	2100% 30–35%	Reddy et al. [67]

Continued

Table 2.1 Continued

Nanomaterial	Content (wt%)	Polymer matrix	Mechanical property	Percent increase		References
Boron nitrate nanotubes	0.2	PPF	Compressive modulus	15%		Farshid et al. [112]
			Compressive yield strength	6%		
Single-walled graphene oxide nanoribbons and multiwalled graphene oxide nanoribbons and graphene nanoplatelets	0.01–0.2	PPF	Compressive modulus	SWGONR	35%	Lalwani et al. [33]
				MWGONR	68%	
			Compressive yield strength	SWGONR	27%	
				MWGONR	60%	
			Flexural modulus	SWGONR	15%	
				MWGONR	24%	
			Flexural yield strength	SWGONR	102%	
				MWGONR	230%	
Graphene oxide (GO)	2.5	Poly(vinyl alcohol)	Compressive strength	60%		Shuai et al. [86]
			Young's modulus	152%		
			Tensile strength	69%		
Poly(vinyl alcohol)-grafted graphene oxide	1	Poly(vinyl alcohol)	Tensile strength	88%		Cheng et al. [87]
			Young's modulus	150%		
			Elongation	22%		
Graphene and nanodiamonds		Poly(vinyl alcohol)	Stiffness and hardness	400%		Prasad et al. [88]
Graphene	5	Polycaprolactone	Specific strength	192%		Sayyar et al. [89]
			Specific modulus	571%		
Graphene	0.1	Chitosan	Elastic modulus	100%		Fan et al. [90]
			Hardness	50%		
Molybdenum disulfide nanoplatelets	0.2	PPF	Young's modulus	108%		Lalwani et al. [33]
			Compressive yield strength	93%		
			Flexural modulus	53%		
			Flexural yield strength	262%		

poly-hydroxylated fullerenes ($C_{60}(OH)_{36}$) [59]. Results show that PC–$C_{60}(OH)_{36}$ nanocomposites have higher mechanical properties compared to PC reinforced with pristine C_{60}. The increased mechanical properties were attributed to the rigid polymer–$C_{60}(OH)_{36}$ interphase region due to hydrophobic interactions and hydrogen bonding. In another study, Sitharaman et al. have reported the use of C_{60} as a reinforcing agent along with single-walled carbon nanotubes (SWCNTs) and ultrashort carbon nanotubes (US tubes) to fabricate injectable nanocomposites of PPF [35]. PPF is a biodegradable, highly viscous polyester of propylene glycol and diethyl fumarate widely used for bone-tissue engineering applications. Dispersion of C_{60} in PPF nanocomposite mix prior to cross-linking decreased the viscosity, thereby improving the injectability for bone-tissue engineering. Ginzburg et al. have reported the mechanical properties of poly(methyl methacrylate) (PMMA) films upon 1 to 10 wt% loading of C_{60} [60]. The authors reported a 5× increase in the strength and 2× increase in the breaking strain and Young's modulus of PMMA–C_{60} films at 1 wt% dispersion of C_{60}. The mechanical properties increased up to 3 wt% loading of C_{60} and declined at higher nanomaterial concentrations. X-ray diffraction (XRD) analysis of PMMA–C_{60} nanocomposite thin films at 10 wt% concentration showed an increase in sample heterogeneity, i.e., formation of C_{60} aggregates that result in the reduction of mechanical properties. The authors propose that at low concentrations (<3 wt%), C_{60} molecules retract the microcrack propagation by covalently bonding with free radicals formed during deformation, thereby resulting in crack healing (Fig. 2.3).

2.2.2 Mechanical properties of 1D nanomaterial-reinforced polymeric nanocomposites

One-dimensional nanomaterials such as carbon nanotubes [33,34,35], titanium oxide nanotubes [61,62], aluminum silicate nanotubes [63], boron nitride nanotubes (BNNTs) [64,112], tungsten disulfide nanotubes [32,34], and cellulose nanofibers [65,66] have been used as reinforcing agents for polymeric networks such as PPF, PMMA, PLA, poly(lactide-co-glycolide acid), chitosan, and PU [32,34,65–70,112]. The Sections 2.2.2.1 and 2.2.2.2 summarize recent studies using 1D carbon and inorganic nanotubes as reinforcing agents for biomedical applications.

2.2.2.1 1D carbon nanomaterial-reinforced polymeric nanocomposites

Several studies have investigated the mechanical properties of single- and multiwalled carbon nanotube (SWCNT and MWCNT)-reinforced polymeric nanocomposites. Shi et al. have reported ~69% increase in flexural modulus (765 MPa) and ~74% increase in compressive modulus (680 MPa) of PPF nanocomposites reinforced with functionalized (dodecylated) SWCNTs (Fig. 2.4) at 0.05 wt%, compared to PPF composites without nanomaterial loading (compressive modulus ~318 MPa, flexural modulus ~456 MPa) [71]. Sitharaman et al. have reported ~70–95% increase in compressive modulus (1100–1300 MPa) and ~10–50% increase in flexural modulus (900–1500 MPa) upon 0.05–1 wt% loading of SWCNTs and US-CNTs, compared to the mechanical

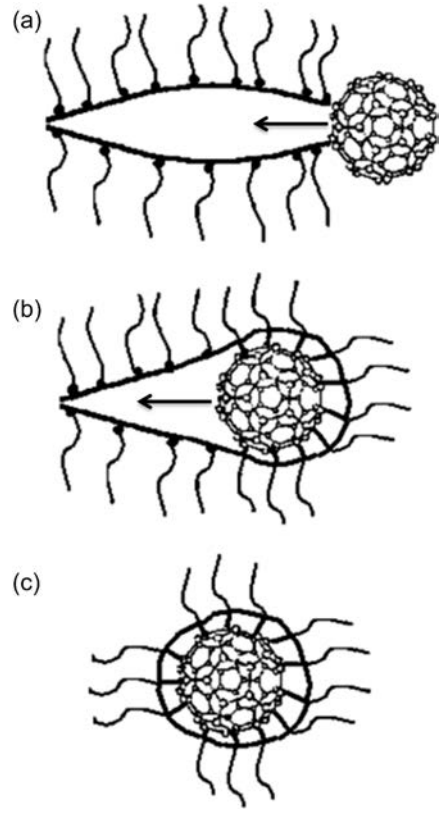

Figure 2.3 Schematic illustration of microcrack healing by fullerene (C_{60}). (a) Initial stage, (b) formation of covalent bonds and movement of C_{60} into microcrack, and (c) intake of C_{60} into microcrack and its healing.
Adapted from Ginzburg B, Pozdnyakov A, Tochil'Nikov D, Tuichiev S, Shepelevskii A. Tribological characteristics of composites based on poly (tetrafluoroethylene) and fullerene carbon. Polymer Science Series A 2008;50:865–73, with permission. Copyright © Springer science and business media, 2008.

properties of cross-linked PPF controls without nanoparticles (compressive modulus ~600 MPa, flexural modulus ~850 MPa) [35]. Lalwani et al. have reported 15–60% increase in mechanical properties (compressive modulus, compressive yield strength, flexural modulus, and flexural yield strength) at 0.05–2 wt% loading of SWCNTs and MWCNTs [33]. The control groups in the above studies were cross-linked PPF composites without addition of SWCNT, MWCNT, or US nanotubes. Zhang et al. have reported the mechanical properties of PLGA–MWCNT nanocomposite scaffolds.

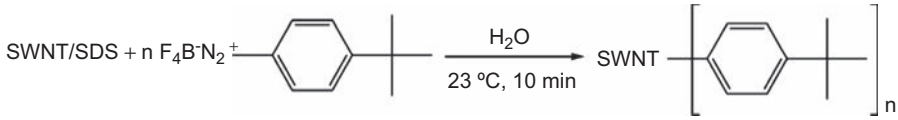

Figure 2.4 Schematic representation of functionalization of individual SWCNTs with sodium dodecyl sulfate (SDS) surfactant.
Adapted from Shi X, Hudson JL, Spicer PP, Tour JM, Krishnamoorti R, Mikos AG. Injectable nanocomposites of single-walled carbon nanotubes and biodegradable polymers for bone tissue engineering. Biomacromolecules 2006;7:2237–42, with permission. Copyright © American Chemical Society, 2006.

In comparison to PLGA composites, addition of 0.25 wt% MWCNTs resulted in ~8% increase in Young's modulus (from ~163 to ~176 MPa), ~80% increase in tensile stress (from ~5 to ~9 MPa), and 13% increase in elongation stress (from ~27% to 40%) for PLGA–MWCNT nanocomposites [72]. In another study, Chen et al. synthesized chitosan–MWCNT nanocomposites. Addition of 0–5 wt% of MWCNTs resulted in a significant increase in elastic modulus (from ~509 to ~1089 MPa) and compressive modulus (from ~33 to 105 MPa) compared to chitosan–hydroxyapatite (HA) composites [73]. Zawadzak et al. synthesized CNT-coated PU foams using electrophoretic deposition technique to fabricate PU–CNT foams as nanostructured matrices for bone-tissue engineering. The porous forms have the potential to be used as bioactive scaffolds due to their nanotopography and bioactivity [74].

2.2.2.2 1D inorganic nanomaterial-reinforced polymeric nanocomposites

Lalwani et al. have reported the synthesis and characterization of mechanical properties of tungsten disulfide nanotubes (WSNT)-reinforced PPF nanocomposites for bone-tissue engineering applications [34]. WSNTs possess high mechanical properties (flexural modulus ~217 GPa, compressive modulus ~150 GPa), functional groups (sulfide, oxysulfide, etc.) and can be readily dispersed in organic solvents. In comparison to CNT-reinforced PPF scaffolds, WSNT loading between 0.01 and 0.2 wt% resulted in a 61% increase in compressive modulus, 55% increase in compressive yield strength, 29% increase in flexural modulus, and a 190% increase in flexural yield strength of PPF nanocomposites (Fig. 2.5). These results were attributed to a uniform dispersion of WSNTs in the PPF matrix (CNTs formed micron-sized aggregates in PPF at high loading concentrations of ~0.2 wt%, Fig. 2.6) and an increased cross-linking density of WSNT–PPF nanocomposites compared to PPF controls. Reddy et al. have synthesized WSNT-embedded PMMA nanocomposites by electrospinning. Compared to pristine PMMA composites, 2 wt% loading of WSNTs resulted in ~22-fold increase in elastic modulus and 30–35% increase in tensile strength and toughness [67]. BNNTs are strong (elastic modulus ~1 TPa) and possess similar tensile strength, mechanical properties, thermal conductivities, and chemical properties to carbon nanotubes [75–77]. Zhi et al. have fabricated BNNT-reinforced PMMA, polystyrene, poly(vinyl butyral) (PVB) and poly(ethylene vinyl alcohol) (PEVA) nanocomposites and evaluated their mechanical properties by the Vickers microhardness test [78–80]. In addition to an increased thermal stability and electrical conductivity upon addition of BNNTs, slight increases in the mechanical properties were also observed. Recently, Farshid et al. have fabricated BNNT-reinforced PPF nanocomposites for bone-tissue engineering applications [112]. In this study, PPF nanocomposites fabricated with 0.2 wt% loading of BNNTs showed ~15% increase in compressive modulus and ~6% increase in compressive yield strength, compared to PPF composites without BNNTs. Furthermore, BNNT-reinforced PPF nanocomposites were cytocompatible; they permit attachment, spreading, and proliferation of MC3T3 preosteoblast cells. The favorable cytocompatibility results along with improved mechanical properties makes BNNT–PPF nanocomposites promising candidates for bone-tissue engineering.

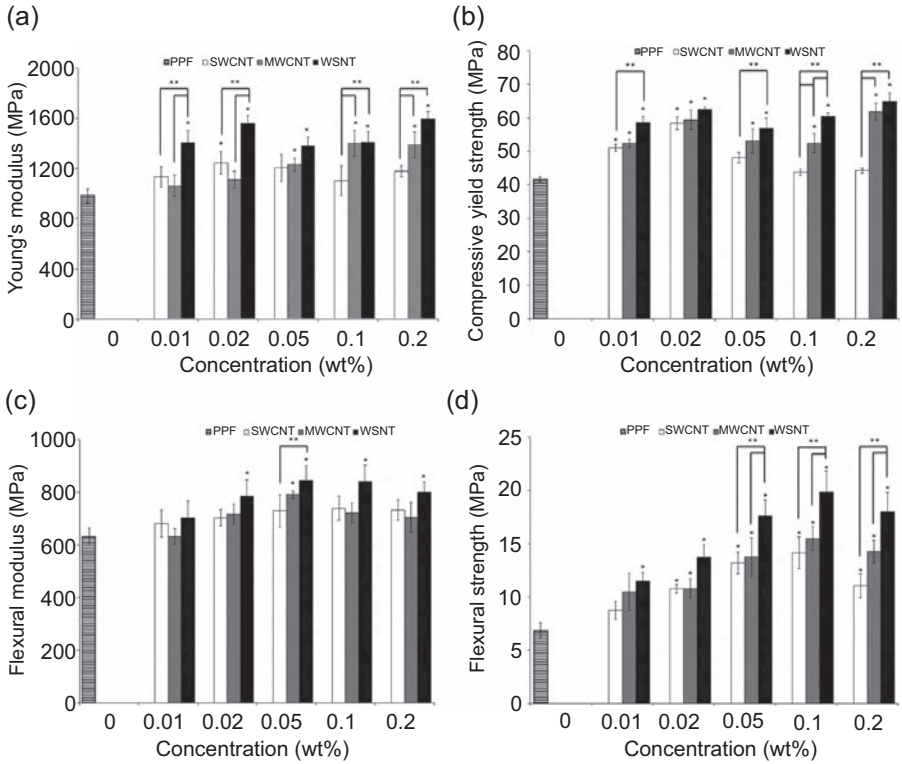

Figure 2.5 (a) Compressive modulus, (b) compressive yield strength, (c) flexural modulus, and (d) flexural yield strength of single-walled carbon nanotubes (SWCNTs), multiwalled carbon nanotubes (MWCNTs), and tungsten disulfide nanotubes (WSNTs) as a function of nanoparticle loading concentration. Data are represented as mean ± standard deviation for $n = 4$ samples. '*' represents significant differences from PPF composites (baseline control) and '**' represents significant difference from SWCNT and MWCNT nanocomposites at $p < 0.05$. Adapted from Lalwani G, Henslee AM, Farshid B, Parmar P, Lin L, Qin YX, et al. Tungsten disulfide nanotubes reinforced biodegradable polymers for bone tissue engineering. Acta Biomater 2013;9:8365–73, with permission. Copyright © Elsevier, 2013.

2.2.3 Mechanical properties of 2D nanomaterial-reinforced polymeric nanocomposites

2D-layered nanomaterials such as pristine graphene, graphene oxide (GO) nanoribbons (prepared by the oxidative unzipping of carbon nanotubes [19]), and nanoplatelets (prepared by Hummer's method and its modifications [11,13]), boron nitride nanoplatelets, molybdenum disulfide nanoplatelets (MSNPs), tungsten disulfide nanosheets, zirconia nanosheets, zinc oxide nanosheets, and titanium nanosheets have been used for several biomedical applications such as bioimaging [11,13,22], drug delivery [25,26], biosensors [81–83], stem cell tracking [84,85] and fabrication of tissue-engineering scaffolds and coatings [32,33,112]. Sections 2.2.3.1 and 2.2.3.2 summarize recent studies using 2D carbon and inorganic nanomaterials as reinforcing agents for tissue-engineering applications.

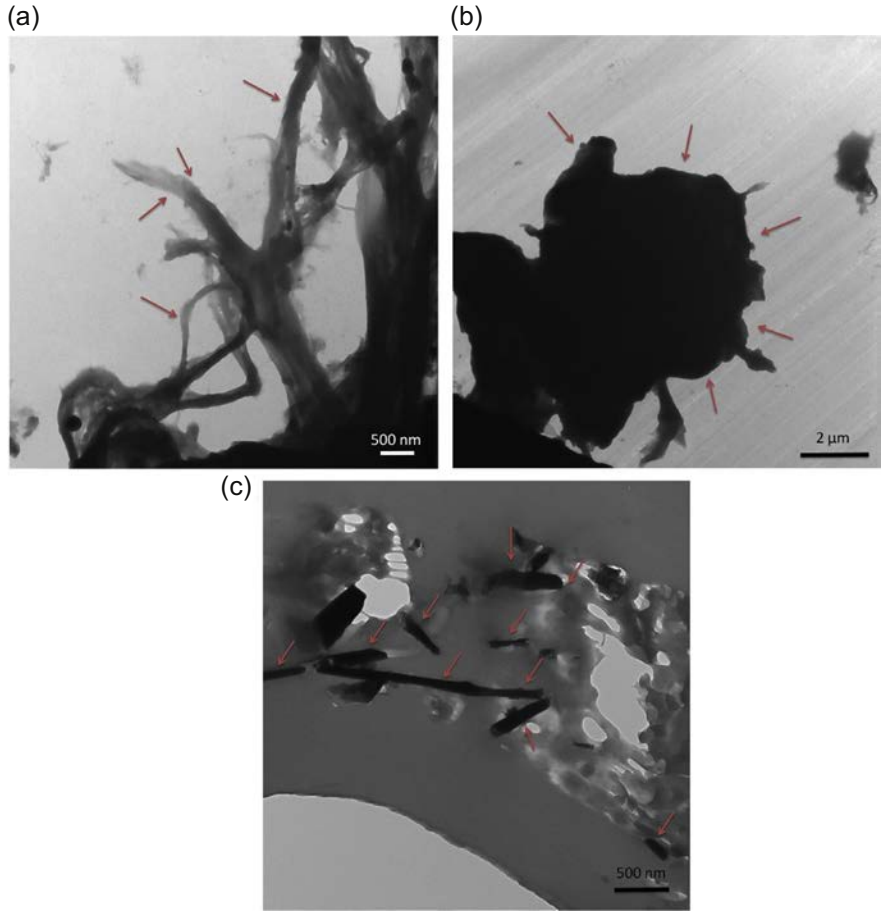

Figure 2.6 Representative transmission electron microscopy images of PPF nanocomposites at 0.1 wt% loading concentration of (a) single-walled carbon nanotubes, (b) multiwalled carbon nanotubes, and (c) tungsten disulfide nanotubes. Red arrows correspond to nanoparticles embedded in the polymer matrix.
Adapted from Lalwani G, Henslee AM, Farshid B, Parmar P, Lin L, Qin YX, et al. Tungsten disulfide nanotubes reinforced biodegradable polymers for bone tissue engineering. Acta Biomater 2013;9:8365–73, with permission.

2.2.3.1 2D carbon nanomaterial-reinforced polymeric nanocomposites

Recently, 2D carbon nanomaterial graphene has been investigated as reinforcing agent for several biocompatible polymers with a focus toward bone-tissue engineering. Lalwani et al. have investigated the mechanical properties of PPF reinforced with single- and multiwalled graphene oxide nanoribbons (SWGONRs and MWGONRs) and graphene nanoplatelets (GNPs) at 0.01 to 0.2 wt% loading

concentrations [33]. Compression and three-point bending tests were performed according to American Society for Testing and Materials (ASTM) standards on cross-linked PPF nanocomposites. Results show that in comparison to 1D carbon nanotubes (SWCNTs and MWCNTs), 2D carbon nanomaterials were better reinforcing agents; addition of SWGONRs, MWGONRs, and GONPs increased the mechanical properties (Young's modulus, compressive yield strength, flexural modulus, and flexural yield strength) by 10–235% depending on the nanomaterial morphology and loading concentration. Specifically, PPF–GONP nanocomposites showed the maximum mechanical reinforcement for various carbon nanomaterial groups investigated. Compared to PPF composites without nanomaterial loading, addition of 0.2 wt% of GONPs increased the Young's modulus by 71% (from ~1000 to ~1700 MPa), compressive yield strength by 63% (from ~41 to ~69 MPa), flexural modulus by 41% (from ~650 to ~925 MPa), and flexural yield strength by 263% (from ~8 to ~27 MPa).

Shuai et al. have investigated the mechanical properties of GO-reinforced poly(vinyl alcohol) (PVA) nanocomposites for tissue-engineering applications [86]. At 2.5 wt% loading of GO, ~60% increase in compressive strength, ~152% increase in Young's modulus, and 69% increase in tensile strength were observed. In another study, Cheng et al. have reported the mechanical properties of PVA nanocomposites reinforced with PVA-grafted GO (PVA-g-GO) [87]. Mechanical properties of PVA-g-GO reinforced PVA nanocomposites were significantly improved; tensile strength, Young's modulus, and elongation at break increased by 88%, 150%, and 22%, respectively at 1 wt% loading of PVA-g-GO. In another study, Prasad et al. have reported ~400% increase in the stiffness and hardness of graphene and nanodiamonds reinforced PVA nanocomposites [88].

Sayyar et al. have investigated the mechanical properties of graphene-reinforced PCL nanocomposites [89]. In this study, the authors used an esterification reaction to covalently link carboxyl groups on graphene sheet with polycaprolactone chains. Results show that 5 wt% loading of graphene resulted in ~192% increase in strength (from 13.5 to 39.5 kN m/kg) and ~571% increase in modulus (from 88.7 to 591.1 kN m/kg) compared to pristine polycaprolactone composites. Fan et al. have reported the mechanical characterization of graphene-reinforced chitosan nanocomposites [90]. Addition of 0.1 wt% graphene resulted in a twofold increase in the elastic modulus and ~1.5-fold increase in the hardness of chitosan–graphene nanocomposites.

2.2.3.2 2D inorganic nanomaterial-reinforced polymeric nanocomposites

Few studies have investigated the application of 2D layered inorganic nanomaterials such as boron nitride nanoplatelets, tungsten disulfide nanosheets, and molybdenum disulfide nanoplatelets as reinforcing agents to improve the mechanical properties of polymeric implants for tissue-engineering applications [33,112]. Other studies have reported the use of 2D tungsten, boron and molybdenum nanosheets as reinforcing agents; however, those nanocomposites were not fabricated toward biomedical applications [91,92].

Farshid et al. have investigated the mechanical properties of boron nitride nanoplatelet (BNNP)-reinforced PPF scaffolds at 0.2 wt% nanomaterial loading [112]. Results show that addition of BNNPs resulted in ~38% increase in the Young's modulus and ~31% increase in compressive yield strength compared to PPF nanocomposites without nanomaterial loading. In another study, Lalwani et al. have reported the mechanical properties of MSNP-reinforced PPF nanocomposites for bone-tissue engineering [33]. PPF nanocomposites at 0.2 wt% loading of MSNPs show ~108% increase in Young's modulus, ~93% increase in compressive yield strength, ~53% increase in flexural modulus, and ~262% increase in flexural yield strength compared to PPF composites without nanomaterials (Fig. 2.7). Transmission electron microscopy analysis shows a uniform dispersion of MSNPs in the polymer matrix (Fig. 2.8), an important factor for efficient mechanical reinforcement.

2.3 Design criteria and nanomaterial properties for maximum mechanical reinforcement

The efficacy of nanomaterials as reinforcing agents depend on several factors such as nanomaterial morphology, aspect ratio, surface area, functionalization state, nanomaterial aggregation, and changes in cross-linking density of polymer matrix. Maximum mechanical reinforcement is achieved as a result of a complex interplay of these several factors. In this section, we will review these parameters and discuss strategies for maximum mechanical reinforcement.

2.3.1 Nanomaterial morphology

Nanomaterial morphology plays an important role in determining the efficacy of mechanical reinforcement. 2D nanomaterials are better reinforcing agents than 1D or 0D nanomaterials. It has been reported that 2D nanomaterials not only have larger surface area compared to 0D and 1D nanomaterials [33], they are more effective in increasing the cross-linking density of polymeric composites, thereby resulting in significant increases in several mechanical properties such as compression strength, tensile strength, creep strain, and fracture toughness [93,94]. Lalwani et al. have compared the efficacies of various 1D and 2D carbon (SWCNTs, MWCNTs, SWGONRs, MWGONRs, and GONPs) and inorganic nanomaterials (WSNTs and MSNPs) as reinforcing agents for PPF polymer used in bone-tissue engineering [33,34]. Their results suggest that inorganic nanomaterials (MSNPs and WSNTs) are better reinforcing agents than carbon nanomaterials (SWCNTs, MWCNTs, SWGONRs, MWGONRs, and GONPs), and in general 2D nanomaterials are better reinforcing agents than 1D nanomaterials.

2.3.2 Aspect ratio and surface area of nanomaterials

Several studies have suggested that a reduction in the aspect ratio of nanoparticles results in improvements in mechanical properties. Sitharaman et al. have shown that

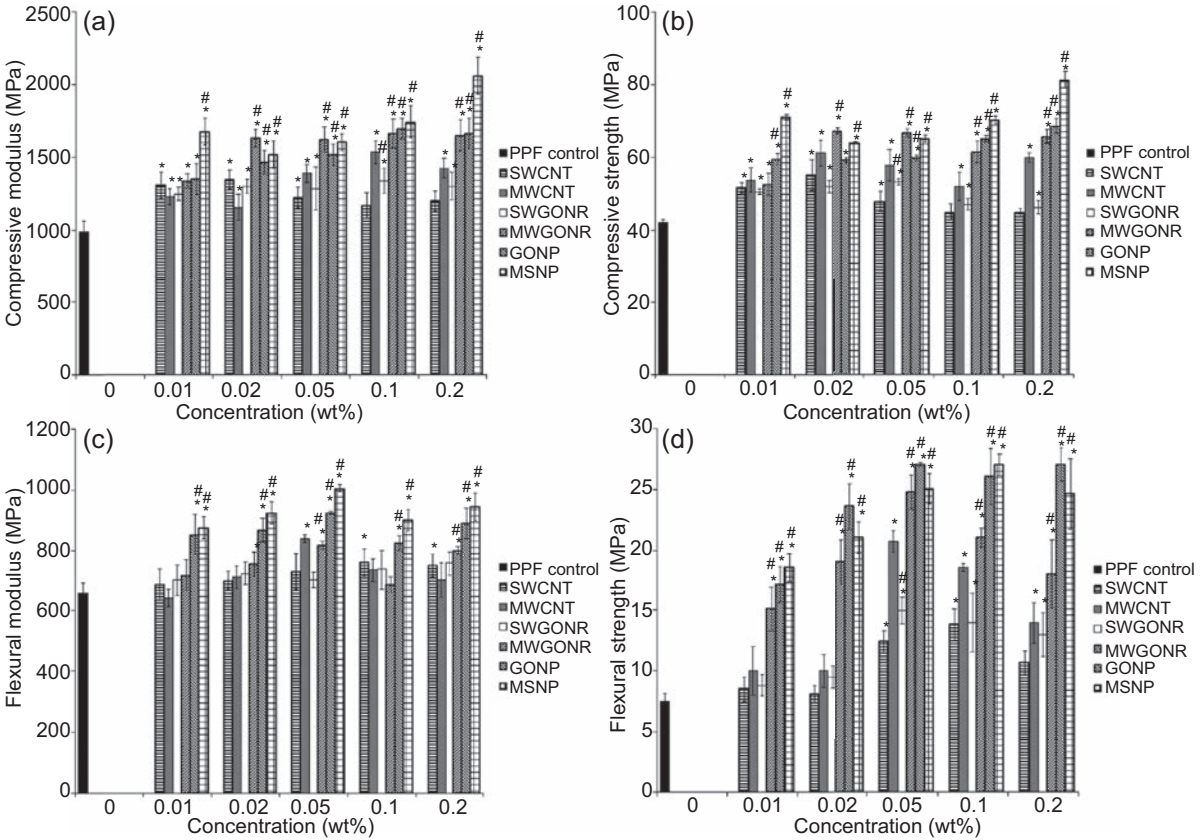

Figure 2.7 (a) Compressive modulus, (b) compressive yield strength, (c) flexural modulus, and (d) flexural yield strength of SWCNT-, MWCNT-, SWGONR-, MWGONR-, GONP-, and MSNP-reinforced PPF scaffolds at 0.01 to 0.2 wt% nanomaterial-loading concentrations. Data are reported as mean ± standard deviation for $n = 5$ samples. '*' represents significant differences from PPF composites (baseline control), and '#' represents significant difference from SWCNT and MWCNT nanocomposites at $p < 0.05$.

Adapted from Lalwani G, Henslee AM, Farshid B, Lin L, Kasper FK, Qin Y-X, et al. Two-Dimensional Nanostructure-Reinforced Biodegradable Polymeric Nanocomposites for Bone Tissue Engineering. Biomacromolecules 2013;14:900–9, with permission. Copyright © American Chemical Society, 2013.

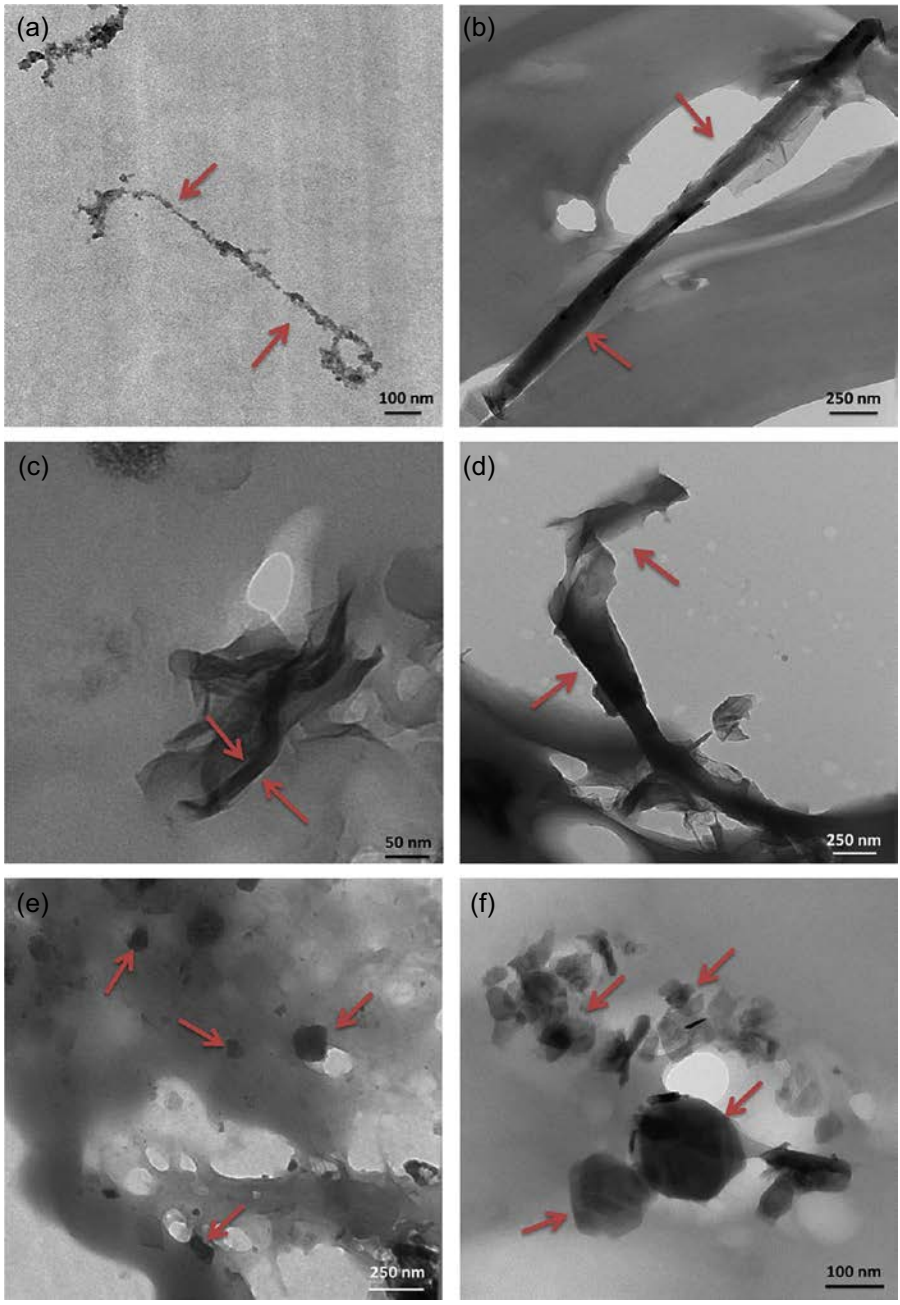

Figure 2.8 Representative transmission electron microscopy images of cross-linked PPF nanocomposites at 0.1 wt% loading of (a) SWCNTs, (b) MWCNTs, (c) SWGONRs, (d) MWGONRs, (e) GONPs, and (f) MSNPs. Nanomaterials embedded in the polymer matrix are marked with red arrows.
Adapted from Lalwani G, Henslee AM, Farshid B, Lin L, Kasper FK, Qin Y-X, et al. Two-Dimensional Nanostructure-Reinforced Biodegradable Polymeric Nanocomposites for Bone Tissue Engineering. Biomacromolecules 2013;14:900–9, with permission. Copyright © American Chemical Society, 2013.

US-SWCNTs are better reinforcing agents than long SWCNTs [35]. Lalwani et al. have shown that 2D carbon and inorganic nanomaterials such as nanoplatelets with low aspect ratio (~1) are better reinforcing agents than long 1D nanomaterials such as nanotubes with higher aspect ratios (>1000) [33,34]. Sitharaman, Rafiee, and others have reported that increasing the surface area of nanomaterials leads to better mechanical reinforcement [35,95]. Nanomaterials with higher surface area provide greater nanomaterial–polymer interaction resulting in a better mechanical reinforcement than nanomaterials with lower surface area.

2.3.3 Nanomaterials chemistry, aggregation state, and cross-linking density of polymer

Presence of functional groups on the surface of nanomaterials can lead to increases in the mechanical properties of nanocomposites due to an increased nanomaterial–polymer interaction. Functionalized nanomaterials are easier to disperse in organic solvents resulting in a uniform dispersion of nanomaterials in the polymer matrix. Micron-sized aggregates of nanomaterials act as points of stress concentration and crack initiation under external loads. Various covalent and noncovalent functional groups such as octadecylamine [96], hyperbranched aromatic polyamide [96], poly(acrylic acid) [97], poly(N-isopropylacrylamide) [97], and nitroxide [98], have been used to improve dispersion of nanomaterials in the polymeric networks. Lalwani et al. and Shi et al. have shown that a uniform dispersion of nanomaterials in the polymer matrix leads to better mechanical reinforcement [33,34,71]. Improvements in the cross-linking density of the polymer can also lead to significant increases in the mechanical properties of nanocomposites. Lalwani et al. have shown that the presence of sulfide, oxysulfide, and oxidative functional groups (hydroxyl, alcohol, and acid) can lead to a greater cross-linking density, which results in improved mechanical properties [33,34]. Lordi et al. have reported that the sliding fractional stresses and binding energies between CNTs and polymeric matrix are minor factors in determining the strength in the interface whereas conformation of the polymeric network around nanotubes is the dominant factor [99]. Furthermore, in addition to covalent and noncovalent functionalization [100,101], by utilizing anisotropy in fabrication of nanocomposites using magnetic and electric fields, it is possible to align nanotubes with the direction of mechanical loading for further mechanical reinforcement [102,103].

2.4 In vitro and in vivo cyto- and biocompatibility of nanomaterial-reinforced polymeric nanocomposites

With increasing applications of nanomaterial-reinforced polymeric nanocomposites in biology and in medicine, there are concerns and debate on the toxicity of these nanocomposites. A better understanding of the toxicity and biocompatibility of these nanocomposites can lead to applications in tissue engineering and regenerative medicine.

In this section, we will review the in vitro and in vivo studies performed to assess the toxicity and biocompatibility of nanomaterial-reinforced polymeric nanocomposites.

2.4.1 *In vitro cytotoxicity of nanomaterial-reinforced polymeric nanocomposites*

In vitro cytotoxicity analysis is typically the first step before more elaborate and expensive in vivo biocompatibility studies. Shi et al. have reported a comparative study of the in vitro cytotoxicity of single-walled nanotubes (SWNTs), functionalized SWNTs (F-SWNTs), and ultrashort SWNTs (US tube)-dispersed PPF nanocomposites for bone-tissue engineering [104]. Tissue culture polystyrene (TCPS) and PPF composites without nanomaterial loading were used as controls, and three different cytotoxicity tests were performed on the cross-linked PPF nanocomposite networks using Fischer rat fibroblast 3T3-like cells (American Type Culture Collection [ATCC], Clinical Reference Laboratory [CRL]-1764). LIVE/DEAD assay was performed after 24 h. Results (Fig. 2.9) show no significant differences in cell viability between experimental (PPF nanocomposites) and control groups; ~100% cell viability was observed. Furthermore, scanning electron microscopy (SEM) images (Fig. 2.10) show that fibroblasts could attach and spread on the nanocomposite surface. Degradation products of PPF nanocomposites showed a dose-dependent cytotoxic response with nearly 0% cell viability at 2× dilution of degradation products which increased to more than 85% cell viability at 100× dilution.

Shi et al. have reported the cytotoxicity of SWCNT, ultrashort SWCNTs (US tubes), and functionalized (dodecylated) US tubes (F-US-tube)-reinforced PPF nanocomposites [105]. In this study, porous PPF nanocomposite scaffolds of four different porosities (75, 80, 85, and 90 vol%) were fabricated using a thermal cross-linking particulate-leaching technique. Rat bone marrow stromal cells (BMSCs) were cultured

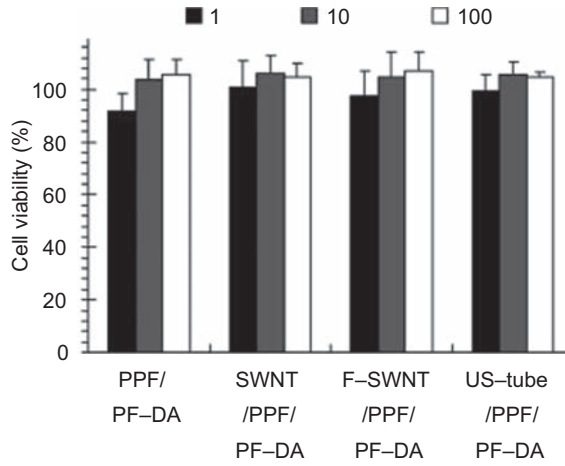

Figure 2.9 Cell viability after 24 h of exposure to 1 to 100× dilutions of cross-linked PPF nanocomposites. (1× dilution = 1 ml media/3 cm^2 network surface). Error bars represent standard deviations for $n = 5$ samples.
Adapted from Shi X, Sitharaman B, Pham QP, Spicer PP, Hudson JL, Wilson LJ, et al. In vitro cytotoxicity of single–walled carbon nanotube/biodegradable polymer nanocomposites. Journal of Biomedical Materials Research Part A 2008;86:813–23, with permission. Copyright © Wiley 2007.

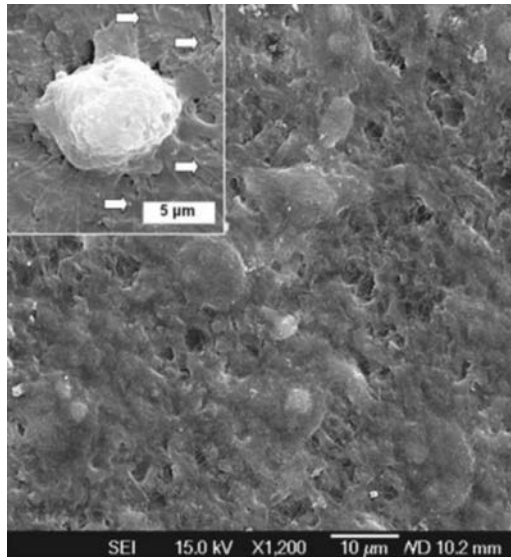

Figure 2.10 Representative SEM image of Fisher 3T3 fibroblasts attached on the surface of F-SWCNT nanocomposites. Inset shows a cell attached to nanocomposite surface with white arrows pointing to carbon nanotubes.
Adapted from Shi X, Sitharaman B, Pham QP, Spicer PP, Hudson JL, Wilson LJ, et al. In vitro cytotoxicity of single–walled carbon nanotube/biodegradable polymer nanocomposites. Journal of Biomedical Materials Research Part A 2008;86:813–23, with permission. Copyright © Wiley 2007.

on scaffolds for 1, 3, and 7 days. PicoGreen assay results showed no significant differences between cellularity of PPF nanocomposites. SEM and fluorescence confocal imaging (Fig. 2.11) showed that cells were able to attach, proliferate, and spread on each nanocomposite group.

Fan et al. have reported the cytotoxicity of chitosan–graphene nanocomposites using L929 cells [90]. 3-(4,5-dimethylthiazol-2-yl)-2,5-diphenyltetrazolium bromide (MTT) assay results showed no reduction in cell viability. Phase-contrast imaging showed that the cells were able to attach and proliferate on chitosan–graphene films. Taken together, these results suggest a good cytocompatibility of graphene–chitosan nanocomposites. Pinto et al. have used GO and GNPs as reinforcing agents to improve the mechanical properties of PLA films [106]. The cytotoxicity of these composite films was tested using mouse embryo fibroblasts 3T3 cells by MTT assay along with evaluation of platelet adhesion and activation. No differences in cellular attachment and morphology were observed between cells on PLA–GO and PLA–GNP nanocomposite surfaces after 48 h. Adsorption of serum proteins such as albumin resulted in reduced platelet activation. In the presence of plasma proteins, PLA–GNP nanocomposite films showed reduced platelet activation compared to PLA and PLA–GO films (Fig. 2.12). These results show that PLA–graphene films are cyto- and hemocompatible.

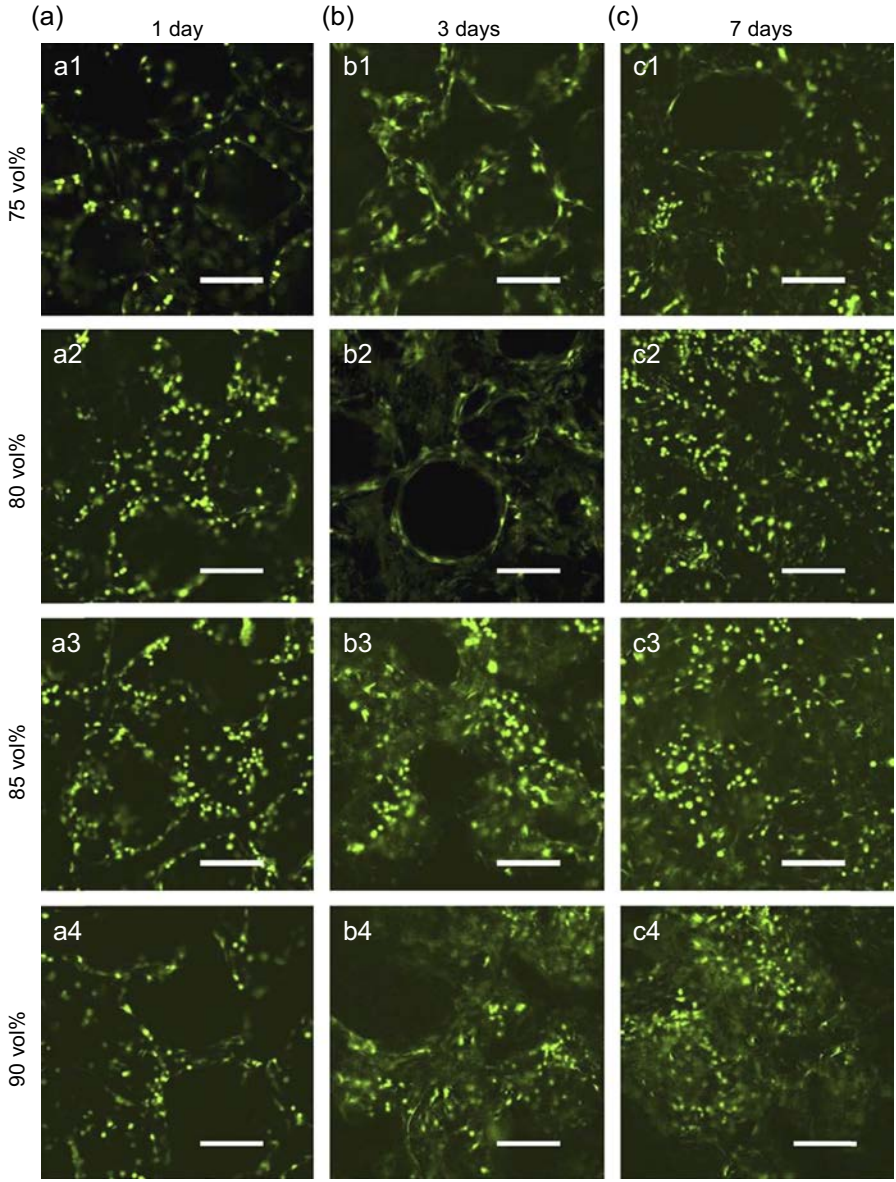

Figure 2.11 Confocal images of F-US-tube-reinforced PPF nanocomposites with porogen fractions of 75, 80, 85, and 90 vol% (top to bottom) after BMSC seeding for 1 day (a1–4), 3 days (b1–4), and 7 days (c1–4) treated with LIVE/DEAD reagent. Scale bars represent 200 μm.

Adapted from Shi X, Sitharaman B, Pham QP, Liang F, Wu K, Billups WE, et al. Fabrication of porous ultra-short single-walled carbon nanotube nanocomposite scaffolds for bone tissue engineering. Biomaterials 2007;28:4078–90, with permission. Copyright © Elsevier, 2007.

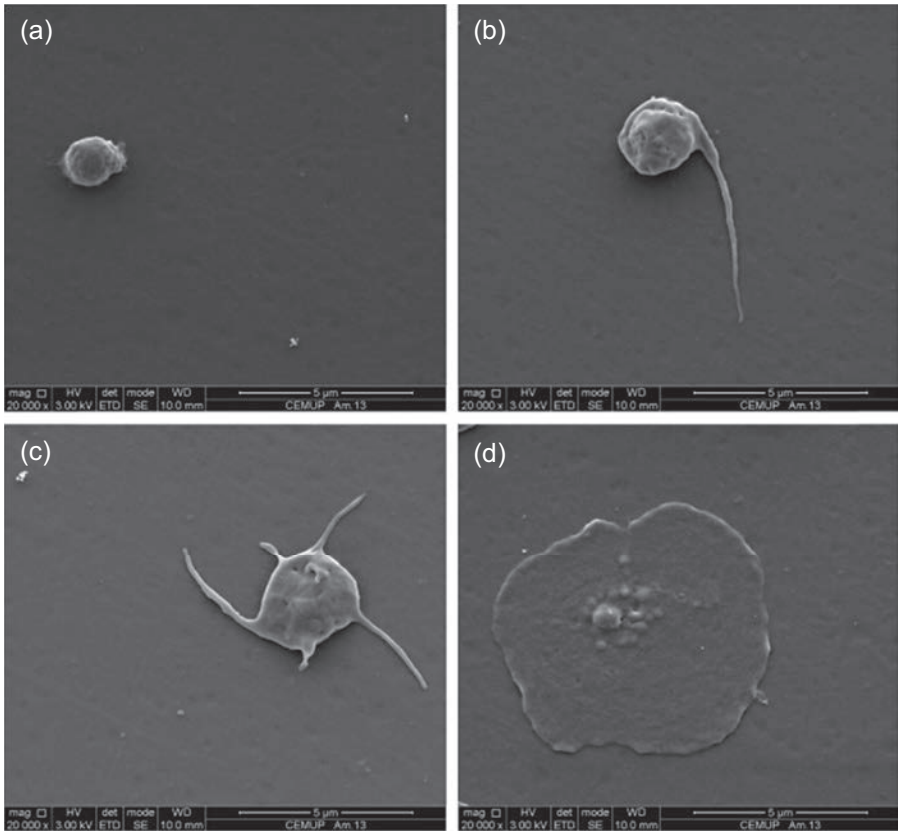

Figure 2.12 Activation degree of platelets at the surface of PLA–GO films. Representative images of nonactivated (a and b) and activated (c and d) platelets at 20,000 × magnification. Adapted from Pinto AM, Moreira S, Gonçalves IC, Gama FM, Mendes AM, Magalhães FD. Biocompatibility of poly (lactic acid) with incorporated graphene-based materials. Colloids and Surfaces B: Biointerfaces 2013;104:229–38, with permission. Copyright © Elsevier, 2012.

Adhikari et al. have reported the cytocompatibility of PLGA films reinforced with GNPs and functionalized GNPs (GNP-NH_2) [107]. Human Embryonic Kidney 293 cells (HEK-293) were cultured on PLGA films containing GNPs (0, 1, or 5 wt%). PLGA–GNP nanocomposites at 1 wt% loading of GNPs showed significant enhancement in HEK-239 cell growth for both GNP and GNP-NH_3 groups; however, higher GNP loading (5 wt%) resulted in increased cytotoxicity. These results show that PLA–GNP nanocomposites at 1 wt% are cytocompatible and are favorable substrates for tissue engineering.

Recently, Farshid et al. have investigated the cytocompatibility of PPF nanocomposites reinforced with various 1D and 2D carbon and inorganic nanomaterials such as SWCNTs, MWCNTs, SWGONRs, MWGONRs, GONPs, WSNTs, and MSNPs at 2 wt% concentrations using NIH3T3 cells and MC3T3 preosteoblast cells towards bone-tissue engineering applications [112]. Cytotoxicity of unreacted components, cross-linked nanocomposites and degradation products were assessed using presto blue and lactate dehydrogenase (LDH) assay. All cross-linked nanocomposites showed high cell viability (78–100%) (Fig. 2.13),

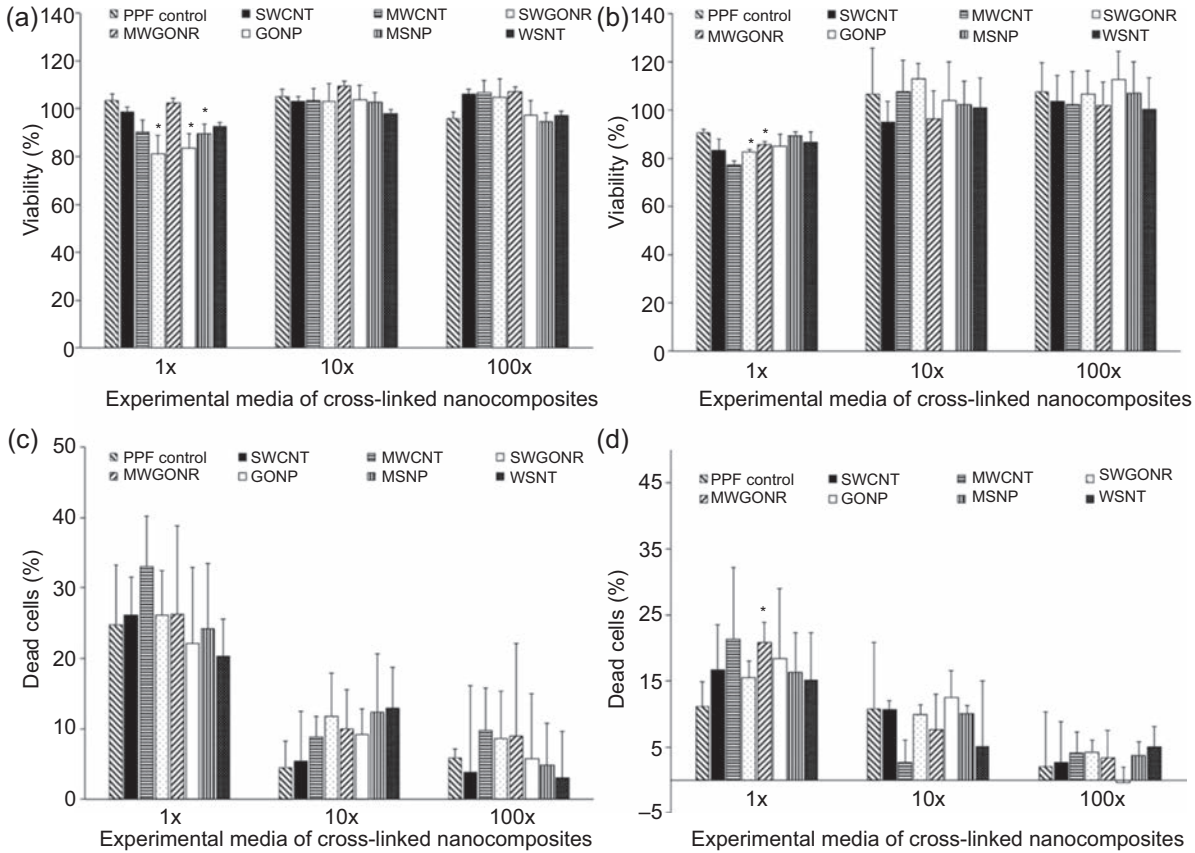

Figure 2.13 Fraction of (a and c) viable and dead NIH3T3 and (b and d) MC3T3 cells after 24 h of exposure to extracts of cross-linked nanocomposites. Data are normalized to live and dead controls and error bars represent standard deviation for $n=6$ samples. The symbol '*' indicates significant difference between PPF baseline and PPF nanocomposites ($p<0.05$).

Adapted from Farshid B, Lalwani G, Sitharaman B. In vitro cytocompatibility of one–dimensional and two–dimensional nanostructure–reinforced biodegradable polymeric nanocomposites. Journal of Biomedical Materials Research Part A 2015;103:2309–21, with permission. Copyright © Wiley, 2015.

robust cellular attachment, and proliferation (Fig. 2.14). However, the unreacted components showed a dose-dependent cytotoxicity, attributed to leaching of cytotoxic components that can be mitigated by their removal from the implant site. These results suggest that nanomaterial-reinforced PPF nanocomposites are cytocompatible and can be used for bone-tissue engineering applications.

Chung et al. and Tayton et al. have reported the cytocompatibility of HA-reinforced poly(1,8-octanediol-co-citrate) (POC) and PLA–PLGA nanocomposites [108,109]. Chung et al. have reported an increased proliferation of human mesenchymal stem cells (hMSCs) with increasing concentrations of HA (40–60 wt%) in POC–HA nanocomposites. Results show that hMSCs were able to attach and proliferate on POC–HA nanocomposites for 21 days for all nanocomposite groups (Fig. 2.15) suggesting a good biocompatibility of POC–HA nanocomposites. Tayton et al. have reported the cytotoxicity of HA-reinforced PLA and PLGA nanocomposites at 10 wt%. After 14 days of incubation with skeletal stem cells (SSCs), an enhanced osteoblastic activity (increased alkaline phosphatase [ALP] expression and Type 1 collagen deposition) was observed, suggesting an osteoinductive and osteogenic capacity of PLA–HA nanocomposites.

Kim et al. have reported the cytotoxicity and osteogenic response of HA-reinforced PPF nanocomposites [110]. Incorporation of HA resulted in an increase in the surface roughness, protein adsorption, hydrophilicity, and cell attachment of rat BMSCs. BMSCs cultured on 3D macroporous PPF–HA scaffolds after 8 days showed increased expression of osteogenic markers such as bone morphogenetic protein-2 (BMP-2), transforming growth factor β1, runx2, alkaline phosphatase activity, calcium deposition, and osteocalcin mRNA expression as a function of HA concentration. These results suggest that PPF–HA nanocomposites designed with tailored HA content and seeding density can be utilized to induce an osteogenic differentiation of stem cells.

Sitharaman et al. have reported the cytotoxicity of gadonanotube (Gd^{3+} doped ultrashort single-walled carbon nanotubes, GdSWCNTs)-reinforced PLGA scaffolds [111]. Rat fibroblasts 3T3 cells were treated with extracts of GdSWCNTs–PLGA scaffolds for 24 h and the cytotoxicity of gadonanotubes, US tubes, and exposure to extracts from the gadonanotubes, US tubes, PLGA scaffolds, and gadonanotube–PLGA nanocomposites was investigated using LIVE/DEAD assay. High cell viability (~100%) was observed for all treatment groups using extract dilution and direct contact analysis (Fig. 2.16).

Recently, Farshid et al. have investigated the mechanical properties of BNNT- and nanoplatelet (BNNP)-reinforced PPF nanocomposites (0.2 wt% nanomaterial loading) and their in vitro cytocompatibility [112]. The cytotoxicity studies were performed using nanocomposite extracts before cross-linking, after cross-linking, and their degradation products. Presto Blue® and LDH assays showed <80% cell viability of MC3T3 cells at 1× dilutions of cross-linked nanocomposites and their degradation products which increased to ~100% for 10× and 100× dilutions. However, the non-cross-linked nanocomposites exhibited a dose-dependent cytotoxicity that may be mitigated by in situ cross-linking. Confocal fluorescence and SEM imaging confirmed excellent cell attachment and ECM deposition on nanocomposite surfaces. These results suggest that BNNT- and BNNP-reinforced PPF nanocomposites are cytocompatible and can be used for bone-tissue engineering applications.

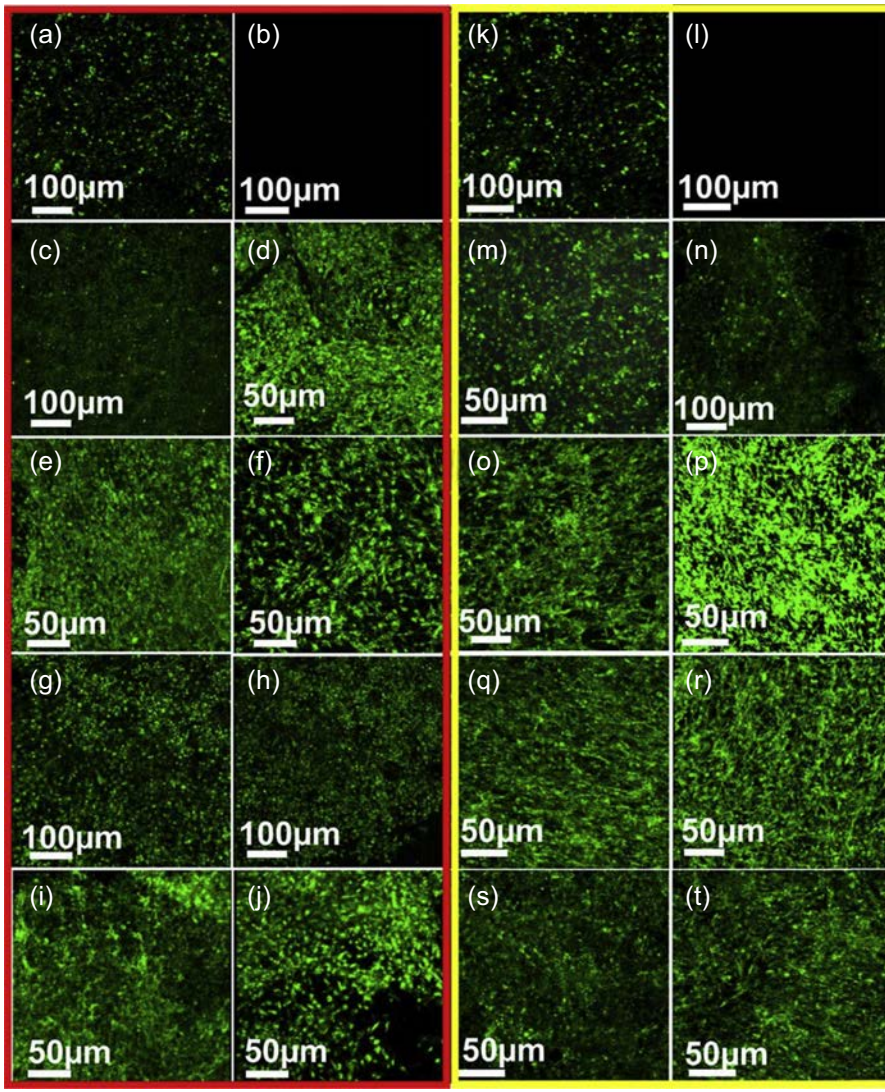

Figure 2.14 Representative fluorescence images of attached cells on cross-linked nanocomposites after 5 days of cell culture of (a–j) NIH3T3 and (k–t) MC3T3 cells, respectively. (a and k) TCPS (positive) control, (b and l) negative control, (c and m) PPF control, (d and n) GONP, (e and o) MWCNT, (f and p) SWCNT, (g and q) MWGONR, (h and r) SWGONR, (i and s) WSNT, and (j and t) MSNP nanocomposites.
Adapted from Farshid B, Lalwani G, Sitharaman B. In vitro cytocompatibility of one–dimensional and two–dimensional nanostructure–reinforced biodegradable polymeric nanocomposites. Journal of Biomedical Materials Research Part A 2015;103:2309–21, with permission. Copyright © Wiley, 2015.

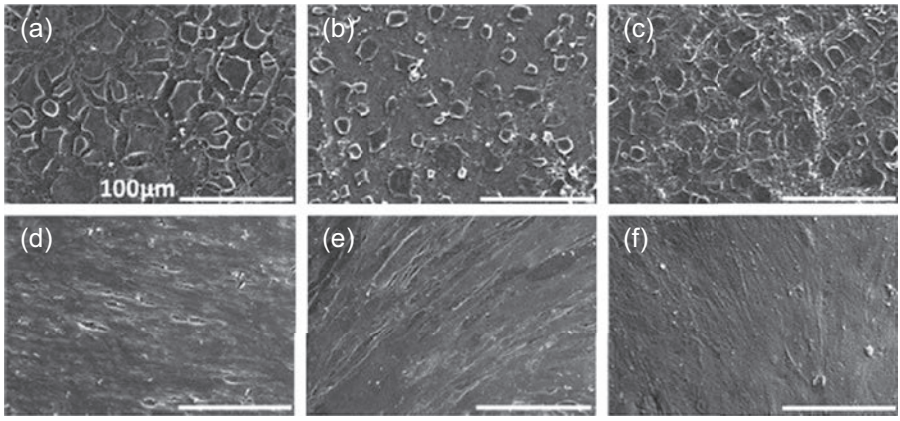

Figure 2.15 Cell adhesion and morphology on (a–c) day 1 and (d–f) day 21 on (a and d) POC–40HA, (b and e) POC–50HA, and (c and f) POC–60HA. Scale bar 100 µm.
Adapted from Chung EJ, Sugimoto MJ, Ameer GA. The role of hydroxyapatite in citric acidbased nanocomposites: Surface characteristics, degradation, and osteogenicity in vitro. Acta biomaterialia 2011;7:4057–63, with permission. Copyright © Elsevier, 2011.

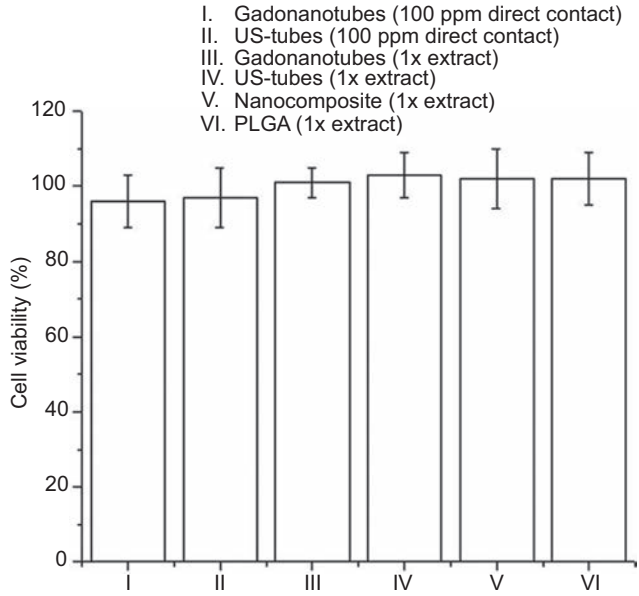

Figure 2.16 Cell viability after 24 h of incubation with extracts of PPF and nanomaterials (direct contact). Error bars represent standard deviations for $n = 6$ samples.
Adapted from Sitharaman B, Van Der Zande M, Ananta JS, Shi X, Veltien A, Walboomers XF, et al. Magnetic resonance imaging studies on gadonanotube–reinforced biodegradable polymer nanocomposites. Journal of Biomedical Materials Research Part A 2010;93:1454–62, with permission. Copyright © Wiley, 2009.

2.4.2 *In vivo biocompatibility of nanomaterial-reinforced polymeric nanocomposites*

Sitharaman et al. have investigated the biocompatibility of US SWCNT-reinforced PPF nanocomposites in a rabbit subcutaneous and femoral defect model [113]. PPF–US-tubes nanocomposite scaffolds were implanted in both left and right femoral condyle defects (4 mm diameter, 8 mm depth) along with subcutaneous pockets created in the dorsum of New Zealand white rabbits (eight rabbits per group) for 4 and 12 weeks. Percentages of bone formation were measured using micro-CT, histology and histomorphometry. As shown in Fig. 2.17, after 12 weeks of implantation, the US-tube–PPF scaffolds showed significantly greater bone healing as compared to the controls (PPF polymer scaffolds without nanomaterials). Histology and histomorphometry analysis (Fig. 2.17) showed new bone-tissue formation along with fibrous tissue and an inflammatory response for the PPF–US-tubes nanocomposites. No significant difference in polymer degradation was observed between all the groups. The results showed that PPF–US-tubes nanocomposite scaffolds after 12 weeks augmented new bone formation (new bone content at the defect site after 12 weeks was ~66% of the surrounding trabecular bone) suggesting that PPF–US-tubes scaffolds are not only osteoconductive but also bioactive assisting osteogenesis.

Kim et al. have investigated the biocompatibility of HA-incorporated PLGA scaffolds fabricated using gas foaming–particulate leaching (GF–PL) and solvent casting–particulate leaching (SC–PL) methods without the use of organic solvents [114]. In this study, a critical sized (8 mm) transosseous defect was produced in the parietal bone and filled with fabricated scaffolds. After 8 weeks, the implants were analyzed by micro-CT and histology for new bone formation. Both types of scaffolds incorporated with HA showed 10–20% higher bone formation than PLGA scaffolds (control) with GF–PL scaffolds showing highest bone-tissue regeneration. These results suggest that incorporation of HA using GF–PL technique to fabricate PLGA-HA nanocomposite scaffolds is promising for bone-tissue engineering.

Tayton et al. have reported the use of PLA and HA-incorporated PLA scaffolds for bone-tissue engineering in vivo [109]. SSCs seeded HA-incorporated (10% loading) PLA scaffolds were implanted in Male MF-1 immunodeficient mice in a 10-mm subcuticular incision over the loin area along with PLA control, PLA with SSCs, PLA, and HA control. After 35 days, micro-CT was performed on all the samples, and quantitative analysis saw a significant increase in bone formation in the SSC-seeded PLA–HA scaffolds when compared to PLA control. Histology analysis confirmed the formation of new bone, suggesting that PLA–HA scaffolds are osteogenic and osteoconductive (Fig. 2.18). In another study, Tayton et al. isolated SSCs from six healthy and skeletally mature Welsh mule ewes and SSCs seeded PLA–HA scaffolds were implanted into a 15 mm cancellous bone defect in ovine (large animal model) [115]. After 13 weeks of bilateral implantation, femoral condyles were harvested along with popliteal lymph nodes and analyzed using micro-CT, histology, and postmortem mechanical testing to assess de novo bone formation. Mechanical testing results show that bone strength of control and SSC-seeded PLA–HA scaffolds were 20% and 11%

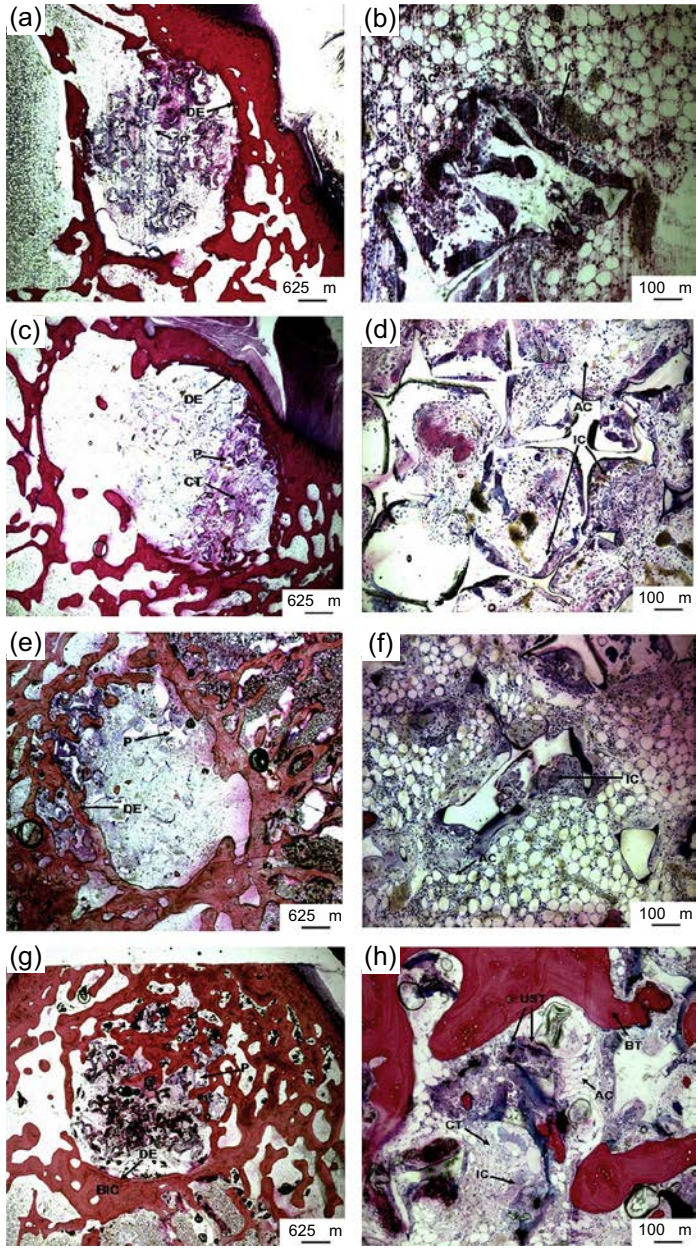

Figure 2.17 Representative histological sections of scaffolds implanted in femoral condyle defects: (a and b) a PPF scaffold 4 weeks after implantation, (c and d) a US-tube–PPF scaffold after 4 weeks, (e and f) a PPF scaffold after 12 weeks, and (g and h) a US-tube–PPF scaffold after 12 weeks' implantation. The images are presented at 1.6Å~ and 10Å~ magnification. The PPF scaffold (P) appears as white areas in all images. The original defect edge (DE) is visible in the low-magnification images. Bone-like tissue (BT) appears red; direct bone implant contact (BIC) occurred with the US-tube–PPF nanocomposite scaffold 12 weeks after implantation. US tubes (UST), connective tissue (CT), adipose cells (AC), and inflammatory cells (IC) are also shown. Adapted from Sitharaman B, Shi X, Walboomers XF, Liao H, Cuijpers V, Wilson LJ, et al. In vivo biocompatibility of ultra-short single-walled carbon nanotube/biodegradable polymer nanocomposites for bone tissue engineering. Bone 2008;43:362–70, with permission.

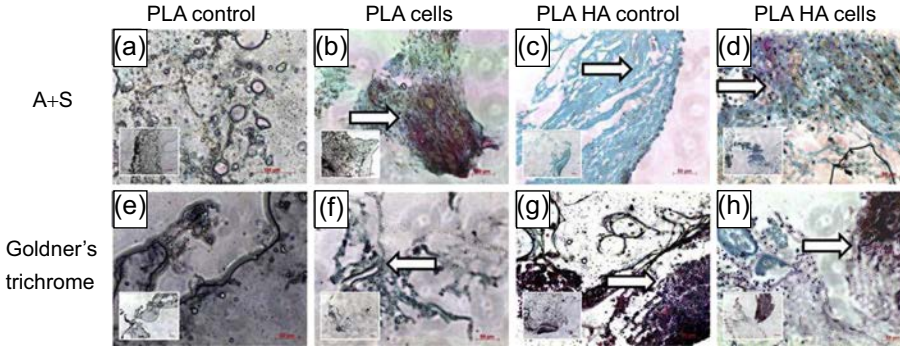

Figure 2.18 Histological sections of specimens viewed under light microscopy (20× magnification, inset = 5× magnification, scale bar = 100 μm) post 5 weeks in vivo period. (a–d) Alcian blue and Sirius red staining for collagen and proteoglycan deposition is negative for (a) the PLA controls but positive for (b–d, *arrows*) other specimens. Similar findings when assessing for (e–h) osteoid (*arrows*) using Goldner's Trichrome stains.
Adapted from Tayton E, Purcell M, Aarvold A, Smith J, Briscoe A, Kanczler J, et al. A comparison of polymer and polymer–hydroxyapatite composite tissue engineered scaffolds for use in bone regeneration. An in vitro and in vivo study. Journal of Biomedical Materials Research Part A 2014;102:2613–24, with permission. Copyright © Wiley, 2013.

greater than native cancellous bone. Micro-CT analysis quantified the new bone formation with a mean increase of 13.4% in SSC-seeded PLA–HA scaffolds compared to control scaffolds. The results of this study demonstrate the osteoconductive nature of PLA–HA scaffolds and highlight the issues and steps for the scale-up and transition of cell-seeded tissue engineering constructs for human trials.

Mistry et al. have demonstrated the biocompatibility and in vivo degradation of porous alumoxane-incorporated PPF scaffolds for bone-tissue engineering applications [116]. In this study, three experimental groups (PPF/propylene fumaratediacrylate [PPF/PF-DA] polymer scaffolds, the macrocomposite PPF/PF-DA polymer scaffolds with micron-sized particles of boehmite, and PPF/PF-DA polymer scaffolds with surface-modified alumoxane nanoparticles) and controls (PPF/PF-DA composites without boehmite–alumoxane loading and low molecular weight PPF composite—degradation control) were implanted in the defects on the lateral side of femoral condyles of adult goats ($n = 6$) for 12 weeks. New bone formation was analyzed by micro-CT and histology (Fig. 2.19). New bone formation was observed within the pores of the scaffolds along with small amounts of soft fibrous tissue and inflammatory cells; however, several pores were empty or filled with fluid. The level of the inflammatory response varied widely between the scaffolds. A direct contact between scaffolds and the neighboring bone tissue was observed along with minimal degradation of the nanocomposite scaffolds in vivo. These results suggest that incorporation of alumoxane nanoparticles in PPF scaffolds does not alter their degradation or in vivo biocompatibility.

Henslee et al. have investigated a two-part bone-tissue engineering scaffold fabricated using a solid PPF intramedullary rod providing mechanical support surrounded

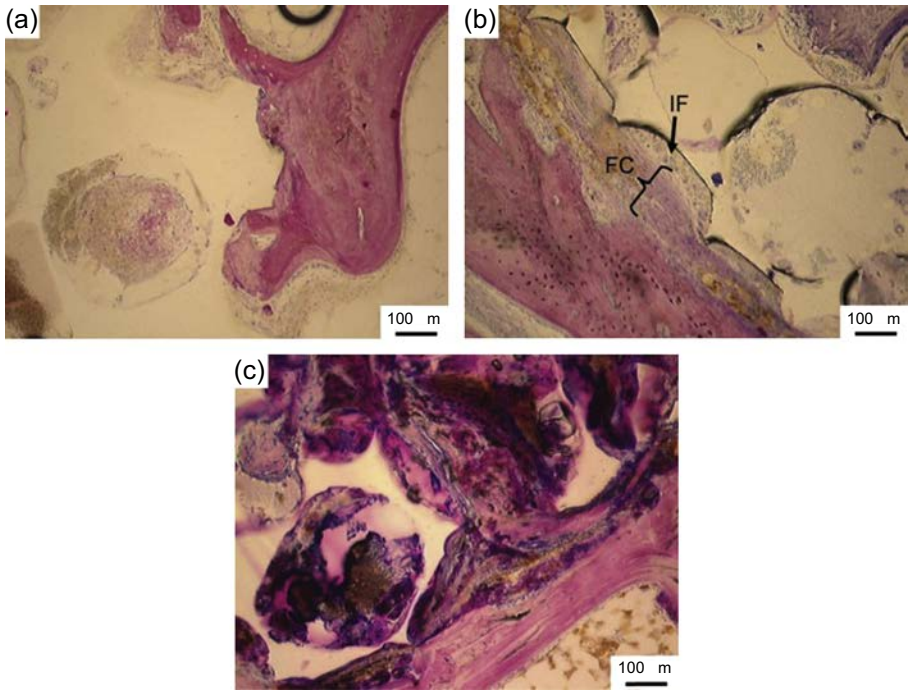

Figure 2.19 (a) Histological section of the middle region of a PPF–PF-DA polymer alone scaffold. The white scaffold is in direct contact with the surrounding bone tissue (pink). Bar is 100 μm. (b) Histological section of the top region of a macrocomposite scaffold showing a thin fibrous capsule (FC) surrounding the scaffold. The porous surface of the scaffold created a pocket in which inflammatory cells (IF) accumulated. Bar is 100 μm. (c) Histological section of the top region of a macrocomposite scaffold showing disorganized tissue and inflammatory cells at the scaffold–tissue interface. Bar is 100 μm.
Adapted from Mistry AS, Pham QP, Schouten C, Yeh T, Christenson EM, Mikos AG, et al. In vivo bone biocompatibility and degradation of porous fumarate–based polymer/alumoxane nanocomposites for bone tissue engineering. Journal of Biomedical Materials Research Part A 2010;92:451–62, with permission. Copyright © Wiley, 2008.

by a porous PPF sleeve containing recombinant human bone morphogenic protein-2 (rhBMP-2)-incorporated PLGA microparticles [117]. The scaffolds were implanted in segmental femoral defects in rats. After 12 weeks, the femurs from the rats were excised and analyzed using radiography, micro-CT, histology, and mechanical testing. The presence of PPF medullary rod inhibited new bone formation; however, the PPF sleeve containing rhBMP-2 microspheres (0, 2, or 8 μg) increased the torsional stiffness of the construct by ~267%. Histological analysis showed the formation of immature cartilage and newly formed bone along the cartilage (Fig. 2.20). These results suggest that, although the scaffolds may provide mechanical support, their presence in a bone defect may hinder new bone formation if they interfere with cellular processes.

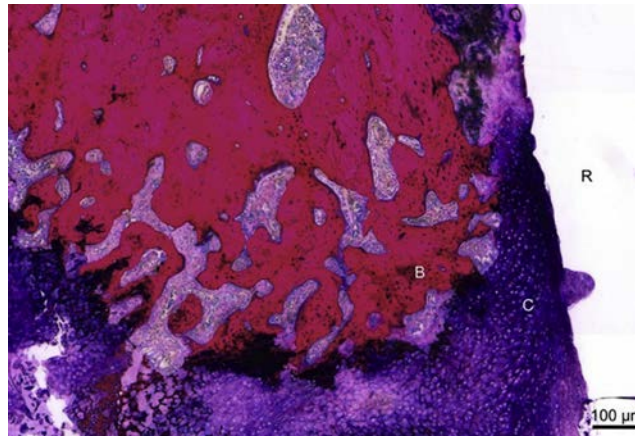

Figure 2.20 Representative histological section of bone implanted with solid intramedullary PPF rod at 12 weeks. Immature cartilage formation (C), indicated by the dark purple matrix with blue cells, was found along the PPF rod surface (R). Newly formed bone (B) was found along the cartilage. Scale bar represents 100 µm.
Adapted from Henslee A, Spicer P, Yoon D, Nair M, Meretoja V, Witherel K, et al. Biodegradable composite scaffolds incorporating an intramedullary rod and delivering bone morphogenetic protein-2 for stabilization and bone regeneration in segmental long bone defects. Acta biomaterialia 2011;7:3627–37, with permission. Copyright © Elsevier, 2011.

2.5 Summary and future perspective

Various 1D and 2D nanomaterials such as carbon nanotubes, graphene, tungsten disulfide nanotubes, HA and alumoxane nanoparticles, graphene nanoribbons and nanoplatelets, and boron nitride nanotubes and nanoplatelets can improve the mechanical properties of polymeric nanocomposites for bone-tissue engineering applications. High surface area and structural defects improve the nanomaterial–polymer interactions and the presence of functional groups on the surface of nanomaterials increases the nanocomposite cross-linking density. These factors along with a uniform dispersion of nanomaterials in the polymer matrix are the key reasons for observed mechanical reinforcement. In vitro cytotoxicity and in vivo biocompatibility studies suggest that nanomaterial-reinforced polymeric nanocomposites are nontoxic and are osteogenic and bioactive favoring de novo bone formation. These results taken together suggest that the incorporation of nanomaterials as reinforcing agents to improve the mechanical properties of polymeric nanocomposite and scaffolds can be harnessed to fabricate the next generation of novel, light-weight, mechanically strong, osteoconductive and osteoinductive bone implants.

Future studies should focus on assessing the long-term stability, toxicity, and degradation profiles of nanocomposites in large animal models to identify the conditions appropriate for first in human clinical trials. Furthermore, the addition of nanomaterials may also be exploited toward the fabrication of multifunctional polymeric

nanocomposites and scaffolds permitting simultaneous therapy (drug delivery) and noninvasive longitudinal monitoring of scaffold degradation and tissue regeneration using clinically relevant imaging modalities such as magnetic resonance imaging (MRI) and computerized tomography (CT). Nanoparticle-reinforced, mechanically stable, nontoxic, biodegradable polymeric nanocomposites show great promise for applications in tissue engineering and regenerative medicine.

References

[1] Betz RR. Limitations of autograft and allograft: new synthetic solutions. Orthopedics 2002;25:S561–70.
[2] Zimmermann G, Moghaddam A. Allograft bone matrix versus synthetic bone graft substitutes. Injury 2011;42:S16–21.
[3] Puleo D, Nanci A. Understanding and controlling the bone–implant interface. Biomaterials 1999;20:2311–21.
[4] Reina A, Jia X, Ho J, Nezich D, Son H, Bulovic V, et al. Large area, few-layer graphene films on arbitrary substrates by chemical vapor deposition. Nano Lett 2009;9:30–5.
[5] Li M, Schnablegger H, Mann S. Coupled synthesis and self-assembly of nanoparticles to give structures with controlled organization. Nature 1999;402:393–5.
[6] Wang X, Zhuang J, Peng Q, Li Y. A general strategy for nanocrystal synthesis. Nature 2005;437:121–4.
[7] Hu J, Odom TW, Lieber CM. Chemistry and physics in one dimension: synthesis and properties of nanowires and nanotubes. Accounts Chem Res 1999;32:435–45.
[8] Hulteen JC, Treichel DA, Smith MT, Duval ML, Jensen TR, Van Duyne RP. Nanosphere lithography: size-tunable silver nanoparticle and surface cluster arrays. J Phys Chem B 1999;103:3854–63.
[9] Corbierre MK, Beerens J, Lennox RB. Gold nanoparticles generated by electron beam lithography of gold (I)-thiolate thin films. Chem Mater 2005;17:5774–9.
[10] Mafuné F, Kohno J-Y, Takeda Y, Kondow T, Sawabe H. Formation and size control of silver nanoparticles by laser ablation in aqueous solution. J Phys Chem B 2000;104:9111–7.
[11] Paratala BS, Jacobson BD, Kanakia S, Francis LD, Sitharaman B. Physicochemical characterization, and relaxometry studies of micro-graphite oxide, graphene nanoplatelets, and nanoribbons. PloS One 2012;7:e38185.
[12] Nicolosi V, Chhowalla M, Kanatzidis MG, Strano MS, Coleman JN. Liquid exfoliation of layered materials. Science 2013;340:1226419.
[13] Lalwani G, Sundararaj JL, Schaefer K, Button T, Sitharaman B. Synthesis, characterization, in vitro phantom imaging, and cytotoxicity of a novel graphene-based multimodal magnetic resonance imaging-X-ray computed tomography contrast agent. J Mater Chem B 2014;2:3519–30.
[14] Stankovich S, Dikin DA, Piner RD, Kohlhaas KA, Kleinhammes A, Jia Y, et al. Synthesis of graphene-based nanosheets via chemical reduction of exfoliated graphite oxide. Carbon 2007;45:1558–65.
[15] Dai H. Carbon nanotubes: synthesis, integration, and properties. Accounts Chem Res 2002;35:1035–44.
[16] Sano N, Nakano J, Kanki T. Synthesis of single-walled carbon nanotubes with nanohorns by arc in liquid nitrogen. Carbon 2004;42:686–8.

[17] Xie J, Zheng Y, Ying JY. Protein-directed synthesis of highly fluorescent gold nanoclusters. J Am Chem Soc 2009;131:888–9.
[18] Huang H, Pierstorff E, Osawa E, Ho D. Protein-mediated assembly of nanodiamond hydrogels into a biocompatible and biofunctional multilayer nanofilm. ACS Nano 2008;2:203–12.
[19] Kosynkin DV, Higginbotham AL, Sinitskii A, Lomeda JR, Dimiev A, Price BK, et al. Longitudinal unzipping of carbon nanotubes to form graphene nanoribbons. Nature 2009;458:872–6.
[20] Terrones M. Sharpening the chemical scissors to unzip carbon nanotubes: crystalline graphene nanoribbons. ACS Nano 2010;4:1775–81.
[21] Costa RD, Lodermeyer F, Casillas R, Guldi DM. Recent advances in multifunctional nanocarbons used in dye-sensitized solar cells. Energy Environ Sci 2014;7:1281–96.
[22] Kanakia S, Toussaint JD, Chowdhury SM, Lalwani G, Tembulkar T, Button T, et al. Physicochemical characterization of a novel graphene-based magnetic resonance imaging contrast agent. Int J Nanomed 2013;8:2821–33.
[23] Surnamelalwani G, Surnamehenslee G, Surnamefarshid G, Surnameparmar G, Surnamelin G, Surnameqin G, et al. Tungsten disulfide nanotubes reinforced biodegradable polymers for bone tissue engineering. Acta Biomater 2013;9(9):8365–73.
[24] Lalwani G, Sitharaman B. Multifunctional fullerene-and metallofullerene-based nanobiomaterials. Nano LIFE 2013;3:1342003-1–1342003-22.
[25] Chowdhury SM, Surhland C, Sanchez Z, Chaudhary P, Suresh Kumar MA, Lee S, et al. Graphene nanoribbons as a drug delivery agent for lucanthone mediated therapy of glioblastoma multiforme. Nanomed Nanotechnol Biol Med 2015;11:109–18.
[26] Mullick Chowdhury S, Lalwani G, Zhang K, Yang JY, Neville K, Sitharaman B. Cell specific cytotoxicity and uptake of graphene nanoribbons. Biomaterials 2013;34:283–93.
[27] Salem AK, Searson PC, Leong KW. Multifunctional nanorods for gene delivery. Nat Mater 2003;2:668–71.
[28] Lalwani G, Sai Pavan G, Mahapatra O, Gopalakrishnan C, Arunachalam KD. Study of effects of tetradotoxin (TTX) on mammalian brain tissue using iron nanoparticle (TTX) conjugate. Int J Mater Sci (IJoMS) 2009;4:529–40.
[29] Lalwani G, Gopalan A, D'Agati M, Srinivas Sankaran J, Judex S, Qin YX, et al. Porous three-dimensional carbon nanotube scaffolds for tissue engineering. J Biomed Mater Res Part A 2015;103(10):3212–25.
[30] Lalwani G, Kwaczala AT, Kanakia S, Patel SC, Judex S, Sitharaman B. Fabrication and characterization of three-dimensional Macroscopic all-carbon scaffolds. Carbon NY 2013;53:90–100.
[31] Patel SC, Lalwani G, Grover K, Qin YX, Sitharaman B. Fabrication and cytocompatibility of in situ crosslinked carbon nanomaterial films. Sci Rep 2015;5:10261. http://dx.doi.org/10.1038/srep10261.
[32] Farshid B, Lalwani G, Sitharaman B. In vitro cytocompatibility of one-dimensional and two-dimensional nanostructure-reinforced biodegradable polymeric nanocomposites. J Biomed Mater Res Part A 2015;103(7):2309–23.
[33] Lalwani G, Henslee AM, Farshid B, Lin L, Kasper FK, Qin Y-X, et al. Two- dimensional nanostructure-reinforced biodegradable polymeric nanocomposites for bone tissue engineering. Biomacromolecules 2013;14:900–9.
[34] Lalwani G, Henslee AM, Farshid B, Parmar P, Lin L, Qin YX, et al. Tungsten disulfide nanotubes reinforced biodegradable polymers for bone tissue engineering. Acta Biomater 2013;9:8365–73.

[35] Sitharaman B, Shi X, Tran LA, Spicer PP, Rusakova I, Wilson LJ, et al. Injectable in situ cross-linkable nanocomposites of biodegradable polymers and carbon nanostructures for bone tissue engineering. J Biomater Sci Polym Ed 2007;18:655–71.
[36] Sai Pavan G, Lalwani G, Arunachalam KD. Synthesis and comparative effect of iron nanoparticles on the antibacterial activity of antibiotics on pathogenic strains of microorganisms. Int J Mater Sci (IJoMS) 2009;4:541–8.
[37] Li Q, Mahendra S, Lyon DY, Brunet L, Liga MV, Li D, et al. Antimicrobial nanomaterials for water disinfection and microbial control: potential applications and implications. Water Res 2008;42:4591–602.
[38] Stephan MT, Irvine DJ. Enhancing cell therapies from the outside in: cell surface engineering using synthetic nanomaterials. Nano Today 2011;6:309–25.
[39] Chen A, Chatterjee S. Nanomaterials based electrochemical sensors for biomedical applications. Chem Soc Rev 2013;42:5425–38.
[40] DeDora DJ, Goenka S, Surhland C, Mullick Chowdhury S, Lalwani G, Mujica-Parodi LR, et al. Sulfobutyl ether β-cyclodextrin (Captisol®) and methyl β-cyclodextrin enhance and stabilize fluorescence of aqueous indocyanine green. J Biomed Mater Res Part B 2015. http://dx.doi.org/10.1002/jbm.b.33496 [Early View Online].
[41] Tang Y-R, Lin D-W, Gao Y, Xu J, Guo B-H. Prominent nucleating effect of finely dispersed hydroxyl-functional hexagonal boron nitride on biodegradable poly (butylene succinate). Ind Eng Chem Res 2014;53(12):4689–96.
[42] Middleton JC, Tipton AJ. Synthetic biodegradable polymers as orthopedic devices. Biomaterials 2000;21:2335–46.
[43] Gogolewski S, Gorna K. Biodegradable polyurethane cancellous bone graft substitutes in the treatment of iliac crest defects. J Biomed Mater Res Part A 2007;80:94–101.
[44] Shi X, Mikos AG. Poly (propylene fumarate). Boca Raton, FL: CRC Press; 2006.
[45] Shin H, Quinten Ruhe P, Mikos AG, Jansen JA. In vivo bone and soft tissue response to injectable, biodegradable oligo (poly (ethylene glycol) fumarate) hydrogels. Biomaterials 2003;24:3201–11.
[46] Jose MV, Thomas V, Johnson KT, Dean DR, Nyairo E. Aligned PLGA/HA nanofibrous nanocomposite scaffolds for bone tissue engineering. Acta Biomater 2009;5:305–15.
[47] Saito N, Okada T, Horiuchi H, Murakami N, Takahashi J, Nawata M, et al. Biodegradable poly-D,L-lactic acid-polyethylene glycol block copolymers as a BMP delivery system for inducing bone. J Bone Jt Surg 2001;83:S92–8.
[48] Kasper FK, Tanahashi K, Fisher JP, Mikos AG. Synthesis of poly (propylene fumarate). Nat Protoc 2009;4:518–25.
[49] Rezwan K, Chen Q, Blaker J, Boccaccini AR. Biodegradable and bioactive porous polymer/inorganic composite scaffolds for bone tissue engineering. Biomaterials 2006;27:3413–31.
[50] Friedrich K, Fakirov S, Zhang Z. Polymer composites: from nano- to macro-scale. Springer Science & Business Media; 2005.
[51] Goenka S, Sant V, Sant S. Graphene-based nanomaterials for drug delivery and tissue engineering. Control Release Off J Control Release Soc 2014;173:75–88.
[52] Harrison BS, Atala A. Carbon nanotube applications for tissue engineering. Biomaterials 2007;28:344–53.
[53] Kalita SJ, Bhardwaj A, Bhatt HA. Nanocrystalline calcium phosphate ceramics in biomedical engineering. Mater Sci Eng C 2007;27:441–9.
[54] Jayakumar R, Menon D, Manzoor K, Nair S, Tamura H. Biomedical applications of chitin and chitosan based nanomaterials—a short review. Carbohydr Polym 2010;82:227–32.
[55] Dykman L, Khlebtsov N. Gold nanoparticles in biomedical applications: recent advances and perspectives. Chem Soc Rev 2012;41:2256–82.

[56] Lalwani G, Talukdar Y, Rashkow J, Sitharaman B. Micro- and nanotechnologies to engineer bone regeneration. Micro Nanotechnol Eng Stem Cells Tissues 2013:220–35.
[57] Lalwani G, Sitharaman B. Carbon nanotechnology in regenerative medicine. World Scientific Press; 2012.
[58] Kalantar-zadeh K, Ou JZ, Daeneke T, Strano MS, Pumera M, Gras SL. Two-dimensional transition metal dichalcogenides in biosystems. Adv Funct Mater 2015;25(32):5086–99.
[59] Saotome T, Kokubo K, Shirakawa S, Oshima T, Hahn HT. Polymer nanocomposites reinforced with C60 fullerene: effect of hydroxylation. J Compos Mater 2011;45(25): 2595–601. http://dx.doi.org/10.1177/0021998311416682.
[60] Ginzburg B, Pozdnyakov A, Tochil'Nikov D, Tuichiev S, Shepelevskii A. Tribological characteristics of composites based on poly (tetrafluoroethylene) and fullerene carbon. Polym Sci Ser A 2008;50:865–73.
[61] Kubota S, Johkura K, Asanuma K, Okouchi Y, Ogiwara N, Sasaki K, et al. Titanium oxide nanotubes for bone regeneration. J Mater Sci Mater Med 2004;15:1031–5.
[62] Wan Y, Chang P, Yang Z, Xiong G, Liu P, Luo H. Constructing a novel three-dimensional scaffold with mesoporous TiO_2 nanotubes for potential bone tissue engineering. J Mater Chem B 2015;3:5595–602.
[63] Yamazaki S, Maeda H, Obata A, Inukai K, Kato K, Kasuga T. Aluminum silicate nanotube coating of siloxane-poly (lactic acid)-vaterite composite fibermats for bone regeneration. J Nanomater 2012;2012:5.
[64] Lahiri D, Rouzaud F, Richard T, Keshri AK, Bakshi SR, Kos L, et al. Boron nitride nanotube reinforced polylactide-polycaprolactone copolymer composite: mechanical properties and cytocompatibility with osteoblasts and macrophages in vitro. Acta Biomater 2010;6:3524–33.
[65] Nasri-Nasrabadi B, Mehrasa M, Rafienia M, Bonakdar S, Behzad T, Gavanji S. Porous starch/cellulose nanofibers composite prepared by salt leaching technique for tissue engineering. Carbohydr Polym 2014;108:232–8.
[66] Wang T, Drzal LT. Cellulose-nanofiber-reinforced poly(lactic acid) composites prepared by a water-based approach. ACS Appl Mater Interfaces 2012;4:5079–85.
[67] Reddy CS, Zak A, Zussman E. WS_2 nanotubes embedded in PMMA nanofibers as energy absorptive material. J Mater Chem 2011;21:16086–93.
[68] Zhang H. Effects of electrospinning parameters on morphology and diameter of electrospun PLGA/MWNTs fibers and cytocompatibility in vitro. J Bioact Compat Polym 2011;26:590–606.
[69] Mallakpour S, Madani M. Effect of functionalized TiO_2 on mechanical, thermal and swelling properties of chitosan-based nanocomposite films. Polym Plast Technol Eng 2015;54(10):1035–42.
[70] Chen X, Chen X, Lin M, Zhong W, Chen X, Chen Z. Functionalized multi-walled carbon nanotubes prepared by in situ polycondensation of polyurethane. Macromol Chem Phys 2007;208:964–72.
[71] Shi X, Hudson JL, Spicer PP, Tour JM, Krishnamoorti R, Mikos AG. Injectable nanocomposites of single-walled carbon nanotubes and biodegradable polymers for bone tissue engineering. Biomacromolecules 2006;7:2237–42.
[72] Zhang H. Electrospun poly (lactic-co-glycolic acid)/multiwalled carbon nanotubes composite scaffolds for guided bone tissue regeneration. J Bioact Compat Polym 2011;26:347–62.
[73] Chen L, Hu J, Shen X, Tong H. Synthesis and characterization of chitosan-multiwalled carbon nanotubes/hydroxyapatite nanocomposites for bone tissue engineering. J Mater Sci Mater Med 2013;24:1843–51.

[74] Zawadzak E, Bil M, Ryszkowska J, Nazhat SN, Cho J, Bretcanu O, et al. Polyurethane foams electrophoretically coated with carbon nanotubes for tissue engineering scaffolds. Biomed Mater 2009;4:015008.
[75] Hernandez E, Goze C, Bernier P, Rubio A. Elastic properties of C and $B_xC_yN_z$ composite nanotubes. Phys Rev Lett 1998;80:4502.
[76] Chang C-W, Han W-Q, Zettl A. Thermal conductivity of B-C-N and BN nanotubes. J Vac Sci Technol B Microelectron Nanom Struct 2005;23:1883.
[77] Chen X, Wu P, Rousseas M, Okawa D, Gartner Z, Zettl A, et al. Boron nitride nanotubes are noncytotoxic and can be functionalized for interaction with proteins and cells. J Am Chem Soc 2009;131:890–1.
[78] Zhi C, Bando Y, Tang C, Honda S, Kuwahara H, Golberg D. Boron nitride nanotubes/polystyrene composites. J Mater Res 2006;21:2794–800.
[79] Zhi C, Bando Y, Terao T, Tang C, Kuwahara H, Golberg D. Towards thermoconductive, electrically insulating polymeric composites with boron nitride nanotubes as fillers. Adv Funct Mater 2009;19:1857–62.
[80] Zhi C, Bando Y, Tang C, Golberg D. Immobilization of proteins on boron nitride nanotubes. J Am Chem Soc 2005;127:17144–5.
[81] Rui Q, Komori K, Tian Y, Liu H, Luo Y, Sakai Y. Electrochemical biosensor for the detection of H_2O_2 from living cancer cells based on ZnO nanosheets. Anal Chim Acta 2010;670:57–62.
[82] Guo Y, Li J, Dong S. Hemin functionalized graphene nanosheets-based dual biosensor platforms for hydrogen peroxide and glucose. Sens Actuators B Chem 2011;160:295–300.
[83] Zhang Y, Chen X, Yang W. Direct electrochemistry and electrocatalysis of myoglobin immobilized in zirconium phosphate nanosheets film. Sens Actuators B Chem 2008;130:682–8.
[84] Talukdar Y, Rashkow JT, Lalwani G, Kanakia S, Sitharaman B. The effects of graphene nanostructures on mesenchymal stem cells. Biomaterials 2014;35:4863–77.
[85] Zhang M, Bai L, Shang W, Xie W, Ma H, Fu Y, et al. Facile synthesis of water-soluble, highly fluorescent graphene quantum dots as a robust biological label for stem cells. J Mater Chem 2012;22:7461–7.
[86] Shuai C, Feng P, Gao C, Shuai X, Xiao T, Peng S. Graphene oxide reinforced poly (vinyl alcohol): nanocomposite scaffolds for tissue engineering applications. RSC Adv 2015;5:25416–23.
[87] Cheng HKF, Sahoo NG, Tan YP, Pan Y, Bao H, Li L, et al. Poly (vinyl alcohol) nanocomposites filled with poly (vinyl alcohol)-grafted graphene oxide. ACS Appl Mater Interfaces 2012;4:2387–94.
[88] Prasad KE, Das B, Maitra U, Ramamurty U, Rao CN. Extraordinary synergy in the mechanical properties of polymer matrix composites reinforced with 2 nanocarbons. Proc Natl Acad Sci USA 2009;106:13186–9.
[89] Sayyar S, Murray E, Thompson BC, Gambhir S, Officer DL, Wallace GG. Covalently linked biocompatible graphene/polycaprolactone composites for tissue engineering. Carbon 2013;52:296–304.
[90] Fan H, Wang L, Zhao K, Li N, Shi Z, Ge Z, et al. Fabrication, mechanical properties, and biocompatibility of graphene-reinforced chitosan composites. Biomacromolecules 2010;11:2345–51.
[91] Wang X, Pakdel A, Zhang J, Weng Q, Zhai T, Zhi C, et al. Large-surface-area BN nanosheets and their utilization in polymeric composites with improved thermal and dielectric properties. Nanoscale Res Lett 2012;7:662.

[92] Kim SK, Wie JJ, Mahmood Q, Park HS. Anomalous nanoinclusion effects of 2D MoS_2 and WS_2 nanosheets on the mechanical stiffness of polymer nanocomposites. Nanoscale 2014;6:7430–5.
[93] Lee D, Song SH, Hwang J, Jin SH, Park KH, Kim BH, et al. Enhanced mechanical properties of epoxy nanocomposites by mixing noncovalently functionalized boron nitride nanoflakes. Small 2013;9:2602–10.
[94] Rafiee MA, Rafiee J, Wang Z, Song H, Yu Z-Z, Koratkar N. Enhanced mechanical properties of nanocomposites at low graphene content. ACS Nano 2009;3:3884–90.
[95] Rafiee MA, Lu W, Thomas AV, Zandiatashbar A, Rafiee J, Tour JM, et al. Graphene nanoribbon composites. ACS Nano 2010;4:7415–20.
[96] Yu J, Huang X, Wu C, Wu X, Wang G, Jiang P. Interfacial modification of boron nitride nanoplatelets for epoxy composites with improved thermal properties. Polymer 2012;53:471–80.
[97] Wang B, Yang D, Zhang JZ, Xi C, Hu J. Stimuli-responsive polymer covalent functionalization of graphene oxide by Ce (IV)-induced redox polymerization. J Phys Chem C 2011;115:24636–41.
[98] Avila-Vega YI, Leyva-Porras CC, Mireles M, Quevedo-López M, Macossay J, Bonilla-Cruz J. Nitroxide-functionalized graphene oxide from graphite oxide. Carbon 2013;63:376–89.
[99] Lordi V, Yao N. Molecular mechanics of binding in carbon-nanotube–polymer composites. J Mater Res 2000;15:2770–9.
[100] Chakoli AN, Wan J, Feng JT, Amirian M, Sui JH, Cai W. Functionalization of multiwalled carbon nanotubes for reinforcing of poly (L-lactide-co-ε-caprolactone) biodegradable copolymers. Appl Surf Sci 2009;256:170–7.
[101] Zhi C, Bando Y, Tang C, Huang Q, Golberg D. Boron nitride nanotubes: functionalization and composites. J Mater Chem 2008;18:3900–8.
[102] Kimura T, Ago H, Tobita M, Ohshima S, Kyotani M, Yumura M. Polymer composites of carbon nanotubes aligned by a magnetic field. Adv Mater 2002;14:1380–3.
[103] Xie X-L, Mai Y-W, Zhou X-P. Dispersion and alignment of carbon nanotubes in polymer matrix: a review. Mater Sci Eng R Rep 2005;49:89–112.
[104] Shi X, Sitharaman B, Pham QP, Spicer PP, Hudson JL, Wilson LJ, et al. In vitro cytotoxicity of single-walled carbon nanotube/biodegradable polymer nanocomposites. J Biomed Mater Res Part A 2008;86:813–23.
[105] Shi X, Sitharaman B, Pham QP, Liang F, Wu K, Billups WE, et al. Fabrication of porous ultra-short single-walled carbon nanotube nanocomposite scaffolds for bone tissue engineering. Biomaterials 2007;28:4078–90.
[106] Pinto AM, Moreira S, Gonçalves IC, Gama FM, Mendes AM, Magalhães FD. Biocompatibility of poly (lactic acid) with incorporated graphene-based materials. Colloids Surf B Biointerfaces 2013;104:229–38.
[107] Adhikari AR, Rusakova I, Haleh A, Luisi J, Panova NI, Laezza F, et al. Thermal property and assessment of biocompatibility of poly (lactic-co-glycolic) acid/graphene nanocomposites. J Appl Phys 2014;115:054701.
[108] Chung EJ, Sugimoto MJ, Ameer GA. The role of hydroxyapatite in citric acid-based nanocomposites: surface characteristics, degradation, and osteogenicity in vitro. Acta Biomater 2011;7:4057–63.
[109] Tayton E, Purcell M, Aarvold A, Smith J, Briscoe A, Kanczler J, et al. A comparison of polymer and polymer–hydroxyapatite composite tissue engineered scaffolds for use in bone regeneration. An in vitro and in vivo study. J Biomed Mater Res Part A 2014;102:2613–24.

[110] Kim K, Dean D, Lu A, Mikos AG, Fisher JP. Early osteogenic signal expression of rat bone marrow stromal cells is influenced by both hydroxyapatite nanoparticle content and initial cell seeding density in biodegradable nanocomposite scaffolds. Acta Biomater 2011;7:1249–64.

[111] Sitharaman B, Van Der Zande M, Ananta JS, Shi X, Veltien A, Walboomers XF, et al. Magnetic resonance imaging studies on gadonanotube-reinforced biodegradable polymer nanocomposites. J Biomed Mater Res Part A 2010;93:1454–62.

[112] Farshid B, Lalwani G, Shir Mohammadi M, Simonsen J, Sitharaman B. Boron nitride nanotubes and nanoplatelets as reinforcing agents of polymeric matrices for bone tissue engineering. J Biomed Mater Res Part B Appl Biomater 2015. http://dx.doi.org/10.1002/jbm.b.33565 [Early View Online].

[113] Sitharaman B, Shi X, Walboomers XF, Liao H, Cuijpers V, Wilson LJ, et al. In vivo biocompatibility of ultra-short single-walled carbon nanotube/biodegradable polymer nanocomposites for bone tissue engineering. Bone 2008;43:362–70.

[114] Kim SS, Ahn KM, Park MS, Lee JH, Choi CY, Kim BS. A poly (lactide-co-glycolide)/hydroxyapatite composite scaffold with enhanced osteoconductivity. J Biomed Mater Res Part A 2007;80:206–15.

[115] Tayton E, Purcell M, Smith JO, Lanham S, Howdle SM, Shakesheff KM, et al. The scale-up of a tissue engineered porous hydroxyapatite polymer composite scaffold for use in bone repair: an ovine femoral condyle defect study. J Biomed Mater Res Part A 2015;103:1346–56.

[116] Mistry AS, Pham QP, Schouten C, Yeh T, Christenson EM, Mikos AG, et al. In vivo bone biocompatibility and degradation of porous fumarate-based polymer/alumoxane nanocomposites for bone tissue engineering. J Biomed Mater Res Part A 2010;92:451–62.

[117] Henslee A, Spicer P, Yoon D, Nair M, Meretoja V, Witherel K, et al. Biodegradable composite scaffolds incorporating an intramedullary rod and delivering bone morphogenetic protein-2 for stabilization and bone regeneration in segmental long bone defects. Acta Biomater 2011;7:3627–37.

Effects of surface modification on polymeric biocomposites for orthopedic applications

3

A.J. Harmata, S.A. Guelcher
Vanderbilt University, Nashville, TN, United States

3.1 Introduction

Often the goal in the development of a composite for any application is to combine the bulk properties of various phased components into a cohesive, uniform structure. It is not surprising then that the interface between two phases within the composite, frequently a liquid and a solid, is a vital relationship that has numerous downstream effects. The surfaces of the individual components can be altered and tailored in numerous ways, before combining them in a composite form, to achieve desired properties of the individual components within the composite or the resultant composite structure as a whole.

This chapter will focus on fundamental concepts related to surface modification of materials utilized within polymeric biocomposites for orthopedic applications. For this chapter, orthopedic applications are defined as medical indications or procedures that benefit from utilization of polymeric biocomposites and/or additional implanted therapeutic material to aid in bone regeneration at a localized site. The term surface modification refers to the physical attachment of molecules, predominantly silanes and/or polymers, to the surface of a solid-phase material. Polymeric biocomposites are a class of biomaterials that comprises a biocompatible bulk polymer and a particulated solid phase, often referred to as a binder and a filler, respectively. As there are vast combinations of polymers and solid materials that fit this definition, this chapter highlights solely those combinations that have been utilized for orthopedic applications, in either the academic or the medical industry settings.

This chapter will not discuss surface modification methods used throughout orthopedic applications not related to polymeric biocomposites. These methods focus on improving the interaction between bulk materials, such as metal implants, and the body through modification of the implant surface. Although this is an important field of study, the effects of these forms of surface modification are not applicable to polymeric biocomposites.

The chapter outline is as follows. The first section provides a general overview of related orthopedic applications as well as the state of materials currently utilized in clinical settings related to these applications. This background information is followed by common approaches and methods for modifying the surface solid-phase materials in the orthopedic field. Next, an overview of the materials including the types of polymers and solid fillers used within polymeric biocomposites for orthopedic applications is given, as well as fabrication methods. Afterward, the effects of surface

Nanocomposites for Musculoskeletal Tissue Regeneration. http://dx.doi.org/10.1016/B978-1-78242-452-9.00003-0

modification on the innate properties of common solid fillers used in orthopedic biomaterials will be discussed with specific focus on their surface properties. Finally, the effects of incorporating surface-modified solid fillers into polymeric biocomposites on the properties of the overall resultant biocomposite are considered. The last sections are dedicated to future trends and sources of additional information on the field of surface modification on polymeric biocomposites for orthopedic applications.

3.2 Orthopedic applications

When a bone fracture occurs, the normal physiological response includes a spontaneous sequence of events to restore function: inflammation, soft callus formation, hard callus formation, and lastly bone remodeling (Khan et al., 2008). If this natural process does not occur, surgical intervention is often warranted. In particular, large bone defects present a significant challenge to reconstructive surgery and often require aid through internal fixation (utilizing bone screws and metal plates) and bone grafting (from either autologous, cadaver, or synthetic sources). Orthopedic conditions that utilize external materials, such as natural or synthetic bone grafts to aid in fracture healing, include screw augmentation (Amendola et al., 2011; Larsson et al., 2012; Larsson and Procter, 2011), open tibial plateau fractures (Russell and Leighton, 2008; Simpson and Keating, 2004), and vertebroplasty (Verlaan et al., 2006). Fig. 3.1 displays X-ray and schematic representative images of these respective procedures. In each image, the white opaque portions of the bone are locations at which external materials were injected into the bone fracture site. In the United States, incidence of osteoporotic

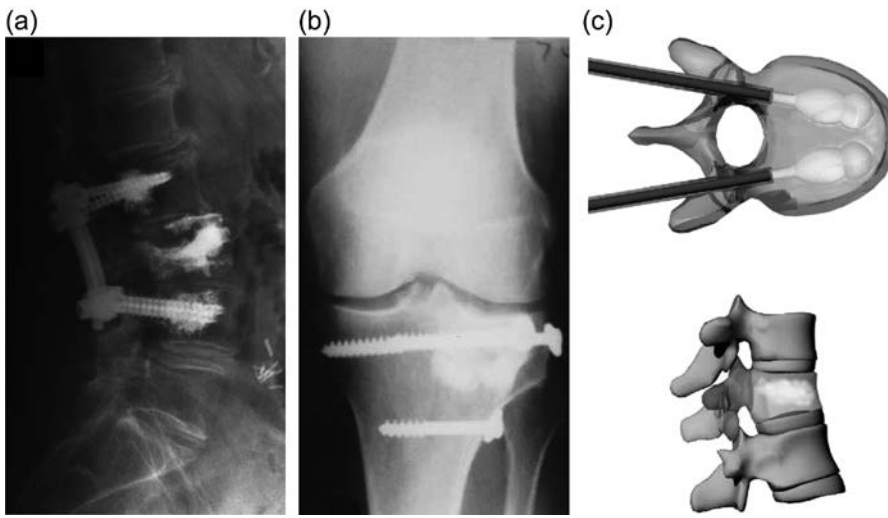

Figure 3.1 Images of orthopedic procedures that currently utilize, or may benefit from use of, polymeric biocomposites. (a) Screw augmentation, (b) tibial plateau fracture, and (c) vertebroplasty.

vertebral fractures is estimated to be at least 700,000 per year (Verlaan et al., 2006). In 2006, there were over 1.6 million bone-graft procedures conducted (US Census Bureau, 2008). Due to a rapidly expanding elderly population, this number is expected to double in the next 25 years (Johnson and Herschler, 2011).

Autologous bone graft is the gold standard for most applications of bone fracture, but it is also associated with numerous complications, including supply limitations, donor site morbidity, loss of function, and limited ability to bear mechanical loads (Damien and Parsons, 1991). One alternative to autograft is allograft, in which tissue is obtained from a cadaver. This source also has associated complications, including risk of disease transmission (Centers for Disease Control and Prevention, 2001, 2002). Attractive alternatives to autograft and allograft include various synthetic graft substitutes that attempt to mimic the physical and mechanical nature of native bone by meeting three desired criteria for bone grafts: osteoconductivity, osteogenicity, and osteoinductivity (El-Amin et al., 2006). Synthetic substitutes have been fabricated from a variety of materials, including polymers, ceramics, and combinations in the form of composites. The ideal bone-graft substitute would be a material that is biocompatible, readily available, easily deliverable to the defect, structurally stable to prevent articular subsidence, and able to remodel to normal bone over time (Greenwald et al., 2001; Johnson and Herschler, 2011).

Since the 1980s, bioceramics have been widely utilized in clinical settings as synthetic bone-graft replacements (Bohner, 2000). Calcium phosphate cements (CPCs), such as commercially available PRO-DENSE® (Wright Medical), have recently proven superior to autografts in tibial plateau fractures. This claim is supported by a retrospective study reporting that 61% of patients treated with buttress plating and autograft experienced loss of reduction after 1 year, compared to 23% of patients treated with a hydroxyapatite (HA) bone cement (Simpson and Keating, 2004). However, the brittleness and low shear strength of CPCs, as well as their slow remodeling, can result in prolonged recovery times, joint stiffness, and increased cost to society, consequently limiting these materials' use in weight-bearing applications (Hall et al., 2009; Johnson and Herschler, 2011; Bohner, 2010). Other CPCs include Norian® SRS® (Synthes), HydroSet (Stryker), and Beta-bsm® (ETEX). Besides CPCs, there has been a recent trend toward the use of highly resorbable bone substitutes. These substitutes include β-tricalcium phosphate (β-TCP) and brushite, which are resorbed by cells and simple dissolution, respectively (Bohner, 2010). Caution is required when designing a bone-graft substitute based on these fillers, as these materials resorb more rapidly than bone can often grow in, which can cause fibrous tissue to fill the defect (Urban et al., 2003).

Polymer-based tissue engineering is a promising approach for meeting the shortcomings of autografts, allografts, and CPCs, in the orthopedic field. Various properties of polymeric materials (including mechanical properties, degradation rate, and microstructure) can be altered over a wide range through variations in composition and structure to meet the needs of a specific application. Originally, both natural and synthetic polymers were often designed to replace heavy metal parts of endoprostheses. Although this disruption did not take in the market, future polymers were designed for biodegradable applications. In general, polymer-based scaffolds and

composites aim to mimic native bone properties at initial implantation as well as at later time points as the body slowly incorporates them. Additionally, the combination of ceramics with polymers in a biocomposite form has been suggested as an alternative approach to designing synthetic bone-graft materials with tougher mechanical properties, improved biological behavior, and modified degradation mechanisms.

3.3 Surface modifications of solid fillers

3.3.1 Silane chemistry

One of the most prominent surface-modification techniques applied to particulated materials (typically with an inorganic composition) within polymer biocomposites is the attachment of organofunctional silanes, which are silicon-based chemicals that contain both organic and inorganic reactivity in the same molecule. Monomeric silicon chemicals (silanes) that contain at least one silicon–carbon bond (Si—C) structure are known as an organosilanes (Khan et al., 2011). The general structure of an organosilane, $R_nSiX_{(4-n)}$, has two classes of functionality, in which X is a hydrolyzable group (typically halogen, alkoxy, acyloxy, or amine), and R is a nonhydrolyzable organic radical that typically possesses the functionality with the exposed desired characteristics (such as a methoxyl or ethoxyl group), with $n=1$ typically (Arkles, 1977). Commonly utilized silanes have one organic substituent.

The attachment of these molecules occurs through four generalized steps, as shown in Fig. 3.2. First (a), hydrolysis of the labile groups occurs, followed by (b) condensation to oligomers. Next (c), oligomers hydrogen-bond to exposed hydroxyl groups on the solid surface. Lastly (d), a covalent linkage is formed between the silicon and filler particle, with the loss of water during curing and drying steps (Arkles, 1977). Subsequently, there is usually one bond from each organosilane silicon to the surface, with the two remaining silanol groups present in the condensed (to other silanols to form siloxane linkages) or free form. Theoretically, a monolayer is sufficient to provide the desired result. However, due to the reactive nature and mechanism of silane molecules, multilayer silane coverage can be attained. To ensure uniform coverage,

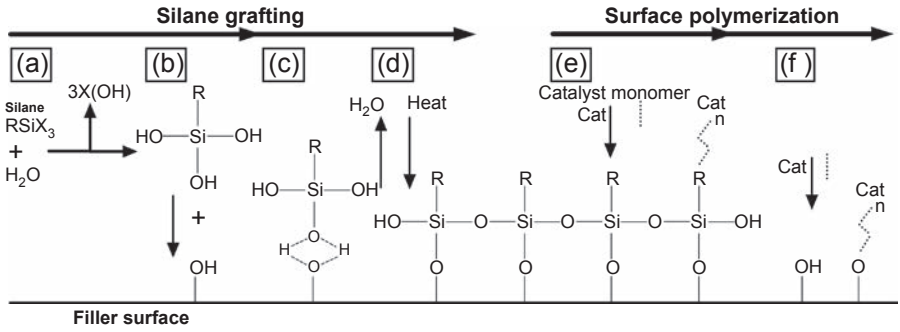

Figure 3.2 Schematics of common surface modification techniques: silane coupling agent grafting and surface polymerization. *R*, reactive species.

often more than one layer is applied to portions (if not all) of the desired surface. The end result is a siloxane polymeric network close to the inorganic surface typically <5 nm thick.

3.3.1.1 Silane grafting methods

Typically, the attachment of silanes (referred to as silanization) to an inorganic surface is done in a polar solution containing water, alcohol (ethanol or methanol (Sousa et al., 2003; Santos et al., 2002)), acetone (Deb et al., 2005), or a combination thereof (Khan et al., 2011; Deb et al., 2005) under dynamic mixing. The ability to silanize surfaces from a non-polar solution containing *n*-propylamine has also been verified (Santos et al., 2002). The hydrolysis reaction rate within the silane-grafting scheme is dependent on the pH of the solution. Certain silanes undergo acid-catalyzed hydrolysis, whereas others are base or neutral-catalyzed (aminosilanes). As the pH of the solution changes, so does the hydrolysis rate. The condensation reaction is also dependent on the pH, and often the ideal pH to catalyze hydrolysis is not the same ideal pH to catalyze the following condensation reaction. Thus, a pH balance must be obtained to optimize the silane attachment. Acidic conditions pH ≃ 4.5 are created by a variety of acids, such as acetic (Sousa et al., 2003) or trifluoroacetic acid (Koleganova et al., 2006).

The hydrolysis and condensation reaction rates determine the time required for incubation in solution. Methods have cited incubation times anywhere from 15 min (Dupraz et al., 1996; Khan et al., 2011) to 4 h (Koleganova et al., 2006). Inducing an increase in pH from acid to basic conditions to induce the condensation reaction and thus the formation of siloxanols (Dupraz et al., 1996) has also been reported. Silanization is typically conducted at room temperature and atmospheric pressure. In addition to the common incubation technique, some have shown the ability to attach silane molecules through a water/methanol spraying method. It was reported that the method of silanization had little effect on the final properties of the silane layer (Sousa et al., 2003). The last step of silanization involves drying and curing the modified inorganic phase, typically at 60 to 120°C in air for 1 h to 2 days, to strengthen polysiloxane network structures (Koleganova et al., 2006; Dupraz et al., 1996).

3.3.1.2 Resultant silane properties

The result of silane surface modification is dependent on the chemical composition of the end group of the silane and the interacting organic phase, as well as their relative chemical compatibility. Potential results include a change in wetting and adhesion characteristics of the solid, as well as the ability to catalyze chemical transformations at a heterogeneous interface. Subsequently, this surface modification technique is applied to a variety of polymer composite systems, motivated by a variety of purposes. There are various applications of silane grafting within a polymer composite system, such as a coupling or dispersal agent, as well as an adhesion promoter or water repellent, or a combination thereof. Surface modification by a silane is often used as a coupling agent between two components linked by the silane molecule, such as organic and inorganics. Within polymer biocomposites, any molecule that enhances adhesion with the polymer phase is technically a coupling agent, but ideally these agents form

a covalent bond between an inorganic (usually the solid phase) and organic (polymer) compound through an intermediary silane (Arkles, 1977). Although, theoretically, the covalent coupling is achieved by matching the reactivity of a (thermoset) polymer with that of the silane, this is difficult to accomplish due to the presence of functional groups that can react with unintended species present in the system.

Additionally, silane coverage provides a method for controlling the surface energy (wetting) of a substrate, and thus can be described as an adhesion promoter. By altering the critical surface tension of a solid, liquids with a surface tension below this critical value will wet the surface, whereas those above will not (Arkles, 1977). In the chapter section entitled *Effects of modifying surface on filler properties*, the relationship between wetting and adhesion is explained in more detail. In polymer biocomposite systems, it is often desired to allow the uncured polymer binder to wet the solid-phase component. The hydrophobicity of the organic group from the silanes will be imparted to the polymer phase. This interaction is leveraged to increase the dispersion of particles within a polymer or to make a polymer more free flowing for injectable systems, thus decreasing its apparent viscosity (Hashimoto et al., 2006). Additionally, organosilanes are frequently used to repel water from a surface or within a composite system. This has been shown through the decreased water uptake of composites made with silanized-HA, compared to those made with unmodified HA (Santos et al., 2002).

Silane molecules are often required for the covalent attachment of additional molecules to the surface of inorganic components. After silanization, various molecules can be chemically bound to the inorganic surface depending on the functional end-group of the silane-coupling agent. These molecules include enzymes immobilized on the surface, but more often are synthetic polymer chains.

3.3.2 Surface-polymerized polymer modification

Polymer attachment can be achieved by the "grafting-to" or "grafting-from" methods. Grafting-to occurs when a polymer is first synthesized and then attached, whereas grafting-from occurs when a polymer is grown from an active surface site through in situ polymerization (Mosse et al., 2009). There are benefits and drawbacks to both methods. The polymer attached in the grafting-to method must have an appropriate anchor sequence that will preferentially attach compared to the rest of the polymer. In contrast, surface-polymerized polymers created by the grafting-from method are not constrained by delivering the polymer to the surface or by the sequence of the polymer. This is because the density of the attached polymer is controlled by the density of initiation sites, often attached silane molecules. Attaching polymer chains to the surface removes the exposed reactive end-group, whether inherently present or via an attached silane, while still altering the surface properties of the inorganic solid.

The most common polymer family to be attached to solid inorganic materials is aliphatic polyesters, such as poly(ε-caprolactone) (PCL). PCL is a thermoplastic, bioresorbable (via hydrolysis), and semicrystalline polymer that is synthesized by the ring-opening polymerization (ROP) of ε-caprolactone monomer (Khan et al., 2010). As depicted in Fig. 3.2(e), this in situ polymerization scheme can be catalyzed by tin(II) 2-ethylhexanoate ($Sn(Oct)_2$) or boron trifluoride dimethyl etherate ($BF_3O(CH_3)_2$)

at 120°C (Khan et al., 2010; Jiang et al., 2005b). A silane-coupling agent is used to polymerize the ε-caprolactone monomer from inorganic solids. The molecular weight of both the surface-polymerized and the bulk PCL is dependent on the polymerization time. Depending on the reaction scheme, a continuous PCL phase can be formed surrounding the inorganic solid of interest. However, the PCL chains remain covalently bound to the surface of silane-modified inorganic solids after solvent dilution of the surrounding continuous PCL phase, as supported by X-ray photoelectron spectroscopy (XPS) analysis. Thus, PCL surface polymerization is a useful method for modifying inorganic solids (Jiang et al., 2005a,b). Furthermore, the molecular weight of the attached PCL chains can be altered by varying the polymerization time (Harmata et al., 2014).

In a similar fashion, others have shown the ability to graft oligo(lactone)s to an inorganic surface without a silane-coupling agent, as depicted in Fig. 3.2(f). This was demonstrated through protonation of a tricalcium phosphate (TCP) surface in an aqueous solution of phosphoric acid, followed by the in situ surface polymerization of lactones, such as PCL or L-lactide (Kunze et al., 2003). In this surface-modification method, surface-polymerized chains were directly attached to exposed hydroxyl reactive groups inherent on the TCP surface.

Other families of polymers are capable of being attached to inorganic phases via silane coupling agents. Polyethylene (PE) was grafted to silanized-HA particles via acrylic acid (Wang and Bonfield, 2001). Although polyethylene is a nonpolar, hydrophobic polymer, it is an effective surface-modification approach for HA in high-density polyethylene (HDPE)-based biocomposites. Separately, nano-apatite (Nap) particles have been modified with an absorbed poly(acrylic acid) (PAA) coupling agent in polyethylene glycol/poly(butylene terephthalate) (PEG/PBT) block copolymer composites (Liu et al., 1997).

3.4 Polymeric biocomposites

Due to their tunable degradability, biocompatibility, processibility, and versatility, polymeric biocomposites are principal materials investigated for the development of synthetic bone scaffolds, cements, and composites (Porter et al., 2009). As previously defined, a polymeric biocomposite is composed of two or more bulk biomaterials (at least one a polymer) of different phases intended for use in the body. There are an unfathomable number of biocomposites that fit this broad criterion. Classic polymeric biocomposites for orthopedic applications are composed of a solid, synthetic ceramic phase that is osteoconductive or -inductive (Sepulveda et al., 2002) and a biocompatible polymer that was at one stage a liquid.

An ideal polymeric biocomposite both initially mimics the properties of the native bone tissue it is intended to replace and also remodels to form new bone. Consequently, choosing the appropriate individual components within a biocomposite, and the manner in which they are combined, is critical. The individual components must be biocompatible, biodegradable, and mechanically robust. The ideal polymeric biocomposite must be fabricated in a manner that allows

it to be safely implanted into the intended defect site and subsequently promote bone remodeling or regeneration. The solid phase is typically one of the following calcium phosphate ceramics: bioactive glass (BG) (Khan et al., 2010, 2011; Koleganova et al., 2006; Jiang et al., 2005a,b; Harmata et al., 2014), HA (Sousa et al., 2003; Santos et al., 2002; Deb et al., 2005; Dupraz et al., 1996; Wang and Bonfield, 2001; Liu et al., 1997, 1998a,b), or biphasic calcium phosphate or TCP (Kunze et al., 2003). These solid-phase fillers come in a variety of shapes and sizes, including macro- and nanorods/fibers (Khan et al., 2010, 2011; Jiang et al., 2005a,b) and particles/powders (Koleganova et al., 2006; Sousa et al., 2003; Santos et al., 2002; Deb et al., 2005; Dupraz et al., 1996; Wang and Bonfield, 2001; Liu et al., 1997, 1998a,b; Kunze et al., 2003; Harmata et al., 2014). The biocompatible polymer phase is typically one (or a copolymer mixture) of the following: polyesters, polyethers, polyanhydrides, or polyurethanes.

Polymeric biocomposites that have utilized techniques to modify the surface of the solid phase before combination with the polymer binder narrow the field. The filler material and polymer binder combinations that fit this criterion and are highlighted in this chapter are paired in Table 3.1. In addition to the surface-modification techniques, what differentiates these biocomposites from one another are the fabrication processes used to combine the polymer and bioactive components and the polymerization of the polymer itself. A general schematic of how surface-modified polymeric

Table 3.1 Surface-modified polymeric biocomposite components

Filler material	Polymer binder
Hydroxyapatite (macro- and nanoparticles) (Dupraz et al., 1996; Garreta et al., 2006; Liu et al., 1998b,c)	Glycidyl dimethacrylate, urethane dimethacrylate, and triethylene glycol dimethacrylate (Deb et al., 1996) Polyethylene glycol and poly(butylene terephthalate) (PEG/PBT) block copolymer (Liu et al., 1997, 1998a) Bisphenol A glycidyl methacrylate (BisGMA) (Santos et al., 2002) Polyethylene (Wang and Bonfield, 2001), high-density polyethylene (HDPE) (Sousa et al., 2003)
Bioactive glass (fibers, particles)	Polyester urethane (Harmata et al., 2014) Poly(ε-caprolactone) (Jiang et al., 2005a,b) Urethane dimethacrylate and 2-hydroxyethyl methacrylate (Koleganova et al., 2006) Poly(L-lactide) (Larranaga et al., 2013; Zhang et al., 2004)
Tricalcium phosphate	Poly(L,DL-lactide) (Kunze et al., 2003)
Phosphate glass	Poly(ε-caprolactone) (Khan et al., 2010, 2011)
TiO_2	HDPE (Hashimoto et al., 2006)

biocomposites are fabricated is shown in Fig. 3.3(a). Fabrication methods utilized for surface-modified polymeric biocomposites include solvent casting, compression molding, monomer transfer molding, monomer-induced polymerization, and reactive liquid molding. The advantages and disadvantages of each of these methods are listed in Table 3.2. All fabrication techniques other than reactive liquid molding require the polymeric biocomposite to be fabricated before in vivo implantation, or "pre-fabricated." Fig. 3.3(b–e) provides cross-section scanning electron microscopy (SEM) images of biocomposites made from a variety of fabrication techniques, with silane and silane + polymer-modified fillers.

Solvent casting is a traditional and commonly utilized technique to fabricate polymer biocomposites for a variety of tissue-engineering purposes. In simplified terms, solidified polymer is dissolved in a solvent, the solid component is mixed into the polymer/solvent solution, the resulting slurry is transferred to the desired mold, and the solvent is evaporated. This method has been used to make PEG/PBT copolymer (Polyactive™ 70/30)–based biocomposites with surface-modified HA (Liu et al., 1998a) or Nap (Liu et al., 1997).

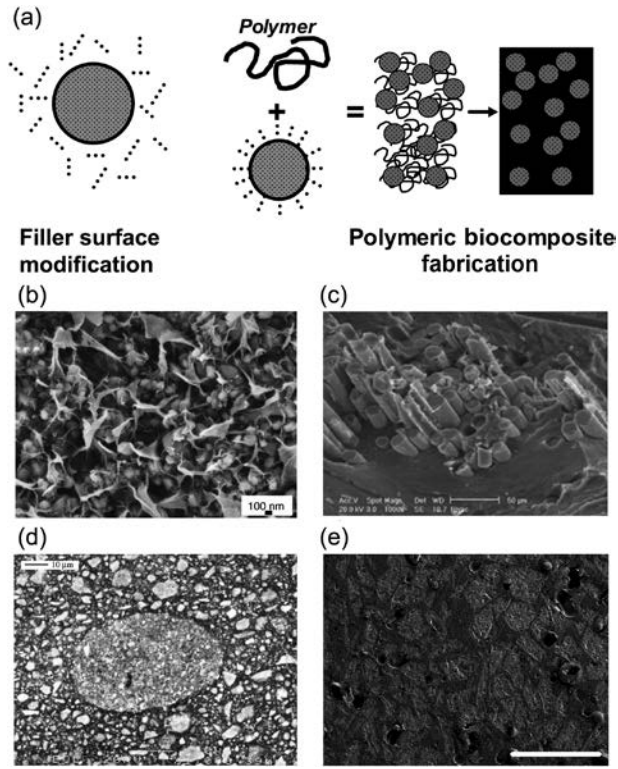

Figure 3.3 Surface-modified polymeric biocomposites. (a) Schematic of general fabrication of polymeric biocomposites. Cross-section SEM images of biocomposites made with silane modified fillers; (b) TiO_2/HDPE; (c) phosphate glass fibers/PCL; (d) modified HA/BisGMA, and silane+PCL modified fillers; (e) BG/PUR.

Table 3.2 Advantages and disadvantages of polymeric composite fabrication methods

Fabrication method	Advantage	Disadvantage	References
Solvent casting	• Exposed to low thermal and mechanical stress • Targeted molecular weight • Control porosity amount, size, and shape via particulate leaching • Alter polymer properties through additives • Typically can be dissolved and reused as raw material • Simple process	• Preformed implant, fabricated before implantation • Limited by mold shape • Must use solvent • Polymer must be soluble in volatile solvent • Residual solvent can be toxic • Often requires additional fabrication techniques, such as compression molding	Siemann (2005), Boccaccini and Blaker (2005), and Liu et al. (2007)
Compression molding	• Control porosity amount, size, and shape via particulate leaching • Low porosity can be achieved • Simple, low cost	• Preformed implant, fabricated before implantation • Poor pore interconnectivity, particularly at low porosities • Difficult to generate large structures (>3 mm thick) • Difficult to leach all particulates in low porosity systems • Fabricate at elevated temperatures	Boccaccini and Blaker (2005), Thomson et al. (1998), and Barick and Tripathy (2011)
Monomer transfer molding	• Covalent linking from solid filler surface to bulk polymer, via coupling agent • Polymerized bulk polymer from solid filler surface improved wetting and thus interfacial bonding between solid filler and polymer	• Preformed implant, fabricated before implantation • Difficult to fabricate at one molecular weight • Polymerization at elevated temperatures	Khan et al. (2010) and Jiang et al. (2005a,b)

Monomer-induced polymerization	• Injectable and settable, filling cavity of targeted defect site • Some monomers are polymerized by photosensitizing agents • Tunable and dependable curing/setting rates • Capable of curing in vivo • Cured polymers generally possess rigid mechanical properties • Minimal water absorption once cured	• Some unreacted monomers can be cytotoxic • Polymerization may exude exotherm that could cause necrosis to surrounding tissue • Polymer can induce inflammatory response • Nondegradable • Cured polymers generally possess rigid mechanical properties	Koleganova et al. (2006) and Sideridou et al. (2003)
Reactive liquid molding	• Can be fabricated and cure in situ, post-implantation in vivo • Injectable and settable, filling cavity of targeted defect site with complex geometry • Tunable setting time, mechanical, degradation, and porosity properties • Carried out at physiological temperature • No detrimental exotherm • Stable, safe precursors	• Formulation optimization required to balance mechanisms of polymer degradation (hydrolytic vs oxidative) • Catalyst required • Curing rate dependent on moisture in defect/wound environment • Difficult to transpose in vitro properties to some in vivo environments	Harmata et al. (2014), Yoshii et al. (2012), Page et al. (2012), and Dumas et al. (2010)

Compression molding is one of the oldest methods of preparing polymer/ceramic biocomposites. Heat and pressure are applied to combine the polymer and solid phases to conform to the desired shape of an open mold cavity. In this process, the polymer and solid are placed in a mold and forced to make contact with all the mold's surfaces, and thus conform to its shape. The polymers used in this method can be thermosetting or plastic. HDPE is a common thermoplastic polymer that is used for a broad range of purposes, including food storage containers, plumbing, and plastic bags. Surface-modified HA and HDPE polymer biocomposites have been fabricated by compression molding (Wang and Bonfield, 2001; Sousa et al., 2003). PCL-based (also a thermoplastic) biocomposites have also been compression molded with surface-modified bioactive glass fibers (Khan et al., 2010, 2011). PCL is a member of the polyester family, one of the most commonly researched family of polymers for bone-regeneration applications.

Monomer transfer molding is similar to compression molding in that a predetermined shape is filled to create a pre-fabricated composite, but instead of utilizing force, monomers are polymerized within a heated mold cavity. The monomer mixture remains enclosed in a mold until it has polymerized and fully cured. Using this method, surface-modified bioglass fiber/PCL biocomposites have been made (Jiang et al., 2005a; Khan et al., 2010), proving there is more than one way to produce a biocomposite with the same basic components.

Another method utilizing unreacted monomers is induced monomer polymerization, in which the polymer phase is formed in the presence of the solid filler to form a polymeric biocomposite. This method is often used to fabricate resin-based biocomposites. Thermosetting resins form irreversible bonds once cured, and thus the shape of the mold is critical, as the polymer phase cannot be reshaped via heating once cured. Various methacrylate biocomposites have been made with surface-modified HA and BG fillers. These materials utilized urethane dimethacrylate (UDMA) (Koleganova et al., 2006; Deb et al., 2005), 2-hydroxyethyl methacrylate (Koleganova et al., 2006), bis-glycidyl dimethacrylate (GMA) (Santos et al., 2002; Deb et al., 2005), and triethylene glycol dimethacrylate (TEGDMA) (Deb et al., 2005; Santos et al., 2002) monomers. Induced monomer polymerization can be initiated by heat and pressure (Santos et al., 2002; Deb et al., 2005) or a photosensitizing agent activated by a light source (Koleganova et al., 2006).

The last polymeric biocomposite fabrication method relies on reactive liquid molding of multiple liquid components that polymerize in situ to fabricate the polymer phase of the biocomposite (Harmata et al., 2014; Yoshii et al., 2012; Page et al., 2012; Dumas et al., 2010). Although the previously outlined prefabricated methods require mold shaping, polymerization, and/or curing before in vivo implantation, polymeric biocomposites fabricated by this form of in situ polymerization can cure postimplantation in vivo. Surface-modified 45S5 BG and poly(ester urethane) (PUR) polymeric biocomposites have been fabricated by this method (Harmata et al., 2014). The PUR polymer network forms in the presence of the BG solid phase through cross-linking of the liquid precursors. This polymeric biocomposite does not require a solvent, heat, pressure, or any other form of energy to set in vivo, and can completely fill the cavity of a targeted defect site.

3.5 Effects of surface modification on filler properties

Attachment of molecules to the surface of a solid filler in polymeric biocomposites affects a variety of innate properties, particularly those related to the surface of the filler material. An overview of the surface modification techniques and how they alter specific filler properties is outlined in Table 3.3. The attachment of molecules affects the immediate physical and chemical composition of a surface, which can alter secondary surface properties related to surface interactions, such as wetting, zeta potential, surface solution reactions including dissolution/degradation, as well as cellular interactions. These primary and secondary properties do not necessarily alter how the filler interacts with polymer binders in a biocomposite setting, but these properties can change the inherent overall properties of the resultant filler.

3.5.1 Primary surface properties

Depending on the density, length, and steric effects of molecules attached to the surface, the apparent chemical composition of the filler has been changed for a given surface depth. Not surprisingly, physical attachment of molecules can also alter the topography, or arrangement of physical features, of solid fillers' surfaces. However, molecular attachment does not necessarily preclude an observed increase in roughness. The attachment of silane molecules to fillers used for orthopedic applications has been reported to smooth surfaces (Koleganova et al., 2006). As verified by SEM images, the attachment of 3-(trimethoxysilyl) propyl methacrylate decreased the roughness of sol–gel-produced BG biocomposite disks compared to those that contained unmodified fillers. This is relevant to polymeric biocomposites because, theoretically, after the surrounding polymer binder has degraded and a filler surface is exposed, the surface topography can affect protein adsorption as well as cell adhesion and spreading.

3.5.2 Secondary surface properties

Zeta potential is the potential difference between the dispersion medium (eg, polymer) and the layer of fluid attached to the dispersed particle (eg, solid filler). This value is used to quantify the electrokinetic potential in a colloidal system and is used to evaluate the stability of colloidal dispersions. The modification of HA powder with methoxysilane coupling agents (possessing a variety of functionalities) was shown to significantly increase the zeta potential (Dupraz et al., 1996).

Wetting is the ability of a liquid to maintain contact with a solid surface. It is an indicator of intermolecular interactions between and relative surface energy of the two phases. Wetting is important in the adhesion between a solid and liquid (eg, a solid filler and polymer binder). As defined from the Young–Dupré relationship, increasing the wettability of a material increases the thermodynamic work of adhesion (Neuendorf et al., 2008). Adhesion between phases in a composite material is one factor that is presumed to alter the mechanical properties of the overall composite. It has been shown that surface modification of HA particles with the silane 3-aminopropyltriethoxy improved wetting of the particles by HDPE polymer binder, and thus the apparent interfacial

Table 3.3 Effects of surface modification on material and polymeric biocomposite properties

Category	Surface modification	Parameter	Effect	References
Filler properties	Silane	Surface topography	Smoothed surface, as determined by SEM	Koleganova et al. (2006)
		Surface zeta potential	Increased 3–16 in H_2O, compared to unmodified control	Dupraz et al. (1996)
		Surface wetting, apparent interfacial adhesion with polymer	Increased compared to unmodified surface, qualitatively determined by SEM	Sousa et al. (2003)
		Degradation rate	Decreased ~15% compared to untreated control, after 7 days incubation in water at 37°C	Khan et al. (2011)
		Cell attachment	No effect compared to unmodified composite control	Koleganova et al. (2006)
		Bioactivity	Minimal, inconclusive effect on disappearance rate of Ca and P from SBF solution	Dupraz et al. (1996)
	Silane–polymer	Bioactivity	Delayed bone-like apatite growth several days when incubated in SBF, determined by SEM and energy-dispersive X-ray diffraction (EDX)	Zhang et al. (2004) and Liu et al. (1997)

Resultant polymeric biocomposite	Silane	Mechanical properties	Increased strength (~10–100%) and stiffness (~20–70%) compared to composite with unmodified filler, determined by either ultrasonic, tensile, or bending test method	Sousa et al. (2003), Zhang et al. (2004), Koleganova et al. (2006), and Khan et al. (2011)
		Mechanical properties (postaqueous incubation)	Maintained bending strength and modulus in similar fashion to composite with unmodified filler after incubation for up to 6 days	Khan et al. (2011)
		Uncured viscosity	Decreased torque, determined by rheometer	Hashimoto et al. (2006)
		Filler incorporation into polymer binder	Improved, determined qualitatively by SEM	Zhang et al. (2004)
		Filler surface polymer adhesion	Improved, determined qualitatively by SEM	Hashimoto et al. (2006) and Khan et al. (2011)
		Degradation rate	Decreased mass loss compared to unmodified filler after incubation in water	Khan et al. (2011)
		Water absorption	Decreased ~50%, determined by change mass	Koleganova et al. (2006) and Santos et al. (2002)
	Polymer	Filler surface polymer adhesion	Improved, determined qualitatively by SEM	Kunze et al. (2003)
		Mechanical properties	Increased strength (~0–400%) and modulus (~0–200%), determined by tensile, compression, or torsion testing	Liu et al. (1998a) and Harmata et al. (2014)

adhesion between the two phases (Sousa et al., 2003). In addition, and in a similar fashion to surface topography, the zeta potential of a surface and its wetting properties alter protein adsorption and cell attachment.

With respect to tissue-regeneration applications, bioactivity refers to controlled chemical release synchronized with the sequence of cellular changes occurring in wound repair (Hench, 2006). Optimal rates of dissolution and reaction are key to stimulating cellular proliferation and differentiation. There are two classes of bioactive materials related to bone repair: Class A bioactivity leads to osteoconduction (bone migration along a surface) and -production, whereas Class B bioactivity includes only osteoconduction (Hench, 2006). Bioactivity is a direct result of surface reactions on a surface of the bioactive material, such as solid fillers utilized in polymeric biocomposites, and is quantified by the release of ions into solution as well as the formation of bone-like apatite onto a surface when in simulated body fluid (SBF) (Dupraz et al., 1996). The surface reactions and subsequent nucleation of bone-like apatite onto a bioactive glass surface submerged in SBF is depicted in Fig. 3.4(a).

It is important to understand how various surface modifications via attachment of surface molecules affect the ability for surface reactions to occur between a solid

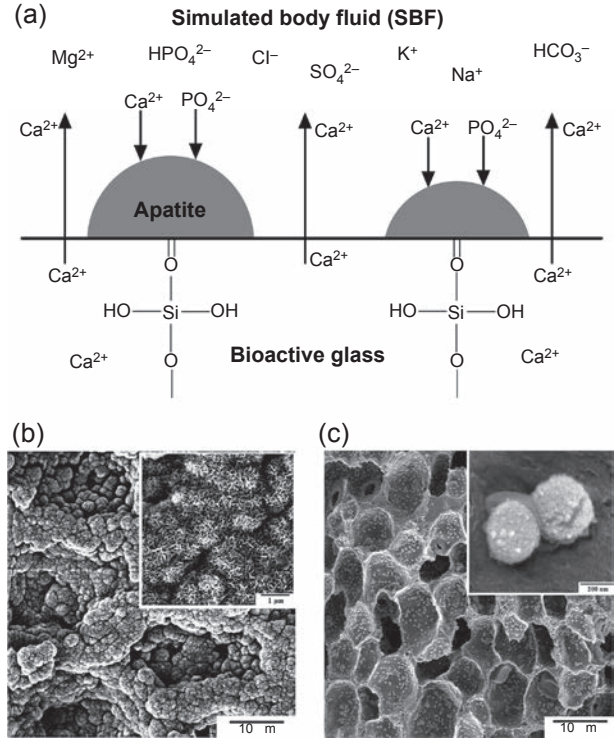

Figure 3.4 Effect of surface modification on solid filler properties: bioactivity. (a) Schematic of surface reaction and subsequent nucleation of apatite on bioactive filler surface. Images from SEM of porous poly(L-lactide) composites made with (b) unmodified BG and (c) silane-treated BG, after 7 days in SBF, showing effect on nucleation of apatite.

surface and fluid within the body, as this can alter the overall properties of the bioactive material, the biocomposite, and their combined ability to aid in bone remodeling. It has been shown that the presence of aminosilane coatings on HA particles initially hindered the release of Ca and P ions in aqueous solution, whereas vinyl- and methacryloxy-silane agents showed no effect compared to unmodified HA (Dupraz et al., 1996). Similarly, porous poly(L-lactide) (PLLA) and surface-modified (with 3-amino propyltrimethoxy silane) BG composites formed less apatite compared to those with nonmodified glass when incubated in SBF (Zhang et al., 2004). SEM images of these PLLA/BG biocomposites (Fig. 3.4(b) and (c)) show the effect of the silane molecules on nucleation of apatite. PAA coating on Nap filler hindered apatite formation compared to nonmodified Nap in Polyactive™ 70:30-based composites (Liu et al., 1997). It is hypothesized that the observed delay is due to decreased diffusivity of released ions from the filler surface through the silane coating to the surrounding fluid. It is important to note that these surface modifications did not completely prevent ionic dissolution or apatite formation, but rather delayed such events.

The majority of solid fillers utilized in polymeric biocomposites for orthopedic applications are capable of being resorbed or degrading after implantation in the body. The ability to degrade, often by dissolution, is often an advantageous quality when its degradation rate is appropriate. For instance, if the mechanical stability of the polymeric biocomposite is dependent on the solid filler, a fast degradation rate may not be desired. Regardless, it is important to understand and characterize the degradation kinetics of surface-modified solids compared to their unmodified counterparts. It has been reported that silane modification (with 3-aminopropyl triethoxysilane) decreased the overall cumulative degradation and degradation rate of phosphate-glass fibers incubated in water (Khan et al., 2011). SEM images of unmodified phosphate-glass fibers immersed in water for 7 days showed signs of hydrolytic surface degradation, whereas silane-treated fibers maintained unaltered surface topography (Fig. 3.5). The maintenance of the original surface topography post water immersion, and thus prevention of surface degradation, was attributed to the presence of a polysiloxane coating on the fiber surface.

Solid bioactive fillers in polymeric biocomposites ideally would not only produce an environment conducive to osteoblast activity via ion release, but would also provide a surface conducive for cell attachment, integration, and proliferation. The presence

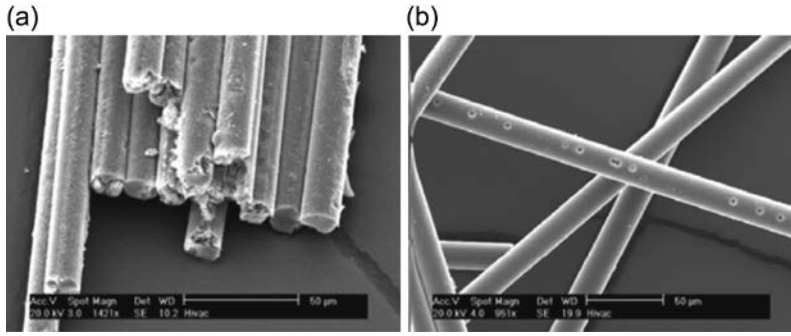

Figure 3.5 Effect of surface modification on solid filler properties: degradation. Images from SEM of phosphate glass fibers, (a) unmodified and (b) silane-treated, degraded for 7 days in water.

of 3-(trimethoxysilyl) propyl methacrylate on the surface of sol–gel BG did not alter cell attachment of osteoblast-like cells to composites (Koleganova et al., 2006). As noted previously, surface modification of bioactive fillers in this biocomposite system decreased roughness compared to the rougher surface of unmodified bioactive-glass biocomposite, which was hypothesized to aid in cell adhesion.

3.6 Effects of surface-modified fillers on the properties of resultant polymeric biocomposites

Modifying the surface of solid fillers used in polymeric biocomposites controls the surface properties (both primary and secondary), which affects both the mechanical and physical properties of the resultant polymeric biocomposite as well as its ability to remodel in vivo. An overview of the surface-modification techniques and how they alter the resultant biocomposite properties is outlined in Table 3.3. The fundamental theory of composite design is to obtain physical properties that lie between those of the individual components. As previously outlined, a primary motivator to modify the surface of a solid filler is to increase adhesion between the solid filler and polymer components, and thus the overall mechanical properties of the biocomposite. This observation has been supported by numerous studies citing an increase in tensile properties. Other overall biocomposite properties that are affected by surface modification of filler components include binding to polymer phase, solid-filler incorporation into polymer binder, water uptake, and degradation.

Surface modification has been noted to improve interaction between the surface of the solid filler and the polymer binder. As outlined previously, this is likely due to improved matching of surface tension and improved wetting by the (initially) liquid polymer. Proper matching can lead to homogenous distribution and improved incorporation of solid fillers into polymer binder, which has been hypothesized to improve related biocomposite properties, such as mechanical strength (Khan et al., 2011; Sousa et al., 2003). One method utilized to determine the interaction between a liquid polymer and solid filler is by calculating the thermodynamic work of adhesion (W_{ad}) from the Young–Dupré relationship (Adamson and Gast, 1997; Neuendorf et al., 2008):

$$W_{ad} = \gamma (1 + \cos \theta)$$

in which γ is the surface tension of the liquid polymer and θ is the equilibrium contact angle between the polymer and solid filler. This calculation is reliable for biocomposites in which dispersion forces are dominant (Mangipudi et al., 1994). In HDPE biocomposites, the viscosity of the overall uncured biocomposite was noted to decrease when [γ-methacryloxypropyl]trimethoxysilane-modified TiO_2 particles were utilized compared to unmodified particles (Hashimoto et al., 2006). Surface modification by 3-aminopropyltrimethoxysilane improved BG incorporation in cured, porous PLLA composites, as evidenced by SEM images (Fig. 3.6(a) and (b); Zhang et al., 2004). It was proposed that this was due to improved interfacial interaction between the

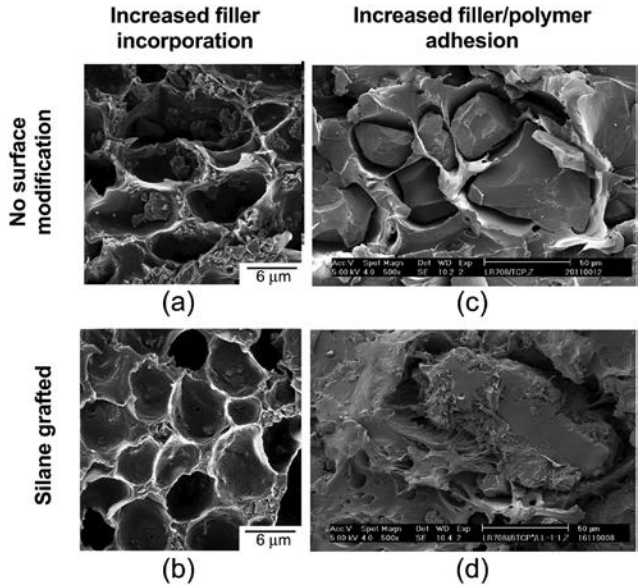

Figure 3.6 Effect of surface modification on resultant polymer biocomposite properties: filler/polymer interaction. Images from SEM of porous poly(L-lactide) composites made with (a) unmodified BG and (b) silane-treated BG, showing increased solid filler incorporation, and poly(L,DL-lactide) composites made with (c) unmodified TCP and (d) polymer surface grafted TCP, showing increased apparent adhesion between filler and polymer.

silane-modified BG particles and PLLA, which was supported by complete coverage of the particles by the polymer binder. Improved qualitative adhesion between solid fillers and binder components has been observed in polymeric biocomposite systems made from HDPE with silane-modified TiO_2 particles (Hashimoto et al., 2006), PCL with silane-modified phosphate-glass fibers (Khan et al., 2011), and poly(L,DL-lactide) with L-lactide-modified TCP particles (Kunze et al., 2003), as shown in Fig. 3.6(c) and (d).

The overall mechanical properties of the resultant biocomposite are the properties most significantly altered by surface modification of the solid-filler surface. In multiple biocomposite systems made with a variety of polymer binders, the presence of surface molecules (silane- and polymer-based) on the solid fillers increased the overall stiffness of the biocomposite, as shown by an increase in the tensile (Liu et al., 1998a; Sousa et al., 2003; Zhang et al., 2004; Koleganova et al., 2006; Khan et al., 2011) and compressive moduli (Harmata et al., 2014). In a similar fashion, the presence of surface silane- and polymer-based molecules on solid fillers increased the ultimate tensile (Liu et al., 1998a; Zhang et al., 2004; Khan et al., 2011; Sousa et al., 2003) and compressive strengths (Harmata et al., 2014) of the various biocomposite systems. Alternatively, some researchers have cited that surface modification of solid fillers does not significantly improve the overall mechanical properties of the biocomposite. These observations were made for polymeric biocomposite systems with a relatively low (<30 vol%) amount of solid filler, in which the total interfacial area (between the

solid filler and the polymer binder) is too low to affect the overall mechanical properties of the resultant polymeric biocomposite (Kunze et al., 2003; Sousa et al., 2003). Surface modification of the solid filler plays a larger role when the total interfacial area in the biocomposite, defined by the volume fraction and the specific surface area of the filler, is sufficient to achieve improvements in strength (Sousa et al., 2003).

The outlined surface-modification techniques have been cited to minimize hydrolytic effects on the solid fillers, polymer binders, the adhesion between these phases, and thus the overall biocomposite properties. In vitro degradation experiments in aqueous solution provide information related to the mechanism and rate of degradation of the biocomposite once placed in the body. In PCL biocomposites with silane-modified phosphate-glass fibers, a decreased rate of mass loss (overall composite degradation) was reported compared to biocomposites made with unmodified phosphate glass (Khan et al., 2011). This altered rate was attributed to an increase in adhesion between the solid filler and polymer binder caused by the presence of siloxane bonds formed at the fiber surface. In the same PCL/BG biocomposite system, inclusion of silane-modified fibers was shown to improve overall biocomposite bending strength when incubated in an aqueous environment (analogous to being in the body) (Khan et al., 2011). Qualitative observations from this study focused on apparent adhesion between the polymer binder and fibers after subjection to incubation in aqueous media followed by mechanical testing. It was noted that biocomposites made with unmodified fibers showed gaps of separation between the polymer and solid phases, whereas the biocomposites made with modified fibers maintained their original integrity with respect to adhesion (Khan et al., 2011). Other systems have reported a decrease in water absorption, which could contribute to maintaining mechanical properties after implantation into the body. In BG and urethane dimethacrylate/2-hydroxyethyl methacrylate biocomposites, utilization of silane-modified BG prevented water absorption by 50% (Koleganova et al., 2006). Additionally, lower water uptake was found for BisGMA-based biocomposites made with silane-modified HA compared to those incorporating unmodified HA (Santos et al., 2002). This may be due to a decrease in porosity and a reduction in water accumulation at the interface caused by an improved adhesion between the solid and polymer phases. The report also cites improved wettability, dispersion, and impregnation into the polymer binder as reasons for decreased water uptake compared to biocomposites made with unmodified HA (Santos et al., 2002).

3.7 Future trends

The fundamental surface-modification methods applied to solid fillers in polymer biocomposites, such as those previously outlined, are based on techniques and surface chemistries that have been utilized for several decades. More recently, new methods have been applied to the surface modification of solid fillers intended for use in polymeric biocomposites for orthopedic applications. Plasma polymerization forms polymeric materials, such as nanoscale-thick polymer coatings, via partially ionized gas (plasma) (Larranaga et al., 2013; Nichols et al., 2007). This rapid and solvent-free alternative approach to the conventional wet-surface modification processes previously described has several advantages that may be particularly appealing for the

large-scale production requirements of the medical device industry, including reduction in required monomer reagents, overall process time, and the effect on the bulk material properties (Larranaga et al., 2013). Additionally, the resultant layer properties (uniformity, thickness, and surface energy) are highly tunable over a wide range, in part because of the ability to control the polymerization process at a molecular level, despite not requiring the use of organic solvents (Nichols et al., 2007; Larranaga et al., 2013). However, plasma polymerization is generalized used for cross-linked polymers. Thus, it may not be appropriate for surface modification with linear polymers with higher targeted molecular weights.

In the past decade, several research groups have utilized surface polymerization of acrylic acid via plasma polymerization to achieve desired properties to the overall resultant polymeric biocomposite, including improved adhesion between solid filler and the surrounding polymer binder. HA powder and nanopowder have been modified with acrylic acid by cold (Garreta et al., 2006) and fluid-bed radio-frequency plasma polymerization (Nichols et al., 2007) techniques, respectively. Surface polymerization of acrylic acid onto both sizes of HA fillers before incorporation into their polymer binders provided a moderately wettable surface that has been shown to be advantageous for the absorption of proteins (Kim et al., 2013). Furthermore, this approach improved the overall tensile strength of the resultant biocomposites, as traditional wet-surface modifications were shown to do in the *Overall biocomposite affects* section (Nichols et al., 2007; Garreta et al., 2006). Additionally, the ability to tailor the biodegradability of the adhered polymer layers and their cytocompatibility with in vitro cell cultures was shown (Nichols et al., 2007). In a similar fashion, the surface modification of BG particles with acrylic acid was performed before inclusion in PLLA, PCL, and poly(L-lactide/ε-caprolactone) composite films (Larranaga et al., 2013). In these composites, the presence of the surface polymer was attributed to improve the thermal stability of the resultant composites by hindering the degradation reaction between the bioactive-glass particle surface and the bulk polymer, which allowed high-temperature thermoplastic composite fabrication techniques to be utilized with desired outcomes (Larranaga et al., 2013).

As an extension to this surface-modification method, researchers have utilized plasma polymerization of acrylic acid to immobilize biologically active molecules, such as recombinant human bone formation protein-2 (rhBMP-2). rhBMP-2 is a signaling molecule that promotes bone formation by osteoinduction that has been utilized for various orthopedic tissue-engineering applications (Kim et al., 2013). One research group modified a PCL scaffold surface with plasma-polymerized acrylic acid (PPAA) and rhBMP-2 via electrostatic interactions (Kim et al., 2013) (which is outside of the scope of this chapter). This interesting approach may be applied to the surface modification of solid fillers and provide additional benefits compared to the surface-modification techniques currently utilized in orthopedic polymeric biocomposite development. The acrylic acid and rhBMP-2-modified surface showed improved cell attachment and adhesion compared to the surface with acrylic acid alone. The ability to modify the surface of a solid-filler particle in a polymeric biocomposite with a bioactive molecule, such as rhBMP-2, provides a delivery vehicle for the bioactive molecule to the polymeric biocomposite and the eventual implantation site of this biomaterial. Such surface-modification and immobilization approaches may provide a method to control the release kinetics of attached molecules to the localized bone-defect site.

Sources of further information and advice

The field of surface modification is not new, and because of this there are abundant sources of further information that provide more detail than what was reviewed in this chapter. There are also many textbooks that expand on particular sections in this chapter. Various volumes of the book *Silane and Other Coupling Agents*, of which Volume 5 was edited by K.L. Mittal in 2009, provides seminal first author journal articles related specifically to the field of coupling agents for diverse purposes. Additionally, others have previously focused on the surface modifications of the polymer, not the inorganic solid, component in biomaterials and other applications. In 1997, Ratner and Castner edited a textbook entitled *Surface Modification of Polymeric Biomaterials* (1997), which covers the proceedings from American Chemical Society Division of Polymer Chemistry International Symposium, and includes sections focused on XPS and static secondary ion mass spectrometry, biomolecule attachment to increase cell adhesion and migration, as well as additional polymer grafting methods not covered in this chapter. Lastly, the *SpecialChem* Website includes online training, information, and networking interactions related to chemicals and materials. This Website offers a section dedicated to silane coupling agents that provides interactive sources for obtaining fundamental information about silane chemistry, application of silanes to surfaces, and how silanes mediate surface interactions.

References

Adamson, A.W., Gast, A.P., 1997. Physical Chemistry of Surfaces. Wiley, New York.

Amendola, L., Gasbarrini, A., Fosco, M., Simoes, C.E., Terzi, S., Delure, F., Boriani, S., 2011. Fenestrated pedicle screws for cement-augmented purchase in patients with bone softening: a review of 21 cases. The Journal of Orthopaedics and Traumatology: Official Journal of the Italian Society of Orthopaedics and Traumatology 12, 193–199.

Arkles, B., 1977. Tailoring surfaces with silanes. ChemTech 7, 766–778.

Barick, A.K., Tripathy, D.K., 2011. Preparation, characterization and properties of acid functionalized multi-walled carbon nanotube reinforced thermoplastic polyurethane nanocomposites. Materials Science and Engineering B-Advanced Functional Solid-State Materials 176, 1435–1447.

Boccaccini, A.R., Blaker, J.J., 2005. Bioactive composite materials for tissue engineering scaffolds. Expert Review of Medical Devices 2, 303–317.

Bohner, M., 2000. Calcium orthophosphates in medicine: from ceramics to calcium phosphate cements. Injury-International Journal of the Care of the Injured 31, S37–S47.

Bohner, M., 2010. Design of ceramic-based cements and putties for bone graft substitution. European Cells & Materials 20, 1–12.

Centers for Disease Control and Prevention, 2001. Septic arthritis following anterior cruciate ligament reconstruction using tendon allografts - Florida and Louisiana. The Morbidity and Mortality Weekly Report 50, 1081–1083.

Centers for Disease Control and Prevention, 2002. Update: allograft-associated bacterial infections - United States. The Morbidity and Mortality Weekly Report 51, 207–210.

Damien, C.J., Parsons, J.R., 1991. Bone-graft and bone-graft substitutes - a review of current technology and applications. Journal of Applied Biomaterials 2, 187–208.

Deb, S., Wang, M., Tanner, K.E., Bonfield, W., 1996. Hydroxyapatite polyethylene composites: effect of grafting and surface treatment of hydroxyapatite. Journal of Materials Science-Materials in Medicine 7, 191–193.

Deb, S., Aiyathurai, L., Roether, J.A., Luklinska, Z.B., 2005. Development of high-viscosity, two-paste bioactive bone cements. Biomaterials 26, 3713–3718.

Dumas, J.E., Zienkiewicz, K., Tanner, S.A., Prieto, E.M., Bhattacharyya, S., Guelcher, S.A., 2010. Synthesis and characterization of an injectable allograft bone/polymer composite bone void filler with tunable mechanical properties. Tissue Engineering Part A 16, 2505–2518.

Dupraz, A.M.P., Dewijn, J.R., Vandermeer, S.A.T., Degroot, K., 1996. Characterization of silane-treated hydroxyapatite powders for use as filler in biodegradable composites. Journal of Biomedical Materials Research 30, 231–238.

El-Amin, S.F., Khan, Y., Laurencin, C., 2006. Bone graft substitutes. Expert Review of Medical Devices 3.

Garreta, E., Tricas, N., Quintana, L., Semino, C.E., Borros, S., 2006. Plasma polymerization on hydroxyapatite powders to increase water dispersibility for biomedical applications. Plasma Processes and Polymers 3, 553–561.

Greenwald, A.S., Boden, S.D., Goldberg, V.M., Khan, Y., Laurencin, C.T., Rosier, R.N., 2001. Bone-graft substitutes: facts, fictions, and applications. Journal of Bone and Joint Surgery-American Volume 83A, 98–103.

Hall, J.A., Beuerlein, M.J., Mckee, M.D., 2009. Open reduction and internal fixation compared with circular fixator application for bicondylar tibial plateau fractures. Surgical technique. Journal of Bone and Joint Surgery-American Volume 91A (Suppl. 2 Pt 1), 74–88.

Harmata, A.J., Ward, C.L., Zienkiewicz, K., Wenke, J.C., Guelcher, S.A., 2014. Investigating the effects of surface-initiated polymerization of ε-caprolactone to bioactive glass particles on the mechanical properties of settable polymer/ceramic composites. Journal of Materials Research 29, 2398–2407.

Hashimoto, M., Takadama, H., Mizuno, M., Kokubo, T., 2006. Enhancement of mechanical strength of TiO_2/high-density polyethylene composites for bone repair with silane-couple treatment. Materials Research Bulletin 41, 515–524.

Hench, L.L., 2006. The story of Bioglass®. Journal of Materials Science-Materials in Medicine 17, 967–978.

Jiang, G., Evans, M.E., Jones, I.A., Rudd, C.D., Scotchford, C.A., Walker, G.S., 2005a. Preparation of poly(epsilon-caprolactone)/continuous bioglass fibre composite using monomer transfer moulding for bone implant. Biomaterials 26, 2281–2288.

Jiang, G., Walker, G.S., Jones, I.A., Rudd, C.D., 2005b. XPS identification of surface-initiated polymerisation during monomer transfer moulding of poly(epsilon-caprolactone)/Bioglass® fibre composite. Applied Surface Science 252, 1854–1862.

Johnson, A.J.W., Herschler, B.A., 2011. A review of the mechanical behavior of CaP and CaP/polymer composites for applications in bone replacement and repair. Acta Biomaterialia 7, 16–30.

Khan, Y., Yaszemski, M.J., Mikos, A.G., Laurencin, C.T., 2008. Tissue engineering of bone: material and matrix considerations. Journal of Bone and Joint Surgery-American Volume 90A, 36–42.

Khan, R.A., Parsons, A.J., Jones, I.A., Walker, G.S., Rudd, C.D., 2010. Preparation and characterization of phosphate glass fibers and fabrication of poly(caprolactone) matrix resorbable composites. Journal of Reinforced Plastics and Composites 29, 1838–1850.

Khan, R.A., Parsons, A.J., Jones, I.A., Walker, G.S., Rudd, C.D., 2011. Effectiveness of 3-aminopropyl-triethoxy-silane as a coupling agent for phosphate glass fiber-reinforced poly(caprolactone)-based composites for fracture fixation devices. Journal of Thermoplastic Composite Materials 24, 517–534.

Kim, B.H., Myung, S.W., Jung, S.C., Ko, Y.M., 2013. Plasma surface modification for immobilization of bone morphogenic protein-2 on polycaprolactone scaffolds. Japanese Journal of Applied Physics 52.

Koleganova, V.A., Bernier, S.M., Dixon, S.J., Rizkalla, A.S., 2006. Bioactive glass/polymer composite materials with mechanical properties matching those of cortical bone. Journal of Biomedical Materials Research Part A 77A, 572–579.

Kunze, C., Freier, T., Helwig, E., Sandner, B., Reif, D., Wutzler, A., Radusch, H.J., 2003. Surface modification of tricalcium phosphate for improvement of the interfacial compatibility with biodegradable polymers. Biomaterials 24, 967–974.

Larranaga, A., Petisco, S., Sarasua, J.R., 2013. Improvement of thermal stability and mechanical properties of medical polyester composites by plasma surface modification of the bioactive glass particles. Polymer Degradation and Stability 98, 1717–1723.

Larsson, S., Procter, P., 2011. Optimising implant anchorage (augmentation) during fixation of osteoporotic fractures: Is there a role for bone-graft substitutes? Injury-International Journal of the Care of the Injured 42, S72–S76.

Larsson, S., Stadelmann, V.A., Arnoldi, J., Behrens, M., Hess, B., Procter, P., Murphy, M., Pioletti, D.P., 2012. Injectable calcium phosphate cement for augmentation around cancellous bone screws. In vivo biomechanical studies. Journal of Biomechanics 45, 1156–1160.

Liu, Q., Dewijn, J.R., Vanblitterswijk, C.A., 1997. Nano-apatite/polymer composites: mechanical and physicochemical characteristics. Biomaterials 18, 1263–1270.

Liu, Q., De Wijn, J.R., Van Blitterswijk, C.A., 1998a. Composite biomaterials with chemical bonding between hydroxyapatite filler particles and PEG/PBT copolymer matrix. Journal of Biomedical Materials Research 40, 490–497.

Liu, Q., De Wijn, J.R., Van Blitterswijk, C.A., 1998b. Covalent bonding of PMMA, PBMA, and poly(HEMA) to hydroxyapatite particles. Journal of Biomedical Materials Research 40, 257–263.

Liu, Q., De Wijn, J.R., Van Blitterswijk, C.A., 1998c. A study on the grafting reaction of isocyanates with hydroxyapatite particles. Journal of Biomedical Materials Research 40, 358–364.

Liu, C., Xia, Z., Czernuszka, J.T., 2007. Design and development of three-dimensional scaffolds for tissue engineering. Chemical Engineering Research & Design 85, 1051–1064.

Mangipudi, V., Tirrell, M., Pocius, A.V., 1994. Direct measurement of molecular-level adhesion between poly(ethylene-terephthalate) and polyethylene films - determination of surface and interfacial energies. Journal of Adhesion Science and Technology 8, 1251–1270.

Mosse, W.K.J., Koppens, M.L., Gengenbach, T.R., Scanlon, D.B., Gras, S.L., Ducker, W.A., 2009. Peptides grafted from solids for the control of interfacial properties. Langmuir 25, 1488–1494.

Neuendorf, R.E., Saiz, E., Tomsia, A.P., Ritchie, R.O., 2008. Adhesion between biodegradable polymers and hydroxyapatite: relevance to synthetic bone-like materials and tissue engineering scaffolds. Acta Biomaterialia 4, 1288–1296.

Nichols, H.L., Zhang, N., Zhang, J., Shi, D., Bhaduri, S., Wen, X., 2007. Coating nanothickness degradable films on nanocrystalline hydroxyapatite particles to improve the bonding strength between nanohydroxyapatite and degradable polymer matrix. Journal of Biomedical Materials Research Part A 82A, 373–382.

Page, J.M., Prieto, E.M., Dumas, J.E., Zienkiewicz, K.J., Wenke, J.C., Brown-Baer, P., Guelcher, S.A., 2012. Biocompatibility and chemical reaction kinetics of injectable, settable polyurethane/allograft bone biocomposites. Acta Biomaterialia 8, 4405–4416.

Porter, J.R., Ruckh, T.T., Popat, K.C., 2009. Bone tissue engineering: a review in bone biomimetics and drug delivery strategies. Biotechnology Progress 25, 1539–1560.

Russell, T.A., Leighton, R.K., 2008. Comparison of autogenous bone graft and endothermic calcium phosphate cement for defect augmentation in tibial plateau fractures. Journal of Bone and Joint Surgery-American Volume 90A, 2057–2061.

Santos, C., Clarke, R.L., Braden, M., Guitian, F., Davy, K.W.M., 2002. Water absorption characteristics of dental composites incorporating hydroxyapatite filler. Biomaterials 23, 1897–1904.

Sepulveda, P., Jones, J.R., Hench, L.L., 2002. Bioactive materials for tissue engineering scaffolds. In: Polak, J.M., Hench, L.L., Kemp, P. (Eds.), Future Strategies for Tissue and Organ Replacement. Imperial College Press.

Sideridou, I., Tserki, V., Papanastasiou, G., 2003. Study of water sorption, solubility and modulus of elasticity of light-cured dimethacrylate-based dental resins. Biomaterials 24, 655–665.

Siemann, U., 2005. Solvent cast technology – a versatile tool for thin film production. Progress in Colloid and Polymer Science 1–14.

Silane and Other Coupling Agents, 2009. Hotei Publishing.

Simpson, D., Keating, J.F., 2004. Outcome of tibial plateau fractures managed with calcium phosphate cement. Injury-International Journal of the Care of the Injured 35, 913–918.

Sousa, R.A., Reis, R.L., Cunha, A.M., Bevis, M.J., 2003. Coupling of HDPE/hydroxyapatite composites by silane-based methodologies. Journal of Materials Science-Materials in Medicine 14, 475–487.

Surface Modification of Polymeric Biomaterials, 1997. Springer.

Thomson, R.C., Yaszemski, M.J., Powers, J.M., Mikos, A.G., 1998. Hydroxyapatite fiber reinforced poly(alpha-hydroxy ester) foams for bone regeneration. Biomaterials 19, 1935–1943.

Urban, R.M., Turner, T.M., Hall, D.J., Infanger, S., Cheema, N., Lim, T.H., 2003. Healing of large defects treated with calcium sulfate pellets containing demineralized bone matrix particles. Orthopedics 26, S581–S585.

US Census Bureau, 2008. Health and Nutrition. US Census Bureau Statistical Abstracts of the United States. US Census Bureau, Washington, DC.

Verlaan, J.J., Oner, F.C., Dhert, W.J.A., 2006. Anterior spinal column augmentation with injectable bone cements. Biomaterials 27, 290–301.

Wang, M., Bonfield, W., 2001. Chemically coupled hydroxyapatite-polyethylene composites: structure and properties. Biomaterials 22, 1311–1320.

Yoshii, T., Dumas, J.E., Okawa, A., Spengler, D.M., Guelcher, S.A., 2012. Synthesis, characterization of calcium phosphates/polyurethane composites for weight-bearing implants. Journal of Biomedical Materials Research Part B-Applied Biomaterials 100B, 32–40.

Zhang, K., Wang, Y.B., Hillmyer, M.A., Francis, L.F., 2004. Processing and properties of porous poly(L-lactide)/bioactive glass composites. Biomaterials 25, 2489–2500.

This page intentionally left blank

Part Two

Polymer nanocomposites for musculoskeletal tissue regeneration

This page intentionally left blank

Toxicity and biocompatibility properties of nanocomposites for musculoskeletal tissue regeneration

4

W. Liu[1,2], *T.J. Webster*[2,3]
[1]Peking University School and Hospital of Stomatology, Beijing, PR China; [2]Northeastern University, Boston, MA, United States; [3]King Abdulaziz University, Jeddah, Saudi Arabia

4.1 Introduction

Novel materials are constantly being developed to improve device performance within all fields of regenerative medicine and tissue regeneration. Tissue engineering is a promising approach to create artificial constructs for regenerating partial or whole musculoskeletal tissue. Due to their superior physicochemical properties, nanosized materials have been widely investigated in tissue engineering, regenerative medicine, and the drug delivery fields (Zhang and Webster, 2009). Musculoskeletal tissues such as bone, cartilage, and ligaments/tendons are highly structured nanocomposites consisting of nanofibers embedded in a matrix of different compositions (Egli and Luginbuehl, 2012). Bone tissue is also a natural nanomaterial, which is composed of collagen fibrils and hydroxyapatite crystals. Articular cartilage ligaments and tendons also have a highly hierarchical micro- and nanostructure. Thus, to mimic the natural structure of orthopedic tissues, nanocomposites made of biocompatible polymers and bioactive inorganic nanoparticles have attracted particular attention (Sun et al., 2011).

One of the many specific requirements for the ideal material for orthopedic tissue engineering is biocompatibility, which means a material with the ability to be compatible with living tissues or living systems without causing harm. Biocompatibility is considered to arise from material chemical structural similarity to the components of musculoskeletal tissue (Sahoo et al., 2013) (Fig. 4.1). The beneficial aspects of nanocomposites are vast; however, there is still a lack of information about the risk and biocompatibility for these materials in the human body. Nanomaterials can vary with respect to composition, size, shape, surface chemistry, and crystal structure. When using a nanophase material, in which at least one surface feature size is less than 100 nm, implant surface properties will change (ie, surface area, energy, topography, and charge). Topography and wettability

Nanocomposites for Musculoskeletal Tissue Regeneration. http://dx.doi.org/10.1016/B978-1-78242-452-9.00004-2

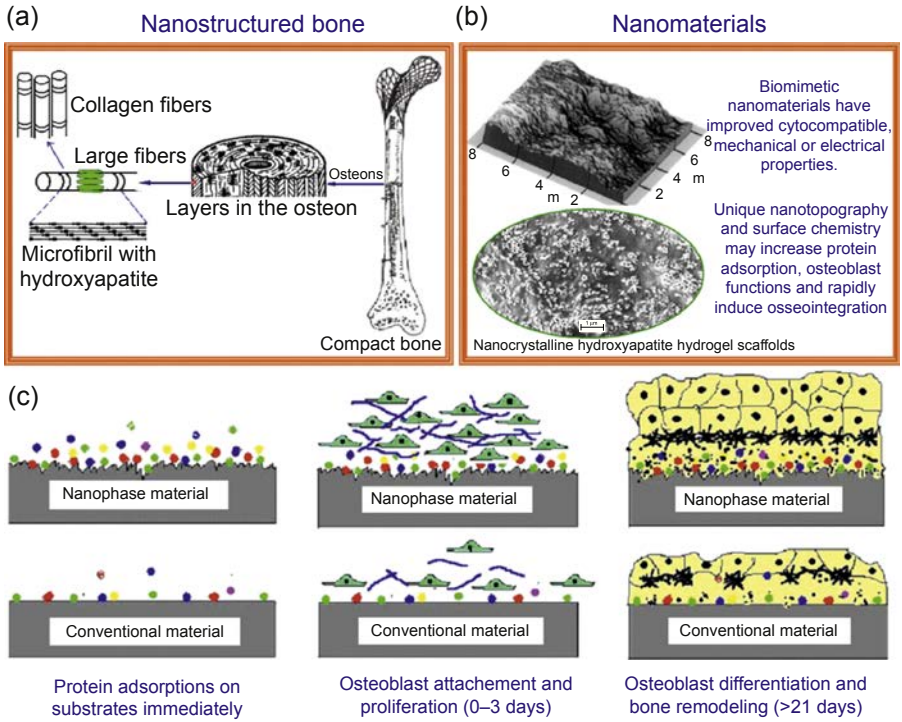

Figure 4.1 The biomimetic advantages of nanomaterials. (a) The nanostructured hierarchical self-assembly of bone. (b) Nanophase titanium (top, atomic force microscopy image) and nanocrystalline HA/ helical rosette nanotube (HRN) hydrogel scaffold (bottom, scanning electron microscopy (SEM) image). (c) Schematic illustration of the mechanism by which nanomaterials may be superior to conventional materials for bone regeneration. The bioactive surfaces of nanomaterials mimic those of natural bones to promote greater amounts of protein adsorption and efficiently stimulate more new bone formation than conventional materials. Zhang, L., Webster, T.J., 2009. Nanotechnology and nanomaterials: promises for improved tissue regeneration. Nano Today 4, 66–80.

are correlated with protein adsorption, which dictates cellular responses. A linear regression-based protein adsorption model was recently developed and used to explain the relationship between protein adsorption and nano surface properties (Egli and Luginbuehl, 2012). Such models confirm experiments which have demonstrated greater cellular functions on nanostructured surfaces due to the enhanced interactions of adherent cells with initially adsorbed proteins (Webster et al., 2001; Miller et al., 2005). This chapter focuses on the toxicity and biocompatibility properties of nanocomposites for various musculoskeletal tissue regeneration applications. It presents state-of-the-art findings as well as poignant thoughts for the future of this field to mature into developing real products that can improve tissue growth.

4.2 Musculoskeletal tissue and natural nanocomposite structures

A nanomaterial is roughly defined as a material with base constituents between 1×10^{-9} and 100×10^{-9} m in length which exhibits at least one property that deviates from equivalent bulk or microstructured materials (Banfield and Navrotsky, 2001). Thus, many biological structures of musculoskeletal tissues, such as bone, collagen fibrils, and hydroxyapatite crystals, are natural nanomaterials by definition. The structural composition of bone, cartilage, and ligaments/tendons is very similar, although these tissues have quite distinct appearances from each other. Bone tissue has a highly nanohierarchical structure consisting mainly of collagen type I fibers and nanohydroxyapatite crystals as the matrix (Egli and Luginbuehl, 2012). The defining features of bone are the mineralized collagen-based extracellular matrix (ECM), which provides bone with its unique biomechanical properties (Haidar, 2010). Ligaments and tendons have a similar building pattern with fibers oriented parallel to the stress axis and consisting mainly of collagen type III embedded in a proteoglycan matrix (Egli and Luginbuehl, 2012). Cartilage is composed of a low percentage of chondrocytes embedded in a dense nanostructured ECM rich with collagen fibers, proteoglycans, and elastin fibers (Zhang and Webster, 2009). Mature articular cartilage has a highly hierarchical structure stratified with collagen fibrils, mainly of collagen type II, embedded in a hydrogel formed by glycosaminoglycans and proteoglycans (Ap Gwynn et al., 2000; Hughes et al., 2005). The hierarchical geometrical structure of bone is critical, not only for macroscopic mechanical properties, but also for cells, which respond to these structural and geometric cues by converting them into intracellular signals which drive cellular activities such as gene expression, protein production, and general phenotypic behavior (Zhang and Webster, 2009; Porter et al., 2009).

Thus, regeneration of organized and multifunctional tissue requires the use of scaffolds presenting a certain degree of nanocompositional and structural complexity (Fig. 4.2).

4.3 Biocompatibility and toxicity of nanocomposites

Nanotechnology research is growing at an exponential rate and is predicted to change the face of the world in which we live. There are many products including sunscreens, anti-wrinkle face creams, sports equipment, bone, and muscular replacement materials which employ nanomaterials to improve functions above those currently observed in conventional or microstructured materials (Henig, 2007).

Nanocomposites are multiphase solid materials which have one to three dimensions less than 100 nm, or structures with nanosized repeat distances in different phases that compose the material (Ajayan et al., 2003). Nanocomposites can be divided into bioceramic nanocomposites, metallic nanocomposites, and polymer nanocomposites. The structure of nanocomposites can be nanofibers, nanoparticles, nanotubes, or scaffolds

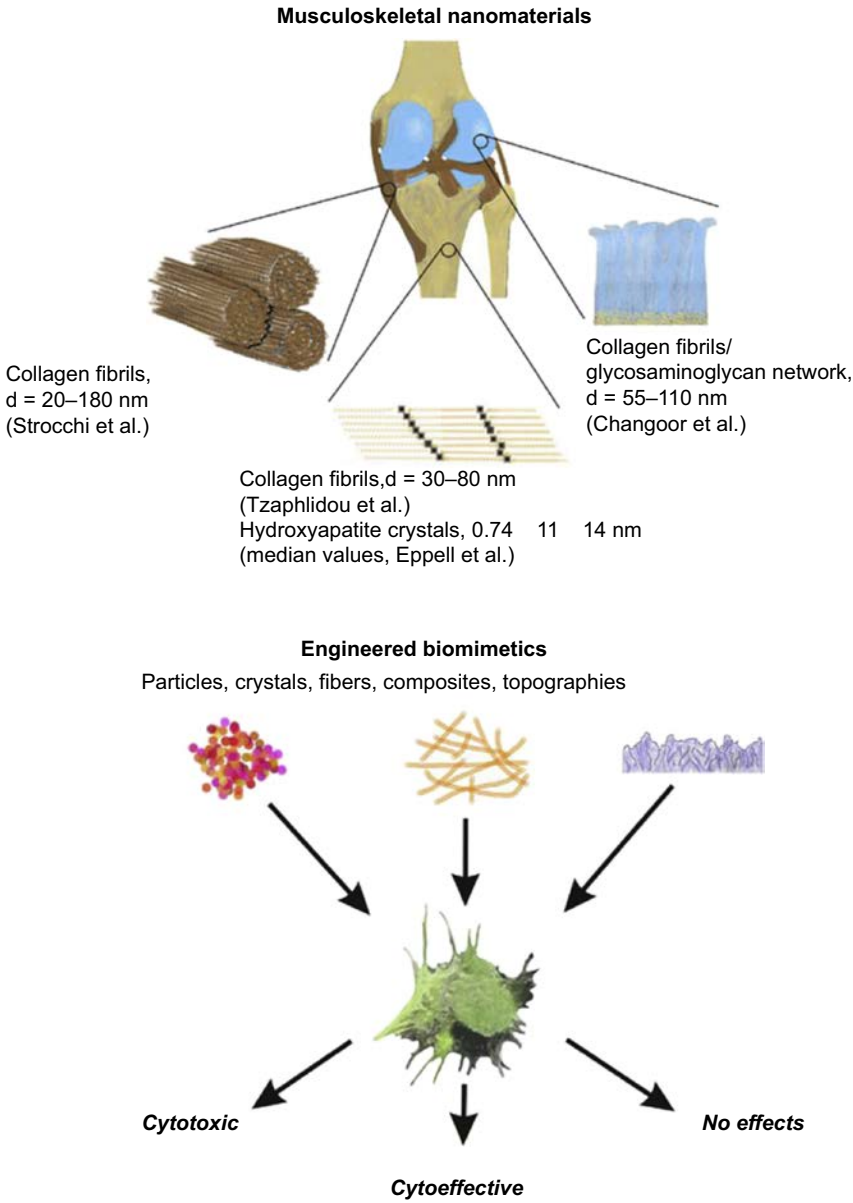

Figure 4.2 Musculoskeletal tissues—the prototypes of nanomaterials. The structural composition of ligaments/tendons, bone, and cartilage is very similar, although these tissues have quite a distinct appearance. In a simplified approach they consist of a characteristic network of collagen fibrils with diameters of approximately 100 nm embedded within a tissue specific matrix. Appropriate engineering of nanobiomaterials making use of particles, crystals, fibers, composites, or surface topographies may lead to biomimetic constructs that exhibit a favorable inductive interplay with the host cells and tissues. Detailed and standardized investigations are necessary to predict the cellular and organ reaction upon exposition to those nanomaterials. Egli, R.J., Luginbuehl, R., 2012. Tissue engineering – nanomaterials in the musculoskeletal system. Swiss Medical Weekly 142, w13647.

with nanostructured surface features. The beneficial aspects of nanocomposites are vast; however, there are some potential risks of nanocomposites due to their small size, such as their capability of penetrating pores in tissues and certainly cells if such constituent nanomaterials become released from the nanocomposites. It has now been well established that different nanostructures may lead to toxicity or have exceptional biocompatibility depending on the chemistry, geometry, and manner into which they are introduced into composites. Toxicity of nanomaterials are such a concern because the reduction in size and corresponding increase in specific surface area and surface energy may cause nanomaterials (more so than conventional or micron materials) to be more biologically active (Warheit, 2006; Oberdorster et al., 2005). Moreover, nanocomposites are smaller than some cells and most cellular organelles, which means they can be taken up within the structures and interfere with cellular processes. Some metal content in nanocomposites may be quite toxic. For example, researches have shown that silver ions induce oxidative stress (Cortese-Krott et al., 2009). Pb, Cu, Ni, Co, Zn, etc. will all show different cytotoxicity in cell culture (Okazaki and Gotoh, 2013). As another example, Zn ion release from TiO_2 nanotubes at a high concentration (0.36 ppm) can lead to stem cell death (Liu et al., 2014).

4.3.1 Ceramic–matrix nanocomposites

Ceramics are broadly used in a large variety of medical device (particularly, orthopedics) applications requiring both structural and functional properties. Ceramic nanocomposites based on ceramic nanomaterials have been studied to improve mechanical properties and alter functional properties, such as beta-$CaSiO_3$/beta-$Ca_3(PO_4)_2$-reinforced composite bioceramic scaffolds, and enhance bone regeneration with great osteoconductivity and osteostimulation (Liu and Webster, 2007; Wang et al., 2012). The ceramic nanocomposites have been broadly defined as either a ceramic nanophase in a ceramic matrix, a carbonaceous nanophase in a ceramic matrix, or to encompass a metal as the second component in a ceramic matrix. This combination of properties can lead to a new generation of medical devices and implants combining mechanical properties with bioactive properties. Calcium phosphate, calcium sulfate, and hydroxyapatite (HA) are clinically used as implant coatings or fillers for their attractive biodegradable, bioactive, and osteoconductive properties to bone (Wang et al., 2012; Luo et al., 2011). Zirconia/alumina nanocomposites, also known as alumina-toughened zirconia because they consist of a zirconia matrix reinforced with alumina nanoparticles, show exceptional resistance and extraordinary toughness. Their biocompatibility is considered to arise from their chemical structure and components similar to natural bone.

Of course, one of the most popular ceramics used in orthopedic tissue engineering is hydroxyapatite (HA). Several researchers have developed HA ceramic-based composites for bone replacements. With different loading conditions of nanohydroxyapatite (nHA) particles, the nanocomposites showed great bioactivity toward bone cells and consequently new bone formation. The bioactivity of HA is due to the close matching of the chemical composition of the ceramic with the natural inorganic phase of bone (Alothman et al., 2013). However, poor resorbability and brittle constructs

are problems that occur when using microsized HA particles. Nanosized HA (nHA) can be incorporated into highly porous collagen scaffolds to produce collagen–nHA biocomposite scaffolds with improved resorbability and mechanical characteristics (Porter et al., 2007).

ZnO and MgO nanoparticles have been shown to increase bone cell functions and decrease infection (Liu et al., 2015; Weng and Webster, 2012). Nano zinc oxide (ZnO) also can induce osteogenic properties from stem cells (Liu et al., 2015). Composites incorporating ZnO nanoparticles with a diameter near 60 nm can form a scaffold for tissue regeneration. The size of laminin, collagen, and fibronectin, which are all major components of the natural ECM, is on the same order of magnitude as a ZnO nanoparticle. Moreover, the piezoelectric and antibacterial properties of ZnO particles make it a good choice for orthopedic implant applications (Seil and Webster, 2008).

4.3.2 Metal–matrix nanocomposites

Metallic matrix composites reinforced with nanoparticles for orthopedic applications are being investigated worldwide. The reduced size of the reinforcement phase down to the nano-scale of the particles results in a remarkable improvement of a composite's mechanical properties (Sanaty-Zadeh, 2012). Different kinds of matrix metals have been coupled with several types of a nanometric phase, such as ceramic compounds, intermetallic materials, and carbon allotropes to reinforce metals and alloys (Casati and Vedani, 2014). The carbon nanotube–metal matrix (Al, Mg, Cu) composite is currently being developed, which is characterized by high strength and stiffness suitable for orthopedic applications (Casati and Vedani, 2014). Carbon nanotubes may be an important tissue engineering material for improved tracking of cells, sensing of microenvironments, delivering of transfection agents, and scaffolding for incorporation within the host's body (Harrison and Atala, 2007). However, as mentioned previously, carbon nanotubes will lead to cytotoxicity in some conditions.

Not only carbon nanotubes, but other carbon-related composites (such as graphene) combined with noble metals also have significant cytotoxicity (Zhou et al., 2014). Metallic ions act to provide an important role in enzymes and cell-signaling pathways in the human body. In health systems, free metallic ion concentrations are maintained at very low levels and the anomalous metallic ion metabolism can contribute to pathological states such as hemochromatosis and Wilson disease (Milman et al., 2003). For example, Zn ions have great osteogenic properties in low concentrations. However, Zn also shows cytotoxicity when released at high levels. Importantly, stem cells showed different morphologies with different concentrations of Zn ions (Fig. 4.3). It has been shown that on pure Ti, the stem cells spread relatively poorly with a round shape. When Zn ion release is lower than 0.3 ppm, stem cells possessed a polygonal morphology and more spread filopodia. The vinculin cell membrane protein was highly expressed. Vinculin formed dot-shaped structures, which indicated the formation of focal contacts between the cells and sample surfaces. The higher Zn ions caused the cells to shrink and agglomerate with poorly expressed vinculin and nonuniform morphologies (Liu et al., 2015). There are also

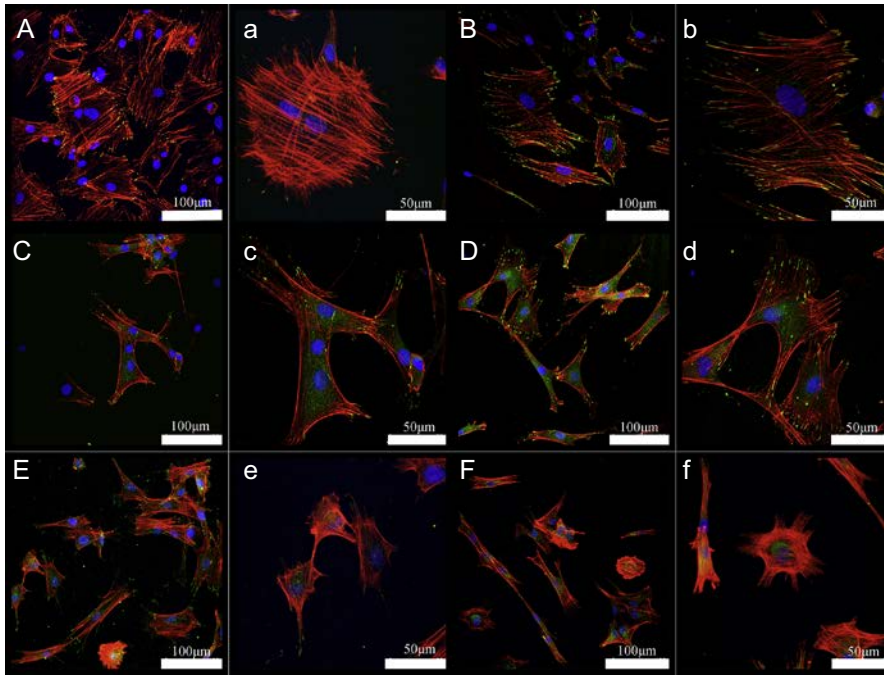

Figure 4.3 Fluorochrome micrography of stem cells cultured for 24 h on (A, a) Ti, (B, b) TNT, (C, c) TNT–Zn 0.005, (D, d) TNT–Zn 0.015, (E, e) TNT–Zn 0.030, and (F, f) TNT–Zn 0.075. Notes: Actin is shown in red, vinculin is shown in green, and the cell nucleus is shown in blue. (a–f) are the magnification of (A–F), respectively. The vinculin protein expressed was more evident on (C) and (D), and there were more extensive filipodia than on the other figures. On (E) and (F), some cells spread poorly. (A) and (B) have fewer polygonal and elongated shapes of cells. Abbreviations: *Ti*, titanium; *TNT*, TiO_2 nanotube.

additional studies, which showed metallic element toxicity. For example, Ag^+ at the concentration of 40 μM will lead to low viability of human skin fibroblasts and at 60 μM will inhibit the proliferation of cells (Liu et al., 2014; Hu et al., 2012). The stability of metallic ion states is important for systemic adverse effects of metallic ion-based composites. This is why some of the most prominent metallic ions oxidize readily in the body, such as Ti, Zn, Mg, etc.

Loading metallic ions into matrices and binding them into a suitable substrate can control the release of metallic ions over long periods to reduce toxicity yet maintain biological activity (Kawashita et al., 2000; Alt et al., 2004). However, caution needs to be taken because although, through such methods, metal release can be controlled at a safe level for cells, some metallic elements have a low corrosion resistance (such as copper) which will compromise the physical properties of materials for tissue engineering (Wan et al., 2007). Thus, incorporating metal elements into a titania nanotube is a method to slow metal ion release and lower the corrosion of metals, such as ZnO particles added to titania nanotubes to modify the surface of an implant to achieve slow Zn ion release (Liu et al., 2014).

Magnesium and its alloys have also been another intriguing metal for orthopedic applications due to its biodegradability and because it occurs naturally in the body. Magnesium undergoes rapid corrosion in physiological conditions and produces magnesium hydroxide ($Mg(OH)_2$), leading to the evolution of hydrogen gas (Keim et al., 2011). Although the corrosion products are nontoxic at low concentrations, mechanical properties and the rate of tissue healing are severely affected due to uncontrolled rapid degradation of magnesium. In addition, the rate of hydrogen evolution affects the healing process due to lower cell activities at the material tissue interface (Li et al., 2010; Ratna Sunil et al., 2014). Therefore, for biodegradable implants based on metallic matrices, it is important to develop a metal or alloy combined with a ceramic or polymer to obtain corrosion resistance composites for orthopedic tissue engineering. Different kinds of matrix metals have been coupled with several types of nanometric phases. Ceramic compounds (SiC, Al_2O_3, etc.), intermetallic materials, and carbon allotropes have all been used to reinforce Al, Mg, Cu, and other metals and alloys (Casati and Vedani, 2014). Also, anodization can improve the anticorrosion properties of Ti, such as anodizing titanium to possess titania nanotubes which showed exceptional properties for orthopedic applications (Liu et al., 2015).

4.3.3 Polymer–matrix nanocomposites

Lastly, polymer–matrix nanocomposites consist of a polymer having nanoparticles or nanofillers dispersed in the polymer matrix. In tissue engineering, polymer nanocomposties can be used for the replacement of orthopedic tissues, which have been destroyed by sickness or accidents, such as musculoskeletal tissue. The polymer nanocomposites can be divided into biodegradable and nonbiodegradable polymer nanocomposites. Nonbiodegradable polymers have been used in bone tissue engineering due to their improved mechanical properties and chemical stability over biodegradable polymers (Sahoo et al., 2013). There are many kinds of nonbiodegradable polymers used for bone tissue engineering such as polyethylene, polypropylene, polytetrafluoroethylene, and polyamide (Kamelger et al., 2004; Fang et al., 2006). However, some of these polymers, such as polyethylene and polypropylene, provoke a severe immune response (Sahoo et al., 2013).

Biodegradable polymers are a specific type of polymer that breaks down after its intended purpose to result in natural by-products (Avérous and Pollet, 2012). Aliphatic polyesters such as polylactide (PLA), poly(glyco-lides) (PGA), and poly (ε- caprolactone) (PCL) have attracted wide attention for their biodegradability and biocompatibility in the human body (Armentano et al., 2010). They have been demonstrated to be biocompatible and degrade into nontoxic components with a controllable degradation rate in vivo (Lin et al., 2003). Nanophase forsterite (Mg_2SiO_4) has been introduced as a bioceramic and combined with PCL to obtain a bioactive nanocomposite (Kharaziha et al., 2013). For example, in just one of many studies, poly(L, DL-lactide) (PLA) and β-tricalcium phosphate (β-TCP) were implanted into the sheep right tibia. Only a mild inflammatory response was observed in the first 12 months. However, after 24 months, a strong inflammatory reaction was reported

(Ignatius et al., 2001). The inflammatory tissue reaction and decreased strength of the PLA nanocomposites were attributed to the degradation of the PLA component, which means that PLA has a risk for tissue regeneration over the long term and perhaps better polymers are needed (Ignatius et al., 2001). Some have tried to improve the properties of bioresorbable lactide-glycolide copolymer (PLGA) blends by combining it with different kinds of fillers of natural and synthetic origin, such as carbon fibers and ceramics based on calcium phosphates (hydroxyapatite, tricalcium phosphate, etc.). Liu et al. (2006) reported the increased dispersion of nanophase titania in PLGA decreased the harmful change in pH normal during PLGA degradation. The modifying phase present in the polymer matrix has an influence on the mechanical properties of the composite, cell response, and the process of its degradation (Cieslik et al., 2009).

As an artificial support in the human body, the biodegradable polymer–matrix nanocomposites should possess both suitable mechanical and biological properties. Because biomaterials are expected to improve the regeneration of new tissues, degradable and absorbable polymer nanocomposites have to be biocompatible and degrade into nontoxic components at a controllable degradation rate. The degradation time and progression of polymer-based composites after performing their functions in the body are significant properties determining their usefulness in orthopedics. The factors determining this phenomenon are, among others, their crystallinity, molar mass, porosity, pH, or environmental temperature (Cieslik et al., 2009). Composites based on HA particles and biodegradable polymers have been used clinically in various forms due to the good osteoconductivity and osteoinductivity of HA and biodegradability of the polymer matrix in the composites. HA has a positive influence upon bone healing and bone restoration because of its ability to initiate and stimulate the processes involved. It plays a particularly important role when long-lasting bone restructuring processes are required (Lin et al., 2003). A study has proved that PLGA combined with HA are fully biocompatible materials (Cieslik et al., 2009). Nanoparticles of metals or carbon nanostructures have also been introduced into a polymer matrix, because they exhibit significant physical, chemical, and biological properties. Silver (Ag) nanoparticles have been investigated for its antibacterial properties (Panacek et al., 2006; Morones et al., 2005; Baker et al., 2005). Drug delivery can be achieved using magnetic nanocomposites, which incorporates biodegradable polymer microspheres with drugs and magnetic nanoparticles. The drug can release through swelling, diffusion, and degradation, such as $(Co_{0.5}Zn_{0.5})\ Fe_2O_4$ in a biodegradable poly (lactic-co-glycolic acid) (PLGA) matrix. However, cytotoxicity may come from the PLGA or metal nanoparticles (Wamocha et al., 2013; Meyer et al., 2012). Carbon nanotubes or carbon nanofibers have special structures, which can improve the composite's mechanical strength (Harrison and Atala, 2007; Shi et al., 2006). However, the toxicity of the metal and carbon nanostructure is still a problem, similar to the other kinds of nanocomposites for tissue regeneration.

Although some potential cytotoxicity occurs with some polymers or metallic ions, there is some research using polymer-based bioactive ceramic composites combined with metals to improve the mechanical and bioactive properties for biomaterials.

High-density polyethylene (HDPE)–hydroxyapatite (HA)–aluminum oxide (Al_2O_3) composite-based implant materials showed great biocompatibility for orthopedic applications, especially for bone replacement (Tripathi et al., 2013) (Table 4.1).

4.4 Biocompatibility and toxicity for musculoskeletal tissue

Now that different nanocomposite systems have been discussed, we will cover their specific applications in musculoskeletal tissue. According to different musculoskeletal tissue and different mechanical properties (Fig. 4.4), the applications of the nanocomposites vary widely. The toxicity and biocompatibility of nanocomposites can, thus, lead to different effects in different muscoskeletal tissues as will be discussed.

4.4.1 Skeletal tissue

The skeletal system provides the shape and form to human bodies and also supports and protects body movement, produces blood, and stores minerals. As mentioned, natural bone tissue possesses a nanocomposite structure that provides appropriate physical and biological properties. Thus, for bone tissue regeneration, it is important to mimic this unique structure for proper bone tissue regeneration. Because no one single material can mimic the structure or function of natural bone, nanocomposites are an optimal choice for skeletal tissue regeneration. For bone fracture repair, there are usually two types of treatment: external and internal fixation (Avérous and Pollet, 2012). External fixation keeps bone fragments aligned by an outside-of-the-body fixation system (Scholz et al., 2011). Internal fixation uses implants to hold bone fragments in place inside the body. A variety of polymer composites are available for internal fixation. The biodegradable polymer composites, such as poly(L-lactic acid) (PLLA), poly(glycolic acid) (PGA), or their copolymers, and poly(L-lactic-co-glycolic acid) (PLGA) have readily been approved for human clinical use (Mano, 2004). However, the selection of matrix polymers must be careful, because some polymers show toxic or extensive inflammatory reactions with human tissues. It is difficult to retain good mechanical properties and at the same time achieve bioactive degradation at an acceptable rate (Fujihara et al., 2004). A biologically inert thermoplastic polymer, poly-ether-ether-ketone (PEEK), a common spinal implant material which possesses mechanical resistance even under extreme body forces, has been studied in recent years (Fujihar et al., 2004). However, in general, the fabrication of high mechanical strength and good fatigue resistance in pure polymers is a challenge compared to metallic materials (Fujihara et al., 2004).

For skeletal defects, defects can be filled with autologous tissue or with biomaterials, which stay in place or are absorbed over time (Egli and Luginbuehl, 2012). Researchers expect nanocomposites to mimic the nanodimensional natural structure of tissues and generate the micro- and nanoenvironment which can induce related cells to form a competent tissue (Engler et al., 2006). Natural bone mainly consists

Table 4.1 **Musculoskeletal applications of various biomaterials**

Biomaterial		Applications			References
Biopolymers					
PLLA	Poly(L-lactic acid)	Bone			Kumbar et al. (2008)
PLGA	Poly(lactic acid-co-glycolic acid)	Bone	Cartilage		Vallet-Regi et al. (2007)
PGA	Poly(glycolic acid)	Bone	Tendon, ligament	Cartilage	Sahoo et al. (2006)
PCL	Poly(ε-caprolactone)	Bone	Muscle	Cartilage	Gogolewski et al. (1993) Singh et al. (2014)
PPF	Poly(propylene fumarate)	Orthopedic			Liu et al. (2010)
PLA	Poly(lactic acid)	Bone	Tendon, ligament	Cartilage	Sahoo et al. (2006) Yang et al. (2013)
PEEK	Poly ether ether ketone	Bone			Fujibayashi et al. (2004)
PMMA	Poly(methyl methacrylate)	Bone			Fujibayashi et al. (2004)
PLAGA	Poly(lactide-co-glycolide)	Muscle	Ligament		Gogolewski et al. (1993) and Sankar et al. (2013)
Bioceramics					
nano HA	Hydroxyapatite	Bone	Cartilage		Jabbari (2009) and Jie et al. (2007)
CaP	Calcium phosphates	Bone			Suchy et al. (2011) and Marmotti et al. (2013)
Metal nanoparticles-base nanocomposites					
Ag	Silver	Bone			Park et al. (2005)
ZnO	Zinc oxide	Bone			Liu et al. (2015)
MgO	Magnesium oxide	Bone	Cartilage		Weng and Webster (2012)
TiO_2	Titanium dioxide	Bone			Liu et al. (2015)
Al_2O_3	Aluminum oxide	Bone			Casati and Vedani (2014)

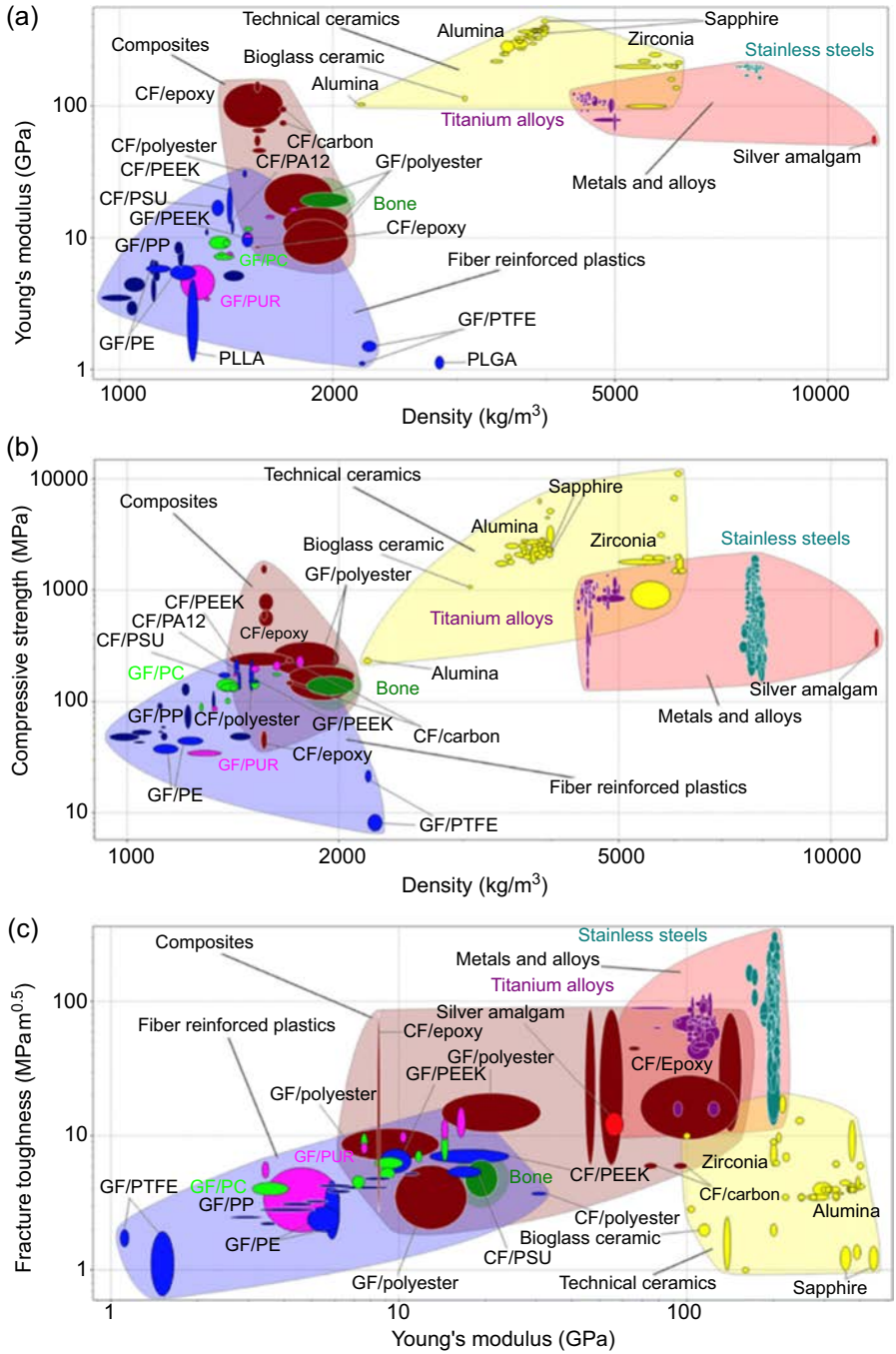

Figure 4.4 Comparison of (a) stiffness, (b) strength, and (c) fracture toughness for metals, technical ceramics, composites, and fiber-reinforced plastics with respect to those of bone. *CF*, carbon fiber; *GF*, glass fiber; *PA12*, polyamide12; *PC*, polycarbonate; *PE*, polyethylene; *PEEK*, poly ether ether ketone; *PLGA*, poly(L-lactic-co-glycolic acid); *PLLA*, poly(L-lactic acid); *PP*, polypropylene; *PSU*, polysulfone; *PTFE*, polytetrafluoroethylene; *PUR*, polyurethane. Scholz, M.S., Blanchfield, J.P., Bloom, L.D., Coburn, B.H., Elkington, M., Fuller, J.D., Gilbert, M.E., Muflahi, S.A., Pernice, M.F., Rae, S.I., Trevarthen, J.A., White, S.C. Weaver P.M., Bond, I.P., 2011. The use of composite materials in modern orthopaedic medicine and prosthetic devices: a review. Composites Science and Technology 71, 1791–1803.

of collagen fibrils mineralized by HA-like calcium phosphate phases. Calcium phosphate phases have been integrated in nanocomposites and investigated with osteoclasts (bone-resorbing cells) and osteoblasts (Heinemann et al., 2013). Extracellular calcium ion concentrations also have an effect on osteoclast dysfunction and is responsible for the ratio between osteoblasts and osteoclasts within a bone multicellular unit (Negishi-Koga and Takayanagi, 2009; Sakai et al., 2010). Calcium phosphates have been used as bioactive materials since the early 20th century to treat bone defects (Egli and Luginbuehl, 2012). Hydroxyapatite (HA)- containing polymers have been proposed for improving the biological properties of bone cements as well. To improve the mechanical properties of these ceramic matrices, a good dispersion of carbon nanotubes in the matrix can be used. Ceramic nanocomposites reinforced with carbon nanotubes improve mechanical properties (Uemura et al., 2003). Although ceramics have good biocompatibility properties for orthopedic applications, the second phase (such as the carbon nanotubes) may cause toxicity concerns which need to be carefully monitored (Liu et al., 2007). The improper incorporation of carbon nanotubes (intratracheal installation of 0.5 mg of carbon nanotubes into mice can induce alveolar macrophage activation) may lead to immunotoxicity and cause some harmful effects such as inflammatory and fibrotic reactions, which will not be good for musculoskeletal structure and tissue regeneration (Yu et al., 2008). Under certain conditions, carbon nanotubes can even enter human cells and accumulate causing cell death (Porter et al., 2007). There have been studies showing that carbon nanotubes can pose a serious risk to humans especially under chronic exposure conditions (Poland et al., 2008; Lam et al., 2006; Mata et al., 2014). On the other hand, there have been reports of using carbon nanotubes to strengthen calcium phosphate (CaP) ceramics showing that hot-pressed carbon nanotubes possess no acute toxicity in a human osteoblastic cell line (Alothman et al., 2013; Mata et al., 2014). Poly(methyl methacrylate) (PMMA) has long been used to secure orthopedic implants to skeletal bone. Studies have proved the PMMA nanofibrous scaffolds combined with HA nanoparticles enhances the biological functions of osteoblasts (Xing et al., 2013) (Fig. 4.5).

Although there is a wealth of knowledge and data concerning how nanocomposites can improve bone growth, there are some cautions to note. When separating from the composites, nanoparticles can lead to a sustained, uninterrupted activation of monocyte cells and, thus, lead to chronic inflammation and even tumor formation through the persistent release of inflammatory cytokines, such as Interleukin (IL)1 and IL12. These inflammatory cytokines will lead to tissue degradation and bone loss. Moreover, nanomaterials in musculoskeletal applications may also be absorbed by the lymphatic system and transported to the lymph nodes and organs (Urban et al., 2000). To be accepted as a comprehensive alternative to natural bone, synthetic bone-graft substitutes need to meet a number of requirements, including providing mechanical support (such as incorporating 15% magnetic nanoparticles in PCL and increasing the scaffolds' tensile strength to 26.2 MPa, yield strength to 15 MPa, and stiffness to 86.7 MPa (Singh et al., 2014)), and bioactivity in terms of osteoinductivity, which is the ability to induct undifferentiated inducible-osteoprogenitor cells to form osteogenic lineage osteoprogenitor cells. Osteoinductivity is essential for the successful healing of large

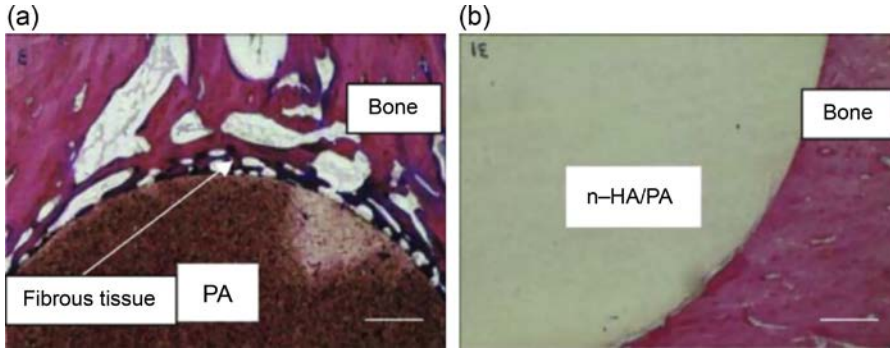

Figure 4.5 Photographs of histological analysis of polyamide (PA) and nHA/PA composite bone implantation, (a) fibrous capsule (*arrow*) around PA implant, (b) composite directly combined with bone, bar = 200 μm.
Jie, W., Hua, H., Lan, W., Yi, H., Yubao, L., 2007. Preliminary investigation of bioactivity of nano biocomposite. Journal of Materials Science. Materials in Medicine 18, 529–533.

critically sized bone defects (Danoux et al., 2014). A number of nanomaterials have shown osteoinductive potential, such as polymers, metals, and biomaterials with calcium phosphate (CaP) ceramics (Winter and Simpson, 1969; Fujibayashi et al., 2004).

A number of studies have addressed the use of composites with CaP which have shown strong osteoinductive potential, and their intrinsic brittleness could be overcome by various combinations of polymers (Tanner, 2010). In vivo, however, polymers still generally cause an inflammatory response. A thin dense fibrous capsule is commonly observed around polymer composite materials, suggesting a mild tissue response (Danoux et al., 2014; Gogolewski et al., 1993). Another problem with polymeric materials is wear debris. When implanting into articulating surfaces, polymeric wear debris is constantly generated, which is recognized as a major initiating event in the development of the periprosthetic osteolysis and aseptic loosening. Without other reinforcement, the poor mechanical properties of a polymeric material will increase the risk of osteolysis (Tripathi et al., 2013). Ceramic content in polymer composites can also induce cytotoxicity properties at a high-volume concentration (more than 15 vol.% of additives), such as hydroxyapatite (HA), and tricalcium phosphate (TCP) (Suchy et al., 2011).

Nanocomposites also can be used as scaffolds for drug delivery for bone regeneration. The scaffold should be biocompatible with osteoconductive properties and allow cells to attach, proliferate, and form an ECM. Drug delivery systems have been developed to be both biodegradable and osteoconductive (such as degradable polymers and calcium phosphate compounds) (Liu et al., 2010; Cunniffe et al., 2010). Many materials such as polyurethane, poly (D,L-lactic acid), collagen, and HA can be synthesized to form scaffolds for drug delivery (Liu et al., 2010; Cunniffe et al., 2010). Bone growth factors or related proteins such as basic fibroblast growth factor (bFGF), recombinant human bone morphogenetic protein-2 (rhBMP2), platelet-derived growth factor (PDGF), and osteonectin can be decorated in the scaffold to improve bone regeneration by release from scaffolds (Jabbari, 2009; Liao et al., 2009). There have

been clinical applications of rhBMP2/ absorbable collagen sponge (ACS) in craniofacial tissue, and it was demonstrated that rhBMP2 was associated with adverse events, such as local swelling, and in preclinical evaluations, sarcoma formation. The frequency and severity of adverse events increase with greater rhBMP2 doses (Wikesjo et al., 2007, 2008).

Controlled drug release systems can overcome the disadvantage of traditional drug dosage forms, offer more effective methods to optimize drug dosage, and deliver drugs to specific sites, or prolong drug delivery duration—and nanomaterials can help in these controlled drug release systems by increasing surface area for loading and/or creating localized drug release even inside cells (Watari et al., 2009). However, direct encapsulation of drugs in scaffolds does not provide a means to control the relative release rates of multiple molecules or biologic agents for sequential delivery. More studies are needed for controlling the rate of drug release (Liu et al., 2010). The high surface area and pore volume of nanoscaffolds are two factors for control of the drug release. So long as the pore size allows the drug to get into the matrix, the higher the surface area, the higher the amount of drug adsorbed. The final drug content can be very sensitive to the surface area (Masami Okamoto and John, 2013). Moreover, the functionalized surface of nanoscaffolds can be used in a drug release control system and develop increased drug surface interaction nanocomposites.

Nanosized composites increase specific surface area, which is one of the aspects that affect biocompatibility. Nanoparticle dissolution and corrosion are important factors for biocompatibility, which are related to the specific surface area. For example, HA–collagen composite coatings can lead to the failure of a dental or bone implant. Apatite dust produced by dropout exfoliation delamination or abrasion can cause inflammation and the resorption of new bone and the coating of apatite. Another typical serious case of apatite dust is osteolysis which is caused by the inflammation induced by abraded particles (Watari et al., 2009).

On the other hand, nanoparticles less than 10 μm can pass through the bronchial epithelial cell. Then, there is the possibility that the uptake of nanoparticles occurs through the respiratory system and the digestive system. The nanoparticles can induce phagocytosis in cells and inflammation in tissue in vivo, which leads to chronic inflammation (Watari et al., 2009).

Thus, although skeletal tissue has been studied for many years, complex materials to regenerate the interactions between tissues and nanocomposites still remain to be discovered.

4.4.2 Muscular tissue

Skeletal muscle can repair by itself, except to restore significant tissue loss, such as the consequence of trauma, congenital defect, tumor ablation, or denervation (Rossi et al., 2010). Skeletal muscle tissues are primarily attached to bones and provide for movement of the skeleton. Tissue engineering is an approach which can mimic organogenesis using cell biology and biomaterials to generate functional muscle tissues by imitating neo-organogenesis from mononucleated stem cells to differentiated myofibers (Stern-Straeter et al., 2007). A variety of biomaterials, such as alginate,

collagen, hyaluronan, hydroxyapatite, and polyethylene glycol are being explored as scaffolds for muscular tissue regeneration. One approach is using fabricated artificial muscle tissue to reimplant the myogenic cell line (Watari et al., 2009). Thus, an ideal orthopedic muscle biomaterial should provide an optimal surface for cell proliferation and differentiation to enhance tissue neogenesis. It also should be biocompatible, bioresorbable, and nonimmunogenic with a high affinity to biological surfaces (Rossi et al., 2010).

In vitro tissue engineering a three-dimensional (3D)-differentiated functional muscle tissue was cultured following a process in a controlled environment (Fig. 4.6). In vivo, the process is shown in Fig. 4.6. The tissue engineering for soft tissue usually demands a scaffold to provide a temporary artificial matrix for cell seeding. The scaffolds should exhibit high porosity, proper pore size, biocompatibility, biodegradability, and proper degradation rate (Sankar et al., 2013). Biopolymer nanocomposites have become the focus for orthopedic muscle regeneration because they can provide the biologically inspired 3D structure for cell seeding. Several polymers such as polyurethane and collagen nanofibers can be used for maintaining the biological and structural integrity of various tissues and organs, such as a PGA fiber seeded with myoblasts, gelatin, and fibronectin-coated electrospun PLLA can be used as muscle tissue grafts (Kumbar et al., 2008; Sahoo et al., 2006).

Mature skeletal muscle tissue is composed of multinucleated, postmitotic fibers that cannot be regenerated. Locally, quiescent populations of myogenic progenitors exist that will fuse with existing or damaged myotubes to form new ones. In major injuries in which the muscle structure is irreversibly compromised, engineered-muscle constructs may overcome problems of muscle transfers and provide a successful replacement device for muscle regeneration (Kumbar et al., 2008). Electrospun-nanofiber scaffolds show morphological similarities to the natural ECM, characterized by ultrafine continuous fibers, high surface-to-volume ratio, high porosity, and variable pore-size distribution, which can be used in the regeneration of skeletal muscle with improved mechanical properties (such as poly (3-hydroxybutyrate-co-3-hydroxyvalerate) (PHBV)). PHBV nanofiber matrices with a specific surface area of 140 m^2/g, and 70% porosity showed a Young's modulus of 350 ± 30 MPa, a tensile strength of 8.6 ± 0.8 MPa, and an elongation at break of 19.5 ± 1.5 mm (Kumbar et al., 2008). An in vitro study showed that multipotent cells are able to start a transdifferentiation process toward very soft tissues according to the elasticity of tissue ECMs, with an intermediate stiffness (~10 kPa). causing stem cells to differentiate toward muscle. Biopolymers presently used in tissue engineering are extremely stiff. Thus, the engineering of soft-tissue replacements needs to be explored by creating biopolymers softer than those presently available today (Masami Okamoto, and John, 2013).

4.4.2.1 Tendons

Tendons and ligaments have similar patterns with fibers, which are oriented parallel to the stress axis and consist of collagen type III embedded in a proteoglycan matrix. The tensile strength of tendon is about 50–150 MPa, and the elastic modulus is about 1200–1800 MPa. Tendons and ligaments have some plasticity to adapt to changing

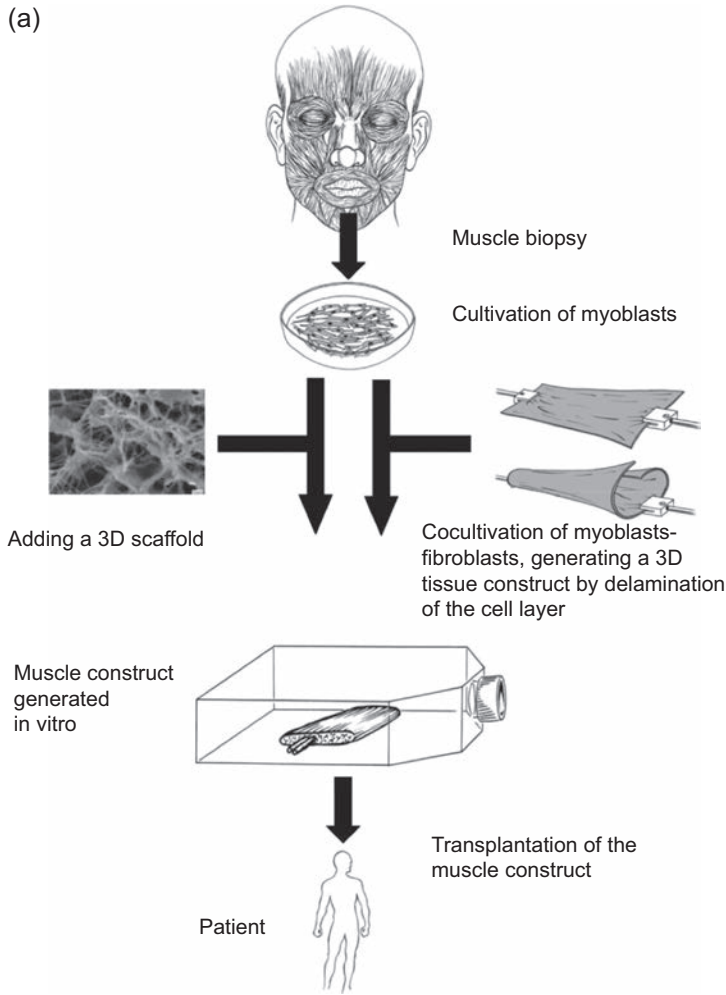

Figure 4.6 (a) The in vitro tissue engineering concept. The in vitro approach to skeletal muscle tissue engineering attempts to create 3D-differentiated, functional muscle tissue with the use of an ECM or by cocultivation of myoblasts and fibroblasts in vitro by extracting stem cells from, eg, muscle biopsies, followed by their expansion and differentiation in a controlled environment. (b) The in vivo tissue engineering concept. The in vivo tissue engineering approach aims to reconstruct functional tissue through the cultivation and expansion of satellite cells in vitro followed by reimplantation using a transport matrix, which allows subsequent differentiation of cells in vivo.

Milman, N., Pedersen, P., Steig, T., Melsen, G.V., 2003. Frequencies of the hereditary hemochromatosis allele in different populations. Comparison of previous phenotypic methods and novel genotypic methods. International Journal of Hematology 77, 48–54.

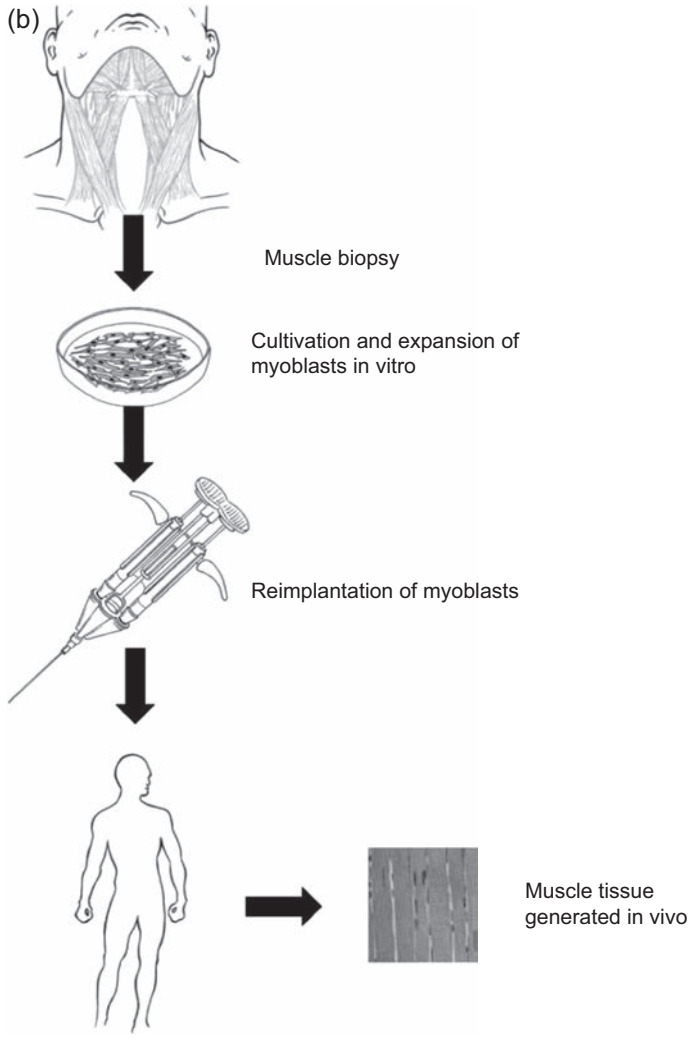

Figure 4.6 Continued.

stresses and for regeneration (Egli and Luginbuehl, 2012). Tendon injuries are the most common body trauma in the young and physically active population. The combination of tendon prostheses with an autologous cell can generate a tendon tissue and provide an approach to current tendon injury problems. Using a biodegradable scaffold, which will functionally support and provide stimuli to the regenerating tissue, is a novel approach (Kumbar et al., 2008). For example, the poly lactide coglycolide polymer (PLAGA) was used to fabricate nanofibrous scaffolds for tendon regeneration (Huang et al., 2006). However, fabricating polymer nanofibers utilizes fluorinated and toxic organic solvents to dissolve polymers. The toxic solvents may affect the structural conformation of biopolymers and proteins and result in cytotoxicity for muscle or tendon regeneration.

4.4.3 Cartilage

Cartilage is a thin dense connective tissue in joints. Thus, the articular cartilage may be considered a soft tissue composed primarily of an ECM with a population of chondrocytes distributed throughout the tissue (Gloria et al., 2010). Cartilage injuries are commonly found in orthopedic surgery, and spontaneous healing of osteochondral lesions leads to the formation of fibrocartilage, a type of functional repair tissue that has different biochemical composition and inferior biomechanical properties from those of hyaline articular cartilage (Marmotti et al., 2013). In cartilage regeneration, chondrocytes are isolated from a cartilage biopsy and then expanded in conventionally cultured monolayers. Cells can be seeded in woven nanocomposites for scaffolds for functional tissue engineering of cartilage. The biocompatible materials should be shown to be conductive to chondrogenesis, such as PGA and agarose or PGA and fibrin (Moutos et al., 2007). Biodegradable polymers such as PLA, PGA, PLGA (poly(lactic-co-glycolic acid)), PCL, and PLCL are the major materials applied for cartilage regeneration (Alves da Silva et al., 2010). PLGA has been combined with calcium sulfate commercially as a biphasic implant that encourages the growth of cartilage and bone (Williams and Gamradt, 2008). Biomimetic rosette nanotubes were also used for the regeneration of cartilage; these nanotubes are obtained through an entropically driven self-assembly process of low-molecular-weight synthetic modules under physiological conditions (Sun and Webster, 2013).

Zhu et al. (2014) reported that NaOH-treated PLGA scaffolds possess created nano surface structures and have significant influence over initial protein interactions that mediate subsequent cell responses (Fig. 4.7). However, NaOH treatment could induce potential harmful chemical changes and alter the properties of PLGA (Park et al., 2005). On the other hand, NaOH-treated PLGA scaffolds may induce stem-cell differentiation into unnecessary cells, which in turn may lead to a relative decrease in the number of chondrocyte-like cells needed for cartilage regeneration (Park et al., 2005). Although the nanocomposites have great biocompatibility, another drawback is possible de-differentiation of the chondrocytes into fibroblast-like cells using some natural polymers (Frenkel and Di Cesare, 2004). Kon et al. reported a type I collagen–hydroxyapatite nanostructured biomimetic osteochondral nanocomposite for osteochondral regeneration, which has been introduced into clinical practice. However, there still have been some slower recovery cases and the subchondral lamina and bone were considered intact in a minority of cases (Kon et al., 2011). The Young's modulus of cartilage is in the range of 0.45 to 0.80 MPa, and, of course, it would be better to make nanocomposites with a similar mechanical value to cartilage. Thus, the engineered repair of cartilaginous tissues still has a way to go.

4.4.4 Ligaments

Ligaments are dense connective tissues constituted by a protein phase (collagen and elastin) and a polysaccharide phase (proteoglycans). The elastic modulus of ligament is about 150–355 MPa, and the tensile strength is less than 50 MPa. Their mechanical properties are determined by the relative amount of the two phases as

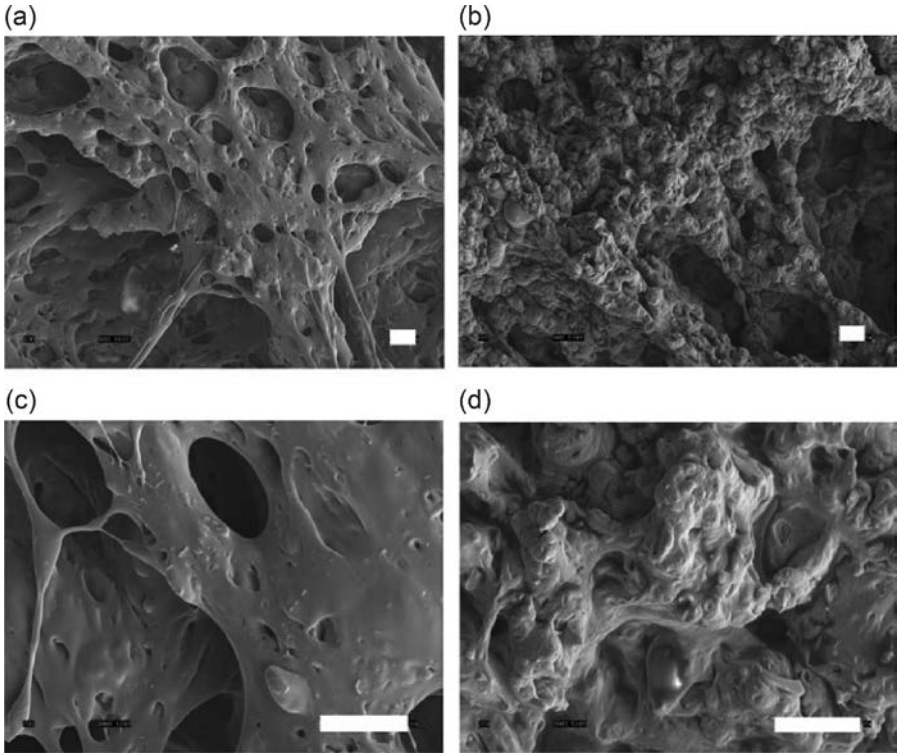

Figure 4.7 SEM images of (b, d) NaOH-treated and (a, c) nontreated PLGA scaffolds. Increased surface roughness was evident on NaOH-treated compared to nontreated PLGA. Top pictures are at a lower magnification, and the bottom pictures are at a higher magnification. Bar = 10 mm.
Park, G.E., Pattison, M.A., Park, K., Webster, T.J., 2005. Accelerated chondrocyte functions on NaOH-treated PLGA scaffolds. Biomaterials 26, 3075–3082.

well as geometrical factors, conformation, and orientation of the individual constituents. Ligaments show a hierarchical structure characterized by different levels of organization, including collagen molecules, fibrils, fibril bundles, and fascicles. In recent years, artificial prostheses were used to repair or replace damaged ligaments in ligament injuries. Benefiting from nanocomposite material science and technology, poly (2-hydroxyethyl methacrylate)-based hydrogels reinforced with poly (ethylene terephthalate) (PET) fibers and PLGA scaffolds characterized by a fibrous hierarchical structure were proposed as high-performance ligament prostheses. Nanotechnology based on 3D fibrous hierarchical designs, utilizing novel braiding techniques which permit the controlled fabrication of substrates with a desired pore diameter, porosity, mechanical properties, and geometry were used to design a scaffold that provided the newly regenerating tissue a temporary site for cell attachment, proliferation, and mechanical stability. This method produces scaffolds for ligament regeneration and showed a positive result (Ambrosio et al., 1998;

Cooper et al., 2005). The polymer content in nanocomposites may also lead to some cytotoxicity. The specific polymers' degradation products reduce local pH, which in turn induces an inflammatory reaction. Moreover, the rapid drop of pH in vivo may accelerate the polymer's degradation rate, which would not be good for tissue regeneration (Liu et al., 2006), such as PLGA, which can be used for ligaments and can also have this adverse effect.

4.5 Conclusions and future perspectives

Nanocomposites in orthopedic tissue engineering mimic the complex nanoarchitecture of natural bone, muscle, cartilage, and tendon tissue, providing a novel and practical approach to tissue regeneration. All ceramic, polymer, and metallic matrix nanocomposites offer a wide range of properties with different chemical and mechanical features; they also exhibit indispensable bioactivity. There is a great potential to improve current biomaterials and nanocomposite scaffolds for musculoskeletal tissue regeneration. However, the variety of different chemical elements and structures of nanocomposites make it difficult to predict unknown outcomes of exposure to musculoskeletal tissue. More research is clearly needed to fully understand favorable nanocomposite chemistries for musculoskeletal tissue.

When using nanomaterials in medical applications, their biocompatibility and performance are improved over conventional or microstructured materials; however, some caution must be taken. Disadvantages of nanocomposites for tissue engineering still exist, such as component stability, long-term stability, and service, structural integrity, mechanical and corrosion properties, and uncertain cytotoxicity (Sahoo et al., 2013). Therefore, the future design of nanocomposites for musculoskeletal tissue regeneration should focus on biocompatibility, mechanical properties, and biostability. Future research, from the biological side, needs to focus on the complex interaction between such materials. To predict the biological outcome, each combination of nanocomposite should be measured separately and determined with cell culture and in vivo approaches. Furthermore, it is essential that for manufacturing, well-defined standardized reference materials with test protocols are included (Egli and Luginbuehl, 2012). From the engineering side, all the biological, mechanical, and chemical properties should be stable over long periods and resorbability carefully controlled. More research is needed to optimize the composition, structure, and different properties of the various components in nanocomposites. More importantly, different musculoskeletal tissue should be applied with a different set of governing rules with fitted nanocomposites using mathematical models. Based on systems biology and a networking science point of view, using a more efficient method to design nanocomposites for tissue regeneration and applying it to clinical and surgical settings is necessary (Yang et al., 2013). Finally, establishing the test procedures to ensure the safe manufacturing and use of nanomaterials is urgently required and achievable. Because nanomaterials vary with respect to composition, size, shape, surface chemistry, and crystal structure, it is not appropriate to establish general safety regulations for all nanomaterials (Ignatius et al., 2001). A great number of novel nanocomposites have been reported

which show potential for the development of nanocomposites with advanced properties. Thus, to achieve the full potential of nanocomposites with great biocompatibility properties for all of musculoskeletal tissue regeneration, more sophisticated techniques and designs are needed; however, nanomaterials may be the answer.

References

Alothman, O.Y., Almajhdi, F.N., Fouad, H., 2013. Effect of gamma radiation and accelerated aging on the mechanical and thermal behavior of HDPE/HA nano-composites for bone tissue regeneration. Biomedical Engineering Online 12, 95.

Alt, V., Bechert, T., Steinrucke, P., Wagener, M., Seidel, P., Dingeldein, E., Domann, E., Schnettler, R., 2004. An in vitro assessment of the antibacterial properties and cytotoxicity of nanoparticulate silver bone cement. Biomaterials 25, 4383–4391.

Alves Da Silva, M.L., Martins, A., Costa-Pinto, A.R., Costa, P., Faria, S., Gomes, M., Reis, R.L., Neves, N.M., 2010. Cartilage tissue engineering using electrospun PCL nanofiber meshes and MSCs. Biomacromolecules 11, 3228–3236.

Ambrosio, L., De Santis, R., Nicolais, L., 1998. Composite hydrogels for implants. Proceedings of the Institution of Mechanical Engineers. Part H 212, 93–99.

Ap Gwynn, I., Wade, S., Kaab, M.J., Owen, G.R., Richards, R.G., 2000. Freeze-substitution of rabbit tibial articular cartilage reveals that radial zone collagen fibres are tubules. Journal of Microscopy 197, 159–172.

Avérous, L., Pollet, E., 2012. Environmental Silicate Nano-biocomposites. http://link.springer.com/book/10.1007%2F978-1-4471-4108-2.

Armentano, I., Dottori, M., Fortunati, E., Mattioli, S., Kenny, J.M., 2010. Biodegradable polymer matrix nanocomposites for tissue engineering: a review. Polymer Degradation and Stability 95, 2126–2146.

Ajayan, P.M., Schadler, L.S., Braun, P.V., 2003. Nanocomposite Science and Technology. Wiley.

Baker, C., Pradhan, A., Pakstis, L., Pochan, D.J., Shah, S.I., 2005. Synthesis and antibacterial properties of silver nanoparticles. Journal of Nanoscience and Nanotechnology 5, 244–249.

Banfield, J.F., Navrotsky, A., 2001. Nanoparticles and the Environment. Reviews in Mineralogy and Geochemistry, vol. 44. Mineralogical Society of America, Washington, DC, pp. 37–62.

Casati, R., Vedani, M., 2014. Metal matrix composites reinforced by nano-particles—a review. Metals 4, 65–83.

Cieslik, M., Mertas, A., Morawska-Chochol, A., Sabat, D., Orlicki, R., Owczarek, A., Krol, W., Cieslik, T., 2009. The evaluation of the possibilities of using PLGA co-polymer and its composites with carbon fibers or hydroxyapatite in the bone tissue regeneration process – in vitro and in vivo examinations. International Journal of Molecular Sciences 10, 3224–3234.

Cooper, J.A., Lu, H.H., Ko, F.K., Freeman, J.W., Laurencin, C.T., 2005. Fiber-based tissue-engineered scaffold for ligament replacement: design considerations and in vitro evaluation. Biomaterials 26, 1523–1532.

Cortese-Krott, M.M., Munchow, M., Pirev, E., Hessner, F., Bozkurt, A., Uciechowski, P., Pallua, N., Kroncke, K.D., Suschek, C.V., 2009. Silver ions induce oxidative stress and intracellular zinc release in human skin fibroblasts. Free Radical Biology and Medicine 47, 1570–1577.

Cunniffe, G.M., Dickson, G.R., Partap, S., Stanton, K.T., O'brien, F.J., 2010. Development and characterisation of a collagen nano-hydroxyapatite composite scaffold for bone tissue engineering. Journal of Materials Science. Materials in Medicine 21, 2293–2298.

Danoux, C.B., Barbieri, D., Yuan, H., de Bruijn, J.D., Van Blitterswijk, C.A., Habibovic, P., 2014. In vitro and in vivo bioactivity assessment of a polylactic acid/hydroxyapatite composite for bone regeneration. Biomatter 4, e27664.

Egli, R.J., Luginbuehl, R., 2012. Tissue engineering – nanomaterials in the musculoskeletal system. Swiss Medical Weekly 142, w13647.

Engler, A.J., Sen, S., Sweeney, H.L., Discher, D.E., 2006. Matrix elasticity directs stem cell lineage specification. Cell 126, 677–689.

Fang, L., Leng, Y., Gao, P., 2006. Processing and mechanical properties of HA/UHMWPE nanocomposites. Biomaterials 27, 3701–3707.

Frenkel, S.R., Di Cesare, P.E., 2004. Scaffolds for articular cartilage repair. Annals of Biomedical Engineering 32, 26–34.

Fujibayashi, S., Neo, M., Kim, H.M., Kokubo, T., Nakamura, T., 2004. Osteoinduction of porous bioactive titanium metal. Biomaterials 25, 443–450.

Fujihara, K., Teo, K., Gopal, R., Loh, P.L., Ganesh, V.K., Ramakrishna, S., Foong, K.W.C., Chew, C.L., 2004. Fibrous composite materials in dentistry and orthopaedics: review and applications. Composites Science and Technology 64, 775–788.

Gloria, A., De Santis, R., Ambrosio, L., 2010. Polymer-based composite scaffolds for tissue engineering. Journal of Applied Biomaterials and Biomechanics 8, 57–67.

Gogolewski, S., Jovanovic, M., Perren, S.M., Dillon, J.G., Hughes, M.K., 1993. Tissue response and in vivo degradation of selected polyhydroxyacids: polylactides (PLA), poly(3-hydroxybutyrate) (PHB), and poly(3-hydroxybutyrate-co-3-hydroxyvalerate) (PHB/VA). Journal of Biomedical Materials Research 27, 1135–1148.

Haidar, Z.S., 2010. Bio-inspired/-functional colloidal core-shell polymeric-based nanosystems: technology promise in tissue engineering, bioimaging and nanomedicine. Polymers 2, 323–352.

Harrison, B.S., Atala, A., 2007. Carbon nanotube applications for tissue engineering. Biomaterials 28, 344–353.

Heinemann, S., Heinemann, C., Wenisch, S., Alt, V., Worch, H., Hanke, T., 2013. Calcium phosphate phases integrated in silica/collagen nanocomposite xerogels enhance the bioactivity and ultimately manipulate the osteoblast/osteoclast ratio in a human co-culture model. Acta Biomaterialia 9, 4878–4888.

Henig, R.M., 2007. Our silver-coated future. OnEarth 29, 22–29.

Hu, H., Zhang, W., Qiao, Y., Jiang, X., Liu, X., Ding, C., 2012. Antibacterial activity and increased bone marrow stem cell functions of Zn-incorporated TiO_2 coatings on titanium. Acta Biomaterialia 8, 904–915.

Huang, N.F., Patel, S., Thakar, R.G., Wu, J., Hsiao, B.S., Chu, B., Lee, R.J., Li, S., 2006. Myotube assembly on nanofibrous and micropatterned polymers. Nano Letters 6, 537–542.

Hughes, L.C., Archer, C.W., Ap Gwynn, I., 2005. The ultrastructure of mouse articular cartilage: collagen orientation and implications for tissue functionality. A polarised light and scanning electron microscope study and review. European Cells and Materials 9, 68–84.

Ignatius, A.A., Betz, O., Augat, P., Claes, L.E., 2001. In vivo investigations on composites made of resorbable ceramics and poly(lactide) used as bone graft substitutes. Journal of Biomedical Materials Research 58, 701–709.

Jabbari, E., 2009. Engineering bone formation with peptidomimetic hybrid biomaterials. Conference Proceedings: Annual International Conference of the IEEE Engineering in Medicine and Biology Society. IEEE Engineering in Medicine and Biology Society 2009, 1172–1175.

Jie, W., Hua, H., Lan, W., Yi, H., Yubao, L., 2007. Preliminary investigation of bioactivity of nano biocomposite. Journal of Materials Science. Materials in Medicine 18, 529–533.

Kamelger, F.S., Marksteiner, R., Margreiter, E., Klima, G., Wechselberger, G., Hering, S., Piza, H., 2004. A comparative study of three different biomaterials in the engineering of skeletal muscle using a rat animal model. Biomaterials 25, 1649–1655.

Kawashita, M., Tsuneyama, S., Miyaji, F., Kokubo, T., Kozuka, H., Yamamoto, K., 2000. Antibacterial silver-containing silica glass prepared by sol-gel method. Biomaterials 21, 393–398.

Keim, S., Brunner, J.G., Fabry, B., Virtanen, S., 2011. Control of magnesium corrosion and biocompatibility with biomimetic coatings. Journal of Biomedical Materials Research. Part B, Applied Biomaterials 96, 84–90.

Kharaziha, M., Fathi, M.H., Edris, H., 2013. Effects of surface modification on the mechanical and structural properties of nanofibrous poly(epsilon-caprolactone)/forsterite scaffold for tissue engineering applications. Materials Science and Engineering. C, Materials for Biological Applications 33, 4512–4519.

Kon, E., Delcogliano, M., Filardo, G., Busacca, M., Di Martino, A., Marcacci, M., 2011. Novel nano-composite multilayered biomaterial for osteochondral regeneration: a pilot clinical trial. American Journal of Sports Medicine 39, 1180–1190.

Kumbar, S.G., James, R., Nukavarapu, S.P., Laurencin, C.T., 2008. Electrospun nanofiber scaffolds: engineering soft tissues. Biomedical Materials 3, 034002.

Lam, C.W., James, J.T., Mccluskey, R., Arepalli, S., Hunter, R.L., 2006. A review of carbon nanotube toxicity and assessment of potential occupational and environmental health risks. Critical Reviews in Toxicology 36, 189–217.

Li, J., Song, Y., Zhang, S., Zhao, C., Zhang, F., Zhang, X., Cao, L., Fan, Q., Tang, T., 2010. In vitro responses of human bone marrow stromal cells to a fluoridated hydroxyapatite coated biodegradable Mg-Zn alloy. Biomaterials 31, 5782–5788.

Liao, S., Ngiam, M., Chan, C.K., Ramakrishna, S., 2009. Fabrication of nano-hydroxyapatite/collagen/osteonectin composites for bone graft applications. Biomedical Materials 4, 025019.

Lin, A.S., Barrows, T.H., Cartmell, S.H., Guldberg, R.E., 2003. Microarchitectural and mechanical characterization of oriented porous polymer scaffolds. Biomaterials 24, 481–489.

Liu, H., Slamovich, E.B., Webster, T.J., 2006. Less harmful acidic degradation of poly(lactic-co-glycolic acid) bone tissue engineering scaffolds through titania nanoparticle addition. International Journal of Nanomedicine 1, 541–545.

Liu, H., Webster, T.J., 2007. Nanomedicine for implants: a review of studies and necessary experimental tools. Biomaterials 28, 354–369.

Liu, H., Zhang, L., Shi, P., Zou, Q., Zuo, Y., Li, Y., 2010. Hydroxyapatite/polyurethane scaffold incorporated with drug-loaded ethyl cellulose microspheres for bone regeneration. Journal of Biomedical Materials Research. Part B, Applied Biomaterials 95, 36–46.

Liu, W., Su, P., Chen, S., Wang, N., Ma, Y., Liu, Y., Wang, J., Zhang, Z., Li, H., Webster, T.J., 2014. Synthesis of TiO nanotubes with ZnO nanoparticles to achieve antibacterial properties and stem cell compatibility. Nanoscale 6, 9050–9062.

Liu, W., Su, P., Gonzales 3rd, A., Chen, S., Wang, N., Wang, J., Li, H., Zhang, Z., Webster, T.J., 2015. Optimizing stem cell functions and antibacterial properties of TiO_2 nanotubes incorporated with ZnO nanoparticles: experiments and modeling. International Journal of Nanomedicine 10, 1997–2019.

Liu, Z., Sun, X., Nakayama-Ratchford, N., Dai, H., 2007. Supramolecular chemistry on water-soluble carbon nanotubes for drug loading and delivery. ACS Nano 1, 50–56.

Luo, D., Sang, L., Wang, X., Xu, S., Li, X., 2011. Low temperature, pH-triggered synthesis of collagen–chitosan–hydroxyapatite nanocomposites as potential bone grafting substitutes. Materials Letters 65, 2395–2397.

Mano, J., 2004. Bioinert, biodegradable and injectable polymeric matrix composites for hard tissue replacement: state of the art and recent developments. Composites Science and Technology 64, 789–817.

Marmotti, A., Bruzzone, M., Bonasia, D.E., Castoldi, F., Von Degerfeld, M.M., Bignardi, C., Mattia, S., Maiello, A., Rossi, R., Peretti, G.M., 2013. Autologous cartilage fragments in a composite scaffold for one stage osteochondral repair in a goat model. European Cells and Materials 26, 15–31 discussion 31–2.

Mata, D., Oliveira, F.J., Ferreira, N.M., Araujo, R.F., Fernandes, A.J., Lopes, M.A., Gomes, P.S., Fernandes, M.H., Silva, R.F., 2014. Processing strategies for smart electroconductive carbon nanotube-based bioceramic bone grafts. Nanotechnology 25, 145602.

Meyer, F., Wardale, J., Best, S., Cameron, R., Rushton, N., Brooks, R., 2012. Effects of lactic acid and glycolic acid on human osteoblasts: a way to understand PLGA involvement in PLGA/calcium phosphate composite failure. Journal of Orthopaedic Research 30, 864–871.

Miller, D.C., Haberstroh, K.M., Webster, T.J., 2005. Mechanism(s) of increased vascular cell adhesion on nanostructured poly(lactic-co-glycolic acid) films. Journal of Biomedical Materials Research. Part A 73, 476–484.

Milman, N., Pedersen, P., Steig, T., Melsen, G.V., 2003. Frequencies of the hereditary hemochromatosis allele in different populations. Comparison of previous phenotypic methods and novel genotypic methods. International Journal of Hematology 77, 48–54.

Morones, J.R., Elechiguerra, J.L., Camacho, A., Holt, K., Kouri, J.B., Ramirez, J.T., Yacaman, M.J., 2005. The bactericidal effect of silver nanoparticles. Nanotechnology 16, 2346–2353.

Moutos, F.T., Freed, L.E., Guilak, F., 2007. A biomimetic three-dimensional woven composite scaffold for functional tissue engineering of cartilage. Nature Materials 6, 162–167.

Negishi-Koga, T., Takayanagi, H., 2009. Ca^{2+}-NFATc1 signaling is an essential axis of osteoclast differentiation. Immunological Reviews 231, 241–256.

Okamoto, M., John, B., 2013. Synthetic biopolymer nanocomposites for tissue engineering scaffolds. Progress in Polymer Science 38, 1487–1503.

Oberdorster, G., Maynard, A., Donaldson, K., Castranova, V., Fitzpatrick, J., Ausman, K., Carter, J., Karn, B., Kreyling, W., Lai, D., Olin, S., Monteiro-Riviere, N., Warheit, D., Yang, H., ILSI Research Foundation/Risk Science Institute Nanomaterial Toxicity Screening Working Group, 2005. Principles for characterizing the potential human health effects from exposure to nanomaterials: elements of a screening strategy. Particle and Fibre Toxicology 2, 8.

Okazaki, Y., Gotoh, E., 2013. Metal ion effects on different types of cell line, metal ion incorporation into L929 and MC3T3-E1 cells, and activation of macrophage-like J774.1 cells. Materials Science and Engineering. C, Materials for Biological Applications 33, 1993–2001.

Panacek, A., Kvitek, L., Prucek, R., Kolar, M., Vecerova, R., Pizurova, N., Sharma, V.K., Nevecna, T., Zboril, R., 2006. Silver colloid nanoparticles: synthesis, characterization, and their antibacterial activity. Journal of Physical Chemistry. B 110, 16248–16253.

Park, G.E., Pattison, M.A., Park, K., Webster, T.J., 2005. Accelerated chondrocyte functions on NaOH-treated PLGA scaffolds. Biomaterials 26, 3075–3082.

Poland, C.A., Duffin, R., Kinloch, I., Maynard, A., Wallace, W.A., Seaton, A., Stone, V., Brown, S., Macnee, W., Donaldson, K., 2008. Carbon nanotubes introduced into the abdominal cavity of mice show asbestos-like pathogenicity in a pilot study. Nature Nanotechnology 3, 423–428.

Porter, A.E., Gass, M., Muller, K., Skepper, J.N., Midgley, P.A., Welland, M., 2007. Direct imaging of single-walled carbon nanotubes in cells. Nature Nanotechnology 2, 713–717.

Porter, J.R., Ruckh, T.T., Popat, K.C., 2009. Bone tissue engineering: a review in bone biomimetics and drug delivery strategies. Biotechnology Progress 25, 1539–1560.

Ratna Sunil, B., Kumar, T.S.S., Chakkingal, U., Nandakumar, V., Doble, M., 2014. Nano-hydroxyapatite reinforced AZ31 magnesium alloy by friction stir processing: a solid state processing for biodegradable metal matrix composites. Journal of Materials Science. Materials in Medicine 25, 975–988.

Rossi, C.A., Pozzobon, M., De Coppi, P., 2010. Advances in musculoskeletal tissue engineering: moving towards therapy. Organogenesis 6, 167–172.

Sahoo, N.G., Pan, Y.Z., Li, L., He, C.B., 2013. Nanocomposites for bone tissue regeneration. Nanomedicine (London) 8, 639–653.

Sahoo, S., Ouyang, H., Goh, J.C., Tay, T.E., Toh, S.L., 2006. Characterization of a novel polymeric scaffold for potential application in tendon/ligament tissue engineering. Tissue Engineering 12, 91–99.

Sakai, H., Moriura, Y., Notomi, T., Kawawaki, J., Ohnishi, K., Kuno, M., 2010. Phospholipase C-dependent Ca^{2+}-sensing pathways leading to endocytosis and inhibition of the plasma membrane vacuolar H^{+}-ATPase in osteoclasts. American Journal of Physiology. Cell Physiology 299, C570–C578.

Sanaty-Zadeh, A., 2012. Comparison between current models for the strength of particulate-reinforced metal matrix nanocomposites with emphasis on consideration of Hall–Petch effect. Materials Science Engineering A 531, 112–118.

Sankar, M.U., Aigal, S., Maliyekkal, S.M., Chaudhary, A., Anshup, Kumar, A.A., Chaudhari, K., Pradeep, T., 2013. Biopolymer-reinforced synthetic granular nanocomposites for affordable point-of-use water purification. Proceedings of National Academy of Sciences of the United States of America 110, 8459–8464.

Scholz, M.S., Blanchfield, J.P., Bloom, L.D., Coburn, B.H., Elkington, M., Fuller, J.D., Gilbert, M.E., Muflahi, S.A., Pernice, M.F., Rae, S.I., Trevarthen, J.A., White, S.C., Weaver, P.M., Bond, I.P., 2011. The use of composite materials in modern orthopaedic medicine and prosthetic devices: a review. Composites Science and Technology 71, 1791–1803.

Seil, J.T., Webster, T.J., 2008. Decreased astroglial cell adhesion and proliferation on zinc oxide nanoparticle polyurethane composites. International Journal of Nanomedicine 3, 523–531.

Shi, X., Hudson, J.L., Spicer, P.P., Tour, J.M., Krishnamoorti, R., Mikos, A.G., 2006. Injectable nanocomposites of single-walled carbon nanotubes and biodegradable polymers for bone tissue engineering. Biomacromolecules 7, 2237–2242.

Singh, R.K., Patel, K.D., Lee, J.H., Lee, E.J., Kim, J.H., Kim, T.H., Kim, H.W., 2014. Potential of magnetic nanofiber scaffolds with mechanical and biological properties applicable for bone regeneration. PLoS One 9, e91584.

Stern-Straeter, J., Riedel, F., Bran, G., Hormann, K., Goessler, U.R., 2007. Advances in skeletal muscle tissue engineering. In Vivo 21, 435–444.

Suchy, T., Balik, K., Sucharda, Z., Sochor, M., Lapcikova, M., Sedlacek, R., 2011. Optimizing and evaluating the biocompatibility of fiber composites with calcium phosphate additives. Wiener Medizinische Wochenschrift 161, 493–502.

Sun, F., Zhou, H., Lee, J., 2011. Various preparation methods of highly porous hydroxyapatite/polymer nanoscale biocomposites for bone regeneration. Acta Biomaterialia 7, 3813–3828.

Sun, L., Webster, T.J., 2013. Self-assembled rosette nanotubes for tissue engineering applications. Conference Proceedings: Annual International Conference of the IEEE Engineering in Medicine and Biology Society. IEEE Engineering in Medicine and Biology Society 2013, 311–313.

Tanner, K.E., 2010. Bioactive ceramic-reinforced composites for bone augmentation. Journal of Royal Society, Interface 7 (Suppl. 5), S541–S557.

Tripathi, G., Gough, J.E., Dinda, A., Basu, B., 2013. In vitro cytotoxicity and in vivo osseointergration properties of compression-molded HDPE-HA-Al_2O_3 hybrid biocomposites. Journal of Biomedical Materials Research. Part A 101, 1539–1549.

Uemura, T., Dong, J., Wang, Y., Kojima, H., Saito, T., Iejima, D., Kikuchi, M., Tanaka, J., Tateishi, T., 2003. Transplantation of cultured bone cells using combinations of scaffolds and culture techniques. Biomaterials 24, 2277–2286.

Urban, R.M., Jacobs, J.J., Tomlinson, M.J., Gavrilovic, J., Black, J., Peoc'h, M., 2000. Dissemination of wear particles to the liver, spleen, and abdominal lymph nodes of patients with hip or knee replacement. Journal of Bone and Joint Surgery. American Volume 82, 457–476.

Vallet-Regi, M., Balas, F., Arcos, D., 2007. Mesoporous materials for drug delivery. Angewandte Chemie (International Edition in English) 46, 7548–7558.

Wamocha, H.L., Misak, H.E., Song, Z., Chu, H.Y., Chen, Y.Y., Asmatulu, R., Yang, S.Y., Ho, J.C., 2013. Cytotoxicity of release products from magnetic nanocomposites in targeted drug delivery. Journal of Biomaterials Applications 27, 661–667.

Wan, Y., Xiong, G., Liang, H., Raman, S., He, F., Y, H., 2007. Modification of medical metals by ion implantation of copper. Applied Surface Science 253, 9426–9429.

Wang, C., Xue, Y., Lin, K., Lu, J., Chang, J., Sun, J., 2012. The enhancement of bone regeneration by a combination of osteoconductivity and osteostimulation using beta-$CaSiO_3$/beta-$Ca_3(PO_4)_2$ composite bioceramics. Acta Biomaterialia 8, 350–360.

Warheit, D.B., 2006. What is currently known about the health risks related to carbon nanotube exposures. Carbon 44, 1064–1069.

Watari, F., Takashi, N., Yokoyama, A., Uo, M., Akasaka, T., Sato, Y., Abe, S., Totsuka, Y., Tohji, K., 2009. Material nanosizing effect on living organisms: non-specific, biointeractive, physical size effects. Journal of Royal Society, Interface 6 (Suppl. 3), S371–S388.

Webster, T.J., Schadler, L.S., Siegel, R.W., Bizios, R., 2001. Mechanisms of enhanced osteoblast adhesion on nanophase alumina involve vitronectin. Tissue Engineering 7, 291–301.

Weng, L., Webster, T.J., 2012. Nanostructured magnesium increases bone cell density. Nanotechnology 23, 485105.

Wikesjo, U.M.E., Qahash, M., Polimeni, G., Susin, C., Shanaman, R.H., Rohrer, M.D., Wozney, J.M., Hall, J., 2008. Alveolar ridge augmentation using implants coated with recombinant human bone morphogenetic protein 2: histologic observations. Journal of of Clinical Periodontology 35, 1001–1010.

Wikesjo, U.M., Huang, Y.H., Polimeni, G., Qahash, M., 2007. Bone morphogenetic proteins: a realistic alternative to bone grafting for alveolar reconstruction. Oral and Maxillofacial Surgery Clinics of North America 19, 535–551, vi-vii.

Williams, R.J., Gamradt, S.C., 2008. Articular cartilage repair using a resorbable matrix scaffold. Instructional Course Lectures 57, 563–571.

Winter, G.D., Simpson, B.J., 1969. Heterotopic bone formed in a synthetic sponge in the skin of young pigs. Nature 223, 88–90.

Xing, Z.C., Han, S.J., Shin, Y.S., Koo, T.H., Moon, S., Jeong, Y., Kang, I.K., 2013. Enhanced osteoblast responses to poly(methyl methacrylate)/hydroxyapatite electrospun nanocomposites for bone tissue engineering. Journal of Biomaterials Science. Polymer Edition 24, 61–76.

Yang, G., Rothrauff, B.B., Tuan, R.S., 2013. Tendon and ligament regeneration and repair: clinical relevance and developmental paradigm. Birth Defects Research, Part C: Embryo Today 99, 203–222.

Yu, Y., Zhang, Q., Mu, Q., Zhang, B., Yan, B., 2008. Exploring the immunotoxicity of carbon nanotubes. Nanoscale Research Letters 3, 271–277.

Zhang, L., Webster, T.J., 2009. Nanotechnology and nanomaterials: promises for improved tissue regeneration. Nano Today 4, 66–80.

Zhou, X., Dorn, M., Vogt, J., Spemann, D., Yu, W., Mao, Z., Estrela-Lopis, I., Donath, E., Gao, C., 2014. A quantitative study of the intracellular concentration of graphene/noble metal nanoparticle composites and their cytotoxicity. Nanoscale 6, 8535–8542.

Zhu, S., Zhang, B., Man, C., Ma, Y., Liu, X., Hu, J., 2014. Combined effects of connective tissue growth factor-modified bone marrow-derived mesenchymal stem cells and NaOH-treated PLGA scaffolds on the repair of articular cartilage defect in rabbits. Cell Transplantation 23, 715–727.

Advanced polymer composites and structures for bone and cartilage tissue engineering

5

P. Sol, A. Martins, R.L. Reis, N.M. Neves
University of Minho, Barco, Guimarães, Portugal; ICVS/3B's – PT Government Associate Laboratory, Braga/Guimarães, Portugal

5.1 Introduction

This chapter intends to provide an overview of the use of polymer composites applied to tissue engineering and regenerative medicine, focused on bone and cartilage. It will describe the constituents and arrangement of the natural extracellular matrix of bone and cartilage and the structure requirements to attain the demands of functional tissues. It will state evidences that polymer composites are the appropriate answer to substitute and restore damaged native tissues, from the more established solutions to the most advanced (Fig. 5.1).

Each section will express in detail features that can impart advanced properties to the polymer composites, with methods of surface modification, the central role of composites as sustained and controlled release systems (of drugs and other bioactive agents), and a part that reports on nanocomposites. The chapter concludes with general remarks and an insight of the likely future trends concerning the use of polymer composites for bone and cartilage tissue engineering.

5.2 The natural extracellular matrix

The extracellular matrix (ECM) of human tissues is a dynamic and hierarchically organized structure composed of water, proteins and polysaccharides (such as the glycosaminoglycans (GAGs): hyaluronic acid, dermatan sulfate, chondroitin sulfate, heparin, heparan sulfate and keratan sulfate), proteins (such as collagen, elastin, fibronectin and laminin) and proteoglycans (including aggrecan, brevican, decorin, keratocan, lumican, neurocan, perlecan, syndecans and versican) synthesized by the adjacent cells (Alberts et al., 2002; Bosman and Stamenkovic, 2003; Frantz et al., 2010; Rosso et al., 2004). In this complex structure, the collagen fibers provide strength to the tissue and, more importantly, have many cell-adhesive peptide moieties intended to allow for cellular anchoring. This hydrated gel composed of proteoglycans and other proteins fills the extracellular space, creating an appropriate microenvironment for ensuring the tissue maintenance and remodeling by cells in response to appropriate stimuli, while allowing for the diffusion of nutrients, metabolites and

Nanocomposites for Musculoskeletal Tissue Regeneration. http://dx.doi.org/10.1016/B978-1-78242-452-9.00005-4

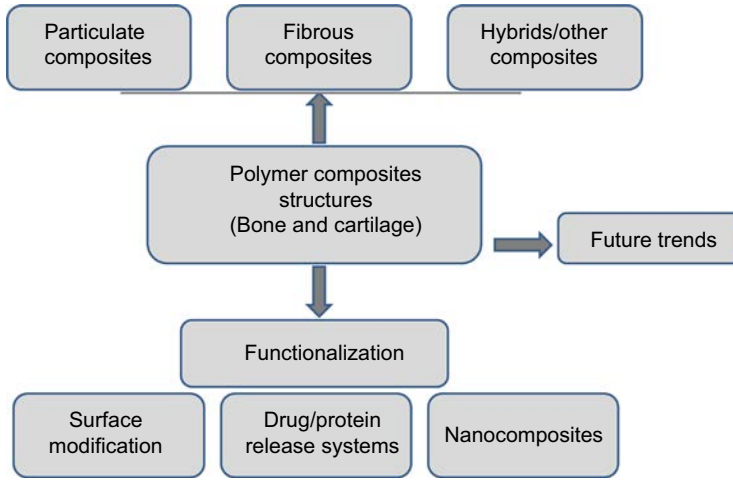

Figure 5.1 Chapter main points.

signaling molecules (Gentili and Cancedda, 2009). These components interact to form an interconnected nano- or micro-ranged fibrous network bound to the membranes of cells. Indeed, tissue ECMs act as a scaffold to support and hold cells together, to control their structure and to regulate cellular functions like adhesion, migration, proliferation, differentiation and ultimately tissue morphogenesis (Zagris, 2001, Rosso et al., 2004). The ECM also serves as a storage depot and a controlled release system for growth factors and signaling molecules.

The ECM interacts with the adjacent cells both mechanically and chemically, remodeling the architecture of the tissues. The structure of different collagen types within the ECM determines its function as a structural element of the connective tissues (Alberts et al., 2002; Frantz et al., 2010). Tendon ECM, for example, is composed of parallel and aligned collagen fibrils, whereas those found on the skin are mesh-like. In most connective tissues, the matrix macromolecules are secreted by fibroblastic cells into the extracellular space. In specialized types of connective tissues, such as cartilage and bone, cells of the fibroblast family (chondrocytes and osteoblasts, respectively) are responsible for ECM deposition. The matrix either becomes calcified into the hard and tough structures of bone and teeth, or can form the transparent matrix of cornea. ECM can also adopt the cord-like organization that gives tendons their tensile strength and elasticity.

Compiling all this information, it is reasonable to conclude that no single material (natural or synthetic) is able to mimic the composition, structure and functionality of natural ECM.

5.2.1 Bone extracellular matrix

Generally, the living bone in the human musculoskeletal system is composed of 10% to 20% collagen, 60% to 70% bone mineral, and 9% to 20% water, by weight (Gentili and Cancedda, 2009; Wu et al., 2014). In addition, other organic materials, such as proteins, polysaccharides and lipids, are also included in small quantities.

Collagen fibers are the main component forming the lamella on the micro level (Fig. 5.2(f)). The diameter of these fibers varies from 100 to 2000 nm, consisting of carefully arranged arrays of tropocollagen molecules that are composed of three left-handed helixes of peptides, which are long, rigid molecules (300 nm long, 1.5 nm wide). Bone mostly contains type-I collagen and small amounts of type-V collagen, the molecules of which are organized into collagen fibrils, which are formed by the assembly of tropocollagen molecules in a 3/4 stagger with a parallel array along the fibrils (Hing, 2004). The basic composition of the bone mineral component can be approximately defined as hydroxyapatite (HAp) with the chemical formula $Ca_{10}(PO_4)_6(OH)_2$. HAp has a Ca:P ratio of 1.67 (5:3); however, the Ca:P ratio in bone minerals actually varies between 1.37 and 1.87, indicating that these varied compositions of bone minerals may contain other additional ions, such as strontium, zinc and carbonate (Hing, 2004). These HAp crystals, which appear in the form of plates or needles, are about 40–60 nm long, 20 nm wide, and 1.5–5 nm thick. The mineral phase in bone is made of a continuous phase of HAp crystals, rather than a discrete aggregation. Indeed, it has been proven that bones retain a good mechanical strength after a complete removal of the organic phase.

5.2.2 Cartilage extracellular matrix

Cartilage is a type of collagen-based connective tissue composed of very large protein–polysaccharide molecules, providing a tough and flexible matrix made of entangled collagen fibers, protein, and sugar (Gentili and Cancedda, 2009). Aggrecan and type II collagen are the most abundant proteins found within the ECM of articular cartilage. They are linked together by a number of collagen-binding proteins including cartilage oligomeric matrix protein (COMP), chondroadherin and other minor collagens on their surface. Aggrecan is a large aggregating proteoglycan, composed of hyaluronan (HA) and link protein (LP), and responsible for the osmotic properties of cartilage, enabling resistance to compressive loads and retention of water. Cartilage also contains a variety of small leucine-rich repeat proteoglycans (SLRPs) as decorin, biglycan, fibromodulin and lumican in which they help maintain the integrity of the tissue and modulate its metabolism (Goldring, 2006; Hunziker et al., 2002).

Articular cartilage is composed of four distinct regions differing in their collagen fibril orientation (Fig. 5.2(b)): (a) the superficial or tangential zone (ca. 200 μm), (b) the middle or transitional zone, (c) the deep or radial zone and (d) the calcified cartilage zone (Eyre, 2002; Poole et al., 2001). The superficial zone is composed of thin collagen fibrils in tangential array mostly parallel to the surface with a high concentration of decorin and lubricin and a low concentration of aggrecan. The middle zone is composed by thicker collagen fibrils more randomly organized. The deep zone is composed by thicker collagen bundles arranged in a radial fashion and orthogonal to the surface. The calcified cartilage zone is located above the subchondral bone and the tidemark that persists after growth plate closure is composed of matrix vesicles, vascularization and innervations irradiating from the subchondral bone. The predominant collagen type in the ECM of the calcified zone is type X as in the hypertrophic zone of the growth plate.

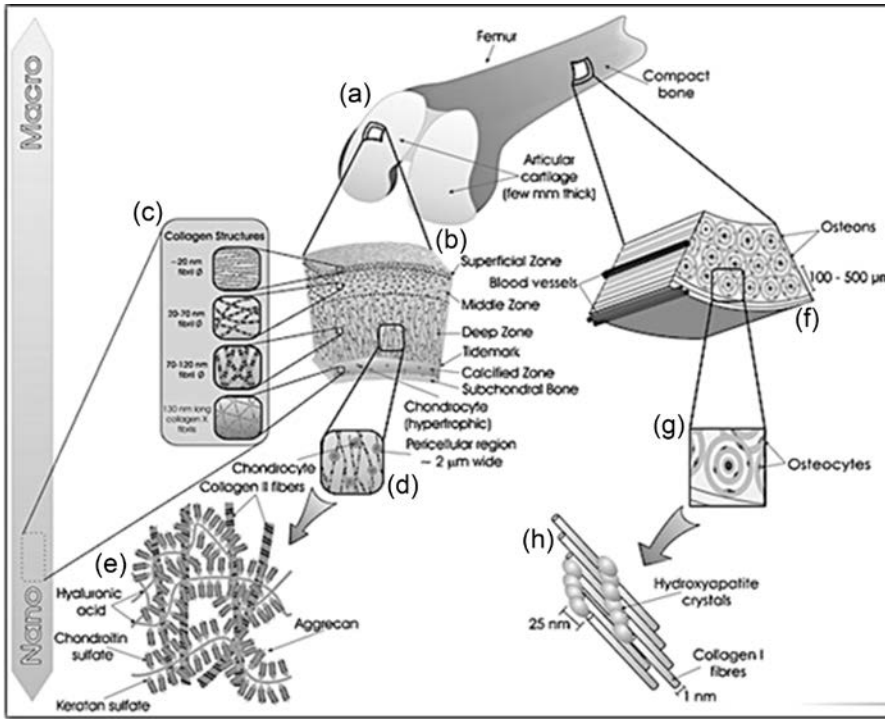

Figure 5.2 Hierarchical organization of cartilage and bone over different length scales. (a) Articular cartilage forms a wear-resistant, load-bearing surface that covers bone in diarthrodial joints. It is organized into (b) distinct zones in which (c) the organization of the collagen structures varies between zones. (d) Resident chondrocytes are encased in pericellular regions, which are surrounded by well-defined matrix nanoarchitecture of (e) aggrecan/hyaluronic acid superaggregates and macrofibrillar collagen networks. Bone mineralizes to form a calcified outer compact layer, which comprises (f) many cylindrical Haversian systems or osteons. (g) The osteocytes within these systems are surrounded by the well-defined nanoarchitecture of the (h) extracellular matrix—a dense network of aligned collagen I fibers, which provide templates for the self-assembly of hydroxyapatite crystals.
Adapted with permission from Mwenifumbo, S., Shaffer, M.S., Stevens, M.M., 2007. Exploring cellular behaviour with multi-walled carbon nanotube constructs. Journal of Materials Chemistry 17, 1894–1902.

5.3 The requirements of structures for tissue engineering

Natural extracellular matrices (ECMs) have been isolated and extracted from various tissues, such as small-intestine submucosa, skin (from cadavers), pancreas and breast (Badylak, 2007). Although these purified ECMs certainly have useful applications, their use is limited in scope owing to the need for well-defined microenvironments in tissue regeneration and stem-cell transplantation, in which animal by-products and contaminants must be limited. Moreover, it has been demonstrated that, besides the spatial framework, tissue-specific ECM cues, namely the constituents and their structural organization, are

decisive factors of their final properties (Muiznieks and Keeley, 2013). Furthermore, it is well established that ECM is dynamic and has an instructive role in building a tissue and in its regeneration after trauma or disease (Muiznieks and Keeley, 2013).

Rarely one material provides all the requirements for a given biomedical application and, in regard to biomaterial/scaffold for tissue engineering of bone and cartilage, this statement is even more accurate. Nevertheless, a set of requirements must be fulfilled, namely adequate mechanical behavior, suitable morphology, and structural/functional properties (Marimuthu and Kim, 2009).

A key requisite of a biomaterial is biocompatibility. Initially, this term was applied to implantable devices that was supposed to remain long periods within an individual, being, at the time, obvious to select the least chemically reactive material to avoid adverse reactions from the body. The term biocompatibility was initially a synonym of nontoxic and nonimmunogenic. The concept that materials should elicit some level of response from tissues, along with issues related to possible products of biodegradability, led biocompatibility to be termed as "the ability to perform with an appropriate host response in a specific situation." More recently, it is stated as "the ability of a biomaterial to perform its desired function with respect to a medical therapy, without eliciting any undesirable local or systemic effects in the recipient or beneficiary of that therapy, but generating the most appropriate beneficial cellular or tissue response in that specific situation, and optimizing the clinically relevant performance of that therapy" (Williams, 2008). This overarching definition almost compelled the extensive use of composite materials, because no material alone could fulfill all the parameters.

The mechanical performance is an essential requirement for any biomedical application. Two features must be considered: the bulk properties should be compatible with, as much as possible, the host mechanical ones, and a proper interface should transfer load from the scaffold to the native tissue. Values of modulus and tensile/compressive strength of the materials determine the final mechanical properties of the scaffolds. The analysis of Fig. 5.3 demonstrates the range of tensile modulus and strength values of biological materials (Mano et al., 2004), and that neither polymers alone, nor ceramics/metals by themselves, provide the necessary array of properties.

Scaffolds are often porous three-dimensional (3D) structures made of degradable materials. The quantity of pores, their size and distribution, along with their interconnectivity, are crucial aspects to provide the environment for bone regeneration. The balance between mechanical support and interconnected porosity is difficult to achieve. The processing methods to obtain scaffolds and the later tune of properties should also be a concern. Once again, polymer composites are an excellent answer to these problems; but why? The next section will present arguments to this question.

5.4 Polymer composite structures for bone and cartilage tissue engineering

Composites are defined as multicomponent materials comprising multiple different phase domains in which at least one type of phase domain is a continuous phase; a polymer composite is a composite in which at least one component is a polymer (Work et al., 2007).

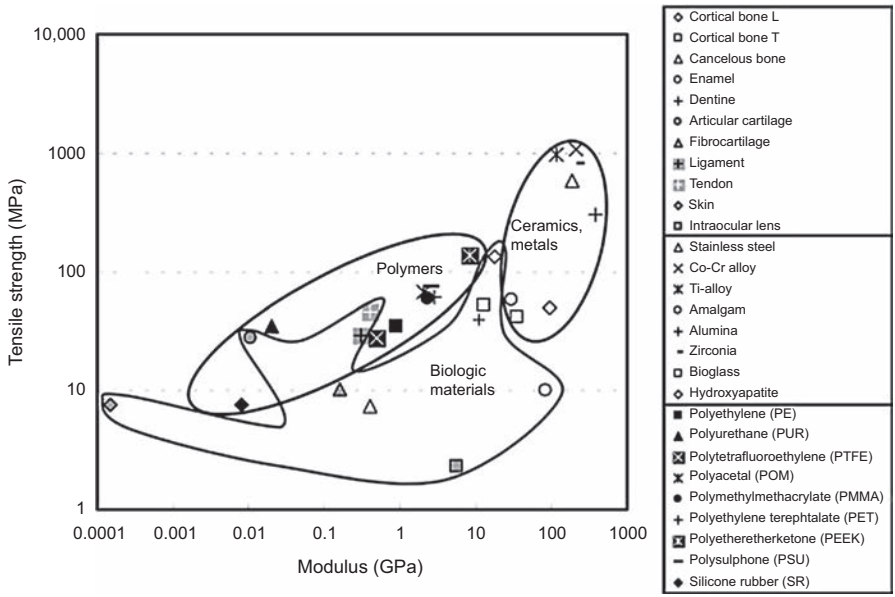

Figure 5.3 Tensile strength versus modulus of materials with relevance for composite design when considering biomedical applications.
From Mano, J.F., Sousa, R.A., Boesel, L.F., Neves, N.M., Reis, R.L., 2004. Bioinert, biodegradable and injectable polymeric matrix composites for hard tissue replacement: state of the art and recent developments. Composites Science and Technology 64, 789–817.

In nature, we can find complex composites with sometimes outstanding mechanical properties, taking into account the individual constituents from which they are built (Meyers et al., 2008; Neves, 2012). As known, polymers are macromolecules with long chains of repetitive monomers mainly composed by carbon atoms, and the variety of polymer matrices (thermoplastic, thermosetting, elastomers and their blends, natural and/or synthetic) as well as the range of processing methods, allow the fine-tuning of properties. The possibility to add fibers and particulates is advantageous by providing to the system added structural and functional properties not attainable by any of the constituents alone. Combine the variety and processability of polymers with the hardness of ceramics, and the stiffness of metals, is not only desired but possible.

Composites can be classified by the form of reinforcement dispersed in the matrix; thus, according to this systematization, it is possible to have particulate composites (when at least one of the constituents is in the particle form), or fibrous composites (when at least one of the constituents is in the fiber form). These main categories are described hereinafter, as well as a third group of hybrid composites.

5.4.1 Particulate composites

The development of composites for bone-tissue engineering very often applies ceramic particles, an obvious option considering the composition of bone, as

mentioned previously. Particles of calcium phosphate (CaP) have been widely used (Mathieu et al., 2006; Wagoner Johnson and Herschler, 2011), precisely due to their resemblance to mineral bone. A range of compositions have been used with greater emphasis on hydroxyapatite, β-tricalcium phosphate and biphasic calcium phosphate, primarily as bone filler or as coating of implants. The industry still provides particles of calcium phosphates (mainly in the form of granules or pastes), but their single use shows reduced ability to repair complex tissues with demanding functionality.

Hydroxyapatite ($Ca_{10}(PO_4)_6(OH)_2$) is the major mineral component of human hard tissues, and both natural and synthetic origins have excellent biocompatibility with bones and teeth. A work reports the melt-compounding of HAp and chitosan (Ch) with several aliphatic polyesters, at several percentages, using a twin-screw extruder (Correlo et al., 2005). The characterization of blends revealed that the HAp addition decreased the crystallinity of the Ch/poly(butylene succinate) (PBS), whereas in the case of Ch/poly(caprolactone) (PCL) blends, the crystallinity increased. However, the addition of HAp decreased the tensile strength and elongation of the polyester/HAp composites, probably due to the weak adhesion between the particles and the matrix. On the other hand, the modulus had an increase in all composites. A more recent work also assessed the effects of HAp addition to biodegradable polymers before clinical translation (Tayton et al., 2014). In this study, high-molecular-weight poly(lactic acid) (PLA) and high-molecular weight poly(lactic-co-glycolic acid) (PLGA) were selected, due to their good resistance to shear forces, and ability to support the survival and proliferation of skeletal stem cells. In a first stage, the addition of HAp aimed to enhance their biological and mechanical properties; after characterization, the best two performing compositions were selected subcutaneously in mice. All polymers had superior mechanical shear strength when compared with allografts, and excellent cell survival; micro-CT analysis revealed increased bone formation for the PLA/HAp composite and excellent neo-vessel formation, confirmed by histology. The authors stated that PLA/HAp showed both enhanced osteoinductive and osteogenic capacity, and for that reason this composite has been selected for scaled-up experimentation before clinical translation (Tayton et al., 2014).

Although bulk properties determine the mechanical and functional properties of scaffolds, the tissue–biomaterials interactions are surface phenomena and have a great influence on cell adhesion as well as on protein adsorption (Anselme, 2000). A study investigated the effect of the addition of chitosan (Ch) powder (that does not melt when processed by melt-based methods, maintaining its shape) to poly(butylene succinate) (PBS) and, in particular, its influence on the surface properties (Coutinho et al., 2012). The adsorption of human serum albumin and human plasma fibronectin onto the Ch/PBS surface was quantified, using tissue culture polystyrene (TCPS) as standard material. The study shows that the location of Ch near the surface promoted the adsorption of proteins, with a preferential adsorption of albumin over fibronectin. The in vitro biological performance of these materials by direct contact assay with an osteoblastic-like cell line showed a synergistic effect; the synthetic polyester promoted the adhesion of the osteoblastic-like cell line, and the presence of chitosan significantly enhanced its osteoblastic activity.

The particle dispersion in the polymer matrices is probably the main problem to solve, and researchers are addressing it and proposing some strategies to overcome this

issue (Supová, 2009) by particle modification or biomimetic approaches. However, the benefits of its inclusion overlap entirely those difficulties.

5.4.2 Fibrous composites

Traditional fibrous composites are composed of a continuous polymer matrix and, embedded in it, fibers as reinforcement components, typically for mechanical improvement. Some studies with different types of reinforcement will be described next.

Thermoplastic composites composed of a poly(lactic acid) (PLA) matrix and reinforcing glass fibers (GF) were prepared (Bühler et al., 2008) to obtain mechanical resistance equivalent to natural bone. The processing steps included the winding of unidirectional forms made of mingled fibers, and subsequent supercritical gas foaming. The foaming of composite forms containing mingled polymer and glass fibers were successfully obtained; the morphological analysis shows that GFs were embedded into the polymer matrix, a result of the melting of the PLA fibers. Most of the GFs were integrated within the cell walls, in which reinforcement is most effective. In addition, as the reinforcing fibers were unidirectional and parallel to the foam expansion direction, the cellular composites were highly anisotropic. The fiber fraction ranged from 0 to 15 vol% and porosity from 50% to 92%; and with up to 1.5 GPa these cellular composites show a higher longitudinal compression modulus when compared with previously suggested foams made of bioresorbable materials (Bühler et al., 2008).

One of the most difficult challenges in tissue engineering is the vascularization of engineered constructs. A recent paper described the development of a scaffold that incorporated silk fibroin fibers into a salt-leached sponge made of poly(D,L-lactic acid) (PDLLA) (Stoppato et al., 2013). The addition of silk fibroin fibers to the PDLLA salt-leached sponge increased the scaffold stiffness and heightened its capacity to support endothelial cells in vitro, and the in vivo perfusion revealed a faster vascularization of the composite scaffolds.

In recent work, activated carbon fibers (ACF), previously obtained via carbon fiber processing in water and nitrogen streams at high temperature, were incorporated into poly(lactic-co-glycolic) acid (PLGA) (Shi et al., 2014). The characterization showed a random distribution of ACF inside the scaffolds with an apparent film formation between ACF and PLGA matrix, denoting benign integration between them. The viability of L929 cell cultured on ACF/PLGA scaffolds was higher than on the control group, probably due to the larger space to wrap cells, which provides a more favorable possibility for cell adhesion and proliferation.

Apart from the more traditional fibrous composite concept (dispersed fibers embedded in a continuous polymer matrix), there are works proposing fibrous scaffolds that are per se polymer composites. Examples of those are electrospinning-based scaffolds with the addition of nanoparticles, which are presented later in this chapter.

5.4.3 Hybrids/other composites

Alternative solutions emerged in the last few years, and hydrogels are one of the most interesting. Hydrogels are 3D water-insoluble, hydrophilic polymer networks, with

the ability to absorb large volumes of water, making them very appealing materials to mimic the ECM (Shapiro and Oyen, 2013). Natural hydrogels, such as collagen and gelatin, have the benefit of innate binding sites for cell adhesion, but may evoke an immune response when used in vivo, whereas synthetic ones are more chemically and structurally uniform, but lack bioactive moieties; both (natural and synthetic) have a common disadvantage, mechanical weakness (Drury and Mooney, 2003). Electrospun fibers are another attractive substrate to be used as scaffold intended to mimic ECM; the fibers with nanometer-to-micrometer scale resemble natural fibrous materials, such as collagen, but with problems with cellular infiltration. Composite scaffolds based on hydrogels and electrospun fibers are an attempt to overcome their individual deficiencies (Bosworth et al., 2013). A paper described the design of a 3D fiber–hydrogel composite, injectable but with macroscale dimensions, for use in an articular cartilage model system. The authors state that the composite enhanced the biological response of adult stem cells, with the accomplishment of near-native levels of ECM with dynamic mechanical stimulation (Coburn et al., 2011).

Laminated composites could be another approach, by stacking sheets of electrospun fibers between layers of hydrogels, to obtain a 3D scaffold (Xu et al., 2010; Yang et al., 2011). Xu et al. attempted to mimic the naturally occurring laminated structure of osteons, found within the outer cortical region of bone; for that they produced a fiber–hydrogel composite based on randomly oriented poly(L-lactic acid) fibers and poly(lactide-co-ethylene oxide fumarate) hydrogel stacked alternately, and further compressed. HAp nanocrystals were added to the precursor solution to produce an osteoconductive matrix for bone marrow stromal (BMS) cells; the results indicate that the laminates have the potential to provide mechanical strength and provide the differentiation of progenitor cells to the osteogenic lineage (Xu et al., 2010). In the work of Yang et al. developed oriented nanofibers of poly(L,D-lactic acid) embedded within collagen type I hydrogels (Yang et al., 2011) and applied this fiber–hydrogel composite as potential intervertebral disc replacement.

Other approaches combine 3D printing and hydrogels, such as the processing of constructs by alternating deposition of thermoplastic fibers and cell-laden hydrogels (Schuurman et al., 2011), or the development of a hybrid scaffold consisting of synthetic biomaterials and a natural hydrogel (collagen), with the latter being infused between the lines of the scaffold (Shim et al., 2011), validated by rat primary hepatocytes and a mouse pre-osteoblast cell line.

5.5 Functionalization of composite structures for bone and cartilage tissue engineering

ECM-like natural biopolymers are usually blended with some synthetic polymers, such as poly(lactic acid) (PLA), poly(glycolic acid) (PGA), poly(lactic acid-co-glycolic acid) (PLGA), and poly (ε-caprolactone) (PCL) to form ECM-like polymer composites/blends, which possess the needed mechanical properties and biological functions. In a recent paper, Wu et al. described the typical polymers for tissue

engineering as well as the typical ECM-like biopolymers used for bone and cartilage scaffolds (Wu et al., 2014).

5.5.1 Surface modification

It is well accepted that surface characteristics are critical for the successful design and medical application of biomaterials, because the surface is the earliest contact with the biological environment. Therefore, the design of scaffolds must take the interactions between cells and the ECM into consideration; which is to say that the surface affinity with receptors on the cytomembrane must also be a concern. Shortly, the surface design of scaffolds includes three types of categories, ie, the tailoring of the surface chemistry and the regulation of the surface structure, as well as the synergistic effects of the two factors (Wu et al., 2014).

Numerous surface techniques are employed to produce different types of coatings to functionalize the surface of the scaffolds and implants. According to their surface chemistry, these coatings can be mainly categorized into three types: inorganic, with HA-derived coatings as preventatives; ECM-derived organic coatings; and other derived-hybrid coatings. Bone mineral-like ceramics, such as apatite and its derived ceramics, are usually deposited on the surface of bone scaffolds to achieve specific biological functions, as reviewed by others (Paital and Dahotre, 2009; Surmenev et al., 2014).

The best-known biofunction is the earlier osteoinduction and osteointegration of HA and its derived coatings. Recent research shows that the form of HA coating significantly influences its biological function (Ye et al., 2013). A mesoporous hydroxyapatite (M-HAp) coating can be prepared on the surface of a porous β-tricalcium phosphate (β-TCP) scaffold by using a sol–gel dip-coating process, using the block copolymer Pluronic F127 as the template. The osteoblasts exhibit a relatively round shape with sphere-like surface evaginations and the microvilli on the nonmesoporous HAp (non-M-HAp) coating. Conversely, more cells are strongly attached to M-HAp and spread in an elongated shape, indicating that the latter is more suitable for osteoblast adhesion and spreading, which is in accordance with the much higher alkaline phosphatase (ALP) and bone sialoprotein (BSP) expression on M-HAp. This is possibly due to the large surface area of M-HAp, providing higher availability of binding sites for receptors in osteoblast filopodia, and thus stimulating cell spread and proliferation (Anselme, 2000; Ye et al., 2013).

Atom transfer radical polymerization (ATRP, one of the living radical polymerization methods) is attracting extensive attention from biomaterial scientists and engineers because of its simplicity and broad applicability, especially for preparing well-defined nanostructured polymer-based materials (Matyjaszewski and Tsarevsky, 2009). Briefly, ATRP is based on alkyl halide initiators or dormant species (RX or PnX) that react with activators consisting of low oxidation-state metal complexes MtzLm (Mtz represents the metal species in oxidation state z, and L refers to a ligand) to achieve a reversible equilibrium between growing radicals (active species) and dormant species. In addition, during ATRP equilibrium, the dormant species can have polymer chains that are able to grow in one or many directions, or polymers that

are attached to functional colloidal particles, surfaces, and biomolecules. Using this method, HA–poly(L-lactide) (PLLA) nanohybrids can be successfully prepared and can exhibit excellent dispersibility in composites, which makes the PLLA–HA-PLLA nanocomposites induce apatite formation much faster than PLLA/HA composites, compared to the aggregated and unmodified HA (He et al., 2012).

5.5.2 Drug/protein release systems

Although biopolymers are versatile in incorporating bioactive factors, bioactive inorganics such as calcium phosphates and glasses have significant limitations in delivering bioactive factors, because they primarily require high-temperature processes in the shape formulation. In this manner, the bioactive inorganics are generally made into composites with natural-origin polymers to allow shape formability (Pérez et al., 2013). Among the bioactive inorganics, calcium phosphate cements (CPCs) are among the most attractive group of inorganic biomaterials to be used as bioactive factor delivery systems. Alpha-tricalcium phosphate-based CPCs can self-harden and be formulated into microspheres with the help of collagen to deliver biomolecules. The addition of alginate into CPC-based calcium carbonate/monocalcium phosphate monohydrate prolonged the release of gentamicin, providing a reservoir system for antibiotic delivery with bone-regeneration capability (David Chen et al., 2011).

Bovine serum albumin (BSA), used as a model protein, was safely loaded within the microspheres and then released sustainably over a month (Park et al., 2011). To stimulate osteoinduction, bone morphogenetic protein 2 (BMP-2) was also incorporated within tetracalcium phosphate/dicalcium phosphate anhydrous-based CPC composite with chitosan, which showed significant improvement of osteoblastic cell functions (Weir and Xu, 2010). Similarly, a composite gelatin/β-TCP sponge loaded with BMP-2 and Wnt1 inducible signaling pathway protein-1 (WISP-1) showed synergistic ectopic bone formation in middle-aged mice, suggesting that a scaffold incorporating multiple osteoinductive agents could be effective in age-related bone disease by inducing new bone formation (Kohara and Tabata, 2011). In a recent study, a composite biomaterial scaffold made of PLA matrix with alginate fibers was developed, in which Vascular Endothelial Growth Factor (VEGF) was loaded into the alginate and the BMP-2 was incorporated into the PLA matrix, aiming at initial VEGF release, and, then, BMP-2 release at a much later stage (Kanczler et al., 2010). When the delivery systems were implanted in mouse segmental femoral defects with human Bone Marrow Stromal Cells (hBMSCs), significantly higher bone regeneration was observed with respect to the composite scaffolds without GFs. In another attempt, the effect of exogenous platelet-derived growth factor homodimer (PDGF-BB) on bone healing was also demonstrated using a collagen (Nash et al., 1994) or a composite of chitosan–tricalcium phosphate (TCP) sponge (Lee et al., 2000) as carriers, in a tibia defect of rabbits or in a calvarial defect of rats, respectively.

Smart biomaterials with stimuli-responsiveness, namely thermosensitive scaffolds, are widely studied for cartilage-tissue engineering. One of the best-known thermoresponsive biopolymers is poly(N-isopropyl acrylamide) (pNIPAAm), which presents a typical sol–gel transition at approximately 32°C (Prabaharan and Mano, 2006).

However, its poor biocompatibility and nondegradability generally requires a composite approach with other biocompatible materials to produce stimuli-responsive and biologically active composite materials. Moreover, composites with natural polymers or hydrophilic synthetic polymers generally modulate the transition point near body temperature, as well as allow the delivery of hydrophilic drugs, enabling better applicability in tissue engineering and drug delivery. For example, a composite of hyaluronic acid with pNIPAAm was exploited to produce thermoreversible hydrogels for cartilage-tissue engineering (Na et al., 2007). Rabbit chondrocytes were encapsulated into the composite gel, which also contained transforming growth factor beta 3 (TGFβ-3). This thermoreversible hydrogel construct was injected subcutaneously in mice, demonstrating enhanced production of cartilage-specific ECM in the cell-growth factor delivering condition than those without the GFs. A hyaluronic acid–pluronic thermosensitive composite was also developed for the delivery of cells and GFs in cartilage-tissue engineering (Jung et al., 2010). Human adipose-derived stem cells and TGF-β1 could be loaded within the composite gel via sol–gel transition at body temperature allowing in vivo injection. The growth factor release was moderate, and the in vivo result of the construct loading into a full-thickness defect of rabbit knee articular cartilage demonstrated the formation of cartilaginous matrix by the tissue-engineered construct.

5.5.3 Nanocomposites

There is a great need for engineering multiphase materials (so-called composites) with structure and composition similar to natural bone. Recently, nanocomposites, particularly hydroxyapatite- and collagen-based, have gained much recognition as bone grafts, not only due to their composition and structural similarity with natural bone, but also because of their unique functional properties, such as larger surface area and superior mechanical strength than their single-phase constituents. By the use of other natural-origin polymers, gelatin–HAp nanocomposite fibers were also processed though the biomimetic precipitation and electrospinning methods, resulting in a biomedical membrane with an HAp composition gradient intended for guided bone-tissue engineering (Kim et al., 2005). The nanocomposite fibrous mesh significantly improved the osteoblastic activity (MG63 cell line) in comparison with the pure gelatin equivalent. Biomimetic nanocomposite nanofibers of HAp–chitosan (Ch) was prepared by a two-step approach that combines an in situ co-precipitation synthesis with an electrospinning process (Zhang et al., 2008). By using an ultrahigh molecular weight poly(ethylene oxide) (PEO) as the fiber-forming facilitating additive, a model nanocomposite HAp-Ch with HAp mass loading of 30 wt% can be readily electrospun into nanofibers from an aqueous acetic acid-dominant solvent system, with proper structural preservation of HAp crystallites. Biological in vitro cell culture with human fetal osteoblast (hFOB) cells indicated that, notwithstanding the occurrences of an initial inhibition, the HAp-incorporated nanofibrous scaffolds as compared to Ch-alone scaffolds appeared to have significantly stimulated the bone-forming ability, as shown by the cell proliferation, mineral deposition and morphology observation. By using a polymer from bacterial origin, poly(hydroxybutyrate-co-hydroxyvalerate) (PHBV)

fibers containing carbonated hydroxyapatite (CHAp) nanoparticles with different CHAp amounts (5, 10 and 15 wt%) were electrospun with the aid of ultrasonic power for dispersing the nanoparticles (Tong et al., 2010). Compared with the PHBV polymer fibrous membranes, the CHAp–PHBV nanocomposite fibrous membranes exhibited improved wettability, whereas their ultimate tensile strength and stiffness were not significantly affected. In vitro studies revealed that both PHBV polymer and CHAp–PHBV nanocomposite fibrous membranes supported the attachment and proliferation of human osteoblastic cells (SaOS-2 cell line). Moreover, compared with cells seeded on the PHBV polymer fibrous membranes, osteoblastic cells seeded on the CHAp–PHBV nanocomposite fibrous membranes exhibited higher ALP activity after 14 days of cell culture, indicating better osteoconductivity with the incorporation of CHAp nanoparticles in electrospun fibers.

Following the previously described approaches for natural-origin polymers, Vohra and collaborators (Thomas et al., 2006; Tyagi et al., 2009) created a nanocomposite scaffold by the co-electrospinning of nanofibrous polycaprolactone (PCL) and nanohydroxyapatite (nHAp) to mimic the physical features of natural bone ECM. A direct correlation was observed between the amount of nHAp and the mechanical (tensile) properties of the composite nanofibrous scaffold. Conversely, the composite fibrous membranes (based on nano-apatite (nAp) and PCL) with a high nAp loading density were mechanically weaker than the one with low nAp loading density, indicating that there is an optimal ratio of nAp to polymer for mechanical reinforcement (Yang et al., 2009). Deng et al. (2007) described the electrospinning of a biomimetic electrospun scaffold made of nHAp and polyesteramide (PEA). The 20%wt nHAp–PEA fibrous scaffold, which is made up of ultrafine fibers with an average diameter 400 ± 50 nm and interconnected pores, was characterized with high surface-to-volume ratio. This biological behavior was confirmed by the culturing of osteoblasts on these nanocomposite scaffolds.

A promising way of fabricating nanocomposite bone grafts using strategies found in nature—the biomimetic process—has recently received much attention and is perceived to be beneficial over conventional methods. Biomimetic processes are defined as the ones that either mimic or are inspired by the biological mechanisms to incorporate desirable nano-features that emulate nature's own structures or functions, aiming to develop the next-generation bone grafts. Nanostructured biomaterials, having less than 100 nm in at least one dimension, in particular nanocomposites, are perceived to be beneficial and potentially adequate for bone applications owing to their nanoscale functional characteristics that facilitate bone cell growth and subsequent tissue formation (Chan et al., 2006). Additionally, it was also stated that synthetic polymers with 3D nanofibrous architecture could provide a better environment for osteogenic differentiation in vitro than 3D microfibrous scaffolds (Binulal et al., 2010) and enhance osteoblast differentiation and bone formation in vivo, when compared to solid-walled 3D scaffolds of the same material (Woo et al., 2009). Accordingly, a work (Schneider et al., 2008) demonstrated the proliferation and osteogenic differentiation of hBMSCs, assessed by the determination of ALP activity and osteocalcin content, when cultured on cotton wool-like poly(lactide-co-glycolide) (PLGA)–amorphous tricalcium phosphate (ATCP) nanocomposite, prepared by electrospinning. Furthermore, a loading of

40% (w/w) ATCP resulted in a triplication of the initial mineral mass formation after 15 days of immersion in simulated body fluid (SBF).

Besides those bioactive inorganic compounds, silica-based bioactive glass (BG) has been considered a promising bone regenerative material because of its excellent cytocompatibility and bioactivity. It is well known that BGs can bond to surrounding bone tissues by the formation of a surface hydroxycarbonate apatite layer in the process of their chemical reactions in body fluids and can promote bone regeneration. A PCL–BG nanocomposite was fabricated using BG nanofibers (BGNFs) and compared with an established composite fabricated using microscale BG particles (BGP) (Jo et al., 2009). The BGNFs were generated using sol–gel precursors via the electrospinning process, chopped into short fibers and then incorporated into the polymeric solution. The BGNFs were reinforced more uniformly and better dispersed than the BGPs in the PCL matrix. The incorporation of the BGNF also significantly enhanced the cytocompatibility, osteoblastic (MC3T3 cell line) activity in vitro, and elastic modulus of the composite when compared with the BGP. Moreover, the results of the in vivo animal experiments using Sprague–Dawley albino rats revealed the bone regeneration capability of the PCL–BGNF composite when implanted in a calvarial bone defect. It was concluded that the improved mechanical and biological properties of the composite are primarily related to the nanoscaled fibrous structure of the incorporated BG. A composite nanofiber of PLA filled with bioactive glass nanoparticles was produced using the electrospinning method (Noh et al., 2010). It was observed that small additions of glass nanofiller, up to 10%, greatly enhanced the in vitro bone bioactivity by inducing calcium phosphate mineral formation at the nanofiber surface in an SBF medium. Osteoblastic cells (MC3T3-E1 cell line) cultured on the nanocomposite fibers showed favorable cellular adhesion and growth.

Submicron electrospun-polymer fibers are also good candidates as reinforcing agents in the development of advanced nanocomposites due to their continuity, orientation, inherent flexibility and potential compatibility with polymeric matrices. However, only a limited number of composites reinforced with electrospun nanofibers have been developed, and mainly for providing some outstanding physical characteristics, ie, optical transparency and mechanical properties (Bergshoef and Vancso, 1999; Chen and Liu, 2008; Dodiuk-Kenig et al., 2008; Fong, 2004; Gao et al., 2008; Lin et al., 2008; Pinho et al., 2009; Tian et al., 2007). Thorough physical characterization of electrospun nanofiber-reinforced composites to be used as dental restorative composites resins was conducted (Bergshoef and Vancso, 1999; Chen and Liu, 2008; Dodiuk-Kenig et al., 2008; Fong, 2004; Gao et al., 2008; Lin et al., 2008; Tian et al., 2007, 2008), but their biological functionality remains to be explored. Recent in vitro results with human bone marrow mesenchymal stem cells cultured on nanofiber-reinforced microfibrous composite scaffolds, under osteogenic induction conditions, showed a sustained ECM deposition and mineralization, as demonstrated by the increased amount of calcium phosphates produced (Martins et al., 2010). All these biological data undoubtedly demonstrated the superior performance of electrospun nanofibrous membranes (NFMs) over the cellular adhesion, proliferation and also differentiation of mesenchymal stem cells (MSCs).

5.6 Conclusions and future trends

The chapter addressed the structural and functional properties conferred by polymer composites to attain the demands of the Tissue Engineering field, which no single material is able to answer, and describes significant features that could be added to composites.

Current concerns are related with a better understanding of the involved mechanisms at different scales, in particular at the micro- and nanoscale, both for human tissue and its biological functions and for engineered materials (Guilak and Baaijens, 2014; Guilak et al., 2014). For particulate and fibrous composites, the dispersion of components and the interface adhesion between particles/fibers and their matrices are highly relevant when mechanical performance is a concern and not completely achieved. The delivery of bioactive agents at the appropriate pace to specific sites is lacking of sufficient knowledge to allow to the researchers the establishment of success criteria.

In recent years, imaging tools such as magnetic resonance imaging (MRI) and computerized tomography (CT), with increased resolution and more sophisticated software, enabled the gathering of data (both from native tissues and engineered structures) allowing a better design and the definition of priority properties. The fast development of additive manufacturing technologies, which include fused-deposition modeling (FDM) and bioprinting, with a wider choice of biomaterials and even the inclusion of growth factors and cells, is enabling the acquisition of structures more similar to the natural tissues (Costa et al., 2014).

In the future, polymer composites and structures should take a leap forward, not only providing better structural properties (a stage almost achieved), but also enhancing biological functionality. An enhanced biological interaction between cells and structures will certainly have a huge influence on the success of engineered biomaterials.

Acknowledgments

The author P. Sol is grateful to Fundação para a Ciência e a Tecnologia (FCT) for the financial support through the grant SFRH/BD/81133/2011 financed by the POPH/FSE programme. The authors would also like to acknowledge the funding through the QREN project “Novel smart and biomimetic materials for innovative regenerative medicine approaches” co-financed by the North Portugal Regional Operational Programme (ON.2, O Novo Norte) under the National Strategic Reference Framework (NSRF), through the European Regional Development Fund (ERDF).

References

Alberts, B., Johnson, A., Lewis, J., Raff, M., Roberts, K., Walter, P., 2002. Molecular Biology of the Cell. Garland Science, London, UK.

Anselme, K., 2000. Osteoblast adhesion on biomaterials. Biomaterials 21, 667–681.

Badylak, S.F., 2007. The extracellular matrix as a biologic scaffold material. Biomaterials 28, 3587–3593.

Bergshoef, M.M., Vancso, G.J., 1999. Transparent nanocomposites with ultrathin, electrospun nylon-4,6 fiber reinforcement. Advanced Materials 11, 1362–1365.

Binulal, N.S., Deepthy, M., Selvamurugan, N., Shalumon, K.T., 2010. Role of nanofibrous poly (caprolactone) scaffolds in human mesenchymal stem cell attachment and spreading for in vitro bone tissue engineering—response to osteogenic regulators. Tissue Engineering Part A 16 (2), 393–404.

Bosman, F.T., Stamenkovic, I., 2003. Functional structure and composition of the extracellular matrix. The Journal of Pathology 200, 423–428.

Bosworth, L.A., Turner, L.-A., Cartmell, S.H., 2013. State of the art composites comprising electrospun fibres coupled with hydrogels: a review. Nanomedicine 9, 322–335.

Bühler, M., Bourban, P.-E., Månson, J.-A.E., 2008. Cellular composites based on continuous fibres and bioresorbable polymers. Composite Part A: Applied Science and Manufacturing 39, 1779–1786.

Chan, C.K., Kumar, T.S., Liao, S., Murugan, R., Ngiam, M., Ramakrishnan, S., 2006. Biomimetic nanocomposites for bone graft applications. Nanomedicine (London) 1, 177–188.

Chen, G., Liu, H., 2008. Electrospun cellulose nanofiber reinforced soybean protein isolate composite film. Journal of Applied Polymer Science 110, 641–646.

Coburn, J., Gibson, M., Bandalini, P.A., Laird, C., Mao, H.Q., Moroni, L., Seliktar, D., Elisseeff, J., 2011. Biomimetics of the extracellular matrix: an integrated three-dimensional fiber-hydrogel composite for cartilage tissue engineering. Smart Structures and Systems 7, 213–222.

Correlo, V.M., Boesel, L.F., Bhattacharya, M., Mano, J.F., Neves, N.M., Reis, R.L., 2005. Hydroxyapatite reinforced chitosan and polyester blends for biomedical applications. Macromolecular Materials and Engineering 290, 1157–1165.

Costa, P.F., Martins, A., Neves, N.M., Gomes, M.E., Reis, R.L., 2014. Automating the processing steps for obtaining bone tissue-engineered substitutes: from imaging tools to bioreactors. Tissue Engineering Part B Reviews 20, 567–577.

Coutinho, D.F., Gomes, M.E., Neves, N.M., Reis, R.L., 2012. Development of micropatterned surfaces of poly(butylene succinate) by micromolding for guided tissue engineering. Acta Biomaterialia 8, 1490–1497.

David Chen, C.-H., Chen, C.-C., Shie, M.-Y., Huang, C.-H., Ding, S.-J., 2011. Controlled release of gentamicin from calcium phosphate/alginate bone cement. Materials Sciences and Engineering: C 31, 334–341.

Deng, X., He, G., Liao, Y.M., Yao, Y.Y., Chen, Z.Q., Li, G., Zhao, Y., Nie, R.R., Liang, Z.H., Qu, Y.L., Tian, K., 2007. Development of ultrafine fibrous hydroxyapatite/polymer scaffold by electrospinning. In: Key Engineering Materials, 336–338, pp. 1703–1706.

Dodiuk-Kenig, H., Lizenboim, K., Roth, S., Zalsman, B., McHale, W.A., Jaffe, M., Griswold, K., 2008. Performance enhancement of dental composites using electrospun nanofibers. Journal of Nanomaterials 2008.

Drury, J.L., Mooney, D.J., 2003. Hydrogels for tissue engineering: scaffold design variables and applications. Biomaterials 24, 4337–4351.

Eyre, D., 2002. Collagen of articular cartilage. Arthritis Research 4, 30–35.

Fong, H., 2004. Electrospun nylon 6 nanofiber reinforced BIS-GMA/TEGDMA dental restorative composite resins. Polymer (Guildford) 45, 2427–2432.

Frantz, C., Stewart, K.M., Weaver, V.M., 2010. The extracellular matrix at a glance. Journal of Cell Science 123, 4195–4200.

Gao, Y., Sagi, S., Zhang, L., Liao, Y., Cowles, D.M., 2008. Electrospun nano-scaled glass fiber reinforcement of Bis-GMA/TEGDMA dental composites. Journal of Applied Polymer Science 110, 2063–2070.

Gentili, C., Cancedda, R., 2009. Cartilage and bone extracellular matrix. Current Pharmaceutical Design 15, 1334–1348.

Goldring, M.B., 2006. Update on the biology of the chondrocyte and new approaches to treating cartilage diseases. Best Practice and Research: Clinical Rheumatology 20, 1003–1025.

Guilak, F., Baaijens, F.P., 2014. Functional tissue engineering: ten more years of progress. Journal of Biomechanics 47, 1931–1932.

Guilak, F., Butler, D.L., Goldstein, S.A., Baaijens, F.P., 2014. Biomechanics and mechanobiology in functional tissue engineering. Journal of Biomechanics 47, 1933–1940.

He, J., Yang, X., Mao, J., Xu, F., Cai, Q., 2012. Hydroxyapatite–poly(L-lactide) nanohybrids via surface-initiated ATRP for improving bone-like apatite-formation abilities. Applied Surface Science 258, 6823–6830.

Hing, K.A., 2004. Bone repair in the twenty-first century: biology, chemistry or engineering? Philosophical Transactions of the Royal Society of London. Series A, Mathematical, Physical, and Engineering Sciences 362, 2821–2850.

Hunziker, E.B., Quinn, T.M., Hauselmann, H.J., 2002. Quantitative structural organization of normal adult human articular cartilage. Osteoarthritis and Cartilage 10, 564–572.

Jo, J.-H., Lee, E.-J., Shin, D.-S., Kim, H.-E., Kim, H.-W., Koh, Y.-H., Jang, J.-H., 2009. In vitro/in vivo biocompatibility and mechanical properties of bioactive glass nanofiber and poly(epsilon-caprolactone) composite materials. Journal of Biomedical Materials Research Part B: Applied Biomaterials 91, 213–220.

Jung, H.H., Park, K., Han, D.K., 2010. Preparation of TGF-β1-conjugated biodegradable pluronic F127 hydrogel and its application with adipose-derived stem cells. Journal of Controlled Release 147, 84–91.

Kanczler, J.M., Ginty, P.J., White, L., Clarke, N.M.P., Howdle, S.M., Shakesheff, K.M., Oreffo, R.O.C., 2010. The effect of the delivery of vascular endothelial growth factor and bone morphogenic protein-2 to osteoprogenitor cell populations on bone formation. Biomaterials 31, 1242–1250.

Kim, H.-W., Song, J.-H., Kim, H.-E., 2005. Nanofiber generation of gelatin-hydroxyapatite biomimetics for guided tissue regeneration. Advanced Functional Materials 15, 1988–1994.

Kohara, H., Tabata, Y., 2011. Enhancement of ectopic osteoid formation following the dual release of bone morphogenetic protein 2 and Wnt1 inducible signaling pathway protein 1 from gelatin sponges. Biomaterials 32, 5726–5732.

Lee, Y.M., Park, Y.J., Lee, S.J., Ku, Y., Han, S.B., Klokkevold, P.R., Chung, C.P., 2000. The bone regenerative effect of platelet-derived growth factor-BB delivered with a chitosan/tricalcium phosphate sponge carrier. Journal of Periodontology 71, 418–424.

Lin, S., Cai, Q., Ji, J., Sui, G., Yu, Y., Yang, X., Ma, Q., Wei, Y., Deng, X., 2008. Electrospun nanofiber reinforced and toughened composites through in situ nano-interface formation. Composites Science and Technology 68, 3322–3329.

Mano, J.F., Sousa, R.A., Boesel, L.F., Neves, N.M., Reis, R.L., 2004. Bioinert, biodegradable and injectable polymeric matrix composites for hard tissue replacement: state of the art and recent developments. Composites Science and Technology 64, 789–817.

Marimuthu, M., Kim, S., 2009. Survey of the state of the art in biomaterials, cells, genes and proteins integrated into micro- and nanoscaffolds for tissue regeneration. Current Nanoscience 5, 189–203.

Martins, A., Pinho, E.D., Correlo, V.M., Faria, S., Marques, A.P., Reis, R.L., Neves, N.M., 2010. Biodegradable nanofibers-reinforced microfibrous composite scaffolds for bone tissue engineering. Tissue Engineering Part A 16, 3599–3609.

Mathieu, L.M., Mueller, T.L., Bourban, P.-E., Pioletti, D.P., Müller, R., Månson, J.-A.E., 2006. Architecture and properties of anisotropic polymer composite scaffolds for bone tissue engineering. Biomaterials 27, 905–916.

Matyjaszewski, K., Tsarevsky, N.V., 2009. Nanostructured functional materials prepared by atom transfer radical polymerization. Nature Chemistry 1, 276–288.

Meyers, M., Chen, P., Lin, A., Seki, Y., 2008. Biological materials: structure and mechanical properties. Progress in Materials Science 53, 1–206.

Muiznieks, L.D., Keeley, F.W., 2013. Molecular assembly and mechanical properties of the extracellular matrix: a fibrous protein perspective. Biochimica et Biophysica Acta Molecular Basis of Disease 1832, 866–875.

Mwenifumbo, S., Shaffer, M.S., Stevens, M.M., 2007. Exploring cellular behaviour with multi-walled carbon nanotube constructs. Journal of Materials Chemistry 17, 1894–1902.

Na, K., Kim, S., Woo, D.-G., Sun, B.K., Yang, H.N., Chung, H.-M., Park, K.-H., 2007. Synergistic effect of TGFbeta-3 on chondrogenic differentiation of rabbit chondrocytes in thermo-reversible hydrogel constructs blended with hyaluronic acid by in vivo test. Journal of Biotechnology 128, 412–422.

Nash, T.J., Howlett, C.R., Martin, C., Steele, J., Johnson, K.A., Hicklin, D.J., 1994. Effect of platelet-derived growth factor on tibial osteotomies in rabbits. Bone 15, 203–208.

Neves, N.M., 2012. Structural Natural Composites. Wiley Encyclopedia of Composites.

Noh, K.-T., Lee, H.-Y., Shin, U.-S., Kim, H.-W., 2010. Composite nanofiber of bioactive glass nanofiller incorporated poly(lactic acid) for bone regeneration. Materials Letters 64, 802–805.

Paital, S.R., Dahotre, N.B., 2009. Calcium phosphate coatings for bio-implant applications: materials, performance factors, and methodologies. Materials Science and Engineering: R 66, 1–70.

Park, J.-H., Lee, G.-S., Shin, U.S., Kim, H.-W., 2011. Self-hardening microspheres of calcium phosphate cement with collagen for drug delivery and tissue engineering in bone repair. Journal of American Ceramic Society 94, 351–354.

Pérez, R.A., Won, J.-E., Knowles, J.C., Kim, H.-W., 2013. Naturally and synthetic smart composite biomaterials for tissue regeneration. Advanced Drug Delivery Reviews 65, 471–496.

Pinho, E.D., Martins, A., Araújo, J.V., Reis, R.L., Neves, N.M., 2009. Degradable particulate composite reinforced with nanofibres for biomedical applications. Acta Biomaterialia 5, 1104–1114.

Poole, A.R., Kojima, T., Yasuda, T., Mwale, F., Kobayashi, M., Laverty, S., 2001. Composition and structure of articular cartilage—a template for tissue repair. Clinical Orthopaedics and Related Research 391, S26–S33.

Prabaharan, M., Mano, J.F., 2006. Stimuli-responsive hydrogels based on polysaccharides incorporated with thermo-responsive polymers as novel biomaterials. Macromolecular Bioscience 6, 991–1008.

Rosso, F., Giordano, A., Barbarisi, M., Barbarisi, A., 2004. From cell-ECM interactions to tissue engineering. Journal of Cellular Physiology 199, 174–180.

Schneider, O.D., Loher, S., Brunner, T.J., Uebersax, L., Simonet, M., Grass, R.N., Merkle, H.P., Stark, W.J., 2008. Cotton wool-like nanocomposite biomaterials prepared by electrospinning: in vitro bioactivity and osteogenic differentiation of human mesenchymal stem cells. Journal of Biomedical Materials Research 84, 350–362.

Schuurman, W., Khristov, V., Pot, M.W., van Weeren, P.R., Dhert, W.J.A., Malda, J., 2011. Bioprinting of hybrid tissue constructs with tailorable mechanical properties. Biofabrication 3.

Shapiro, J.M., Oyen, M.L., 2013. Hydrogel composite materials for tissue engineering scaffolds. JOM 65, 505–516.

Shi, Y., Han, H., Quan, H., Zang, Y., Wang, N., Ren, G., Xing, M., Wu, Q., 2014. Activated carbon fibers/poly(lactic-co-glycolic) acid composite scaffolds: preparation and characterizations. Material Science and Engineering: C 43, 102–108.

Shim, J.H., Kim, J.Y., Park, M., Park, J., Cho, D.W., 2011. Development of a hybrid scaffold with synthetic biomaterials and hydrogel using solid freeform fabrication technology. Biofabrication 3.

Stoppato, M., Stevens, H.Y., Carletti, E., Migliaresi, C., Motta, A., Guldberg, R.E., 2013. Effects of silk fibroin fiber incorporation on mechanical properties, endothelial cell colonization and vascularization of PDLLA scaffolds. Biomaterials 34, 4573–4581.

Supová, M., 2009. Problem of hydroxyapatite dispersion in polymer matrices: a review. The Journal of Materials Science: Materials in Medicine 20, 1201–1213.

Surmenev, R.A., Surmeneva, M.A., Ivanova, A.A., 2014. Significance of calcium phosphate coatings for the enhancement of new bone osteogenesis—a review. Acta Biomaterialia 10, 557–579.

Tayton, E., Purcell, M., Aarvold, A., Smith, J.O., Briscoe, A., Kanczler, J.M., Shakesheff, K.M., Howdle, S.M., Dunlop, D.G., Oreffo, R.O.C., 2014. A comparison of polymer and polymer-hydroxyapatite composite tissue engineered scaffolds for use in bone regeneration. An in vitro and in vivo study. Journal of Biomedical Materials Research Part A 102, 2613–2624.

Thomas, V., Jagani, S., Johnson, K., Jose, M.V., Dean, D.R., Vohra, Y.K., Nyairo, E., 2006. Electrospun bioactive nanocomposite scaffolds of polycaprolactone and nanohydroxyapatite for bone tissue engineering. Journal of Nanoscience and Nanotechnology 6, 487–493.

Tian, M., Gao, Y., Liu, Y., Liao, Y., Hedin, N.E., Fong, H., 2008. Fabrication and evaluation of Bis-GMA/TEGDMA dental resins/composites containing nano fibrillar silicate. Dental Materials 24, 235–243.

Tian, M., Gao, Y., Liu, Y., Liao, Y., Xu, R., Hedin, N.E., Fong, H., 2007. Bis-GMA/TEGDMA dental composites reinforced with electrospun nylon 6 nanocomposite nanofibers containing highly aligned fibrillar silicate single crystals. Polymer (Guildford) 48, 2720–2728.

Tong, H.W., Wang, M., Li, Z.Y., Lu, W.W., 2010. Electrospinning, characterization and in vitro biological evaluation of nanocomposite fibers containing carbonated hydroxyapatite nanoparticles. Biomedical Materials 5.

Tyagi, P., Catledge, S.A., Stanishevsky, A., Thomas, V., Vohra, Y.K., 2009. Nanomechanical properties of electrospun composite scaffolds based on polycaprolactone and hydroxyapatite. Journal of Nanoscience and Nanotechnology 9, 4839–4845.

Wagoner Johnson, A.J., Herschler, B.A., 2011. A review of the mechanical behavior of CaP and CaP/polymer composites for applications in bone replacement and repair. Acta Biomaterialia 7, 16–30.

Weir, M.D., Xu, H.H.K., 2010. Osteoblastic induction on calcium phosphate cement-chitosan constructs for bone tissue engineering. Journal of Biomedical Materials Research Part A 94, 223–233.

Williams, D.F., 2008. On the mechanisms of biocompatibility. Biomaterials 29, 2941–2953.

Woo, K.M., Chen, V.J., Jung, H.M., Kim, T.I., Shin, H.I., Baek, J.H., Ryoo, H.M., Ma, P.X., 2009. Comparative evaluation of nanofibrous scaffolding for bone regeneration in critical-size calvarial defects. Tissue Engineering Part A 15, 2155–2162.

Work, W.J., Horie, K., Hess, M., Stepto, R.F.T., 2007. Definitions of Terms Related to Polymer Blends, Composites, and Multiphase Polymeric Materials, 76, pp. 1985–2007.

Wu, S., Liu, X., Yeung, K.W.K., Liu, C., Yang, X., 2014. Biomimetic porous scaffolds for bone tissue engineering. Material Science and Engineering: R 80, 1–36.

Xu, W., Ma, J., Jabbari, E., 2010. Material properties and osteogenic differentiation of marrow stromal cells on fiber-reinforced laminated hydrogel nanocomposites. Acta Biomaterialia 6, 1992–2002.

Yang, F., Both, S.K., Yang, X., Walboomers, X.F., Jansen, J.A., 2009. Development of an electrospun nano-apatite/PCL composite membrane for GTR/GBR application. Acta Biomaterialia 5, 3295–3304.

Yang, Y., Wimpenny, I., Ahearne, M., 2011. Portable nanofiber meshes dictate cell orientation throughout three-dimensional hydrogels. Nanomedicine 7, 131–136.

Ye, X., Cai, S., Xu, G., Dou, Y., Hu, H., Ye, X., 2013. Preparation and in vitro evaluation of mesoporous hydroxyapatite coated β-TCP porous scaffolds. Materials Science and Engineering. C, Materials for Biological Applications 33, 5001–5007.

Zagris, N., 2001. Extracellular matrix in development of the early embryo. Micron 32, 427–438.

Zhang, Y., Venugopal, J.R., El-Turki, A., Ramakrishna, S., Su, B., Lim, C.T., 2008. Electrospun biomimetic nanocomposite nanofibers of hydroxyapatite/chitosan for bone tissue engineering. Biomaterials 29, 4314–4322.

Bioactive polymer nanocomposites for spinal cord tissue engineering

6

P. Kumar, Y.E. Choonara, G. Modi, V. Pillay
University of the Witwatersrand, Johannesburg, South Africa

6.1 Introduction

Tissue engineering is an evolving field still at a nascent stage and hence has ample scope of trials and tribulations at an infinite level. One of the most challenging areas in this domain is neural tissue engineering owing to the inherent complexity of the nervous system (or more precisely the injured or degenerated nervous system) as well as its direct effect on quality of life (Yang et al., 2004). For the potential restoration of neuronal function after traumatic spinal cord injuries, currently the most common strategies involve administration of glucocorticoids such as methylprednisolone (MP) at a very high dose (up to 2 g within 24 h) or more recently transplantation of precursor cells directly at the site of injury. The controversial high-dose MP administration has shown moderate benefits and is encountered with serious side effects, whereas the directly implanted precursor cells have shown minimal survival owing to the unavailability of supportive environment (Kumar et al., 2014a). The above limitations can be overcome by advanced nerve-tissue engineering strategies whereby the glucocorticoids and several other bioactive agents can be locally delivered to the injury site either by an intrathecally administered drug-loaded three-dimensional (3D) biomaterial scaffold or by incorporating drug-loaded nanoparticles into the scaffold for sustained delivery. The aforementioned 3D archetypes can additionally act as physicomechanical support for the efficient proliferation of and biofactor production by the implanted precursor cells (Kumar et al., 2015). The chapter highlights several biomaterial and polymeric archetypes, such as in situ gelling intrathecally implantable systems consisting of hyaluronic acid–methylcellulose or agarose; extracellular matrix (ECM)-mimicking scaffolds composed of collagen, chondroitin sulfate or silk fibroin; 3D-solid substrates made up of block copolymers or poly(acrylic acid); and nerve guidance channels fabricated from polyhydroxy acids. Furthermore, the effect of adding pristine or drug-loaded nanomaterials such as carbon nanotubes, nanoparticles, microtubules, nanofibers, and piezoelectric nanomaterials on the nanotopographical features and bioactive releasing functionality of polymeric archetypes is discussed. A special attention is given to various biological (human embryonic/mesenchymal/progenitor stem cells), biofactor (glial-derived/brain-derived/vascular endithelial neurotrophic factors, neurotrophin-3, fibroblast growth factor-2, and chondroitinase ATP-binding

Nanocomposites for Musculoskeletal Tissue Regeneration. http://dx.doi.org/10.1016/B978-1-78242-452-9.00006-6

cassette (chABC)), and bioactive (dexamethasone (DEX) and methylprednisolone (MP)) components employed by leading research groups for restriction, repair, regeneration, restoration and reorganization of neuronal tissue after traumatic spinal cord injury. The chapter is broadly divided into two sections: nanoenclatherated polymer composites loaded with bioactives and biomaterial–carbon nanotube composites with no therapeutic agent loaded.

6.2 Bioactive-loaded nanoenclatherated polymer composites

The incorporation of micro- or nanoparticles in polymer hydrogels, scaffolds or coatings has a long history, but the last 10 years has seen the majority of developments in the field of micro–nanoenclatherated-polymer composites for neural tissue engineering. In this section, we provide a brief account of some important research studies having direct or indirect implications toward spinal cord injury interventions. For example, in a very basic but mechanistic study, Kim and Martin (2006) investigated the release of a model anti-inflammatory glucocorticoid (dexamethasone) from poly(lactic-co-glycolic acid) (PLGA) nanoparticles (oil-in-water emulsion technique; arguably the most widely researched polymer nanoparticulate system) embedded in alginate hydrogel matrices. The researchers proposed that the initial burst release characteristic of the PLGA nanoparticles can be contained by the buffering effect of hydrogels thereby preventing the early loss of DEX from the nanoparticles and precisely controlling the release of dexamethasone from the nanocomposite. Although the drug was uniformly distributed in and onto the PLGA nanoparticles, the hydrophobic nature of DEX led to the formation of molecular aggregates after being released from PLGA nanoparticles (NPs) into the alginate matrix—further retarding the release of DEX from the nanocomposite-coated neural electrodes (Fig. 6.1).

The major limitation of the system was the nonuniform distribution and aggregation of PLGA nanoparticles within the hydrogel matrix which was attributed to the hydrophobic nature of PLGA and DEX (Kim and Martin, 2006). In a possible solution to this limitation, Kokai et al. (2010) employed a polymer composite system comprising poly-L-lactide acid (PLLA)-walled poly(lactic-co-glycolic acid) (PLGA) microspheres loaded with glial cell line-derived neurotrophic factor (GDNF) and embedded in a polycaprolactone (PCL) nerve conduit making it an all-poly(hydroxy acid)-based polymeric archetype. The PLLA wall acted as the burst-release barrier, whereas the PCL matrix, being compatible with PLLA–PLGA, allowed uniform dispersion of the microspheres within the conduit. Due to the salt-leaching method of conduit fabrication, the PCL nerve conduit was porous in nature, and hence no loss in final cumulative protein release was observed while sustaining GDNF release over five weeks. Although the researchers tested the composite in a peripheral injury model, this simplified approach has implications reaching to spinal cord injury (SCI) intervention, because GDNF treatment after traumatic SCI is known for its preventative action on reactive astrocytosis and macrophage accumulation (Kokai et al., 2010). Bioactive growth factor-loaded polymeric particles may further form a niche micro- or nanoenvironment within the

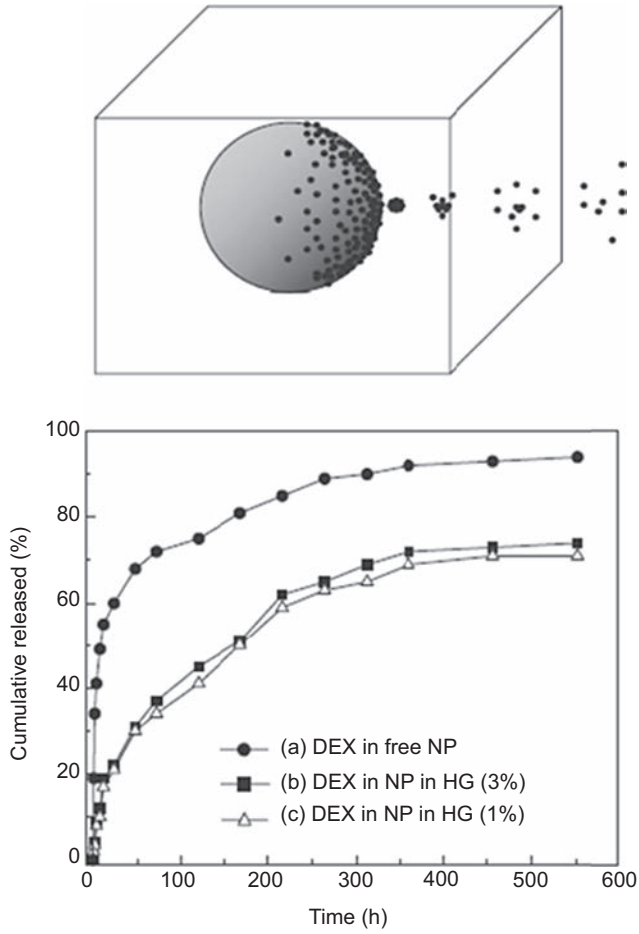

Figure 6.1 (Top) The schematic of release mechanism of encapsulated substance in the micro/NPs through the pores of hydrogel network; and (Bottom) the release of dexamethasone from either (a) free NPs or NPs entrapped within hydrogels with different alginate concentrations (b) 3% and (c) 1%, respectively.
Kim, D.H., Martin D.C., 2006. Sustained release of dexamethasone from hydrophilic matrices using PLGA nanoparticles for neural drug delivery. Biomaterials 27, 3031–3037. Reproduced with permission from Elsevier BV Ltd. © 2006.

outer artificial ECM-mimicking matrix, thereby providing topographical, structural and reservoir support. PLGA microspheres when embedded in a hyaluronic acid hydrogel produced a biocompatible and -degradable system capable of loading and releasing bioactive brain-derived neurotrophic factor (BDNF) and vascular endothelial growth factor (VEGF) within the central nervous system (CNS) environment. In addition to promoting the proliferation and migration of neural stem cells (NSCs), the biomaterial composite stimulated angiogenesis on the materials and produced a neurorescue paradigm for CNS injuries. In terms of physicomechanical properties, the addition of PLGA

microspheres enhanced the elasticity and microroughness of the HYA hydrogel matrix and hence improved the neuronal cell adherence and proliferation. The biofactors, BDNF and VEGF, were consistently released (≈20–30% within 150 h) for a prolonged period forming a neurodurable neuromimicking environment wherein the release (extent and duration) and mechanical properties (soft to hard hydrogel) can be controlled by modulating the amount of cross-linker and/or particles added (Wang et al., 2011). Citing the shortcomings of "impregnated fibronectin mats, fibrin matrices, fibrin sealant, gelatin-tricalcium, phosphate membranes, growth factor eluting conduits, subcutaneous reservoir implantation, and infusion at coaptation site and mini osmotic pumps," de Boer et al. (2011) from Mayo Clinic College of Medicine designed PLGA 50/50 microspheres for incorporation into a PLGA 85/15 nerve conduit. Employing microspheres/conduits of similar polymer formed an "in situ compatible material system" and hence no microspheric interference to regeneration was observed. The researchers observed no significantly enhanced nerve regeneration at all concentration tested conduits (filled with saline and nerve growth factor (NGF) microspheres (5 mg/mL; 20 ng/mL; 50 ng/mL; and 100 ng/mL)) possible due to suboptimal concentrations of nerve growth factor released from the microspheres or conduits. We propose that moving from micro to nano might resolve this issue without compromising the mechanical and functional aspects of the delivery system (de Boer et al., 2011).

In one of the pioneering studies involving polymer neuronanocomposites, Seil and Webster (2008) tested Zinc oxide (ZnO) piezoelectric nanomaterials embedded in polyurethane as potential nerve guidance channels for neuroregeneration after traumatic spinal cord injury. The study was based on three fundamental properties of nanomaterials applicable in tissue engineering, namely (1) biomimetism: nanoscale surface features analogous to nanoscale biological proteins, (2) nanoroughness: enhanced functional area for selective protein adsorption and hence cell adhesion, and (3) grain boundaries with high surface energy—ideal for protein adsorption as well as conformation and hence superior bioactivity. The ZnO–PU nanocomposite provided nanotopographic and piezoelectric properties characterized by nanoroughness and electrical stimulus (generated by mechanical deformation of the scaffold), respectively. Interestingly, an increase in ZnO concentration increased the surface energy of the polymer nanocomposite and significantly reduced the adhesion, proliferation and cell density of astrocytes—a first report proving the scar inhibitory activity of a polymer nanocomposite—thereby providing a conducive environment for axonal growth and neuronal regeneration (Seil and Webster, 2008).

Over the last decade, the research group led by Professor Molly Shoichet at the Donnelly Centre for Cellular and Biomolecular Research (University of Toronto, Toronto, Canada) has published substantial research related to polymer micro- and nanocomposites for neural injury interventions. An environmentally responsive injectable hydrogel composed of hyaluronic acid and methylcellulose (HYAMC) formed the "umbrella neuroarchetype" into which were added bioactive-loaded PLGA nanostructures to achieve CNS repair after traumatic neural injury. The salient findings of these bioactive/HYAMC–PLGA polymer nanocomposite drug delivery systems are detailed below in chronological order:

1. *NBQX, FGF-2, dbcAMP, EGF, NT-3, and anti-NogoA*: In an innovative approach, Baumann et al. (2009) directly loaded HYAMC (2:3:HYA:MC) hydrogels with two neuroprotective

molecules (NBQX and FGF-2), while four neuroregenerative therapeutic molecules (dbcAMP, epidermal growth factor (EGF), and proteins analogous to neuroactive agents NT-3 and anti-NogoA (IgG)) were encapsulated in PLGA nano- and microparticles. In this way, NBQX and FGF-2 were completely released within one and four days, respectively, thereby providing early neuroprotection to the severed spinal cord—the first desirable feature of an effective SCI intervention. Because the HYAMC hydrogel is capable of holding the molecules for maximum four days, the PLGA nanomatrices were employed as a sustained-release mechanism for the efficient delivery of dbcAMP, EGF, NT-3 and anti-NogoA, achieving a linear and controlled release of the biofactors over 28 days. The HYAMC–PLGA polymer nanocomposite proved to be a versatile drug delivery system capable of delivering small to large molecular weight bioactives over 1 through 4–28 days with a high nanoparticle loading of up to 15% without disturbing the injectability of the HYAMC hydrogel. Furthermore, ≈80% of all therapeutic molecules were released locally at the site of administration and ≈95% of PLGA nanoparticles were retained in the HYAMC hydrogel over the study period (Baumann et al., 2009).

2. *Particle-mediated hydrogel stabilization*: Furthering the above research, Baumann et al. (2010) studied the in vivo biosafety and biocompatibility of HYAMC–PLGA polymer nanocomposites, the mechanism inherent to the formation and performance of polymer nanocomposite, and in vitro stabilization of the HYAMC hydrogel by PLGA nanoparticles. The addition of hydrophobic PLGA to HYAMC resulted in a time-dependent increase in gel modulus suggestive of the formation of physical cross-links either by H-bonding or ionic bonding or even via hydrophobic interactions (Fig. 6.2). In contrast to previous reports, the PLGA nanoparticles in this study demonstrated no microglial activation even at twice the concentration and smaller size range which can be attributed to the unique composition of the polymer composite. With respect to biosafety, the composite initiated some inflammation after implantation into the spinal cavity which was attributed to the increase in modulus of the hydrogel. Additionally, no astrocyte activation (astrogliosis) and increase in cystic cavity volume was reported for nanocomposite or the individual components. Although the polymer nanocomposite demonstrated excellent neurocompatibility and durability, no improvement in locomotor function was reported with drug-free (blank) polymer nanocomposite corroborating the nonbioactivity of this injectable neural implant (Baumann et al., 2010).
3. *Hydrogel–electrospun-fiber composites*: In a first study in this domain, Hsieh et al. (2010) amalgamated poly(caprolactone-co-D,L-lactide) (P(CL:DLLA)) or collagen-electrospun nanofibers with thermoreversible/shear-thinning HYAMC hydrogel for potential cell replacement therapy employing neural stem/progenitor cells (NSPCs). The HYAMC hydrogel maintained the homogeneity of the NSPCs in vitro, in contrast to media alone in which the cells showed substantial aggregation. In comparison to HYAMC, collagen–HYAMC composites reduced the survival, proliferation and differentiation of NSPCs, whereas the (P(CL:DLLA))–HYAMC polymer composites maintained the proliferation while enhancing the differentiation in vitro. Interestingly and for the first time (as claimed by the researchers), NSPCs generated higher "total plasma ATP content" while proliferating as compared to while differentiating. The above results contrasted with earlier reports and will require further investigation in support of the argument. In conclusion, (P(CL:DLLA))–HYAMC polymer composites may serve as an effective nanohydrotemplate for efficient neuronal adhesion, proliferation, survival, and differentiation due to their nanotopographical features which can be easily and precisely controlled by modulating the diameter, surface morphology, composition, and strength of the constituent fibers (Hsieh et al., 2010).

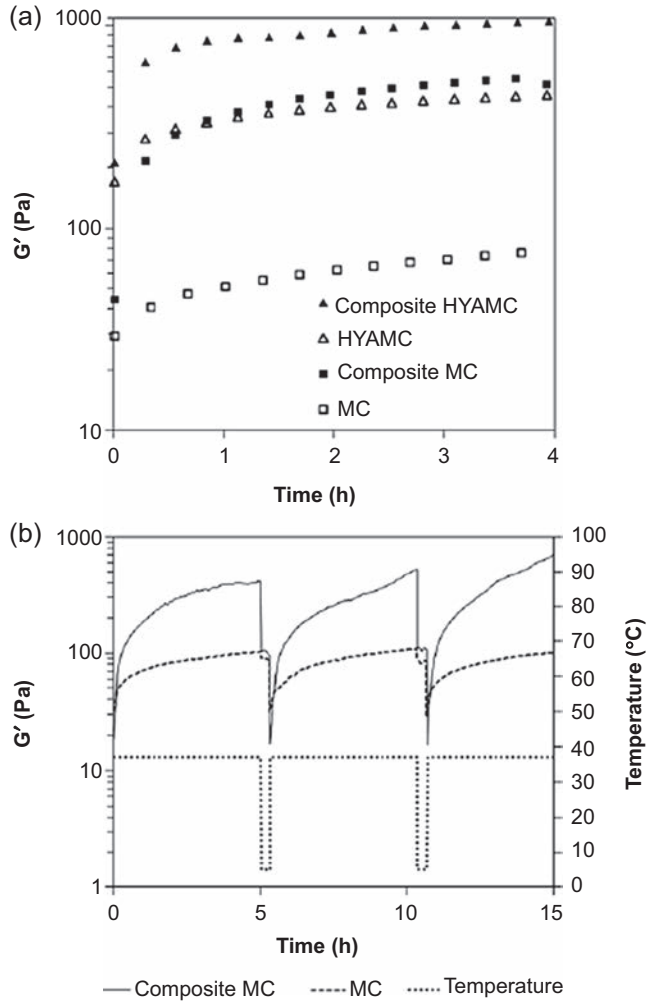

Figure 6.2 Hyaluronic acid (HYA) and nanoparticles dramatically stiffen methylcellulose (MC), but through different mechanisms. In (a), the intrinsic salting out of MC by HYA is immediately evident in a six-fold increase in initial G′(storage modulus) . The effect of nanoparticles on MC is of similar magnitude, and likely due to a hydrophobic association similar to the MC–MC interactions responsible for the inverse thermal gelation of MC. The reversible gelation of MC and composite MC is shown in (b), in which the presence of nanoparticles enhances G′(t, T) at 37°C but not 4°C.
Baumann, M.D., Kang, C.E., Tator C.H., Shoichet M.S., 2010. Intrathecal delivery of a polymeric nanocomposite hydrogel after spinal cord injury. Biomaterials 30, 7631–7639. Reproduced with permission from Elsevier BV Ltd. © 2010.

4. *Neurotrophin-3 bioactivity and release*: Stanwick et al. (2012) tested the HYAMC–PLGA polymer nanocomposite for potential sustained delivery of neurotrophin-3 (NT-3) in vitro with implications reaching to in vivo studies. The careful selection of formulation excipients played a determining role on NT-3 stability and bioactivity, and release with trehalose

significantly enhanced the NT-3 stability during sonication and lyophilization, poly(ethylene glycol) (PEG) enhanced the detection of the encapsulated NT-3 (74%) while increasing the NT-3 release, and co-encapsulated magnesium carbonate sustained the release and bioactivity of NT-3 over 28 days. However, trehalose and PEG were removed from the final formulation because of similar results being obtained from excipient-free formulations. Magnesium carbonate, due to its pH-neutralizing effect on degrading PLGA particles, prevented the autocatalysis of PLGA and hence prolonged the stay and release of NT-3 in and from the particles. This pH adjustment additionally maintained the bioactivity of pH-sensitive NT-3 in and around the nanoparticles. The mathematical continuum model developed for elucidation of bioactive release confirmed that "the linear drug release observed from HYAMC/PLGA polymer nanocomposite was due to a diffusion-limiting layer of methyl cellulose on the particle surface" (Stanwick et al., 2012). In a recent study, Donaghue et al. (2015) established the applicability of HYAMC–PLGA polymer nanocomposite for spinal cord injury intervention in a moderate compressive injury model and intricately determined the release of NT-3 in vitro and in vivo. NT-3 was encapsulated in PLGA nanoparticles (220 nm) at efficiency and loading of ≈50% and 1.03 μg/mg nanoparticle, respectively. The bioactive showed a triphasic release pattern from the HYAMC–PLGA drug delivery system (DDS) over 50 days with initial slow release (10 days), intermediate faster release (10–28 days) and final slow release (28–60 days) with ≈85% drug being released in 28 days. During in vivo testing, NT-3 was detected over 28 days at the lesion site with a total of 3% of the delivered drug detected at the lesion site. Additionally, NT-3 was detected throughout the depth of the spinal cord confirming ventral diffusion of NT-3 from the lesion site. The in vivo NT-3 release results corroborated well with the in vitro studies. According to Basso Beattie Bresnahan (BBB) locomotor scale, the behavioral studies demonstrated "frequent to consistent forelimb–hindlimb coordination" in comparison to drug-free scaffold and untreated control group (Donaghue et al., 2015).

5. *Sustained delivery of FGF-2*: Fibroblast growth factor-2 (FGF-2), when applied locally, can lead to reduction in vasoconstriction along with initiation of angiogenetic response in vicinity of primary SCI area. Kang et al. (2012) encapsulated FGF-2 within PLGA nanoparticles which were then embedded in injectable HYAMC hydrogel to fill the SCI defect. The FGF-2 was released in a controlled and programmed manner from the HYAMC–PLGA DDS within 8 days postimplantation, thereby achieving vasoprotection and increased vascular density within the posttraumatic angiogenesis time frame (Kang et al., 2013).

Over the years, a research team led by Ravi V. Bellamkonda (Wallace H. Coulter Department of Biomedical Engineering, Georgia Institute of Technology/Emory University, USA) has made remarkable contributions toward polymer micro- and nanocomposites for spinal cord injury interventions. They employed in situ gelling 3D agarose scaffolds as the micro- and nanocarrier system due to its (1) biocompatibility: minimal inflammatory response when implanted in vivo; (2) neuroapplicability: easy manipulation of the axonal outgrowth by varying the porosity and physicomechanical properties; (3) reservoirability: storage and delivery of trophic factors either via direct loading or through secondary enclatherated carriers; (4) ability to support cell migration; and (5) protein-binding property for spatial control of therapeutic macromolecules such as BDNF. Initially, self-assembled lipid microtubules synthesized from 1,2-bis-(triscosa-10,12-diynoyl)-sn-glycero-3-phosphocholine ($DC_{8,9}PC$) were loaded with BDNF followed by enclatheration into the agarose hydrogel. Due to the high gelation temperature of hydroethylated agarose, the agarose gel composite was exposed to cold nitrogen rendering rapid in situ gelation of the delivery system. The

BDNF released from the scaffold retained its bioactivity as evident from the resultant "no axonal bulbed-up morphology" along with significantly higher interfacial crossing of the growing axons into and over the hydrogel architecture. Additionally, BDNF assisted in (1) neurite outgrowth within the scaffold; (2) reduction of astrocyte reactivity; (3) inhibition of chondroitin sulfate proteoglycans (CSPGs) production; (4) the entry and crossing of regenerating axons into and across, respectively, the agarose scaffold; (5) enhancing the biocompatibility of the scaffold by attenuating the minimal inflammatory response (Jain et al., 2006). Furthering the agarose–microtubule paradigm, Lee et al. (2010) encapsulated chondroitinase ABC (chABC; a glycosaminoglycan-digesting enzyme) into the lipid microtubules to attain minimally invasive, sustained, and localized delivery of chABC in a dorsal-over-hemisection injury model. Due to the thermal sensitivity of chABC (complete loss of activity at 37°C within three to five days), it was thermostabilized employing a novel method involving a sugar, wherein trehalose conformationally stabilized chABC against thermal degradation and prolonged the in vivo enzymatic activity of chABC against chondroitin sulfate proteoglycans (CSPGs) over two weeks. Interestingly, agarose-microtubule–chABC scaffolds in combination with neurotrophin-3 resulted in enhanced axonal sprouting (sensory axons and serotonergic fibers) and functional recovery (locomotor function) following topical delivery as compared to once-off injection of unstabilized chABC. Furthermore, sustained release of bioactive chABC kept CSPG levels significantly low for approximately six weeks postinjury, thereby overcoming the CSPG-mediated regenerative failure (Lee et al., 2010). In a recent study, Jain et al. (2011) targeted CSPG-mediated inhibition of axonal regeneration through agarose–microtubule-based localized delivery of constitutively active (CA) Rho GTPases (CA-Rac1 and CA-Cdc42) together with BDNF. The cumulative release of bioactives in vitro and in vivo showed a major burst release of 3 and 4 mg on the first and the next three days, respectively, followed by a sustained release of 3 ng/day for a further 11 days—perfectly mimicking the therapeutic paradigm involving a bolus dose followed by a high- and low-dose infusion. The spatial distribution analysis confirmed the presence of BDNF up to 2 mm proximal to the lesion site. Additionally, the immunohistochemcal profiling of the extracted tissue revealed the uptake of BDNF by the ED-1+ cells together with the presence of neurotrophins along the lesion site. The hydrogel–microtubule acted as a "barrier removal system" wherein the localized delivery of CA-Cdc42 and CA-Rac1 decreased the sensitivity of growth cones to CSPGs promoting axonal growth across the otherwise inaccessible CSPG-rich regions (Jain et al., 2011). In conclusion, the hydrogel–microtubule composite system allowed (1) conformal filling of the lesion cavity due to its thermosensitivity; and (2) slow and localized release of neuroprotective or axonal migration bioactives.

Taking leads from the above composite system, Bellamkonda and co-workers designed and tested the applicability of an injectable polymer nanocomposite for localized delivery of methylprednisolone to the lesion site in a contusion injury model (Fig. 6.3). Chvatal et al. (2008) reported the spatial distribution and the acute inflammatory effect of MP after release from MP-loaded PLGA nanoparticles dispersed in an agarose gel. The drug was coupled with Texas-red cadaverine (Tx, Biotium) to make its visualization possible in the areas surrounding spinal cord. This

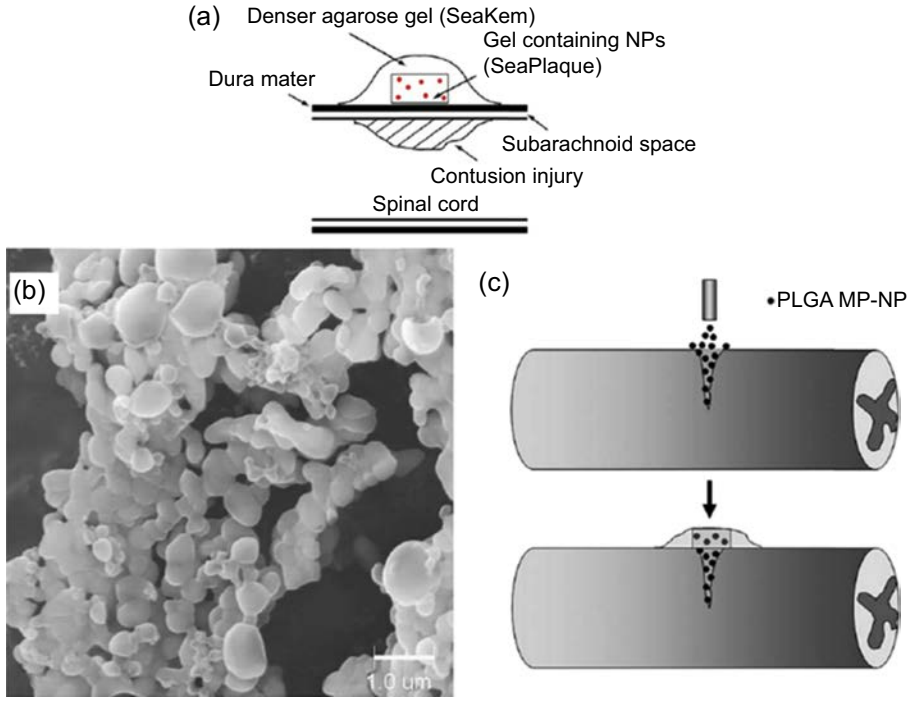

Figure 6.3 (a) Schematic showing the Tx-MP-NP-embedded gel is placed directly onto the injury site, on top of the dura. The denser gel is injected on top and quickly cooled to hold the NP-embedded gel in place and minimize outward diffusion of Tx-MP. (b) Methylprednisolone-encapsulating PLGA nanoparticles (PLGA MP-NP): scanning electron microscopy (SEM) image of the lyophilized PLGA MP-NPs. (c) Schematic of topical and local delivery of the PLGA MP-NPs onto dorsal-over-hemisection-lesioned spinal cord.
Chvatal, S.A., Kim, Y.T., Bratt-Leal, A.M., Lee, H., Bellamkonda, R.V., 2008. Spatial distribution and acute anti-inflammatory effects of methylprednisolone after sustained local delivery to the contused spinal cord. Biomaterials 29 (12), 1967–1975; Kim, Y.T., Caldwell, J.M., Bellamkonda, R.V., 2009. Nanoparticle-mediated local delivery of methylprednisolone after spinal cord injury. Biomaterials 30 (13), 2582–2590. Reproduced with permission from Elsevier BV Ltd. © 2008 and 2009.

was followed by preparation of PLGA nanoparticles which were then incorporated into agarose gel. The release pattern of Tx–MP from the gel-embedded NPs was measured by release of drug–indicator conjugate over six days which was due to gradual degradation of PLGA. This system provided lipid-peroxidation inhibition during the initial and acute phase of secondary injury via continual delivery of MP to the injured spinal cord in a single administration. Further, in vitro release studies were carried out by co-incubation with lipopolysaccharide (LPS)-stimulated primary rat microglia and nitric oxide (NO) released from the microglia at different time points was measured. The results validated that cells treated with Tx-PLGA MP-NPs had significant reduction in NO produced as compared to the negative control. Decreased

early inflammation, lower number of ED-1 macrophages/activated microglia, reduced expression of proinflammatory proteins and eventually reduced lesion volume within a week after contusion injury was observed in this study (Chvatal et al., 2008). In 2009, Kim and co-workers extended the above study by carrying out histological and behavioral study of MP delivery by the use of biodegradable polymer-based nanoparticles and observed decreased reactivity of proapoptotic proteins, increased reactivity of antiapoptotic protein and reduced inducible nitric oxide synthase (iNOS) indicating that MP treatment lowered the mitochondria-mediated cell-death pathway. This proved that sustained MP delivery by slow release PLGA MP-NP can decrease the reactivity of the injury-related proteins. Hence it could be deduced that PLGA MP-NP local delivery has improved therapeutic effect as compared to the systemic MP delivery and has more efficient targeted delivery to the injured site in a significantly lower dose. In addition, delivery rate and duration could be adjusted as the MP release profile from nanoparticles can be manipulated through the composition of the biodegradable polymer. It also gives advantage of stable formulation in the form of injectable and lyophilized powder formulation. The lyophilized formulation could be stored as a powder and easily suspended in saline or implanted in hydrogel when required to be delivered onto the lesion site (Kim et al., 2009).

6.3 Biomaterial carbon nanotube composites

Carbon nanotubes (CNTs) are one-dimensional nanomaterials employed in various bio-devices owing to their excellent tensile strength and electroconductive properties. Although their aggressive aggregation behavior limits their use in large concentrations, appropriately functionalized and encapsulated–embedded CNTs offer distinctive biocompatible advantages (Sridharan et al., 2009; Cho and Borgens, 2010). The stand-out aspect of CNTs, as compared to other nanomaterials such as graphene, is that their size is analogous to neuronal ECM components (collagens and laminins) together with aspect ratios matching with those of nerve fibers, axonal growth cones and synapses—making them a perfect candidate for the design of polymeric nanocomposites for neural tissue engineering, especially spinal cord injury interventions wherein neurogenesis and/or neuronal lineage is an important aspect for the survival and success of stem cell transplantation. In addition to size, CNTs offer excellent mechanical strength while being flexible, are conductive in nature, help maintain scaffold structural integrity by providing "organized fractal-like nanostructure," are not affected by environmental conditions, and can initiate signal transmission among growing axons (electrical shortcuts) (Serrano et al., 2014; Chen et al., 2012; Chao et al., 2009).

The physical environment in the form of ECM plays a critical role in stem cell differentiation, proliferation and lineage selection. The ECM can be closely mimicked by designing scaffolds derived from native ECM components such as collagen and elastin or by incorporating biopolymers such as silk fibroin. However, the ECM matrices so produced demonstrate weak physical strength due to the absence of "naturally inherent" inter- and intracomponent linkages. Sridharan et al. (2009) compared a composite system comprising type I collagen and CNT with respect to soft gelatin matrices for

their ability to induce differentiation in human Embryonic Stem Cell (hESC) culture. Although the gelatin matrices showed full differentiation into all three endoderm, mesoderm and ectoderm lineages, the collagen–CNT composite demonstrated focused neurogenic ectodermal lineage over the coarsely aligned matrix microstructure proving its potential as an advanced "neural-cell based bio-device." In addition to providing anisotropic local stresses, the incorporation of CNT to collagen rendered improved collagen–collagen interaction along with the nanostructurization of collagen and formation of thick, resilient and nonwoven fibrillar architecture (Sridharan et al., 2009). The neuroapplicability of collagen–CNT was further demonstrated by Cho and Borgens (2010), wherein the researchers incorporated multiwall carbon nanotubes (MWCNTs) in collagen scaffolds and evaluated the effect of their electroconductivity on neurite outgrowth. The uniformly distributed MWCNTs imparted enhanced electroactivity even at very low concentrations of less than 1%. Furthermore, the electrical stimulation immensely affected the adhesion, metabolic activity, and neurite extension of pheochromocytoma (PC12) cells leading to electroguidance-based neurite outgrowth characterized by the presence of soma, neurites, and growth cones outlined by microspikes and filopodia. The addition of MWCNTs to collagen augmented the attachment between the neurocytoskeleton and the nanocomposite surface as revealed by fluorescence microscopy analysis of sprouting focal adhesions (Cho and Borgens, 2010). In addition to collagen, another important component of natural neural architecture under extensive investigation is chondroitin sulfate (CS). When combined with MWCNTs, CS scaffolds form a "synergistic neural-permissive platform" capable of promoting the formation of a neuron-enriched network within a neuronal lesion and hence restricting the transitory glial content. The inherent nanofeatures and adsorptive properties of MWCNTs contributed toward the formation of a 3D reservoir of growth factors and allowed (1) differentiation of embryonic neural progenitor cells (ENPCs) without the usual coating with neuron adhesion-promoting molecules such as poly-L-lysine or laminin, (2) higher neurons–glial cells ratios, (3) activation of Ca^{++} signaling, and (4) maintenance of mitochondrial membrane potential and function (Serrano et al., 2014).

It is apparent that natural ECM components such as collagen and chondroitin sulfate provide better neuronal viability and adhesion as compared to natural and synthetic non-ECM biomaterials. However, if coated with neuron adhesion-promoting molecules, non-ECM biomaterials can be employed to produce neuroarchetypes perfectly mimicking the neuro-ECM. Based on the above proposition, Chen et al. (2012) designed laminin-coated silk–MWCNT composite scaffolds for potential spinal cord injury intervention. The hydrophobic component of the silk fibroin (75% of total fibroin protein) demonstrated excellent compatibility with the hydrophobic MWCNTs, whereas the hydrophilic component acted as a dispersant for MWCNTs within the silk scaffold. Human embryonic stem cells (hESCs) seeded on silk–CNT substrates showed distinctive neuronal somas along with longer, high-density axonal sprouting forming "complex 3-D axonal bundle networks" as characterized by upregulation of β-III tubulin and nestin. Furthermore, the biodegradability of silk–CNT scaffolds provided a porous architecture with large surface area for efficient cell–scaffold interaction and adequate space conducive for extensive axonal sprouting and extension (Chen et al., 2012).

Although it is feasible to uniformly disperse CNTs within a scaffold by employing selective polymers with selective hydrophobic–hydrophilic–compatible–dispersant balance, a perfectly uniform polymer nanocomposite can only be achieved by covalent interaction between the CNT and the polymer chain. In an interesting study published by Chao et al. (2009), the researchers demonstrated the selective differentiation of hESCs into neuronal cells in the presence of CNTs grafted on poly(acrylic acid) substrate. In comparison to a poly-L-ornithine surface, a well-known neuronal culture substrate, the poly(acrylic acid)–CNT films demonstrated enhanced neuronal differentiation (about two times) accompanied by excellent cellular viability and maturity due to their protein-adsorption and cell-attachment properties augmented by topological (robust yet flexible nanotube architecture) and biological (obtained by polymer grafting) cues offered by poly(acrylic acid)–CNT films (Fig. 6.4; Chao et al., 2009).

The neuroperformance and compatibility of polymer–nanotube composites can be enhanced by focused functionalization of nanotubes as described as follows:

1. Carboxylic functionalized single-walled carbon nanotubes (SWCNTs): Carbon nanotubes if appropriately functionalized can provide desired microenvironment conducive to neurogenesis (Sridharan et al., 2009). Tay et al. (2010) from Nanyang Technological University,

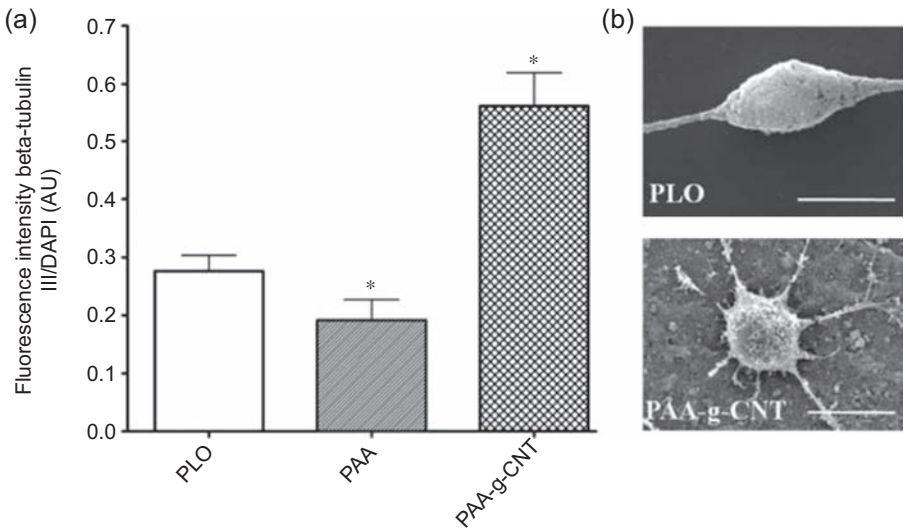

Figure 6.4 Enhanced neuron differentiation on poly(acrylic acid) (PAA)-grafted (g)-CNT 2D scaffolds. (a) Neuron differentiation efficiency characterization. Cells were stained with neuron specific marker β-tubulin III (1:500) and nuclei were counter-stained with DAPI (1:5000). Images were acquired by using fixed exposure time in every field. Differentiation efficiency was acquired by calculating fluorescence intensity of immunopositive cells against DAPI-stained cells. Values were shown as mean ± SEM. (b) SEM images of cells on poly-L-ornithine (PLO) and PAA–CNT (PAA-g-CNT) surfaces, seven days after attachment.
Chao, T.I., Xiang, S., Chen, C.S., Chin, W.C., Nelson, A.J., Wang, C., Lu, J., 2009. Carbon nanotubes promote neuron differentiation from human embryonic stem cells. Biochem. Biophys. Res. Commun, 384, 426–430. Reproduced with permission from Elsevier BV Ltd. © 2009.

Singapore, chemofunctionalized SWCNTs with carboxylic acid (—COOH), enhancing their biocompatibility and cell-adherence capability. With no induction medium employed, the carboxylic-functionalization additionally provided topographical cues in the form of nanoroughness leading to neurogenetic lineage in human mesenchymal stem cells (hMSCs) as evidenced from the formation of microspikes and the upregulation of neurogenic gene markers (nestin, glial fibrillary acidic protein and microtubule-associated protein 2) (Tay et al., 2010).

2. Pluronic-coated carbon nanotubes: The applicability of carbon nanotubes for neural tissue engineering was further proved by Bardi et al. (2009), wherein the carbon nanotubes when coated with Pluronic F127 (PF127), a PPO–PEO–PPO block copolymer, showed more distinctive biocompatibility properties than the individual components. The researchers proposed that PF127 stabilized and solubilized the CNTs due to its surfactant action, whereas CNTs circumvented the PF127-induced apoptosis by the so-called surfactant sequestration mechanism (Bardi et al., 2009).

6.4 Future trends

From the aforementioned discussion, it is evident that combinatorial strategies involving "precursor cells or growth factors + ECM-mimiking [sic] scaffolds + nanomaterials" have demonstrated immense potential in improving the neurological, neurochemical, and behavioral outcome after implantation post-TSCI. However, these "bioactive polymer nanocomposites" are still far from being designated as "all-in-one neuroprotective and therapeutic systems" because of the following limitations: (1) the localized delivery of the composite system requires adjuvant stabilizers for administration; (2) unavailability of complete in vivo toxicity profile of one-dimensional nanomaterials such as carbon nanotubes or graphenes; (3) complicated fabrication of functionalized chemical surfaces and related bioconjugation; (4) nano-with-scaffold incompatibility along with co-fabrication challenges; (5) nonuniform distribution of nanostructures within the scaffold; (6) narrow therapeutic window of the administered bioactives; (7) pH- and cross-linking-dependent fabrication, stability and degradation of polymeric scaffolds; (8) immunological responses to implanted precursor cells; (9) surface localization of nanoparticles due to hydrophobic–hydrophilic imbalance (Kumar et al., 2014b). We hereby propose two different strategies, bioactive nanostructures and nanostructured biomaterials, which, if merged together, may provide the scientific and clinical community with novel "bioactive nanoenabled neuroplatforms." First, the constituent nanostructures may be (1) developed with neuroactive polymers such as ferulic acid/glycol chitosan nanoparticles (Wu et al., 2014), (2) capable of external modulation such as magnetic polymeric nanoliposomes so that they can be localized to the desired area (Wang et al., 2010), and (3) self-propelled for targeting the activated microglia and macrophages (Papa et al., 2014). The aforementioned nanostructures may be combined with specialized scaffolds, or the 3D neurosupport platforms, designed with intrinsic nanofeatures. This may provide the much needed nanotopographical cues to the regenerating axons. Typical examples of such platforms include (1) assembling electrospun nanofibers and self-assembling peptides into composite guidance channels

(Gelain et al., 2011); (2) electrically conductive polymeric nanofiber composites composed of polypyrrole coating (Lee et al., 2009); (3) microgrooved nerve conduits made of chitosan–gold nanocomposites (Lin et al., 2008); (4) double-layered scaffold in which the nanofibers in each layer are aligned along a different direction (Xie et al., 2009); and (5) composite aligned and random nanofibrous substrates (Gupta et al., 2009). If applied together, these multicomponent and multifunctional systems have implications reaching to clinical application for traumatic neural injuries as well as neurodegenerative conditions; neurite outgrowth, growth cone guidance, and axonal regeneration are key to therapeutic benefits.

List of abbreviations

3D Three–dimensional
AMP Adenosine monophosphate
ATP Adenosine triphosphate
BBB Basso Beattie Bresnahan
BDNF Brain-derived neurotrophic factor
CA Constitutively active
chABC Chondroitinase ABC
CNS Central nervous system
CNT Carbon nanotube
COOH Carboxylic acid
CS Chondroitin sulfate
CSPGs Chondroitin sulfate proteoglycans
dbcAMP Dibutyryl cyclic-AMP
$DC_{8,9}PC$ 1,2-bis-(triscosa-10,12-diynoyl)-sn-glycero-3-phosphocholine
DDS Drug delivery system
DEX Dexamethasone
ECM Extracellular matrix
EGF Epidermal growth factor
ENPC Embryonic neural progenitor cell
FGF-2 Fibroblast growth factor-2
g Grafted
GDNF Glial-derived neurotrophic factor
HYAMC Hyaluronic acid–methylcellulose
hESC Human Embryonic Stem Cell
hMSC Human mesenchymal stem cells
iNOS Inducible nitric oxide synthase
LPS Lipopolysaccharide
MC Methylcellulose
MP Methylprednisolone
MWCNT Multiwalled carbon nanotube
NBQX 2,3-Dioxo-6-nitro-1,2,3,4-tetrahydrobenzo[f]quinoxaline-7-sulfonamide
NGF Nerve growth factor
NO Nitric oxide

NP Nanoparticle
NSC Neural stem cell
NSPC Neural stem/progenitor cell
NT-3 Neurotrophic factor-3
PAA Poly(acrylic acid)
P(CL:DLLA) Poly(caprolactone-co-D,L-lactide)
PC12 Pheochromocytoma cell
PCL Polycaprolactone
PEG Poly(ethylene glycol)
PF127 Pluronic F127
PLGA Poly(lactic-co-glycolic acid)
PLLA poly-L-lactide acid
PLO Poly-L-ornithine
PU Polyurethane
SCI Spinal cord injury
SWCNTs Single-walled carbon nanotubes
TSCI Traumatic spinal cord injury
VEGF Vascular endothelial growth factor
ZnO Zinc oxide

References

Bardi, G., Tognini, P., Ciofani, G., Raffa, V., Costa, M., Pizzorusso, T., 2009. Pluronic-coated carbon nanotubes do not induce degeneration of cortical neurons in vivo and in vitro. Nanomedicine: Nanotechnology Biology and Medicine 5, 96–104.

Baumann, M.D., Kang, C.E., Stanwick, J.C., Wang, Y., Kim, H., Lapitsky, Y., Shoichet, M.S., 2009. An injectable drug delivery platform for sustained combination therapy. Journal of Controlled Release 138 (3), 205–213.

Baumann, M.D., Kang, C.E., Tator, C.H., Shoichet, M.S., 2010. Intrathecal delivery of a polymeric nanocomposite hydrogel after spinal cord injury. Biomaterials 30, 7631–7639.

Chao, T.I., Xiang, S., Chen, C.S., Chin, W.C., Nelson, A.J., Wang, C., Lu, J., 2009. Carbon nanotubes promote neuron differentiation from human embryonic stem cells. Biochemical and Biophysical Research Communications 384, 426–430.

Chen, C.S., Soni, S., Le, C., Biasca, M., Farr, E., Chen, Y.E.T., Chin, W.C., 2012. Human stem cell neuronal differentiation on silk-carbon nanotube composite. Nanoscale Research Letters 7, 126.

Cho, Y., Borgens, R.B., 2010. The effect of an electrically conductive carbon nanotube/collagen composite on neurite outgrowth of PC12 cells. Journal of Biomedical Materials Research Part A 95A, 510–517.

Chvatal, S.A., Kim, Y.T., Bratt-Leal, A.M., Lee, H., Bellamkonda, R.V., 2008. Spatial distribution and acute anti-inflammatory effects of methylprednisolone after sustained local delivery to the contused spinal cord. Biomaterials 29 (12), 1967–1975.

de Boer, R., Knight, A.M., Borntraeger, A., Hébert-Blouin, M.N., Spinner, R.J., Malessy, M.J., Yaszemski, M.J., Windebank, A.J., 2011. Rat sciatic nerve repair with a poly-lactic-co-glycolic acid scaffold and nerve growth factor releasing microspheres. Microsurgery 31 (4), 293–302.

Donaghue, I.E., Tator, C.H., Shoichet, M.S., 2015. Sustained delivery of bioactive neurotrophin-3 to the injured spinal cord. Biomaterials Science 3, 65–72.

Gelain, F., Panseri, S., Antonini, S., Cunha, C., Donega, M., Lowery, J., Taraballi, F., Cerri, G., Montagna, M., Baldissera, F., Vescovi, A., 2011. Transplantation of nanostructured composite scaffolds results in the regeneration of chronically injured spinal cords. ACS Nano 5 (1), 227–236.

Gupta, D., Venugopal, J., Prabhakaran, M.P., Dev, V.R., Low, S., Choon, A.T., Ramakrishna, S., 2009. Aligned and random nanofibrous substrate for the in vitro culture of Schwann cells for neural tissue engineering. Acta Biomater 5 (7), 2560–2569.

Hsieh, A., Zahir, T., Lapitsky, Y., Amsden, B., Wan, W., Shoichet, M.S., 2010. Hydrogel/electrospun fiber composites influence neural stem/progenitor cell fate. Soft Matter 6, 2227–2237.

Jain, A., Kim, Y.T., McKeon, R.J., Bellamkonda, R.V., 2006. In situ gelling hydrogels for conformal repair of spinal cord defects, and local delivery of BDNF after spinal cord injury. Biomaterials 27 (3), 497–504.

Jain, A., McKeon, R.J., Brady-Kalnay, S.M., Bellamkonda, R.V., 2011. Sustained delivery of activated Rho GTPases and BDNF promotes axon growth in CSPG-rich regions following spinal cord injury. PLoS One 6 (1), e16135.

Kang, C.E., Baumann, M.D., Tator, C.H., Shoichet, M.S., 2013. Localized and sustained delivery of fibroblast growth factor-2 from a nanoparticle-hydrogel composite for treatment of spinal cord injury. Cells Tissues Organs 197 (1), 55–63.

Kim, D.H., Martin, D.C., 2006. Sustained release of dexamethasone from hydrophilic matrices using PLGA nanoparticles for neural drug delivery. Biomaterials 27, 3031–3037.

Kim, Y.T., Caldwell, J.M., Bellamkonda, R.V., 2009. Nanoparticle-mediated local delivery of methylprednisolone after spinal cord injury. Biomaterials 30 (13), 2582–2590.

Kokai, L.E., Ghaznavi, A.M., Marra, K.G., 2010. Incorporation of double-walled microspheres into polymer nerve guides for the sustained delivery of glial cell line-derived neurotrophic factor. Biomaterials 31, 2313–2322.

Kumar, P., Choonara, Y.E., Modi, G., Naidoo, D., Pillay, V., 2014a. Cur(Que)min: a neuroactive permutation of curcumin and quercetin for treating spinal cord injury. Medical Hypotheses 82, 437–441.

Kumar, P., Choonara, Y.E., Modi, G., Naidoo, D., Pillay, V., 2014b. Nanoparticulate strategies for the five R's of traumatic spinal cord injury intervention: restriction, repair, regeneration, restoration and reorganization. Nanomedicine (London) 9 (2), 331–348.

Kumar, P., Choonara, Y.E., Modi, G., Naidoo, D., Pillay, V., 2015. Multifunctional therapeutic delivery strategies for effective neuro-regeneration following traumatic spinal cord injury. Current Pharmaceutical Design 21, 1517–1528.

Lee, H., McKeon, R.J., Bellamkonda, R.V., 2010. Sustained delivery of thermostabilized chABC enhances axonal sprouting and functional recovery after spinal cord injury. Proceedings of the National Academy of Sciences of the United States of America 107 (8), 3340–3345.

Lee, J.Y., Bashur, C.A., Goldstein, A.S., Schmidt, C.E., 2009. Polypyrrole-coated electrospun PLGA nanofibers for neural tissue applications. Biomaterials 30 (26), 4325–4335.

Lin, Y.L., Jen, J.C., Hsu, S.H., Chiu, I.M., 2008. Sciatic nerve repair by microgrooved nerve conduits made of chitosan-gold nanocomposites. Surgical Neurology 70 (S1), 9–18.

Papa, S., Ferrari, R., De Paola, M., Rossi, F., Mariani, A., Caron, I., Sammali, E., Peviani, M., Dell'Oro, V., Colombo, C., Morbidelli, M., Forloni, G., Perale, G., Moscatelli, D., Veglianese, P., 2014. Polymeric nanoparticle system to target activated microglia/macrophages in spinal cord injury. Journal of Controlled Release 174, 15–26.

Seil, J.T., Webster, T.J., 2008. Decreased astroglial cell adhesion and proliferation on zinc oxide nanoparticle polyurethane composites. International Journal of Nanomedicine 3 (4), 523–531.

Serrano, M.C., Nardecchia, S., García-Rama, C., Ferrer, M.L., Collazos-Castro, J.E., del Monte, F., Gutiérrez, M.C., 2014. Chondroitin sulphate-based 3D scaffolds containing MWCNTs for nervous tissue repair. Biomaterials 35, 1543–1551.

Sridharan, I., Kim, T., Wang, R., 2009. Adapting collagen/CNT matrix in directing hESC differentiation. Biochemical and Biophysical Research Communications 381, 508–512.

Stanwick, J.C., Baumann, M.D., Shoichet, M.S., 2012. Enhanced neurotrophin-3 bioactivity and release from a nanoparticle-loaded composite hydrogel. Journal of Controlled Release 160 (3), 666–675.

Tay, C.Y., Gu, H., Leong, W.S., Yu, H., Li, H.Q., Heng, B.C., Tantang, H., Loo, H.C.J., Li, L.L., Tan, L.P., 2010. Cellular behavior of human mesenchymal stem cells cultured on single-walled carbon nanotube film. Carbon 48, 1095–1104.

Wang, H., Zhang, S., Liao, Z., Wang, C., Liu, Y., Feng, S., Jiang, X., Chang, J., 2010. PEGlated magnetic polymeric liposome anchored with TAT for delivery of drugs across the blood-spinal cord barrier. Biomaterials 31 (25), 6589–6596.

Wang, Y., Wei, Y.T., Zu, Z.H., Ju, R.K., Guo, M.Y., Wang, X.M., Xu, Q.Y., Cui, F.Z., 2011. Combination of hyaluronic acid hydrogel scaffold and PLGA microspheres for supporting survival of neural stem cells. Pharmaceutical Research 28, 1406–1414.

Wu, W., Lee, S.Y., Wu, X., Tyler, J.Y., Wang, H., Ouyang, Z., Park, K., Xu, X.M., Cheng, J.X., 2014. Neuroprotective ferulic acid (FA)-glycol chitosan (GC) nanoparticles for functional restoration of traumatically injured spinal cord. Biomaterials 35 (7), 2355–2364.

Xie, J., MacEwan, M.R., Li, X., Sakiyama-Elbert, S.E., Xia, Y., 2009. Neurite outgrowth on nanofiber scaffolds with different orders, structures, and surface properties. ACS Nano 3 (5), 1151–1159.

Yang, F., Murugan, R., Ramakrishna, S., Wang, X., Ma, Y.X., Wang, S., 2004. Fabrication of nano-structured porous PLLA scaffold intended for nerve tissue engineering. Biomaterials 25, 1891–1900.

This page intentionally left blank

Chitosan–nanohydroxyapatite nanocomposite for bone-tissue regeneration

7

J. Venkatesan[1], *R. Jayakumar*[1,2], *S. Anil*[3], *S.-K. Kim*[1]
[1]Pukyong National University, Busan, South Korea; [2]Amrita Institute of Medical Sciences and Research Centre, Kochi, India; [3]King Saud University, Riyadh, Saudi Arabia

7.1 Introduction

Bone consists of nanohydroxyapatite (nHA) and collagen major proportions with a hierarchical arrangement. Bone loss or defects are serious concerns for humans worldwide due to motor accidents, birth defects, osteoporosis, and so on. Autograft and allograft are the best-known remedies to treat the loss or defects of bone tissue. Both methods have advantages and disadvantages; the drawbacks are insufficient donor site and transfer of immune disease. In recent years, significant progress has been made to develop artificial organs by synthetic and naturally derived biomaterials. The preparation of artificial bone is one of the biggest challenges for the biomaterials scientist, biologist and orthopedic surgeon. A new field in this science is known as Tissue Engineering (Langer and Vacanti, 1993; Barth et al., 2011). Several biological materials have been prepared and are checked to mimic the natural function of bone. Biopolymers with bioceramics are one of the best approaches to prepare artificial bone. The biopolymers include alginate, chitin/chitosan, hyaluronic acid, poly (lactic acid), poly(glycolic acid), poly(lactic-co-glucolide) copolymers, polypropylene fumarate and poly(ε-caprolactone), and the bioceramics are hydroxyapatite and bioactive bioglass (Rezwan et al., 2006; Jayakumar et al., 2010; Venkatesan and Kim, 2012a,b; Venkatesan et al., 2012b, 2010; Pallela et al., 2012; Ramya et al., 2012).

7.2 Nanohydroxyapatite

Hydroxyapatite [$Ca_{10}(PO_4)_6(OH)_2$] (HA) is one of the most stable forms of calcium phosphate (Kim and Mendis, 2006) and is used in variety of areas, including orthopedic, dental and maxillofacial applications. HA has recently emerged as an important compound for artificial bone preparation due to its osteoconductive properties. The structural similarity of HA with the bone has proven that it can mimic the natural function of bone due to its biocompatibility and osteoconductive nature. However, the mechanical strength of HA is a serious concern when it is used to replace or treat bone loss or defects (Zhou and Lee, 2011). Composite scaffold of

Nanocomposites for Musculoskeletal Tissue Regeneration. http://dx.doi.org/10.1016/B978-1-78242-452-9.00007-8

HA with the biopolymers is a new strategy, and it is reported that it can mimic the natural function of bone (Jeong et al., 2013).

7.3 Chitosan

Chitosan is a structurally linear polysaccharide and one of the most widely reported polymers with HA (Venkatesan and Kim, 2010; Venkatesan et al., 2011, 2012a; Thein-Han and Misra, 2009; Chesnutt et al., 2009; Muzzarelli et al., 2012; Reves et al., 2012); it is found in crustaceans and insects and consists of 2-acetamido-2-deoxy-β-D-glucose (Fig. 7.1(a)). Great importance has been given to marine-derived chitosan for making artificial organs due to its biodegradable, biocompatible, porous structure, suitable for cell growth, and an intrinsic antibacterial easily available from natural sources (Di Martino et al., 2005). Chitosan can be modified into different forms such as fibers, beads, scaffolds, gels, and microspheres according to the shape of the artificial organ.

7.4 Chitosan–nHA composite scaffolds

Remarkable research has been conducted on chitosan–nHA (Fig. 7.1(b)) in past decades. However, still more advanced investigative research is needed to design a

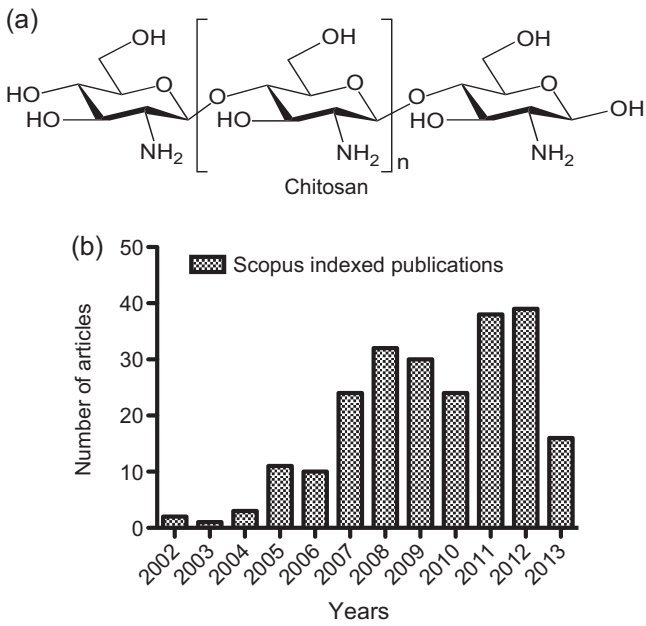

Figure 7.1 (a) Structure of chitosan and (b) scopus indexed articles on chitosan–nHA.

commercial method of production. The combination of chitosan with nHA is one of the best approaches for the preparation of artificial bone. In the present book chapter, we attempted to explore the preparative method, mechanical strength, cellular interaction and in vivo studies of chitosan–nHA composite and its possible future applications.

7.4.1 Production of chitosan–nHA

In situ chemical method is one of the best ways to get the chitosan–nHA nanocomposite biomaterials into pure form (Fig. 7.2). Chemically, nHA can be synthesized using the solution of $Ca(NO_3)_2$ (calcium nitrate) and $NH_4H_2PO_4$ (ammonium dihydrogen phosphate) using ammonia hydroxide solution at pH greater than 10 with the stoichiometric ratio of 1.67. The prepared chitosan–nHA nanocomposite is characterized using different analytical techniques such as Fourier transform-infrared spectroscopy (FT-IR), X-ray diffraction analysis, scanning electron microscopy, transmission electron microscopy and energy dispersive X-ray spectroscopy (Fig. 7.3). Using the chemical method, the formation of nHA in chitosan solution is uniform and significantly reduces the brittleness and crystallinity of HA (Chen et al., 2002; Murugan and Ramakrishna, 2004; Rusu et al., 2005). The mechanical properties of bending strength and modulus of the composite are 86 MPa and 3.4 GPa, which is two to three times stronger than poly(methyl methacrylate) cement (Hu et al., 2004). The biocompatibility of the chitosan–nHA scaffold was assessed with MC3T3-E1 osteoblastic cells. The composite scaffolds showed better biocompatibility than the pure chitosan scaffold (Kong et al., 2005). Manjubala et al. (2006), suggested that

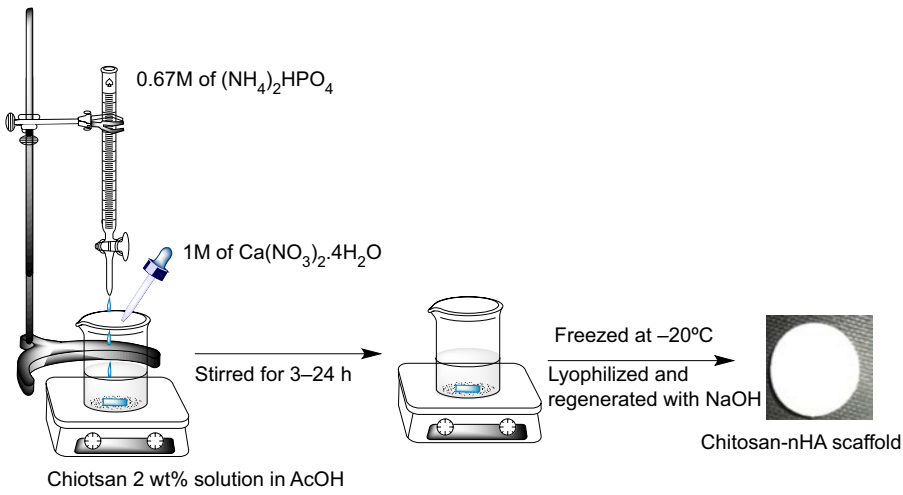

Figure 7.2 Preparative procedure of chitosan–nHA by in situ chemical method.

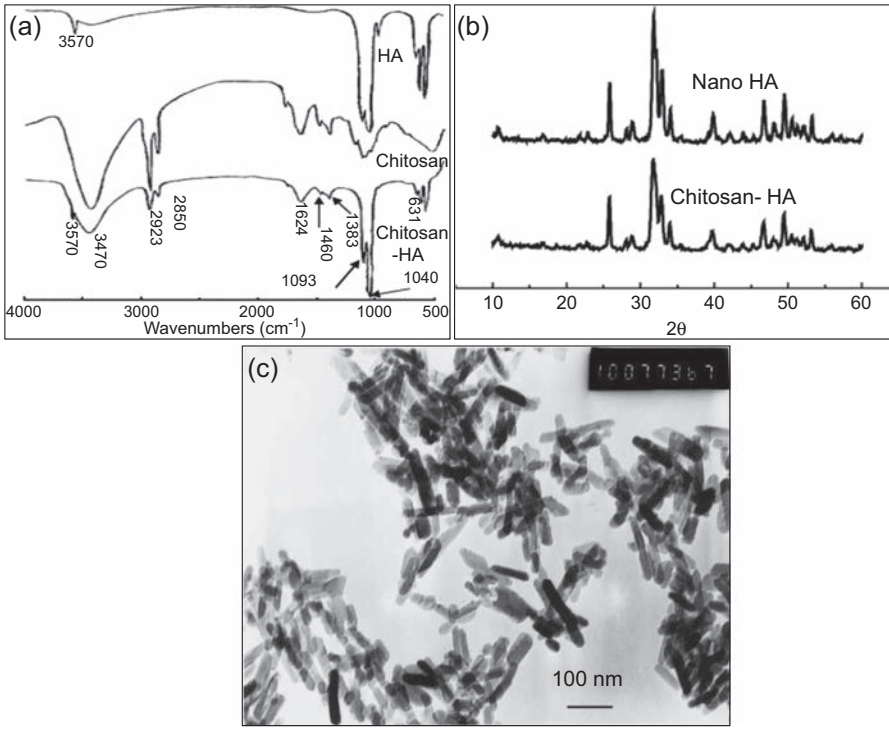

Figure 7.3 Chemical characterization of chitosan–nHA. (a) Fourier Transform-Infrared Spectrum (FT-IR). (b) X-ray diffraction spectrum (c) transmission images of nHA and chitosan–nHA.
Reproduced the figure with permission from Elsevier. (Chen et al., 2002)

double diffusion technique might be a better approach to make the chitosan–nHA scaffold for bone-tissue engineering.

In the literature, some other methods are suggested by a few researchers for the preparation of the nanocomposite of chitosan–nHA: in situ method (Kong et al., 2006), in situ mineralization method (Verma et al., 2008a,b), solvent casting (Murugan and Ramakrishna, 2004), coprecipitation method (Yamaguchi et al., 2003; Teng et al., 2009), simple in situ hybridization (Hu et al., 2004), double diffusion method (Manjubala et al., 2006), biocomposite (Ma et al., 2011), hydroxypropylated chitosan and ethylene glycol functionalized nHA (Depan et al., 2011), homogeneous microstructure (Chen et al., 2002), sol–gel method (Su et al., 2009), and evaporation methods (Xianmiao et al., 2009). Normal bone is made up of approximately 30% organic material and 70% nHA. Li et al. (2005) prepared the composite materials with a 30/70 ratio of chitosan–nHA, and showed a better compressive strength of 120 MPa and higher biodegradability when immersed in a simulated body fluid (SBF) solution. nHA with chitosan can be prepared by using SBF solution. The mineralization of Ca and P ions on the composites was observed with higher chitosan concentration with longer period of exposure (Mohamed et al., 2011a,b; Shi et al., 2012). Li et al. (2012b) used a simple

casting solvent evaporation method that develops chitosan with different amounts of nHA content (1, 5, 10, 15, 20 and 30%). FT-IR results suggest that possible interaction was observed between chitosan and nHA (Li, Nan, et al., 2012b).

Chitosan–nHA composites with different compositions of 0 to 70% were prepared by in situ hybridization methods. The average diameter of the fibers was about 3 nm, whereas the length of the fibers increases from 20 to 60 nm when the nHA content increased from 10 to 70%. Compressive strength and Young's modulus of the nHA composites increases with the nHA content reaching the highest value of 170 and 1.7 GPa (Zhang et al., 2012a). Chitosan with nHA composite was also prepared using in situ chemical method. The particle size of nHA is 40–100 nm (Nikpour et al., 2012).

The effect of chlorotrimethylsilane on bonding of nHA with chitosan–polyacrylamide matrix which was prepared using physical mixing method (Bhat Kalambettu et al., 2012). Chitosan–nHA was prepared by a supercritical fluid-assisted process, and different amounts of nHA (0.25, 0.5, and 1.00%) were added to chitosan solution (Karakeçili and Arıkan, 2012). Hyaluronic acid and collagen with chitosan–nHA were prepared with zearalanol for better bone-tissue formation (Liu et al., 2012). nHA with chitosan film was developed with an in situ combined method (Sun et al., 2012), whereas chitosan with nHA was prepared with an in situ hybridization method. The highest degree of bone regeneration potential observed in nHA powder, with the bone regeneration lowest in nHA with 6 g of chitosan (Tavakol et al., 2013).

Chitosan with nHA macrosphere has also been prepared using a water-in-oil emulsion by in situ generation method. The availability of nHA in the microsphere is poorly crystalline in nature, similar to biological apatite (Ding et al., 2012). Electrospun scaffolds of chitosan and nHA composite were prepared using SBF solution (Thien et al., 2013). nHA–chitosan–poly(L-lactic acid) ternary composite were prepared by physical mixing (Zhang et al., 2013). Chitosan–nHA and polycaprolactone scaffold were checked for bone periodontal tissue engineering. They suggest that bioactive glass incorporation is an important parameter to improve the function of chitosan–nHA for bone-tissue engineering (Shalumon et al., 2013). Chitosan–nHA gelatin preparation (Mohamed et al., 2013), nHA–Si–Mg–Zn–chitosan–collagen scaffold (Tomoaia et al., 2012), chitosan gelatin were prepared by following wet chemical methods (Rajkumar et al., 2013).

The porosity, biocompatibility, mechanical strength and osteogenesis are much more important parameters to keep in mind while preparing the chitosan–nHA composite scaffold for bone-tissue engineering. The fact is, increasing the porosity of the composite scaffold generally decreases the mechanical strength of the scaffolds. To overcome this issue, multilayer scaffold chitosan–nHA can be prepared with the pore size of 15 to 40 μm, which is sufficient for blood and nutrient supplementation (Kong et al., 2007).

Particle size of HA plays an important role in bone regeneration. The additions of nano HA and micro HA in the chitosan matrix were developed with freeze dry lyophilization method. Lee et al. reported on the effects of the surface characteristics of nHA and micro-HA films on the behavior of human mesenchymal stem cells (hMSCs) in vitro. The cell proliferation of hMSC in chitosan with nHA shows better performance than micro-HA with chitosan due to higher surface area of nHA (Lee et al., 2011). The tensile modulus increases more for composites containing nHA than composites containing micro-HA due to nHA being uniformly distributed in the matrix

(chitosan–starch) when compared to micro-HA. However, the swelling percentage decreased for the samples containing nHA (Ai et al., 2011).

The chemical interaction between chitosan and HA is due to an coordination bond which is usually observed by FT-IR spectroscopy, indicating that chitosan interacts with nHA through NH^{3+} groups, whereas in polygalacturonic acid/HA dissociated carboxylate groups (COO-) form unidentate chelate with calcium atoms (Verma et al., 2008a). Chemical bond interaction exists between Ca ions and —OH^- groups of nHA and —NH_2 or —OH groups of chitosan (Xianmiao et al., 2009; Hu et al., 2004). The carboxylic and amino groups play crucial roles for the HA formation on chitosan–gelatin polymer matrix in the presence of citric acid. The formation of nHA particles and the size of the crystals are increased with an increase in the amount of chitosan and gelatin, whereas they are decreased with citric acid addition (Mohamed et al., 2011a,b).

7.4.2 Ternary composites of chitosan–nHA

Saravanan et al. (2011) have suggested that addition of nanosilver (nAg) to the chitosan–nHA composite scaffold significantly improved antimicrobial properties; those composite scaffolds, which are nontoxic to rat osteoprogenitor cells and human osteosarcoma cell line, were prepared by the freeze-dry method. Zinc has been proven to have an antimicrobial property; the addition of nanozinc in nHA to chitosan showed better performance toward bone-tissue engineering (Tripathi et al., 2012). Chen et al. reported two methods for the preparation of chitosan–nHA, the in situ and sol–gel methods. In situ additions of HA possess better performance in elastic modulus, compressive strength, cell proliferation and alkaline phosphatase activity. This may be because, uniformly dispersed and chemical interaction may be possible in in situ formation of HA in the chitosan matrix (Chen et al., 2011).

Chitosan–nHA alone may not be not enough to mimic the natural function of bone. To improve the function of chitosan–nHA, there are several other substances that have to be incorporated. Those materials are from gelatin (Li et al., 2007; Peter et al., 2010), poly(lactic acid) (Zhang et al., 2012b), Konjac glucomannan (Gang et al., 2007), poly(galacturonic acid) (Verma et al., 2008a,b, 2010), β-glycerophosphate (Huang et al., 2009), polyamide 66 (Huang et al., 2012), sodium carboxymethyl cellulose (Jiang et al., 2008, 2009, 2011; Liuyun et al., 2008, 2009), collagen (Wang et al., 2009), starch (Jafar et al., 2011), zinc oxide (Li et al., 2010), collagen gels (Huang et al., 2011), hyaluronic acid (Chen et al., 2012a), poly(vinyl alcohol) (Yang et al., 2008), pectin (Li et al., 2011), magnetite (Cui et al., 2008), genipin (Li et al., 2012b), poly(caprolactone) (Zhou et al., 2007) and gelatin (nHCG) (Li et al., 2009) for bone-tissue engineering. Gel of carboxymethyl chitosan–gelatin–nHA is susceptible to tyrosinase/p-cresol physiological temperature (Mishra et al., 2011).

Hyaluronic acid–chitosan–collagen and nHA was prepared by physical mixing and checked for mechanical strength and its effect on cellular morphology and cell proliferation (Lu et al., 2011). A pulsed electrochemical deposition method has been reported to produce chitosan–nHA with chitosan composite coating on titanium (Ti) substrate. It has been proven that Ti is well known for orthopedic use. The addition of chitosan–nHA substance on the Ti substrate improves biocompatibility, and composites favored

the attachments (Wang et al., 2011). Highly porous scaffold of nHA–polyamide 66 with chitosan coating was investigated for physical and cytological properties. The chitosan coating in the composite scaffold is significantly effective and nontoxic with better cell proliferation (Huang et al., 2012).

7.4.3 *In vitro and in vivo study of chitosan–nHA*

Chitosan and hyaluronic acid with nHA polyelectrolyte sample were prepared by in situ chemical method. The addition of hyaluronic acid to the chitosan–nHA significantly increased the cell proliferation and alkaline phosphatase activity (Chen et al., 2012a). Chitosan–nHA–collagen were checked for cytotoxicity; cell proliferation, alkaline phosphatase, type 1 collagen, RUNX-2 and osteocalcin assay were found to be greater than in chitosan–nHA scaffold compared to chitosan alone in MC3T3-E1 mouse calvarial preosteoblast cells (Chen et al., 2012b). In situ synthesis of nHA with diameter 27 nm and length around 150 nm to chitosan functionalized graphene oxide nHA were produced. Compared with HA, the prepared graphene-incorporated HA composite shows increased elasticity and hardness. The in vitro cytotoxicity assay reveals that the nanocomposite showed better cell proliferation and alkaline phosphatase activity (Li et al., 2013). The cell adhesion and proliferation was 1.5 times higher on chitosan–nHA scaffold compared to chitosan scaffold alone (Thein-Han and Misra, 2009) (Fig. 7.4).

The use of osteoconductive agents is one of the ways to cure bone-related diseases. Bone morphogenetic protein-2 (BMP-2) has been proven as one of the best proteins to solve several bone-related diseases. Stem cell incorporation in the composite scaffold is a better way to improve the function of bone scaffold; nHA with chitosan with bone

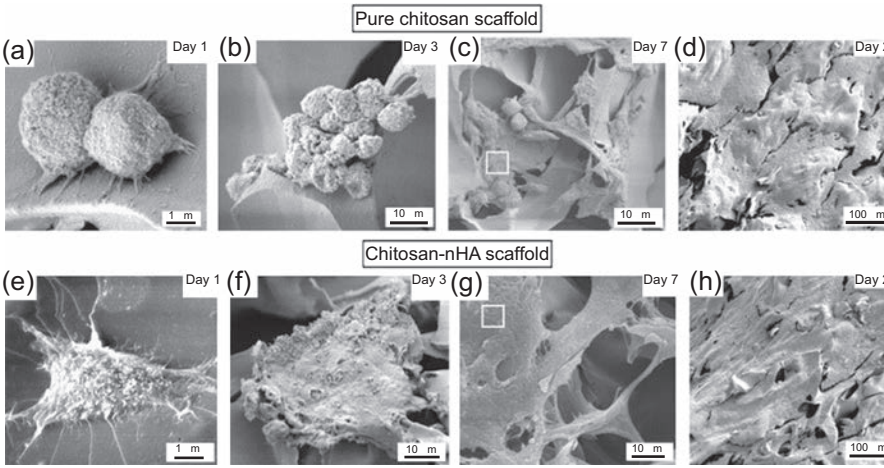

Figure 7.4 Scanning electron micrographs (SEM) of preosteoblasts on chitosan surface after (a) day 1, (b) day 3, (c) day 7 and (d) day 21 of cell culture; and on chitosan–nHA surface after (e) day 1, (f) day 3, (g) day 7 and (h) day 21 of cell culture.
Reproduced the figure with permission from Elsevier. (Thein-Han and Misra, 2009)

marrow mesenchymal stem cells (BMSCs) unregulated the bone markers (Liu et al., 2013). Icariin is plant-derived flavonol glycoside, and has osteoinductive properties for bone regeneration. Chitosan with nHA can be used as a scaffold to release the icariin in specific to enhance bone repair (Fan et al., 2012). Li et al. reported that in vivo study of chitosan–nHA composite was checked in osteochondral defects of rabbits. Bone marrow mesenchymal stem cells were cultivated in chrondrogenic differentiation medium for 2 weeks. The rates were harvested at 4th and 12th week by postoperation; BMSC induced chondrocytes after cultivation with chondrogenic differentiation medium. The scaffolds have good adhesion with chondrocyte (Li et al., 2012a).

Critical-size bone defects (6 mm diameter, 10 mm length) were created in the left femoral condyles of 43 adult New Zealand white rabbits. The femoral condyle bone defects were repaired by nHA–chitosan composite; 8 weeks after surgery, irregular osteon development was detected in the group treated with nHA with chitosan composites compared to pure chitosan; 12 weeks after surgery, complete healing of the segmental bone defects was observed in the nHA group. The injectable form of nHA with chitosan scaffold is a potential candidate for regeneration of bone loss (Zhang et al., 2012c). nHA, chitosan and collagen tricomponent scaffold has been synthesized using in situ-forming hydrogel. Chitosan–nHA hydrogel was injected into rat intravenous tissue and assessed for 28 days. Chitosan–nHA scaffold showed a better stiffness, lower degradation rate, and greater blood supply in the in vivo evaluation than chitosan scaffold (Chen et al., 2012c).

7.5 Future directions

- The addition of a third component in the chitosan–nHA composite will be essential to improve its properties towards cell proliferation, alkaline phosphatase, mineralization and type one collagen production. Synthetic materials, natural polymers, bone morphogenetic protein, glycerol phosphate, antimicrobial substances (zinc, copper, and silver), non-collagenous protein can be 3rd components.
- The addition of stem cells is one of the best approaches to overcome the problems.
- The wet chemical, sol-gel and freeze-drying methods are widely used techniques; still more advanced techniques need to be developed.
- There are significant drawbacks in chitosan purity, degree of deacetylation, viscosity, and molecular weight that play major roles in fabricating scaffolds. The bioactivity of chitosan mainly depends on several things.
- Increasing the mechanical strength of the chitosan–nHA composite is a burning question; it can be overcome by the addition of a very strong component, such as carbon nanotube or graphene.

7.6 Conclusion

Chitosan–nHA nanocomposites have been proven to increase cell proliferation, porosity, increase the osteogenic marker and bone formation. However, the numbers of in vivo studies suggest that addition of a third component in the chitosan–nHA composite is necessary for better bone formation. Proper utilization with

the required property of chitosan–nHA will result in promising biomaterials for bone-tissue regeneration.

Acknowledgments

This research was supported by a grant from Marine Bioprocess Research Center of the Marine Biotechnology Program funded by the Ministry of Oceans and Fisheries, Republic of Korea.

References

Ai, J., Rezaei-Tavirani, M., Biazar, E., Heidari, K.S., Jahandideh, R., 2011. Mechanical properties of chitosan-starch composite filled hydroxyapatite micro-and nanopowders. Journal of Nanomaterials 2011 16.

Barth, H.D., Zimmermann, E.A., Schaible, E., Tang, S.Y., Alliston, T., Ritchie, R.O., 2011. Characterization of the effects of x-ray irradiation on the hierarchical structure and mechanical properties of human cortical bone. Biomaterials 32 (34), 8892–8904.

Bhat Kalambettu, A., Rajangam, P., Dharmalingam, S., 2012. The effect of chlorotrimethylsilane on bonding of nano hydroxyapatite with a chitosan–polyacrylamide matrix. Carbohydrate Research 352, 143–150.

Chen, F., Wang, Z.-C., Lin, C.-J., 2002. Preparation and characterization of nano-sized hydroxyapatite particles and hydroxyapatite/chitosan nano-composite for use in biomedical materials. Materials Letters 57 (4), 858–861.

Chen, J., Zhang, G., Yang, S., et al., 2011. Effects of in situ and physical mixing on mechanical and bioactive behaviors of nano hydroxyapatite–chitosan scaffolds. Journal of Biomaterials Science, Polymer Edition 22 (15), 2097–2106.

Chen, J., Yu, Q., Zhang, G., Yang, S., Wu, J., Zhang, Q., 2012a. Preparation and biocompatibility of nanohybrid scaffolds by in situ homogeneous formation of nano hydroxyapatite from biopolymer polyelectrolyte complex for bone repair applications. Colloids and Surfaces B: Biointerfaces 93 (1), 100–107.

Chen, Y., Huang, Z., Li, X., et al., 2012b. In vitro biocompatibility and osteoblast differentiation of an injectable chitosan/nano-hydroxyapatite/collagen scaffold. Journal of Nanomaterials 2012 3.

Chen, Y., Li, S., Li, X., et al., 2012c. Noninvasive evaluation of injectable chitosan/nano-hydroxyapatite/collagen scaffold via ultrasound. Journal of Nanomaterials 2012 5.

Chesnutt, B.M., Yuan, Y., Buddington, K., Haggard, W.O., Bumgardner, J.D., 2009. Composite chitosan/nano-hydroxyapatite scaffolds induce osteocalcin production by osteoblasts in vitro and support bone formation in vivo. Tissue Engineering Part A 15 (9), 2571–2579.

Cui, W., Hu, Q., Wu, J., Li, B., Shen, J., 2008. Preparation and characterization of magnetite/hydroxyapatite/chitosan nanocomposite by in situ compositing method. Journal of Applied Polymer Science 109 (4), 2081–2088.

Depan, D., Venkata Surya, P., Girase, B., Misra, R., 2011. Organic/inorganic hybrid network structure nanocomposite scaffolds based on grafted chitosan for tissue engineering. Acta Biomaterialia 7 (5), 2163–2175.

Di Martino, A., Sittinger, M., Risbud, M.V., 2005. Chitosan: a versatile biopolymer for orthopaedic tissue-engineering. Biomaterials 26 (30), 5983–5990.

Ding, C.-C., Teng, S.-H., Pan, H., 2012. In-situ generation of chitosan/hydroxyapatite composite microspheres for biomedical application. Materials Letters 79, 72–74.

Fan, J., Bi, L., Wu, T., et al., 2012. A combined chitosan/nano-size hydroxyapatite system for the controlled release of icariin. Journal of Materials Science: Materials in Medicine 23 (2), 399–407.

Gang, Z., Yubao, L., Li, Z., et al., 2007. The study of tri-phasic interactions in nano-hydroxyapatite/konjac glucomannan/chitosan composite. Journal of Materials Science 42 (8), 2591–2597.

Hu, Q., Li, B., Wang, M., Shen, J., 2004. Preparation and characterization of biodegradable chitosan/hydroxyapatite nanocomposite rods via in situ hybridization: a potential material as internal fixation of bone fracture. Biomaterials 25 (5), 779–785.

Huang, Z., Tian, J., Yu, B., Xu, Y., Feng, Q., 2009. A bone-like nano-hydroxyapatite/collagen loaded injectable scaffold. Biomedical Materials 4, 055005.

Huang, Z., Yu, B., Feng, Q., Li, S., Chen, Y., Luo, L., 2011. In situ-forming chitosan/nano-hydroxyapatite/collagen gel for the delivery of bone marrow mesenchymal stem cells. Carbohydrate Polymers 85, 261–267.

Huang, D., Zuo, Y., Zou, Q., et al., 2012. Reinforced nanohydroxyapatite/polyamide 66 scaffolds by chitosan coating for bone tissue engineering. Journal of Biomedical Materials Research Part B: Applied Biomaterials 100 (1), 51–57.

Jafar, A., Mostafa, R.T., Esmaeil, B., Saeed, H.K., Rahim, J., 2011. Mechanical properties of chitosan-starch composite filled hydroxyapatite micro-and nanopowders. Journal of Nanomaterials 2011, 5:391596.

Jayakumar, R., Prabaharan, M., Nair, S., Tamura, H., 2010. Novel chitin and chitosan nanofibers in biomedical applications. Biotechnology Advances 28 (1), 142–150.

Jeong, H.-S., Venkatesan, J., Kim, S.-K., 2013. Hydroxyapatite-fucoidan nanocomposites for bone tissue engineering. International Journal of Biological Macromolecules 57, 138–141.

Jiang, H., Zuo, Y., Cheng, L., Wang, H., Gu, A., Li, Y., 2011. A homogenous CS/NaCMC/n-HA polyelectrolyte complex membrane prepared by gradual electrostatic assembling. Journal of Materials Science: Materials in Medicine 22 (2), 289–297.

Jiang, L., Li, Y., Wang, X., Zhang, L., Wen, J., Gong, M., 2008. Preparation and properties of nano-hydroxyapatite/chitosan/carboxymethyl cellulose composite scaffold. Carbohydrate Polymers 74 (3), 680–684.

Jiang, L.Y., Li, Y.B., Zhang, L., Wang, X.J., 2009. Preparation and characterization of a novel composite containing carboxymethyl cellulose used for bone repair. Materials Science and Engineering: C 29 (1), 193–198.

Karakeçili, A., Arıkan, A., 2012. Preparation of chitosan-nanohydroxyapatite composite scaffolds by a supercritical CO_2 assisted process. Polymer Composites 33 (7), 1215–1223.

Kim, S.-K., Mendis, E., 2006. Bioactive compounds from marine processing byproducts—a review. Food Research International 39 (4), 383–393.

Kong, L., Ao, Q., Wang, A., et al., 2007. Preparation and characterization of a multilayer biomimetic scaffold for bone tissue engineering. Journal of Biomaterials Applications 22, 223–239.

Kong, L., Gao, Y., Cao, W., Gong, Y., Zhao, N., Zhang, X., 2005. Preparation and characterization of nano-hydroxyapatite/chitosan composite scaffolds. Journal of Biomedical Materials Research Part A 75 (2), 275–282.

Kong, L., Gao, Y., Lu, G., Gong, Y., Zhao, N., Zhang, X., 2006. A study on the bioactivity of chitosan/nano-hydroxyapatite composite scaffolds for bone tissue engineering. European Polymer Journal 42 (12), 3171–3179.

Langer, R., Vacanti, J., 1993. Tissue engineering. Science 260 (5110), 920–926.

Lee, Y.-T., Yu, B.-Y., Shao, H.-J., et al., 2011. Effects of the surface characteristics of nano-crystalline and micro-particle calcium phosphate/chitosan composite films on the behavior of human mesenchymal stem cells in vitro. Journal of Biomaterials Science, Polymer Edition 22 (17), 2369–2388.

Li, J., Chen, Y.P., Yin, Y., Yao, F., Yao, K., 2007. Modulation of nano-hydroxyapatite size via formation on chitosan–gelatin network film in situ. Biomaterials 28 (5), 781–790.

Li, J., Dou, Y., Yang, J., et al., 2009. Surface characterization and biocompatibility of micro-and nano-hydroxyapatite/chitosan-gelatin network films. Materials Science and Engineering: C 29 (4), 1207–1215.

Li, J., Sun, H., Sun, D., Yao, Y., Yao, F., Yao, K., 2011. Biomimetic multicomponent polysaccharide/nano-hydroxyapatite composites for bone tissue engineering. Carbohydrate Polymers 85, 885–894.

Li, J.R., Zha, Z.G., Liu, N., et al., 2012a. An experimental research of repairing osteochondral defect in a rabbit model with tissue-engineered nanohydroxyapatite/chitosan graft. Applied Mechanics and Materials 140, 17–23.

Li, X., Nan, K., Shi, S., Chen, H., 2012b. Preparation and characterization of nano-hydroxyapatite/chitosan cross-linking composite membrane intended for tissue engineering. International Journal of Biological Macromolecules 50 (1), 43–49.

Li, M., Wang, Y., Liu, Q., et al., 2013. In situ synthesis and biocompatibility of nano hydroxyapatite on pristine and chitosan functionalized graphene oxide. Journal of Materials Chemistry B 1 (4), 475–484.

Li, Z., Yubao, L., Aiping, Y., Xuelin, P., Xuejiang, W., Xiang, Z., 2005. Preparation and in vitro investigation of chitosan/nano-hydroxyapatite composite used as bone substitute materials. Journal of Materials Science: Materials in Medicine 16 (3), 213–219.

Li, Z., Yubao, L., Yi, Z., Lan, W., Jansen, J.A., 2010. In vitro and in vivo evaluation on the bioactivity of ZnO containing nano-hydroxyapatite/chitosan cement. Journal of Biomedical Materials Research Part A 93 (1), 269–279.

Liu, H., Peng, H., Wu, Y., et al., 2013. The promotion of bone regeneration by nanofibrous hydroxyapatite/chitosan scaffolds by effects on integrin-BMP/Smad signaling pathway in BMSCs. Biomaterials 32 (18), 4404–4417.

Liu, L., Guo, Y., Chen, X., et al., 2012. Three-dimensional dynamic culture of pre-osteoblasts seeded in HA-CS/Col/nHAP composite scaffolds and treated with α-ZAL. Acta Biochimica et Biophysica Sinica 44 (8), 669–677.

Liuyun, J., Yubao, L., Chengdong, X., 2009. Preparation and biological properties of a novel composite scaffold of nano-hydroxyapatite/chitosan/carboxymethyl cellulose for bone tissue engineering. Journal of Biomedical Science 16, 65.

Liuyun, J., Yubao, L., Li, Z., Jianguo, L., 2008. Preparation and properties of a novel bone repair composite: nano-hydroxyapatite/chitosan/carboxymethyl cellulose. Journal of Materials Science: Materials in Medicine 19 (3), 981–987.

Lu, L., Rui-xin, L., Li, Z., et al., 2011. Mechanical properties of hyaluronic acid modifying chitosan/collagen/nano-hydroxyapatite composite scaffold and its effect on osteoblast proliferation. Journal of Clinical Rehabilitative Tissue Engineering Research 15 (38).

Ma, X., Wang, Y., Guo, H., Wang, J., 2011. Nano-hydroxyapatite/chitosan sponge-like biocomposite for repairing of rat calvarial critical-sized bone defect. Journal of Bioactive and Compatible Polymers 26 (4), 335–346.

Manjubala, I., Scheler, S., Bössert, J., Jandt, K.D., 2006. Mineralisation of chitosan scaffolds with nano-apatite formation by double diffusion technique. Acta Biomaterialia 2 (1), 75–84.

Mishra, D., Bhunia, B., Banerjee, I., Datta, P., Dhara, S., Maiti, T.K., 2011. Enzymatically crosslinked carboxymethyl–chitosan/gelatin/nano-hydroxyapatite injectable gels for in situ bone tissue engineering application. Materials Science and Engineering: C 31 (7), 1295–1304.

Mohamed, K.R., Beherei, H.H., El-Rashidy, Z.M., 2013. In vitro study of nano-hydroxyapatite/chitosan–gelatin composites for bio-applications. Journal of Advanced Research 5 (2), 201–208.

Mohamed, K.R., El-Rashidy, Z.M., Salama, A.A., 2011a. In vitro properties of nano-hydroxyapatite/chitosan biocomposites. Ceramics International 37 (8), 3265–3271.

Mohamed, K.R., El-Rashidy, Z.M., Salama, A.A., 2011b. Preparation and characterization of nano hydroxyapatite/polymeric composites materials. Part I. Materials Chemistry and Physics 130 (1), 561–568.

Murugan, R., Ramakrishna, S., 2004. Bioresorbable composite bone paste using polysaccharide based nano hydroxyapatite. Biomaterials 25 (17), 3829–3835.

Muzzarelli, R.A., Greco, F., Busilacchi, A., Sollazzo, V., Gigante, A., 2012. Chitosan, hyaluronan and chondroitin sulfate in tissue engineering for cartilage regeneration: a review. Carbohydrate Polymers 89 (3), 723–739.

Nikpour, M., Rabiee, S., Jahanshahi, M., 2012. Synthesis and characterization of hydroxyapatite/chitosan nanocomposite materials for medical engineering applications. Composites Part B: Engineering 43 (4), 1881–1886.

Pallela, R., Venkatesan, J., Janapala, V.R., Kim, S.K., 2012. Biophysicochemical evaluation of chitosan-hydroxyapatite-marine sponge collagen composite for bone tissue engineering. Journal of Biomedical Materials Research Part A 100 (2), 486–495.

Peter, M., Ganesh, N., Selvamurugan, N., et al., 2010. Preparation and characterization of chitosan-gelatin/nanohydroxyapatite composite scaffolds for tissue engineering applications. Carbohydrate Polymers 80 (3), 687–694.

Rajkumar, M., Kavitha, K., Prabhu, M., Meenakshisundaram, N., Rajendran, V., 2013. Nano-hydroxyapatite–chitosan–gelatin polyelectrolyte complex with enhanced mechanical and bioactivity. Materials Science and Engineering: C 33 (6), 3237–3244.

Ramya, R., Venkatesan, J., Kim, S.K., Sudha, P., 2012. Biomedical applications of chitosan: an overview. Journal of Biomaterials and Tissue Engineering 2 (2), 100–111.

Reves, B.T., Jennings, J.A., Bumgardner, J.D., Haggard, W.O., 2012. Preparation and functional assessment of composite chitosan-nano-hydroxyapatite scaffolds for bone regeneration. Journal of Functional Biomaterials 3 (1), 114–130.

Rezwan, K., Chen, Q., Blaker, J., Boccaccini, A.R., 2006. Biodegradable and bioactive porous polymer/inorganic composite scaffolds for bone tissue engineering. Biomaterials 27 (18), 3413–3431.

Rusu, V.M., Ng, C.-H., Wilke, M., Tiersch, B., Fratzl, P., Peter, M.G., 2005. Size-controlled hydroxyapatite nanoparticles as self-organized organic–inorganic composite materials. Biomaterials 26 (26), 5414–5426.

Saravanan, S., Nethala, S., Pattnaik, S., Tripathi, A., Moorthi, A., Selvamurugan, N., 2011. Preparation, characterization and antimicrobial activity of a bio-composite scaffold containing chitosan/nano-hydroxyapatite/nano-silver for bone tissue engineering. International Journal of Biological Macromolecules 49 (2), 188–193.

Shalumon, K.T., Sowmya, S., Sathish, D., Chennazhi, K.P., Nair, S.V., Jayakumar, R., 2013. Effect of incorporation of nanoscale bioactive glass and hydroxyapatite in PCL/chitosan nanofibers for bone and periodontal tissue engineering. Journal of Biomedical Nanotechnology 9 (3), 430–440.

Shi, H., Wang, W., Lu, D., et al., 2012. Cellular biocompatibility and biomechanical properties of N-carboxyethylchitosan/nanohydroxyapatite composites for tissue-engineered trachea. Artificial Cells, Blood Substitutes and Biotechnology 40 (1–2), 120–124.

Su, W., Sun, K., Chu, C., 2009. The behavior of rhBMP2 gene transfecting cells on nanometer hydroxyapatite/chitosan scaffold. Journal of Medical and Biological Engineering 29, 290–295.

Sun, F., Koh, K., Ryu, S.-C., Han, D.-W., Lee, J., 2012. Biocompatibility of nanoscale hydroxyapatite-embedded chitosan films. Bulletin of the Korean Chemical Society 33 (12).

Tavakol, S., Nikpour, M., Amani, A., et al., 2013. Bone regeneration based on nano-hydroxyapatite and hydroxyapatite/chitosan nanocomposites: an in vitro and in vivo comparative study. Journal of Nanoparticle Research 15 (1), 1–16.

Teng, S.H., Lee, E.J., Yoon, B.H., Shin, D.S., Kim, H.E., Oh, J.S., 2009. Chitosan/nanohydroxyapatite composite membranes via dynamic filtration for guided bone regeneration. Journal of Biomedical Materials Research Part A 88 (3), 569–580.

Thein-Han, W., Misra, R., 2009. Biomimetic chitosan–nanohydroxyapatite composite scaffolds for bone tissue engineering. Acta Biomaterialia 5 (4), 1182–1197.

Thien, D.V.H., Hsiao, S.W., Ho, M.H., Li, C.H., Shih, J.L., 2013. Electrospun chitosan/hydroxyapatite nanofibers for bone tissue engineering. Journal of Materials Science 48 (4), 1640–1645.

Tomoaia, G., Soritau, O., Tomoaia-Cotisel, M., et al., 2012. Scaffolds made of nanostructured phosphates, collagen and chitosan for cell culture. Powder Technology 238, 99–107.

Tripathi, A., Saravanan, S., Pattnaik, S., Moorthi, A., Partridge, N.C., Selvamurugan, N., 2012. Bio-composite scaffolds containing chitosan/nano-hydroxyapatite/nano-copper–zinc for bone tissue engineering. International Journal of Biological Macromolecules 50 (1), 294–299.

Venkatesan, J., Kim, S.-K., 2010. Chitosan composites for bone tissue engineering—an overview. Marine Drugs 8 (8), 2252–2266.

Venkatesan, J., Kim, S.K., 2012a. Nanostructured hydroxyapatite-chitosan composite biomaterial for bone tissue engineering. Advanced Materials Research 584, 212–216.

Venkatesan, J., Kim, S.K., 2012b. Stimulation of minerals by carbon nanotube grafted glucosamine in mouse mesenchymal stem cells for bone tissue engineering. Journal of Biomedical Nanotechnology 8 (4), 676–685.

Venkatesan, J., Pallela, R., Bhatnagar, I., Kim, S.-K., 2012a. Chitosan-amylopectin/hydroxyapatite and chitosan-chondroitin sulphate/hydroxyapatite composite scaffolds for bone tissue engineering. International Journal of Biological Macromolecules 51 (5), 1033–1042.

Venkatesan, J., Ryu, B., Sudha, P.N., Kim, S.-K., 2012b. Preparation and characterization of chitosan–carbon nanotube scaffolds for bone tissue engineering. International Journal of Biological Macromolecules 50 (2), 393–402.

Venkatesan, J., Pangestuti, R., Qian, Z.-J., Ryu, B., Kim, S.-K., 2010. Biocompatibility and alkaline phosphatase activity of phosphorylated chitooligosaccharides on the osteosarcoma MG63 cell line. Journal of Functional Biomaterials 1 (1), 3–13.

Venkatesan, J., Qian, Z.-J., Ryu, B., Ashok Kumar, N., Kim, S.-K., 2011. Preparation and characterization of carbon nanotube-grafted-chitosan—natural hydroxyapatite composite for bone tissue engineering. Carbohydrate Polymers 83 (2), 569–577.

Verma, D., Katti, K.S., Katti, D.R., 2008a. Effect of biopolymers on structure of hydroxyapatite and interfacial interactions in biomimetically synthesized hydroxyapatite/biopolymer nanocomposites. Annals of Biomedical Engineering 36 (6), 1024–1032.

Verma, D., Katti, K.S., Katti, D.R., Mohanty, B., 2008b. Mechanical response and multilevel structure of biomimetic hydroxyapatite/polygalacturonic/chitosan nanocomposites. Materials Science and Engineering: C 28 (3), 399–405.

Verma, D., Katti, K.S., Katti, D.R., 2010. Osteoblast adhesion, proliferation and growth on polyelectrolyte complex–hydroxyapatite nanocomposites. Philosophical Transactions of the Royal Society A: Mathematical, Physical and Engineering Sciences 368 (1917), 2083–2097.

Wang, X., Wang, X., Tan, Y., Zhang, B., Gu, Z., Li, X., 2009. Synthesis and evaluation of collagen–chitosan–hydroxyapatite nanocomposites for bone grafting. Journal of Biomedical Materials Research Part A 89 (4), 1079–1087.

Wang, Y., Lu, X., Li, D., Feng, B., Qu, S., Weng, J., 2011. Hydroxyapatite/chitosan composite coatings on titanium surfaces by pulsed electrochemical deposition. Acta Polymerica Sinica 011 (11), 1244–1252 11004.

Xianmiao, C., Yubao, L., Yi, Z., Li, Z., Jidong, L., Huanan, W., 2009. Properties and in vitro biological evaluation of nano-hydroxyapatite/chitosan membranes for bone guided regeneration. Materials Science and Engineering: C 29 (1), 29–35.

Yamaguchi, I., Iizuka, S., Osaka, A., Monma, H., Tanaka, J., 2003. The effect of citric acid addition on chitosan/hydroxyapatite composites. Colloids and Surfaces A: Physicochemical and Engineering Aspects 214 (1–3), 111–118.

Yang, D., Jin, Y., Ma, G., Chen, X., Lu, F., Nie, J., 2008. Fabrication and characterization of chitosan/PVA with hydroxyapatite biocomposite nanoscaffolds. Journal of Applied Polymer Science 110 (6), 3328–3335.

Zhang, C., Chen, J., Zhuang, Z., Zhang, T., Wang, X., Fang, Q., 2012a. In situ hybridization and characterization of fibrous hydroxyapatite/chitosan nanocomposite. Journal of Applied Polymer Science 124 (1), 397–402.

Zhang, C., Zhang, C., Wang, J., et al., 2012b. Fabrication and in vitro investigation of nanohydroxyapatite, chitosan, poly (L-lactic acid) ternary biocomposite. Journal of Applied Polymer Science 127 (3). http://dx.doi.org/10.1002/app.37795.

Zhang, X., Zhu, L., Lv, H., et al., 2012c. Repair of rabbit femoral condyle bone defects with injectable nanohydroxyapatite/chitosan composites. Journal of Materials Science: Materials in Medicine 23 (8), 1941–1949.

Zhang, C.Y., Zhang, C.L., Wang, J.F., et al., 2013. Fabrication and in vitro investigation of nanohydroxyapatite, chitosan, poly(L-lactic acid) ternary biocomposite. Journal of Applied Polymer Science 127 (3), 2152–2159.

Zhou, G., Li, Y., Zhang, L., Zuo, Y., Jansen, J.A., 2007. Preparation and characterization of nano-hydroxyapatite/chitosan/konjac glucomannan composite. Journal of Biomedical Materials Research Part A 83 (4), 931–939.

Zhou, H., Lee, J., 2011. Nanoscale hydroxyapatite particles for bone tissue engineering. Acta Biomaterialia 7 (7), 2769–2781.

Polymer nanocomposites for drug delivery applications in bone tissue regeneration

8

V. Mouriño
University of Buenos Aires, Buenos Aires, Argentina; A CONICET, Buenos Aires, Argentina

8.1 Introduction and challenges

Tissue engineering and bioactive molecule delivery are closely related fields (Bonassar and Vacanti, 1998; Langer and Vacanti, 1993). Research in tissue engineering as well as controlled drug delivery has progressed greatly in recent years (Goldberg et al., 2007). In particular, the development of scaffolds for bone tissue engineering has progressed from the preparation of porous materials hydrolytically degradable in its beginnings to current alternatives that emphasize the use of multifunctional matrices with the capability to reproduce more closely the topography and functions of bone extracellular matrix (Mouriño et al., 2013a,b; Goldberg et al., 2007). A convenient approach being increasingly investigated to enhance the multifunctional matrix functionality is to load bioactive molecules in the matrix to enhance and accelerate functional bone tissue regeneration and/or to treat a nearby disease; which is leading to a novel research field called tissue engineering (TE) therapeutics (Baroli, 2009; Mouriño and Boccaccini, 2010). In this regard, polymer nanocomposites (PNCs)—combining biodegradable polymers with bioceramics—have established themselves as a promising type of nanocomposite biomaterials for regenerative medicine and drug delivery applications and are widely researched as multifunctional nanomaterials (see Fig. 8.1).

In particular, the possibility of using PNCs in bone tissue engineering (BTE) to serve as both three-dimensional (3D) scaffolds of bone cell proliferation, differentiation, and attachment, and matrices for in situ release of bioactive molecules to enhance cellular activity during bone tissue repair, could represent a versatile approach (Baroli, 2009; Mouriño and Boccaccini, 2010; Goldberg et al., 2007). The multiple capabilities of PNCs originate from the large variety of natural and synthetic biopolymers and a range of nanoparticles available to researchers. Existing biopolymers include, but are not limited to, starch, cellulose, alginate, chitosan, collagen, gelatin, and fibrin, poly (vinyl alcohol) (PVA), poly (ethylene glycol) (PEG), poly (caprolactone) (PCL), poly (lactic-co-glycolic acid) (PLGA), and poly (glycerol sebacate) (PGS). A range of nanoparticles including nanobioceramics, nanohydroxyapatite, mesoporous silica nanoparticles, and metal nanoparticles are incorporated as fillers within the biopolymeric network to design a PNC with the desired property combinations. It is well known that a PNC matrix must meet

Nanocomposites for Musculoskeletal Tissue Regeneration. http://dx.doi.org/10.1016/B978-1-78242-452-9.00008-X

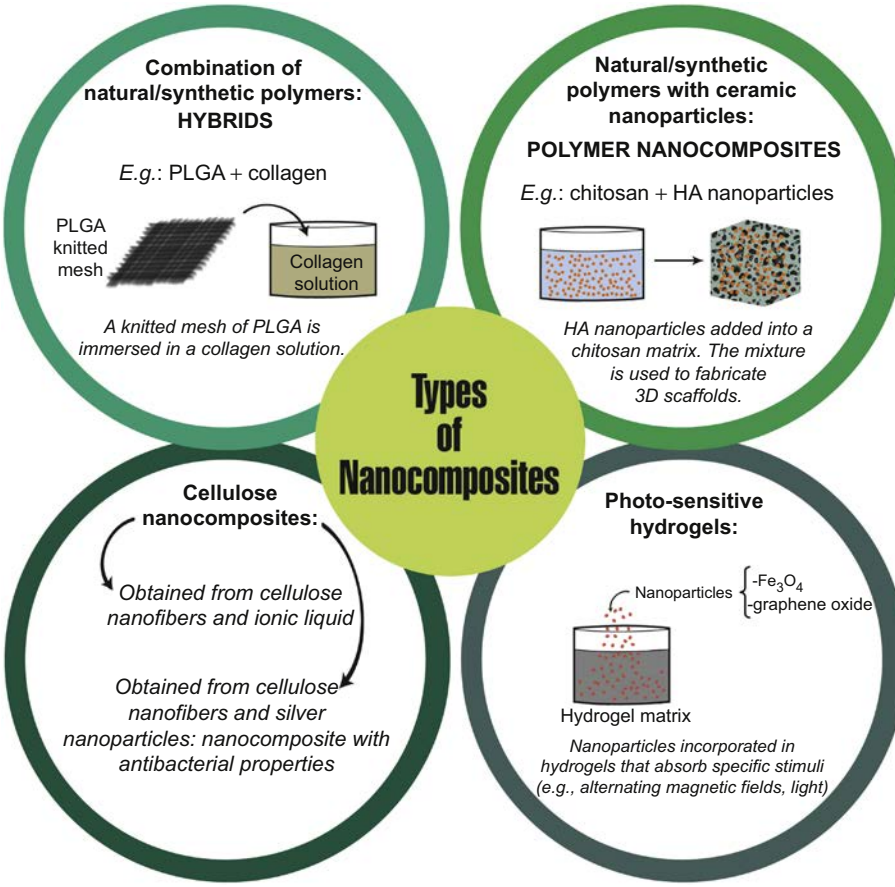

Figure 8.1 Type of nanocomposite biomaterials for regenerative medicine and drug delivery applications.

certain design and functional criteria to be useful as a 3D scaffold for BTE, including mechanical properties, biodegradability, biocompatibility, and absence of immune response (Freed et al., 1994; Rezwan et al., 2006). In addition, due to unique interactions between biopolymers and nanoparticles, different property combinations can be engineered to control the delivery of a loaded bioactive molecule locally and in a sustained manner from a 3D PNC scaffold for BTE (Mouriño et al., 2013a,b; Mouriño and Boccaccini, 2010; Baroli, 2009).

Among the techniques currently used for the development of 3D scaffolds for BTE made from PNCs are polymer coating, slurry dipping, electrospinning, and 3D printing (see Fig. 8.2). Most of the elaboration techniques involve different mechanisms such as temperature, mechanical agitation, using organic solvents, and ultrasonication which can degrade the bioactive molecule. Thus, the matrix system should be rationally designed to prevent bioactive molecule damage.

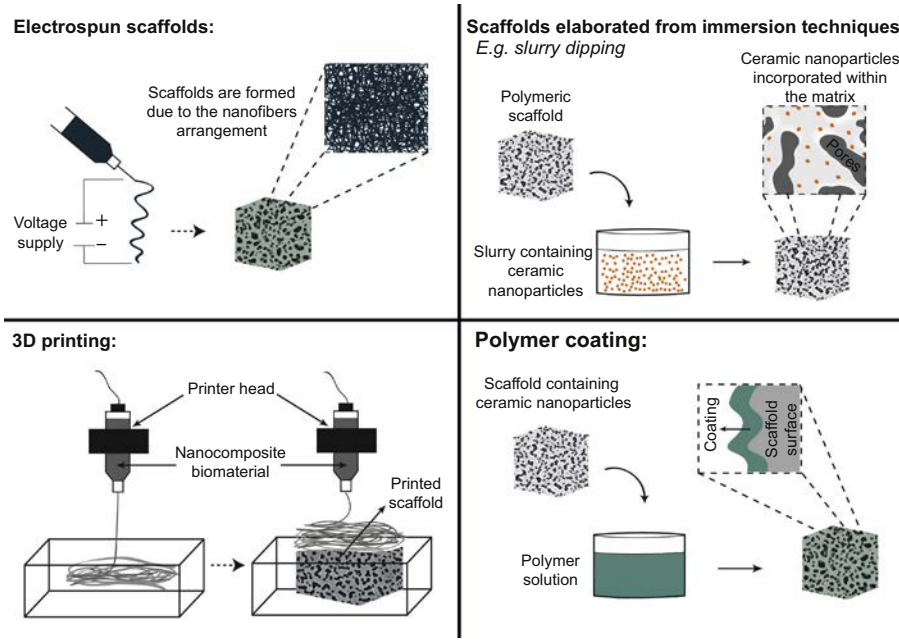

Figure 8.2 Techniques currently used for the development of 3D scaffolds for BTE made from PNCs.

Further, a critical factor underlying 3D multifunctional nanocomposite scaffolds for drug delivery applications in BTE is the interaction between the chosen matrix and the loaded bioactive molecules; different chemistries and compositions can lead to the delivery of a loaded bioactive molecule from burst to sustained release. Burst release is commonly ineffective from both therapeutic and economic viewpoints. Thus, it is needed to control the release kinetics of the loaded biomimetic molecule to optimize its therapeutic effect and particularly overcome the burst release usually observed. From this point of view, the main challenge for the next generation of 3D PNC scaffolds for BTE, therefore, focuses on achieving the right combination of physical support and morphological direction for cell proliferation, differentiation, and attachment. At the same time, they must serve as matrices for the sustained release of bioactive molecules with the adequate therapeutic concentration level, which may require spatiotemporal variations (Lee and Shin, 2007; Baroli, 2009; Gomes and Reis, 2004; Habraken et al., 2007; Duarte et al., 2007; Mouriño and Boccaccini, 2010; Wende and Guelcher, 2011). Moreover, multifunctional scaffolds must be easy to sterilize without either loss of their mechanical function or causing denaturation of the loaded bioactive molecules. In addition, to achieve clinical application, the safety and toxicity of novel PNCs should be evaluated before their utilization as biomaterials in regenerative medicine in general and in controlled drug delivery for bone tissue regeneration in particular.

In this chapter, which follows from previous review papers (Mouriño et al., 2013a,b; Mouriño and Boccaccini, 2010), special attention has been paid to

discuss current efforts and key research challenges in the development of PNC scaffolds with potential drug delivery applications in BTE. The document is organized as follows: Section 8.2 details efforts and care adopted to develop PNC scaffolds as drug delivery vehicles in terms of drug encapsulation efficiency and controlled and sustained drug release. Finally, the remaining challenges in the field are summarized in Section 8.3, in which also directions for future research efforts are highlighted.

8.2 Bioactive molecule-releasing scaffolds for bone tissue engineering

Multifunctional PNC matrices for regenerative medicine should be designed rationally with the challenge to envisage a dual function of them: (1) to act as scaffold for promoting cellular infiltration and proliferation for tissue regeneration, and (2) to act as a carrier system to deliver bioactive molecules in a localized, spatiotemporal manner mimicking the natural healing process.

In the case of BTE, 3D multifunctional scaffolds may be useful as carrier systems for localized controlled delivery of bioactive molecules such as bone tissue inductive molecules and therapeutic drugs to enhance and accelerate functional bone tissue regeneration and/or to treat a nearby disease. The successful utilization of grown factors depends on the rational design of the matrix in terms of delivery technology because growth factors commonly have short half-lives, and cells are sensitive to their concentration (Lee and Shin, 2007; Blackwood et al., 2012; Baroli, 2009; Wende and Guelcher, 2011; Chung and Park, 2007; Vo et al., 2012; Ekenseair et al., 2013). In the case of therapeutic drugs used in the treatment of bone diseases, their local administration has potential advantages over systemic administration to minimize side effects and risk of overdose and to improve bioavailability of the drug, with the appropriate therapeutic concentration level achieved effectively in situ for a desired time frame (Baroli, 2009; Mouriño and Boccaccini, 2010; Somayaji et al., 1998). Further, bioactive molecule delivery at the target site reduces the possibilities of immune system attacks and thus increases its bioavailability (Saltzman and Olbricht, 2002). In addition, local delivery of antimicrobial agents could prevent the competition between the process of integrating the 3D scaffold with its neighbouring tissue and bacterial adhesion, with the consequent formation of biofilms on its surface after implantation (Mouriño and Boccaccini, 2010; Gristina, 1987; Hetrick and Schoenfisch, 2006; Zilberman & Elsner, 2008). The desired characteristics of 3D scaffold for BTE and their manufacturing technologies are described in other chapters of this book and in several review articles (for example, in the following references: Hutmacher, 2000; Rezwan et al., 2006; Blackwood et al., 2012; Liu et al., 2012; Guarino et al., 2007). Although characteristics and features of scaffold considered in its design may influence tissue formation, addition of appropriate bioactive molecules such as growth factors, cytokines, or therapeutic drugs can significantly enhance the cellular response required to speed up the process of functional tissue regeneration, and/or treat a nearby infection or disease,

Table 8.1 Bioactive molecules commonly loaded on 3D scaffolds for bone tissue engineering

Bioactive molecule	Type of molecule delivered	References
Alendronate	Inhibition of osteoclastic resorption	Wang et al. (2010) and Mondal et al. (2012)
Amoxicilin	Antimicrobial	Sotoudeh et al. (2012)
Ceftazidime	Antimicrobial	Liu et al. (2010)
Clodronate	Inhibition of osteoclastic resorption	Puppi et al. (2011)
Colistin	Antimicrobial	Shi et al. (2010)
Dexamethasone	Inductive effect in osteogenic culture	Duarte et al. (2009) and Son et al. (2011)
Doxorubicin	Antibiotic/antitumoral	Chen et al. (2012)
Gallium	Antimicrobial	Mouriño et al. (2011)
Gatifloxacin	Antimicrobial	Miyai et al. (2008)
Gentamicin	Antimicrobial	Zhang and Zhang (2002), Francis et al. (2010), and Shi et al. (2010)
Ibuprofen	Antiinflammatory	Mortera et al. (2008)
rhBMP2	Growth factor	Kale et al. (2000), Nie et al. (2008), and Fu et al. (2008)
Tetracycline	Antimicrobial	Teng et al. (2009), Kim et al. (2004), and Medvecky et al. (2007)
Vancomycin	Antimicrobial	Zhou et al. (2012), Kim et al. (2005), and Zhang et al. (2008)

as indicated previously. When a bioactive molecule is loaded into a PNC scaffold, drug encapsulation efficiency and controlled and sustained drug release—allowing a localized and desired spatiotemporal drug delivery—are needed. Table 8.1 lists bioactive molecules commonly loaded on 3D scaffolds for BTE to facilitate cell infiltration and proliferation for bone tissue regeneration and/or for local disease treatments in the aim of mimicking host's natural healing process (Salvay and Shea, 2006; Kolambkar et al., 2011).

8.2.1 Bioactive molecule entrapment efficiency

Drug entrapment is achieved via physical interaction between the bioactive molecule and the carrier system usually by attachment to the matrix surface, by entrapment within it by the aim of a covalent binding, or by drug preencapsulation. Table 8.2 lists general basic approaches for drug encapsulation into 3D PNC scaffolds for BTE.

In all cases, entrapment efficiency will be determined by the affinity of molecular interactions but also will be influenced by the environments in terms of pH and ionic strength. In addition, understanding the efforts to increase drug entrapment

Table 8.2 General basic approaches for drug encapsulation into 3D PNC scaffolds for BTE and their predominant drug mechanism

Drug encapsulation system	Main characteristics of the system	Drug encapsulation efficiency	Predominant drug release mechanism
Preencapsulation	Steps 1. Encapsulation of bioactive molecules in micro/nanospheres or hydrogels 2. Loading of encapsulating system into the polymer nanocomposite carrier system	++++	Polymer matrix degradation • Uncontrolled diffusion of bioactive molecule is prevented through a physical barrier until the encapsulation system has been sufficiently degraded
Multilayered polymer coatings	Steps 1. Bioactive molecules is entrapped through multi-layered loaded-polymer coatings 2. Loading of encapsulating system into the polymer nanocomposite carrier system	++	Swelling control and polymer matrix degradation
Surface immobilization by nonspecific mechanism	Nonspecific bindings (eg, hydrophobic, electrostatic, van der Waals) based on the composition of the bioactive molecule as well as the carrier system (eg, polymer, protein, sugar, lipid) and the presence of functional groups Also depends on swelling ratio and density of the polymer nanocomposite	++	Diffusion
Surface immobilization by addition of functional groups	Functional groups can be introduced on the bioactive molecule or in the polymer nanocomposite carrier system	+++	Swelling control and diffusion

efficiency will be useful in achieving a controlled bioactive molecule release as mostly formulation parameters that drive the initial burst and the entrapment efficiency are overlapped.

8.2.2 Controlled and sustained bioactive molecule release

The ultimate goal for drug releasing PNC scaffolds for BTE is the emergence of a nanofabricated bioactive molecule release matrix with the capability to hold and release the active agent locally and on demand. Further, a major challenge for future generations of 3D multifunctional scaffolds for BTE should be the sustained release of more than one bioactive molecule, which should ideally be a coordinated spatiotemporal delivery according to the requirements of bone tissue regeneration.

As stated in the previous subsection, initial burst release is commonly ineffective from both therapeutic and economic viewpoints. Burst release is often unwanted because the bioactive molecule released in this early period is usually wasted (thus, not available for sustained release) and can lead to harmful side effects in vivo. In general, initial burst is subordinate to how efficiently the bioactive molecule is entrapped within the scaffold. Diffusion drives delivery of adsorbed bioactive molecule on the scaffold surface, which does not usually provide adequate (sustained) release behaviour. Loosely associated bioactive molecules with the scaffold surface produce limited control over the release kinetics, delivering by diffusion great percentage of the bioactive molecule at very initial stages in high release rates followed by a very slow release rate (decreasing rate of bioactive molecule release with time) (Mouriño and Boccaccini, 2010; Mouriño et al., 2013a,b; Sah et al., 1994; O'Hagan et al., 1994; Igartua et al., 1997; Rafati et al., 1997). In addition, nonhomogeneous bioactive molecule distribution generally contributes to initial burst release.

Aside pure diffusion, swelling control and polymer degradation are commonly drug release mechanisms for bioactive molecules entrapped or encapsulated within PNCs. To control the release profiles efficiently, it would be essential to utilize polymers with a desirable degradation profile when designing the multi-functional scaffold. However, it is important to highlight that, in BTE, the scaffold needs to warrant robust mechanical properties and functional backup for integrative tissue repair which often requires slow degradation of the matrix to guarantee its mechanical integrity for cellular infiltration and proliferation during tissue regeneration (Blackwood et al., 2012; Porter et al., 2009; Woodruff et al., 2012).

Considering the previous, drug release behaviour should be disengaged from the constitutional scaffold degradation pattern to maximize the efficiency of a multifunctional PNC scaffold. Progress in this sense can be observed by bioactive molecule preencapsulation in nano-/microspheres and hydrogels or by the entrapment of the molecular agent through multilayered loaded-polymer coatings onto the preformed scaffold surface (see Table 8.2); polymers employed are generally degradable biopolymers able to generate networks (Kim et al., 2005; Francis et al., 2010). In addition, it can be envisaged that the release of multiple bioactive molecules follow a sequential pattern which can be tuned

according to the degradation characteristics of each polymer layer. Moreover, a bioactive molecule immersed in a polymer solution can be electrospun within the innermost part of a nanofiber by using coaxial electrospinning (see Table 8.2).

8.3 Conclusions and future trends

Research focused on the application of PNC scaffolds for BTE (PNC-BT scaffolds) has shown their great potential as a single platform with multifunctional capabilities for bone regeneration emerging as an attractive approach. PNC-BT scaffolds with the added value of bioactive molecule-delivery capability appear particularly promising.

However, despite the significant progress already made, significant challenges remain to achieve clinical applications. In this sense, more data are needed regarding the effective dose at local level for the majority of the bioactive molecules currently loaded into multifunctional scaffolds. Further attempts should be made in developing strategies to establish the required concentration of a particular bioactive molecule needing to be reached when it is entrapped within a scaffold for successful results. In addition, there is still the necessity to accomplish significant in vivo results which can offer sensible basis for the improvement of drug delivery from PNC-BT.

Moreover, there is a lack of drug dosage management capability as well as reported clinical efficiency of a large number of novel PNC-BT scaffolds reported in literature. Further, many of the proposed PNC-BT scaffolds prototypes cannot be scaled up in terms of cost-effective manufacture processes. In this sense, PNC-BT scaffolds should be easy to fabricate and sterilize and need to fulfil the requirements to obtain approval from regulatory authorities including long-term evaluation of their clinical performance through validated and standardized in vivo trials.

In addition, it is important to highlight that the utmost clinical impact of PNC-BT scaffolds might rely not only on the capability to adjust and perfect the variables that drive the controlled and sustained bioactive molecule delivery process from the developed matrix, but also on the ability to develop bioactive composite scaffolds that suit the specific needs of bone tissue regeneration. Even though the above challenges should be overcome, it is clear that PNC-BT scaffolds outstrip traditional scaffolds, and future progress in BTE approaches will benefit from the further optimization of the multifunctionality of these matrices. In this regard, the next major challenge for PNC-BT would be the incorporation of a complex multibioactive molecule delivery system able to mimick the necessary patterns for an effective osseointegration and bone tissue regeneration. Finally, the ultimate goal of bioactive delivery using PNC-BTE scaffolds could widen the range of application from BTE, including multidrug releasing system, to other fields of regenerative medicine.

It seems clear that this interdisciplinary field will expand with more intensive cooperation among various disciplines such as biology, biomaterials science, chemistry, medicine, and pharmacy to deal with the further work required toward the development of more effective multifunctional bone TE.

References

Baroli, B., 2009. From natural bone graft to tissue engineering therapeutics: brainstorming on pharmaceutical formulative requirements and challenges. Journal of Pharmaceutical Sciences 98, 1317–1375.

Blackwood, K., Bock, N., Dargaville, Y., et al., 2012. Scaffolds for growth factor delivery as applied to bone tissue engineering. International Journal of Polymer Science 2012, 174942.

Bonassar, J., Vacanti, C., 1998. Tissue engineering: the first decade and beyond. Journal of Cellular Biochemistry. Supplement 30, 297–303.

Chen, M., Le, D., Hein, S., et al., 2012. Fabrication and characterization of a rapid prototyped tissue engineering scaffold with embedded multicomponent matrix for controlled drug release. International Journal of Nanomedicine 7, 4285–4297.

Chung, H.J., Park, T.G., 2007. Surface engineered and drug releasing pre-fabricated scaffolds for tissue engineering. Advanced Drug Delivery Reviews 59, 249–262.

Duarte, A.R., Simplicio, A.L., Vega-Gonzalez, A., et al., 2007. Supercritical fluid impregnation of a biocompatible polymer for ophthalmic drug delivery. Journal of Supercritical Fluids 42, 373–377.

Duarte, A.R.C., Mano, J.F., Reis, R.L., 2009. Dexamethasone-loaded scaffolds prepared by supercritical-assisted phase inversion. Acta Biomaterialia 5, 2054–2062.

Ekenseair, A., Kasper, F., Mikos, A., 2013. Perspectives on the interface of drug delivery and tissue engineering. Advanced Drug Delivery Reviews 65, 89–92.

Francis, L., Meng, D., Knowles, J., et al., 2010. Multi-functional P(3HB) microsphere/45S5 bioglass-based composite scaffolds for bone tissue engineering. Acta Biomaterialia 6, 2773–2786.

Freed, L., Vunjak-Novakovic, G., Biron, R., et al., 1994. Biodegradable polymer scaffolds for tissue engineering. Nature Biotechnology 12, 689–693.

Fu, Y.C., Nie, H., Ho, M.L., et al., 2008. Optimized bone regeneration based on sustained release from three-dimensional fibrous PLGA/HAp composite scaffolds loaded with BMP-2. Biotechnology and Bioengineering 99, 996–1006.

Goldberg, M., Langer, R., Jia, X., 2007. Nanostructured materials for applications in drug delivery and tissue engineering. Journal of Biomaterials Science. Polymer Edition 18 (3), 241–268.

Gomes, M.E., Reis, R.L., 2004. Biodegradable polymers and composites in biomedical applications from catgut to tissue engineering. Part II: systems for temporary replacement and advanced tissue regeneration. International Materials Reviews 49, 274–285.

Gristina, A.G., 1987. Biomaterial-centered infection: microbial adhesion versus tissue integration. Science 237, 1588–1595.

Guarino, V., Causa, F., Ambrosio, L., 2007. Bioactive scaffolds for bone and ligament tissue. Expert Review of Medical Devices 4, 405–418.

Habraken, W.J., Wolke, J.G., Jansen, J.A., 2007. Ceramic composites as matrices and scaffolds for drug delivery in tissue engineering. Advanced Drug Delivery Reviews 59, 234–248.

Hetrick, E.M., Schoenfisch, M.H., 2006. Reducing implant-related infections: active release strategies. Chemical Society Reviews 35, 780–789.

Hutmacher, D.W., 2000. Scaffolds in tissue engineering bone and cartilage. Biomaterials 21, 2529–2543.

Igartua, M., Hernandez, R.M., Esquisabel, A., Gascon, A.R., Calvo, M.B., Pedraz, J.L., 1997. Influence of formulation variables on the in vitro release of albumin from biodegradable microparticulate systems. Journal of Microencapsulation 14, 349–356.

Kale, S., Biermann, S., Edwards, C., 2000. Three-dimensional cellular development is essential for ex vivo formation of human bone. Nature Biotechnology 18, 954–958.

Kim, H., Knowles, J., Kim, H., 2004. Hydroxyapatite/poly(ε-caprolactone) composite coatings on hydroxyapatite porous bone scaffold for drug delivery. Biomaterials 25, 1279–1287.

Kim, H.W., Knowles, J.C., Kim, H.E., 2005. Hydroxyapatite porous scaffold engineered with biological polymer hybrid coating for antibiotic Vancomycin release. Journal of Materials Science. Materials in Medicine 16, 189–195.

Kolambkar, Y.M., Dupont, K.M., Boerckel, J.D., et al., 2011. An alginate-based hybrid system for growth factor delivery in the functional repair of large bone defects. Biomaterials 32, 65–74.

Langer, R., Vacanti, J., 1993. Tissue engineering. Science 260, 920–926.

Lee, S.H., Shin, H., 2007. Matrices and scaffolds for delivery of bioactive molecules in bone and cartilage tissue engineering. Advanced Drug Delivery Reviews 59, 339–359.

Liu, H., Zhang, L., Shi, P., et al., 2010. Hydroxyapatite/polyurethane scaffold incorporated with drug-loaded ethyl cellulose microspheres for bone regeneration. Journal of Biomedical Materials Research. Part B, Applied Biomaterials 95, 36–46.

Liu, Y., Lim, J., Teoh, S., 2012. Review: development of clinically relevant scaffolds for vascularised bone tissue engineering. Biotechnology Advances pii:S0734–9750(12), 00184-X.

Medvecky, L., Stulajterova, R., Briancin, J., 2007. Study of controlled tetracycline release from porous calcium phosphate/polyhydroxybutyrate composites. Chemical Papers 61, 477–484.

Miyai, T., Ito, A., Tamazawa, G., et al., 2008. Antibiotic-loaded poly-e-caprolactone and porous beta-tricalcium phosphate composite for treating osteomyelitis. Biomaterials 29, 350–358.

Mondal, T., Sunny, M.C., Khastgir, D., et al., 2012. Poly (L-lactide-co-epsilon caprolactone) microspheres laden with bioactive glass-ceramic and alendronate sodium as bone regenerative scaffolds. Materials Science and Engineering C 32, 697–706.

Mortera, R., Onida, B., Fiorilli, S., et al., 2008. Synthesis and characterization of MCM-41 spheres inside bioactive glass–ceramic scaffold. Chemical Engineering Journal 137, 54–61.

Mouriño, V., Boccaccini, A.R., 2010. Bone tissue engineering therapeutics: controlled drug delivery in three-dimensional scaffolds. Journal of the Royal Society, Interface 7, 209–227.

Mouriño, V., Cattalini, J.P., Wei, L., Boccaccini, A.R., Lucangioli, S.L., 2013a. Multifunctional scaffolds for bone tissue engineering and *in situ* drug delivery. In: Boccaccini, A.R. (Ed.), Tissue Engineering Using Ceramics and Polymers. Woodhead Publishing, Cambridge, RU, pp. 648–674.

Mouriño, V., Cattalini, J.P., Roether, J.A., Dubey, P., Roy, I., Boccaccini, A.R., 2013b. Composite polymer-bioceramic scaffolds with drug delivery capability for bone tissue engineering. Expert Opinion on Drug Delivery 10 (10), 1353–1356.

Mouriño, V., Newby, P., Pishbin, F., et al., 2011. Physicochemical, biological and drug-release properties of gallium crosslinked alginate/nanoparticulate bioactive glass composite films. Soft Matter 7, 6705–6712.

Nie, H., Beng, W.S., Fu, Y.C., et al., 2008. Three-dimensional fibrous PLGA/HAp composite scaffold for BMP-2 delivery. Biotechnology and Bioengineering 99, 223–234.

O'Hagan, D.T., Jeffery, H., Davis, S.S., 1994. The preparation and characterization of PLGA microspheres: III. Microparticle/polymer degradation rates and the in vitro release of a model protein. International Journal of Pharmaceutics 103, 37–45.

Porter, J.R., Ruckh, T.T., Popat, K.C., 2009. Bone tissue engineering: a review in bone biomimetics and drug delivery strategies. Biotechnology Progress 25, 1539–1560.

Puppi, D., Piras, A., Chiellini, F., et al., 2011. Optimized electro- and wet-spinning techniques for the production of polymeric fibrous scaffolds loaded with bisphosphonate and hydroxyapatite. Journal of Tissue Engineering and Regenerative Medicine 5, 253–263.

Rafati, H., Coombes, A.G.A., Adler, J., Holland, J., Davis, S.S., 1997. Protein-loaded PLGA microparticles for oral administration: formulation, structural and release characteristics. Journal of Controlled Release 43, 89–102.

Rezwan, K., Chen, Q.Z., Blaker, J.J., et al., 2006. Biodegradable and bioactive porous polymer/inorganic composite scaffolds for bone tissue engineering. Biomaterials 27, 3413–3431.

Saltzman, W.M., Olbricht, W.L., 2002. Building drug delivery into tissue engineering. Nature Reviews. Drug Discovery 1, 177–186.

Salvay, D.M., Shea, L.D., 2006. Inductive tissue engineering with protein and DNA-releasing scaffolds. Molecular Biosystems 2, 36–48.

Sah, H., Toddywala, R., Chien, Y.W., 1994. The influence of biodegradable microcapsule formulations on the controlled release of a protein. Journal of Controlled Release 30, 201–211.

Shi, M., Kretlow, J., Nguyen, A., et al., 2010. Antibiotic-releasing porous polymethylmethacrylate constructs for osseous space maintenance and infection control. Biomaterials 31, 4146–4156.

Somayaji, B.V., Jariwala, U., Jayachandran, P., et al., 1998. Evaluation of antimicrobial efficacy and release pattern of tetracycline and metronidazole using a local delivery system. Journal of Periodontology 69, 409–413.

Son, J., Appleford, M., Ong, J., et al., 2011. Porous hydroxyapatite scaffold with three-dimensional localized drug delivery system using biodegradable microspheres. Journal of Controlled Release 153, 133–140.

Sotoudeh, S., Barati, A., Davarnejad, R., et al., 2012. Antibiotic release process from hydrogel nano zeolite composites. Middle East Journal of Scientific Research 12, 392–396.

Teng, S.-H., Lee, E.-J., Wang, P., et al., 2009. Functionally gradient chitosan/hydroxyapatite composite scaffolds for controlled drug release. Journal of Biomedical Materials Research 90B, 275–282.

Vo, T., Kasper, F., Mikos, A., 2012. Strategies for controlled delivery of growth factors and cells for bone regeneration. Advanced Drug Delivery Reviews 64, 1292–1309.

Wang, Y., Shi, X., Ren, L., et al., 2010. In vitro osteogenesis of synovium mesenchymal cells induced by controlled release of alendronate and dexamethasone from a sintered microspherical scaffold. Journal of Biomaterials Science. Polymer Edition 21, 1227–1238.

Wende, J., Guelcher, S., 2011. Dual delivery of an antibiotic and a growth factor addresses both the microbiological and biological challenges of contaminated bone fractures. Expert Opinion on Drug Delivery 8, 1555–1569.

Woodruff, M.A., Lange, L., Reichert, J., et al., 2012. Bone tissue engineering: from bench to bedside. Materials Today 15, 430–435.

Zhang, Y., Zhang, M., 2002. Calcium phosphate/chitosan composite scaffolds for controlled in vitro antibiotic drug release. Journal of Biomedical Materials Research 62, 378–386.

Zhang, L., Yang, D., Chen, H., et al., 2008. An ionically crosslinked hydrogel containing vancomycin coating on a porous scaffold for drug delivery and cell culture. Internation Journal of Pharmaceutics 353, 74–87.

Zilberman, M., Elsner, J., 2008. Antibiotic-eluting medical devices for various applications. Journal of Controlled Release 130, 202–215.

Zhou, J., Fang, T., Wang, Y., et al., 2012. The controlled release of vancomycin in gelatin/beta-TCP composite scaffolds. Journal of Biomedical Materials Research 100A, 2295–2301.

Further reading

Baroli, B., 2009. From natural bone graft to tissue engineering therapeutics: brainstorming on pharmaceutical formulative requirements and challenges. Journal of Pharmaceutical Sciences 98, 1317–1375.

Habraken, W.J., Wolke, J.G., Jansen, J.A., 2007. Ceramic composites as matrices and scaffolds for drug delivery in tissue engineering. Advanced Drug Delivery Reviews 59, 234–248.

Mouriño, V., Boccaccini, A.R., 2010. Bone tissue engineering therapeutics: controlled drug delivery in three-dimensional scaffolds. Journal of the Royal Society, Interface 7, 209–227.

Mouriño, V., Cattalini, J.P., Wei, L., Boccaccini, A.R., Lucangioli, S.L., 2013a. Multifunctional scaffolds for bone tissue engineering and *in situ* drug delivery. In: Boccaccini, A.R. (Ed.), Tissue Engineering Using Ceramics and Polymers. Woodhead Publishing, Cambridge, RU, pp. 648–674.

Mouriño, V., Cattalini, J.P., Roether, J.A., Dubey, P., Roy, I., Boccaccini, A.R., 2013b. Composite polymer-bioceramic scaffolds with drug delivery capability for bone tissue engineering. Expert Opinion on Drug Delivery 10 (10), 1353–1356.

Fabrication of cellulosic composite scaffolds for cartilage tissue engineering

9

A.G. Nandgaonkar[1], W.E. Krause[1], L.A. Lucia[1,2]
[1]North Carolina State University, Raleigh, NC, United States; [2]Key Laboratory of Pulp & Paper Science and Technology of the Ministry of Education, Jinan, People's Republic of China

9.1 Introduction

Cartilage injuries and associated diseases are frequent and cause extensive health issues in the United States. The rupture of such tissue causes pain, reduction in joint mobility, and billions of dollars in medical and surgical treatment costs (Yelin et al., 2007) alone. Unfortunately, articular cartilage (AC) has a limited intrinsic capacity to self-repair because it has an avascular nature and relatively very low cellular mitotic activity. Various techniques have been implemented to repair damaged cartilage tissue that include microfracture, autologous chondrocyte transplantation, and prosthetic joint replacement (Redma et al., 2005). However, despite the application of these techniques, the progression of cartilage degeneration is inevitable and ultimately gives rise to fibrous or osseous cartilage which is biomechanically inferior to hyaline cartilage (Marsano et al., 2007).

The current trend for a more robust and successful treatment of damaged or diseased cartilage is within the domain of tissue engineering (TE), a relatively new discipline, which is based on the principles of the life sciences and engineering. This discipline aims to elaborate the basic science, engineering, and technology required to regenerate damaged tissue instead of wholesale replacing it, by fabricating a substrate (scaffold) onto which targeted guest cells can restore, maintain, or improve tissue functions (O'Brien, 2011). The major criteria that characterize a successful tissue scaffold are sufficient mechanical properties (relative to the type of biomechanical stresses exerted), high porosity (for cell percolation and adhesion, nutrient delivery, and waste expulsion), good biocompatibility (within the temporal window necessary for successful tissue incorporation), and ultimately, but not trivially, biodegradability (to ensure its sorption or removal without interfering with the natural regenerated tissue). In addition to these major criteria, the extracellular matrix's (ECM) complex biochemical environment within tissue, the individual components of which are arranged in a particular organizational motif within a hierarchical zonal organization of cartilage, makes it extremely difficult to mimic cartilaginous structure

Nanocomposites for Musculoskeletal Tissue Regeneration. http://dx.doi.org/10.1016/B978-1-78242-452-9.00009-1

without compromising other unique, select properties of the scaffold (Murugan and Ramakrishna, 2007; Steward et al., 2011).

Our current attention has been focused on utilizing cellulosic materials for tissue-engineering applications because its native chemical structure is quite similar to that of the fibrous collagen molecule which provides the requisite tensile strength to AC and, quite feasibly, can be used as collagen-mimicking substrate (Bäckdahl et al., 2008; Bhosale and Richardson, 2008). Various studies as early as 2000 have been executed in which cellulose for cartilage TE has been exploited (Ko and Iwata, 2001). Within a short time, cellulosic materials were modified chemically and physically to meet specific scaffolding (biochemical and biophysical) requirements. Our current overview focuses on the science and engineering of cellulosic materials for fabricating scaffolds such as cellulose fabrics, sponges, hydrogels, composite materials, and the unique nanofibrous material known as bacterial cellulose (BC). We will show that the overall biocompatibility of the cellulose fabric and sponge were enhanced through the additions of calcium phosphate and collagen types, respectively. We will also demonstrate that cellulose nanocrystals can be effectively used to improve the mechanical properties of the latter materials. Various derivatives of cellulose such as methylcellulose (MC), hydroxypropylcellulose (HPC), ethyl cellulose (EC), and carboxymethylcellulose (CMC) have already been used as injectable hydrogels after chemical modification through silane grafting. Cellulosic composite hydrogels have been prepared with organic and inorganic materials that include polymers, biomolecules, and mineral particles. Various in vivo and in vitro studies will be discussed as feasible cartilage repair systems. We were able to compare the properties of these cellulosic materials with unique BC, a substance that possesses superior properties to plant-derived cellulose. Various examples of in vivo and in vitro studies of BC and its associated scaffold preparations are discussed with respect to biocompatibility, mechanical strength, and biodegradation.

9.2 Structure, composition, and anatomy of articular cartilage

Cartilage is a flexible connective tissue that can be found principally in three histologically distinct regions in the body: (1) hyaline cartilage in articular joints, invertible disks; (2) elastic cartilage in tendons and ligaments; and (3) fibrocartilage in ears. AC covers the surface of long bones and tends to be translucent (glass-like) with a high opalescence due to high proteoglycan content that absorbs copious amounts of water. Because of its high water-holding capacity, AC acts as a shock absorber, gliding surface, and load distribution nexus between the articulation of two bones during motion (Spiller et al., 2011; Athanasiou et al., 2009).

AC is an avascular tissue that is mainly composed of ECM and water. Approximately 70–80% of the tissue is composed of water (constituting a gel) which helps to transfer nutrients and distribute loads. The solid contents of the cartilage are embedded inside the ECM in addition to residence of a single population of chondrocytes. The ECM and chondrocytes correspond to 20–30% of the AC, whereas the ECM consists

of different types of macromolecules such as proteoglycans (15–30%), collagen type II (main type), IX, and XI, water, and other noncollagenous components which are normally synthesized by the chondrocytes. All these components embedded inside the network provide the mechanical strength and elasticity to the AC during joint motion (Steward et al., 2011; Athanasiou et al., 2009; García-Carvajal et al., 2013).

ECM has a molecular porous structure which retains water and synovial fluid ingredients. The main component of the synovial fluid is water (70–80% of total mass) and other lubricating molecules such as hyaluronan and proteoglycans that provide a low-friction gliding surface to prevent two articulating bones from interabrasion (Schmidt et al., 2007). The water percent is different in different zones for load deformation. However, the water content increases to 90% during an osteoarthritis (OA) stage and causes degradation of the ECM to result in an inferior mechanical strength of cartilage (Bhosale and Richardson, 2008; Newman, 1998).

The main component of the ECM is collagen, which is a fibrous molecule having a triple helix structure and constituting 60% of the dry weight of the AC. The collagen fibrils are distributed uniformly throughout the AC and are arranged in a specific order according to the different zones. In general, these biomaterials provide the stiffness and mechanical strength of the AC. In one of the clinical studies of cow, the mechanical and biochemical properties of the juvenile cartilage increases with increases in collagen content and cross-linking (Williamson et al., 2003). There are different collagen types present in AC; however, collagen type II corresponds to 90% of the total collagen content responsible for the tensile strength of AC (Bhosale and Richardson, 2008; Buckwalter et al., 2005). Proteoglycans correspond to the 15–20% of the dry weight which is responsible for providing compressive strength to the AC. Proteoglycans have a protein core and many sulfated polysaccharide glycosaminoglycan (GAG) chains. The different types of proteoglycans are chondroitin sulfate, keratan sulfate, and hyaluronan (see Fig. 9.1). These GAGs are disaccharide molecules bound to the protein core by sugar bonds ultimately forming an *aggrecan* molecule. The hyaluronan, which is nonsulfated, is attached to the protein core to stabilize this chain and form an intricate GAG molecule. Because proteoglycans are negatively charged, they attract ions which maintain the fluid and electrolyte balance in the AC. The negatively charged carboxylate groups and sulfates provide a net negative charge that is known as the fixed charge density of the cartilage ECM. The negative charge causes osmotic imbalances, and the proteoglycans are compressed by the collagen framework. The damaged collagen fibers then allow the proteoglycans to expand which leads to absorption of water to help hydrate, thus inducing swelling of the tissue, which in turn increases the resistance of the tissue against compression (Steward et al., 2011; Bhosale and Richardson, 2008; Buckwalter and Mankin, 1998).

The ECM molecules discussed above are synthesized by the chondrocyte cells which correspond to 1–5% by volume with a wide distribution throughout the AC (Bhosale and Richardson, 2008). The articular chondrocytes from different regions have specific morphologies and functions. In addition, the cells have different shapes and diameters according to their specific zonal functions (Aydelotte and Kuettner, 1988).

As mentioned earlier, AC is a highly ordered structure which is divided into different zones. These zones differ in the composition and orientation of the collagen fibers

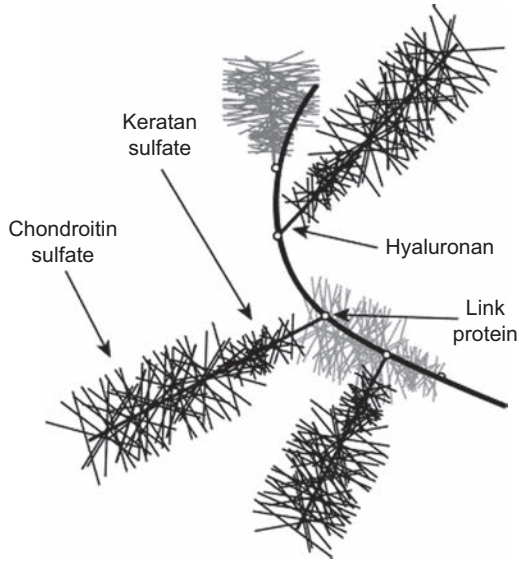

Figure 9.1 Sketch of proteoglycan aggregate. It consists of a central hyaluronan chain on which glycosaminoglycan (GAG) molecules such as chondroitin and keratin sulfate are attached by central link protein.
Reprinted with permission from Morgan & Claypool Publishers (Athanasiou, K., Darling, E., Hu, J., 2009. Articular Cartilage Tissue Engineering 1 (1), 1–182).

with respect to their proliferation from the upper surface of cartilage to the bone. In each zone, the cells have a different shape, size, and orientation, all of which contribute to specific metabolic activity and, thus, the AC properties change according to the depth of each of the zones that are listed below (see Fig. 9.2).

- Superficial zone
- Transitional zone
- Middle or deep zone
- Calcified cartilage zone

The superficial zone is the thinnest layer of all zones consisting of 10–20% of the total cartilage thickness. This zone has a high collagen and low proteoglycan content. The collagen fibers are densely packed and arranged parallel to the surface so that they can resist shear stresses (Jadin et al., 2007). Any alteration to the native parallel assembly can substantially reduce the mechanical strength and thus give rise to osteoarthritis. In general, the cells are flattened and ellipsoidal in shape arranged parallel to the collagen fibers, and are covered by synovial fluid. This provides the requisite gliding surface to avoid friction between articulating bones during joint movement (Bhosale and Richardson, 2008; Buckwalter et al., 2005). It was also found out that the local compressive modulus in this zone was around 0.03 and 0.15 MPa for fetal and juvenile bovine cartilage, respectively (Mauck and Burdick, 2011). The transitional zone is the middle zone between the superficial and deep zone. It constitutes 40–50% of the total AC thickness. The cells there display a spheroidal shape with a concomitant low density

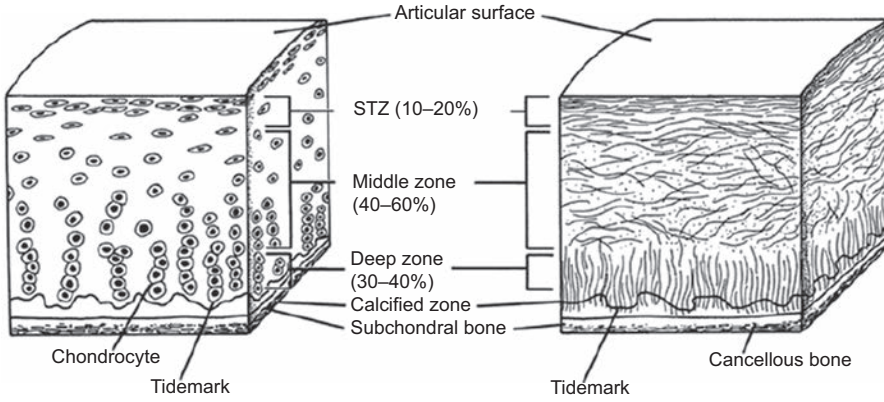

Figure 9.2 Structure of the articular cartilage. Left side: Chondrocyte arrangement in different zones, Right side: Collagen fiber arrangement and distribution throughout the articular cartilage. *STZ*, superficial tangential zone.
Reprinted from Journal of the American Academy of Orthopedic Surgeons (Buckwalter, J.A., Mow, V.C., Ratcliffe, A., 1994. Restoration of injured or degenerated articular cartilage. The Journal of the American Academy of Orthopaedic Surgeons 2 (4), 192–201). Copyright © Wolters Kluwer Health.

and are embedded in the ECM. These cells produce larger diameter collagen fibers (30–80 nm) and higher proteoglycan content both of which are arranged randomly relative to the superficial zone. In the middle zone, the collagen fibers are more or less randomly arranged. The random arrangement of the collagen fibers and chondrocytes in this zone facilities load distribution. The cells possess a spheroidal shape with a relatively low density as compared to those in the superficial zone. The deep zone is the last zone of AC and by default contributes to 30–40% of the AC thickness. The water content and cell density is the lowest of all three zones. The cells and collagen fibers are arranged perpendicularly relative to the surface of the AC to resist the compressive forces exerted (Bhosale and Richardson, 2008; Athanasiou et al., 2009; Jadin et al., 2007). The local compressive modulus in the middle and deep zone was found to be around 0.13 and 0.65 MPa for fetal and juvenile bovine cartilage, respectively (Mauck and Burdick, 2011). The calcified zone separates the AC from the subchondral bone. It consists of only 5–10% thickness of the total AC. The collagen fibers therein provide the needed mechanical support from the cartilage to the bone. The cartilage in the calcified zone is separated from the deep zone by a thin demarcation termed as "tidemark," a volume space that is rich in collagen fibers and hyaluronic acid (Bhosale and Richardson, 2008; Weiss et al., 2010).

9.3 Motivation for cartilage tissue engineering

Senescence is one of the major factors which can lead to OA. In addition, AC injuries can be caused in many ways from repeated loading, aging, trauma, and mechanical misalignment of the joint. These types of injuries often lead to osteoarthritis

over time. The rupture of this tissue can cause pain, reduction in mobility, and billions of dollars in medical costs and associated surgeries (Athanasiou et al., 2009). The degradation and degeneration of AC from excessive mechanical stresses such as high-impact sports, aging, and genetic factors may all give rise to OA (Athanasiou et al., 2009). It is the second most common disease after cardiovascular disease and affects nearly 15% of the US population with an annual cost of around $128 billion to the US economy (Yelin et al., 2007). With a burgeoning aging population, this value is expected to only continue to rise in the coming years (Hootman and Helmick, 2006). Articulate cartilage lacks a good arterial blood supply, venous and lymphatic drainage, and obtains its nutrition only from synovial fluid. Therefore, it has a very limited capacity for self-repair because of its avascular nature and low cellular mitosis activity. Osteochondral lesions tend to form fibrocartilage which is mechanically inferior and can break down under normal shear. Numerous techniques have been used to repair the damaged cartilage tissue: microfracture, autologous implants, chondrocyte transplantation, and prosthetic joint replacement (Redman et al., 2005; Newman, 1998). However, each technique has distinct limitations. Autografting is expensive and is limited due to patient morbidity. Allografts show a high risk of rejection of donor tissue, in addition to contracting infections (O'Brien, 2011). Moreover, these techniques have limited success in producing long-lasting cartilage. Cartilage produced from these methods results in the formation of a mixture of collagen type I that is biochemically inferior (Marsano et al., 2007; Chung and Burdick, 2008). Remarkably, cartilage tissue is considered a simple tissue, but biomedical scientists have always faced very high barriers and challenges in engineering this tissue. What is the basis for the lack of adequate engineering? Although a complex question, the solution lies mainly in the fact that the tissue has a hierarchical structure composed of different molecules. The main type of cell in this avascular cartilage tissue is the chondrocyte cell. However, no one fully understands how the cells maintain their population. An ideal cell source, a three-dimensional network with controlled porosity, more specifically a suitable scaffold material, and the necessary growth factors are among the parameters required for maintaining chondrocyte differentiation and proliferation. Therefore, an ideal approach in cartilage TE is to regenerate the damaged tissue instead of replacing it.

9.4 Cartilage tissue engineering

Tissue Engineering is an emerging field the objective for which is to regenerate damaged tissue by seeding appropriate cell types onto a specific biomimetic (ECM-like) substrate (scaffold). Developing a successfully engineered tissue requires certain factors such as (1) appropriate cell type (2) scaffolds that can behave as substrates for cell seeding and structural support, and (3) cell–matrix interactions for tissue growth with appropriate biomechanical and biochemical signals to maintain cell metabolism and cell phenotype (Murugan and Ramakrishna, 2007; Steward et al., 2011).

9.4.1 Requirement of scaffold

AC tissue engineering is based on the principle of seeding the chondrocytes or differentiated stem cells onto biodegradable/bioresorbable scaffolds that are implanted at the joint defect site. The scaffold is a three-dimensional (3-D), interconnected, and porous network supporting cellular growth, proliferation, and differentiation to form new cartilage. Factors related to nutrient supply such as porosity, pore size, pore structure, and void volume are critical. Improving these factors is beneficial for cellular attachment, growth, and ECM production (Dutta et al., 2011). Without question, and sometimes overlooked, the mechanical properties of scaffolds greatly affect the biological functions of cells within the implanted tissue scaffold (Carletti et al., 2011). During the construction of scaffolds for tissue-engineering applications, material properties, porosity, surface area, morphology, biodegradability, and mechanical properties are paramount. Keeping these properties in mind, different types of natural and synthetic material were used to fabricate cartilage tissue scaffold as listed in Table 9.1. Natural and synthetic materials possess their own advantages and disadvantages. Natural material have the advantage of biocompatibility; however, it has difficult processing conditions and can produce allergic reactions. Synthetic materials can be processed easily with tailored mechanical properties and degradation time. However, they lack the biocompatibility which is essential for cell growth.

Yet, there is no such characteristic set of requirements that define an ideal scaffold. The ECM of our bodies displays a complex microenvironment with specific tissue functions. The scaffold should match with the native ECM properties possessing nanopore dimensions. However, mimicking the natural ECM is nontrivial, but with current advances in TE certain basic characteristics of the scaffolds can be achieved.

The scaffold should be biocompatible; ie, it should be nonallergenic and thus not provoke any immune or inflammatory responses. It should have 3-D architecture to guide the cell and ingrowths and should transport promote nutrients and oxygen through its interconnected porous structure. The porous structure helps the cell to attach, migrate, proliferate or differentiate. The second requirement of a scaffold is that it should be biodegradable. It should not remain in the body after a cell regenerates its own ECM of tissue. The by-product of the scaffold should also be nontoxic, ie, it should not compromise the function of the developing tissue or other organs. Scaffolds must be mechanically strong enough to withstand in vitro biological forces. The mechanical properties of the scaffolds can be achieved at the expense of losing their porosity or vice versa. There is a trade-off between mechanical properties and the porosity of the scaffold (for infiltration) (O'Brien, 2011; Murugan and Ramakrishna, 2007).

9.5 Cellulose-based materials for cartilage tissue engineering

Cellulosic materials are ubiquitous in the plant kingdom and can also be found in many different animal-based organisms. They have already seen traditional use in the tissue-engineering field such as cotton for wound dressing and sutures. Though

Table 9.1 Different scaffolds used for cartilage tissue engineering and their properties

Scaffold material	Advantages	Disadvantages	References
Natural			
Chitosan	• Similar to various GAG molecules • High biocompatibility and biodegradability	• Low solubility • Require cross-linking and cell cannot infiltrate due to lower pore size	Correia et al. (2011) and Montembault et al. (2006)
Collagen	• Main component of cartilage tissue • Support chondrogenesis • Maintain chondrocyte phenotype and glycosaminoglycans production.	• Rapid degradation and poor mechanical property	Matsiko et al. (2012) and Yan et al. (2010)
Hyaluronic acid	• Main glycosaminoglycans molecule of ECM • Good biocompatibility and degradability	• Negative charge can lead to lower cell adhesion • High water absorption and lower mechanical strength	Correia et al. (2011), Barbucci et al. (2002), and Ren et al. (2009)
Fibrin	• Natural component of intravascular area • Spontaneous repair activities with abundant type II collagen and sulfate GAGs	• Lower mechanical strength • Rapid degradation	Hendrickson et al. (1994) and Petersen et al. (2004)
Silk	• Support growth of chondrocytes • Superior mechanical property and slower biodegradation	• Allergic reactions	Hofmann et al. (2006) and Gellynck et al. (2008)
Cellulose	• Mechanical strength superior than the natural cartilage	• Low cell growth when used alone and therefore requires coating with other biopolymer • Low biocompatibility	Torres et al. (2012) and Pulkkinen et al. (2006)
Synthetic			
Polylactic acid (PLA) and Polylactic-co-glycolic acid (PLGA)	• Promotes chondrocytes proliferation and glycosaminoglycans • Satisfactory biocompatibility • Good mechanical strength	• Induced inflammation due to polymer hydrolysis, inconsistent biodegradation rates	Chen and Su (2011) and Munirah et al. (2008)

cellulose is naturally occurring and has found a number of applications inside and outside of the medical field, it is not typically produced in its neat state. A lengthy process is required to separate lignin, hemicelluloses, and other molecules from the cellulose in most renewables (wood, agricultural fibers such as cotton, grasses, etc.). Other sources to obtain cellulose are from the biosynthetic processes of microorganisms such as algae, fungi, and bacteria. There are many highly desirable traits for cellulose that can validate its potential as a tissue-engineering scaffold:

1. the chemical composition of cellulose is biocompatible for use in a 3-D tissue-engineering application. Regenerated cellulose having a high amount of hydroxyl groups possesses a sufficiently enhanced surface activity that allows the immobilization of fibronectin to help cells attach well compared to native cellulose (Ko and Iwata, 2001).
2. because of the high hydroxyl group content, cellulose tends to absorb water and create a humid environment for the cellulose scaffold. In addition, cellulose shows a high mechanical property even under a wet state, a property that is essential for cartilage regeneration (Svensson et al., 2005; Petersen and Gatenholm, 2011).
3. the chemical structure of cellulose fiber is similar to that of collagen and therefore it can be used as a collagen-mimicking substrate given that the AC composition consists of 60% by dry weight of collagen, responsible for providing the requisite mechanical strength (Bäckdahl et al., 2008).
4. because cellulose is hard to degrade in vivo, it can be removed from the implant site when it is no longer needed (Ko and Iwata, 2001).
5. cellulose can undergo etherification, ie, the hydroxyl groups of cellulose chemically react with relatively electropositive carbons in specific organic species (eg, alkyl halides) to give rise to cellulose derivatives such as MC, hydroxypropylcellulose (HPC), EC and CMC (Sannino et al., 2009). These functionalities have found wide applications in different arenas including cartilage TE. Several of the applications and properties of these materials will be discussed in the latter half of this chapter.

9.5.1 Cellulose fabric and sponge

Cellulose can be engineered into different shapes and sizes as found in knitted, nonwoven, woven, or sponges depending upon the application. The biocompatibility of pure cellulose can be improved by coating it with other biomaterials. Muller et al. (2006) used fabric consisted of regenerated cellulose II monofilament fibers coated with calcium phosphate for cartilage regeneration. The coating layer consists of calcium-deficient carbonated apatite having similar composition of the inorganic material of bone which is biocompatible. The coating made the scaffold more hydrophilic as compared to untreated one and triggered the adhesion of chondrocyte cells. It was evidenced by the homogenous distribution and collagen type II expression, an observation that proves the biocompatibility of cellulose fabric as a potential biomaterial for cartilage TE (Muller et al., 2006). Pulkkeinen et al. (2006) used a viscose cellulose sponge into which was incorporated collagen type II. In this case, the human type II collagen turned out to be the best coating material as it was able to maintain chondrocyte morphology. The results showed that after 4 weeks of cultivation with chondrocytes, cell attachment was only 60% due to small pore sizes. However, the sponges coated with collagen type II maintained chondrocyte phenotype. Nevertheless, it induced stiffness in the scaffold and lacked proper ECM composition (Pulkkinen et al., 2006).

9.5.2 Cellulose nanocrystals

Cellulose nanocrystals (CNCs) have been used as a reinforcement agent in composite materials or hydrogels to improve their mechanical properties, thermal stability, and/or water absorption properties. In one of the studies (Wang and Chen, 2011), CNCs were used to prepare an all-cellulose composite material by adding CNCs from 0 to 50 wt-% via rapid thermally induced phase separation. The CNCs acted as a bridge to cross-link the cellulose chains during the gel formation process. The resultant gels showed a very porous structure with improved mechanical properties similar to those of polylactic acid (PLA)–polyethylene oxide (PEO)–PLA hydrogels and PLA–fibrin gels that were conjectured to be cartilage TE materials (Sanabria-DeLong et al., 2008; Zhao et al., 2009).

Hydrogels of hemicellulose and CNCs were prepared by in situ radical polymerization. The hemicelluloses were modified by reaction with 2-hydroxyethylmethacrylate before adsorption onto the CNCs. The resulting hydrogels showed improved toughness, good recovery behavior, and acceptable swelling and mechanical properties. Based on these properties, it has been hypothesized that these hydrogels have potential for use in load-bearing biomedical applications such as AC replacement (Karaaslan et al., 2011).

9.5.3 Chemically modified cellulose–based hydrogels

Hydroxypropylmethylcellulose (HPMC) is a precursor of cellulose and is modified with small amounts of propylene glycol ether groups attached to the anhydroglucose terminus of the cellulose. It is a self-hardening hydrogel having silane grafted along the hydroxypropyl methylcellulose grafted with silanol group (Si-HPMC) chains (Fatimi et al., 2008). Vinatier et al. (2005) were among the first to mention its use as a potential cartilage tissue material. They have done singular research on injectable and self-setting hydrogels of Si-HPMC for cartilage TE. The cross-linking and the self-hardening of the hydrogels depend upon the pH of the environment and also on the silanol condensation from the silane grafted onto the cellulose backbone. The chondrocytes isolated from rabbit AC and two human chondrocytic cell lines maintain a chondrocyte-specific phenotype and express type II collagen and aggrecan. Although the hydrogel showed its potential for cartilage regeneration, its actual pH as an injectable hydrogel during the time of injection will differ from the physiological pH of the implant site (Vinatier et al., 2005). A later study by Vinatier et al. (2007) showed that the Si-HPMC encouraged the maintenance and recovery of human nasal chondrocytic phenotypes. After 3 weeks of in vivo culturing of cells in nude mice, the hydrogel was able to form a cartilaginous tissue, an appreciable result that demonstrates a feasible approach for cartilage TE (Vinatier et al., 2007). Extended work with injectable self-setting cellulose-based Si-HPMCs has been carried out to repair AC defects of rabbits in which Si-HPMC-containing autologous rabbit nasal chondrocytes are used. An analysis of the postoperative recovery of the articular cavity within 6 weeks revealed no signs of inflammation and found that the site has a structurally organized tissue resembling hyaline-like

cartilage (Vinatier et al., 2009). This innovative hydrogel could be used as a transplantation hydrogel for in vivo cartilage TE.

The same research group extended their work on adipose tissue stem cells (ATSC) with Si-HPMC in the presence of a chondrogenic culture medium and under hypoxia (5% O_2). The ATSC underwent a chondrogenic differentiation and favored type II collagen and aggrecan mRNA expression. An in vivo experiment was carried out in which an ATSC/Si-HPMC system was injected into subcutaneous pockets in nude mice. After 21 days of culture, ATSC was able to form a cartilaginous tissue when implanted with Si-HPMC hydrogel (Merceron et al., 2010). Again, the same group carried out further research exploring oxygen tension to determine its effect on the regenerative potential of mesenchymal stem cell (MSC) for cartilage repair. MSC from human and rabbit adipose stromal cells that was injected in Si-HPMC hydrogel and later preconditioned formed a cartilaginous tissue regardless of the oxygen tension. In a 3-D in vitro culture, 5% O_2 enhances the chondrogenic differentiation; however, it does not enhance its in vivo chondrogenesis. This confirms the potential of Si-HPMC in cartilage repair when used with preconditioned appropriate cells (Portron et al., 2013).

Chondrocytes cell culture studies were carried out on two and three dimensional Si-HPMC scaffolds incorporated with two GAG-like marine exopolysaccharides (HE800 and GY785, with hyaluronic acid as control). The incorporation of exopolysaccharides significantly improved gelation time and the mechanical properties (10.25 KPa) which were similar to native cartilage and with a better dispersion of cells on the surface of these hydrogels in a 2-D culture. Although in a 3-D culture, the chondrocyte cells dispersed in the environment, leading to cluster formation. This happened because of the small pore sizes in the course of the preparation of the scaffold; however, the scaffold showed higher mechanical properties compared with the Si-HPMC scaffold alone (Rederstorff et al., 2011). Therefore, from the latter work, it can be deduced that an ideal scaffold should have an open porous structure to help cells to infiltrate and migrate within the scaffold and allow for adequate mechanical strength.

One particular cellulose derivative, CMC, had been modified by converting a large percentage of the native carboxylic groups (50%) into amidic groups and trying to mimic the hyaluronan macromolecule which is an essential component of AC. The resultant modified polysaccharide was further cross-linked to obtain hydrogels containing NH_2 groups. The hydrogels showed a viscous–elastic solid-like behavior as verified by rheological characterization and can serve as potential filler for cartilage defects (Leone et al., 2008a). In later studies on the same hydrogels, the thixotropic (flow) behavior showed that the hydrogels can recover their original shape after removing a mechanical stressor, a finding that proves their potential to be injectable. This hydrogel was further analyzed by in vitro studies of normal human articular chondrocytes obtained from the human knee. The results showed that the hydrogels with chondrocytes showed increased production of ECM components rich in collagen and proteoglycans. This hydrogel also compared well with hyaluronan hydrogels as a substitute. An in vivo study carried out on adult male rabbit for 50 days showed from the results of histological sectioning that the amidated carboxymethylcellulose (CMCA)-treated defect had a layer of mixed fibrocartilaginous and hyaline-like tissue

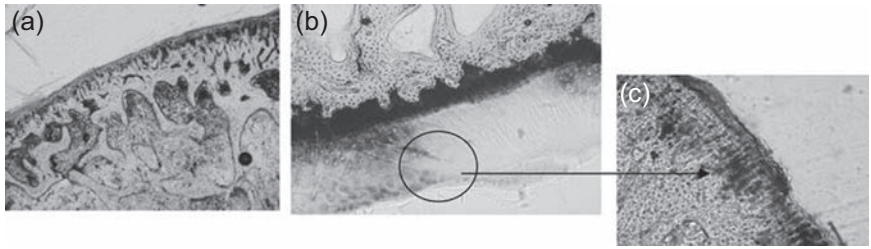

Figure 9.3 Histological section of the chondral defects of a male rabbit after 50 days of in vivo studies. (a) Control defect with no hydrogels; (b) amidated carboxymethylcellulose (CMCA) hydrogels showed a mixed layer of fibrocartilaginous and hyaline-like tissue. (c) Chondrocytes showing cluster and columnar formations in new hyaline-like matrix (magnification: 5×).
Reprinted with kind permission from Springer Science and Business Media (Leone, G., Fini, M., Torricelli, P., Giardino, R., Barbucci, R., 2008b. An amidated carboxymethylcellulose hydrogel for cartilage regeneration. Journal of Materials Science: Materials in Medicine 19 (8), 2873–2880).

with a regular and smooth surface. The chondrocytes showed cluster and columnar formations in the new hyaline cartilage as seen in Fig. 9.3(c). The hydrogels showed similar behavior compared to hyaline hydrogels (Leone et al., 2008b).

9.5.4 Cellulose organic and inorganic composite hydrogels

Cellulosic composite materials have been prepared to enhance the functional as well as the biological properties of the cellulose fraction. Alone, cellulose cannot overcome limitations such as low mechanical properties and no antibacterial properties; therefore, cellulose has been endowed with more bioactivity by combination with other natural biopolymers and nanomaterials.

Injectable polymers has gained interest because these polymer solutions can encapsulate live cells and form gels at body temperature and ambient physiological conditions without invasive surgeries and are known to accommodate the defect at the required shape and size. A composite scaffold of chitosan–glycerol–phosphate solution with hydroxyethylcellulose (HEC) was prepared. The gel proved its worth by engaging in cartilage-matrix deposition with articular chondrocytes and was able to partly retain the full thickness of the chondral defects in a living rabbit for 1–7 days (Hoemann et al., 2002, 2005). A small amount of glyoxal permitted the gel formation, viable cell encapsulation, and cell proliferation. However, the gelation temperature was 70°C beyond that of normal body temperature (Hoemann et al., 2007).

Because the physical and chemical properties of a number of injectable polymer hydrogels are pH and temperature dependent, a new copolymer of poly (*N*-isopropylacrylamide)-*g*-methylcellulose (PNIPAAm-*g*-MC) has been explored as a 3-D scaffold for AC regeneration. In this system, PNIPAAm has a lower critical solution temperature (LCST) of approximately 33°C and undergoes a liquid-to-gel reversible phenomenon while also having the added advantage of an LCST very close

to body temperature. Fig. 9.4 shows the images of PNIPAAm hydrogel at different temperatures. Encapsulated ATDC5 chondrogenic cells within the hydrogel are able to retain their viability and maintain their chondrogenic phenotype, spherical morphology, while promoting ECM production (Sá–Lima et al., 2011).

A novel, thermally sensitive pH-dependent hydrogel of CMC–chitosan has been prepared as an injectable hydrogel for cartilage repair. This gel is in the liquid state at room temperature into which living chondrocytes are encapsulated. Remarkably, at physiological pH and body temperature during in vivo injection, the liquid became a hydrogel (implant) in situ. Therefore, this novel polyelectrolyte hydrogel demonstrated great potential as an injectable hydrogel under physiological conditions (Chen and Fan, 2008).

Hydrogels should demonstrate adequate mechanical strength along with biocompatibility. A composite hydrogel of poly(acrylamide) and cellulose was prepared mainly for its mechanical characteristics compared to various natural ACs. The hydrogels were quite similar to cartilage in terms of compressive properties while simultaneously demonstrating very good viscoelastic behavior (Buyanov et al., 2013). A composite scaffold of cellulose and gelatin was prepared because gelatin can impart a 3-D architecture to the scaffold by virtue of its own structure, it is a derivative of

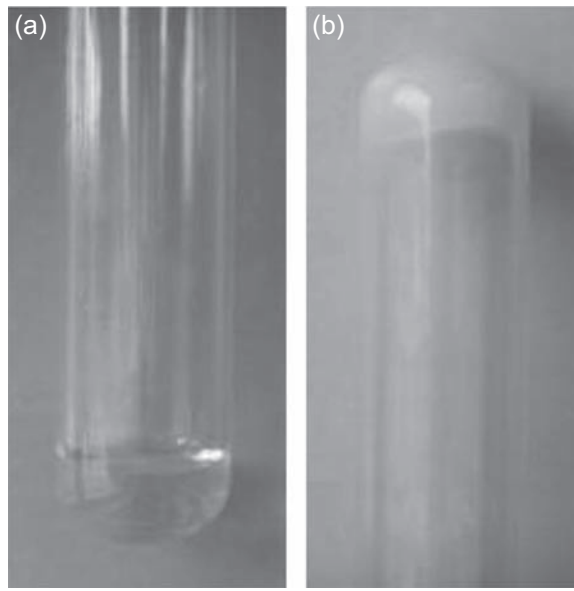

Figure 9.4 Images of poly (*N*-isopropylacrylamide)-*g*-methylcellulose (PNIPAAm-*g*-MC) copolymer system at (a) room temperature, and (b) at body temperature 37°C.
Reprinted from permission of Journal of Biomedical Materials Research (Sá-Lima, H., Tuzlakoglu, K., Mano, J.F., Reis, R.L., 2011. Thermoresponsive poly (N–isopropylacrylamide)–g–methylcellulose hydrogel as a three–dimensional extracellular matrix for cartilage–engineered applications. Journal of Biomedical Materials Research Part A 98 (4), 596–603). Copyright © 2011 Wiley Periodicals, Inc.

collagen (an essential component of the AC), and it is biodegradable. The scaffold had an open porous and rough structure, factors which played important roles in cell adhesion. The scaffold showed three to eight times greater mechanical strength as a function of the increase in the amount of added cellulose. The scaffold supported human mesenchymal stem cells and ECM formation with extensive F-actin expression (Xing et al., 2010). Starch-based scaffolds have been prepared with incorporation of cellulose nanofibers using film casting, salt leaching, and freeze-drying methods. The scaffolds have adequate mechanical strength and possess among the highest compressive moduli (10.41 MPa), in the range of the window of compressive moduli for human articulate cartilage (1.9–14.4 MPa). Chondrocytes from rabbit knee after 4 days culture showed spherical morphology, were well attached to the scaffold, and the MTT assay showed no toxicity from salt leaching that proves the biocompatibility of cellulose/gelatin scaffolds (Nasri-Nasrabadi et al., 2014).

Other than polymers, other biomolecules were also incorporated into cellulose such as chondroitin 4-sulfate (C-4S), a sulfated and carboxylated GAG that has already been delineated as an important structural component of cartilage. Cellulose was modified with quaternary amino groups to make it more highly cationic in nature and thus interact more strongly with oppositely charged C-4S. This kind of complex system may serve as a treatment for osteoarthritis and articular degenerative diseases (Bierbrauer et al., 2014).

Other inorganic materials, such as biphasic calcium phosphate (BCP) with CMC have been prepared for new classes of composite materials. Multiphasic materials such as bioceramic show high compressive properties in addition to containing water-soluble polymers and are considered good ionic carriers for the formation of ECM. This composite material provided adequate injectable properties and nontoxic responses, demonstrating its potential for the repair of AC (De Freitas et al., 2012).

9.6 Bacterial cellulose properties and suitability as a medical implant for cartilage tissue engineering

Although BC displays a similar chemical structure to plant cellulose, it has a much higher natural availability because of the absence of lignin and hemicelluloses, which require a lot of energy and chemicals for their removal from their native lignocellulosic "cage." This is rather big distinction between the cellulose found in bacteria versus that found in plants. The macromolecular structure of BC is also quite different from plant cellulose. BC chains combine to form subfibrils of a width of approximately 2 nm at most. These subfibrils then crystallize into microfibrils, and further into ribbons of approximately 4 to 100 nm, a size much smaller than what is found in wood cellulose (Yamanaka and Sugiyama, 2000). BC is produced from various species of bacteria such as *Acetogluconobacter xylinus* (a gram-negative bacterial strain) during the fermentation process. Due to the high water uptake of cellulose, it has a tendency to form gels. It has high tensile strength, a high crystallinity index, excellent

biocompatibility, and very high purity. BC has found applications in fields as diverse as pulp and paper products, audio components (the diaphragm for speakers), and soft-TE (Petersen and Gatenholm, 2011; Malcolm, 2013). BC has a unique 3-D fibril structural network similar to the ECM component (collagen) of naturally occurring tissue. It is approximately of the same size (100 nm in diameter) (Backdahl et al., 2006) and has a mesh-like appearance and woven network structure that result in high porosity and an attendant large surface area. In addition, such an arrangement of fibrils gives rise to high mechanical properties (Yamanaka and Sugiyama, 2000; Malcolm, 2013).

9.6.1 Biocompatibility

BC has been investigated for a number of biomedical applications such as wound dressing, blood-vessel formation, and bone reconstruction (Czaja et al., 2007). Recently, an in vivo study of subcutaneous BC implantation in rats was carried for 12 weeks, and no microscopic signs of inflammation, exudation, fibrotic capsulation, or giant cell formations were observed, proving its biocompatibility (Helenius et al., 2006). The biocompatibility of a BC scaffold has already been well studied (Muller et al., 2006; Pulkkinen et al., 2006; Kim et al., 2010).

Svensson et al. (2005) used unmodified and modified (by chemical sulfation and phosphorylation) BC to study the cell culture of bovine chondrocytes with incorporation of collagen and alginate. They found that unmodified BC supports chondrocyte proliferation on 50% of the collagen type II substrate. Fig. 9.5(a) shows the SEM image of chondrocytes attached to a BC scaffold that show a round morphology. Modified BC showed no effect on chondrocyte growth after chemical sulfation and phosphorylation (Svensson et al., 2005). Andersson et al. (2010) used human chondrocytes

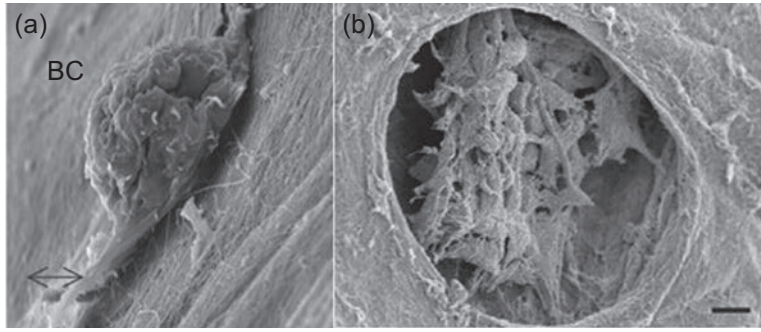

Figure 9.5 (a) SEM image of chondrocyte attached to the surface of bacterial cellulose (BC) scaffold. Reprinted with permission from Elsevier *(Svensson, A., Nicklasson, E., Harrah, T., Panilaitis, B., Kaplan, D.L., Brittberg, M., Gatenholm, P., 2005. Bacterial cellulose as a potential scaffold for tissue engineering of cartilage. Biomaterials 26 (4), 419–431).*
(b) SEM image of chondrocytes filling the single pore of BC scaffold. Reprinted from permission of Journal of Biomedical Materials Research *(Andersson, J., Stenhamre, H., Backdahl, H., Gatenholm, P., 2010. Behavior of human chondrocytes in engineered porous bacterial cellulose scaffolds. Journal of Biomedical Materials Research Part A 94A (4), 1124–1132).*

on porous BC scaffolds to regenerate AC. Paraffin wax microparticles were incorporated in glass tube bioreactors with a silicone tube to generate larger pore sizes in the scaffold. The pore size of the scaffold was around 15–300 μm, but was not evenly distributed. Also, the cell seeding was uneven throughout the scaffold due to an uneven surface of the material. However, the interconnectivity of the pores allowed cells to enter deeply into the scaffold. The chondrocytes were also able to produce ECM within the scaffold. Fig. 9.5(b) shows the SEM image of the chondrocytes filling a single pore of a BC scaffold (Andersson et al., 2010). BC sponges with a hierarchical pore structure were prepared by an emulsion freeze-drying technique to give a high surface area of $92.81 \pm 2.02\ m^2/g$ and a high porosity of $90.42 \pm 0.25\%$. The synovial-derived MSCs were cultured on sponges and after 7 days, it was found out that MSCs can proliferate well and grow inside the BC sponges with a maximum ingrowth of 150 μm (Zhijiang et al., 2012). A 3-D scaffold of BC seeded with equine bone marrow mesenchymal stem cells showed excellent biocompatibility for bone and cartilage TE. The scaffolds were cytocompatible and supported cellular adhesion and proliferation. The cells spread out fully on the surface of the BC nanofibers, maintained a round morphology, and allowed osteogenic and chondrogenic differentiation after 14 days of culture (Favi et al., 2013).

In another study, a composite 3-D scaffold of BC and agarose showed better cell attachment and proliferation because of the higher surface area of the scaffold. The higher porosity promoted cell viability and agarose helped phenotype maintenance in addition to improving the strength and biocompatibility of the scaffold compared to a pure BC scaffold (Yang et al., 2011). Other studies have shown the incorporation of biomolecules such as growth factor TGF-β1, which helps in differentiation, proliferation, and matrix synthesis. A new method was proposed for in vitro bovine cartilage regeneration using a punch model for focal cartilage defects in which a central defect was filled with nonresorbable BC. The chondrocytes on the surface of the BC showed redifferentiation with increased aggrecan–collagen type II mRNA expression over time. However, the chondrocytes did not immigrate into the central BC area because of small pore sizes (2–5 μm) (Pretzel et al., 2013).

Very recently, the problem of small size and heterogeneity of the pores in BC was overcome by a laser perforation technique. Fig. 9.6 illustrates the preparation technique of unidirectional and 3-D laser perforation in BC. The right column shows how BC was prepared in culture plates over 14 days, the middle column shows how the unidirectional perforation were performed, and the last column shows the 3-D perforation in which the laser cutting was done on the other side of the cuboids. This technique is versatile in that it is able to fabricate different shapes and architectural patterns. Compared with in situ modification of BC such as paraffin wax, this method had the added advantage of timesaving while providing a controlled architecture and rapid prototyping. Fig. 9.7 shows an SEM image of a 3-D laser-modified BC hydrogel which shows a channeled pattern. This scaffold showed high biocompatibility with cartilage-specific matrix production and indicated that the chondrocytes differentiated to provide a compressive strength similar to that of unmodified BC. The perforation of the resulting channels provided a short diffusion distance for nutrients and ECM components. Therefore, this technique, when done in conjunction with BC hydrogels, is well suited for in vivo cartilage repair (Ahrem et al., 2014).

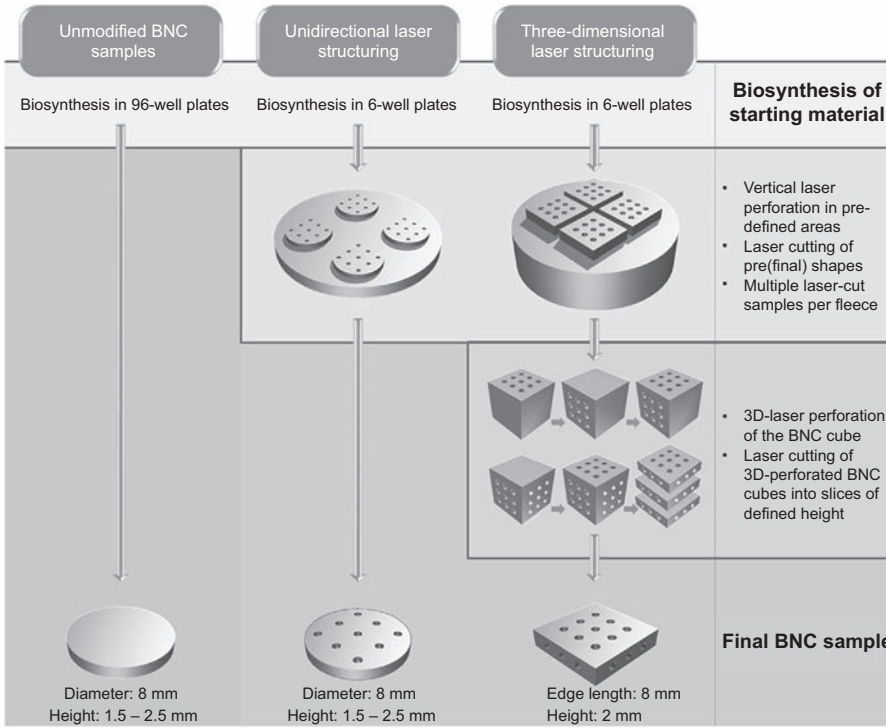

Figure 9.6 Schematic illustration of the preparation technique of unmodified and laser-structured bacterial nano cellulose (BNC) samples. The holes of the modified BNC do not represent the actual size in the experimental section. *BNC*, bacterial nanocellulose.
Reprinted with permission from Elsevier (Ahrem, H., Pretzel, D., Endres, M., Conrad, D., Courseau, J., Müller, H., Jaeger, R., Kaps, C., Klemm, D.O., Kinne, R.W., 2014. Laser-structured bacterial nanocellulose hydrogels support ingrowth and differentiation of chondrocytes and show potential as cartilage implants. Acta Biomaterialia 10 (3), 1341–1353).

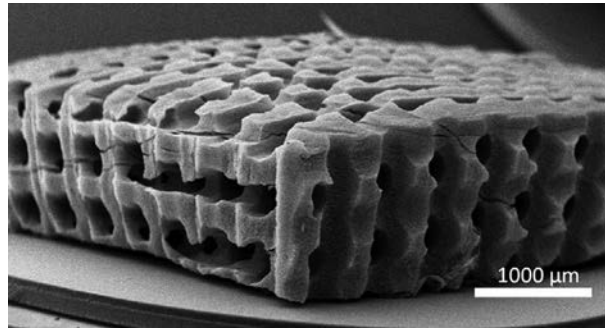

Figure 9.7 SEM image of structural 3-D laser-modified BC scaffold.
Reprinted with permission from Elsevier (Ahrem, H., Pretzel, D., Endres, M., Conrad, D., Courseau, J., Müller, H., Jaeger, R., Kaps, C., Klemm, D.O., Kinne, R.W., 2014. Laser-structured bacterial nanocellulose hydrogels support ingrowth and differentiation of chondrocytes and show potential as cartilage implants. Acta Biomaterialia 10 (3), 1341–1353).

9.6.2 Mechanical properties

Articulated cartilage (AC) is a very hydrated connective tissue providing low friction, good load bearing, and high wear resistance at the synovial joints, while also showing characteristically good mechanical properties. During a normal walking cycle, AC can bear up to four times its own weight, but as such, it can endure significant abrasive/friction forces depending on the load and speed. In one of the studies, the friction and wear behavior of BC was investigated in AC by studying the tribological response. Synovial fluid is a lubricating agent in AC to help facilitate the sliding of two articulating bones through reducing the coefficients of friction. In this study, BC exhibited values in the range of 0.046 to 0.058, with decreasing friction coefficient as the contact pressure increased, thus acting as an excellent biomimetic of the lubricating effect. This might be due to the 3-D nanofibril network and its excellent water-holding capacity given that BC consists of more than 90% water and only 1% solid (Klemm et al., 2011). Therefore, it can be reasonably concluded that BC (gel) can be used as a potential AC scaffold for articular joints (Lopes et al., 2011).

BC-based scaffolds have excellent tensile strengths and Young's moduli; however, they exhibit low compressive properties in the perpendicular direction. This prevents more extensive use of BC because of its lack of compression and shear resistance. Currently, there are numerous studies to improve these properties by the incorporation of fillers or other polymers. Additionally, BC has an asymmetric network structure composed of many lamellar layers that give rise to many small voids. Therefore, a uniform pore structure is also needed for cellular infiltration without compensating mechanical properties. Scaffolds of 2,2,6,6-tetramethylpiperidine-1-oxyl (TEMPO)-mediated BC mixed with chitosan have already been prepared by a two-step chemical modification. The scaffolds showed lower compressive moduli than human and animal cartilage specimens because of lower cellulose content. Therefore, a better fabrication method is still needed to overcome this deficiency (Nge et al., 2010).

Hydrogels with an interpenetrating polymer network have been developed with polyacrylamide (PAAm) and BC which has demonstrated mechanical properties similar to natural cartilage. Concentrated PAAm solution impregnated into a BC layer and cross-linked with N,N′–methylene–*bis*–acrylamide (MBA), a component which governs the swelling and mechanical properties. The hydrogels showed anisotropic behavior as shown by the higher resilience of specimens cut in a direction perpendicular to the top and bottom parts of BC as compared to a specimen cut in the parallel direction. Also, hydrogels with a higher BC content showed higher moduli and strengths. These samples were subjected to fatigue tests up to 6000 cyclic compression-unloading to compare with natural AC and showed no large depression. This anisotropic behavior was due to the unique BC 3-D structure. BC possesses tunnel-like lacunae, normal to the surface of the BC pellicle, arranged in the axis perpendicular to the surface of BC pellicles, a very unusual property of BC compared to plant cellulose. These hydrogels have a compression in the range of 1.9 to 14 MPa, quite similar to the compressive modulus of a human joint cartilage (Buyanov et al., 2010).

Articulated cartilage (AC) displays nonlinear, viscoelastic, and strain rate-dependent properties, in addition to the anisotropy properties. These strain-rate properties

are important because they enable continuous joint function throughout the wide range of loads from walking, running, and other physical activities. Polyvinyl alcohol (PVA) has limited strain-rate dependence under unconfined compression and also shows very low wear resistance and friction compared to a clinically available material of ultrahigh molecular weight polyethylene (UHMWPE). Adding a small amount of BC with a PVA matrix increased the viscoelasticity and stiffness when the number of cycles increased from one to six compared to pure PVA, a trend quite similar to natural cartilage. However, the stiffest PVA–BC scaffold showed a slightly lower elastic modulus than that of AC. Therefore, by altering the number of thermal cycles and PVA or BC concentration, it is possible to increase the range of moduli (Millon et al., 2009). Other promising candidates include methacrylate for the preparation of BC–composite hydrogels. BC–methacrylate hydrogel composites were prepared by UV radical cross-linking polymerization. The compression moduli ranged from 2 to 5.5 MPa for composites swollen to equilibrium having 20–70 wt-% water by simply introducing 1–2% BC. Thus, BC can be a reinforcing biomaterial with strong interfacial interactions with other polymer matrices (Hobzova et al., 2012).

Another commonplace strategy is to make double network (DN) hydrogels that are quite different than a common interpenetrated-polymer network for fiber-reinforced hydrogels. DN hydrogels consist of two hydrophilic polymers with a combination of a stiff and brittle first network and a soft and ductile second network. One such DN hydrogel was prepared by combining BC and poly dimethylacrylamide (PDMAA), the wear property for which was evaluated by a pin-on-flat-type wear test. These hydrogels showed excellent cyclic friction that was quite comparable to that of (UHMWPE) and showed a greater degree of resistance to wear (Yasuda et al., 2005). Therefore, by improving the processing strategies, concentration, and polymer chemical structures, an ideal hydrogel can be prepared that mimics the natural cartilage in terms of friction, wear, viscoelastic, and load-bearing properties.

9.6.3 Biodegradation

In addition to biocompatibility and high mechanical strength, a scaffold for cartilage TE should demonstrate adequate biodegradability. BC is very crystalline with a compact structure. It is susceptible to cellulolysis induced by various fungi and bacterial species. However, these enzymes are not present in animals and the degradation of cellulose is limited in vivo because of the absence of the required cellulase. BC has varying surface and structural characteristics depending upon its cultivation conditions that can imbue it with varying degrees of degradation. Various in vivo and in vitro studies have been carried out to evaluate the degradability of BC: an in vivo study of subcutaneous BC implantation in rats was carried for 12 weeks that showed no sign of BC degradation; however, 12 weeks was a very short time to claim any biodegradability (Helenius et al., 2006). The enhancement of biodegradation of BC was done in vitro (in water, phosphate buffer saline, simulated body fluid). Yet, BC showed negligible degradation compared to biodegradable polymers like polyglycolic acid and polylactic acid (Li et al., 2009).

One of the biggest mysteries for a scaffold for cartilage TE is whether it should be biodegradable. A major problem with a biodegradable scaffold is that it follows a non-synchronized degradation of the seeded scaffold and subsequent regeneration of damaged tissue. However, for cartilage to be fully functional, it usually requires months or even years. Thus, BC is a suitable candidate. Therefore, a BC scaffold should have adequate mechanical strength and a porous structure with an architectural pattern for the migration of local cells in the defect-filling implants to synthesize new cartilage matrix (Pretzel et al., 2013).

On the other hand, the degradation of the BC can be changed metabolically by the incorporation of *N*-acetylglucosamine (GlcNAc) residues during de novo synthesis from *Gluconacetobacter xylinus*. This modified BC is less crystalline, but more susceptible to lysozyme (an enzyme found in human body) compared to a control BC (Yadav et al., 2010, 2011). Adult human mesenchymal stem cells (ahMSCs) were successfully adhered, proliferated, and differentiated in these modified scaffolds. The chondrocytes were able to synthesize ECM containing proteoglycan and type II collagen with the added advantage of lysozyme susceptibility for degradation, an outcome that can prove useful for in vivo studies (Yadav et al., 2013).

9.7 Conclusions and future outlook

The goal of this chapter was to give an overview of cartilage-related health diseases and injuries and develop an understanding of cellulosic materials for their potential fabrication as scaffolds for cartilage TE. Cellulose appears to be a suitable candidate for this application because of its chemical structural similarity to collagen. The properties of the scaffold can be tuned by various chemical modifications, architectural patternings, and combination with other polymers to improve the biocompatibility and mimic the natural ECM. Injectable hydrogels of cellulose derivatives (Si-HPMC) appear to provide a potent combination of ECM environment with an ability to fill the defect area by in situ cross-linking under physiological regimes, provide viable cell encapsulation, and are able to support chondrocyte proliferation and adhesion for cartilage regeneration. However, the problem of limited cell migration because of small pore size and lower mechanical strength is persistent with this type of scaffold. A combination with other natural polymers such as chitosan, gelatin, and starch can improve the mechanical strength and biocompatibility; however, the collapse of the porous structure can be observed because of the solubility of these latter polysaccharides. This problem can be solved by introducing an interpenetrating polymer network to form a stable hydrogel (Buyanov et al., 2010). Another interesting biopolymer that has gained tremendous attention is BC which had proven a suitable candidate because of its smaller fibril size (ranging from 20 to 100 nm) and 3-D nanofibrous architecture that remarkably mimics the ECM of cartilage. However, in addition to very small pore sizes, an in vivo characterization and the performance of the BC scaffold (for a long period of time in a large animal model) is still needed to address the future clinical suitability application for cartilage tissue regeneration.

Noting the ever-increasing research in cartilage TE using cellulose materials, an improved and alternative method is still needed, and there is plenty of room for improvements. Researchers should consider the following aspects for preparing practical scaffolds that mimic the natural ECM: (1) Improving the porous structure of the BC scaffold. Recently, new technique was developed which can create a 3-D porous scaffold by laser perforation. This scaffold has porous channels that can help transfer nutrients and other essential ECM components. This technique does not induce any toxicity and is free of the residual solvent removal problem. The added advantage of rapid prototyping with consistent pore size makes this technique a viable process at the industrial scale (Ahrem et al., 2014). (2) Biocompatibility can be further enhanced by incorporation of ECM-supporting molecules and growth factors such as chondroitin 4-sulfate and TGF-β1, respectively, to favor cartilage regeneration. The cell–scaffold interaction should be monitored to fully understand cell attachment and cartilage formation during the early stage of implantation. Again, the interaction will depend upon scaffold architecture properties such as pore size and surface area; (3) scaffold biodegradation for cartilage regeneration is still questionable. Cartilage needs at least several months to 1 year to fully recover. During this period, the scaffold should support ECM formation without degradation. Therefore, the degradation proprieties of cellulose may be tuned by either chemical (Li et al., 2009) or biological means (Yadav et al., 2010).

References

Ahrem, H., Pretzel, D., Endres, M., Conrad, D., Courseau, J., Müller, H., Jaeger, R., Kaps, C., Klemm, D.O., Kinne, R.W., 2014. Laser-structured bacterial nanocellulose hydrogels support ingrowth and differentiation of chondrocytes and show potential as cartilage implants. Acta Biomaterialia 10 (3), 1341–1353.

Andersson, J., Stenhamre, H., Backdahl, H., Gatenholm, P., 2010. Behavior of human chondrocytes in engineered porous bacterial cellulose scaffolds. Journal of Biomedical Materials Research Part A 94A (4), 1124–1132.

Athanasiou, K., Darling, E., Hu, J., 2009. Articular Cartilage Tissue Engineering, vol. 1 (1), pp. 1–182.

Aydelotte, M.B., Kuettner, K.E., 1988. Differences between sub-populations of cultured bovine articular chondrocytes.1. Morphology and cartilage matrix production. Connective Tissue Research 18 (3), 205–222.

Bäckdahl, H., Esguerra, M., Delbro, D., Risberg, B., Gatenholm, P., 2008. Engineering microporosity in bacterial cellulose scaffolds. Journal of Tissue Engineering and Regenerative Medicine 2 (6), 320–330.

Backdahl, H., Helenius, G., Bodin, A., Nannmark, U., Johansson, B.R., Risberg, B., Gatenholm, P., 2006. Mechanical properties of bacterial cellulose and interactions with smooth muscle cells. Biomaterials 27 (9), 2141–2149.

Barbucci, R., Lamponi, S., Borzacchiello, A., Ambrosio, L., Fini, M., Torricelli, P., Giardino, R., 2002. Hyaluronic acid hydrogel in the treatment of osteoarthritis. Biomaterials 23 (23), 4503–4513.

Bhosale, A.M., Richardson, J.B., 2008. Articular cartilage: structure, injuries and review of management. British Medical Bulletin 87 (1), 77–95.

Bierbrauer, K.L., Alasino, R.V., Strumia, M.C., Beltramo, D.M., 2014. Cationic cellulose and its interaction with chondroitin sulfate. Rheological properties of the polyelectrolyte complex. European Polymer Journal 50, 142–149.

Buckwalter, J.A., Mankin, H.J., 1998. Articular cartilage: degeneration and osteoarthritis, repair, regeneration, and transplantation. Instructional Course Lectures 47, 487–504.

Buckwalter, J.A., Mankin, H.J., Grodzinsky, A.J., 2005. Articular cartilage and osteoarthritis. Instructional Course Lectures-American Academy of Orthopaedic Surgeons 54, 465.

Buckwalter, J.A., Mow, V.C., Ratcliffe, A., 1994. Restoration of injured or degenerated articular cartilage. The Journal of the American Academy of Orthopaedic Surgeons 2 (4), 192–201.

Buyanov, A., Gofman, I., Khripunov, A., Tkachenko, A., Ushakova, E., 2013. High-strength biocompatible hydrogels based on poly (acrylamide) and cellulose: synthesis, mechanical properties and perspectives for use as artificial cartilage. Polymer Science Series A 55 (5), 302–312.

Buyanov, A., Gofman, I., Revel'skaya, L., Khripunov, A., Tkachenko, A., 2010. Anisotropic swelling and mechanical behavior of composite bacterial cellulose–poly (acrylamide or acrylamide–sodium acrylate) hydrogels. Journal of the Mechanical Behavior of Biomedical Materials 3 (1), 102–111.

Carletti, E., Motta, A., Migliaresi, C., 2011. Scaffolds for tissue engineering and 3D cell culture. 3D Cell Culture: Methods in molecular and Protocols 695, 17–39.

Chen, H., Fan, M., 2008. Novel thermally sensitive pH-dependent chitosan/carboxymethyl cellulose hydrogels. Journal of Bioactive and Compatible Polymers 23 (1), 38–48.

Chen, J., Su, C., 2011. Surface modification of electrospun PLLA nanofibers by plasma treatment and cationized gelatin immobilization for cartilage tissue engineering. Acta Biomaterialia 7 (1), 234–243.

Chung, C., Burdick, J.A., 2008. Engineering cartilage tissue. Advanced Drug Delivery Reviews 60 (2), 243–262.

Correia, C.R., Moreira-Teixeira, L.S., Moroni, L., Reis, R.L., van Blitterswijk, C.A., Karperien, M., Mano, J.F., 2011. Chitosan scaffolds containing hyaluronic acid for cartilage tissue engineering. Tissue Engineering Part C-Methods 17 (7), 717–730.

Czaja, W.K., Young, D.J., Kawecki, M., Brown, R.M., 2007. The future prospects of microbial cellulose in biomedical applications. Biomacromolecules 8 (1), 1–12.

De Freitas, D.G., Osthues, R.M., da Silva, S.N., 2012. Study of the cytotoxicity of a composite of carboxymethylcellulose (CMC) and a BioCeramic (Biphasic calcium phosphate-BCP) injection for use in articular cartilage repair. Key Engineering Materials 493, 703–708.

Dutta, P.K., Rinki, K., Dutta, J., 2011. Chitosan: a promising biomaterial for tissue engineering scaffolds. Chitosan for Biomaterials II 244, 45–79.

Fatimi, A., Axelos, M.A., Tassin, J.F., Weiss, P., 2008. Rheological characterization of self–hardening hydrogel for tissue engineering applications: gel point determination and viscoelastic properties. Macromolecular Symposia 12 Wiley Online Library.

Favi, P.M., Benson, R.S., Neilsen, N.R., Hammonds, R.L., Bates, C.C., Stephens, C.P., Dhar, M.S., 2013. Cell proliferation, viability, and *in vitro* differentiation of equine mesenchymal stem cells seeded on bacterial cellulose hydrogel scaffolds. Materials Science and Engineering: C 33 (4), 1935–1944.

García-Carvajal, Z.Y., Garciadiego-Cázares, D., Parra-Cid, C., Aguilar-Gaytán, R., Velasquillo, C., Ibarra, C., Carmona, J.S.C., 2013. Cartilage Tissue Engineering: The Role of Extracellular Matrix (ECM) and Novel Strategies. , pp. 365–397.

Gellynck, K., Verdonk, P.C., Van Nimmen, E., Almqvist, K.F., Gheysens, T., Schoukens, G., Van Langenhove, L., Kiekens, P., Mertens, J., Verbruggen, G., 2008. Silkworm and spider silk scaffolds for chondrocyte support. Journal of Materials Science: Materials in Medicine 19 (11), 3399–3409.

Helenius, G., Bäckdahl, H., Bodin, A., Nannmark, U., Gatenholm, P., Risberg, B., 2006. In vivo biocompatibility of bacterial cellulose. Journal of Biomedical Materials Research Part A 76 (2), 431–438.

Hendrickson, D.A., Nixon, A.J., Grande, D.A., Todhunter, R.J., Minor, R.M., Erb, H., Lust, G., 1994. Chondrocyte–fibrin matrix transplants for resurfacing extensive articular cartilage defects. Journal of Orthopaedic Research 12 (4), 485–497.

Hobzova, R., Duskova–Smrckova, M., Michalek, J., Karpushkin, E., Gatenholm, P., 2012. Methacrylate hydrogels reinforced with bacterial cellulose. Polymer International 61 (7), 1193–1201.

Hoemann, C., Chenite, A., Sun, J., Hurtig, M., Serreqi, A., Lu, Z., Rossomacha, E., Buschmann, M., 2007. Cytocompatible gel formation of chitosan–glycerol phosphate solutions supplemented with hydroxyl ethyl cellulose is due to the presence of glyoxal. Journal of Biomedical Materials Research Part A 83 (2), 521–529.

Hoemann, C.D., Sun, J., Chrzanowski, V., Buschmann, M.D., 2002. A multivalent assay to detect glycosaminoglycan, protein, collagen, RNA, and DNA content in milligram samples of cartilage or hydrogel-based repair cartilage. Analytical Biochemistry 300 (1), 1–10.

Hoemann, C., Sun, J., Legare, A., McKee, M., Buschmann, M., 2005. Tissue engineering of cartilage using an injectable and adhesive chitosan-based cell-delivery vehicle. Osteoarthritis and Cartilage 13 (4), 318–329.

Hofmann, S., Knecht, S., Langer, R., Kaplan, D.L., Vunjak-Novakovic, G., Merkle, H.P., Meinel, L., 2006. Cartilage-like tissue engineering using silk scaffolds and mesenchymal stem cells. Tissue Engineering 12 (10), 2729–2738.

Hootman, J.M., Helmick, C.G., 2006. Projections of US prevalence of arthritis and associated activity limitations. Arthritis and Rheumatism 54 (1), 226–229.

Jadin, K.D., Bae, W.C., Schumacher, B.L., Sah, R.L., 2007. Three-dimensional (3-D) imaging of chondrocytes in articular cartilage: growth-associated changes in cell organization. Biomaterials 28 (2), 230–239.

Karaaslan, M.A., Tshabalala, M.A., Yelle, D.J., Buschle-Diller, G., 2011. Nanoreinforced biocompatible hydrogels from wood hemicelluloses and cellulose whiskers. Carbohydrate Polymers 86 (1), 192–201.

Kim, J., Cai, Z., Chen, Y., 2010. Biocompatible bacterial cellulose composites for biomedical application. Journal of Nanotechnology in Engineering and Medicine 1 (1) 011006.

Klemm, D., Kramer, F., Moritz, S., Lindström, T., Ankerfors, M., Gray, D., Dorris, A., 2011. Nanocelluloses: a new family of nature–based materials. Angewandte Chemie International Edition 50 (24), 5438–5466.

Ko, I.K., Iwata, H., 2001. An approach to constructing three–dimensional tissue. Annals of the New York Academy of Sciences 944 (1), 443–455.

Leone, G., Delfini, M., Di Cocco, M.E., Borioni, A., Barbucci, R., 2008a. The applicability of an amidated polysaccharide hydrogel as a cartilage substitute: structural and rheological characterization. Carbohydrate Research 343 (2), 317–327.

Leone, G., Fini, M., Torricelli, P., Giardino, R., Barbucci, R., 2008b. An amidated carboxymethylcellulose hydrogel for cartilage regeneration. Journal of Materials Science: Materials in Medicine 19 (8), 2873–2880.

Li, J., Wan, Y., Li, L., Liang, H., Wang, J., 2009. Preparation and characterization of 2, 3-dialdehyde bacterial cellulose for potential biodegradable tissue engineering scaffolds. Materials Science and Engineering: C 29 (5), 1635–1642.

Lopes, J., Machado, J., Castanheira, L., Granja, P., Gama, F., Dourado, F., Gomes, J., 2011. Friction and wear behaviour of bacterial cellulose against articular cartilage. Wear 271 (9), 2328–2333.

Malcolm, B., 2013. Microbial Cellulose: A New Resource for Wood, Paper, Textiles, Food and Specialty Products. http://www.botany.utexas.edu/facstaff/facpages/mbrown/position1.htm May, 2013.

Marsano, A., Millward-Sadler, S.J., Salter, D.M., Adesida, A., Hardingham, T., Tognana, E., Kon, E., Chiari-Grisar, C., Nehrer, S., Jakob, M., Martin, I., 2007. Differential cartilaginous tissue formation by human synovial membrane, fat pad, meniscus cells and articular chondrocytes. Osteoarthritis and Cartilage 15 (1), 48–58.

Matsiko, A., Levingstone, T.J., O'Brien, F.J., Gleeson, J.P., 2012. Addition of hyaluronic acid improves cellular infiltration and promotes early-stage chondrogenesis in a collagen-based scaffold for cartilage tissue engineering. Journal of the Mechanical Behavior of Biomedical Materials 11, 41–52.

Mauck, R.L., Burdick, J.A., 2011. Engineering cartilage tissue. In: Tissue Engineering. Springer, pp. 493–520.

Merceron, C., Portron, S., Masson, M., Fellah, B., Gauthier, O., Lesoeur, J., Cherel, Y., Weiss, P., Guicheux, J., Vinatier, C., 2010. Cartilage tissue engineering: from hydrogel to mesenchymal stem cells. Bio-Medical Materials and Engineering 20 (3), 159–166.

Millon, L.E., Oates, C.J., Wan, W., 2009. Compression properties of polyvinyl alcohol–bacterial cellulose nanocomposite. Journal of Biomedical Materials Research Part B: Applied Biomaterials 90 (2), 922–929.

Montembault, A., Tahiri, K., Korwin-Zmijowska, C., Chevalier, X., Corvol, M.T., Domard, A., 2006. A material decoy of biological media based on chitosan physical hydrogels: application to cartilage tissue engineering. Biochimie 88 (5), 551–564.

Muller, F.A., Muller, L., Hofmann, I., Greil, P., Wenzel, M.M., Staudenmaier, R., 2006. Cellulose-based scaffold materials for cartilage tissue engineering. Biomaterials 27 (21), 3955–3963.

Munirah, S., Kim, S., Ruszymah, B., Khang, G., 2008. The use of fibrin and poly (lactic-co-glycolic acid) hybrid scaffold for articular cartilage tissue engineering: an in vivo analysis. European Cells & Materials 15 (41), e52.

Murugan, R., Ramakrishna, S., 2007. Design strategies of tissue engineering scaffolds with controlled fiber orientation. Tissue Engineering 13 (8), 1845–1866.

Nasri-Nasrabadi, B., Mehrasa, M., Rafienia, M., Bonakdar, S., Behzad, T., Gavanji, S., 2014. Porous starch/cellulose nanofibers composite prepared by salt leaching technique for tissue engineering. Carbohydrate Polymers 108, 232–238.

Newman, A.P., 1998. Articular cartilage repair. The American Journal of Sports Medicine 26, 309–324.

Nge, T.T., Nogi, M., Yano, H., Sugiyama, J., 2010. Microstructure and mechanical properties of bacterial cellulose/chitosan porous scaffold. Cellulose 17 (2), 349–363.

O'Brien, F.J., 2011. Biomaterials & scaffolds for tissue engineering. Materials Today 14 (3), 88–95.

Petersen, B., Barkun, A., Carpenter, S., Chotiprasidhi, P., Chuttani, R., Silverman, W., Hussain, N., Liu, J., Taitelbaum, G., Ginsberg, G.G., 2004. Tissue adhesives and fibrin glues: NOVEMBER 2003. Gastrointestinal Endoscopy 60 (3), 327–333.

Petersen, N., Gatenholm, P., 2011. Bacterial cellulose-based materials and medical devices: current state and perspectives. Applied Microbiology and Biotechnology 91 (5), 1277–1286.

Portron, S., Merceron, C., Gauthier, O., Lesoeur, J., Sourice, S., Masson, M., Fellah, B.H., Geffroy, O., Lallemand, E., Weiss, P., 2013. Effects of in vitro low oxygen tension preconditioning of adipose stromal cells on their in vivo chondrogenic potential: application in cartilage tissue repair. PloS One 8 (4), e62368.

Pretzel, D., Linss, S., Ahrem, H., Endres, M., Kaps, C., Klemm, D., Kinne, R.W., 2013. A novel in vitro bovine cartilage punch model for assessing the regeneration of focal cartilage defects with biocompatible bacterial nanocellulose. Arthritis Research & Therapy 15 (3), R59.

Pulkkinen, H., Tiitu, V., Lammentausta, E., Hamalainen, E.R., Kiviranta, I., Lammi, M.J., 2006. Cellulose sponge as a scaffold for cartilage tissue engineering. Bio-Medical Materials and Engineering 16 (4), S29–S35.

Rederstorff, E., Weiss, P., Sourice, S., Pilet, P., Xie, F., Sinquin, C., Colliec-Jouault, S., Guicheux, J., Laïb, S., 2011. An in vitro study of two GAG-like marine polysaccharides incorporated into injectable hydrogels for bone and cartilage tissue engineering. Acta Biomaterialia 7 (5), 2119–2130.

Redman, S.N., Oldfield, S.F., Archer, C.W., 2005. Current strategies for articular cartilage repair. European Cells & Materials 9, 23.

Ren, Y., Zhou, Z., Liu, B., Xu, Q., Cui, F., 2009. Preparation and characterization of fibroin/hyaluronic acid composite scaffold. International Journal of Biological Macromolecules 44 (4), 372–378.

Sanabria-DeLong, N., Crosby, A.J., Tew, G.N., 2008. Photo-cross-linked PLA-PEO-PLA hydrogels from self-assembled physical networks: mechanical properties and influence of assumed constitutive relationships. Biomacromolecules 9 (10), 2784–2791.

Sannino, A., Demitri, C., Madaghiele, M., 2009. Biodegradable cellulose-based hydrogels: design and applications. Materials 2 (2), 353–373.

Sá-Lima, H., Tuzlakoglu, K., Mano, J.F., Reis, R.L., 2011. Thermoresponsive poly (N–isopropylacrylamide)–g–methylcellulose hydrogel as a three–dimensional extracellular matrix for cartilage–engineered applications. Journal of Biomedical Materials Research Part A 98 (4), 596–603.

Schmidt, T.A., Gastelum, N.S., Nguyen, Q.T., Schumacher, B.L., Sah, R.L., 2007. Boundary lubrication of articular cartilage: role of synovial fluid constituents. Arthritis & Rheumatism 56 (3), 882–891.

Spiller, K.L., Maher, S.A., Lowman, A.M., 2011. Hydrogels for the repair of articular cartilage defects. Tissue Engineering Part B: Reviews 17 (4), 281–299.

Steward, A.J., Liu, Y., Wagner, D.R., 2011. Engineering cell attachments to scaffolds in cartilage tissue engineering. JOM 63 (4), 74–82.

Svensson, A., Nicklasson, E., Harrah, T., Panilaitis, B., Kaplan, D.L., Brittberg, M., Gatenholm, P., 2005. Bacterial cellulose as a potential scaffold for tissue engineering of cartilage. Biomaterials 26 (4), 419–431.

Torres, F.G., Commeaux, S., Troncoso, O.P., 2012. Biocompatibility of bacterial cellulose based biomaterials. Journal of Functional Biomaterials 3 (4), 864–878.

Vinatier, C., Gauthier, O., Fatimi, A., Merceron, C., Masson, M., Moreau, A., Moreau, F., Fellah, B., Weiss, P., Guicheux, J., 2009. An injectable cellulose–based hydrogel for the transfer of autologous nasal chondrocytes in articular cartilage defects. Biotechnology and Bioengineering 102 (4), 1259–1267.

Vinatier, C., Magne, D., Moreau, A., Gauthier, O., Malard, O., Vignes–Colombeix, C., Daculsi, G., Weiss, P., Guicheux, J., 2007. Engineering cartilage with human nasal chondrocytes and a silanized hydroxypropyl methylcellulose hydrogel. Journal of Biomedical Materials Research Part A 80 (1), 66–74.

Vinatier, C., Magne, D., Weiss, P., Trojani, C., Rochet, N., Carle, G.F., Vignes-Colombeix, C., Chadjichristos, C., Galera, P., Daculsi, G., 2005. A silanized hydroxypropyl methylcellulose hydrogel for the three-dimensional culture of chondrocytes. Biomaterials 26 (33), 6643–6651.

Wang, Y., Chen, L., 2011. Impacts of nanowhisker on formation kinetics and properties of all-cellulose composite gels. Carbohydrate Polymers 83 (4), 1937–1946.

Weiss, P., Fatimi, A., Guicheux, J., Vinatier, C., 2010. Hydrogels for cartilage tissue engineering. Biomedical Applications of Hydrogels Handbook, vol. 3, pp. 247–268.

Williamson, A.K., Chen, A.C., Masuda, K., Thonar, E.J., Sah, R.L., 2003. Tensile mechanical properties of bovine articular cartilage: variations with growth and relationships to collagen network components. Journal of Orthopaedic Research 21 (5), 872–880.

Xing, Q., Zhao, F., Chen, S., McNamara, J., DeCoster, M.A., Lvov, Y.M., 2010. Porous biocompatible three-dimensional scaffolds of cellulose microfiber/gelatin composites for cell culture. Acta Biomaterialia 6 (6), 2132–2139.

Yadav, V., Panilaitis, B., Shi, H., Numuta, K., Lee, K., Kaplan, D.L., 2011. N-acetylglucosamine 6-phosphate deacetylase (nagA) is required for N-acetyl glucosamine assimilation in *Gluconacetobacter xylinus*. PloS One 6 (6), e18099.

Yadav, V., Paniliatis, B.J., Shi, H., Lee, K., Cebe, P., Kaplan, D.L., 2010. Novel in vivo-degradable cellulose-chitin copolymer from metabolically engineered *Gluconacetobacter xylinus*. Applied and Environmental Microbiology 76 (18), 6257–6265.

Yadav, V., Sun, L., Panilaitis, B., Kaplan, D.L., 2013. In vitro chondrogenesis with lysozyme susceptible bacterial cellulose as a scaffold. Journal of Tissue Engineering and Regenerative Medicine 9 (12), 276–288.

Yamanaka, S., Sugiyama, J., 2000. Structural modification of bacterial cellulose. Cellulose 7 (3), 213–225.

Yang, C., Gao, C., Wan, Y., Tang, T., Zhang, S., Dai, K., 2011. Preparation and characterization of three-dimensional nanostructured macroporous bacterial cellulose/agarose scaffold for tissue engineering. Journal of Porous Materials 18 (5), 545–552.

Yan, L., Wang, Y., Ren, L., Wu, G., Caridade, S.G., Fan, J., Wang, L., Ji, P., Oliveira, J.M., Oliveira, J.T., Mano, J.F., Reis, R.L., 2010. Genipin-cross-linked collagen/chitosan biomimetic scaffolds for articular cartilage tissue engineering applications. Journal of Biomedical Materials Research Part A 95A (2), 465–475.

Yasuda, K., Ping Gong, J., Katsuyama, Y., Nakayama, A., Tanabe, Y., Kondo, E., Ueno, M., Osada, Y., 2005. Biomechanical properties of high-toughness double network hydrogels. Biomaterials 26 (21), 4468–4475.

Yelin, E., Cisternas, M., Foreman, A., Pasta, D., Murphy, L., Helmick, C.G., 2007. National and state medical expenditures and lost earnings attributable to arthritis and other rheumatic conditions - United States, 2003 (Reprinted from MMWR, vol. 56, pg 4–7, 2007) Jama-Journal of the American Medical Association 297 (15), 1649–1650.

Zhao, H., Ma, L., Gong, Y., Gao, C., Shen, J., 2009. A polylactide/fibrin gel composite scaffold for cartilage tissue engineering: fabrication and an in vitro evaluation. Journal of Materials Science: Materials in Medicine 20 (1), 135–143.

Zhijiang, C., Chengwei, H., Guang, Y., 2012. Preparation and characterization of a bacterial cellulose/chitosan composite for potential biomedical application (vol. 121, pg 1488, 2011) Journal of Applied Polymer Science 126 (6), 2078.

Electrospun scaffolds for cartilage regeneration

10

C.B. Horner, K. Low, J. Nam
University of California-Riverside, Riverside, CA, United States

10.1 Introduction

10.1.1 Cartilage regeneration

Cartilage is an avascular and aneural tissue with minimal intrinsic repair capabilities (Buckwalter and Mankin, 1997). Even the slightest damage to the tissue due to disease or injury results in an unrecoverable decline in tissue health and functionality. The societal costs associated with cartilage degeneration total approximately $128 billion, and are attributed to clinical treatments, lost productivity in the workplace, and decline in the quality of life (Yelin et al., 2007; Birnbaum et al., 2010). Therefore, urgent action for devising engineering tools to restore the functionality of cartilage is necessary for our increasingly aging population.

Cartilage degeneration commonly occurs in high load-bearing joints of the body such as the knee or hip. A significant attribute for any type of tissue regeneration requires the presence of blood vessels for progenitor cell migration (ie, stem-cell homing), proper nutrient transport and waste removal. Therefore, the lack of vasculature in cartilage will impede the native ability for self-regeneration of the tissue due to the limited cell source and metabolic processes within the innate tissue. Additionally, without the presence of nerves, the gradual degeneration of cartilage is typically unnoticed until the tissue is severely damaged and patients experience pain due to friction between the bones of their joints (Wang et al., 2006). This ultimately leads to the formation of bone spurs that replace injured cartilage, which further progresses the degeneration of the cartilage tissue.

Due to the limited self-healing capability of cartilage, current treatments require invasive procedures to restore physiological functions. There are only a few clinical techniques for cartilage treatment, other than the use of prostheses, which include autologous chondrocyte implantation (ACI) and microfracture of the subchondral bone (Smith et al., 2005). Limitations of the use of ACI, which harvests chondrocytes from the patient, expand and implant them directly into cartilage defects, include the complexity of the surgical procedure, leakage of transplanted chondrocytes from the defect site, uneven distribution of the mature cells, periosteal hypertrophy, limited availability of autologous chondrocytes, as well as dedifferentiation of the primary chondrocytes in monolayer culture. When considering the treatment of damaged or diseased cartilage via microfracture procedure to initiate mobilization of mesenchymal stems cells from subchondral bone for localized repair of the damaged tissue, the formation of undesired fibrocartilage becomes a clinical concern (Iwasa et al., 2009).

Nanocomposites for Musculoskeletal Tissue Regeneration. http://dx.doi.org/10.1016/B978-1-78242-452-9.00010-8

In contrast, tissue-engineering approaches provide an opportunity to precisely place proper cells into the defect site in a controlled cellular microenvironment to maintain/enhance chondrocyte phenotype and increase cell-delivery efficiency for facilitated tissue regeneration.

To repair or replace the damaged cartilage with tissue-engineering approaches, it is important to consider the local structure of the cartilage for appropriate biomechanical functions (Wilson et al., 2006). The solution of this complex problem should be based upon a combinatory effort of proper material selection, adequate cell sourcing, and incorporation of biochemical/biophysical cues (Vinatier et al., 2009).

10.1.2 Structure–function relationship of cartilage

The body is composed of three primary types of cartilage: elastic, fibro-, and hyaline cartilage. Each serves specific functions within the musculoskeletal system. Elastic cartilage is a structural cartilaginous tissue for non-load-bearing body parts, such as ears, nose, and epiglottis (Hutmacher et al., 2003). It typically does not experience high mechanical loads for prolonged periods of time. Therefore, the damage of this tissue is not common or chronic, as compared to other types of cartilage found in the body. On the other hand, fibrocartilage acts as a mechanical supporting tissue in the intervertebral discs of the spine, the temporomandibular joint (TMJ) of the jaw, and the meniscus of the knee (Palmer and Werner, 1981). This type of cartilage contains a combination of both fibrous and cartilaginous tissue to serve as a tough, yet flexible supporting tissue for the musculoskeletal system. The directional woven structure of collagen type I, as well as the more common collagen type II typically found in hyaline cartilage, provides the greatest mechanical strength among different cartilages (Eyre and Wu, 1983). Although the regeneration of elastic and fibrocartilage is also of interest for medicine, this chapter will primarily focus on the most easily injured, thus the most widely studied type of cartilage, hyaline cartilage.

Hyaline cartilage is located along the surface of the ends of long bones in the joints and within the rib cage and the trachea, providing low-friction surfaces throughout the body (Poole et al., 2001). This particular musculoskeletal tissue is highly susceptible to damage from injury or degenerative diseases due to its exposure to severe mechanical loadings. Although there have been a large number of reported successes for experimental in vitro neocartilage production, there have been little to no reports for long-term clinical efficacy of the implanted engineered tissues (Francis Suh and Matthew, 2000; Mauck et al., 2006; Eyrich et al., 2007).

The articular cartilage (AC), composed of hyaline cartilage tissue, plays an important role for joint functions; AC acts as a shock absorber, alleviates the friction between bones within joints, and maintains a biochemical homeostasis with the subchondral bone (Sophia Fox et al., 2009). The composition and structure of hyaline cartilage are closely related to the tissue functions. Although this tissue is avascular and aneural, the high glycosaminoglycan (GAG), collagen and water contents within the tissue act as an essential microenvironment for chondrocyte homeostasis and provide the necessary mechanical integrity for articulation of the limbs.

Due to its role in the body's daily movements, AC is highly susceptible to damage or disease by physiological wear and tear, and traumatic injuries. With the end goal of repairing or regenerating cartilage through various tissue-engineering strategies, the biochemical and biomechanical requirements of the native tissue must be taken into account for long-term success. Therefore, a thorough understanding of the structure–function relationship of native articular cartilage with a comprehensive analysis of the physiochemical parameters is a prerequisite for engineering cartilage.

10.1.3 Physiochemical requirements of engineered cartilage

To engineer functional AC, the physiological requirements should closely mimic the characteristics of the native tissue in both biochemical composition and mechanical integrity. The native structure of AC comprises three primary zones including the superficial, middle and deep zones (Fig. 10.1). Each of the zones independently, yet cohesively, contribute specific functions of cartilage such as lubrication and compressive resistance, due to the organization and composition of the extracellular matrix (ECM) accompanied by cells.

The superficial zone of AC contains the largest cell population while only being roughly 10–20% by volume. The tissue primarily acts as the area for friction reduction in the tissue (Pearle et al., 2005). In this zone, the chondrocytes have a flat morphology and run parallel to the surface of the joint along with the collagen fibers. In addition to these structural characteristics, the chondrocytes in this zone secrete lubricin, a lubricant protein, reducing friction experienced from joint movement (Buckwalter and Mankin, 1997).

The middle zone acts as the primary shock absorbing layer in AC. In this portion of cartilage, mature chondrocytes are round in morphology and are sparsely dispersed through a proteoglycan-rich ECM consisting of approximately 40–60% of AC by

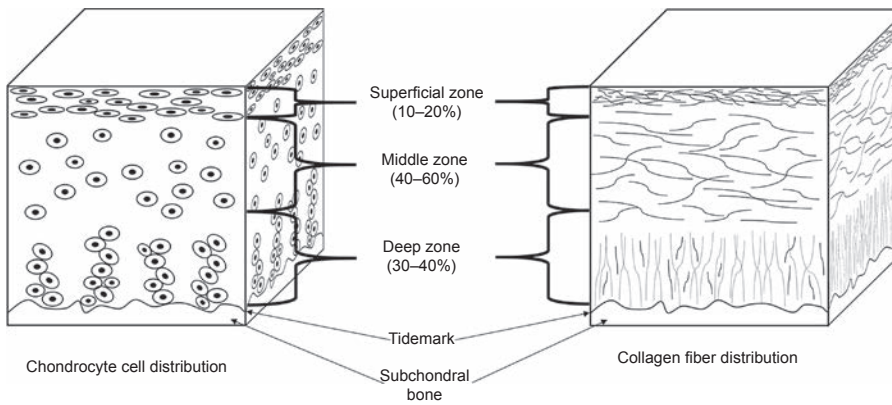

Figure 10.1 Cross-sectional schematic of articular cartilage. The tissue consists of the superficial, middle/transitional, and deep zones with a distinct tidemark of calcified cartilage and the underlying subchondral bone (from top to bottom). Both cellular organization and collagen-fiber orientation are shown with respect to the zonal structure of cartilage.

volume. The cells are perpendicularly aligned to the joint surface along with collagen fibers, which provides the structural integrity of AC. Additionally, although aggrecan is prominent throughout the tissue, the middle zone contains the highest content of this proteoglycan by volume, which helps contribute to the intrinsic compressive strength of AC (Bhosale and Richardson, 2008).

The closest zone to the underlying subchondral bone is the deep zone, which makes up about 30–40% of AC by volume. Located at the interface of cartilage and bone, this transitional zone possesses the characteristic feature known as the tidemark. The tidemark is the boundary of the calcification of the tissue and allows for proper integration between AC and the underlying subchondral bone. Beyond the definitive tidemark, while still contributing to ECM production, chondrocytes begin to show signs of hypertrophy. There is a gradual increase in mineral content in the transition from interfacial cartilage to bone. This transitional calcified cartilage zone is important for proper neocartilage tissue integration because of its close proximity to vasculature in subchondral bone (Bhosale and Richardson, 2008). The calcified cartilage also mediates the mechanical stresses and biological stimuli between the interfacial tissues, in addition to providing interstitial fluid transport to the cartilage above (Oegema et al., 1997).

Chondrocytes, the only cell type found in cartilage, are responsible for producing and maintaining the ECM in AC, and the subsequent resulting anisotropic biomechanics in the mature tissue. Considering the fact that chondrocytes compose only 1–5% of the total volume and that they require an extensive duration for the maturation of cell-secreted ECM, designing a scaffold with zonal structure is a key component to provide proper initial microenvironmental cues for the facilitated regeneration of cartilage tissue (Sharma et al., 2007; Bhosale and Richardson, 2008). In this regard, electrospinning has shown to be an attractive method for cartilage tissue engineering due to its ability to tailor both the structure and function of the scaffolds with high porosity.

This chapter will discuss electrospinning as a promising fabrication technique for scaffolding, current applications of electrospun scaffolds for cartilage tissue engineering, as well as limitations with the use of such scaffolds for translational applications.

10.2 Synthesis of electrospun scaffolds

Electrospinning is a simple, yet powerful method for synthesizing highly porous nano- and microfibrous scaffolds for cartilage tissue engineering. This easily tunable process for synthesizing scaffolds with tightly regulated microstructures is ideal for controlling cell–scaffold interactions and subsequent tissue development. In comparison to scaffolds fabricated by other techniques, such as hydrogel-based materials (Kim et al., 2011), porogen leaching of polymeric materials (Ma et al., 2003) or three-dimensional (3D) printing (Reiffel et al., 2013), electrospun scaffolds provide several mechanical and biochemical advantages, which will be further discussed in this section.

10.2.1 Electrospinning overview

Electrospinning is a versatile technique with a variety of finely tunable parameters to achieve desired material, chemical, and mechanical properties of a nonwoven nano- or microfibrous mesh (Fig. 10.2). This common term has been developed from the early description "electrostatic spinning," and has been widely studied and used in both academic and industrial settings (Park, 2010). Electrospinning provides a means for synthesizing a network of elongated one-dimensional nanostructures, which mimics the native nanoscale ECM present in AC.

Electrospinning requires a polymer to be soluble in a solvent at specific ranges of viscosity, conductivity, vapor pressure, and other solution properties. The solution is fed to a spinneret, a small orifice to generate a droplet at the tip, at a known flow rate. A high voltage is applied to the solution droplet to form what is known as the Taylor cone. In the Taylor cone, the charges which are carried throughout the solution mixture begin to separate. This charge separation elongates and ejects the polymer solution in the stable jet region of the Taylor cone to the direction of the electric field. As the ejected polymer jet begins to dry within the distance of travel from the spinneret to the collection substrate, the current flow changes from ohmic to convection as the charges begin to move toward the outer surface of the fiber. Beyond a critical point at which the energy of these charges overcomes the surface tension of the mixture, the solution experiences an electrostatic repulsion from one another causing a whipping instability, known as 'spinning,' to occur. This instability of the ejected polymer solution results in the rapid evaporation of the solvent creating nano- and microfibers. Finally, these fibers are then collected on a grounded substrate of desired geometry, producing vertically deposited nonwoven fiber mats.

One of the greatest advantages of electrospinning is its processing capacity of various materials to yield scaffolds with diverse chemical and mechanical properties, which can invoke various biological responses from the cells. Natural polymers such as collagen, gelatin, fibrinogen, elastin, and fibrin have been electrospun for tissue-engineering applications (Geng et al., 2005; Matthews et al., 2003). A plethora of synthetic biodegradable polymers such as poly(lactic acid) (PLA), poly(glycolic acid)

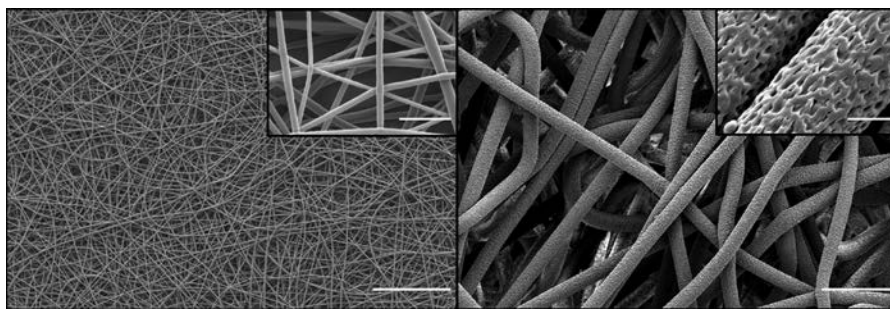

Figure 10.2 Scanning electron microscopy (SEM) images of electrospun nano- and microfibrous poly(ε-caprolactone) scaffolds demonstrating fiber dimensions of different orders of magnitude (scale bars: 5 μm for subset and 50 μm for full images).

Table 10.1 Common polymers used in electrospinning

Natural polymers	Synthetic polymers
Collagen	PGA—poly(glycolic acid)
Gelatin	PLA—poly(lactic acid)
Chitosan	PLLA—poly(L-lactic acid)
Fibrin	PLGA—poly(lactic-co-glycolic acid)
Hyaluronic acid	PCL—poly(ε-caprolactone)
	PEO—poly(ethylene oxide)
	PEG—poly(ethylene glycol)

(PGA), poly(ε-caprolactone) (PCL), and composites of the monomer units (Huang et al., 2003; Gunatillake and Adhikari, 2003; Marin et al., 2013) were also utilized for electrospinning. Table 10.1 lists commonly used polymers for electrospinning in the applications of cartilage tissue engineering. Many of these polymers have been approved by the Food and Drug Administration (FDA) for various in vivo applications, and can be selectively used to tailor the mechanical, chemical and degradation properties of electrospun scaffolds.

There are various configurations to produce electrospun scaffolds having different compositional and microstructural characteristics (eg, coelectrospinning, coaxial electrospinning, and blend electrospinning). Such diversity in electrospun fibers enables synthesis of scaffolds with tailored properties. By selectively determining materials and methodologies for electrospinning, scaffolds can be engineered to induce cell/tissue-specific responses, facilitate tissue morphogenesis, and maintain phenotypical characteristics of the tissue.

Coelectrospinning is a technique in which two or more polymeric solutions are simultaneously collected onto a single collection device (Fig. 10.3). This is an attractive method for producing fibers that are on different orders of magnitude in fiber diameters or chemical compositions contained within a monolithic scaffold (Wu et al., 2010; Francis et al., 2010; Ding et al., 2004). By modifying the collection medium or materials used for electrospinning, cellular responses can be tailored to address shortcomings of a single polymeric material.

Coaxial electrospinning, also referred to as core–shell or core–sheath electrospinning, is the process of enclosing one material around the other through the use of concentric needles (Fig. 10.4). It has been demonstrated that this procedure can incorporate materials that are unable to be processed alone, when the sheath acts as a carrier of the core solution (Bazilevsky et al., 2007). With this method, unspinnable materials can be used for tuning the intrinsic mechanical properties of the fibers, or a drug of interest can be loaded into the core material to control tissue morphogenesis (Han et al., 2008; Qu et al., 2013).

Blend electrospinning occurs when two or more miscible solutions are combined into a single feed system and fed through a common spinneret for desired final material properties (Fig. 10.5). Although this procedure is not the most common technique, the advantage of this particular method is its ability to modify the chemical

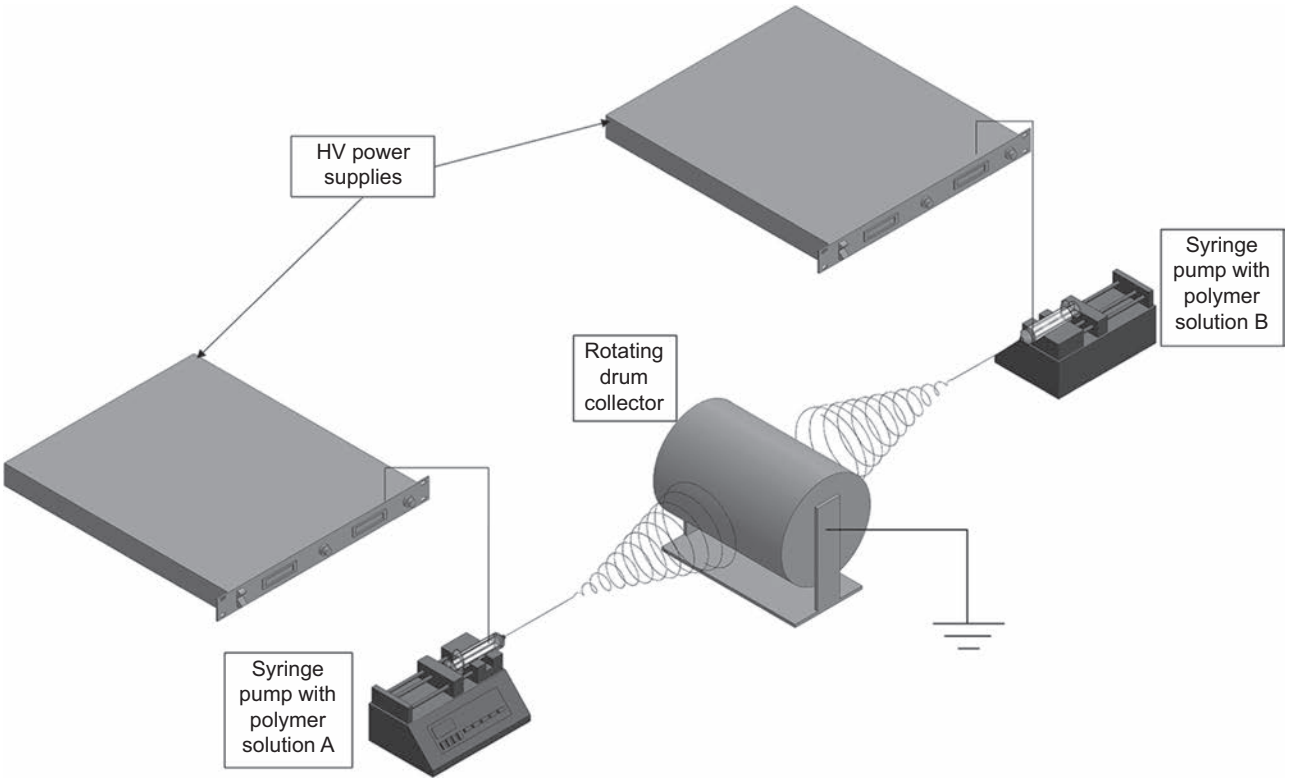

Figure 10.3 A schematic of coelectrospinning setup in which two different solutions are simultaneously electrospun and acquired on a common collector.

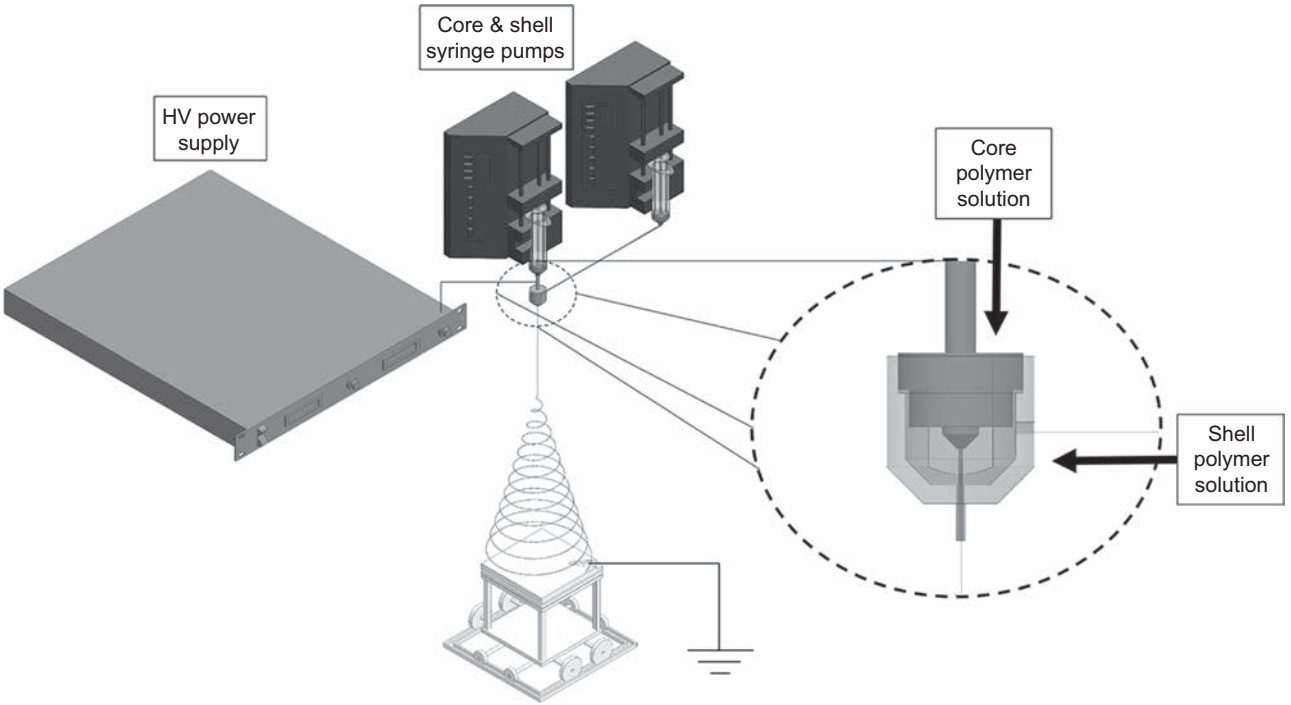

Figure 10.4 A schematic of coaxial or core–shell electrospinning setup in which one polymeric solution is fed into an inner reservoir (core), while a secondary polymer is fed to the surrounding reservoir (shell).

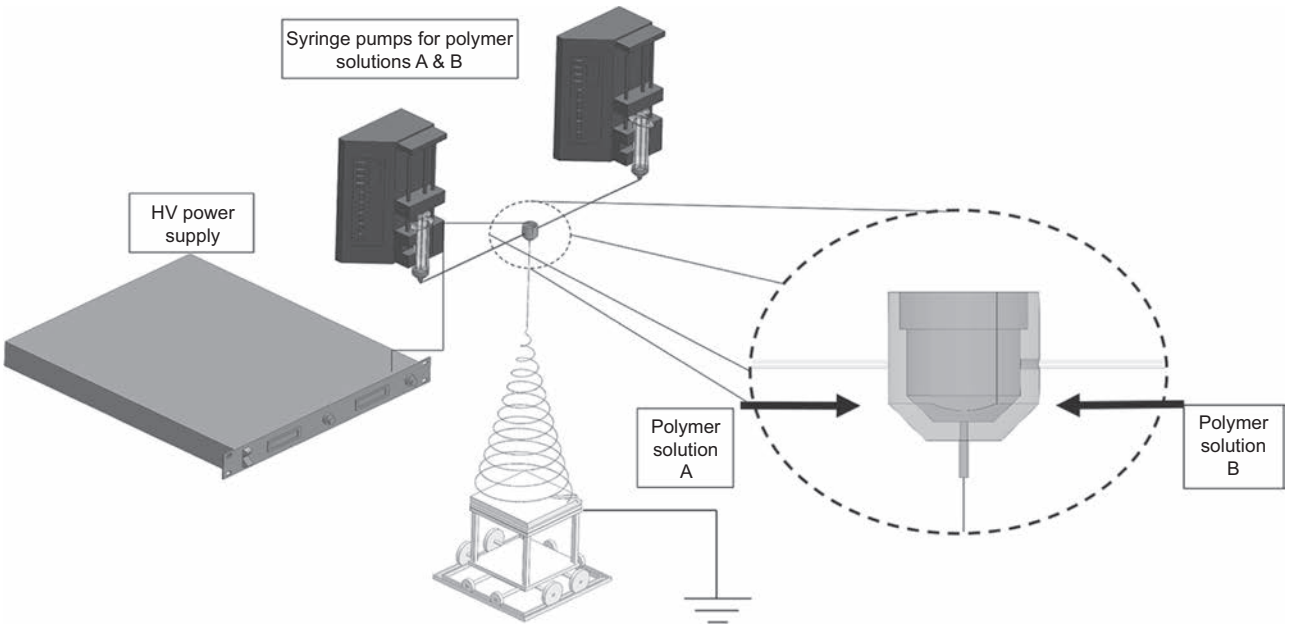

Figure 10.5 A schematic of blend electrospinning in which two different polymeric solutions are independently fed into the same reservoir, mixed together, and are emitted through a single capillary.

and mechanical properties of the scaffolds for aiding in cell proliferation, differentiation, and survivability (Bazilevsky et al., 2007; Zhang et al., 2006b; Gupta and Wilkes, 2003).

There are many variables which need to be carefully determined for successful electrospinning. The detailed description of electrospinning parameters that determine the structural and morphological characteristics of electrospun fibers, as well as spinnability, is as follows in the subsequent section.

10.2.2 Fundamental principles of electrospinning

The fundamental principles of electrospinning are dictated by three primary parameters including solution, processing, and environmental conditions (Table 10.2). Each process setting must be taken into close consideration to properly synthesize a scaffold with structural and functional characteristics similar to native cartilage.

10.2.2.1 Solution parameters: User-defined variables

The first step to determine the properties of the final end product is the selection of solution parameters, which consist of the polymer and solvent material properties, as well as those of the solution mixture. The high solubility of the polymer of interest in a particular solvent is a prerequisite for uniform electrospinning. The major scaffold characteristics such as chemical composition, mechanical integrity, degradation rate and by-products will be determined by polymeric materials. On the other hand, the solvent properties will primarily determine morphological characteristics of electrospun scaffolds such as fiber size, porosity and fiber morphology.

Table 10.2 List of parameters addressed during the electrospinning process

Parameter	Subparameters
Solution: User-defined variables	Polymer–solvent solubility
	Polymer–solvent concentration
	Polymer molecular weight
	Solution viscosity
	Solution conductivity
	Dielectric constant
Processing: Experimental variables	Polymer solution flow rate
	Electric field strength
	Working distance
	Applied voltage
	Fiber collection geometry and composition
Ambient: Environmental variables	Temperature
	Relative humidity
	Air cabin velocity

Different polymeric materials have different solubility characteristics in any given solvent. Some polymers are fully, partially, or even insoluble in different solvents, which will impact the electrospinnability of those materials. The selected solvent, or combination of solvents, also has varying intrinsic chemical, electrical, and solubility characteristics that will significantly affect the fabrication of the fibers (Luo et al., 2010). There is a critical range of polymer concentration which determines electrospinnability (Greiner and Wendorff, 2007). Below a certain threshold, there is an insufficient amount of polymer-chain entanglement to generate continuous fibers, resulting in fragmented polymer droplets called electrospraying. This critical concentration depends on a balance among the polymer chemical composition, chain length, the accompanying solvents and the solution viscosity. In contrast, an extremely high polymer concentration results in overly large polymer-chain entanglements, and entrapped solvent prevents the fibers from sufficiently drying before being collected. This results in wet fibers binding to one another, creating a thin film rather than porous fibrous membranes (Pillay et al., 2013). Similarly, when the polymer molecular weight increases, large, smooth, continuous fibers are formed, whereas a low molecular-weight polymer is insufficient in forming fibers due to low polymer-chain entanglement (Xu et al., 2007).

Another solution parameter for electrospinning is the conductivity of the fluid. The polymer solution conductivity (ie, charge density) assists in the jet formation from the Taylor cone and resulting whipping instability of the electrospun fibers. As the conductivity increases, the distribution of the charge density overcomes the tangential electric field along the surface of the solution droplet (Angammana and Jayaram, 2011). Therefore, higher solution conductivities will result in smaller fiber diameters, whereas lower values generate larger electrospun-fiber diameters. When the polymer solution conductivity is too low, surface charging is insufficient to form a Taylor cone failing the electrospinning process. In contrast, when the solution conductivity is too high the reduced tangential electric field also resists the formation of the Taylor cone (Angammana and Jayaram, 2011). The addition of ionic salts such as KH_2PO_4 and NaCl in the solution can increase the ion contents, which enhances the surface-charge density of the solution, and improves the electrospinnability of the insulating solution (Fong et al., 1999).

Finally, the dielectric properties of the solvent used in electrospinning polymers also affect the electrospinnability of the polymer solution in conjunction with the conductivity. The dielectric constant of a solvent represents the amount of “free” charge that can be induced into the polymer solution during electrospinning (Sun et al., 2012). Polymer–solvent solutions consisting of low dielectric constants limit the initiation of the whipping instability and thinning of the polymer jet. By reducing the available charge on the surface of the polymer jet, the electrostatic repulsive force which initiates the whipping instability of the fiber is also decreased. This results in an extended duration for the charge density to migrate to the surface of the fluid, ultimately leading to the formation of larger electrospun fiber diameters or loss of electrospinnability. This suggests that there is a critical window of “free” charge available to initiate the whipping instability that induces spinning of any polymer–solvent systems.

10.2.2.2 Process parameters: Experimental variables

Process parameters are defined as experimental variables to control the electrospinning process. These parameters include the polymer-solution flow rate, the working distance from the tip of the spinneret to the collection target, the type of grounded collection target, as well as the applied voltage at the spinneret.

The polymer solution flow rate has been shown to influence the overall fiber diameters. Although low flow rates typically result in smaller fiber diameters and vice versa for higher flow rates, there is a range of optimal flow rates for any given polymer–solvent combination (Zargham et al., 2012; Ganan-Calvo et al., 2013). If the flow rate is too low for a given solution, an overcharging of the solution may occur, resulting in electrospraying to deposit particles on the collector. If the solution flow rate is too high, the applied electric field cannot generate a whipping instability within the polymer jet, preventing "spinning" of the polymer solution. In addition, the solvent contained within the solution will not evaporate rapidly enough to form fibers.

The working distance between the spinneret tip and the collection substrate dictates the resulting fiber morphology. By changing the working distance, the applied electric field between the tip and collector is also altered, impacting the formation of the fibrous membranes. As the distance increases, the fibers are continually stretched and thinned within the whipping region, resulting in smaller fiber diameters (Milleret et al., 2011). However, a critical voltage threshold can be applied to the spinneret that is proportional to the increased working distance without causing instability in the Taylor cone formation. The applied voltage that creates an electric field between the spinneret and the collector is the key driving factor for electrospinning, determining the electrospun-fiber diameter (Sener et al., 2011; Liu et al., 2011). High applied-voltage levels increase the surface-charge density of the polymer solution resulting in greater repulsion of the fibers, which in turn increases the whipping instability and thinning of the jet formation, thus ultimately generating fibers on a smaller dimensional scale.

Finally, the collection target has significant effects on the macrostructure of the synthesized scaffolds (Kumar, 2012). Although the most common collection substrate is a grounded static metallic collection plate, a wide variety of collectors including grounded solution baths (Pant et al., 2011), rotating mandrels (Errico et al., 2011), and patterned devices (Neves et al., 2007) have been used. Each of these result in patterns or macro-structures allowing for tailored cellular responses in migration, proliferation, and differentiation of the cells. The macrostructure of electrospun scaffolds is especially important for cellular migration including angiogenesis, thus determining engineered tissue integration to native tissues (Santos et al., 2008; Telemeco et al., 2005).

10.2.2.3 Ambient parameters: Environmental variables

Although the ambient parameters have a distinct impact on electrospun fibers, these systemic parameters present challenges for dynamic control. Furthermore, the effects of these environmental factors depend on polymer–solution combinations (ie, sensitivity to temperature, hygroscopic nature of solution and optimum vapor pressure)

and simultaneously influence solution properties (ie, viscosity and evaporation rate). Therefore, it is difficult to make direct correlations between final scaffold production and these variables.

The temperature during electrospinning has been shown to influence the final fiber diameters. Both the solvent evaporation rate and the intrinsic solution viscosity are affected by ambient temperature during electrospinning (Su et al., 2011). There have been two proposed mechanisms on the effects of environmental temperature on electrospinning, both of which affect fiber diameters in a biphasic manner. First, as the temperature decreases, the solvent evaporation is reduced. The prolonged solidification of the polymer induces increased fiber elongation and jet thinning, resulting in smaller fiber diameters. Second, at higher temperatures the polymer chains have greater freedom to move, resulting in lower solution viscosity, also reducing the fiber diameters (De Vrieze et al., 2009). In most cases, ambient room temperature (20–23°C) conditions are used, unless more specific conditions are required to successfully generate fibers.

Next, the relative humidity also determines the morphological characteristics of electrospun fibers. When the environmental humidity is too low, the solvent evaporation rate increases and can completely dry the solvent before proper solution elongation to form fibers. In contrast, when the humidity is too high, the solvent cannot entirely evaporate resulting in continuing elongation of the fibers resulting in small diameters. Therefore, depending on the polymer–solvent selection, there is an ideal range of relative humidity for successful continuous fiber formation (De Vrieze et al., 2009). The humidity has also been shown to impact the surface morphology of the electrospun fibers in which lower levels of humidity generate smooth fibers, whereas higher humidity levels create pores on the surface of the fibers (Casper et al., 2004). Although the exact mechanism for surface pore formation is unclear, it was proposed that the evaporation of the solvent cools the fibers during electrospinning, and ambient moisture condenses on the surface of the fiber resulting in pitting and pore formation. Similarly, the cabin air velocity also has an influence on fiber generation by affecting solvent evaporation (Doshi and Reneker, 1993). When the cabin air velocity is too low, solvent evaporation is decreased resulting in insufficient drying of the fibers.

10.3 Electrospun scaffolds for cartilage regeneration

Designing scaffolds with appropriate chemical, mechanical and biological properties is essential for inducing proper functionality and integration of engineered cartilage. Therefore, the scaffolds should strive to address the following criteria.

- Scaffold materials are biocompatible to minimize any immunogenic response of the surrounding tissues.
- Scaffolds are biodegradable at a designed degradation rate, resulting in proper integration of the engineered tissue to the native tissues while maintaining structural and mechanical integrity during maturation.
- The microstructure and composition of scaffolds provide proper microenvironments to either differentiate native progenitor cells to the necessary phenotype of the tissue or maintain the phenotype of cultured mature cells within the scaffolds.

These prerequisites ensure the development of the engineered tissue to match the mechanical and biochemical properties of the native tissue.

Electrospinning has shown to be an attractive method to produce chondroinductive scaffolds that meet the above criteria due to its ability to tailor the structural, mechanical, and chemical parameters simulating the extracellular microenvironments for cell migration, proliferation, and/or differentiation of chondrocytes or their precursor cells. Herein, a discussion of the materials used in the synthesis of electrospun scaffolds will be given, followed by the effects of such scaffolds on directing cellular behavior for cartilage regeneration.

10.3.1 Materials selection

When selecting proper polymers to be used for cartilage regeneration, it is important to consider how the chemical and mechanical properties of these materials correlate to the structure and function of articular cartilage. The appropriate materials selection is essential for controlling cellular behaviors and the impacts on the surrounding native tissues. The following will describe biocompatible materials that are most commonly used for electrospun scaffolds for cartilage regeneration.

10.3.1.1 Natural/biological materials

The use of natural or biological polymers for electrospun scaffolds is advantageous due to their biocompatible and biodegradable properties. The balance between hydrophilicity for proper cellular interaction and hydrophobicity for structural maintenance during tissue maturation is critical for cartilage regeneration. Additionally, the by-products from these biodegradable scaffolds induce little to no innate immune responses from the surrounding tissues. Although a few promising natural polymers may not have intrinsic material properties to be electrospun individually, coaxial electrospinning and/or postmodification techniques can provide an opportunity to exploit excellent biological properties of these natural polymers to elicit the desired cellular interactions.

As one of the primary components within cartilage, collagen is commonly used because of its ability to impart natural bioactivity on the localized cell population as arginine-glycine-aspartic acid (RGD)-binding domains present in collagen promote cellular attachment and proliferation (Hashimoto et al., 1997). Furthermore, electrospinning of collagen typically produces nanofibers ranging from 50 to 500 nm, similar to the sizes of native collagen fibrils (Matthews et al., 2002). The degradation rate of the as-spun collagen-nanofiber mats can be controlled by in situ cross-linking to enhance the mechanical integrity of the scaffold, a typical shortcoming of natural products (Meng et al., 2012). Electrospinning of collagen has been studied extensively (Matthews et al., 2003), along with the combinatory blends of other natural materials such as chitosan, elastin, and silk fibroin for various tissue-engineering applications (Buttafoco et al., 2006; Chen et al., 2007; Zhou et al., 2010). In addition to its use as an electrospinning material, this natural protein can be conjugated to the surface of synthetic electrospun fibers, which may possess critical mechanical characteristics necessary for cartilage tissue engineering, to enhance cellular attachment. Gelatin, a

denatured collagen product, is also a naturally derived protein extracted from a variety of tissues in xenogenic sources. It is commonly used for electrospinning due to its biocompatibility and chemical composition similar to collagen while providing economic advantages over the high costs associated with pure collagen (Chen and Su, 2011). The mechanical properties of electrospun gelatin can be modulated by tailoring the degree of cross-linking similarly to collagen (Zhang et al., 2006a).

Hyaluronic acid (HA) is a glycosaminoglycan found in the ECM of many soft connective tissues. The function of HA is especially important for cartilage as its charged nature attracts water molecules to render resistance to compressive forces. However, the polyelectrolytic nature, in addition to very high molecular weight that significantly increases solution viscosity, inhibits the use of HA as a stand-alone material for electrospinning. Therefore, many studies have focused on blending HA with uncharged carrier polymers such as gelatin (Li et al., 2006) and poly(ethylene oxide) (PEO) (Ji et al., 2006) to enable electrospinning. Recently, Brenner et al. (2012) demonstrated that the use of aqueous ammonium solutions can overcome these limiting characteristics of HA for electrospinning, making it an attractive material for cartilage regeneration.

Finally, chitosan, a polysaccharide, is another natural material commonly used for electrospinning. Electrospun chitosan has been shown to enhance chondrocyte attachment, proliferation, and conservation of the chondrocyte phenotype when compared to a chitosan-based film (Shim et al., 2009). More commonly, blending of chitosan and other natural or synthetic components have been shown to be beneficial for cell attachment, proliferation, and viability (Subramanian et al., 2005; Bhattarai et al., 2005).

10.3.1.2 Synthetic polymers

Although there are numerous synthetic materials successfully used for electrospinning in various tissue-engineering applications such as vascular (Hasan et al., 2014), bone (Jang et al., 2009), neural (Lee et al., 2009), and tendon/ligament (Ladd et al., 2011), the following will focus on three of the main polymers for cartilage tissue regeneration. Synthetic polymers typically have enhanced mechanical properties over their natural counterparts, as well as a customizable chemical structure through modification in functional groups to control cell–scaffold interactions.

Poly(lactic acid) (PLA), poly(glycolic acid) (PGA), and poly(ε-caprolactone) (PCL) have all been approved by the FDA for various in vivo applications. Therefore, each of these synthetic polymers is attractive for cartilage regeneration to address specific cellular responses based on its chemical and mechanical traits. These materials have been shown beneficial in promoting or maintaining chondrogenic phenotype over commonly used cell-culture methods, such as chondrogenic differentiation of mesenchymal stem cells (MSCs) on PCL nanofibers over tissue culture polystyrene (TCPS) (Nam et al., 2011) or providing a suitable substrate for chondrocyte culture without dedifferentiation (Li et al., 2003).

The use of PLA alone for electrospun scaffolds in cartilage regeneration has had little to no attention probably due to the slow clearance rates of the material during rapid biodegradation, which accumulate the acidic by-products of the polymers in the native tissue. Thus, it has been typically used as a component for blends or

co-block polymers in electrospinning applications (Xu et al., 2009; Luu et al., 2003). Additionally, different techniques were incorporated to PLA electrospinning to optimize the scaffolds for cartilage applications. Laser ablation was used on electrospun nanofibrous PLA scaffolds to increase the pore dimensions, which could enhance cell infiltration for tissue engineering (Mccullen et al., 2011). In addition, nanofibrous PCL fibers were coated on microfibrous PLA fibers in an attempt to fabricate highly porous scaffold with nanofibrous topographical features for cartilage generation (Thorvaldsson et al., 2008).

Poly(glycolic acid) (PGA), a semicrystalline polyester, is an attractive polymer for scaffolding material due to the relatively quick degradation period of only a few weeks in vivo (Aghdam et al., 2012). Prior to the popularity of electrospinning for tissue-engineering applications, the method of nonwoven microfibrous mesh via extrusion of fine fibers of PGA was developed. Using isolated chondrocytes, these fibrous scaffolds were shown to induce the formation of cartilaginous tissue consisting of high GAG and collagen content (Freed et al., 1994).

Another polyester-based synthetic polymer, PCL, has been extensively studied in electrospinning for cartilage applications. Although the degradation time for this material is much slower than PGA (>24 months), this may be an ideal polymer due to the low required clearance rate of acidic by-products in native cartilage. With this relatively soft material characteristic in consideration, nanofibrous scaffolds have been developed for two-dimensional (2D) cell culture to enhance cartilage tissue formation (Li et al., 2003, 2005; Nam et al., 2011). Additionally, its excellent processability in a variety of organic and inorganic solvents increases its utility as a composite material for cartilage tissue applications (Cipitria et al., 2011).

10.3.1.3 Composite materials

Alloying materials among natural and synthetic polymers provides an opportunity to tune the chemical, mechanical and biological properties of scaffolds to modulate functionality of the final chondroinductive scaffold and the subsequent cellular behaviors. To facilitate cartilage regeneration, the composites utilize the beneficial aspects of the various natural and synthetic polymers by incorporating their mechanical properties, biocompatibility, and degradation rates. These composites are typically fabricated by simple blending or using the coaxial or coelectrospinning procedures as previously described.

Additional common examples of composite materials used for cartilage regeneration utilize a combination of both synthetic and natural polymers, such as chitosan–PEO (Bhattarai et al., 2005), gelatin–PCL (Zheng et al., 2014), or gelatin–PLLA (Chen and Su, 2011). Although each of these composites addresses a different application of cartilage regeneration, it combines the chemical and mechanical strengths of the two materials to alleviate the limitations of its counterpart. Therefore, the optimization of composition, whether it be combinations of synthetic–synthetic or natural–synthetic polymers, is critical for potential uses in cartilage regeneration as well as electrospinning processability.

In addition to simple alloy of materials, synthesis of co-block polymers from the previously mentioned synthetic materials (PLA, PGA, and PCL) are commonly used

to tailor the chemical and mechanical properties of electrospun fibers. One example of synthetic co-block polymers used for cartilage regeneration is poly(D,L-lactide-co-glycolide) (PLGA). This copolymer has been investigated for the mechanical properties, degradation, and cellular responses to different lactic acid to glycolic acid ratios, and has been used in the fabrication of both 2D (Shin et al., 2006) and 3D (Toyokawa et al., 2010) nanofibrous scaffolds for cartilage reconstruction.

10.3.2 Applications of electrospun scaffolds for cartilage regeneration

The capability of synthesizing scaffolds with highly tunable chemical and mechanical characteristics positions electrospinning as one of the viable methods to produce a tightly regulated microenvironment for desired cellular behaviors. Applicability to a wide variety of materials and mass-scalability add significant value to electrospun scaffolds for therapeutic applications. Typical use of these electrospun scaffolds includes cell-culture substrates for chondrocyte expansion or MSC differentiation to chondrocytes, and 3D tissue scaffolds for cartilage tissue engineering.

10.3.2.1 Electrospun cell-culture systems

Limited cell source is a primary concern for cartilage regeneration (Chung and Burdick, 2008). Mature primary chondrocytes dedifferentiate or lose their phenotypic characteristics during typical in vitro expansion involving common cell-culture platforms (Schulze-Tanzil et al., 2004; Schulze-Tanzil, 2009). They change their morphology, a feature that is closely linked to the functions of the cells, from round to flat shape primarily due to changes in the configuration of cell–ECM adhesion from 3D to 2D (Caron et al., 2012). By this reason, hydrogel systems such as agarose or alginate have been used to culture chondrocytes to maintain their phenotype. However, their application in the mass production of chondrocytes is limited by its difficulty in cell retrieval from 3D matrices. On the other hand, topographical features associated with the nonwoven nature of electrospun fibers provide a microenvironment suitable for maintaining chondrocytes' natural morphology and functionality in a 2D format ideal for cell retrieval.

In an earlier study by Li et al. (2003), electrospun PCL nanofibers showed enhanced maintenance of chondrocytic phenotype over TCPS systems. A rounder or more spindle shape of chondrocytes with less actin stress-fiber formation was observed on the nanofibrous scaffolds, in contrast to a flatter morphology on the TCPS. This morphological difference was related to the cells' functionality, demonstrated by greater expression of chondrocytic proteins including collagen II and IX, aggrecan, and cartilage oligomeric matrix protein on the electrospun scaffolds. This enhancement in maintaining phenotypic characteristics of chondrocytes is likely due to physical features of electrospun fibrous structure rather than specific chemical traits. The superiority of electrospun fibrous structure as a cell-culture system for chondrocytes was demonstrated when a chitosan and poly(ethylene oxide) (PEO) blend of nanofibers was compared to a thin film of similar composition (Bhattarai et al., 2005).

Interestingly, in addition to the topographical feature of electrospun scaffolds, the fiber size significantly affects the phenotypic stability of chondrocytes. Noriega et al. (2012) reported that submicron-size topography was preferential for chondrocyte culture when compared to larger micron-sized fibers. Although the differences in the fiber size did not induce significant changes in Ras homolog gene family, member A (RhoA) activity, which governs cytoskeletal organization, the increased Rho-associated, coiled-coil containing protein kinase (ROCK) expression in nanofibers appears to enhance chondrocytic protein expression and phenotypic maintenance (Noriega et al., 2012). RhoA is a central protein that is regulated by integrin-related cell–ECM interactions and mechanotransduction (Shyy and Chien, 2002). It is unclear whether the enhanced chondrocytic activity on nanofibers is due to the increased binding sites that change the quantity of cell–matrix adhesion or the decreased substrate stiffness that frustrates stress-fiber formation. Nevertheless, the study by Noriega et al. (2012) provides insight to the influence of fiber diameter on cellular behaviors and confirms the utility of electrospun nanofibers as a promising substrate for chondrocyte culture systems.

One of the approaches to overcome limited quantities of native chondrocytes from a patient for cartilage regeneration is to use various types of stem cells by differentiating them into chondrocytes. In this regard, electrospun scaffolds demonstrated a great potential promoting chondrocytic differentiation of stem cells. Utilizing PCL nanofibrous scaffolds, Li et al. (2005) demonstrated the enhanced differentiation potential of MSCs toward chondrocytes. More specifically, the results showed that the high MSC-seeding density, similar to commonly used differentiation protocols such as micro mass (Ahrens et al., 1977) or pellet culture (Johnstone et al., 1998), may not be required when an electrospun system is used. This observation further signifies the beneficial effects of topographical features in electrospun fibrous structure for promoting the differentiation of stem cells toward chondrocytes and the subsequent maintenance of mature chondrocytic phenotype.

Among many physiochemical properties of electrospun fibers, the mechanical properties of a fibrous network are one of the dominant factors that delineate the enhanced chondrogenesis of stem cells on electrospun scaffolds. Nam et al. (2011) showed that softer electrospun scaffolds exhibited greater chondrogenesis as compared to stiffer scaffolds when the same surface chemistry was maintained by utilizing core–shell electrospinning. MSCs cultured on soft PCL nanofibrous scaffolds exhibit a rounder chondrocyte-like morphology with less actin stress-fiber formation, in contrast to the elongated fibroblast-like structure of the MSCs cultured on TCPS shown in Fig. 10.6. These results indicate that the compliance or pliability of individual electrospun fibers controls the cell morphology and its subsequent differentiation, which further emphasizes the importance of material selection for optimized mechanical properties.

The topographical cues of nanofibrous scaffolds have been shown to significantly influence cellular signaling of stem cells during chondrogenic differentiation. Nanofibers provide adequate focal points for stem cell adhesion, proliferation, and chondrogenic differentiation (Shafiee et al., 2014). Zhong et al. (2013) investigated the roles of the RhoA/ROCK and Yes-associated protein (YAP)/transcriptional coactivator with Psd-95 (Post Synaptic Density Protein), DlgA (Drosophila Disc Large Tumor Suppressor) and ZO1 (Zonula Occludens-1 Protein) (PDZ)-binding motif (TAZ) signaling

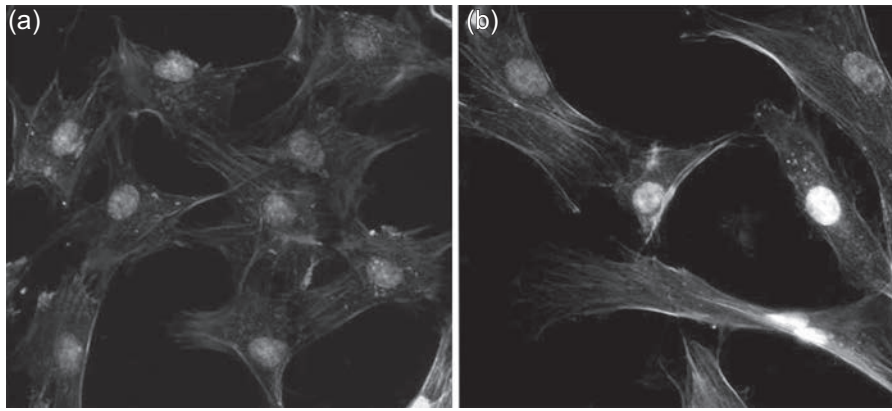

Figure 10.6 Immunofluorescence images of mesenchymal stem cells (MSCs) cultured on (a) nanofibrous poly(ε-caprolactone) scaffolds and (b) tissue culture polystyrene plate showing different cytoskeletal organization (actin and nucleus were stained with Phalloidin and 4′,6-diamidino-2-phenylindole [DAPI]).

pathways in fibrochondrogenic differentiation of MSCs, showing that these signaling pathways play an imperative role in cytoskeletal dynamics and stem cell differentiation (Woods and Beier, 2006). The activation of ROCK on nanofibers enhances SRY (sex determining region Y) activity, which is a primary transcription factor necessary for promoting chondrogenesis (Ghosh et al., 2009). Simultaneously, the YAP/TAZ signaling that upregulates Runt-related transcription factor 2 (RUNX2) and collagen I, while downregulating SRY, collagen II, and aggrecan gene expression, was effectively suppressed, further enhancing chondrogenesis. This study provides a critical insight on the cell-signaling responses of stem cells to their local microenvironment, demonstrating the utility of electrospun nanofibers for directing chondrogenesis.

Overall, these results demonstrate the superiority of electrospun scaffolds over typical tissue-culture plates as a cell-culture platform for cartilage regeneration. The nanofibrous structure not only enhances the phenotypic maintenance of mature chondrocytes, but also promotes the differentiation of stem cells toward chondrocytes.

10.3.2.2 Electrospun scaffolds for cartilage tissue engineering

In contrast to the monolayer culture systems described above, the construction of engineered cartilage requires placement of appropriate cells within a 3D electrospun scaffold while maintaining the mechanical integrity in the defect site of the host under physiological conditions. Considering the main function of cartilage being load bearing, it is important to consider promoting tissue morphogenesis while maintaining structural integrity during the maturation of the engineered tissue, both of which associate with the porosity and degradation rate of scaffolds. For cartilage tissue engineering, two main approaches include (1) the use of acellular scaffolds followed by the recruitment of endogenous cells into the scaffolds and (2) the culture of appropriate cells within scaffolds in vitro and their subsequent implantation after tissue maturation.

To assess the feasibility of utilizing electrospun scaffolds for cartilage regeneration, acellular electrospun PLGA scaffolds were implanted into osteochondral defects in the femoral condyles of rabbits (Toyokawa et al., 2010). The results showed the ingrowth of endogenous cells into the scaffolds and enhanced tissue formation over untreated tissue damage. However, the degree of regeneration depended on the availability of macropores for cellular infiltration; scaffolds having a cannulated configuration induced greater tissue morphogenesis as compared to a solid form, indicating that intrinsically small pore size in electrospun nanofibers is a limiting factor impeding tissue regeneration. A recent study using an in vitro cell–scaffold culture approach demonstrated a similar observation regarding cellular infiltration-dependent cartilage regeneration by electrospun scaffolds (Zheng et al., 2014). Different ratios of gelatin to PCL electrospun scaffolds were implanted in vivo in a rodent model to evaluate their potential for 3D cartilage regeneration. PCL enhanced the mechanical integrity of the scaffolds, whereas the biocompatibility and facilitated biodegradation of gelatin increased the cellular infiltration and subsequent tissue morphogenesis. It was shown that scaffolds with high PCL content were less favorable for 3D cartilage regeneration due to limited cellular infiltration demonstrating the importance of the balance between chondrogenesis-favorable nanofiber structure and cell ingrowth-allowing macroporous structure.

To overcome the shortcoming of electrospun nanofibrous structure, various methods have been incorporated into the electrospinning process to increase pore size for enhanced cellular infiltration. Some of these methods of enlarging pore dimensions include removing salt particles incorporated into the fibers during the synthesis (Nam et al., 2007; Ekaputra et al., 2008), ultrasonication to enlarge the interfiber spacing (Lee et al., 2011), as well as the selective dissolution of sacrificial fibers after scaffold fabrication (Guimaraes et al., 2010). Another approach includes the utilization of microfibers to increase intrinsic pore size in electrospun scaffolds (Nam et al., 2009). Fig. 10.7 shows articular chondrocytes cultured in 3D microfibrous PCL scaffolds, secreting their own nanofibrous ECM within the microfiber networks. One of the

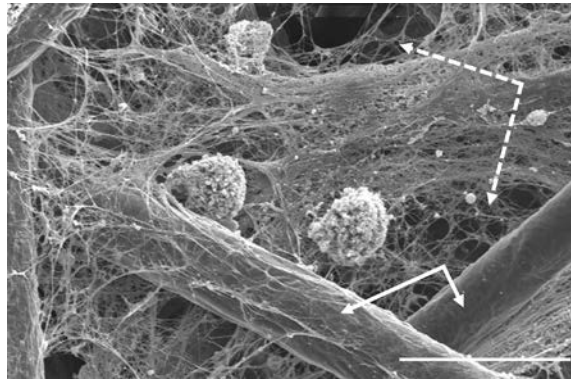

Figure 10.7 SEM images of articular chondrocytes culture on microfibrous poly(ε-caprolactone) scaffolds. *Dashed arrows* indicate cell-secreted collagen fibers. *Solid arrows* indicate poly(ε-caprolactone) microfibers (scale bar: 20 μm).

caveats utilizing microfibers, however, is extensive culture period for tissue maturation due to the large pore volume that needs to be filled by the cells.

A novel method for addressing the benefits and pitfalls of solely using electrospun nano- or microfibers is to employ a multiscale or multidimensional electrospun fiber approach. The benefits of a multiscale approach stem from the cell-favorable topographical scales accomplished by nanofibers and the cellular infiltration enhancing macropores by microfibers. One method used to address this multiscale approach was achieved via combining fibrin nanofibers and PCL microfibers by utilizing the coelectrospinning technique on a rotating mandrel (Levorson et al., 2013). The combination of using both nano- and microfibers in a 3D scaffold demonstrated the enhancement of cellular proliferation throughout the scaffold while enabling the cells to maintain cellularity and secrete chondrocytic ECM. Another similar study utilizing multiscale electrospun fibers to enhance the porosity of 3D scaffolds employed nanofiber-coated microfibers. A combination of PCL nanofibers electrospun onto PLA microfibers was utilized to synthesize highly porous scaffolds ranging 95–97% porosity while providing nanotopography for cell–scaffold interactions (Thorvaldsson et al., 2008). Although the authors did not focus on the biochemical aspects of maintaining chondrocyte phenotype or enhancing chondrogenesis, this study demonstrated a possibility of inducing synergistic effects between nanofibers and microfibers for enhanced cellular behaviors and infiltration, which may be applicable for cartilage regeneration.

As previously described, AC is structured to exhibit depth-wise anisotropy in cell population, morphology, orientation as well as ECM composition and structure. This gradient structure is essential for depth-dependent cartilage functions such as load bearing and joint lubrication. In an effort to address the structure and function for this zonal architecture, a combinatory approach for sequential electrospinning has been attempted to produce distinct fiber dimensions and organizations in a depth-dependent manner (Mccullen et al., 2012). Varying the polymer concentration and velocity of a rotating mandrel collector, a 3D trilaminar composite microfibrous culture system mimicking the articular cartilage zonal architecture was developed. Culture of mature chondrocytes in this scaffold over the course of a 5-week period resulted in cartilage-like ECM deposition with a depth-dependent organization.

Overall, electrospinning finds a great utility in the fabrication of in vitro cell culture systems and in vivo tissue-engineering scaffolds. However, there are still limitations and drawbacks that need to be overcome to further enhance therapeutic applications of electrospun scaffolds in cartilage regeneration.

10.4 Current limitations of electrospun scaffolds in cartilage tissue engineering

Many key factors must be considered and incorporated into material selection and fabrication process to ensure proper cartilage regeneration. For example, different scales of electrospun fibers (ie, nano- and microsize) exhibit both benefits and shortcomings for cartilage regeneration. Nanofibrous structure produces a high surface-area-to-volume ratio which promotes cellular adhesion and proliferation, ideal for

2D cell culture. However, its intrinsically small pore size restricts cellular infiltration, limiting its use in 3D culture systems. In contrast, the microfibers allow for greater cellular penetration in 3D, but do not provide nanofiber-based topographical cues mimicking the ECM components present in the native tissue (Levorson et al., 2013).

Although most studies focus on scaffold materials for electrospinning, the structural configuration of such as-spun fibers does not depict the 3D spatial orientation of cartilage ECM. Because cartilage is a complex tissue with varying ECM arrangements, both parallel and perpendicular to the surface to the joint, electrospinning techniques to mimic these organizations are currently limited to layered-fiber networks (Li et al., 2014). Such a layered approach may impede its therapeutic applications due to compromised structural integrity between layers. Therefore, a monolithic scaffold having gradient changes in structural and mechanical properties would present a more appropriate platform for cartilage regeneration. Another aspect to consider for electrospun scaffolds as a vehicle to drive cartilage regeneration is the size and shape of the implant. So far, most studies have been limited to the size of local cartilage lesion with a cylindrical shape. To further facilitate the adaption of electrospun scaffolds for cartilage tissue engineering, methods that can scale up the size of scaffolds to full cartilage with a patient-specific shape need to be devised.

In conclusion, electrospun scaffolds demonstrate exemplary promise for cartilage regeneration. Electrospinning is a versatile technique which produces fibers on different orders of magnitude in size and mechanical properties, providing an opportunity to fabricate physiochemically tuned scaffolds for cartilage regeneration. Future focus for the field will likely address the zonal architecture of articular cartilage in both structure and function of engineered tissue through a thorough consideration of materials to match the chemical and mechanical aspects of physiological cartilage tissue.

References

Aghdam, R.M., Najarian, S., Shakhesi, S., Khanlari, S., Shaabani, K., Sharifi, S., 2012. Investigating the effect of PGA on physical and mechanical properties of electrospun PCL/PGA blend nanofibers. Journal of Applied Polymer Science 124, 123–131.

Ahrens, P.B., Solursh, M., Reiter, R.S., 1977. Stage-related capacity for limb chondrogenesis in cell culture. Developmental Biology 60, 69–82.

Angammana, C.J., Jayaram, S.H., 2011. Analysis of the effects of solution conductivity on electrospinning process and fiber morphology. IEEE Transactions on Industry Applications 47, 1109–1117.

Bazilevsky, A.V., Yarin, A.L., Megaridis, C.M., 2007. Co-electrospinning of core-shell fibers using a single-nozzle technique. Langmuir 23, 2311–2314.

Bhattarai, N., Edmondson, D., Veiseh, O., Matsen, F.A., Zhang, M.Q., 2005. Electrospun chitosan-based nanofibers and their cellular compatibility. Biomaterials 26, 6176–6184.

Bhosale, A.M., Richardson, J.B., 2008. Articular cartilage: structure, injuries and review of management. British Medical Bulletin 87, 77–95.

Birnbaum, H., Pike, C., Kaufman, R., Marynchenko, M., Kidolezi, Y., Cifaldi, M., 2010. Societal cost of rheumatoid arthritis patients in the US. Current Medical Research and Opinion 26, 77–90.

Brenner, E.K., Schiffman, J.D., Thompson, E.A., Toth, L.J., Schauer, C.L., 2012. Electrospinning of hyaluronic acid nanofibers from aqueous ammonium solutions. Carbohydrate Polymers 87, 926–929.

Buckwalter, J.A., Mankin, H.J., 1997. Articular cartilage.1. Tissue design and chondrocyte-matrix interactions. Journal of Bone and Joint Surgery-American Volume 79A, 600–611.

Buttafoco, L., Kolkman, N.G., Engbers-Buijtenhuijs, P., Poot, A.A., Dijkstra, P.J., Vermes, I., Feijen, J., 2006. Electrospinning of collagen and elastin for tissue engineering applications. Biomaterials 27, 724–734.

Caron, M.M., Emans, P.J., Coolsen, M.M., Voss, L., Surtel, D.A., Cremers, A., Van Rhijn, L.W., Welting, T.J., 2012. Redifferentiation of dedifferentiated human articular chondrocytes: comparison of 2D and 3D cultures. Osteoarthritis Cartilage 20, 1170–1178.

Casper, C.L., Stephens, J.S., Tassi, N.G., Chase, D.B., Rabolt, J.F., 2004. Controlling surface morphology of electrospun polystyrene fibers: effect of humidity and molecular weight in the electrospinning process. Macromolecules 37, 573–578.

Chen, J.P., Su, C.H., 2011. Surface modification of electrospun PLLA nanofibers by plasma treatment and cationized gelatin immobilization for cartilage tissue engineering. Acta Biomaterialia 7, 234–243.

Chen, Z., Mo, X., Qing, F., 2007. Electrospinning of collagen–chitosan complex. Materials Letters 61, 3490–3494.

Chung, C., Burdick, J.A., 2008. Engineering cartilage tissue. Advanced Drug Delivery Reviews 60, 243–262.

Cipitria, A., Skelton, A., Dargaville, T., Dalton, P., Hutmacher, D., 2011. Design, fabrication and characterization of PCL electrospun scaffolds—a review. Journal of Materials Chemistry 21, 9419–9453.

De Vrieze, S., Van Camp, T., Nelvig, A., Hagström, B., Westbroek, P., De Clerck, K., 2009. The effect of temperature and humidity on electrospinning. Journal of Materials Science 44, 1357–1362.

Ding, B., Kimura, E., Sato, T., Fujita, S., Shiratori, S., 2004. Fabrication of blend biodegradable nanofibrous nonwoven mats via multi-jet electrospinning. Polymer 45, 1895–1902.

Doshi, J., Reneker, D.H., 1993. Electrospinning process and applications of electrospun fibers. In: Industry Applications Society Annual Meeting, 1993, Conference Record of the 1993 IEEE. IEEE, pp. 1698–1703.

Ekaputra, A.K., Prestwich, G.D., Cool, S.M., Hutmacher, D.W., 2008. Combining electrospun scaffolds with electrosprayed hydrogels leads to three-dimensional cellularization of hybrid constructs. Biomacromolecules 9, 2097–2103.

Errico, C., Detta, N., Puppi, D., Piras, A.M., Chiellini, F., Chiellini, E., 2011. Polymeric nanostructured items electrospun on a cylindrical template: a simple procedure for their removal. Polymer International 60, 1162–1166.

Eyre, D.R., Wu, J.J., 1983. Collagen of fibrocartilage: a distinctive molecular phenotype in bovine meniscus. FEBS Letters 158, 265–270.

Eyrich, D., Wiese, H., Mailer, G., Skodacek, D., Appel, B., Sarhan, H., Tessmar, J., Staudenmaier, R., Wenzel, M.M., Goepferich, A., Blunk, T., 2007. In vitro and in vivo cartilage engineering using a combination of chondrocyte-seeded long-term stable fibrin gels and polycaprolactone-based polyurethane scaffolds. Tissue Engineering 13, 2207–2218.

Fong, H., Chun, I., Reneker, D.H., 1999. Beaded nanofibers formed during electrospinning. Polymer 40, 4585–4592.

Francis, L., Venugopal, J., Prabhakaran, M.P., Thavasi, V., Marsano, E., Ramakrishna, S., 2010. Simultaneous electrospin-electrosprayed biocomposite nanofibrous scaffolds for bone tissue regeneration. Acta Biomaterials 6, 4100–4109.

Francis Suh, J.K., Matthew, H.W.T., 2000. Application of chitosan-based polysaccharide biomaterials in cartilage tissue engineering: a review. Biomaterials 21, 2589–2598.

Freed, L.E., Vunjak-Novakovic, G., Biron, R.J., Eagles, D.B., Lesnoy, D.C., Barlow, S.K., Langer, R., 1994. Biodegradable polymer scaffolds for tissue engineering. Biotechnology (Nature Publishing Company) 12, 689–693.

Ganan-Calvo, A.M., Rebollo-Munoz, N., Montanero, J.M., 2013. The minimum or natural rate of flow and droplet size ejected by Taylor cone-jets: physical symmetries and scaling laws. New Journal of Physics 15, 033035.

Geng, X., Kwon, O.H., Jang, J., 2005. Electrospinning of chitosan dissolved in concentrated acetic acid solution. Biomaterials 26, 5427–5432.

Ghosh, S., Laha, M., Mondal, S., Sengupta, S., Kaplan, D.L., 2009. In vitro model of mesenchymal condensation during chondrogenic development. Biomaterials 30, 6530–6540.

Greiner, A., Wendorff, J.H., 2007. Electrospinning: a fascinating method for the preparation of ultrathin fibers. Angewandte Chemie International Edition in English 46, 5670–5703.

Guimaraes, A., Martins, A., Pinho, E.D., Faria, S., Reis, R.L., Neves, N.M., 2010. Solving cell infiltration limitations of electrospun nanofiber meshes for tissue engineering applications. Nanomedicine (London) 5, 539–554.

Gunatillake, P.A., Adhikari, R., 2003. Biodegradable synthetic polymers for tissue engineering. European Cells and Materials 5, 1–16 discussion 16.

Gupta, P., Wilkes, G.L., 2003. Some investigations on the fiber formation by utilizing a side-by-side bicomponent electrospinning approach. Polymer 44, 6353–6359.

Han, D., Boyce, S.T., Steckl, A.J., 2008. Versatile core-sheath biofibers using coaxial electrospinning. In: MRS Proceedings. Cambridge University Press. 1094-DD06-02.

Hasan, A., Memic, A., Annabi, N., Hossain, M., Paul, A., Dokmeci, M.R., Dehghani, F., Khademhosseini, A., 2014. Electrospun scaffolds for tissue engineering of vascular grafts. Acta Biomaterials 10, 11–25.

Hashimoto, K., Noshiro, M., Ohno, S., Kawamoto, T., Satakeda, H., Akagawa, Y., Nakashima, K., Okimura, A., Ishida, H., Okamoto, T., 1997. Characterization of a cartilage-derived 66-kDa protein (RGD-CAP/beta ig-h3) that binds to collagen. Biochimica et Biophysica Acta (BBA)-Molecular Cell Research 1355, 303–314.

Huang, Z.-M., Zhang, Y.-Z., Kotaki, M., Ramakrishna, S., 2003. A review on polymer nanofibers by electrospinning and their applications in nanocomposites. Composites Science and Technology 63, 2223–2253.

Hutmacher, D.W., Ng, K.W., Kaps, C., Sittinger, M., Klaring, S., 2003. Elastic cartilage engineering using novel scaffold architectures in combination with a biomimetic cell carrier. Biomaterials 24, 4445–4458.

Iwasa, J., Engebretsen, L., Shima, Y., Ochi, M., 2009. Clinical application of scaffolds for cartilage tissue engineering. Knee Surgery, Sports Traumatology, Arthroscopy 17, 561–577.

Jang, J.H., Castano, O., Kim, H.W., 2009. Electrospun materials as potential platforms for bone tissue engineering. Advanced Drug Delivery Reviews 61, 1065–1083.

Ji, Y., Ghosh, K., Shu, X.Z., Li, B., Sokolov, J.C., Prestwich, G.D., Clark, R.A., Rafailovich, M.H., 2006. Electrospun three-dimensional hyaluronic acid nanofibrous scaffolds. Biomaterials 27, 3782–3792.

Johnstone, B., Hering, T.M., Caplan, A.I., Goldberg, V.M., Yoo, J.U., 1998. In vitro chondrogenesis of bone marrow-derived mesenchymal progenitor cells. Experimental Cell Research 238, 265–272.

Kim, I.L., Mauck, R.L., Burdick, J.A., 2011. Hydrogel design for cartilage tissue engineering: a case study with hyaluronic acid. Biomaterials 32, 8771–8782.

Kumar, P., 2012. Effect of Colletor on Electrospinning to Fabricate Aligned Nano Fiber Thesis. National Institute of Technology, Rourkela.

Ladd, M.R., Lee, S.J., Stitzel, J.D., Atala, A., Yoo, J.J., 2011. Co-electrospun dual scaffolding system with potential for muscle-tendon junction tissue engineering. Biomaterials 32, 1549–1559.

Lee, J.B., Jeong, S.I., Bae, M.S., Yang, D.H., Heo, D.N., Kim, C.H., Alsberg, E., Kwon, I.K., 2011. Highly porous electrospun nanofibers enhanced by ultrasonication for improved cellular infiltration. Tissue Engineering Part A 17, 2695–2702.

Lee, J.Y., Bashur, C.A., Goldstein, A.S., Schmidt, C.E., 2009. Polypyrrole-coated electrospun PLGA nanofibers for neural tissue applications. Biomaterials 30, 4325–4335.

Levorson, E.J., Raman Sreerekha, P., Chennazhi, K.P., Kasper, F.K., Nair, S.V., Mikos, A.G., 2013. Fabrication and characterization of multiscale electrospun scaffolds for cartilage regeneration. Biomedical Materials 8, 014103.

Li, G., Zhang, T., Li, M., Fu, N., Fu, Y., Ba, K., Deng, S., Jiang, Y., Hu, J., Peng, Q., Lin, Y., 2014. Electrospun fibers for dental and craniofacial applications. Current Stem Cell Research and Therapy 9, 187–195.

Li, J.X., He, A.H., Zheng, J.F., Han, C.C., 2006. Gelatin and gelatin-hyaluronic acid nanofibrous membranes produced by electrospinning of their aqueous solutions. Biomacromolecules 7, 2243–2247.

Li, W.J., Danielson, K.G., Alexander, P.G., Tuan, R.S., 2003. Biological response of chondrocytes cultured in three-dimensional nanofibrous poly(epsilon-caprolactone) scaffolds. Journal of Biomedical Materials Research Part A 67, 1105–1114.

Li, W.J., Tuli, R., Huang, X., Laquerriere, P., Tuan, R.S., 2005. Multilineage differentiation of human mesenchymal stem cells in a three-dimensional nanofibrous scaffold. Biomaterials 26, 5158–5166.

Liu, Y., Dong, L.A., Fan, J., Wang, R., Yu, J.Y., 2011. Effect of applied voltage on diameter and morphology of ultrafine fibers in bubble electrospinning. Journal of Applied Polymer Science 120, 592–598.

Luo, C.J., Nangrejo, M., Edirisinghe, M., 2010. A novel method of selecting solvents for polymer electrospinning. Polymer 51, 1654–1662.

Luu, Y.K., Kim, K., Hsiao, B.S., Chu, B., Hadjiargyrou, M., 2003. Development of a nanostructured DNA delivery scaffold via electrospinning of PLGA and PLA-PEG block copolymers. Journal of Controlled Release 89, 341–353.

Ma, Z., Gao, C., Gong, Y., Shen, J., 2003. Paraffin spheres as porogen to fabricate poly(L-lactic acid) scaffolds with improved cytocompatibility for cartilage tissue engineering. Journal of Biomedical Materials Research Part B: Applied Biomaterials 67, 610–617.

Marin, E., Briceño, M.I., Caballero-George, C., 2013. Critical evaluation of biodegradable polymers used in nanodrugs. International Journal of Nanomedicine 8, 3071.

Matthews, J.A., Boland, E.D., Wnek, G.E., Simpson, D.G., Bowlin, G.L., 2003. Electrospinning of collagen type II: a feasibility study. Journal of Bioactive and Compatible Polymers 18, 125–134.

Matthews, J.A., Wnek, G.E., Simpson, D.G., Bowlin, G.L., 2002. Electrospinning of collagen nanofibers. Biomacromolecules 3, 232–238.

Mauck, R.L., Yuan, X., Tuan, R.S., 2006. Chondrogenic differentiation and functional maturation of bovine mesenchymal stem cells in long-term agarose culture. Osteoarthritis Cartilage 14, 179–189.

Mccullen, S.D., Autefage, H., Callanan, A., Gentleman, E., Stevens, M.M., 2012. Anisotropic fibrous scaffolds for articular cartilage regeneration. Tissue Engineering Part A 18, 2073–2083.

Mccullen, S.D., Gittard, S.D., Miller, P.R., Pourdeyhimi, B., Narayan, R.J., Loboa, E.G., 2011. Laser ablation imparts controlled micro-scale pores in electrospun scaffolds for tissue engineering applications. Annals of Biomedical Engineering 39, 3021–3030.

Meng, L.H., Arnoult, O., Smith, M., Wnek, G.E., 2012. Electrospinning of in situ crosslinked collagen nanofibers. Journal of Materials Chemistry 22, 19412–19417.

Milleret, V., Simona, B., Neuenschwander, P., Hall, H., 2011. Tuning electrospinning parameters for production of 3D-fiber-fleeces with increased porosity for soft tissue engineering applications. European Cells and Materials 21, 286–303.

Nam, J., Huang, Y., Agarwal, S., Lannutti, J., 2007. Improved cellular infiltration in electrospun fiber via engineered porosity. Tissue Engineering 13, 2249–2257.

Nam, J., Johnson, J., Lannutti, J.J., Agarwal, S., 2011. Modulation of embryonic mesenchymal progenitor cell differentiation via control over pure mechanical modulus in electrospun nanofibers. Acta Biomaterials 7, 1516–1524.

Nam, J., Rath, B., Knobloch, T.J., Lannutti, J.J., Agarwal, S., 2009. Novel electrospun scaffolds for the molecular analysis of chondrocytes under dynamic compression. Tissue Engineering Part A 15, 513–523.

Neves, N.M., Campos, R., Pedro, A., Cunha, J., Macedo, F., Reis, R.L., 2007. Patterning of polymer nanofiber meshes by electrospinning for biomedical applications. International Journal of Nanomedicine 2, 433–448.

Noriega, S.E., Hasanova, G.I., Schneider, M.J., Larsen, G.F., Subramanian, A., 2012. Effect of fiber diameter on the spreading, proliferation and differentiation of chondrocytes on electrospun chitosan matrices. Cells Tissues Organs 195, 207–221.

Oegema Jr., T.R., Carpenter, R.J., Hofmeister, F., Thompson Jr., R.C., 1997. The interaction of the zone of calcified cartilage and subchondral bone in osteoarthritis. Microscopy Research and Technique 37, 324–332.

Palmer, A.K., Werner, F.W., 1981. The triangular fibrocartilage complex of the wrist—anatomy and function. The Journal of Hand Surgeryery 6, 153–162.

Pant, H.R., Neupane, M.P., Pant, B., Panthi, G., Oh, H.J., Lee, M.H., Kim, H.Y., 2011. Fabrication of highly porous poly (varepsilon-caprolactone) fibers for novel tissue scaffold via water-bath electrospinning. Colloids and Surfaces B, Biointerfaces 88, 587–592.

Park, J.-S., 2010. Electrospinning and its applications. Advances in Natural Sciences: Nanoscience and Nanotechnology 1, 043002.

Pearle, A.D., Warren, R.F., Rodeo, S.A., 2005. Basic science of articular cartilage and osteoarthritis. Clinics in Sports Medicine 24, 1–12.

Pillay, V., Dott, C., Choonara, Y.E., Tyagi, C., Tomar, L., Kumar, P., Du Toit, L.C., Ndesendo, V.M.K., 2013. A review of the effect of processing variables on the fabrication of electrospun nanofibers for drug delivery applications. Journal of Nanomaterials 2013.

Poole, A.R., Kojima, T., Yasuda, T., Mwale, F., Kobayashi, M., Laverty, S., 2001. Composition and structure of articular cartilage: a template for tissue repair. Clinical Orthopaedics and Related Research S26–S33.

Qu, H., Wei, S., Guo, Z., 2013. Coaxial electrospun nanostructures and their applications. Journal of Materials Chemistry A 1, 11513–11528.

Reiffel, A.J., Kafka, C., Hernandez, K.A., Popa, S., Perez, J.L., Zhou, S., Pramanik, S., Brown, B.N., Ryu, W.S., Bonassar, L.J., Spector, J.A., 2013. High-fidelity tissue engineering of patient-specific auricles for reconstruction of pediatric microtia and other auricular deformities. PloS One 8, e56506.

Santos, M.I., Tuzlakoglu, K., Fuchs, S., Gomes, M.E., Peters, K., Unger, R.E., Piskin, E., Reis, R.L., Kirkpatrick, C.J., 2008. Endothelial cell colonization and angiogenic potential of combined nano- and micro-fibrous scaffolds for bone tissue engineering. Biomaterials 29, 4306–4313.

Schulze-Tanzil, G., 2009. Activation and dedifferentiation of chondrocytes: implications in cartilage injury and repair. Annals of Anatomy 191, 325–338.

Schulze-Tanzil, G., Mobasheri, A., De Souza, P., John, T., Shakibaei, M., 2004. Loss of chondrogenic potential in dedifferentiated chondrocytes correlates with deficient Shc-Erk interaction and apoptosis. Osteoarthritis Cartilage 12, 448–458.

Sener, A., Altay, A.S., Altay, F., 2011. Effect of voltage on morphology of electrospun nanofibers. In: Electrical and Electronics Engineering (ELECO), 2011 7th International Conference on 2011. IEEE. I-324-I-328.

Shafiee, A., Seyedjafari, E., Sadat Taherzadeh, E., Dinarvand, P., Soleimani, M., Ai, J., 2014. Enhanced chondrogenesis of human nasal septum derived progenitors on nanofibrous scaffolds. Materials Science and Engineering C: Materials for Biological Applications 40, 445–454.

Sharma, B., Williams, C.G., Kim, T.K., Sun, D., Malik, A., Khan, M., Leong, K., Elisseeff, J.H., 2007. Designing zonal organization into tissue-engineered cartilage. Tissue Engineering 13, 405–414.

Shim, I.K., Suh, W.H., Lee, S.Y., Lee, S.H., Heo, S.J., Lee, M.C., Lee, S.J., 2009. Chitosan nano-/microfibrous double-layered membrane with rolled-up three-dimensional structures for chondrocyte cultivation. Journal of Biomedical Materials Research Part A 90, 595–602.

Shin, H.J., Lee, C.H., Cho, I.H., Kim, Y.J., Lee, Y.J., Kim, I.A., Park, K.D., Yui, N., Shin, J.W., 2006. Electrospun PLGA nanofiber scaffolds for articular cartilage reconstruction: mechanical stability, degradation and cellular responses under mechanical stimulation in vitro. Journal of Biomaterials Science Polymer Edition 17, 103–119.

Shyy, J.Y., Chien, S., 2002. Role of integrins in endothelial mechanosensing of shear stress. Circulation Research 91, 769–775.

Smith, G.D., Knutsen, G., Richardson, J.B., 2005. A clinical review of cartilage repair techniques. Journal of Bone and Joint Surgery British Volume 87, 445–449.

Sophia Fox, A.J., Bedi, A., Rodeo, S.A., 2009. The basic science of articular cartilage: structure, composition, and function. Sports Health: A Multidisciplinary Approach 1, 461–468.

Su, Y., Lu, B., Xie, Y., Ma, Z., Liu, L., Zhao, H., Zhang, J., Duan, H., Zhang, H., Li, J., Xiong, Y., Xie, E., 2011. Temperature effect on electrospinning of nanobelts: the case of hafnium oxide. Nanotechnology 22, 285609.

Subramanian, A., Vu, D., Larsen, G.F., Lin, H.Y., 2005. Preparation and evaluation of the electrospun chitosan/PEO fibers for potential applications in cartilage tissue engineering. Journal of Biomaterials Science Polymer Edition 16, 861–873.

Sun, Z.C., Deitzel, J.M., Knopf, J., Chen, X., Gillespie, J.W., 2012. The effect of solvent dielectric properties on the collection of oriented electrospun fibers. Journal of Applied Polymer Science 125, 2585–2594.

Telemeco, T.A., Ayres, C., Bowlin, G.L., Wnek, G.E., Boland, E.D., Cohen, N., Baumgarten, C.M., Mathews, J., Simpson, D.G., 2005. Regulation of cellular infiltration into tissue engineering scaffolds composed of submicron diameter fibrils produced by electrospinning. Acta Biomaterialia 1, 377–385.

Thorvaldsson, A., Stenhamre, H., Gatenholm, P., Walkenstrom, P., 2008. Electrospinning of highly porous scaffolds for cartilage regeneration. Biomacromolecules 9, 1044–1049.

Toyokawa, N., Fujioka, H., Kokubu, T., Nagura, I., Inui, A., Sakata, R., Satake, M., Kaneko, H., Kurosaka, M., 2010. Electrospun synthetic polymer scaffold for cartilage repair without cultured cells in an animal model. Arthroscopy-the Journal of Arthroscopic and Related Surgery 26, 375–383.

Vinatier, C., Mrugala, D., Jorgensen, C., Guicheux, J., Noel, D., 2009. Cartilage engineering: a crucial combination of cells, biomaterials and biofactors. Trends in Biotechnology 27, 307–314.

Wang, Y., Ding, C., Wluka, A.E., Davis, S., Ebeling, P.R., Jones, G., Cicuttini, F.M., 2006. Factors affecting progression of knee cartilage defects in normal subjects over 2 years. Rheumatology 45, 79–84.

Wilson, W., Van Burken, C., Van Donkelaar, C., Buma, P., Van Rietbergen, B., Huiskes, R., 2006. Causes of mechanically induced collagen damage in articular cartilage. Journal of Orthopaedic Research 24, 220–228.

Woods, A., Beier, F., 2006. RhoA/ROCK signaling regulates chondrogenesis in a context-dependent manner. Journal of Biological Chemistry 281, 13134–13140.

Wu, L., Li, H., Li, S., Li, X., Yuan, X., Zhang, Y., 2010. Composite fibrous membranes of PLGA and chitosan prepared by coelectrospinning and coaxial electrospinning. Journal of Biomedical Materials Research Part A 92, 563–574.

Xu, J., Zhang, J.H., Gao, W.Q., Liang, H.W., Wang, H.Y., Li, J.F., 2009. Preparation of chitosan/PLA blend micro/nanofibers by electrospinning. Materials Letters 63, 658–660.

Xu, W., He, X., Sarvestani, A.S., Jabbari, E., 2007. Effect of a low-molecular-weight cross-linkable macromer on electrospinning of poly(lactide-co-glycolide) fibers. Journal of Biomaterials Science Polymer Edition 18, 1369–1385.

Yelin, E., Cisternas, M., Foreman, A., Pasta, D., Murphy, L., Helmick, C., 2007. National and state medical expenditures and lost earnings attributable to arthritis and other rheumatic conditions—United States, 2003. MMWR. Morbidity and Mortality Weekly Report 56, 4.

Zargham, S., Bazgir, S., Tavakoli, A., Rashidi, A.S., Damerchely, R., 2012. The effect of flow rate on morphology and deposition area of electrospun Nylon 6 nanofiber. Journal of Engineered Fibers and Fabrics 7, 42–49.

Zhang, Y.Z., Venugopal, J., Huang, Z.M., Lim, C.T., Ramakrishna, S., 2006a. Crosslinking of the electrospun gelatin nanofibers. Polymer 47, 2911–2917.

Zhang, Y.Z., Wang, X., Feng, Y., Li, J., Lim, C.T., Ramakrishna, S., 2006b. Coaxial electrospinning of (fluorescein isothiocyanate-conjugated bovine serum albumin)-encapsulated poly(epsilon-caprolactone) nanofibers for sustained release. Biomacromolecules 7, 1049–1057.

Zheng, R., Duan, H., Xue, J., Liu, Y., Feng, B., Zhao, S., Zhu, Y., He, A., Zhang, W., Liu, W., Cao, Y., Zhou, G., 2014. The influence of Gelatin/PCL ratio and 3-D construct shape of electrospun membranes on cartilage regeneration. Biomaterials 35, 152–164.

Zhong, W., Zhang, W., Wang, S., Qin, J., 2013. Regulation of fibrochondrogenesis of mesenchymal stem cells in an integrated microfluidic platform embedded with biomimetic nanofibrous scaffolds. PloS One 8, e61283.

Zhou, J., Cao, C., Ma, X., Lin, J., 2010. Electrospinning of silk fibroin and collagen for vascular tissue engineering. International Journal of Biological Macromolecules 47, 514–519.

Nanocomposites for bone repair and osteointegration with soft tissues

11

W. Jiang, H. Liu
University of California, Riverside, CA, United States

11.1 Introduction

Biomaterials as an emerging category of materials have been developed and used for treating bone diseases and repairing bone tissue. Implants and fixations, for example, have been successfully used for treating bone injuries, but the ideal biocompatibility and bioactivity have not yet been fully achieved. The inflammations and foreign-body responses are still undermining the efficacy of the implants for orthopedic applications. The traditional implants like prostheses and tissue substitutes still cannot compete with original tissue. However, the idea of guided tissue regeneration has attracted increasing attention with more and more researchers realizing the potential of tissue engineering and stem cell therapy. Advances in materials, the keystone of engineering technologies, are therefore needed to meet the requirements in tissue engineering. Biomaterials for orthopedic applications and bone-tissue regeneration are usually processed into prostheses, fixation devices, scaffolds or fillers. Their applications may vary, but there are some fundamental requirements shared by all orthopedic applications, such as the mechanical properties, biocompatibility, bioactivity and machinability.

To better design biomaterials, it is greatly necessary to combine the knowledge in both bone biology and engineering. For the bone-biology part, chemical composition, structural arrangements and biological mechanism of bone are the basic knowledge to introduce. For the engineering part, principles of materials design and advanced-fabrication approaches are discussed.

11.2 Bone composition and structures

Bone is a heterogeneous, anisotropic and hierarchical composite with different structural arrangements at many scales (Liu and Webster, 2007b; Weiner and Traub, 1992; Rho et al., 1998). Each scale has unique structural units and chemical composition. The understanding of bone physiological structure and composition is indispensable for designing biomaterials, implants and devices.

Nanocomposites for Musculoskeletal Tissue Regeneration. http://dx.doi.org/10.1016/B978-1-78242-452-9.00011-X

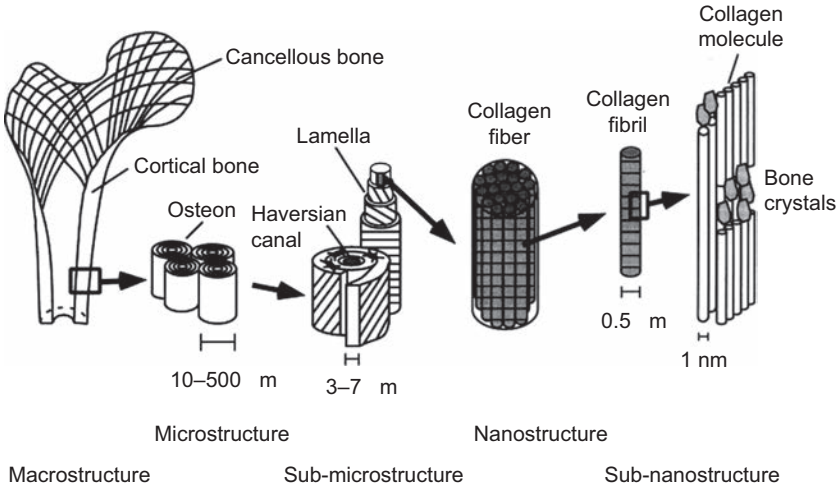

Figure 11.1 Hierarchical structures of bone in varied length scales (Rho et al., 1998).

11.2.1 Bone physiological structures

Bone structures are hierarchical. At different length scales, bone has different building blocks. Such delicate arrangements enable the integration of excellent mechanical properties as well as multiple biological functions. Rho et al. (1998) described bone structures at five length scales: macrostucrture, microstructure, sub-microstructure, nanostructure and subnanostructure. Fig. 11.1 (Rho et al., 1998) presented bone structures at different scales. It can be seen from Fig. 11.1 that bone has highly hierarchical structures. Each level, from macroscale to subnanoscale, has particular units and arrangements supporting and affecting larger and smaller scales. At macroscopic scale, bone is categorized by cortical and cancellous bone. Cortical bone is the denser outer part of the bone. Cancellous bone is the inner part of the bone with sponge-like structures. At microscopic scale (10–500 μm), osteon is the basic unit of cortical bone, whereas trabecula is the basic unit of cancellous bone. Osteon is a cylindrical structure formed by concentric lamellae. In the middle of the lamellae is the Harversian canal which allows the vessels and nerves to pass through. Trabecula is a rod- or plate-shaped tissue forming a sponge-like porous network. This structure makes the porosity of the cancellous bone higher than that of cortical bone. At submicroscopic scale (1–10 μm), both cortical and cancellous bone consist of lamellae, but the immature (newly formed) bone consists of collagen fibers. At nanoscopic scale (100–1000 nm) and sub-nanoscopic scale (less than 100 nm), collagen fibers are the building blocks forming the lamellae. Minerals are attached discontinuously to the collagen fibers.

The complexity of bone structure is rarely seen in the inorganic world, hence sound knowledge of bone structures is necessary for designing scaffolds, implants, prostheses and other devices for bone regeneration. For example, Ma (2008) points out in a review that simply replicating natural structure without a proper understanding may result in an ineffective materials design. One reason presented is that the extracellular

matrix conditions for normal tissue may not necessarily be optimal for tissue-engineering materials which require the function of accelerating tissue regeneration. In general, the structural features of bone are important considerations for understanding the difference between bone and humanmade materials. Moreover, the structures designed by nature may greatly inspire innovation in the biomimetic materials area.

11.2.2 Bone chemical composition

Apart from the hierarchy of bone structures discussed in the last section, bone chemical composition is another important aspect. Bone in nature is a nanostructured composite with an organic matrix and an inorganic reinforcing phase (Liu and Webster, 2007a). Bone chemical composition varies with many factors, such as age and individual health status. Calcified bone is composed of 25% organic matter and 75% inorganic matter (70% minerals and 5% water) by weight (Sommerfeldt and Rubin, 2001).

11.2.2.1 Organic phase

The organic phase of bone mainly contains Type I collagen (90%) and noncollagenous proteins (10%) (Liu and Webster, 2007a). A single Type I collagen molecule is formed by three polypeptide chains in a helix space arrangement (Weiner and Traub, 1992). Periodicity of the structure is approximately 67 nm with 40 nm for spacing (Rho et al., 1998).

11.2.2.2 Inorganic phase

The main inorganic composition of bone is hydroxyapatite (HA). The chemical formula of HA is $Ca_{10}(PO_4)_6(OH)_2$. The ratio of Ca atoms and P atoms (Ca/P ratio) is an important parameter of the bone chemistry. The Ca/P ratio of pure HA is 1.67, calculated by the chemical formula. In bone, however, impurities of sodium, carbonate and other ions often appear (Termine, 1988).

11.3 Healing mechanism of bone injury

The healing process of bone has been intensively studied and summarized (Carano and Filvaroff, 2003; Kalfas, 2001). Right after fracture, the injury causes inflammatory responses and hematoma. This stage may last hours to days. Then, the angiogenesis process will begin and collagen matrix will be deposited. The result is the formation of the soft callus. In the first 4–6 weeks, the soft callus is not strong enough to provide adequate mechanical support, so fixations are needed to secure it. Next, the soft callus is mineralized into hard callus. Notably, the ossification may fail if the necessary immobilization is not provided. The final stage is the slow recovery and remodeling of the fractured bone. This stage lasts over months to years.

Understanding the healing process helps to better design biomaterials. For example, biodegradable fixations for orthopedic applications may undergo decrease in

mechanical properties after implantation. It is necessary for the fixations to maintain certain mechanical properties before the damaged bone tissue can provide adequate mechanical support (for bone fracture, the time period is typically 3–6 months (Kalfas, 2001)). Another aspect that should be carefully considered is the inflammatory response. Injury induces inflammatory responses which are also affected by the implanting materials. Proper design and refinement of materials hopefully regulates the healing process by regulating the inflammatory response.

11.4 Bone-tissue repair and regeneration

Principal therapies for bone defects and injuries include bone-tissue transplantation, artificial prosthesis implantation and tissue-engineering treatments. Autologous transplantation of cells and tissue is the gold standard (Healy and Guldberg, 2007). The scarcity of autologous tissue, however, limits its further application (Healy and Guldberg, 2007). Therefore, much effort has been put into the development of other approaches.

Artificial prostheses serve as substitutes for damaged bone tissue. Although these can significantly improve the quality of life of many patients, failure often occurs (Rose and Oreffo, 2002). Unsatisfactory long-term biocompatibility and chronic inflammation are major challenges.

Tissue engineering as a rapidly growing domain attracts much attention in academia. Rather than attempt to transplant or fabricate bone tissue, tissue engineering focuses on regeneration of the damaged tissue. Tissue engineering promises to address the aforementioned problems. It does not require tissue donors, avoids undesired chronic foreign body responses and reaches the maximum degree of recovery of the damaged tissue.

In situ regeneration is an inspiring idea, which requires that implanted materials or scaffolds stimulate local bone-tissue regeneration (Griffith and Naughton, 2002). Combining growth factors with scaffolds is a potential approach to stimulate bone-tissue regeneration and growth (Mistry and Mikos, 2005). When materials degrade, growth factors are released to stimulate new bone formation (Mistry and Mikos, 2005). Still, this realm is new and needs further exploration and development.

11.5 Materials for bone repair and regeneration

Biomaterials directly contact and interact with the body environment. Chemical composition, microstructure, surface properties and mechanical and biological performance are considered the most important aspects for designing and developing biomaterials. They serve as the building blocks for the fixations, prostheses, scaffolds, biosensors or other devices for various medical applications.

Decades ago, scientists and engineers sought for materials that mechanically match human tissue, remain stable in contact with human tissue and do not induce severe

immunological responses. However, with no materials being inert, the long-term presence of biomaterials in the body raises the concern of their safety profile. Now the burgeoning concept of tissue engineering raises more stringent standards, in addition to minimal foreign body responses and safety profile, those materials should be able to degrade or be absorbed and concurrently guide tissue regeneration. Big challenges remain and much research needs to be done in the biomaterials area to meet clinical requirements and fulfill better tissue repair and regeneration. This ambitious goal also requires high-degree convergence and integration of medicine, bioengineering and materials science.

For bone repair and regeneration, understanding the structures, composition, and mechanical, chemical and biological properties of bone is necessary to design biomaterials and medical devices. The basics of bone physiology and healing mechanism were introduced in previous sections. In this section, the rationale for design and the major types of currently used biomaterials for bone repair and regeneration will be discussed.

11.5.1 Principles of designing biomaterials for bone repair and regeneration

Bone-repair biomaterials must be mechanically matched with bone tissue, avoid serious immunological response and be nontoxic to the human body (Hench and Polak, 2002). These standards, however still important, cannot meet future clinical requirements. Today, ideal biomaterials used for bone repair and regeneration should be osteoinductive (induce bone formation and differentiation), osteoconductive (allow bone tissue to attach and pass through) and have a good osteointegration (adequately strong bonding to bone tissue). The three principles, in addition to traditional criteria, are also the major considerations of materials design for bone-tissue engineering.

Polymers, ceramics, glass, metals and their composites have all been intensively investigated as candidate for bone-repair materials and substitutes. Knowledge and techniques of these materials are imparted from conventional materials science. However, it is extremely difficult to replicate living tissue of such high delicacy and complexity. Rational strategy is to mimic the living tissue, such as to develop materials with composition and structure close to the target tissue. For example, HA has been widely used for orthopedic applications. One reason is the fact that HA crystals are widely distributed in bone-collagen fibers.

Single-phase materials cannot satisfyingly mimic bone tissues which are in nature multiphase nanocomposites (Liu and Webster, 2007a). Nanocomposites, therefore, draw much attention due to their compositions and structures resembling bone tissue. Nanomaterials are those with structural features between 1 and 100 nm in at least one dimension. Nanomaterials have a high surface energy due to their large surface area. The quantum effects of nanomaterials also give them novel properties. Nanocomposites mimic bone tissue not only in chemical composition, but also in microstructure. It has been proved that nanocomposites can promote cell adhesion and proliferation (Webster et al., 2001, 2000; Kim et al., 2010).

11.5.2 Polymeric biomaterials for bone repair and regeneration

Polymers are the most intensively investigated materials for biomedical applications. Polymers have similar chemical compositions to living tissue. Their flexibility and versatility in structure and composition enable precise control and modification of properties. Polymers can be categorized into synthetic and natural polymers. The field of synthetic polymers has been intensively explored for years and remarkable progress has been achieved (Stevens, 2008; Langer and Tirrell, 2004; Bose et al., 2012; Puppi et al., 2010), and the related knowledge is, therefore, comprehensive and easily available. Natural polymers have a high degree of complexity and better biological properties, but availability is often limited, the control of its structures and compositions is far from sufficiently developed and industrial production is still in the early stage. Besides, natural polymers deriving from other living creatures possibly lead to immunological problems (Seal et al., 2001; Cheung et al., 2007).

11.5.2.1 Synthetic polymers

Poly(lactic-co-glycolic) acid (PLGA) is the copolymer of poly(lactic acid) (PLA) and poly(glycolic acid) (PGA). It has been approved by FDA for biomedical applications. It is biodegradable and has been reported to be nontoxic to human body (Athanasiou et al., 1996). The repeat unit of PLGA is shown in Fig. 11.2. The repeat unit of PLGA consists of lactic acid (LA) and glycolic acid (GA) monomers. PLGA is usually expressed as PLGA (x:y) in which x and y represent the percentage of the numbers of LA and GA monomers, respectively, in each repeat unit. For example, PLGA (50:50) has 100 LA monomers and 100 GA monomers in every 100 repeat units. PLGA undergoes hydrolytic degradation when contacting body fluids. LA has one more methyl side group than GA. This side group has a steric shielding effect which makes LA more hydrophobic. The hydrophilicity–hydrophobicity and the crystallinity of PLGA are tunable by changing the LA/GA ratio. PLGA has a long history of clinical uses, which attracts many researchers to further explore its applications in implants, scaffolds and drug delivery. Another property that makes PLGA a popular candidate is that PLGA can be easily processed into three-dimensional (3D) porous bulk (Seal et al., 2001). However, the mechanical properties of PLGA cannot compete with those of metallic materials, which limits its possible uses in orthopedic applications.

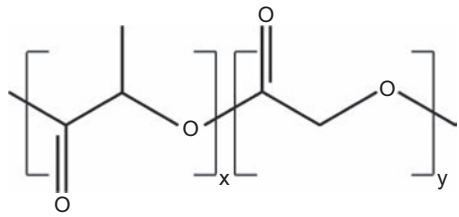

Figure 11.2 Structure of repeat unit of PLGA. x represents LA monomer, y represents GA monomer.

Polycaprolactone (PCL) is another biodegradable polymer approved by FDA for medical uses. It can be processed into porous structures. A long-term in vivo degradability study indicated that PCL capsules can remain mechanically intact for 2 years (Sun et al., 2006). PCL is highly crystalline and hydrophobic, which accounts for its slow degradation. In fact, this slow degradation makes PCL more hopeful as long-term implants than as scaffolds (Liu and Webster, 2007a).

Polyethylene (PE) is used as prostheses and implants. PE can be categorized into low molecular weight polyethylene, high molecular weight polyethylene and ultra-high molecular weight polyethylene (UHMWPE). UHMWPE has high strength and high Young's modulus, which allow its wide application in orthopedic surgery. PE is nondegradable, so it is usually used for permanent implants.

Cross-linked polyanhybrides are emerging as new orthopedic biomaterials attaining both degradability and high strength (Muggli et al., 1999). Interestingly, cross-linked polyanhybrides have a surface-degrading mechanism (Muggli et al., 1999). Unlike bulk degradation, the surface degradation allows polymers to maintain mechanical property and integrity after a significant mass loss (Muggli et al., 1999).

11.5.2.2 Natural polymers

Lessons from nature have been incorporated into many research outcomes in the field of natural polymeric biomaterials. Natural polymers perform nicely as scaffold materials. Their chemical compositions and structural arrangements more closely resemble living tissue, and they have excellent biological properties. Nonetheless, because the natural polymers are derived from other living creatures, the pathogens and the potential immunological responses they stimulate may be concerns. Besides, it is very difficult to precisely control the fabrication of natural polymers. The limited number of sources is another challenge.

One strategy to derive natural polymers is to directly "modify" living tissue. Demineralized bone matrix (DBM), for example, is obtained from natural bone by removing the mineral composition of bone, with acid demineralization being the major step to remove the minerals (Gruskin et al., 2012). The removal of minerals maximally preserves the structure of the nonmineralized part of the original bone and the bioactive factors such as collagen and growth factors, but mechanical strength is compromised (Kao and Scott, 2007; Gruskin et al., 2012).

Collagen is the fibrous protein distributed in bone tissue. About 90% of the organic phase in bone is collagen (Liu and Webster, 2007a). Varying in chemistry and structure, up to 28 types of collagen exist. Three polypeptides form a triple helix of collagenous fiber (Weiner and Traub, 1992). Despite the biomolecular composition in nature that resembles to living tissue, collagen has poor mechanical properties. A possible solution is combination with a reinforcing component such as ceramics (Lawson and Czernuszka, 1998).

Another attractive natural polymer that occurs in the human body is hyaluronic acid. Hyaluronic acid possesses excellent biocompatibility. Jansen et al. (2004) investigated a hyaluronan-based conduit, and no cytotoxicity was found. Cross-linking is very important in tailoring the properties and the application of hyaluronic acid. For

example, cross-linked hyaluronic acid with slow degradation and excellent biocompatibility has been achieved (Liu et al., 2005).

The advantage of collagen and hyaluronic acid for bone-tissue engineering can be easily seen because of their abundant presence in the human body. However, there are natural polymers deriving from other animals that also hold great potential for this application. Chitosan, a natural polymer usually obtained from shrimp shell, is a linear chain polymer the repeat unit for which is D-glucosamine. The amino group of D-glucosamine can be acetylated, and the degree of acetylation greatly affects the properties of chitosan. Chitosan has been reported to be biocompatible (VandeVord et al., 2002; Mi et al., 2002). Despite the excellent biological performance, its poor mechanical strength seriously limits its applications in bone-tissue engineering (El-Sherbiny and El-Baz, 2015).

11.5.3 Bioactive ceramics and bioactive glass for bone repair and regeneration

Although ceramics are brittle, they have created wide interest in their applications as orthopedic biomaterials due to chemical composition similar to bone, the major constituent for which is inorganic minerals (Sommerfeldt and Rubin, 2001). Research also demonstrated the capacity of bioactive ceramics to stimulate new bone formation (Yuan et al., 1998).

11.5.3.1 Calcium phosphate ceramics

Calcium phosphate ceramics constitute the majority of bone minerals. For this reason, it is rational to select calcium phosphate ceramics as candidate for orthopedic applications. Research revealed that calcium phosphate is biocompatible, osteoconductive and potentially osteoinductive (LeGeros et al., 2003; Yuan et al., 1998; LeGeros, 2008). Hydroxyapatite (HA) is the most common phase in bone minerals. The chemical formula of HA is $Ca_{10}(PO_4)_6(OH)_2$. The Ca/P ratio affects the properties of materials such as grain size and porosity, nitric oxide production and influence on cell behaviors (Liu et al., 2008). HA particles can be fabricated into different morphologies (Zhou and Lee, 2011), which further increase the degree they mimic human bone tissue in which HA presents a rod-like shape (Zhou and Lee, 2011). HA particles with various morphologies also show potential in fabricating scaffolds, coatings and enhancing osteoinductivity (Zhou and Lee, 2011). HA as a drug carrier is another increasingly interesting topic in academia. For most drug carrier matrices, polymers are ideal materials, but in bone-tissue regeneration, HA has particular applications (Ginebra et al., 2006). HA also has applications in bone fillers. Normally, HA is mixed with aqueous phase to fabricate cement fillers which are then injected into defect sites. In summary, it can be predicted that interdisciplinary research on HA concerning biofunctionalization, improvement of mechanical properties and combinations with other phases will continue, which may broaden its applications in the orthopedic domain.

Tricalcium phosphate (TCP), with chemical formula $Ca_3(PO_4)_2$, is another calcium phosphate ceramic. There are two types of TCP: α-TCP and β-TCP. β-TCP is more

thermodynamically stable below 1100°C (Kamitakahara et al., 2008). β-TCP is more often investigated, but α-TCP still attracts much attention due to its higher solubility (Kamitakahara et al., 2008).

11.5.3.2 Bioactive glass

The bioactive glass for orthopedic applications was first conceived by Professor Larry Hench and his colleagues in the late 1960s (Hench, 2006). He investigated the Na_2O–CaO–SiO_2–P_2O_5 system. Bioactive glass then grew rapidly as a new category of biomaterials. For glass, the chemical composition and degradation rate are easy to control, but its brittleness impedes its further application (Fu et al., 2011).

There are three types of bioactive glass: silicate-based, borate-based and phosphate-based glass. Typical silicate-based bioactive glass, 45S5, has low SiO_2 content and high Na_2O and CaO content (Rahaman et al., 2011). Once 45S5 glass is implanted, a carbonate-substituted hydroxyapatite (HCA) layer will be formed, which explains the tight bonding to bone (Rahaman et al., 2011). This 45S5 glass also demonstrates good biocompatibility (Wilson et al., 1981). Borate-based glass substitutes B_2O_3 for SiO_2. Borate-based glass shows the potential to match the degradation rate of bone (Rahaman et al., 2011) and capacity of supporting osteogenic differentiation (Marion et al., 2005). Phosphate-based glass contains P_2O_5. P_2O_5–CaO–Na_2O–TiO_2 glass was found to be nontoxic (Navarro et al., 2004), but another study (Franks et al., 2000; Salih et al., 2000) investigating Na_2O–CaO–P_2O_5 glass demonstrated the inhibiting effects on human osteoblast cell lines when solubility is high, and promoting effects when solubility is low, suggesting the ion release and pH increase caused by degradation significantly influence cytotoxicity.

11.5.4 Metallic biomaterials for bone substitutes and implants

Metallic biomaterials have a long history of medical uses. Metals and alloys have enough strength for heavy-load implant applications, and less brittleness compared with ceramics. Metallic biomaterials are also relatively easier to be processed into the desired shape. Nevertheless, metallic biomaterials normally have poor biocompatibility.

11.5.4.1 Nondegradable metals

The conventional solution to the poor biocompatibility of metallic materials is to select the materials inert in the human body. Stainless steel, for example, has nice resistance to corrosion due to the addition of Cr, which results in its broad clinical uses. The only implant material entering clinical treatments is 316L stainless steel, an austenitic stainless steel (Niinomi, 2008). Co-based alloys have favorable behavior for fabricating wear-bearing devices (Niinomi, 2008). Co alloys often need addition of Ni to increase the processibility (Niinomi, 2008), which remains a challenge.

Ti and Ti alloys have even better mechanical properties, and do not contain Ni. Ti and Ti alloys are also extremely stable in the human body. Pure Ti and Ti-6Al-4V are

the most common two materials for biomedical applications. Surface modifications are also widely investigated to improve the biocompatibility and bioactivity of Ti and Ti alloys (Liu et al., 2004; Niinomi, 2003).

11.5.4.2 Biodegradable metals: new category

Unlike the nondegradable metals with a bioinertness property as the gold standard, biodegradable metals are designed to be biocompatible and bioactive. It is expected that the degradable metals can be absorbed after a certain time period to (1) eliminate the need of secondary surgery to remove the implants, and (2) avoid chronic complications. In the orthopedic area, Mg and Mg alloys are hopeful candidates due to their degradability, excellent biocompatibility and mechanical properties (Zeng et al., 2008). Their degradation, however, is too rapid to meet the clinical need. The fast degradation also produces hydrogen and increases pH (degradation produces OH^-). The solution includes alloying (Zhang et al., 2010; Hanzi et al., 2009) and surface modification (Johnson et al., 2013; Iskandar et al., 2013). Mg-based metallic glasses are also developed to address these problems (Zberg et al., 2009; Yu et al., 2013). Zinc alloys are also biodegradable. Zn–Mg alloy of slower degradation was prepared as alternative to Mg (Vojtěch et al., 2011). Besides, although iron as another biodegradable metal was used for cardiovascular application (Peuster et al., 2001), there is little report for its orthopedic application.

11.5.5 Nanocomposites for bone repair and regeneration

Two aspects should be considered to approach satisfactory nanocomposites: how to fabricate composites and how to nanoscale them. To fabricate composites, several principles should be observed. First, the components should be mutually chemically stable. Second, the combination between different components should be sufficiently strong. Third, in composite materials science, thermal expansion coefficients of each component should be matched. For composites used in the human body, the temperature should be maintained around 37°C. However, it still needs to be considered whether the fabrication process should undergo a significant temperature change. To make materials nanoscaled, top-down and bottom-up methods are both available. The former obtains nanomaterials from macroscopic bulk materials, whereas the latter assembles from molecules or atoms. Mechanical, chemical or biomimicking methods can obtain desired nanomaterials. For example, ball milling is used to obtain micro- and nanoparticles via mechanical impact. It is a mature process in industry, so high production can be reached. Wet chemistry methods, including the sol–gel method, the homogeneous precipitation method and the hydrothermal method, not only can obtain uniform particle size and controllable particle morphology, but also allow accurate control of chemical composition. Their costs are also low in the laboratory. Biomimicking methods are promising in meeting the higher requirements of nanocomposites in the future, but

their studies are just in the beginning stage. Such approaches include self-assembly, biomineralization, and so forth.

11.5.5.1 Ceramic–polymer nanocomposites

Most research in synthetic nanocomposites dominantly focus on ceramic–polymers and ceramic–biomolecular composite systems. Specifically, the latter disperse ceramic particles or fibers into polymers or biomolecular matrix. Nano-HA is a hopeful candidate for dispersion because (1) nano-HA is the major constituent in bone, and (2) ceramics can reinforce the mechanical properties of polymers. HA–polymer nanocomposites have been intensively studied and used to fabricate scaffolds: composites that have nanosized needle-like HA particles in PLA matrix were developed to fabricate 3D porous scaffolds (Kothapalli et al., 2005). Nanofibrous HA–PLGA nanocomposite scaffolds were also obtained (Jose et al., 2009). To achieve better dispersion of HA in PLGA matrix, high-power sonication was used to fabricate nano-HA–PLGA as coating materials (Johnson et al., 2013). HA–PLGA was also developed with microspheric morphology for a controlled delivery system with improved osteoinductivity (Shi et al., 2009). Apart from nano-HA–PLA systems, other composites have also been investigated, such as nano-HA–PCL composites (Hao et al., 2003) and nano-HA–polyanhydride composites (Li et al., 2003).

In addition to HA, silica has been used to improve PCL mechanical properties without compromising biocompatibility (Calandrelli et al., 2010). In this study, PCL and silica surfaces were modified to chemically bond to each other, which reflects the criterion that nanocomposites should have a strong combination between components. Another study (Wei et al., 2009) observed the formation of apatite and the promoted cell proliferation on a calcium–silica-reinforced PCL, which further justifies the use of silica–polymer composite for bone-tissue engineering.

Cheng et al. (2013) incorporated carbon nanotube (CNT) into PLGA matrix to improve its overall properties as scaffold materials for bone-tissue engineering. The results showed that the incorporation of CNT increased the compressive modulus and roughness of PLGA scaffolds. It was also observed that osteoblast adhesion, growth and osteogenic differentiation were increased on CNT–PLGA composites.

11.5.5.2 Ceramic–biomolecules nanocomposites

Biomolecules are the desired matrix materials for fabricating nanocomposites. Biomolecules are a suitable platform for cells to attach and proliferate, which comes from their structures and compositions that more closely resemble to extracellular matrix. Their highly hierarchical and anisotropic structures are particularly difficult to replicate on synthetic materials. Therefore, biomolecule matrix is a much easier way toward high biological performance of nanocomposite. Because of well-established material technologies that can successfully incorporate, reinforce, and precisely control the structure and properties of different phases (nanoparticles, nanotubes, nanofibers, etc.), ceramic–biomolecule nanocomposites are promising to achieve both superior biological performance and desired mechanical properties. For example, to

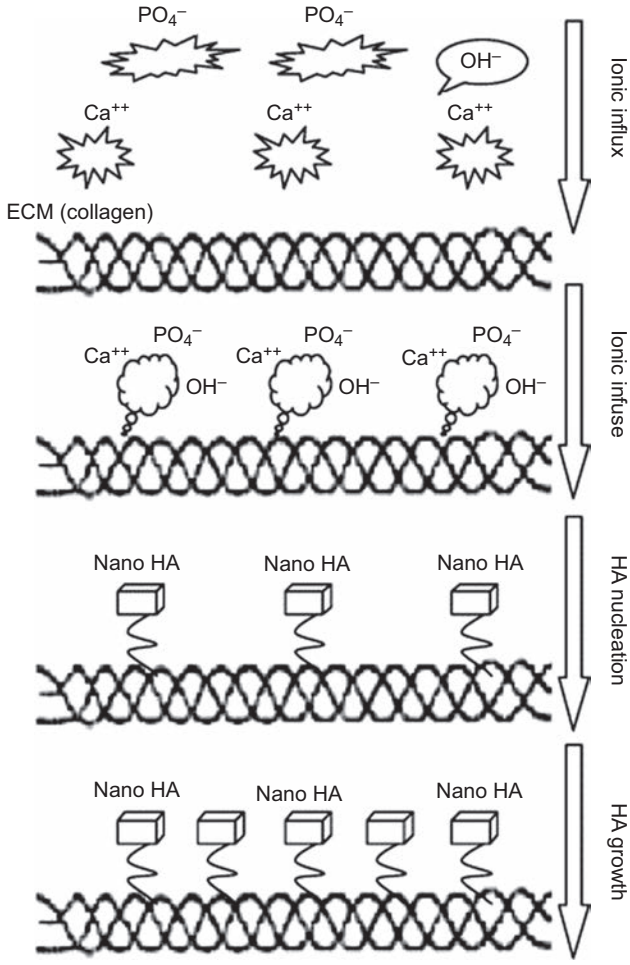

Figure 11.3 Procedure of self-assembly nano-HA on collagen (Murugan and Ramakrishna, 2005).

achieve better bonding between collagen and HA, a self-assembly method in which HA nucleates and grows onto collagen was developed (Murugan and Ramakrishna, 2005). Fig. 11.3 (Murugan and Ramakrishna, 2005) shows this procedure. This work reported improved mechanical properties, excellent biocompatibility and bioactivity. Moreover, ceramic–biomolecule nanocomposites themselves can be used as the reinforcement phase into synthetic polymer matrix. Liao et al. (2004) dispersed nano-HA–collagen nanocomposites into PLA matrix. This design overcomes the weak mechanical strength of nano-HA–collagen nanocomposites and compensates for the poor biological performance of PLA. These hierarchical composites show controllable mechanical properties and bioactivity.

11.5.6 Nanocomposites osteointegration with soft tissue

Nanocomposites demonstrate the hope of enhancing osteointegration and osteoinductivity. This effect also applies to the soft tissue in bone. Nano-HA–PLA has been proved to have good cell attachment to human cartilage (Cheng et al., 2006). Type II collagen at nanoscale size can support chondrocyte growth (Matthews et al., 2003). In terms of metals, cell attachment on anodized Ti shows a strong dependence on tube diameter (Park et al., 2007). The mechanism of how scaling affects osteointegration still needs further investigation, but one point is clear in that the selection of components and the design of microstructures will determine the osteointegration of nanocomposites with soft tissue. Therefore, (1) designing nanocomposites with constituent materials already known to have good osteointegration with cartilage tissue, and (2) fabricating biomimetic nanostructures are two hopeful approaches to obtain the desired osteointegration with soft tissue.

11.6 Conclusion

Biomaterials are essential for orthopedic implants and bone-tissue regeneration. Implants, fillers and fixation devices will continue taking the dominant position in the orthopedic devices market, which generates a big demand for implant materials. Biomedical metals, ceramics and polymers need further improvement of their mechanical properties and biocompatibility. Nanocomposites are especially hopeful candidates for future implant materials. With tissue engineering progressing from concept into practice, biodegradable and bioactive materials will attract increasing attention. The research into biodegradable scaffolds and implants, biomimetic materials, nanocomposites for biomedical applications, and their osteoconductivity, osteoinductivity and osteointegration will show considerable progress in the foreseeable future. In this author's opinion, the current synthetic materials, despite their great success in the past, have intrinsic limitations. It is almost impossible for them to replace naturally grown tissue and organs without any loss of biological functions. The living tissues are far more complicated than any contemporary humanmade materials. The burgeoning tissue-engineering field, however, which attempts to guide tissue regeneration, in vitro or in vivo, shows the best promise in the foreseeable future. This trend raises rigid requirements for materials design, fabrication and characterization. As in the case of bone, the mechanical properties should be especially considered, which pushes the requirements even higher. It was widely known in the past that the urgent needs of the aviation industry stimulated the development of composites. A similar thing is happening again. Higher material requirements are urged by tissue engineering, and conventional single-phase materials can no longer compete. Therefore, it is expected that nanocomposites will strongly intrigue academia and industry due to their scaling effects and diversity in composition, structure and morphology. These superiorities still have not been fully exploited.

References

Athanasiou, K.A., Niederauer, G.G., Agrawal, C., 1996. Sterilization, toxicity, biocompatibility and clinical applications of polylactic acid/polyglycolic acid copolymers. Biomaterials 17, 93–102.

Bose, S., Roy, M., Bandyopadhyay, A., 2012. Recent advances in bone tissue engineering scaffolds. Trends in Biotechnology 30, 546–554.

Calandrelli, L., Annunziata, M., Della Ragione, F., Laurienzo, P., Malinconico, M., Oliva, A., 2010. Development and performance analysis of PCL/silica nanocomposites for bone regeneration. Journal of Materials Science: Materials in Medicine 21, 2923–2936.

Carano, R.A., Filvaroff, E.H., 2003. Angiogenesis and bone repair. Drug Discovery Today 8, 980–989.

Cheng, L., Zhang, S.M., Chen, P., Huang, S., Cao, R.R., Zhou, W., Liu, J., Luo, Q., Gong, H., 2006. Fabrication and characterization of nano-hydroxyapatite/poly (D,L-lactide) composite porous scaffolds for human cartilage tissue engineering. Key Engineering Materials 309, 943–948.

Cheng, Q., Rutledge, K., Jabbarzadeh, E., 2013. Carbon nanotube–poly (lactide-co-glycolide) composite scaffolds for bone tissue engineering applications. Annals of Biomedical Engineering 41, 904–916.

Cheung, H.-Y., Lau, K.-T., Lu, T.-P., Hui, D., 2007. A critical review on polymer-based bio-engineered materials for scaffold development. Composites Part B: Engineering 38, 291–300.

El-Sherbiny, I.M., El-Baz, N.M., 2015. A Review on Bionanocomposites Based on Chitosan and Its Derivatives for Biomedical Applications. Eco-friendly Polymer Nanocomposites. Springer.

Franks, K., Abrahams, I., Knowles, J., 2000. Development of soluble glasses for biomedical use Part I: in vitro solubility measurement. Journal of Materials Science: Materials in Medicine 11, 609–614.

Fu, Q., Saiz, E., Rahaman, M.N., Tomsia, A.P., 2011. Bioactive glass scaffolds for bone tissue engineering: state of the art and future perspectives. Materials Science and Engineering: C 31, 1245–1256.

Ginebra, M., Traykova, T., Planell, J., 2006. Calcium phosphate cements as bone drug delivery systems: a review. Journal of Controlled Release 113, 102–110.

Griffith, L.G., Naughton, G., 2002. Tissue engineering–current challenges and expanding opportunities. Science 295, 1009–1014.

Gruskin, E., Doll, B.A., Futrell, F.W., Schmitz, J.P., Hollinger, J.O., 2012. Demineralized bone matrix in bone repair: history and use. Advanced Drug Delivery Reviews 64, 1063–1077.

Hanzi, A., Sologubenko, A.S., Uggowitzer, P.J., 2009. Design strategy for new biodegradable Mg-Y-Zn alloys for medical applications. International Journal of Materials Research 100, 1127.

Hao, J., Liu, Y., Zhou, S., Li, Z., Deng, X., 2003. Investigation of nanocomposites based on semi-interpenetrating network of [l-poly (ε-caprolactone)]/[net-poly (ε-caprolactone)] and hydroxyapatite nanocrystals. Biomaterials 24, 1531–1539.

Healy, K., Guldberg, R., 2007. Bone tissue engineering. Journal of Musculoskeletal and Neuronal Interactions 7, 328.

Hench, L.L., 2006. The story of Bioglass®. Journal of Materials Science: Materials in Medicine 17, 967–978.

Hench, L.L., Polak, J.M., 2002. Third-generation biomedical materials. Science Signaling 295, 1014.

Iskandar, M.E., Aslani, A., Liu, H., 2013. The effects of nanostructured hydroxyapatite coating on the biodegradation and cytocompatibility of magnesium implants. Journal of Biomedical Materials Research Part A 101 (8), 2340–2354.

Jansen, K., Van Der Werff, J., Van Wachem, P., Nicolai, J.A., De Leij, L., Van Luyn, M., 2004. A hyaluronan-based nerve guide: in vitro cytotoxicity, subcutaneous tissue reactions, and degradation in the rat. Biomaterials 25, 483–489.

Johnson, I., Akari, K., Liu, H., 2013. Nanostructured hydroxyapatite/poly (lactic-co-glycolic acid) composite coating for controlling magnesium degradation in simulated body fluid. Nanotechnology 24, 375103.

Jose, M.V., Thomas, V., Johnson, K.T., Dean, D.R., Nyairo, E., 2009. Aligned PLGA/HA nanofibrous nanocomposite scaffolds for bone tissue engineering. Acta Biomaterialia 5, 305–315.

Kalfas, I.H., 2001. Principles of bone healing. Neurosurgical Focus 10, 1–4.

Kamitakahara, M., Ohtsuki, C., Miyazaki, T., 2008. Review paper: behavior of ceramic biomaterials derived from tricalcium phosphate in physiological condition. Journal of Biomaterials Applications 23, 197–212.

Kao, S.T., Scott, D.D., 2007. A review of bone substitutes. Oral and Maxillofacial Surgery Clinics of North America 19, 513–521.

Kim, T.G., Park, S.-H., Chung, H.J., Yang, D.-Y., Park, T.G., 2010. Microstructured scaffold coated with hydroxyapatite/collagen nanocomposite multilayer for enhanced osteogenic induction of human mesenchymal stem cells. Journal of Materials Chemistry 20, 8927–8933.

Kothapalli, C.R., Shaw, M.T., Wei, M., 2005. Biodegradable HA-PLA 3-D porous scaffolds: effect of nano-sized filler content on scaffold properties. Acta Biomaterialia 1, 653–662.

Langer, R., Tirrell, D.A., 2004. Designing materials for biology and medicine. Nature 428, 487–492.

Lawson, A.C., Czernuszka, J., 1998. Collagen-calcium phosphate composites. Proceedings of the Institution of Mechanical Engineers, Part H: Journal of Engineering in Medicine 212, 413–425.

LeGeros, R., Lin, S., Rohanizadeh, R., Mijares, D., Legeros, J., 2003. Biphasic calcium phosphate bioceramics: preparation, properties and applications. Journal of Materials Science: Materials in Medicine 14, 201–209.

LeGeros, R.Z., 2008. Calcium phosphate-based osteoinductive materials. Chemical Reviews 108, 4742–4753.

Li, H., Chen, Y., Xie, Y., 2003. Photo-crosslinking polymerization to prepare polyanhydride/needle-like hydroxyapatite biodegradable nanocomposite for orthopedic application. Materials Letters 57, 2848–2854.

Liao, S., Cui, F., Zhang, W., Feng, Q., 2004. Hierarchically biomimetic bone scaffold materials: nano–HA/collagen/PLA composite. Journal of Biomedical Materials Research Part B: Applied Biomaterials 69, 158–165.

Liu, H., Webster, T.J., 2007a. Bioinspired nanocomposites for orthopedic applications. In: Nanotechnology for the Regeneration of Hard and Soft Tissues. World Scientific Publishing Company, Toh Tuck Link, Singapore.

Liu, H., Webster, T.J., 2007b. Nanomedicine for implants: a review of studies and necessary experimental tools. Biomaterials 28, 354–369.

Liu, H., Yazici, H., Ergun, C., Webster, T.J., Bermek, H., 2008. An in vitro evaluation of the Ca/P ratio for the cytocompatibility of nano-to-micron particulate calcium phosphates for bone regeneration. Acta Biomaterialia 4, 1472–1479.

Liu, X., Chu, P.K., Ding, C., 2004. Surface modification of titanium, titanium alloys, and related materials for biomedical applications. Materials Science and Engineering: R: Reports 47, 49–121.

Liu, Y., Shu, X.Z., Prestwich, G.D., 2005. Biocompatibility and stability of disulfide-cross-linked hyaluronan films. Biomaterials 26, 4737–4746.

Ma, P.X., 2008. Biomimetic materials for tissue engineering. Advanced Drug Delivery Reviews 60, 184–198.

Marion, N.W., Liang, W., Reilly, G.C., Day, D.E., Rahaman, M.N., Mao, J.J., 2005. Borate glass supports the in vitro osteogenic differentiation of human mesenchymal stem cells. Mechanics of Advanced Materials and Structures 12, 239–246.

Matthews, J.A., Boland, E.D., Wnek, G.E., Simpson, D.G., Bowlin, G.L., 2003. Electrospinning of collagen type II: a feasibility study. Journal of Bioactive and Compatible Polymers 18, 125–134.

Mi, F.-L., Tan, Y.-C., Liang, H.-F., Sung, H.-W., 2002. In vivo biocompatibility and degradability of a novel injectable-chitosan-based implant. Biomaterials 23, 181–191.

Mistry, A.S., Mikos, A.G., 2005. Tissue Engineering Strategies for Bone Regeneration. Regenerative Medicine II. Springer.

Muggli, D.S., Burkoth, A.K., Anseth, K.S., 1999. Crosslinked polyanhydrides for use in orthopedic applications: degradation behavior and mechanics. Journal of Biomedical Materials Research 46, 271–278.

Murugan, R., Ramakrishna, S., 2005. Development of nanocomposites for bone grafting. Composites Science and Technology 65, 2385–2406.

Navarro, M., Del Valle, S., Martínez, S., Zeppetelli, S., Ambrosio, L., Planell, J.A., Ginebra, M.P., 2004. New macroporous calcium phosphate glass ceramic for guided bone regeneration. Biomaterials 25, 4233–4241.

Niinomi, M., 2003. Recent research and development in titanium alloys for biomedical applications and healthcare goods. Science and Technology of Advanced Materials 4, 445–454.

Niinomi, M., 2008. Metallic biomaterials. Journal of Artificial Organs 11, 105–110.

Park, J., Bauer, S., Von Der Mark, K., Schmuki, P., 2007. Nanosize and vitality: TiO_2 nanotube diameter directs cell fate. Nano Letters 7, 1686–1691.

Peuster, M., Wohlsein, P., Brügmann, M., Ehlerding, M., Seidler, K., Fink, C., Brauer, H., Fischer, A., Hausdorf, G., 2001. A novel approach to temporary stenting: degradable cardiovascular stents produced from corrodible metal—results 6–18 months after implantation into New Zealand white rabbits. Heart 86, 563–569.

Puppi, D., Chiellini, F., Piras, A., Chiellini, E., 2010. Polymeric materials for bone and cartilage repair. Progress in Polymer Science 35, 403–440.

Rahaman, M.N., Day, D.E., Sonny Bal, B., Fu, Q., Jung, S.B., Bonewald, L.F., Tomsia, A.P., 2011. Bioactive glass in tissue engineering. Acta Biomaterialia 7, 2355–2373.

Rho, J.-Y., Kuhn-Spearing, L., Zioupos, P., 1998. Mechanical properties and the hierarchical structure of bone. Medical Engineering & Physics 20, 92–102.

Rose, F.R., Oreffo, R.O., 2002. Bone tissue engineering: hope vs hype. Biochemical and Biophysical Research Communications 292, 1–7.

Salih, V., Franks, K., James, M., Hastings, G., Knowles, J., Olsen, I., 2000. Development of soluble glasses for biomedical use Part II: the biological response of human osteoblast cell lines to phosphate-based soluble glasses. Journal of Materials Science: Materials in Medicine 11, 615–620.

Seal, B., Otero, T., Panitch, A., 2001. Polymeric biomaterials for tissue and organ regeneration. Materials Science and Engineering: R: Reports 34, 147–230.

Shi, X., Wang, Y., Ren, L., Gong, Y., Wang, D.-A., 2009. Enhancing alendronate release from a novel PLGA/hydroxyapatite microspheric system for bone repairing applications. Pharmaceutical Research 26, 422–430.

Sommerfeldt, D., Rubin, C., 2001. Biology of bone and how it orchestrates the form and function of the skeleton. European Spine Journal 10, S86–S95.

Stevens, M.M., 2008. Biomaterials for bone tissue engineering. Materials Today 11, 18–25.

Sun, H., Mei, L., Song, C., Cui, X., Wang, P., 2006. The in vivo degradation, absorption and excretion of PCL-based implant. Biomaterials 27, 1735–1740.

Termine, J.D., 1988. Non-collagen proteins in bone. In: Cell and Molecular Biology of Vertebrate Hard Tissues, Ciba Foundation Symposium, pp. 178–190.

Vandevord, P.J., Matthew, H.W., Desilva, S.P., Mayton, L., Wu, B., Wooley, P.H., 2002. Evaluation of the biocompatibility of a chitosan scaffold in mice. Journal of Biomedical Materials Research 59, 585–590.

Vojtěch, D., Kubásek, J., Šerák, J., Novák, P., 2011. Mechanical and corrosion properties of newly developed biodegradable Zn-based alloys for bone fixation. Acta Biomaterialia 7, 3515–3522.

Webster, T.J., Ergun, C., Doremus, R.H., Siegel, R.W., Bizios, R., 2000. Enhanced functions of osteoblasts on nanophase ceramics. Biomaterials 21, 1803–1810.

Webster, T.J., Ergun, C., Doremus, R.H., Siegel, R.W., Bizios, R., 2001. Enhanced osteoclast-like cell functions on nanophase ceramics. Biomaterials 22, 1327–1333.

Wei, J., Heo, S., Liu, C., Kim, D., Kim, S., Hyun, Y., Shin, J.W., Shin, J.W., 2009. Preparation and characterization of bioactive calcium silicate and poly (ε-caprolactone) nanocomposite for bone tissue regeneration. Journal of Biomedical Materials Research Part A 90, 702–712.

Weiner, S., Traub, W., 1992. Bone structure: from angstroms to microns. The FASEB Journal 6, 879–885.

Wilson, J., Pigott, G., Schoen, F., Hench, L., 1981. Toxicology and biocompatibility of bioglasses. Journal of Biomedical Materials Research 15, 805–817.

Yu, H.J., Wang, J.Q., Shi, X.T., Louzguine−Luzgin, D.V., Wu, H.K., Perepezko, J.H., 2013. Ductile biodegradable Mg−based metallic glasses with excellent biocompatibility. Advanced Functional Materials 23 (38), 4793–4800.

Yuan, H., Yang, Z., Li, Y., Zhang, X., De Bruijn, J., De Groot, K., 1998. Osteoinduction by calcium phosphate biomaterials. Journal of Materials Science: Materials in Medicine 9, 723–726.

Zberg, B., Uggowitzer, P.J., Löffler, J.F., 2009. MgZnCa glasses without clinically observable hydrogen evolution for biodegradable implants. Nature Materials 8, 887–891.

Zeng, R., Dietzel, W., Witte, F., Hort, N., Blawert, C., 2008. Progress and challenge for magnesium alloys as biomaterials. Advanced Engineering Materials 10, B3–B14.

Zhang, S., Zhang, X., Zhao, C., Li, J., Song, Y., Xie, C., Tao, H., Zhang, Y., He, Y., Jiang, Y., 2010. Research on an Mg–Zn alloy as a degradable biomaterial. Acta Biomaterialia 6, 626–640.

Zhou, H., Lee, J., 2011. Nanoscale hydroxyapatite particles for bone tissue engineering. Acta Biomaterialia 7, 2769–2781.

This page intentionally left blank

Biomimetic nanocomposite hydrogels for cartilage regeneration

12

N.J. Castro, L.G. Zhang
The George Washington University, Washington, DC, United States

12.1 Introduction

Acute and chronic orthopedic injuries to articulating joints (knee, shoulder, and hip) typically affect and compromise the structural integrity of cartilage tissue. In severe cases, these injuries may lead to progressive degeneration of not only the compliant and soft cartilage tissue, but the stiff and highly mineralized subchondral bone. Degenerative joint disease (such as osteoarthritis) and trauma present a common and serious clinical problem. Currently, 48 million Americans are afflicted with osteoarthritis and 67 million Americans are projected to suffer from this condition by 2030 (Lawrence et al., 2008; CDC, 2008) leading to a pressing need for new treatment options to address these defects. Clinically, osteoarthritis is defined as the gradual loss of hyaline cartilage leading to structural and functional failure at the bone–cartilage interface (Buckwalter et al., 2000). Not surprisingly, bone-on-bone contact leads to inhibited joint motion and increased pain. Currently, there are limited options to treat and no methods to cure osteoarthritis.

12.1.1 Clinical challenges

Traditional surgical treatment options are determined by the severity, type, size, and location of the cartilage defect site. Clinically viable options to treat focal defects (<5 mm in diameter) include autografts, autologous chondrocyte implantation, debridement (Aaron et al., 2006), microfracture (Chuckpaiwong et al., 2008), and mosaicplasty (Robert, 2011). Even though they have shown acceptable success, several limitations persist. The "gold standard" for cartilage repair (autograft) largely involves the harvest and transplantation of autologous tissue. In this procedure, cylindrical "plugs" which include cartilage and subchondral bone are harvested from minimal-to-non load-bearing sites within the patient's body and transplanted to the defect site(s) wherein greater mechanical stress is experienced (Robert, 2011). This procedure is considerably limited due to insufficient donor tissue and donor-site morbidity. For patients with severe and advanced osteoarthritis, total joint arthroplasty (TJA) is a common treatment option (Tavazoie et al., 2008). It is an invasive procedure wherein the articulating surfaces of the joint are replaced by complex systems comprising metallic, ceramic, and/or polymeric components. Although generally minor

Nanocomposites for Musculoskeletal Tissue Regeneration. http://dx.doi.org/10.1016/B978-1-78242-452-9.00012-1

in prevalence, complications such as infection, particulate-induced bone loss (osteolysis), implant loosening and reaction to metal ions can affect the longevity of TJA.

12.1.2 Tissue engineering

The interdisciplinary field of tissue engineering (TE) holds great promise for the development of novel therapeutic approaches for the treatment of traumatic injuries, diseases and congenital defects that may overcome the body's natural healing capacity (Langer and Vacanti, 1993; Santo et al., 2012). For patients with an increasingly active lifestyle, TE approaches to cartilage repair may also offer a favorable alternative that enables patients to return to high-impact activities or competitive sports, which are not recommended for patients with TJA. TE approaches may one day offer the possibility of treating and potentially curing the progression of degenerative joint disease in younger patients minimizing the need for TJA.

Current cartilage TE strategies commonly employ a combination of cells, a biocompatible/biodegradable three-dimensional (3D) support structure, and chemical or biological factor(s) to promote cell function during de novo tissue formation (Zhang et al., 2009a). The basic premise relies on the introduction or elicitation of cells to the defect site by means of an appropriate scaffold, which results in directed spatial and temporal tissue remodeling. Several key scaffold parameters shown to affect the success of scaffolds for tissue regeneration are: (1) biocompatibility and bioactivity to maximize tissue growth, (2) appropriate mechanical properties to enable the patient's rapid return to mobility while protecting developing tissue, (3) controllable biodegradability in which degradation rates closely match the rate of new tissue formation, and (4) interconnected porous structure to improve nutrient diffusion and waste transport (Hutmacher, 2000). In addition, two distinct approaches exist within the area of tissue regeneration (Fig. 12.1). The first approach typically referred to as a top–down strategy employs the use of prefabricated scaffolds exhibiting the aforementioned characteristics. The second, bottom–up approach, utilizes extended cell-culture periods in combination with high-seeding densities and morphogenetic factors to induce cellular differentiation leading to extracellular matrix (ECM) deposition.

Owing to the aforementioned differences in TE approaches, scaffold-based top–down studies can readily manufacture scaffolds displaying homogeneous composition and tunable mechanical properties within a univariate system. Therefore, the base materials employed in the fabrication of cartilage scaffolds must be chosen from biomaterials that exhibit similar mechanical and physical properties to the native tissue (Ge et al., 2012). For example, natural polymers, such as collagen and polysaccharides or water soluble low-molecular weight synthetic polymers such as poly(ethylene) glycol (PEG) and poly(ethylene) oxide that allow for easy incorporation of tissue-specific morphogenetic factors, have been used for cartilage regeneration (Madry et al., 2014; Xu et al., 2011; Spiller et al., 2011; Park et al., 2011; Gupta et al., 2011; Aulin et al., 2011).

Advances in materials and scaffold design have also included biochemical cues that mimic those found within articular cartilage exhibiting improved cell adhesion, proliferation, directed differentiation, and phenotypic expression (Chen et al., 2011; Guo et al., 2010). Extended culture approaches, in which cartilage-like tissue is secreted by

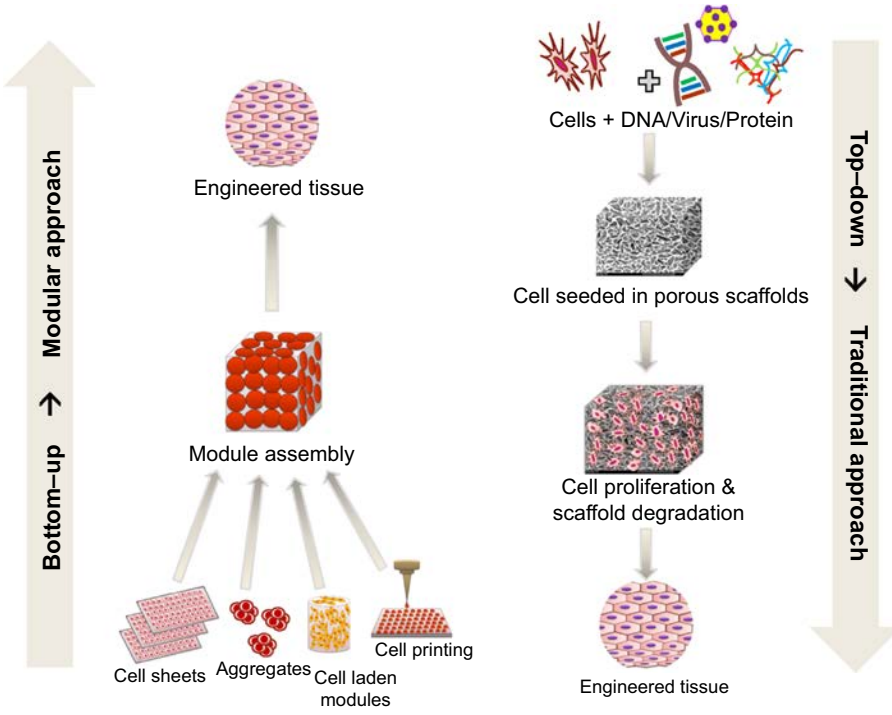

Figure 12.1 Bottom–up and top–down scaffold fabrication approaches.
Image is adapted from Tiruvannamalai-Annamalai, R., Armant, D.R., Matthew, H.W., 2014. A glycosaminoglycan based, modular tissue scaffold system for rapid assembly of perfusable, high cell density, engineered tissues. PLoS One 9, e84287.

mature cells, have also been employed to overcome the inherent complexity of manufacturing functional tissue in combination with scaffold-based strategies, but limitations with these approaches persist. In addition to biomaterial limitations of traditional TE approaches with respect to spatial and temporal control of tissue formation, the mechanical properties of single tissue-specific constructs has also proven challenging. Therefore, applying nanotechnology (ie, nanomaterials and 3D nanofabrication) to manufacture novel biomimetic cartilage constructs within certain biological and mechanical constraints merits considerable focused attention. In the following sections, we will explore the material requirements of cartilage tissue and cutting-edge advances in nanotechnology and 3D fabrication for cartilage tissue regeneration.

12.2 Hydrogels for cartilage regeneration

Hydrogels have been used in two forms for the purpose of replacing articular cartilage—as permanent implants to replace damaged cartilage, or as cell-carrier materials to encourage tissue regeneration. As cell-free implants, hydrogels can be structurally and

mechanically similar to cartilage and allow efficient load transfer (Gonzalez and Alvarez, 2014; Obradovic et al., 2012; Lee et al., 2009). As cell-seeded tissue-engineering scaffolds, hydrogels are also extremely useful: they promote chondrocyte attachment in a manner that is similar to the cartilage ECM (Tibbitt and Anseth, 2009; Lin and Anseth, 2009; Cushing and Anseth, 2007; Cushing et al., 2007), they maintain the chondrocyte phenotype in a way that is impossible in monolayer culture, and their viscoelastic nature permits effective transfer of loads to the chondrocytes, which depend on mechanical signals for survival (Mesallati et al., 2014; Mauck et al., 2000; Elisseeff et al., 2000). There are several design parameters that can be readily modified to affect the performance of a hydrogel-based cartilage scaffold. The main parameters include type of hydrogel, cross-linking density, degradation profile, porosity, mechanical properties and loading regimen, source and density of cells, concentrations of growth factors, and so on.

12.2.1 Naturally derived hydrogels

Hydrogels formed from naturally derived polymers, such as agarose, alginate, chitosan, hyaluronan, collagen, fibrin, and polysaccharides, are attractive because they are biochemically similar to natural cartilage. Scaffolds prepared from naturally derived hydrogels have been used in matrix-assisted autologous chondrocyte implantation, including collagen type I/III (Schneider et al., 2011; Benthien and Behrens, 2011), hyaluronan (Gobbi et al., 2009), and fibrin (Kim et al., 2010). Although naturally derived hydrogels normally lack the necessary mechanical properties to withstand physiological loads, they still have the high potential to support the formation of healthy cartilage. In the following, several typical hydrogels will be discussed.

Agarose and alginate, both derived from marine algae, were among the first hydrogels studied for tissue engineering due to the ease of gelation and cell encapsulation (Overhauser, 1992; Sittinger et al., 1994). Alginate gels in the presence of divalent ions and agarose undergo spontaneous gelation under mild conditions due to hydrogen bonding (Shoichet et al., 1996). They have been used extensively as model systems to study the effects of dynamic loading and other conditions on cell behavior (Elder et al., 2006; Liu et al., 2011; Chahine et al., 2009; Freeman et al., 1994) and have supported the formation of cartilage tissue with similar mechanical properties to native cartilage (Ghahramanpoor et al., 2011).

Hydrogels can also be formed from collagen of type I or type II, the latter being the dominant component of articular cartilage. Collagen hydrogels are chemically biomimetic, have high swelling ratios, and promote cartilage formation by encapsulated cells (Yamaoka et al., 2006). Chondrocytes interact with collagen gels via integrins, which promote proliferation and production of ECM components, and can remodel collagen through the secretion of collagenase (Yamaoka et al., 2006). In 1994, the landmark study by Wakitani et al. (1994) reported that mesenchymal stem cells (MSCs) embedded in type I collagen gels differentiated into chondrocytes and repaired cartilage defects in rabbits with hyaline-like cartilage, but with areas of incomplete integration with the surrounding cartilage. Type I collagen gels have also been used as cell-delivery vehicles for the transplantation of bone marrow stem cells into cartilage defects in humans (Wakitani et al., 2011).

Fibrin hydrogels can be prepared from fibrinogen in the presence of thrombin, isolated from a patient's own blood, reducing the risk of a foreign body reaction, and exhibit excellent adhesion to surrounding tissue (Ahmed et al., 2008; Zhao et al., 2008). MSCs differentiated into chondrocytes and produced more cartilage tissue when encapsulated in fibrin hydrogels when compared to alginate hydrogels (Watts et al., 2013). Fibrin hydrogels have poor mechanical properties (Haugh et al., 2012). They have been investigated as carriers in autologous chondrocyte transplantation (Wysocka et al., 2010; Kim et al., 2010).

Hyaluronic acid (HA) is a natural glycosaminoglycan (GAG) found in articular cartilage and synovial fluid and is also involved in the regulation of wound healing, cell motility, ECM organization, and cell differentiation (Kim et al., 2011). HA is degraded by cell-secreted hyaluronidase, and the rate of degradation can be readily tuned (Khetan et al., 2009). Cartilage formation by chondrocytes and by MSCs was enhanced in HA hydrogels in comparison to fibrin and to PEG hydrogels, emphasizing the role of biochemical cues in cartilage formation (Callahan et al., 2012; Chung and Burdick, 2009). HA hydrogels supported cartilage formation by human embryonic stem cells in non-weight-bearing defects in a rat model, with good integration with the surrounding cartilage after 12 weeks (Toh et al., 2010). The addition of HA to cell-culture medium increased deposition of type II collagen and GAG, markers of the cartilage phenotype, by chondrocytes encapsulated in alginate hydrogels (Akmal et al., 2005), but decreased such markers by chondrocytes encapsulated in collagen hydrogels (Yoon et al., 2009). Other studies have shown that the addition of HA to alginate hydrogels caused an increase in the expression of type I collagen, a marker of fibrous scar-like cartilage formation. Interestingly, this trend was reversed in the presence of exogenous insulin-like growth factor-1 (IGF-1), suggesting a role for HA in the modulation of IGF-1 signaling by entrapped chondrocytes.

Chitosan is prepared by partial N-deacetylation of chitin, derived from the exoskeleton of arthropods, and is structurally similar to the GAG found in cartilage (Chandy and Sharma, 1990; Abarrategi et al., 2010). The gelation of chitosan can be induced by ionic cross-linking (Cai and Lapitsky, 2013; Aiedeh et al., 2007). Chitosan has been modified to increase biochemical similarity to cartilage and to prepare injectable scaffolds (Yang et al., 2012; Tigli and Gumusderelioglu, 2009; Marsich et al., 2008; Hoemann et al., 2005; Xia et al., 2004).

12.2.2 Synthetic hydrogels

The primary underlying issue limiting the full capabilities of naturally derived hydrogels (such as mechanical strength) has prompted the use and investigation of synthetic hydrogels derived from intermediate molecules of the Krebs cycle and other polyesters. Synthetic hydrogels prepared from PEG, also known as poly(ethylene oxide), modified with methacrylate groups to allow photo-crosslinking, were first introduced by Elisseeff et al. (1999) as an injectable and transdermally photopolymerizable hydrogel for cartilage tissue regeneration. PEG hydrogels can be easily modified and have been useful in studying the effects of hydrogel properties on cartilage formation (Nguyen et al., 2011a,b; Hwang et al., 2011). PEG

macromers have also been modified with moieties that made the hydrogels more biomimetic. The addition of collagen-mimetic peptides resulted in enhanced retention of cell-secreted collagen and increased production of both collagen and proteoglycans by MSCs (Mhanna et al., 2014). The incorporation of chondroitin sulfate to PEG hydrogels resulted in enhanced ECM deposition by encapsulated chondrocytes when compared to pure chondroitin sulfate hydrogels and increased expression of chondrogenic markers by encapsulated MSCs (Varghese et al., 2008; Hwang et al., 2007; Villanueva et al., 2010; Park et al., 2009).

The PEG macromer has also been modified with fumaric acid to form hydrogels made of oligo(poly(ethylene glycol) fumarate) (OPF), which are photo-cross-linkable, injectable, and can be prepared with compressive moduli as high as cartilage (Henke et al., 2014; Temenoff et al., 2002). When MSCs were encapsulated in the hydrogels, the quality of deposited tissue was improved (Lam et al., 2014). These hydrogels have also been used to evaluate the effects of the controlled release of various growth factors on cartilage formation in vitro and in vivo (Kim et al., 2013; Park et al., 2005; Holland et al., 2003; Kasper et al., 2005). Hydrogels contain several inherent attractive features which can be modulated to display tunable physical characteristics. In the following section, we will discuss several of these parameters.

12.2.3 Physical properties of hydrogels

Cross-linking density: The network cross-linking density of a hydrogel controls many of its properties, such as diffusion coefficients, mechanical behavior, and rate of degradation (Bryant et al., 2004; Nicodemus and Bryant, 2008; Bian et al., 2013). The swelling ratio of a hydrogel, the ratio of its swollen weight to its dry weight, is related to the cross-linking density and is a measure of how much water is retained by the hydrogel (Nguyen et al., 2012). Less cross-linked hydrogels have a larger mesh size, or the distance between cross-links, which allows faster diffusion of nutrients and waste to and from encapsulated cells. The cross-linking density of the common PEG hydrogels can be enhanced by increasing the concentration of the PEG solutions, decreasing the molecular weight of the PEG macromers, or by using branched PEG structures instead of linear structures, with corresponding increases in compressive modulus. Because of the facility of modulating the properties of PEG hydrogels, many studies on the effects of hydrogel properties have been performed using PEG hydrogels.

Degradation rate: Higher swelling ratios are beneficial for cartilage matrix production but decrease the mechanical properties of the hydrogels. Degradable hydrogels exhibit an increase in swelling ratio through the degradation process allowing for initial mechanical support which is transferred to the evolving cartilage matrix over time and has shown to have a direct influence on MSC behavior (Hudalla et al., 2008; Martens et al., 2003). Control over hydrogel degradation also allows control over nutrient and waste diffusion in a growing cartilage construct (Dhote et al., 2013). The degradation of PEG hydrogels has also been varied by cross-linking with biodegradable genipin (Ferretti et al., 2006), phosphate-releasing groups (Gandavarapu et al., 2013; Wang et al., 2003), and by dextran-based hydrogels (Jin et al., 2011).

12.3 Nanocomposite-cartilage scaffold fabrication

With the advent of novel nanomaterials, the design of biomimetic and bioactive tissue scaffolds with improved biocompatibility and functional properties (Zhang et al., 2008b; Zhang and Webster, 2009; Holmes et al., 2013) has greatly increased. The underlying advantage of nanoscaled structures is the ability to mimic the native-tissue ECM environment, as well as favorably modulate cell function. Several proposed mechanisms for the improved nanomaterial–cell interaction have been correlated to structural (surface topography and surface area) and physicochemical (surface chemistry, energy, and wettability) cues that can regulate cellular behavior, but the basic principles have yet to be identified (Streicher et al., 2007). In the following, we will discuss several bottom–up and top–down cartilage scaffold fabrication approaches as well as introduce several promising nanomaterials for cartilage regeneration.

12.3.1 Bottom–up self-assembling nanomaterials-based cartilage constructs

Because natural tissues are constructed via a bottom–up self-assembly method, self-assembling supramolecular nanomaterials holds great potential to facilitate the construction of complex tissue environments (Huebsch and Mooney, 2009). Advances in nanotechnology are greatly increasing the design of these types of sophisticated nanobiomaterials. Hartgerink et al. (2001) reported that a peptide-amphiphile (PA) with cell-adherent RGD (Arg-Gly-Asp) peptide can self-assemble into supramolecular nanofibers and align nanohydroxyapatite (nHA) along their long axis similar to the pattern of bone ECM. Hosseinkhani et al. (2006) showed significantly enhanced MSC differentiation of stem cells in a 3D PA scaffold when compared to 2D static tissue culture. Also, Shah et al. (2010) recently designed PA nanofibers which display a high density of transforming growth factor β1 (TGF-β1) binding sites for improved cartilage regeneration (Aida et al., 2012).

In addition to the promising results obtained with self-assembling PA nanofibers, another promising direction is the development of new self-assembling nanotubes that mimic cellular (such as DNA) and ECM components while displaying signals in a spatiotemporally controlled manner. Our lab has developed these types of highly innovative self-assembling rosette nanotubes (RNTs) with controllable surface chemistry. Specifically, RNTs are a new class of biologically inspired supramolecular nanobiomaterials obtained through the self-assembly of low-molecular-weight DNA base-pair motifs (Guanine^Cytosine, G^C) in an aqueous solution. Fig. 12.2 illustrates the morphology of two types of twin DNA-based RNTs. For the twin DNA-based RNTs, two covalently linked G^C bases can self-assemble into a six-member twin rosette maintained by 36 hydrogen bonds. The RNTs have a very stable nanotubular structure with a hydrophobic core and hydrophilic outer surface via electrostatic forces, base-stacking interactions, and hydrophobic effects. The outer diameter and the length of all nanotubes are ~3–4 nm and several 100 nm, respectively. Another intriguing feature of RNTs is their flexibility in design, which makes their length, diameter, and surface chemistry tunable. In our previous work, we designed multiple

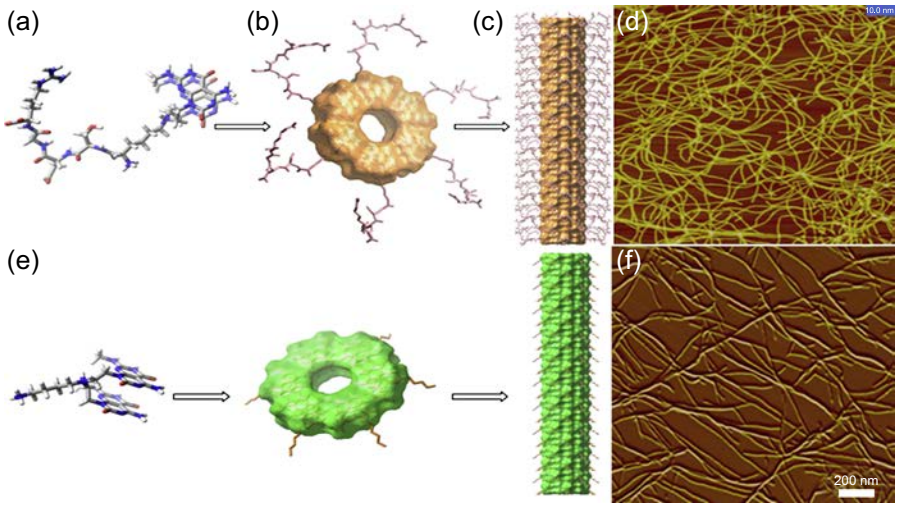

Figure 12.2 Schematic illustration of self-assembly process of RNTs. (a) Twin G^C motifs with an RGDSK peptide; (b) rosette-like supermacrocycle assembled from six motifs; and (c) rosettes stacked up into stable helical nanotubes with an 11 Å hollow core, 3–4 nm in diameter and up to several μm long. Atomic force microscopy image of (d) twin DNA-based RNTs with RGDSK peptide. (e and f) twin DNA-based RNTs with an aminobutane linker (TBL).

DNA-based RNTs with varying peptide and amino-acid side chains via a bottom–up self-assembly method, which has shown great potential for cartilage and bone regeneration (Sun et al., 2012; Zhang et al., 2010, 2009b,c, 2008a; Fine et al., 2009; Childs et al., 2013). We explored human bone marrow MSC adhesion, proliferation and 4-week chondrogenic differentitiaon in twin-based RNTs conjugated with cell-adherent arginine-glycine-aspartic acid-serine-lysine (RGDSK) (tunable bone rosette nanotube(TB-RNT)-RGDSK) peptide in poly-L-lactic acid (PLLA) scaffolds (Childs et al., 2013). Our results demonstrated that these biomimetic twin-based nanotubes can significantly enhance MSC adhesion, proliferation and chondrogenic differentiation (such as GAG, collagen and protein synthesis) when compared to controls. Histological examination (Fig. 12.3) confirmed that TB-RNT-RGDSK can greatly improve tissue formation when compared to controls without nanotubes. Theoretically, any cell-favorable short peptide can be conjugated onto the G^C motifs to modulate surface chemistry, rendering RNTs as a biomimetic nanotemplate for tissue regeneration. Based on the currently available studies, supramolecular biomimetic self-assembling nanomaterials have great potential in regenerating cartilage tissue.

12.3.2 Top–down cartilage-scaffold fabrication techniques

Generally, traditional TE efforts have focused on the manufacture of homogenous constructs exhibiting mechanical properties and characteristics similar to those of one particular tissue type. Although good results have been obtained, current research has focused on the fabrication of 3D spatiotemporal stratified/graded nanocomposite

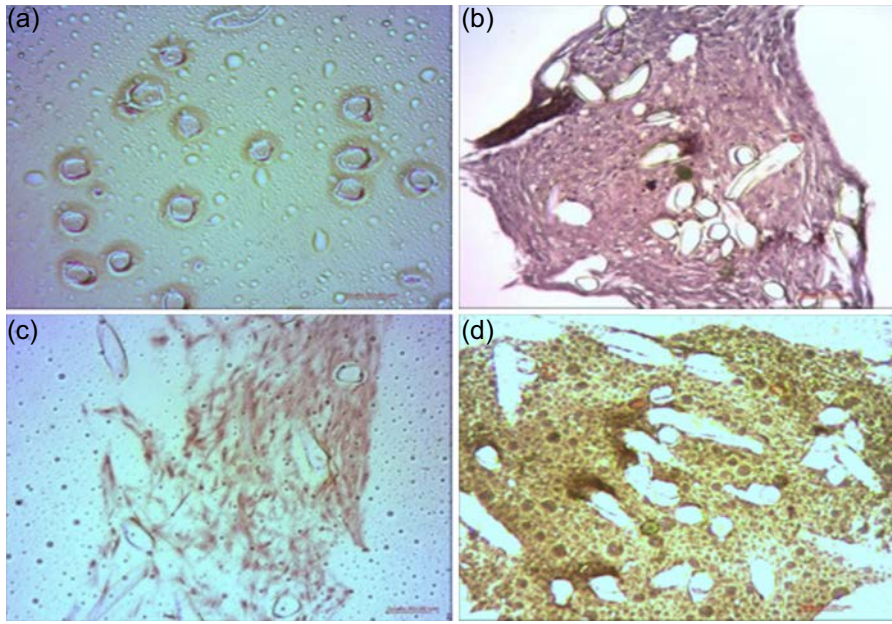

Figure 12.3 Hemotoxylin and eosin staining of (a and c) PLLA controls; and (b and d) TB-RNT-RGDSK PLLA scaffolds for MSC chondrogenic differentiation at weeks 1 and 2.

scaffolds that better mimic native cartilage tissue. In the following, we will explore traditional and contemporary scaffold fabrication techniques of homogeneous and stratified scaffolds for cartilage regeneration.

12.3.2.1 Gas foaming/particle leaching

Three-dimensional scaffold architecture and geometric cues play a major role in directing cell behavior and tissue regeneration (Kilian et al., 2010). For cartilage studies, conventional 3D scaffold fabrication methods such as gas foaming, particle leaching and freeze-drying have been used to fabricate 3D scaffolds and have shown to influence cell behavior and improve tissue regeneration (Castro et al., 2012, 2014; Dormer et al., 2010; Holmes et al., 2012). Specifically, gas foaming is a process for scaffold fabrication similar to solvent casting in which a foam-forming agent, such as ammonium bicarbonate, is added to a polymer-solvent solution. The polymer-solvent foam is then dried, and the solvent evaporates, leaving a rigid and porous structure. Ji et al. (2012) used gas foaming to create highly porous poly-DL-lactide and PEG copolymer scaffolds foamed with CO_2. Chen et al. used a novel method to seed calcium phosphate cement with human umbilical cord cells encapsulated in hydrogel spheres. The calcium phosphate–hydrogel-sphere mixture was then foamed with a porogen to achieve high porosity and good cellular dispersion (Chen et al., 2012a,b). Zhou et al. (2011) employed a new technique in which "solid-state" foaming (SSF) was combined with immiscible polymer blends to achieve a variety of different pore sizes and distributions within the same structure. That is to say, highly interconnected micro- and nanopores were observed (Zhou et al., 2011).

Other available systems have also focused on the fabrication of stratified scaffolds through novel methods of adhering discrete tissue-specific layers (Oliveira et al., 2006; Jiang et al., 2007) to address specific mechanical requirements. Wang et al. (2009) developed a silk microsphere/scaffold gradient system wherein recombinant BMP-2 and IGF-1 were encapsulated within silk microspheres for controlled release and spatially distributed within the silk scaffold for directed human MSC differentiation. This study showed that MSCs exhibited osteogenic and chondrogenic phenotypic expression along the BMP-2 gradient and combination of BMP-2/IGF-1 after culturing the seeded scaffolds in a medium containing morphogenetic factors.

12.3.2.2 Three-dimensional printing

Conventional 3D scaffold fabrication methods often offer limited control over scaffold geometry, pore size and distribution, pore interconnectivity, as well as internal channel construction. Random, spontaneously generated and disconnected pores significantly decrease nutrient transportation, cell migration, and survival especially in the center of the scaffold limiting their clinical feasibility (Hollister, 2005). As an emerging technology, 3D printing (such as inkjet printing, stereolithography (SL), and bioplotting) offers great precision and control of the internal architecture and outer shape of a scaffold, allowing for the fabrication of complicated structures that closely mirror the architecture of biological tissue (Derby, 2012). Based on computer-aided design (CAD) data reconstructed from medical images of defects, 3D printers can easily fabricate a construct with anatomically relevant gross shape for a near-perfect fit within a defect site (Fukui et al., 2003; Holmes et al., 2014).

Inkjet bioprinting

Inkjet printers have been employed in a process called "bioprinting," which involves the printing of cells, biomolecules or hydrogels based on a digital pattern (Seidi et al., 2011). In this 3D printing process, a binding material is deposited into a material stream and onto a powder bed, causing the particles to join to form the desired object (Bártolo et al., 2011). Then, a new layer of powder is deposited and can be selectively joined to the previous layer, a process which repeats until the entire scaffold is complete (Bártolo et al., 2011) as shown in Fig. 12.4. This process has several advantages. As the ink nozzle does not contact the printed surface, risk of cross-contamination is low (Ilkhanizadeh et al., 2007). Furthermore, inkjet bioprinting is programmable and requires no significant modification of substrates for printing (Phillippi et al., 2008). Recently, Cui et al. (2012a) successfully inkjet bioprinted a poly(ethylene glycol) dimethacrylate solution containing chondrocytes into a defect formed in an osteochondral plug. They observed greater proteoglycan deposition at the interface of the printed implant and native tissue.

Inkjet bioprinting has been employed to print ECM, cells, proteins, and DNA at low cost in many biomedical applications (Ilkhanizadeh et al., 2007). Gradients can be obtained by employing grayscale patterns of different intensities in the CAD (Ilkhanizadeh et al., 2007), or by applying different number of overprints

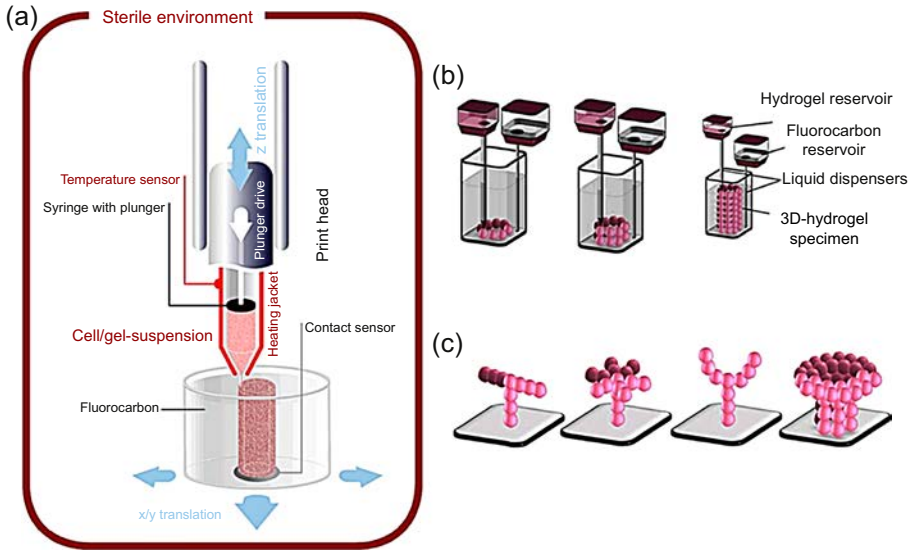

Figure 12.4 Schematic view of the layer-by-layer inkjet/bioplotting deposition technique. Image is adapted from Campos, D.F.D., Blaeser, A., Weber, M., Jäkel, J., Neuss, S., Jahnen-Dechent, W., Fischer, H., 2013. Three-dimensional printing of stem cell-laden hydrogels submerged in a hydrophobic high-density fluid. Biofabrication 5, 015003.

to achieve higher concentration in specified regions (Phillippi et al., 2008). Collagen I scaffolds with defined microchannels and internal structures have been created with inkjet bioprinting (Wahl et al., 2007). Processing did not affect the structural stability of the collagen, and this scaffold was able to be further applied for tissue-engineering applications (Wahl et al., 2007). Inkjet bioprinting can also be used to precisely pattern cells. Cellular printing was achieved using a layer-by-layer bioprinting assembly to print PEG mixed with human chondrocytes to fabricate osteochondral plugs (Cui et al., 2012b). Photopolymerization was simultaneously employed to maintain chondrocyte position (Cui et al., 2012b). This system achieved specific placement of individual cells, high cell viability, maintenance of chondrogenic phenotype as ascertained through aggrecan and collagen type I and II gene expression, and integration with host tissue, assessed by push-out testing to determine interface failure stress (Cui et al., 2012b). By further modifying inkjet printers to be more suitable for printing cells and ECM hydrogel materials, this technique has the potential to create structures with very specific internal structures, soluble factor placement, and cell patterning. The extension of 3D printing technologies in the design and fabrication of spatiotemporal scaffolds can further aid in the development of raw and composite nanomaterials designed specifically for the technology employed. Manufacturing constraints and available nanomaterials with suitable physical and biological properties have limited the clinical applicability of bioprinted constructs, but more focused investigations have leveraged nanomaterials such as those previously described in fabricating more biomimetic scaffolds.

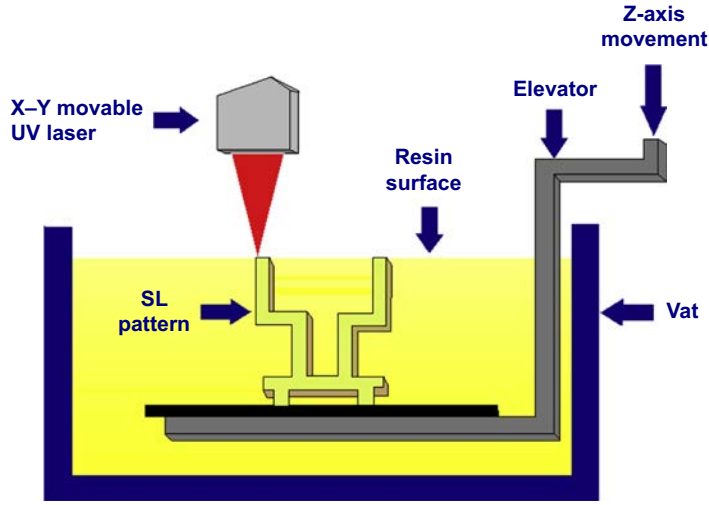

Figure 12.5 Schematic illustration of stereolithography 3D printing.
Image is adapted from Cooke, M.N., 2004. Novel Stereolithographic Manufacture of Biodegradable Bone Tissue Scaffolds, Case Western Reserve University.

Stereolithography

Stereolithography (SL)-based 3D printing provides precise control of the gross geometry of fabricated scaffolds as well as allows for the incorporation and spatial placement of incorporated nanomaterials. Fig. 12.5 illustrates the process of SL. Briefly, a photocurable hydrogel (such as PEG derivatives) is placed in a vat or reservoir whereby mirror-directed or fiber optic-coupled ultraviolet energy is exposed to the material surface leading to solidification of the liquid and attachment to the subsequent layer. Our laboratory has developed a table-top SL apparatus for the manufacture of bioactive biomimetic scaffolds containing morphogenetic factors for cartilage tissue regeneration. Based on the flexibility in designing photocurable and functional hydrogels, SL has garnered greater attention for the manufacture of bioactive 3D scaffolds (Sharifi et al., 2012; Seck et al., 2010; Lee et al., 2007, 2008; Arcaute et al., 2006). Grogan et al. (2013) synthesized and fabricated 3D methacrylated gelatin scaffolds which illustrated good tissue integration and the formation of de novo meniscal fibrocartilage in an organ explant model. Schuller-Ravoo et al. (2013) similarly synthesized a novel branched monomer based on trimethyl carbonate. Scaffolds were fabricated with the use of a digital mirror device allowing for layer thickness of ~25 μm. In addition, synthetic polymers with tunable physical properties can be readily synthesized and fabricated through alterations of the "resin" mixture and density of photo-cross-linkable moieties (Timmer et al., 2003).

12.4 In vitro testing considerations: cell sources

Through the course of our discussion, we have elucidated key biomaterial and scaffold fabrication considerations necessary for cartilage regeneration. In addition,

one must consider culture conditions when evaluating fabricated constructs in vitro. Many preliminary analyses of tissue-engineered scaffolds employ immature chondrocytes due to the ease of cell isolation and expansion. However, compared to mature chondrocytes, immature chondrocytes tend to proliferate more, produce more ECM components, and respond more to the application of growth factors (Kopesky et al., 2010; Anderson and Athanasiou, 2009). Adult chondrocytes have been successful in developing a cartilage-like matrix in agarose hydrogels when used to repair non-weight-bearing defects in a canine model with good host-tissue integration (Ng et al., 2010). Stem cells can also be isolated from adipose tissue, bone marrow, and other sources with each differing slightly in behavior, response to external forces, and potential to produce new cartilage tissue (Roux et al., 2013; Salamon et al., 2013; Maumus et al., 2013; Burk et al., 2013). In any case, the isolation of chondrocytes from any of the cartilages causes considerable damage to the donor site. In contrast, stem cells isolated from mesenchymal tissues can produce cartilage tissue under the right conditions. Although immature chondrocytes produced greater levels of cartilage tissue than immature bone marrow-derived MSCs encapsulated in hyaluronic acid, agarose, and peptide hydrogels (Erickson et al., 2009), MSCs derived from skeletally mature horses produced superior cartilage tissue compared to mature chondrocytes in peptide hydrogels (Lee et al., 2010; Kisiday et al., 2008). It is important that future studies utilize cells from clinically relevant sources to determine the effectiveness of tissue-engineering strategies. These studies suggest that MSCs derived from a variety of sources are suitable for cartilage tissue regeneration. The seeding density of chondrocytes or MSCs in hydrogels also affects the quality of engineered cartilage tissue (Buckley et al., 2009; Park et al., 2007). In addition, the presence of mechanical loading showed a marked difference in ECM accumulation and mechanical properties between hydrogels (Haugh et al., 2012; Bian et al., 2012). Therefore, cell seeding density and mechanical stimulation may result in greater cartilage-specific ECM production.

12.5 Conclusion

Significant research has focused on the use of hydrogels in the repair and regeneration of cartilage tissue. Materials from naturally derived sources contain inherent benefits with regard to biocompatibility with minimized deleterious cell–material interactions. Synthetic materials exhibit greater flexibility in the control of physical and mechanical properties as well as lend themselves to be modified and employed in the manufacture of predesigned 3D scaffolds. The ideal cartilage scaffold should exhibit properties conducive to withstand direct physiological loading and degrade at a rate efficient for cellular infiltration and subsequent tissue formation. With the combination of prefabricated 3D structures and biomimetic nanomaterials, enhanced tissue integration can be achieved. Although much research has been conducted in an effort to recapitulate the complex nature of cartilage tissue, a better understanding of the effects of morphological and spatiotemporal cues is still required.

Acknowledgments

This work was supported by Award Number 1510561 from NSF BME program and by the George Washington Institute for Biomedical Engineering and Institute for Nanotechnology.

References

Aaron, R.K., Skolnick, A.H., Reinert, S.E., Ciombor, D.M., 2006. Arthroscopic debridement for osteoarthritis of the knee. Journal Bone and Joint Surgery-American 88, 936–943.

Abarrategi, A., Lopiz-Morales, Y., Ramos, V., Civantos, A., Lopez-Duran, L., Marco, F., Lopez-Lacomba, J.L., 2010. Chitosan scaffolds for osteochondral tissue regeneration. Journal of Biomedical Materials Research, Part A 95, 1132–1141.

Ahmed, T.A., Dare, E.V., Hincke, M., 2008. Fibrin: a versatile scaffold for tissue engineering applications. Tissue Engineering Part B Reviews 14, 199–215.

Aida, T., Meijer, E.W., Stupp, S.I., 2012. Functional supramolecular polymers. Science 335, 813–817.

Aiedeh, K.M., Taha, M.O., AL-Hiari, Y., Bustanji, Y., Alkhatib, H.S., 2007. Effect of ionic crosslinking on the drug release properties of chitosan diacetate matrices. Journal of Pharmaceutical Sciences 96, 38–43.

Akmal, M., Singh, A., Anand, A., Kesani, A., Aslam, N., Goodship, A., Bentley, G., 2005. The effects of hyaluronic acid on articular chondrocytes. Journal of Bone and Joint Surgery-British 87, 1143–1149.

Anderson, D.E.J., Athanasiou, K.A., 2009. A comparison of primary and passaged chondrocytes for use in engineering the temporomandibular joint. Archives of Oral Biology 54, 138–145.

Arcaute, K., Mann, B.K., Wicker, R.B., 2006. Stereolithography of three-dimensional bioactive poly(ethylene glycol) constructs with encapsulated cells. Annals of Biomedical Engineering 34, 1429–1441.

Aulin, C., Bergman, K., Jensen-Waern, M., Hedenqvist, P., Hilborn, J., Engstrand, T., 2011. In situ cross-linkable hyaluronan hydrogel enhances chondrogenesis. Journal of Tissue Engineering and Regenerative Medicine 5, e188–e196.

Bártolo, P.J., Domingos, M., Patrício, T., Cometa, S., Mironov, V., 2011. Biofabrication Strategies for Tissue Engineering. Springer Netherlands, Dordrecht.

Benthien, J.P., Behrens, P., 2011. The treatment of chondral and osteochondral defects of the knee with autologous matrix-induced chondrogenesis (AMIC): method description and recent developments. Knee Surgery, Sports Traumatology Arthroscopy: Official Journal of the ESSKA 19, 1316–1319.

Bian, L., Hou, C., Tous, E., Rai, R., Mauck, R.L., Burdick, J.A., 2013. The influence of hyaluronic acid hydrogel crosslinking density and macromolecular diffusivity on human MSC chondrogenesis and hypertrophy. Biomaterials 34, 413–421.

Bian, L., Zhai, D.Y., Zhang, E.C., Mauck, R.L., Burdick, J.A., 2012. Dynamic compressive loading enhances cartilage matrix synthesis and distribution and suppresses hypertrophy in hMSC-laden hyaluronic acid hydrogels. Tissue Engineering Part A 18, 715–724.

Bryant, S.J., Chowdhury, T.T., Lee, D.A., Bader, D.L., Anseth, K.S., 2004. Crosslinking density influences chondrocyte metabolism in dynamically loaded photocrosslinked poly(ethylene glycol) hydrogels. Annals of Biomedical Engineering 32, 407–417.

Buckley, C.T., Thorpe, S.D., O'brien, F.J., Robinson, A.J., Kelly, D.J., 2009. The effect of concentration, thermal history and cell seeding density on the initial mechanical properties of agarose hydrogels. Journal of the Mechanical Behavior Biomedical Materials 2, 512–521.

Buckwalter, J.A., Martin, J., Mankin, H.J., 2000. Synovial joint degeneration and the syndrome of osteoarthritis. Instructional Course Lectures 49, 481–489.

Burk, J., Ribitsch, I., Gittel, C., Juelke, H., Kasper, C., Staszyk, C., Brehm, W., 2013. Growth and differentiation characteristics of equine mesenchymal stromal cells derived from different sources. Veterinary Journal 195, 98–106.

Cai, Y., Lapitsky, Y., 2013. Formation and dissolution of chitosan/pyrophosphate nanoparticles: Is the ionic crosslinking of chitosan reversible? Colloids and Surfaces B Biointerfaces 115C, 100–108.

Callahan, L.A., Ganios, A.M., Mcburney, D.L., Dilisio, M.F., Weiner, S.D., Horton Jr., W.E., Becker, M.L., 2012. ECM production of primary human and bovine chondrocytes in hybrid PEG hydrogels containing type I collagen and hyaluronic acid. Biomacromolecules 13, 1625–1631.

Campos, D.F.D., Blaeser, A., Weber, M., Jäkel, J., Neuss, S., Jahnen-Dechent, W., Fischer, H., 2013. Three-dimensional printing of stem cell-laden hydrogels submerged in a hydrophobic high-density fluid. Biofabrication 5, 015003.

Castro, N.J., Hacking, S.A., Zhang, L.G., 2012. Recent progress in interfacial tissue engineering approaches for osteochondral defects. Annals of Biomedical Engineering 40, 1628–1640.

Castro, N.J., O'brien, C., Zhang, L.G., 2014. Biomimetic biphasic 3D nanocomposite scaffold for osteochondral regeneration. AICHE Journal 60, 432–442.

CDC, 2008. National Center for Chronic Disease Prevention and Health Promotion. http://www.cdc.gov/arthritis/arthritis/osteoarthritis.htm.

Chahine, N.O., Albro, M.B., Lima, E.G., Wei, V.I., Dubois, C.R., Hung, C.T., Ateshian, G.A., 2009. Effect of dynamic loading on the transport of solutes into agarose hydrogels. Biophysical Journal 97, 968–975.

Chandy, T., Sharma, C.P., 1990. Chitosan–as a biomaterial. Biomaterials Artificial Cells and Artificial Organs 18, 1–24.

Chen, J., Chen, H., Li, P., Diao, H., Zhu, S., Dong, L., Wang, R., Guo, T., Zhao, J., Zhang, J., 2011. Simultaneous regeneration of articular cartilage and subchondral bone in vivo using MSCs induced by a spatially controlled gene delivery system in bilayered integrated scaffolds. Biomaterials 32, 4793–4805.

Chen, W., Zhou, H., Tang, M., Weir, M.D., Bao, C., Xu, H.H., 2012a. Gas-foaming calcium phosphate cement scaffold encapsulating human umbilical cord stem cells. Tissue Engineering Part A 18, 816–827.

Chen, W., Zhou, H., Weir, M.D., Bao, C., Xu, H.H., 2012b. Umbilical cord stem cells released from alginate-fibrin microbeads inside macroporous and biofunctionalized calcium phosphate cement for bone regeneration. Acta Biomaterialia 8, 2297–2306.

Childs, A., Hemraz, U.D., Castro, N.J., Fenniri, H., Zhang, L.G., 2013. Novel biologically-inspired rosette nanotube PLLA scaffolds for improving human mesenchymal stem cell chondrogenic differentiation. Biomedical Materials 8, 065003.

Chuckpaiwong, B., Berkson, E.M., Theodore, G.H., 2008. Microfracture for osteochondral lesions of the ankle: outcome analysis and outcome predictors of 105 cases. Arthroscopy-The Journal of Arthroscopic and Related Surgery 24, 106–112.

Chung, C., Burdick, J.A., 2009. Influence of three-dimensional hyaluronic acid microenvironments on mesenchymal stem cell chondrogenesis. Tissue Engineering Part A 15, 243–254.

Cooke, M.N., 2004. Novel Stereolithographic Manufacture of Biodegradable Bone Tissue Scaffolds. Case Western Reserve University.

Cui, X., Breitenkamp, K., Finn, M.G., Lotz, M., D'lima, D.D., 2012a. Direct human cartilage repair using three-dimensional bioprinting technology. Tissue Engineering Part A 18, 1304–1312.

Cui, X., Breitenkamp, K., Finn, M.G., Lotz, M., D'lima, D.D., 2012b. Direct human cartilage repair using three-dimensional bioprinting technology. Tissue Engineering. Part A 18, 1–9.

Cushing, M.C., Anseth, K.S., 2007. Materials science. Hydrogel cell cultures. Science 316, 1133–1134.

Cushing, M.C., Liao, J.T., Jaeggli, M.P., Anseth, K.S., 2007. Material-based regulation of the myofibroblast phenotype. Biomaterials 28, 3378–3387.

Derby, B., 2012. Printing and prototyping of tissues and scaffolds. Science 338, 921–926.

Dhote, V., Skaalure, S., Akalp, U., Roberts, J., Bryant, S.J., Vernerey, F.J., 2013. On the role of hydrogel structure and degradation in controlling the transport of cell-secreted matrix molecules for engineered cartilage. Journal of the Mechanical Behavior of Biomedical Materials 19, 61–74.

Dormer, N.H., Singh, M., Wang, L., Berkland, C.J., Detamore, M.S., 2010. Osteochondral interface tissue engineering using macroscopic gradients of bioactive signals. Annals of Biomedical Engineering 38, 2167–2182.

Elder, S.H., Sanders, S.W., Mcculley, W.R., Marr, M.L., Shim, J.W., Hasty, K.A., 2006. Chondrocyte response to cyclic hydrostatic pressure in alginate versus pellet culture. Journal of Orthopaedic Research 24, 740–747.

Elisseeff, J., Anseth, K., Sims, D., Mcintosh, W., Randolph, M., Yaremchuk, M., Langer, R., 1999. Transdermal photopolymerization of poly(ethylene oxide)-based injectable hydrogels for tissue-engineered cartilage. Plastic and Reconstructive Surgery 104, 1014–1022.

Elisseeff, J., Mcintosh, W., Anseth, K., Riley, S., Ragan, P., Langer, R., 2000. Photoencapsulation of chondrocytes in poly(ethylene oxide)-based semi-interpenetrating networks. Journal of Biomedical Materials Research 51, 164–171.

Erickson, I.E., Huang, A.H., Chung, C., Li, R.T., Burdick, J.A., Mauck, R.L., 2009. Differential maturation and structure-function relationships in mesenchymal stem cell and chondrocyte-seeded hydrogels. Tissue Engineering Part A 15, 1041–1052.

Ferretti, M., Marra, K.G., Kobayashi, K., Defail, A.J., Chu, C.R., 2006. Controlled in vivo degradation of genipin crosslinked polyethylene glycol hydrogels within osteochondral defects. Tissue Engineering 12, 2657–2663.

Fine, E., Zhang, L., Fenniri, H., Webster, T.J., 2009. Enhanced endothelial cell functions on rosette nanotube-coated titanium vascular stents. International Journal of Nanomedicine 4, 91–97.

Freeman, P.M., Natarajan, R.N., Kimura, J.H., Andriacchi, T.P., 1994. Chondrocyte cells respond mechanically to compressive loads. Journal of Orthopaedic Research 12, 311–320.

Fukui, N., Ueno, T., Fukuda, A., Nakamura, K., 2003. The use of stereolithography for an unusual patellofemoral disorder. Clinical Orthopaedics and Related Research 169–174.

Gandavarapu, N.R., Mariner, P.D., Schwartz, M.P., Anseth, K.S., 2013. Extracellular matrix protein adsorption to phosphate-functionalized gels from serum promotes osteogenic differentiation of human mesenchymal stem cells. Acta Biomaterialia 9, 4525–4534.

Ge, Z., Li, C., Heng, B.C., Cao, G., Yang, Z., 2012. Functional biomaterials for cartilage regeneration. Journal of Biomedical Materials Research, Part A 100, 2526–2536.

Ghahramanpoor, M.K., Hassani Najafabadi, S.A., Abdouss, M., Bagheri, F., Baghaban Eslaminejad, M., 2011. A hydrophobically-modified alginate gel system: utility in the repair of articular cartilage defects. Journal of Materials Science Materials in Medicine 22, 2365–2375.

Gobbi, A., Kon, E., Berruto, M., Filardo, G., Delcogliano, M., Boldrini, L., Bathan, L., Marcacci, M., 2009. Patellofemoral full-thickness chondral defects treated with second-generation autologous chondrocyte implantation: results at 5 years' follow-up. The American Journal of Sports Medicine 37, 1083–1092.

Gonzalez, J.S., Alvarez, V.A., 2014. Mechanical properties of polyvinylalcohol/hydroxyapatite cryogel as potential artificial cartilage. Journal of Mechanical Behavior of Biomedical Materials 34C, 47–56.

Grogan, S.P., Chung, P.H., Soman, P., Chen, P., Lotz, M.K., Chen, S., D'lima, D.D., 2013. Digital micromirror device projection printing system for meniscus tissue engineering. Acta Biomaterialia 9, 7218–7226.

Guo, X., Park, H., Young, S., Kretlow, J.D., Van Den Beucken, J.J., Baggett, L.S., Tabata, Y., Kasper, F.K., Mikos, A.G., Jansen, J.A., 2010. Repair of osteochondral defects with biodegradable hydrogel composites encapsulating marrow mesenchymal stem cells in a rabbit model. Acta Biomaterialia 6, 39–47.

Gupta, M.S., Cooper, E.S., Nicoll, S.B., 2011. Transforming growth factor-beta 3 stimulates cartilage matrix elaboration by human marrow-derived stromal cells encapsulated in photocrosslinked carboxymethylcellulose hydrogels: potential for nucleus pulposus replacement. Tissue Engineering Part A 17, 2903–2910.

Hartgerink, J.D., Beniash, E., Stupp, S.I., 2001. Self-assembly and mineralization of peptide-amphiphile nanofibers. Science 294, 1684–1688.

Haugh, M.G., Thorpe, S.D., Vinardell, T., Buckley, C.T., Kelly, D.J., 2012. The application of plastic compression to modulate fibrin hydrogel mechanical properties. Journal of Mechanical Behavior of Biomedical Materials 16, 66–72.

Henke, M., Baumer, J., Blunk, T., Tessmar, J., 2014. Foamed oligo(poly(ethylene glycol)fumarate) hydrogels as versatile prefabricated scaffolds for tissue engineering. Journal of Tissue Engineering and Regenerative Medicine 8, 248–252.

Hoemann, C.D., Sun, J., Legare, A., Mckee, M.D., Buschmann, M.D., 2005. Tissue engineering of cartilage using an injectable and adhesive chitosan-based cell-delivery vehicle. Osteoarthritis Cartilage 13, 318–329.

Holland, T.A., Tabata, Y., Mikos, A.G., 2003. In vitro release of transforming growth factor-beta 1 from gelatin microparticles encapsulated in biodegradable, injectable oligo(poly(ethylene glycol) fumarate) hydrogels. Journal of Controlled Release 91, 299–313.

Hollister, S.J., 2005. Porous scaffold design for tissue engineering. Nature Materials 4, 518–524.

Holmes, B., Castro, N.J., Li, J., Keidar, M., Zhang, L.G., 2013. Enhanced human bone marrow mesenchymal stem cell functions in novel 3D cartilage scaffolds with hydrogen treated multi-walled carbon nanotubes. Nanotechnology 24, 365102.

Holmes, B., Castro, N.J., Zhang, L.G., Zussman, E., 2012. Electrospun fibrous scaffolds for bone and cartilage tissue generation: recent progress and future developments. Tissue Engineering Part B Reviews 18, 478–486.

Holmes, B., Zhu, W., Li, J., Lee, J.D., Zhang, L.G., 2014. Development of biomimetic 3D printed scaffolds for osteochondral regeneration. Tissue Engineering Part A 21 under revision.

Hosseinkhani, H., Hosseinkhani, M., Tian, F., Kobayashi, H., Tabata, Y., 2006. Osteogenic differentiation of mesenchymal stem cells in self-assembled peptide-amphiphile nanofibers. Biomaterials 27, 4079–4086.

Hudalla, G.A., Eng, T.S., Murphy, W.L., 2008. An approach to modulate degradation and mesenchymal stem cell behavior in poly(ethylene glycol) networks. Biomacromolecules 9, 842–849.

Huebsch, N., Mooney, D.J., 2009. Inspiration and application in the evolution of biomaterials. Nature 462, 426–432.

Hutmacher, D.W., 2000. Scaffolds in tissue engineering bone and cartilage. Biomaterials 21, 2529–2543.

Hwang, N.S., Varghese, S., Lee, H.J., Theprungsirikul, P., Canver, A., Sharma, B., Elisseeff, J., 2007. Response of zonal chondrocytes to extracellular matrix-hydrogels. FEBS Letters 581, 4172–4178.

Hwang, N.S., Varghese, S., Li, H., Elisseeff, J., 2011. Regulation of osteogenic and chondrogenic differentiation of mesenchymal stem cells in PEG-ECM hydrogels. Cell and Tissue Research 344, 499–509.

Ilkhanizadeh, S., Teixeira, A.I., Hermanson, O., 2007. Inkjet printing of macromolecules on hydrogels to steer neural stem cell differentiation. Biomaterials 28, 3936–3943.

Ji, C., Annabi, N., Hosseinkhani, M., Sivaloganathan, S., Dehghani, F., 2012. Fabrication of poly-DL-lactide/polyethylene glycol scaffolds using the gas foaming technique. Acta Biomaterialia 8, 570–578.

Jiang, C.C., Chiang, H., Liao, C.J., Lin, Y.J., Kuo, T.F., Shieh, C.S., Huang, Y.Y., Tuan, R.S., 2007. Repair of porcine articular cartilage defect with a biphasic osteochondral composite. Journal of Orthopaedic Research 25, 1277–1290.

Jin, R., Teixeira, L.S.M., Dijkstra, P.J., Van Blitterswijk, C.A., Karperien, M., Feijen, J., 2011. Chondrogenesis in injectable enzymatically crosslinked heparin/dextran hydrogels. Journal of Controlled Release 152, 186–195.

Kasper, F.K., Kushibiki, T., Kimura, Y., Mikos, A.G., Tabata, Y., 2005. In vivo release of plasmid DNA from composites of oligo(poly(ethylene glycol)fumarate) and cationized gelatin microspheres. Journal of Controlled Release 107, 547–561.

Khetan, S., Chung, C., Burdick, J.A., 2009. Tuning hydrogel properties for applications in tissue engineering. Conference Proceedings: Annual International Conference of the IEEE Engineering in Medicine and Biology Society 2009, 2094–2096.

Kilian, K.A., Bugarija, B., Lahn, B.T., Mrksich, M., 2010. Geometric cues for directing the differentiation of mesenchymal stem cells. Proceedings of the National Academy of Sciences of the United States of America 107, 4872–4877.

Kim, I.L., Mauck, R.L., Burdick, J.A., 2011. Hydrogel design for cartilage tissue engineering: a case study with hyaluronic acid. Biomaterials 32, 8771–8782.

Kim, K., Lam, J., Lu, S., Spicer, P.P., Lueckgen, A., Tabata, Y., Wong, M.E., Jansen, J.A., Mikos, A.G., Kasper, F.K., 2013. Osteochondral tissue regeneration using a bilayered composite hydrogel with modulating dual growth factor release kinetics in a rabbit model. Journal of Controlled Release 168, 166–178.

Kim, M.K., Choi, S.W., Kim, S.R., Oh, I.S., Won, M.H., 2010. Autologous chondrocyte implantation in the knee using fibrin. Knee Surgery, Sports Traumatology Arthroscopy: Official Journal of the ESSKA 18, 528–534.

Kisiday, J.D., Kopesky, P.W., Evans, C.H., Grodzinsky, A.J., Mcilwraith, C.W., Frisbie, D.D., 2008. Evaluation of adult equine bone marrow- and adipose-derived progenitor cell chondrogenesis in hydrogel cultures. Journal of Orthopaedic Research 26, 322–331.

Kopesky, P.W., Lee, H.Y., Vanderploeg, E.J., Kisiday, J.D., Frisbie, D.D., Plaas, A.H.K., Ortiz, C., Grodzinsky, A.J., 2010. Adult equine bone marrow stromal cells produce a cartilage-like ECM mechanically superior to animal-matched adult chondrocytes. Matrix Biology 29, 427–438.

Lam, J., Lu, S., Meretoja, V.V., Tabata, Y., Mikos, A.G., Kasper, F.K., 2014. Generation of osteochondral tissue constructs with chondrogenically and osteogenically predifferentiated mesenchymal stem cells encapsulated in bilayered hydrogels. Acta Biomaterialia 10, 1112–1123.

Langer, R., Vacanti, J.P., 1993. Tissue engineering. Science 260, 920–926.

Lawrence, R.C., Felson, D.T., Helmick, C.G., Arnold, L.M., Choi, H., Deyo, R.A., Gabriel, S., Hirsch, R., Hochberg, M.C., Hunder, G.G., Jordan, J.M., Katz, J.N., Kremers, H.M., Wolfe, F., 2008. Estimates of the prevalence of arthritis and other rheumatic conditions in the United States. Part II. Arthritis and Rheumatism 58, 26–35.

Lee, H.Y., Kopesky, P.W., Plaas, A., Sandy, J., Kisiday, J., Frisbie, D., Grodzinsky, A.J., Ortiz, C., 2010. Adult bone marrow stromal cell-based tissue-engineered aggrecan exhibits ultrastructure and nanomechanical properties superior to native cartilage. Osteoarthritis Cartilage 18, 1477–1486.

Lee, S.J., Kang, T., Rhie, J.W., Cho, D.W., 2007. Development of three-dimensional hybrid scaffold using chondrocyte-encapsulated alginate hydrogel. Sensors and Materials 19, 445–451.

Lee, S.J., Rhie, J.W., Cho, D.W., 2008. Development of three-dimensional alginate encapsulated chondrocyte hybrid scaffold using microstereolithography. Journal of Manufacturing Science and Engineering-Transactions of the Asme 130.

Lee, S.Y., Pereira, B.P., Yusof, N., Selvaratnam, L., Yu, Z., Abbas, A.A., Kamarul, T., 2009. Unconfined compression properties of a porous poly(vinyl alcohol)-chitosan-based hydrogel after hydration. Acta Biomaterialia 5, 1919–1925.

Lin, C.C., Anseth, K.S., 2009. PEG hydrogels for the controlled release of biomolecules in regenerative medicine. Pharmaceutical Research 26, 631–643.

Liu, Q., Subhash, G., Moore, D.F., 2011. Loading velocity dependent permeability in agarose gel under compression. Journal of the Mechanical Behavior of Biomedical Materials 4, 974–982.

Madry, H., Rey-Rico, A., Venkatesan, J.K., Johnstone, B., Cucchiarini, M., 2014. Transforming growth factor beta-releasing scaffolds for cartilage tissue engineering. Tissue Engineering Part B Reviews 20, 106–125.

Marsich, E., Borgogna, M., Donati, I., Mozetic, P., Strand, B.L., Salvador, S.G., Vittur, F., Paoletti, S., 2008. Alginate/lactose-modified chitosan hydrogels: a bioactive biomaterial for chondrocyte encapsulation. Journal of Biomedical Materials Research, Part A 84, 364–376.

Martens, P.J., Bryant, S.J., Anseth, K.S., 2003. Tailoring the degradation of hydrogels formed from multivinyl poly(ethylene glycol) and poly(vinyl alcohol) macromers for cartilage tissue engineering. Biomacromolecules 4, 283–292.

Mauck, R.L., Soltz, M.A., Wang, C.C., Wong, D.D., Chao, P.H., Valhmu, W.B., Hung, C.T., Ateshian, G.A., 2000. Functional tissue engineering of articular cartilage through dynamic loading of chondrocyte-seeded agarose gels. Journal of Biomechanical Engineering 122, 252–260.

Maumus, M., Manferdini, C., Toupet, K., Peyrafitte, J.A., Ferreira, R., Facchini, A., Gabusi, E., Bourin, P., Jorgensen, C., Lisignoli, G., Noel, D., 2013. Adipose mesenchymal stem cells protect chondrocytes from degeneration associated with osteoarthritis. Stem Cell Research 11, 834–844.

Mesallati, T., Buckley, C.T., Kelly, D.J., 2014. A comparison of self-assembly and hydrogel encapsulation as a means to engineer functional cartilaginous grafts using culture expanded chondrocytes. Tissue Engineering Part C Methods 20, 52–63.

Mhanna, R., Ozturk, E., Vallmajo-Martin, Q., Millan, C., Muller, M., Zenobi-Wong, M., 2014. GFOGER-modified MMP-sensitive polyethylene glycol hydrogels induce chondrogenic differentiation of human mesenchymal stem cells. Tissue Engineering Part A 20 (7–8), 1165–1174.

Ng, K.W., Lima, E.G., Bian, L., O'conor, C.J., Jayabalan, P.S., Stoker, A.M., Kuroki, K., Cook, C.R., Ateshian, G.A., Cook, J.L., Hung, C.T., 2010. Passaged adult chondrocytes can form engineered cartilage with functional mechanical properties: a canine model. Tissue Engineering Part A 16, 1041–1051.

Nguyen, L.H., Kudva, A.K., Guckert, N.L., Linse, K.D., Roy, K., 2011a. Unique biomaterial compositions direct bone marrow stem cells into specific chondrocytic phenotypes corresponding to the various zones of articular cartilage. Biomaterials 32, 1327–1338.

Nguyen, L.H., Kudva, A.K., Saxena, N.S., Roy, K., 2011b. Engineering articular cartilage with spatially-varying matrix composition and mechanical properties from a single stem cell population using a multi-layered hydrogel. Biomaterials 32, 6946–6952.

Nguyen, Q.T., Hwang, Y., Chen, A.C., Varghese, S., Sah, R.L., 2012. Cartilage-like mechanical properties of poly (ethylene glycol)-diacrylate hydrogels. Biomaterials 33, 6682–6690.

Nicodemus, G.D., Bryant, S.J., 2008. The role of hydrogel structure and dynamic loading on chondrocyte gene expression and matrix formation. Journal of Biomechanics 41, 1528–1536.

Obradovic, B., Stojkovska, J., Jovanovic, Z., Miskovic-Stankovic, V., 2012. Novel alginate based nanocomposite hydrogels with incorporated silver nanoparticles. Journal of Materials Science Materials in Medicine 23, 99–107.

Oliveira, J.M., Rodrigues, M.T., Silva, S.S., Malafaya, P.B., Gomes, M.E., Viegas, C.A., Dias, I.R., Azevedo, J.T., Mano, J.F., Reis, R.L., 2006. Novel hydroxyapatite/chitosan bilayered scaffold for osteochondral tissue-engineering applications: scaffold design and its performance when seeded with goat bone marrow stromal cells. Biomaterials 27, 6123–6137.

Overhauser, J., 1992. Encapsulation of cells in agarose beads. Methods in Molecular Biology 12, 129–134.

Park, H., Guo, X., Temenoff, J.S., Tabata, Y., Caplan, A.I., Kasper, F.K., Mikos, A.G., 2009. Effect of swelling ratio of injectable hydrogel composites on chondrogenic differentiation of encapsulated rabbit marrow mesenchymal stem cells in vitro. Biomacromolecules 10, 541–546.

Park, H., Temenoff, J.S., Holland, T.A., Tabata, Y., Mikos, A.G., 2005. Delivery of TGF-beta1 and chondrocytes via injectable, biodegradable hydrogels for cartilage tissue engineering applications. Biomaterials 26, 7095–7103.

Park, H., Temenoff, J.S., Tabata, Y., Caplan, A.I., Mikos, A.G., 2007. Injectable biodegradable hydrogel composites for rabbit marrow mesenchymal stem cell and growth factor delivery for cartilage tissue engineering. Biomaterials 28, 3217–3227.

Park, J.S., Yang, H.N., Woo, D.G., Jeon, S.Y., Park, K.H., 2011. The promotion of chondrogenesis, osteogenesis, and adipogenesis of human mesenchymal stem cells by multiple growth factors incorporated into nanosphere-coated microspheres. Biomaterials 32, 28–38.

Phillippi, J.A., Miller, E., Weiss, L., Huard, J., Waggoner, A., Campbell, P., 2008. Microenvironments engineered by inkjet bioprinting spatially direct adult stem cells toward muscle- and bone-like subpopulations. Stem Cells 26, 127–134.

Robert, H., 2011. Chondral repair of the knee joint using mosaicplasty. Orthopaedics and Traumatology Surgery and Research 97, 418–429.

Roux, C., Pisani, D.F., Yahia, H.B., Djedaini, M., Beranger, G.E., Chambard, J.C., Ambrosetti, D., Michiels, J.F., Breuil, V., Ailhaud, G., Euller-Ziegler, L., Amri, E.Z., 2013. Chondrogenic potential of stem cells derived from adipose tissue: a powerful pharmacological tool. Biochemical and Biophysical Research Communications 440, 786–791.

Salamon, A., Jonitz-Heincke, A., Adam, S., Rychly, J., Muller-Hilke, B., Bader, R., Lochner, K., Peters, K., 2013. Articular cartilage-derived cells hold a strong osteogenic differentiation potential in comparison to mesenchymal stem cells in vitro. Experimental Cell Research 319, 2856–2865.

Santo, V.E., Gomes, M.E., Mano, J.F., Reis, R.L., 2012. From nano- to macro-scale: nanotechnology approaches for spatially controlled delivery of bioactive factors for bone and cartilage engineering. Nanomedicine (Lond) 7, 1045–1066.

Schneider, U., Rackwitz, L., Andereya, S., Siebenlist, S., Fensky, F., Reichert, J., Loer, I., Barthel, T., Rudert, M., Noth, U., 2011. A prospective multicenter study on the outcome of type I collagen hydrogel-based autologous chondrocyte implantation (CaReS) for the repair of articular cartilage defects in the knee. The American Journal of Sports Medicine 39, 2558–2565.

Schuller-Ravoo, S., Teixeira, S.M., et al., 2013. Flexible and elastic scaffolds for cartilage tissue engineering prepared by stereolithography using poly(trimethylene carbonate)-based resins. Macromolecular Bioscience 13(12), 1711–1719.

Seck, T.M., Melchels, F.P.W., Feijen, J., Grijpma, D.W., 2010. Designed biodegradable hydrogel structures prepared by stereolithography using poly(ethylene glycol)/poly(D,L-lactide)-based resins. Journal of Controlled Release 148, 34–41.

Seidi, A., Ramalingam, M., Elloumi-Hannachi, I., Ostrovidov, S., Khademhosseini, A., 2011. Gradient biomaterials for soft-to-hard interface tissue engineering. Acta biomaterialia 7, 1441–1451.

Shah, R.N., Shah, N.A., Del Rosario Lim, M.M., Hsieh, C., Nuber, G., Stupp, S.I., 2010. Supramolecular design of self-assembling nanofibers for cartilage regeneration. Proceedings of the National Academy of Sciences of the United States of America 107, 3293–3298.

Sharifi, S., Blanquer, S.B.G., Van Kooten, T.G., Grijpma, D.W., 2012. Biodegradable nanocomposite hydrogel structures with enhanced mechanical properties prepared by photo-crosslinking solutions of poly(trimethylene carbonate)-poly(ethylene glycol)-poly(trimethylene carbonate) macromonomers and nanoclay particles. Acta Biomaterialia 8, 4233–4243.

Shoichet, M.S., Li, R.H., White, M.L., Winn, S.R., 1996. Stability of hydrogels used in cell encapsulation: an in vitro comparison of alginate and agarose. Biotechnology and Bioengineering 50, 374–381.

Sittinger, M., Bujia, J., Minuth, W.W., Hammer, C., Burmester, G.R., 1994. Engineering of cartilage tissue using bioresorbable polymer carriers in perfusion culture. Biomaterials 15, 451–456.

Spiller, K.L., Maher, S.A., Lowman, A.M., 2011. Hydrogels for the repair of articular cartilage defects. Tissue Engineering Part B Reviews 17, 281–299.

Streicher, R.M., Schmidt, M., Fiorito, S., 2007. Nanosurfaces and nanostructures for artificial orthopedic implants. Nanomedicine (Lond) 2, 861–874.

Sun, L., Zhang, L., Hemraz, U.D., Fenniri, H., Webster, T.J., 2012. Bioactive rosette nanotube-hydroxyapatite nanocomposites improve osteoblast functions. Tissue Engineering Part A 18, 1741–1750.

Tavazoie, S.F., Alarcon, C., Oskarsson, T., Padua, D., Wang, Q., Bos, P.D., Gerald, W.L., Massague, J., 2008. Endogenous human microRNAs that suppress breast cancer metastasis. Nature 451, 147–152.

Temenoff, J.S., Athanasiou, K.A., Lebaron, R.G., Mikos, A.G., 2002. Effect of poly(ethylene glycol) molecular weight on tensile and swelling properties of oligo(poly(ethylene glycol) fumarate) hydrogels for cartilage tissue engineering. Journal of Biomedical Materials Research 59, 429–437.

Tibbitt, M.W., Anseth, K.S., 2009. Hydrogels as extracellular matrix mimics for 3D cell culture. Biotechnology and Bioengineering 103, 655–663.

Tigli, R.S., Gumusderelioglu, M., 2009. Chondrogenesis on BMP-6 loaded chitosan scaffolds in stationary and dynamic cultures. Biotechnology and Bioengineering 104, 601–610.

Timmer, M.D., Ambrose, C.G., Mikos, A.G., 2003. Evaluation of thermal- and photo-crosslinked biodegradable poly(propylene fumarate)-based networks. Journal of Biomedical Materials Research, Part A 66A, 811–818.

Tiruvannamalai-Annamalai, R., Armant, D.R., Matthew, H.W., 2014. A glycosaminoglycan based, modular tissue scaffold system for rapid assembly of perfusable, high cell density, engineered tissues. PLoS One 9, e84287.

Toh, W.S., Lee, E.H., Guo, X.M., Chan, J.K., Yeow, C.H., Choo, A.B., Cao, T., 2010. Cartilage repair using hyaluronan hydrogel-encapsulated human embryonic stem cell-derived chondrogenic cells. Biomaterials 31, 6968–6980.

Varghese, S., Hwang, N.S., Canver, A.C., Theprungsirikul, P., Lin, D.W., Elisseeff, J., 2008. Chondroitin sulfate based niches for chondrogenic differentiation of mesenchymal stem cells. Matrix Biology 27, 12–21.

Villanueva, I., Gladem, S.K., Kessler, J., Bryant, S.J., 2010. Dynamic loading stimulates chondrocyte biosynthesis when encapsulated in charged hydrogels prepared from poly(ethylene glycol) and chondroitin sulfate. Matrix Biology 29, 51–62.

Wahl, D.A., Sachlos, E., Liu, C., Czernuszka, J.T., 2007. Controlling the processing of collagen-hydroxyapatite scaffolds for bone tissue engineering. Journal of Materials Science Materials in Medicine 18, 201–209.

Wakitani, S., Goto, T., Pineda, S.J., Young, R.G., Mansour, J.M., Caplan, A.I., Goldberg, V.M., 1994. Mesenchymal cell-based repair of large, full-thickness defects of articular cartilage. The Journal of Bone Joint Surgery-American Volume 76, 579–592.

Wakitani, S., Okabe, T., Horibe, S., Mitsuoka, T., Saito, M., Koyama, T., Nawata, M., Tensho, K., Kato, H., Uematsu, K., Kuroda, R., Kurosaka, M., Yoshiya, S., Hattori, K., Ohgushi, H., 2011. Safety of autologous bone marrow-derived mesenchymal stem cell transplantation for cartilage repair in 41 patients with 45 joints followed for up to 11 years and 5 months. Journal of Tissue Engineering and Regenerative Medicine 5, 146–150.

Wang, D.A., Williams, C.G., Li, Q., Sharma, B., Elisseeff, J.H., 2003. Synthesis and characterization of a novel degradable phosphate-containing hydrogel. Biomaterials 24, 3969–3980.

Wang, X., Wenk, E., Zhang, X., Meinel, L., Vunjak-Novakovic, G., Kaplan, D.L., 2009. Growth factor gradients via microsphere delivery in biopolymer scaffolds for osteochondral tissue engineering. Journal of Controlled Release 134, 81–90.

Watts, A.E., Ackerman-Yost, J.C., Nixon, A.J., 2013. A comparison of three-dimensional culture systems to evaluate in vitro chondrogenesis of equine bone marrow-derived mesenchymal stem cells. Tissue Engineering Part A 19, 2275–2283.

Wysocka, A., Mann, K., Bursig, H., Dec, J., Gazdzik, T.S., 2010. Chondrocyte suspension in fibrin glue. Cell Tissue Bank 11, 209–215.

Xia, W., Liu, W., Cui, L., Liu, Y., Zhong, W., Liu, D., Wu, J., Chua, K., Cao, Y., 2004. Tissue engineering of cartilage with the use of chitosan-gelatin complex scaffolds. Journal of Biomedical Materials Research, Part B, Applied Biomaterials 71, 373–380.

Xu, X., Jha, A.K., Duncan, R.L., Jia, X., 2011. Heparin-decorated, hyaluronic acid-based hydrogel particles for the controlled release of bone morphogenetic protein 2. Acta Biomaterialia 7, 3050–3059.

Yamaoka, H., Asato, H., Ogasawara, T., Nishizawa, S., Takahashi, T., Nakatsuka, T., Koshima, I., Nakamura, K., Kawaguchi, H., Chung, U.I., Takato, T., Hoshi, K., 2006. Cartilage tissue engineering using human auricular chondrocytes embedded in different hydrogel materials. Journal of Biomedical Materials Research, Part A 78, 1–11.

Yang, Z., Wu, Y., Li, C., Zhang, T., Zou, Y., Hui, J.H., Ge, Z., Lee, E.H., 2012. Improved mesenchymal stem cells attachment and in vitro cartilage tissue formation on chitosan-modified poly(L-lactide-co-epsilon-caprolactone) scaffold. Tissue Engineering Part A 18, 242–251.

Yoon, D.M., Curtiss, S., Reddi, A.H., Fisher, J.P., 2009. Addition of hyaluronic acid to alginate embedded chondrocytes interferes with insulin-like growth factor-1 signaling in vitro and in vivo. Tissue Engineering Part A 15, 3449–3459.

Zhang, L., Hemraz, U.D., Fenniri, H., Webster, T.J., 2010. Tuning cell adhesion on titanium with osteogenic rosette nanotubes. Journal of Biomedical Materials Research, Part A 95, 550–563.

Zhang, L., Hu, J., Athanasiou, K.A., 2009a. The role of tissue engineering in articular cartilage repair and regeneration. CRC Critical Reviews in Bioengineering 37, 1–57.

Zhang, L., Rakotondradany, F., Myles, A.J., Fenniri, H., Webster, T.J., 2009b. Arginine-glycine-aspartic acid modified rosette nanotube-hydrogel composites for bone tissue engineering. Biomaterials 30, 1309–1320.

Zhang, L., Ramsaywack, S., Fenniri, H., Webster, T.J., 2008a. Enhanced osteoblast adhesion on self-assembled nanostructured hydrogel scaffolds. Tissue Engineering Part A 14, 1353–1364.

Zhang, L., Rodriguez, J., Raez, J., Myles, A.J., Fenniri, H., Webster, T.J., 2009c. Biologically inspired rosette nanotubes and nanocrystalline hydroxyapatite hydrogel nanocomposites as improved bone substitutes. Nanotechnology 20, 175101.

Zhang, L., Sirivisoot, S., Balasundaram, G., Webster, T.J., 2008b. Nanoengineering for bone tissue engineering. In: Khademhosseini, A., Borenstein, J., Toner, M., Takayama, S. (Eds.), Micro and Nanoengineering of the Cell Microenvironment: Technologies and Applications. Artech House.

Zhang, L., Webster, T.J., 2009. Nanotechnology and nanomaterials: promises for improved tissue regeneration. Nanotoday 4, 66–80.

Zhao, H., Ma, L., Zhou, J., Mao, Z., Gao, C., Shen, J., 2008. Fabrication and physical and biological properties of fibrin gel derived from human plasma. Biomedical Materials 3, 015001.

Zhou, C., Ma, L., Li, W., Yao, D., 2011. Fabrication of tissue engineering scaffolds through solid-state foaming of immiscible polymer blends. Biofabrication 3, 045003.

This page intentionally left blank

Part Three

Ceramic and glass nanocomposites for musculoskeletal tissue regeneration

This page intentionally left blank

Biomimetic phosphate nanocomposites for bone-tissue regeneration

13

J. Buschmann
University Hospital Zurich, Zurich, Switzerland

13.1 Introduction

One hundred years ago, the German philosopher Walter Benjamin (1892–1940) understood mimesis as a crucial step in the development of a child; children mimic what they see and hear [1]. Moreover, Benjamin also asked the question how it could be possible to "read in the book of nature"— and again (perhaps in a more general way to understand) suggested closely looking at nature and thereby getting oneself a little bit alike what we are observing. In that sense, looking closely at natural-bone tissue, approaches for regenerative medicine with respect to bone replacement should include different levels of mimesis; mimesis with respect to structure, function and mechanical behavior.

13.2 Biomimesis of bone tissue

13.2.1 Natural bone

Many studies have been performed to analyze the material "bone" [2,3], to be able to closely mimic the natural material when fabricating biomaterials aimed at bone regeneration. The main building block of bone is a mineralized collagen fibril; with the mineral phase consisting of ~60 wt% hydroxyapatite (HA; $Ca_{10}(PO_4)_6(OH)_2$), dahllite (DA; Ca_5 (PO_4, $CO_3)_3(OH)$), carbonate (4 wt%) and additionally citrate (1 wt%) which plays a critical role in crystal thickening and stabilizing mineral crystals in bone [4,5]. The organic phase on the other hand is primarily composed of collagen I fibrils (about 80–100 nm in diameter). Type I collagen is formed by a triple helix pattern of two α1 and one α2 chains. Although collagen I makes up around 20 wt% of the whole bone substance, other organic components such as osteocalcin, osteonectin, osteopontin, thrombospondin, morphogenetic protein, sialoprotein, serum proteins, polysaccharides, lipids and cytokines among others, do only amount to a total of around 3 wt% [5].

Worthwhile to stress is another inorganic component of bone: water. With its 9 wt% of total bone mass, it is essential and crucial—and in bone-tissue engineering studies an often neglected component, because many studies include tests of

Nanocomposites for Musculoskeletal Tissue Regeneration. http://dx.doi.org/10.1016/B978-1-78242-452-9.00013-3

"dry" bone grafting materials [6] and not "wet" materials—scaffolds swollen by water mimicking the real in vivo situation [7].

Besides these basic building blocks, bone cells populated on those structures are fundamental for keeping the bone material alive—osteoblasts and the mature osteocytes producing extracellular matrix (ECM) including the mineralized collagen fibrils; and osteoclasts, the bone-resorbing cells [8]. Finally, bone-marrow stromal cells have the important role of differentiation into preosteoblasts—and in case of injury—play pivotal benefits in bone regeneration [9].

With this knowledge of bone composition in background, it should theoretically be easy to engineer artificial bone. However, it is not done with providing all the aforementioned components. As the different hierarchical levels of bone lead to a very wide range of biomechanical properties, tissue engineering encounters many difficulties in terms of stability. Although the mineral components should provide toughness and rigidity to a tissue-engineered bone graft, the organic component should add tensile strength and flexibility. Moreover, the new generation of phosphate nanocomposites should synergistically combine the advantages of polymers such as biocompatibility, desired shape and resistance to corrosion with the bioactive properties of the phosphate nanoparticles. Usually when speaking of natural bone, two large subgroups are considered: cancellous bone as well as cortical bone. Their biomechanical properties are completely different and do vary in a wide range within each subgroup. For example, Young's moduli of 0.05 to 0.5 GPa are determined for cancellous bone and 14 to 20 GPa for cortical bone (Table 13.1). Furthermore, the tensile and compressive strength found for the two kinds of natural bone vary remarkably, with tensile strength of 10 to 20 and 50 to 150 MPa and compressive strength of 7 to 10 and 170 to 193 MPa for cancellous and cortical bone, respectively. Studies including functional grading try to overcome problems of mechanical stability [10]; however, no study so far reached a mimesis level at which all the structures of bone organization such as osteons and different collagen-fibril array patterns are considered in detail and in which the mechanical behavior adequately resembles natural bone in all its characteristics.

Table 13.1 Physical properties of natural bone (Ref. [5] and references therein)

Property	Cancellous bone	Cortical bone
Young's modulus (GPa)	0.05–0.5	14–20
Tensile strength (MPa)	10–20	50–150
Compressive strength (MPa)	7–10	170–193
Strain to failure (%)	5–7	1–3
Density (g/cm^3)	0.1–1.0	18–22
Surface/bone volume (mm^2/mm^3)	20	2.5

Murugan R, Ramakrishna S. Development of nanocomposites for bone grafting. Compos Sci Technol 2005;65(15–16):2385–2406.

13.2.2 Mimesis of inorganic phosphate phases

13.2.2.1 Calcium phosphates

Crystalline alpha-tricalcium phosphate and beta-tricalcium phosphate

Tricalcium phosphate (TCP, $Ca_3(PO_4)_2$) occurs in two crystalline modifications, as alpha-TCP which is formed at high temperatures and as beta-TCP (Table 13.2). Alpha-TCP can be prepared by precipitation of $Ca(OH)_2$ and *ortho*-H_3PO_4 and a calcining program at 1400°C [6]. It has been used in combination with poly-L-lactic acid (PLLA) to form a biomimetic nanocomposite for bone regeneration [6]. The authors prepared the polylactic acid (PLA)–alpha-TCP nanocomposite with two different injection molding conditions; either with a mold temperature of 40°C (quenched samples) or of 110°C (annealed samples). The annealed samples showed a higher crystallinity, a higher storage modulus and glass transition temperature, which implies a higher energy to resist deformation in vivo. Compared to cortical bone of bovine femur which has a storage modulus of ~8 GPa, storage moduli of dry PLA/alpha-TCP (30 wt% of TCP nanoparticles) reached values of ~5.5 GPa, probably preventing stress shielding during bone regeneration [11]. It was concluded that according to the need of the load-bearing conditions at a specific bone defect site, different approaches in the preparation of PLA/alpha-TCP may offer a wide range of bone-replacement material characteristics [6].

The second modification, beta-TCP, is widely used in combinations with polymers to mimic the phosphate phase in bone. Regarding this combination, there have been several reports lately. Yeo et al. produced a composite scaffold material based on polycaprolactone (PCL)–beta-TCP by melt plotting and embedding in electrospun collagen I nanofibers [12]—with the beta-TCP particles being in the size range of 100 nm to 12 µm. Osteoblast-like cells (MG_{63}) were shown to attach better and proliferate doubly as fast in the PCL–beta-TCP collagen nanocomposite compared to PCL–beta-TCP alone [12]. The authors concluded to have a synergistic effect in their hierarchically composed scaffold by the beta-TCP particles and the collagen I nanofibers. In another study, beta-TCP nanoparticles combined with PCL served as a basic composite material to produce functionally graded nanocomposites via twin-screw-extrusion/spiral-winding process [10]. Rather large scaffolds were fabricated, with radial gradations in porosity, pore size, chemical and mechanical properties. In vitro experiments with human fetal osteoblasts were successful; not only did the cells attach well to the scaffold and proliferate into the three-dimensional (3D) structure, but also was a Ca^{2+} deposition observed by early mineralized-matrix synthesis during the first 8 days [10].

Rakovsky et al. also chose beta-TCP as a phosphate phase for the production of a nanocomposite. They produced the 50–150-nm sized beta-TCP nanoparticles via calcination of the previously prepared HA [13]. Attrition milling with PLA disintegrated the agglomerates and led to uniformly dispersed nanoparticles. Variation of attrition-milling time and different PLA volume fractions were shown to give nanocomposites with a very wide range of compressive-strength strain curves [13]. For example, when the attrition-milling time was increased from 12 to 24 h, the compressive strength of beta-TCP–PLA with 40 vol% of PLA in the composite increased from

Table 13.2 Inorganic phosphate phases used for biomimetic nanocomposites aimed at bone-tissue engineering

	alpha-TCP	beta-TCP	amorphous TCP	HA	OCP
Chemical formula	$Ca_3(PO_4)_2$	$Ca_3(PO_4)_2$	$Ca_xH_y(PO_4)_z{\cdot}nH_2O$; n = 3–4.5	$Ca_{10}(PO_4)_6(OH)_2$	$Ca_8H_2(PO_4)_6{\cdot}4H_2O$
Ca/P molar ratio	1.48 [27]	1.48 [27]	1.2–2.2 [22]	1.67 [27]	1.33 [27]
Elastic modulus (GPa)	104 [77] 189 [76]	33 [78] 64 [76] 80–90 [79]	–	114 [75] 80–110 [22]	–
Compressive strength (MPa)	–	–	–	400–900 [5] 350–917 [22]	–
Solubility, 25°C, gL^{-1}	0.0025 [22]	0.0005 [22]	–	0.0003 [22]	0.00081 [22]
Cell compatibility (biocompatibility)	Human MSCs [80]	Human MG_{63} cells [12]	Human MSCs [17]	Human dermal fibroblasts [81]	Human bone marrow stromal cells [82]

Besides, biphasic calcium phosphate (BCPs) are bioceramics consisting of two different calcium phosphate phases which are mixed. Typically, BCPs used in nanocomposites aimed at bone regeneration consist of a low solubility calcium phosphate phase such as hydroxyapatite (HA) and a more soluble one such as beta-tricalcium phosphate (TCP) [22]. *MSCs*, mesenchymal stem cells; *OCP*, octacalcium phosphate.

250 to 270 MPa. However, the volume fraction of PLA had a much more pronounced impact on the compressive strength. Although it was 270 MPa for a 40 vol% of PLA, it was increased to 410 MPa for a 20 vol% of PLA (both having an attrition milling time of 24 h). Although the reported compressive-strength values are beyond the values found for natural cortical bone (Table 13.1), it is nicely exemplified how processing conditions may drastically influence the biomechanical properties of tissue-engineering phosphate nanocomposites and as such offer the option of tuning and tailoring the desired material properties.

Finally, beta-TCP nanoparticles with a size of 100 nm were blended with DL-poly (lactide-co-glycolic acid) (DL-PLGA) and filaments of nanocomposite material were produced with extrusion [14]. Implanted in rabbit femoral defects, osteoconduction and new bone formation was limited to the periphery of the nanocomposite. The results obtained with an additional HA coating of the DL-PLGA–beta-TCP filaments were similar compared to the filaments having no coating [14].

Amorphous tricalcium phosphate

Compared to crystalline TCPs, amorphous TCP is much more reactive with respect to HA formation in contact with water [15], which is indeed an important feature to render a bone-mimetic nanocomposite bioactive [16]. Therefore, Schneider et al. combined amorphous TCP nanoparticles with poly(lactic-co-glycolic acid) (PLGA) in a bone-regeneration composite material [17], which allowed osteogenic differentiation when human mesenchymal stem cells were seeded on the scaffold and cultured in osteogenic differentiation medium. Moreover, the same material was used in drill-hole defects of long bone in sheep and had a successful outcome 8 weeks postsurgery with respect to new bone formation [18]. Compared to the porous bovine-derived mineral Bio-Oss® (Geistlich, Wolhusen, Switzerland), the PLGA/amorphous TCP nanocomposite resulted in cancellous bone-mimetic structures, whereas Bio-Oss®-treated defects in a rabbit calvarial model afforded solid cortical bone [19]. Recently, amorphous TCP nanoparticles were also combined with poly(D,L-lactic acid) (PDLLA) by electrospinning [20]—and in vitro performance was tested with MG_{63} osteoblast-like cells. Attachment of the cells and proliferation were satisfactory. Also, bioactivity tests in simulated body fluid (SBF) ended up in HA deposition [20]. In addition, with a double diffusion method into gelatin hydrogel, a bone-biomimetic nanocomposite consisting of amorphous TCP and brushite ($CaHPO_4 \cdot 2H_2O$) was produced which was successfully transformed to nanocrystalline HA in SBF [21].

13.2.2.2 Hydroxyapatite

Biomimetic phosphate nanocomposites do sometimes include—besides other phosphate phases—HA, as for example in the next paragraph dealing with biphasic calcium phosphate (BCP) nanocomposites, consisting of beta-TCP and HA (Table 13.2).

13.2.2.3 Biphasic calcium phosphate

BCPs are bioceramics consisting of two different calcium phosphate phases which are mixed. Typically, BCPs used in nanocomposites aimed at bone regeneration consist of

a low-solubility calcium phosphate phase such as HA and a more soluble one such as beta-TCP [22]. BCP nanocomposites based on HA nanofibers and porous beta-TCP matrix had significantly better mechanical properties compared to beta-TCP alone [23] and attained a compressive strength of 9.8 MPa like cancellous bone (Table 13.1). Lin et al. reported that rat adipose-derived stem cells (ASCs) seeded onto a nano-BCP (HA nanofibers in a beta-TCP matrix) resulted in ectopic bone formation when implanted subcutaneously in nude mice; moreover, they stimulated in vivo bone formation when used in critical-size cranial defects in rats [24]. BCP nanocomposites including gelatin are reported to be successfully osteoblast seeded [25]. Moreover, the coating of BCP with a layer of PCL and HA nanoparticles was reported to be well populated with human osteoblasts in co-culture with human ASCs, which triggered osteogenic differentiation of the latter—being an advantage of a biomimetic-bone nanocomposite material [26].

13.2.2.4 Octacalcium phosphate

Octacalcium phosphate (OCP) has a low Ca/P molar ratio with 1.33 and favors faster dissolution of the Ca^{2+} and PO_4^{3-} ions compared to higher Ca/P ratios as in beta-TCP (1.5), or HA (1.67) which is insoluble in SBF [27]. Because an impact of free Ca^{2+} ion concentration on osteoinduction was reported [28], OCP might be an interesting inorganic phase in nanocomposites aimed at bone reconstruction [29].

13.2.2.5 Best biomimetic inorganic phase?

After presenting a diverse set of inorganic phosphate phases used in nanocomposites aimed at bone regeneration, the question arises which phosphate phase is mimicking frank bone the best. This is not an easy question, and the huge amount of literature dealing with research in this field suggests that no clear answer has yet been found. In terms of biomineralization capability, the crystallinity of a phosphate compound plays a pivotal role. From this point of view, introducing amorphous rather than crystalline calcium phosphate phases into organic carriers is advantageous; amorphous TCP in contact with water is more quickly transformed into HA compared to alpha-TCP or beta-TCP. Biomineralization capacity is coupled to dissolution rates of the corresponding phosphate phase. For the presented phosphate phases, the relative dissolution rates are amorphous TCP > alpha-TCP > beta-TCP > HA [30]. Moreover, the extent of bone mimesis lies also in the mechanical properties which may vary considerably relative to the ratio of the phosphate phase and the chosen organic phase. It has been shown in many studies that variation of this ratio can lead to the desired bone-mimicking mechanical properties. The porosity also plays a pivotal role. For example, TCP tends to be more porous compared to HA, because the surface formation energies are lower than those for HA [31]. However, such porosity considerations are often given for the pure phosphate compounds [31] and may be completely different in the composite material. As bone is a heterogeneous material in terms of porosity, graded materials are suggested to mimic bone the best. Finally, integration of the bone graft into the living surrounding tissue is also important. Therefore, reports on osteoinduction as well as osteoconduction in animal models should be considered while choosing a specific combination of inorganic and organic phase for bone reconstruction.

13.2.3 Mimesis of organic phases

13.2.3.1 Cellulose

Cellulose, a polysaccharide based on β-D-glucose monomers, is the most abundant biopolymer in the biosphere [32] (Table 13.3). Cellulose and its derivative carboxymethylated cellulose were used as an organic carrier for calcification to generate a macroporous matrix for bone regeneration [33]. Three different precalcification methods were used before immersing the precalcified scaffolds into SBF for biomimetic mineralization and HA formation during 2 weeks. All three approaches, (1) incubation in $CaCl_2$ and $(NH_4)_2HPO_4$; (2) carboxymethylation and NaOH; (3) calcium silicate for silanolization, were successful with respect to subsequent mineralization; however, the carboxymethylated cellulose showed the best results with respect to mineralization rate and amount of deposited HA; moreover, DNA of MG_{63} osteoblasts grown on the respective matrices was highest for the cellulose that had been carboxymethylated [33]. In another study, microbial cellulose was alternately incubated in $CaCl_2$ and Na_2HPO_4 to form HA; the nanocomposite was applied in noncritical size defects of the rat tibia and analyzed 1, 4 and 16 weeks postsurgery [27]. Results showed completely repaired mature bone after 16 weeks with a clear cell infiltration of osteoblasts and osteoclasts as well as sufficient vascularization. At that time point, the cellulose-based bone graft was not yet fully degraded [27].

13.2.3.2 Chitosan

High and medium molecular weight chitosan was used in combination with HA nanoparticles for bone-tissue engineering [34]. Different weight fractions of HA in the HA–chitosan nanocomposites were characterized, with increasing compression moduli determined for higher HA fractions. Moreover, preosteoblast cell behavior was better on HA–chitosan nanocomposites compared to pure chitosan—improved attachment and higher proliferation of the cells were found [34]. In another study, chitosan was combined with orthophosphoric acid to yield chitosan phosphate; this was then further modified with HA nanoparticles as a filler in 10–60 wt% [35]. The impact of phosphatation of chitosan lies in the fact that HA nanoparticles are better and more homogeneously distributed in the polymer due to particle–phosphate interactions. The nanocomposite was beneficial with respect to osteocompatibility and osteogenesis when primary murine osteoblasts were seeded and cultured on this bioanalog composite material [35]. Finally, also blends of chitosan with other polymers such as PLLA and combined with calcium phosphate nanoparticles aimed at bone-tissue engineering were fabricated [36]. The elastic moduli of the corresponding materials were tunable, with 4 to 15.6 MPa (chitosan:PLLA 20:80), 12.2 to 53.1 MPa (chitosan:PLLA 50:50) and 15.5 to 82.6 MPa (chitosan:PLLA 80:20). As such, the elastic modulus of these blended nanocomposites were comparable to cancellous bone [36] (Table 13.1)—no in vitro or in vivo experiments were reported.

13.2.3.3 Collagen

Using collagen I as the organic phase in bone-biomimetic nanocomposites comes to nature the nearest. Collagen initiates and orientates HA crystal growth and is reported to be responsible for size and distribution of HA crystals in natural bone [37].

Table 13.3 Organic phases used for biomimetic phosphate nanocomposites intended for bone-tissue engineering

	Structure	Formula	Cell study	Further properties
Cellulose	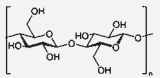	$(C_6H_{10}O_5)_n$	Human MG_{63} cells [33]	Density: 1.5 g/cm^3 Melting point: 260–270°C "Sugar of plant cell wall"
Chitosan	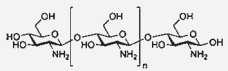	$(C_6H_6O_4N)_n$	Mouse Preosteoblasts MC 3T3-E1 [34]	M_w = 3800–20,000 da Rapidly clots blood Antibacterial agent
Collagen	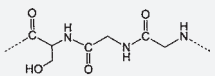 (Example of a polypeptide structure)	Protein with each third amino acid = glycine	Human MSCs [42]	Triple-stranded helix of collagen polypeptide alpha chains
Gelatin	Irreversibly partially hydrolyzed collagen	Rich in glycine and proline	Rabbit ASCs [43]	Hemostatic; activates coagulation
Polycaprolactone	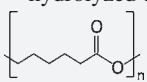	$(C_6H_{10}O_2)_n$	Human MG_{63} cells [50]	Density: 1.1 g/cm^3 Melting point: 60°C Tensile strength: 16–400 MPa [83]
Polylactic acid	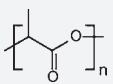	$(C_3H_4O_2)_n$	Mouse Preosteoblasts MC 3T3-E1 [56]	Density: 1.2–1.4 g/cm^3 Melting point: 150–160°C Tensile strength: 28–50 MPa [83]
Poly(lactic-co-glycolic acid)	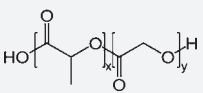	x, number of units of lactic acid; y, number of units of glycolic acid	Human MSCs [61]	The higher the glycolide content, the faster the degradation.
Polyvinyl alcohol	$(CH_2—CHOH)_n$	$(C_2H_4O)_n$	Human MG_{63} cells [68]	Tensile strength: 25–35 MPa [83]

M_w, molecular weight; *MSCs*, mesenchymal stem cells; *ASCs*, adipose-derived stem cells.

Therefore, many researchers used collagen successfully in combination with HA [3,7,38–41]. For example, collagen–apatite nanocomposite foams were used in a critical-size defect of pig tibia and resulted in new bone formation 6 months postoperation [41]. Although having low mechanical properties with compressive strength at maximum of 0.14 MPa compared to cancellous bone having values of 7 to 10 MPa (Table 13.1), a collagen-foam scaffold with in situ-generated calcium phosphate crystals, has been proposed to serve as a biomimetic-bone graft. This is because in vitro studies with human mesenchymal stem cells from two different sources (Wharton's jelly and menstrual blood) had significantly higher alkaline phosphatase (ALP) activity and showed osteogenesis when seeded onto the calcium phosphate–collagen nanocomposite compared to the collagen foam alone [42].

13.2.3.4 Gelatin

Gelatin, as a derivative of collagen, is a polymer obviously useful to biomimic the organic phase of bone. To generate an ideal HA–gelatin nanocomposite, Hwang et al. studied different ratios of HA:gelatin, and determined the impact of glutaraldehyde (GA) addition [43]. Rabbit ASCs were seeded on those nanocomposites, with the 10 g HA:3 g gelatin ratio (without GA) leading to the best response with respect to attachment, proliferation and osteogenic differentiation of ASCs. A subsequent study with the same nanocomposite resulted in a clear final differentiation step from human osteoblasts into osteocytes [44].

At a physiologically relevant pH of 7.4, a gelatin hydrogel was placed in the middle of two solutions, $CaCl_2$ and Na_2HPO_4, which resulted—after diffusion and precipitation—in HA nanoparticles on the gelatin [21]. Compared to microsized HA on gelatin, an enhanced reinforcing ability of the HA nanoparticles was proposed, suggested by the significantly higher compressive strength of the material. In another study, gelatin from bovine skin type B was stabilized by cross-linking with N-(3-dimethyl aminopropyl)-N′-ethyl carbodiimide (EDC) and combined with BCP [25]. Such a stabilization by cross-linking was also favorably applied by Li and Aparicio [3]. The influence of gelatin on the mechanical properties of biphasic nanocomposite materials aimed at bone regeneration was examined also by Babaei et al. [45]. They found a positive influence of gelatin on the mechanical properties of the scaffold when gelatin–chitosan/HA nanocomposites were compared to chitosan–HA nanocomposites—significant improvements of the elastic modulus and compressive strength were achieved [45].

13.2.3.5 Heliobond®

Heliobond® is a polymer mixture of 60% bisphenol-a-diglycidyl ether methacrylate (Bis-GMA) and 40% of triethylene glycol dimethacrylate (TEGDMA), which turns into an adhesive polymer under blue light of $\lambda = 450$ nm [46]. From its chemical structure, it is not biomimetic due to predominant ether functionality. However, Heliobond® was successfully combined with amorphous TCP, which was changed into HA after in vitro biomineralization in SBF. Adhesion to wet cow bone was tested, and the incorporation of 20 wt% of amorphous TCP significantly improved it compared to

Heliobond® alone. In addition, the compressive strength of 205 MPa was determined to be very similar to human femoral bone [46].

13.2.3.6 Hydrogel

Hydrogels consisting of oligo(poly(ethylene glycol) fumarate) (OPF) were either physically or chemically mixed with calcium phosphate of varying crystallinity. Although the physical mixing resulted in irreproducible dispersion of the calcium phosphate components, the chemical mixing lead to a homogeneous distribution of the calcium phosphates in the hydrogel [47]. In another study, 3D-bioplotted hydrogels consisting of PLGA, collagen or chitosan and spiked with TCP nanoparticles were successfully used as cranial critical-size defect fillers in sheep [48].

13.2.3.7 Polycaprolactone

In a study by Mavis et al., PCL was immersed in 10SBF-like solutions (10 times as concentrated as simulated body fluid) based on a variety of protocols [49]. The nanofibers were coated with biomimetic calcium phosphate components including HA and $CaHPO_4$. The coatings were optimized according to thermodynamic modeling results and cell seeding was shown beneficial [49]. An in vivo study by Liang et al. showed histologically that new bone tissue was observed in a rabbit mandible defect, when a PCL scaffold with 60 wt% nonstoichiometric apatite particles was implanted [50]. In contrast, PCL scaffolds containing only 20 wt% or no apatite performed less beneficially. In addition, the authors also did cell studies using MG_{63} osteoblasts. After 7 days, a clear increase in ALP and nitric oxide in the presence of 60 wt% nonstoichiometric apatite compared to mere PCL corroborated the in vivo findings [50].

A functionally graded PCL–beta-TCP scaffold for bone regeneration was established by varying the beta-TCP:PCL ratio in different layers of a cylindrical radially graded material [10]. Such graded scaffold materials with varying porosity were shown beneficial with respect to proliferation of human fetal osteoblast.

Differentiation studies of ASCs toward osteoblasts were performed on PCL-coated BCP [26]. It was shown that either the addition of nano-HA particles in the PCL coating, or a co-culture system with osteoblasts using only PCL coating, was essential for this differentiation process. Similarly, Roohani-Esfahani et al. used a BCP scaffold with a PCL coating containing nano-HA particles. They studied the impact of nanoparticle size and shape (needles, rods and spheres) on osteogenesis and also on biomechanical properties [51]. Scaffolds coated with needle-shaped nano-HA particles in PCL showed the best osteogenic differentiation profile compared to microcomposite-coated scaffolds. Moreover, with respect to biomechanics, the best scaffold material had a maximum compressive strength of 2.1 MPa which is 20 times higher than unmodified merely PCL-coated scaffolds, but four times lower than cancellous bone [51].

13.2.3.8 Peptides

Bone-biomimetic nanocomposite materials based on peptides potentially aimed at orthopedic applications are rather seldom reported; a thermoreversibly gelling block copolymer conjugated to HA-nucleating peptides, however, has been reported similar

to the apatite present in bone [52]. The thermoreversible gelation properties of this material could enable it to serve as an injectable biomaterial for bone regeneration—no cell studies or in vivo studies have been performed so far [53].

13.2.3.9 Polylactic acid

Homogenous and dense beta-TCP–PLA nanocomposites with very high compressive strengths of up to 400 MPa with high-volume fractions of beta-TCP (60–80%) were produced with the intention of using it for bone regeneration [13]. Other nanocomposites including PLA as an organic carrier material for HA nanorods [54] and for HA nanoparticles [55] were reported and mostly differ in their preparation methods (see Section 13.3 in the following). A special approach including carbon nanotubes adsorbed onto nano-calcium phosphate powder mixed with PLA was shown beneficial in an in vitro study with respect to cell proliferation, osteogenesis and mechanical properties [56]. In addition, blends of PLA with collagen (1:1) that are reinforced with calcium phosphate nanoparticles through a flow-mineralization process were reported beneficial with respect to bone-mimicking regenerative purposes [57].

13.2.3.10 Poly(lactic-co-glycolic acid)

Combined with calcium phosphate compounds, biodegradable PLGA is one of the mostly used organic polymers in orthopedic applications [58]. The copolymer has been approved by the Food and Drug Administration (FDA). Its properties can be varied with the variation of the ratio of the two constituents. As the degradation of PLGA is acidic, addition of calcium phosphate compounds may compensate the pH drop induced by PLGA—making it an ideal implant material [14,18,59,60]. Moreover, such nanocomposites have been shown to trigger stem-cell osteogenesis [61]; which is a valuable characteristic as stem-cell therapies are becoming more and more attractive in bone-regenerative medicine [62–64].

An interesting approach with the intention to tailor the release dosage of recombinant human bone morphogenetic protein (rhBMP-2) was reported by Wang et al. [65]. In a dual-source electrospinning process, the authors were able to control the fibrous component ratio, which was primarily based on a PDLLA-nanofibers component (see next chapter) including rhBMP-2 and, as a second component, nanosized calcium phosphate particles in a PLGA matrix. The in vitro behavior of this bicomponent nanocomposite has been shown to be different compared to the monocomponent materials as the degradation behavior—and, going along with this, the release kinetics of the corresponding bone growth factor—could be varied [65].

13.2.3.11 Polyvinyl alcohol

There has been increasing interest in polyvinyl alcohol (PVA) nanocomposites recently [66]. For bone-regeneration purposes, PVA-based biomimetic phosphate compounds were produced by electrospinning [67]. The polymer solution aimed at electrospinning was treated by $Ca(NO_3)_2$ addition to incorporate Ca^{2+} ions in PVA. Such an introduction of Ca^{2+} ions into PVA nanofibers was reported beneficial for the distribution, the nucleation and the crystallinity of subsequent HA forming when alternately

soaking these nanofibers in calcium ($Ca(NO_3)_2$)- and phosphate ($(NH_4)_2HPO_4$)-containing solutions [67]. PVA is also used successfully in combination with gelatin; after testing different ratios of BCP incorporation into these composites, 50% BCP-loaded electrospun PVA–gelatin fibers were reported to give the best results in vitro (MG_{63} cell attachment and growth, and protein expression) and in vivo (5-mm deep hole in the cranium of rats) [68].

13.2.3.12 Best biomimetic organic phase?

From the presented organic-carrier phases for phosphate nanocomposites, collagen type I mimicks true bone the best, because natural bone's organic phase primarily consists of this protein. Moreover, it makes up around 20 wt% of the whole bone substance [5]. Nevertheless, natural polysaccharides such as cellulose or chitosan, both having excellent biocompatibility, are as well beneficial organic carriers for phosphate phases. Other merits of choosing a particular organic phase for phosphate nanocomposites may lie in a high tensile strength, for instance found for PCL, or in thermoreversible gelation properties, enabling injection at the defect site [53].

13.3 Fabrication of biomimetic phosphate nanocomposites

13.3.1 Immersion/soaking/precipitation

Immersion or soaking is one of the simplest methods to incorporate calcium phosphate compounds into organic carriers (Figure 13.1(a)). The basic interaction between such precipitated calcium phosphate species and the organic compound is based on adhesion, in other words on ion–dipole interactions or van der Waals forces (dispersion forces) between the two major components. Hence, many studies include this simple processing step in their protocols [20,45,49].

For example, successful formation of nano-HA in cognate with native apatite on electrospun PLGA, as well as on electrospun PLGA–collagen blend, has been reported to be achieved by a three-cycle process of alternately dipping the electrospun fibers for 5 to 10 min in 0.5 M $CaCl_2$ (pH 7.20) and 0.3 M Na_2HPO_4 (pH 8.96), respectively, properly washing the scaffolds after each immersion step [69]. Also, collagen foams have been beneficially modified to give phosphate nanocomposites by alternate immersion for 2 h into 0.1 M $NaNH_4HPO_4$ (pH 7.20) and 0.1 M $CaCl_2$ (pH 7.20), respectively, without washing in between [42]. Moreover, immersion into a solution—although metastable—containing both the calcium as well as the phosphate component, for 48 h has been reported to lead to successful in situ crystal growth [70].

13.3.2 Electrospinning

As for the organic carrier in the biomimetic nanocomposites, electrospinning is a method that is very often used to generate nanofibers of organic polymers [71]. Briefly, fibers are generated by dissolving the polymer in a suitable solvent which is then loaded in

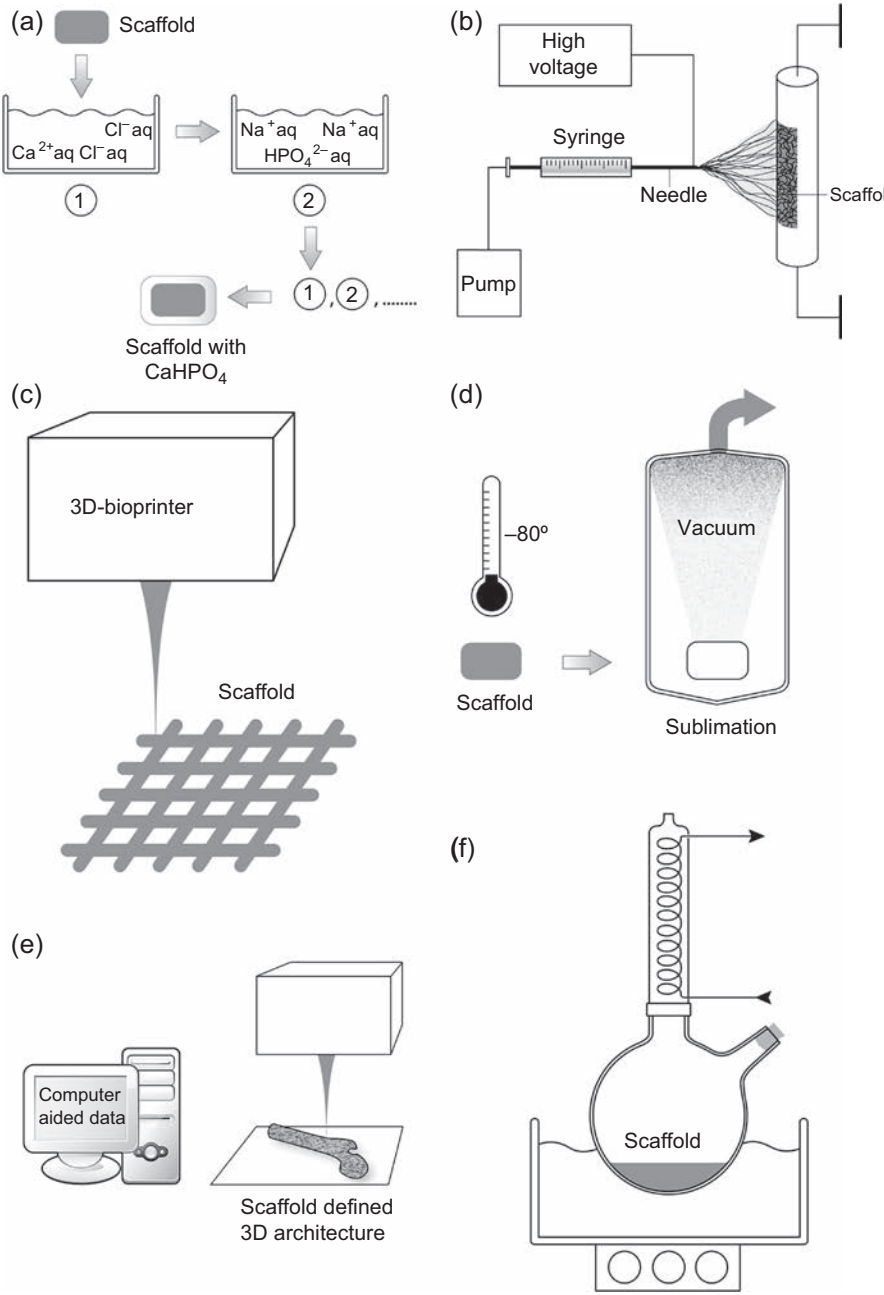

Figure 13.1 Different fabrication processes for phosphate nanocomposites: (a) immersion, soaking, precipitation; (b) electrospinning; (c) (bio)plotting; (d) freeze-casting; (e) rapid prototyping from computer-aided data; and (f) chemical synthesis.

a syringe fitted to a needle (Figure 13.1(b)). A collector often consisting of a round cylindrical target at a distance of usually 20 ± 5 cm to the needle is then covered by fibers emerging from the jet of the needle under high voltage (in the range of 15–20 kV).

In this technique, not only pure polymers can be electrospun, but also polymers in combination with nanoparticles, as realized for example with PLGA and HA nanoparticles [61,72]. Moreover, surfactants can be added to the nanoparticle–polymer–solvent mixture to facilitate the dissolution process and overcome the different polarities of hydrophilic nanoparticles such as HA and the hydrophobic polymer–solvent solutions such as chloroform-dissolved PLA [55].

13.3.3 Plotting

The (bio)plotting technique is also often used for the fabrication of nanocomposites aimed at bone-tissue engineering (Figure 13.1(c)). For example, in melt-plotting, TCP particles were mixed with PCL particles and finally plotted with a 3D robot system to give a grid with square-pore morphology [12]. Although not including an organic carrier, another example for 3D plotting is the report of Xu et al. in which they generated a Nagel scaffold ($Ca_7Si_2P_2O_{16}$) and found that square-pore morphology is better than triangular- or parallelogram-pore morphologies with respect to compressive strength and modulus aimed at bone reconstruction [73].

13.3.4 Freeze-casting

The process of freeze-casting consists of freezing a slurry or blend, usually based on water at low temperatures, and removing the solvent by sublimation under low pressure [36] (Figure 13.1(d)). In the preparation of bone-biomimetic nanocomposites, the technique of freeze-casting has been claimed to lead to adequate mechanical properties and desired pore structure of the so-prepared scaffolds compared to other techniques like dip coating of polymer foams by ceramics or foaming of aqueous ceramic powder suspensions among others [36]. The technique of freeze-casting was applied in the fabrication of a BCP–gelatin nanocomposite. During the freezing, the gelatin that filled the pores of the BCP scaffold became frigid, whereas during the subsequent freeze-drying process the distilled water of the gelatin was sublimated so that a gelatin network was deposited on the surface of the pores—leading to a porous structure of the biomimetic nanocomposite [25]. Another example of successful bone-biomimetic nanocomposite fabrication via freeze-casting is reported by Thein-Han and Misra, in which they used chitosan in acetic acid aqueous solvent and dispersed nano-HA [34].

13.3.5 Rapid prototyping: selective laser sintering

Rapid prototyping comprises a group of techniques that can generate a physical model directly from computer-aided data (Figure 13.1(e)). One of these techniques is selective laser sintering (SLS). It is an additive manufacturing technique used for the low-volume production of prototype models and functional components. SLS uses lasers as its power source to sinter powdered material, binding it together to create

a solid structure. For example, Duan et al. report successful fabrication of a multifunctional tissue-engineered biomimetic nanocomposite based on calcium phosphate and polyhydroxybutyrate-co-hydroxyvalerate by SLS [74]. Moreover, this scaffold material has a surface coating consisting of gelatin and immobilized heparin [74]. The authors claim that such a surface modification provided a suitable binding site for bone morphogenetic protein-2 (BMP-2)—leading to enhanced ALP activity and osteogenesis of mesenchymal stem cells [74].

13.3.6 Synthesis

A rather seldom chosen approach is to chemically synthesize new polymers to mimic processes occurring in nature during bone generation (Figure 13.1(f)). For example, Yusufoglu et al. synthesized new peptides by conjugating polymers into block copolymers offering HA-nucleating sites [52]. Another synthetic approach included the introduction of phosphate groups into chitosan, thereby offering easier nucleation sites for HA generation and also facilitating the addition of HA nanoparticles as a filler material for chitosan due to higher intermolecular forces [35].

13.3.7 Comparison of fabrication processes

Immersion, soaking or (alternatively) dipping accompanied with subsequent precipitation is one of the simplest methods to incorporate calcium phosphate compounds into organic carriers and is therefore widely used and reported. In contrast, chemical synthesis of polymers that mimic natural processes such as HA nucleation or phosphatation are rather seldom reported because large chemical background knowledge as well as a special equipment are needed.

From a cost perspective, electrospinning, plotting and rapid prototyping under the use of computer-aided data are rather expensive methods and have the prerequisite of elaborate and special machines. In the case of electrospinning, such machines may be homemade with rather low costs; however, very sophisticated and expensive apparatus are on the market for which not only all variables can be programmed as a function of time, but also humidity in the electrospinning chamber can be tuned automatically. Compared to these methods, soaking and freeze-drying are low-cost methods with nevertheless very convincing results as shown previously.

From a structure and architecture point of view, discrete 3D architectures are achieved by plotting and prototyping, whereas electrospinning, freeze-casting and also chemical synthesis provide materials that have to be further processed to get the desired final architecture for the implant device.

List of abbreviations

ALP Alkaline phosphatase
ASCs Adipose-derived stem cells
BCP Biphasic calcium phosphate

Bis-GMA Bisphenol-a-diglycidyl ether methacrylate
DA $Ca_5 (PO_4, CO_3)_3 (OH)$, dahllite
ECM Extracellular matrix
EDC N-(3-dimethyl aminopropyl)-N′-ethyl carbodiimide)
FDA Food and Drug Administration
GA Glutaraldehyde
HA $Ca_{10}(PO_4)_6(OH)_2$, hydroxyapatite
OCP Octacalcium phosphate
OPF Oligo(poly(ethylene glycol) fumarate)
PCL Polycaprolactone
PDLLA Poly(D,L-lactic acid)
PLA Polylactic acid
PLLA Poly-L-lactic acid
PLGA Poly(lactic-co-glycolic acid)
PVA Polyvinyl alcohol
rhBMP-2 Recombinant human bone morphogenetic protein-2
SBF Simulated body fluid
SLS Selective laser sintering
10SBF 10 times as concentrated as simulated body fluid
TCP $Ca_3(PO_4)_2$, tricalcium phosphate
TEGDMA Triethylene glycol dimethacrylate

References

[1] Benjamin W. Ueber das mimetische Vermoegen. Gesammelte Schriften. II. Frankfurt am Main 1933:204–13.
[2] Weiner S, Wagner HD. The material bone: structure mechanical function relations. Annu Rev Mater Sci 1998;28:271–98.
[3] Li Y, Aparicio C. Discerning the subfibrillar structure of mineralized collagen fibrils: a model for the ultrastructure of bone. PLoS One 2013;8(9):e76782.
[4] Hu YY, Rawal A, Schmidt-Rohr K. Strongly bound citrate stabilizes the apatite nanocrystals in bone. Proc Natl Acad Sci USA 2010;107(52):22425–9.
[5] Murugan R, Ramakrishna S. Development of nanocomposites for bone grafting. Compos Sci Technol 2005;65(15–16):2385–406.
[6] Wilberforce SI, Finlayson CE, Best SM, Cameron RE. A comparative study of the thermal and dynamic mechanical behaviour of quenched and annealed bioresorbable poly-L-lactide/α-tricalcium phosphate nanocomposites. Acta Biomater 2011;7(5):2176–84.
[7] Gelinsky M, Welzel PB, Simon P, Bernhardt A, Konig U. Porous three-dimensional scaffolds made of mineralised collagen: preparation and properties of a biomimetic nanocomposite material for tissue engineering of bone. Chem Eng J 2008;137(1):84–96.
[8] Akiyama N, Takemoto M, Fujibayashi S, Neo M, Hirano M, Nakamura T. Difference between dogs and rats with regard to osteoclast-like cells in calcium-deficient hydroxyapatite-induced osteoinduction. J Biomed Mater Res Part A 2011;96A(2):402–12.
[9] Heinemann C, Heinemann S, Worch H, Hanke T. Development of an osteoblast/osteoclast co-culture derived by human bone marrow stromal cells and human monocytes for biomaterials testing. Eur Cells Mater 2011;21:80–93.

[10] Ozkan S, Kalyon DM, Yu X. Functionally graded beta-TCP/PCL nanocomposite scaffolds: in vitro evaluation with human fetal osteoblast cells for bone tissue engineering. J Biomed Mater Res A 2010;92(3):1007–18.
[11] Wang T, Feng Z. Dynamic mechanical properties of cortical bone: the effect of mineral content. Mater Lett 2005;59(18):2277–80.
[12] Yeo M, Lee H, Kim G. Three-dimensional hierarchical composite scaffolds consisting of polycaprolactone, β-tricalcium phosphate, and collagen nanofibers: fabrication, physical properties, and in vitro cell activity for bone tissue regeneration. Biomacromolecules 2011;12(2):502–10.
[13] Rakovsky A, Gotman I, Rabkin E, Gutmanas EY. Strong bioresorbable Ca phosphate-PLA nanocomposites with uniform phase distribution by attrition milling and high pressure consolidation. J Mech Behav Biomed Mater 2013;18:37–46.
[14] Kim J, McBride S, Tellis B, Alvarez-Urena P, Song Y-H, Dean DD, et al. Rapid-prototyped PLGA/β-TCP/hydroxyapatite nanocomposite scaffolds in a rabbit femoral defect model. Biofabrication 2012;4(2). [online].
[15] Brunner TJ, Bohner M, Dora C, Gerber C, Stark WJ. Comparison of amorphous TCP nanoparticles to micron-sized alpha-TCP as starting materials for calcium phosphate cements. J Biomed Mater Res Part B 2007;83B(2):400–7.
[16] Brunner TJ, Grass RN, Bohner M, Stark WJ. Effect of particle size, crystal phase and crystallinity on the reactivity of tricalcium phosphate cements for bone reconstruction. J Mater Chem 2007;17(38):4072–8.
[17] Schneider OD, Loher S, Brunner TJ, Uebersax L, Simonet M, Grass RN, et al. Cotton wool-like nanocomposite biomaterials prepared by electrospinning: in vitro bioactivity and osteogenic differentiation of human mesenchymal stem cells. J Biomed Mater Res Part B 2008;84B(2):350–62.
[18] Schneider OD, Mohn D, Fuhrer R, Klein K, Kämpf K, Nuss KMR, et al. Biocompatibility and bone formation of flexible, cotton wool-like PLGA/calcium phosphate nanocomposites in sheep. Open Orthop J 2011;5(1):63–71.
[19] Schneider OD, Weber F, Brunner TJ, Loher S, Ehrbar M, Schmidlin PR, et al. In vivo and in vitro evaluation of flexible, cottonwool-like nanocomposites as bone substitute material for complex defects. Acta Biomater 2009;5(5):1775–84.
[20] Ma Z, Chen F, Zhu YJ, Cui T, Liu XY. Amorphous calcium phosphate/poly(D,L-lactic acid) composite nanofibers: electrospinning preparation and biomineralization. J Colloid Interface Sci 2011;359(2):371–9.
[21] Azami M, Moosavifar MJ, Baheiraei N, Moztarzadeh F, Ai J. Preparation of a biomimetic nanocomposite scaffold for bone tissue engineering via mineralization of gelatin hydrogel and study of mineral transformation in simulated body fluid. J Biomed Mater Res A 2012;100(5):1347–55.
[22] Acros D. Calcium phosphate bioceramics. In: Vallet-Regi M, editor. Bio-ceramics with clinical applications. 2014. p. 465.
[23] Ramay HRR, Zhang M. Biphasic calcium phosphate nanocomposite porous scaffolds for load-bearing bone tissue engineering. Biomaterials 2004;25(21):5171–80.
[24] Lin Y, Wang T, Wu L, Jing W, Chen X, Li Z, et al. Ectopic and in situ bone formation of adipose tissue-derived stromal cells in biphasic calcium phosphate nanocomposite. J Biomed Mater Res A 2007;81(4):900–10.
[25] Bakhtiari L, Rezaie HR, Hosseinalipour SM, Shokrgozar MA. Investigation of biphasic calcium phosphate/gelatin nanocomposite scaffolds as a bone tissue engineering. Ceram Int 2010;36(8):2421–6.

[26] Lu Z, Roohani-Esfahani S-I, Wang G, Zreiqat H. Bone biomimetic microenvironment induces osteogenic differentiation of adipose tissue-derived mesenchymal stem cells. Nanomedicine 2012;8(4):507–15.
[27] Saska S, Barud HS, Gaspar AM, Marchetto R, Ribeiro SJ, Messaddeq Y. Bacterial cellulose-hydroxyapatite nanocomposites for bone regeneration. Int J Biomater 2011;2011. 175362.
[28] Chai YC, Roberts SJ, Schrooten J, Luyten FP. Probing the osteoinductive effect of calcium phosphate by using an in vitro biomimetic model. Tissue Eng Part A 2011;17(7–8):1083–97.
[29] Lebourg M, Suay Anton J, Gomez Ribelles JL. Characterization of calcium phosphate layers grown on polycaprolactone for tissue engineering purposes. Compos Sci Technol 2010;70(13):1796–804.
[30] Park J, editor. Bioceramics properties, characterizations, and applications. 2008.
[31] Liang L, Rulis P, Ching WY. Mechanical properties, electronic structure and bonding of α- and β-tricalcium phosphates with surface characterization. Acta Biomater 2010;6(9):3763–71.
[32] Kumbar SG, Laurencin CT, Deng M, editors. Natural and synthetic biomedical polymers. 2014.
[33] Petrauskaite O, Gomes PDS, Fernandes MH, Juodzbalys G, Stumbras A, Maminskas J, et al. Biomimetic mineralization on a macroporous cellulose-based matrix for bone regeneration. Biomed Res Int 2013;2013. [online].
[34] Thein-Han WW, Misra RD. Biomimetic chitosan-nanohydroxyapatite composite scaffolds for bone tissue engineering. Acta Biomater 2009;5(4):1182–97.
[35] Pramanik N, Mishra D, Banerjee I, Maiti TK, Bhargava P, Pramanik P. Chemical synthesis, characterization, and biocompatibility study of hydroxyapatite/chitosan phosphate nanocomposite for bone tissue engineering applications. Int J Biomater 2009;1–8. 2009.
[36] Jafarkhani M, Fazlali A, Moztarzadeh F, Moztarzadeh Z, Mozafari M. Fabrication and characterization of PLLA/chitosan/nano calcium phosphate scaffolds by freeze-casting technique. Ind Eng Chem Res 2012;51(27):9241–9.
[37] Wang Y, Azais T, Robin M, Vallee A, Catania C, Legriel P, et al. The predominant role of collagen in the nucleation, growth, structure and orientation of bone apatite. Nat Mater 2012;11(8):724–33.
[38] Li X, Chang J. Preparation of bone-like apatite-collagen nanocomposites by a biomimetic process with phosphorylated collagen. J Biomed Mater Res A 2008;85(2):293–300.
[39] Lin X, Li X, Fan H, Wen X, Lu J, Zhang X. In situ synthesis of bone-like apatite/collagen nano-composite at low temperature. Mater Lett 2004;58(27–28):3569–72.
[40] Bodhak S, Kikuchi M, Sogo Y, Tsurushima H, Ito A, Oyane A. Calcium phosphate coating on a bioresorbable hydroxyapatite/collagen nanocomposite for surface functionalization. Chem Lett 2013;42(9):1029–31.
[41] Pek YS, Gao S, Arshad MS, Leck KJ, Ying JY. Porous collagen-apatite nanocomposite foams as bone regeneration scaffolds. Biomaterials 2008;29(32):4300–5.
[42] Karadas O, Yucel D, Kenar H, Torun Kose G, Hasirci V. Collagen scaffolds with in situ-grown calcium phosphate for osteogenic differentiation of Wharton's jelly and menstrual blood stem cells. J Tissue Eng Regen Med June 28, 2012;8(7):534–45.
[43] Hwang D-S, Kim U-K, Chang M-C, Kim Y-D, Shin S-H, Chung I-K. Osteogenic differentiation of stem cells in a gelatin-hydroxyapatite nanocomposite. Tissue Eng Regen Med 2009;6(12):1107–13.
[44] Lee J-M, Choi B, Choi J-H, Kim G-C, Hwang D-S, Chang M, et al. Osteoblastic response to the hydroxyapatite/gelatin nanocomposite and bio-calcium phosphate cement. Tissue Eng Regen Med 2013;10(2):47–52.

[45] Babaei Z, Jahanshahi M, Rabiee SM. The fabrication of nanocomposites via calcium phosphate formation on gelatin–chitosan network and the gelatin influence on the properties of biphasic composites. Mater Sci Eng C 2013;33(1):370–5.
[46] Schneider OD, Stepuk A, Mohn D, Luechinger NA, Feldman K, Stark WJ. Light-curable polymer/calcium phosphate nanocomposite glue for bone defect treatment. Acta Biomater 2010;6(7):2704–10.
[47] Leeuwenburgh SCG, Jansen JA, Mikos AG. Functionalization of oligo(poly(ethylene glycol)fumarate) hydrogels with finely dispersed calcium phosphate nanocrystals for bone-substituting purposes. J Biomater Sci Polym Ed 2007;18(12):1547–64.
[48] Haberstroh K, Ritter K, Kuschnierz J, Bormann KH, Kaps C, Carvalho C, et al. Bone repair by cell-seeded 3D-bioplotted composite scaffolds made of collagen treated tricalciumphosphate or tricalciumphosphate-chitosan-collagen hydrogel or PLGA in ovine critical-sized calvarial defects. J Biomed Mater Res Part B 2010;93B(2):520–30.
[49] Mavis B, Demirtaş TT, Gümüşderelioğlu M, Gündüz G, Çolak Ü. Synthesis, characterization and osteoblastic activity of polycaprolactone nanofibers coated with biomimetic calcium phosphate. Acta Biomater 2009;5(8):3098–111.
[50] Liang Y, Xinchen Z, Haojiang L, Zhe W. Fabrication and biocompatibility of porously bioactive scaffold of nonstoichiometric apatite and poly(-caprolactone) nanocomposite. J Appl Polym Sci 2009;116(2):762–70.
[51] Roohani-Esfahani SI, Nouri-Khorasani S, Lu Z, Appleyard R, Zreiqat H. The influence hydroxyapatite nanoparticle shape and size on the properties of biphasic calcium phosphate scaffolds coated with hydroxyapatitePCL composites. Biomaterials 2010;31(21):5498–509.
[52] Yusufoglu Y, Hu Y, Kanapathipillai M, Kramer M, Kalay YE. Bioinspired synthesis of self-assembled calcium phosphate nanocomposites using block copolymer-peptide conjugates. J Mater Res 2008;23(12):3196–212.
[53] Hu YY, Yusufoglu Y, Kanapathipillai M, Yang CY, Wu YQ, Thiyagarajan P, et al. Self-assembled calcium phosphate nanocomposites using block copolypeptide templates. Soft Matter 2009;5(21):4311–20.
[54] Aydin E, Planell JA, Hasirci V. Hydroxyapatite nanorod-reinforced biodegradable poly(L-lactic acid) composites for bone plate applications. J Mater Sci Mater Med 2011;22(11):2413–27.
[55] Kim HW, Lee HH, Knowles JC. Electrospinning biomedical nanocomposite fibers of hydroxyapatite/poly(lactic acid) for bone regeneration. J Biomed Mater Res A 2006;79(3):643–9.
[56] Lee H-H, Shin US, Lee J-H, Kim H-W. Biomedical nanocomposites of poly(lactic acid) and calcium phosphate hybridized with modified carbon nanotubes for hard tissue implants. J Biomed Mater Res B Appl Biomater 2011;98(2):246–54.
[57] Teo WE, Liao S, Chan C, Ramakrishna S. Fabrication and characterization of hierarchically organized nanoparticle-reinforced nanofibrous composite scaffolds. Acta Biomater 2011;7(1):193–202.
[58] Zhou H, Lawrence JG, Bhaduri SB. Fabrication aspects of PLA-CaP/PLGA-CaP composites for orthopedic applications: a review. Acta Biomater 2012;8(6):1999–2016.
[59] Nie H, Ho ML, Wang CK, Wang CH, Fu YC. BMP-2 plasmid loaded PLGA/HAp composite scaffolds for treatment of bone defects in nude mice. Biomaterials 2009;30(5):892–901.
[60] Hild N, Schneider OD, Mohn D, Luechinger NA, Koehler FM, Hofmann S, et al. Two-layer membranes of calcium phosphate/collagen/PLGA nanofibres: in vitro biomineralisation and osteogenic differentiation of human mesenchymal stem cells. Nanoscale 2011;3(2):401–9.

[61] Lee JH, Rim NG, Jung HS, Shin H. Control of osteogenic differentiation and mineralization of human mesenchymal stem cells on composite nanofibers containing poly[lactic-co-(glycolic acid)] and hydroxyapatite. Macromol Biosci 2010;10(2):173–82.
[62] Buschmann J, Härter L, Gao S, Hemmi S, Welti M, Hild N, et al. Tissue engineered bone grafts based on biomimetic nanocomposite PLGA/amorphous calcium phosphate scaffold and human adipose-derived stem cells. Injury 2012;43(10):1689–97.
[63] Gao SP, Calcagni M, Welti M, Hemmi S, Hild N, Stark WJ, et al. Proliferation of ASC-derived endothelial cells in a 3D electrospun mesh: Impact of bone-biomimetic nanocomposite and co-culture with ASC-derived osteoblasts. Injury Int J Care Inj 2014;45(6): 974–80.
[64] Baumgartner W, Welti M, Hild N, Hess SC, Stark WJ, Bürgisser GM, et al. Tissue mechanics of piled critical size biomimetic and biominerizable nanocomposites: formation of bioreactor-induced stem cell gradients under perfusion and compression. J Mech Behav Biomed Mater 2015;47.
[65] Wang C, Wang M. Dual-source dual-power electrospinning and characteristics of multifunctional scaffolds for bone tissue engineering. J Mater Sci Mater Med 2012;23(10): 2381–97.
[66] Rescignano N, Fortunati E, Montesano S, Emiliani C, Kenny JM, Martino S, et al. PVA bio-nanocomposites: a new take-off using cellulose nanocrystals and PLGA nanoparticles. Carbohydr Polym 2014;99:47–58.
[67] Chang W, Mu X, Zhu X, Ma G, Li C, Xu F, et al. Biomimetic composite scaffolds based mineralization of hydroxyapatite on electrospun calcium-containing poly(vinyl alcohol) nanofibers. Mater Sci Eng C 2013;33(7):4369–76.
[68] Linh NTB, Lee KH, Lee BT. Functional nanofiber mat of polyvinyl alcohol/gelatin containing nanoparticles of biphasic calcium phosphate for bone regeneration in rat calvaria defects. J Biomed Mater Res Part A 2013;101A(8):2412–23.
[69] Ngiam M, Liao S, Patil AJ, Cheng Z, Chan CK, Ramakrishna S. The fabrication of nano-hydroxyapatite on PLGA and PLGA/collagen nanofibrous composite scaffolds and their effects in osteoblastic behavior for bone tissue engineering. Bone 2009;45(1):4–16.
[70] Sikirić MD, Gergely C, Elkaim R, Wachtel E, Cuisinier FJ, Füredi-Milhofer H. Biomimetic organic-inorganic nanocomposite coatings for titanium implants. J Biomed Mater Res A 2009;89(3):759–71.
[71] Chae T, Yang H, Ko F, Troczynski T. Bio-inspired dicalcium phosphate anhydrate/poly (lactic acid) nanocomposite fibrous scaffolds for hard tissue regeneration: In situ synthesis and electrospinning. J Biomed Mater Res Part A 2013;102(2):514–22.
[72] Jose MV, Thomas V, Johnson KT, Dean DR, Nyairo E. Aligned PLGA/HA nanofibrous nanocomposite scaffolds for bone tissue engineering. Acta Biomater 2009;5(1):305–15.
[73] Xu M, Zhai D, Chang J, Wu C. In vitro assessment of three-dimensionally plotted nagelschmidtite bioceramic scaffolds with varied macropore morphologies. Acta Biomater 2014;10(1):463–76.
[74] Duan B, Wang M. Customized Ca-P/PHBV nanocomposite scaffolds for bone tissue engineering: design, fabrication, surface modification and sustained release of growth factor. J R Soc Interface 2010;7(Suppl. 5):S615–29.
[75] Gilmore RS, Katz JL. Elastic properties of apatites. J Mater Sci 1982;17(4):1131–41.
[76] Lopes MA, Silva RF, Monteiro FJ, Santos JD. Microstructural dependence of Young's and shear moduli of P_2O_5 glass reinforced hydroxyapatite for biomedical applications. Biomaterials 2000;21(7):749–54.

[77] Sax M, Zografou C, Telle R, Kalawrytimos G. Properties of sintered apatite ceramics. 1995.
[78] Jarcho M, Salsbury RL, Thomas MB, Doremus RH. Synthesis and fabrication of beta-tricalcium phosphate (Whitlockite) ceramics for potential prosthetic applications. J Mater Sci 1979;14(1):142–50.
[79] Akao M, Aoki H, Kato K, Sato A. Dense polycrystalline beta-tricalcium phosphate for prosthetic applications. J Mater Sci 1982;17(2):343–6.
[80] Schloegl W, Marschall V, Witting MY, Volkmer E, Drosse I, Leicht U, et al. Porosity and mechanically optimized PLGA based in situ hardening systems. Eur J Pharm Biopharm 2012;82(3):554–62.
[81] Shi X-H, Wang S-L, Zhang Y-M, Wang Y-C, Yang Z, Zhou X, et al. Hydroxyapatite-coated sillicone rubber enhanced cell adhesion and it may be through the interaction of EF1 beta and gamma-actin. Plos One 2014;9(11).
[82] Zorin VL, Komlev VS, Zorina AI, Khromova NV, Solovieva EV, Fedotov AY, et al. Octa-calcium phosphate ceramics combined with gingiva-derived stromal cells for engineered functional bone grafts. Biomed Mater 2014;9(5).
[83] Dumitriu S, Popa V, editors. Polymeric biomaterials. 3rd ed. 2013.

This page intentionally left blank

Hydroxyapatite nanocomposites for tendon repair

14

J. Xie[1], *J. Jiang*[1], *M.J. Teusink*[1], *F.D. Shuler*[2]
[1]University of Nebraska Medical Center, Omaha, NE, United States; [2]Marshall University, Huntington, WV, United States

14.1 Introduction

Tendon injuries are generally attributed to attritional wear from overuse and/or aging. Repetitive motion in work, sports, or daily activities may lead to higher chances of tendon injuries. An example of this is shoulder rotator-cuff tendon and elbow medial collateral ligament injuries in baseball pitchers due to the repetitive high stresses placed on these structures during the pitching motion. Approximately 100,000 to 200,000 anterior cruciate ligament (ACL) injuries occur in the United States each year (Evans et al., 2014). Rotator-cuff injuries occur as partial-thickness and full-thickness tears. They are present in 30% to 50% of the population age over 50 (Riley, 2004) and are one of the most common shoulder conditions affecting more than 17 million people in the United States (Yamaguchi et al., 2006). Because most rotator-cuff tears occur as a result of degeneration, their incidence is expected to rise as the population ages. Although some tears are asymptomatic, rotator-cuff tears often result in debilitating pain, reduced shoulder function, and weakness. Rotator-cuff repair involves reattachment of the torn tendon edge to the bone with either suture anchors or with sutures through bone tunnels. It is one of the most common orthopedic surgical procedures with approximately 300,000 rotator-cuff tendon surgical repairs performed each year in the United States (Aurora et al., 2007; Vitale et al., 2007). The greatest clinical challenge with this procedure continues to be achieving reliable tendon-to-bone healing as is evidenced by high failure rates ranging from 20% to 94% (Vitale et al., 2007; Cummins and Murrell, 2003; Galatz et al., 2004).

One of the reasons for poor healing rates is the spatially graded matrix component (eg, linearly graded mineral content) and fiber organization at the natural attachment of tendon to bone generate high levels of concentrated stress at the transitional interface (Yang and Temenoff, 2009). This concentrated stress inhibits an effective transfer of mechanical loads at the interface during healing. The gradations in both composition and structure cannot be reconstructed during surgical treatment of rotator-cuff tears, which lead to transitional interface failure, thus highlighting the critical importance of this transitional junction. The healing of tendon to bone represents a great challenge due to the mismatch of mechanical properties between a soft compliant material (tendon) and a stiff material (bone).

Nanocomposites for Musculoskeletal Tissue Regeneration. http://dx.doi.org/10.1016/B978-1-78242-452-9.00014-5

In this chapter, we first describe the basic properties of the tendon–bone interface including unique features in fiber organization, composition, and extracellular matrix components, the role of minerals in the development of this interface, and current strategies for repairing tendon to bone. We then discuss the mechanism of hydroxyapatite nanocomposites in tendon-to-bone insertion repair highlighting recent advances of hydroxyapatite nanocomposites in repairing tendon-to-bone insertion sites. Finally, we conclude this chapter with a discussion on perspectives in this field.

14.2 Basics of tendon-to-bone insertion

The transitional tissue interface of tendons- and ligaments-to-bone attachment, also called the "enthesis," is classified as either fibrous or fibrocartilaginous. As the rotator-cuff tendon inserts into the proximal humerus, there is a transition of four distinct

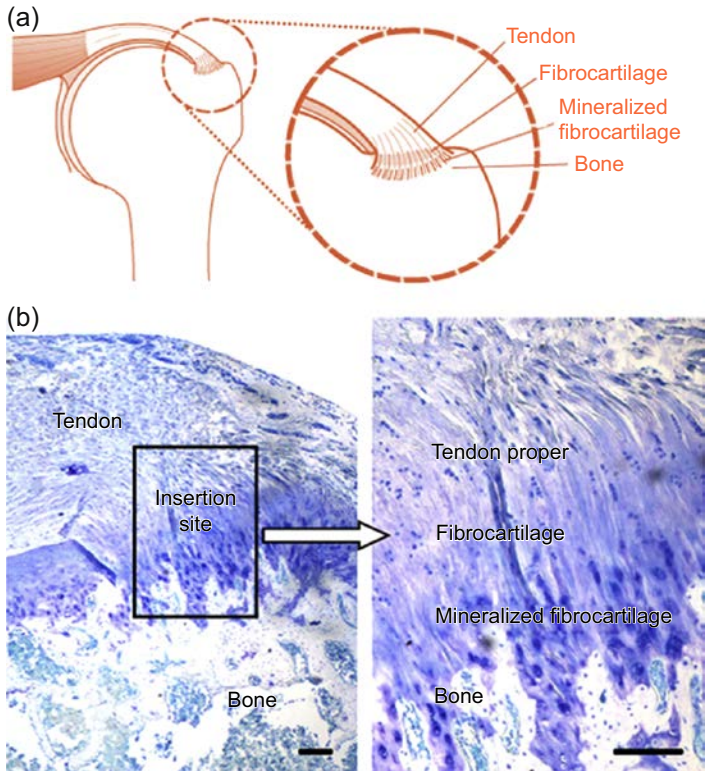

Figure 14.1 Basic of tendon-to-bone insertion site. (a) Schematic illustrating the attachment from tendon to bone. (b) Histology of tendon-to-bone insertion site illustrating the four zones: tendon, fibrocartilage, mineralized cartilage and bone.
Adapted from Thomopoulos, S., 2011. The role of mechanobiology in the attachment of tendon to bone. IBMS BoneKEy 8, 271–285. http://dx.doi.org/10.1138/20110515, with permission from Nature Publishing Group.

tissue zones: tendon, nonmineralized fibrocartilage, fibrocartilage, and bone as indicated in Fig. 14.1 (Thomopoulos, 2011). None of the current repair strategies replicates this normal transitional zone, which leads to stress concentrations that weaken the healed tendon-to-bone insertion, contributing to the high failure rates observed (Thomopoulos et al., 2003b, 2006, 2008). The stress concentrations are mainly attributed to the mechanical mismatch between tendon, a soft tissue with a Young's modulus of 200 MPa, and bone, a hard tissue with a Young's modulus of 20 GPa, one of the biggest mechanical mismatches in nature (Rho et al., 1998; Maganaris and Paul, 1999). Mature tendon-to-bone insertion site presents three unique features. One is the change of organization of collagen fibers: the collagen fibers are significantly more organized at the musculotendinous junction than at the bony insertion (Thomopoulos et al., 2003a). Another is the variation in extracellular matrix compositions (Thomopoulos et al., 2002, 2003a). The final is the gradual change of mineral content from tendon to bone (Fig. 14.2(a)) (Wopenka et al., 2008; Genin et al., 2009). The degree of fiber mineralization affects stiffness of the fibers (Fig. 14.2(b)). All these attributes contribute to the unique mechanical functions such as dissipating stress concentrations at tendon-to-bone interfaces. The graded mineral content is believed to play a critical role for transferring the load efficiently at the interface.

A similar characterization of ACL-to-bone insertion has been reported (Moffat et al., 2008, 2009). Fig. 14.3(a–c) shows the basics of ACL–bone insertion, exhibiting spatial variations in matrix major composition: ligament proper containing types I and III collagen matrix, nonmineralized fibrocartilage matrix consisting of types I and II collagen and proteoglycan, the matrix in mineralized fibrocartilage containing type X collagen and minerals, and the matrix in the bone region containing type I collagen and minerals. Fig. 14.3(d) shows the mineral content in nonmineralized and mineralized fibrocartilage and the corresponding Young's modulus. The increase in compressive modulus and axial stress from the nonmineralized to mineralized fibrocartilage may be attributed to the presence of minerals in the calcified fibrocartilage region.

Understanding the role of minerals in the development of the enthesis may provide valuable information to design hydroxyapatite composites for repairing the tendon-to-bone insertion site (Thomopoulos et al., 2010). The development of the enthesis is initially driven by endochondral ossification: cartilage mineralizes to form bone, and a fibrocartilaginous transition then develops at the interfaces between the bone and connective tissues (Lu and Thomopoulos, 2013). Thomopoulos et al. demonstrated the development of graded mineralized interface at the murine supraspinatus tendon entheses was related to endochondral bone formation starting postnatally and completed by postnatal day 28 (Schwartz et al., 2012). They also quantified micrometer-scale patterns of mineralization in the gradient region at different time points postnatally (Fig. 14.4). It was suggested that the magnitudes of the mineral gradients along the insertion were similar for the five postnatal time points tested, and the length of tendon with mineral gradient also remained approximately the same at about 25 μm from postnatal day (P)7 to P56 (Fig. 14.4(a)). They further investigated the mineralized interface in the supraspinatus tendon enthesis by transmission electron microscopy (TEM), and found gradual increase in size and density of mineral nanoclusters along the insertion at different time points postnatally (Fig. 14.5).

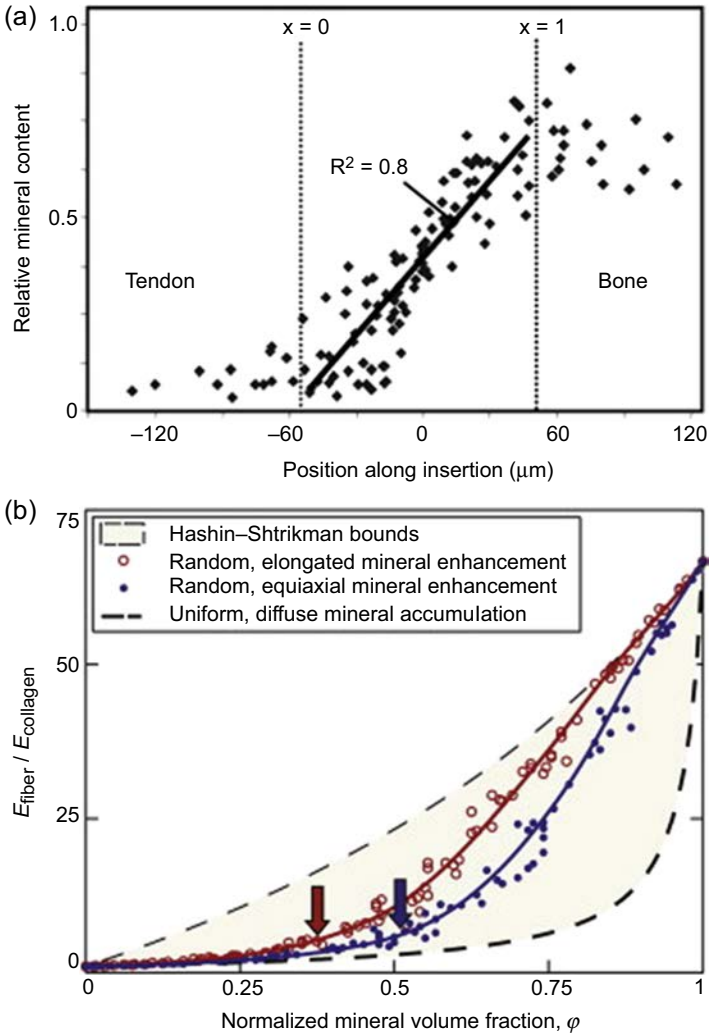

Figure 14.2 The compositional change at tendon-to-bone insertion site and the corresponding change of mechanical properties. (a) Relative mineral content evaluated from confocal Raman microprobe spectroscopy measurements, showing the ratio of the areas of the 960 Δcm^{-1} PO_4 peak to the 2940 Δcm^{-1} collagen peak, across the tendon-to-bone insertion. (b) Bounds and estimates for the axial elastic modulus (E) of a partially mineralized fiber. Mineral stiffens fibers dramatically at volume fraction above the percolation threshold ($\phi \approx 0.5$), indicated by the *arrows*. Percolation occurs at lower volume fraction for regions of enhanced mineralization elongated parallel to the fiber axis.
Adapted from Genin, G.M., Kent, A., Birman, V., Wopenka, B., Pasteris, J.D., Marquez, P.J., Thomopoulos, S., 2009. Functional grading of mineral and collagen in the attachment of tendon to bone. Biophysical Journal 97, 976–985. http://dx.doi.org/10.1016/j.bpj.2009.05.043, with permission from Elsevier.

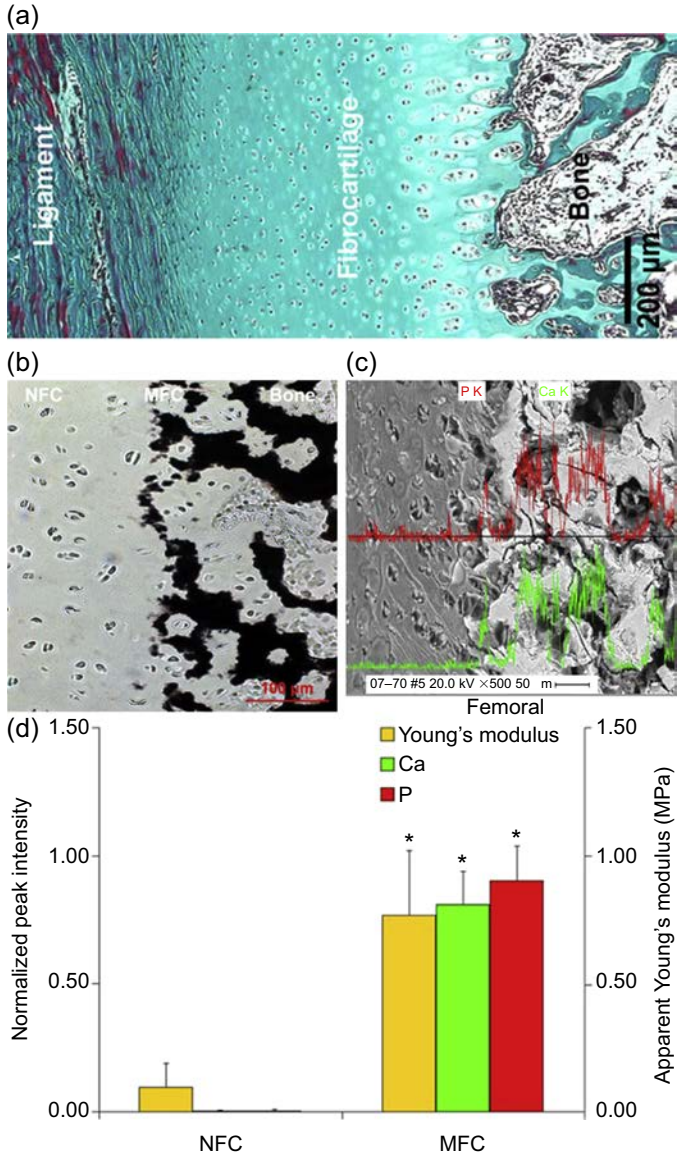

Figure 14.3 Basics of anterior cruciate ligament (ACL)–bone insertion. (a) Modified Goldner Masson trichrome staining of the native neonatal bovine ACL–bone interface indicating the existence of contiguous yet distinct tissue regions including ligament, fibrocartilage (nonmineralized and mineralized fibrocartilage), and bone. (b) von Kossa staining indicating mineral presence and distribution at the interface. (c) Backscattered scanning electron microscopy (SEM) images for the ACL–bone insertion site indicating the distribution of calcium and phosphorous across the insertion. (d) The mineral content in nonmineralized and mineralized fibrocartilage and the corresponding Young's modulus.

Adapted from Moffat, K.L., Sun, W.H.S., Pena, P.E., Chahine, N.O., Doty, S.B., Ateshian, G.A., Hung, C.T., Lu, H.H., 2008. Characterization of the structure-function relationship at the ligament-to-bone interface. Proceedings of the National Academy of Sciences of the United States of America 105 (23), 7947–7952. http://dx.doi.org/10.1073/pnas.0712150105, with permission from The National Academy of Sciences.

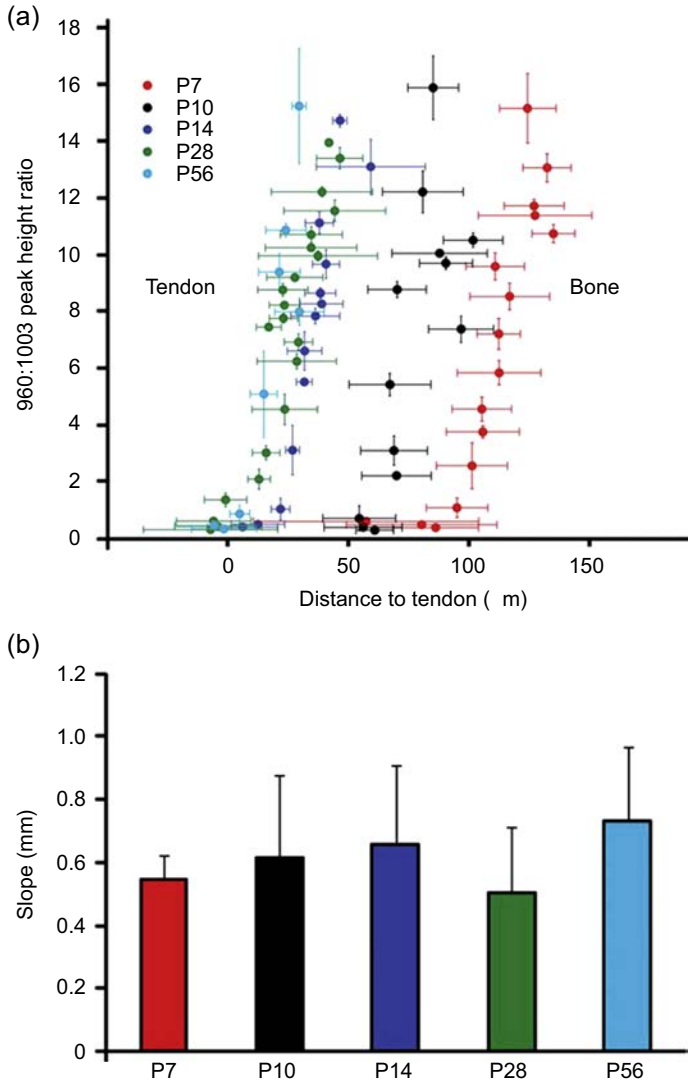

Figure 14.4 Mineral gradients in the developing enthesis. (a) The average mineral content relative to collagen concentration evaluated by the ratio of the heights of 960 Δcm^{-1} PO_4 peak to the 1003 Δcm^{-1} collagen peak across the tendon-to-bone insertion site at day 7, 10, 14, 28, and 56 postnatally. (b) The slope of the data in (a) means the steepness of the mineral gradient. Adapted from Schwartz, A.G., Pasteris, J.D., Genin, G.M., Daulton, T.L., Thomopoulos, S., 2012. Mineral distributions at the developing tendon enthesis. PLoS One 7 (11), e48630. http://dx.doi.org/10.1371/journal.pone.0048630.

The current treatment and subsequent rehabilitation strategies for tendon-to-bone insertion site can be classified into three categories: surgical or technical, biological and biophysical (Atesok et al., 2014; Lui et al., 2010). The surgical or technical strategy includes enveloping the grafts with periosteum, natural matrix patches (eg, acellular

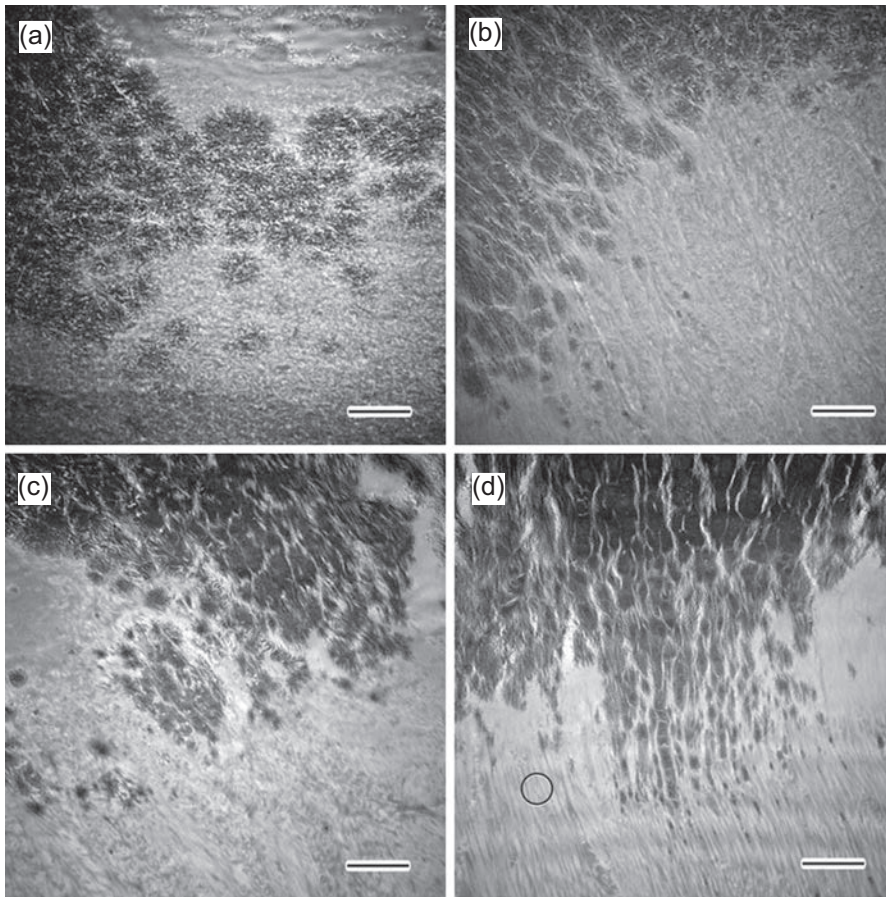

Figure 14.5 TEM images showing the mineralization of the supraspinatus tendon entheses at different developmental times: (a) P10, (b) P14; (c) P28, and (d) P56. Scale bar: 2 μm. Adapted from Schwartz, A.G., Pasteris, J.D., Genin, G.M., Daulton, T.L., Thomopoulos, S., 2012. Mineral distributions at the developing tendon enthesis. PLoS One 7 (11), e48630. http://dx.doi.org/10.1371/journal.pone.0048630.

human dermal matrix, and porcine small-intestine submucosa), synthetic and biodegradable scaffolds/biomimetic patches, osteoconductive materials (eg, Ca^{2+}-, Mg^{2+}-, and Sr^{2+}-based materials), and coated sutures and interference screws. The biological strategy includes the use of osteoinductive growth factors (eg, transforming growth factor [TGF], bone morphogenic protein [BMP], fibroblast growth factor [FGF], granulocyte-colony stimulating factor [G-CSF], platelet-rich plasma [insulin-like growth factor 1 (IGF-1)], platelet-derived growth factor [PDGF] and vascular endothelial growth factor [VEGF]), gene therapy (BMP-2 plasmid), osteoconductive materials (eg, Ca^{2+}, PO_4^{3-}, and Sr^{2+}), or coated sutures and interference screws (delivering biological molecules). The biophysical approach includes the application of low-intensity pulsed ultrasound, extracorporeal shock-wave treatment, or various loading methods and immobilization.

14.3 Mechanism of hydroxyapatite minerals for tendon-to-bone insertion repair

As stated previously, a mineral gradient exists at the interface of the tendon-to-bone insertion. Graded minerals at the insertion result in varying mechanical properties at different locations across the tendon-to-bone insertion. In addition, it has been demonstrated that hydroxyapatite minerals that dissociate to Ca^{2+} and PO_4^{3-} play important roles in osteogenic differentiation of osteoblasts and progenitor cells and promote bone healing. However, the molecular mechanism of the osteogenicity and osteoinductivity of calcium phosphate minerals has not been revealed until recently. Different factors including the ability to modulate extracellular calcium and phosphate ions and the adsorption and release of osteoinductive growth factors like bone morphogenic proteins (BMPs) have been proposed to account for the osteogenicity and osteoinductivity of calcium phosphate minerals. It was found that influx of extracellular Ca^{2+} through L-type calcium channels enhanced the proliferation and osteogenic differentiation of bone marrow mesenchymal stem cells (Wen et al., 2012). In another work, it was demonstrated that extracellular phosphate uptake through solute carrier family 20 member 1 (SLC20a1) (a phosphate transporter) supported osteogenic differentiation of human mesenchymal stem cells via adenosine, an ATP metabolite, which acted as an autocrine/paracrine signaling molecule through A2b adenosine receptor (Fig. 14.6) (Shih et al., 2014).

14.4 Hydroxyapatite nanocomposites for tendon-to-bone insertion repair

Local administration of hydroxyapatite powder at the tendon–bone interface in both a 3-week delayed-repair rat model and an acute-repair model showed improvement in healing the injured rotator cuff (Zhao et al., 2014; Kovacevic et al., 2011). Calcium phosphate nanocomposites for tendon-to-bone interface repair can be categorized as the following.

14.4.1 Mineralized tendon grafts

The use of tendinous autografts fails to provide strong integration at the orthopedic interface (Rodeo et al., 1993; Weiler et al., 2002). To reestablish the native orthopedic interface, mineralization of tendons has been investigated for regeneration of tendon-to-bone insertion. Mutsuzaki et al. (2004) showed the improvement of tendon–bone attachment using mineralized flexor digitorum longus (FDL) tendons as ACL grafts in an acute-repair rabbit model. The mineralized tendons were generated by alternately soaking 10 times in a Ca^{2+}-containing solution and a PO_4^{3-}-containing solution for 30 s each. After implantation of mineralized tendons, the tendon-to-bone healing process was significantly enhanced in terms of histological analysis, and the regenerated interface (fibrocartilage layer) was akin to a native ACL insertion in a shorter time frame compared to the control (unmineralized tendons). Despite

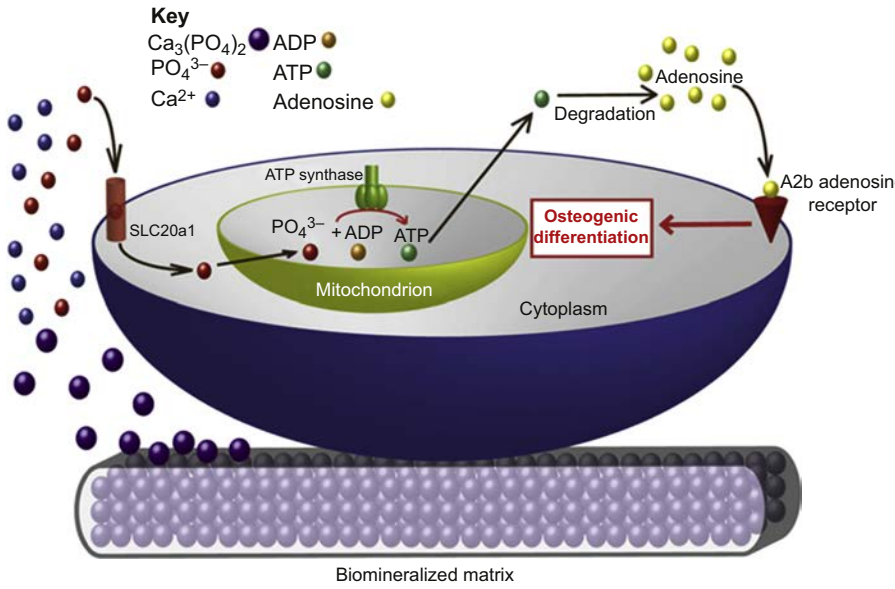

Figure 14.6 Schematic illustrating a molecular mechanism of osteogenic differentiation that is induced by phosphate ions released from calcium phosphate minerals.
Adapted from Shih, Y.R.V., Hwang, Y.S., Phadke, A., Kang, H., Hwang, N.S., Caro, E.J., Nguyen, S., Siu, M., Theodorakis, E.A., Gianneschi, N.C., Vecchio, K.S., Chien, S., Lee, O.K., Varghese, S., 2014. Calcium phosphate-bearing matrices induce osteogenic differentiation of stem cells through adenosine signaling. Proceedings of the National Academy of Sciences of the United States of America 111 (3), 990–995. http://dx.doi.org/10.1073/pnas.1321717111, with permission from The National Academy of Sciences.

promising histologic data, biomechanical testing is needed to examine the effect of calcium phosphate hybridization on functional recovery of repaired tendons. A later study by the same group demonstrated the formation of a direct bond between the calcium phosphate-hybridized tendon graft and the regenerated neobone in femoral- and tibial-bone tunnels in a goat ACL reconstruction model (Mutsuzaki et al., 2009). Their further biomechanical test indicated that the strength of the tendon–bone interface in the calcium phosphate-hybridized tendon group was superior to that of control group (unmineralized tendons) (Mutsuzaki et al., 2011). In a separate study, they demonstrated that calcium phosphate-hybridized tendon grafts could reduce bone-tunnel enlargement after ACL reconstruction in goats which may reduce the number of clinical failures (Mutsuzaki et al., 2012b). They also examined the long-term effect of hybridized calcium phosphate–tendon graft on the healing of the tendon–bone interface after ACL reconstruction in a goat model (Mutsuzaki and Sakane, 2011). The hybridized graft enhanced the tendon–bone healing 2 years after ACL reconstruction. They recently performed a randomized controlled trial to examine the effect of calcium phosphate-hybridized tendon graft in ACL reconstruction in human patients (Mutsuzaki et al., 2012a). Compared with the conventional hamstring tendon autograft ACL reconstruction, the calcium phosphate-hybridized tendon graft showed

improvement of anterior knee stability and Lysholm scores at the 2-year follow-up and reduction of bone-tunnel enlargement at 1-year follow-up. This concept was also tested in a separate study, to transform the tendon-to-bone interface to a 'bone-to-bone' interface for repairing utilizing flexor digitorum profundus (FDP) tendons isolated from dogs (Qu et al., 2013). In another study, a combination of extraction and fetuin (an inhibitor of mineral nucleation) resulted in significant increase of calcium phosphate mineral content in tendons; however, an in vivo study needs to be carried out to demonstrate this proof of concept (Price et al., 2009).

14.4.2 Demineralized bone grafts

Alternatively, cancellous bone regionally demineralized as a scaffold with a continuous transition from soft to hard tissue was examined for tendon-to-bone repair (Fig. 14.7(a)) (Dickerson et al., 2013). It was shown that the mineral content in cancellous bone can be completely removed after treatment in a demineralizing solution (1.0 M HCl, 1.9 mM ethylene diamine tetra-acetic acid) for 4.5 h. During the process of mineral removal, one end of the sample was coated with a polymer to prevent the regions from being demineralized (58 ± 17.3% of the mineral). Histological sections of supraspinatus tendons in sheep revealed that the normal entheses displayed a typical bone-calcified fibrocartilage–fibrocartilage interface (Fig. 14.7(b)). However, in control repairs, the transition is from bone directly into scar tissue after 16 weeks postsurgically (Fig. 14.7(c)). In contrast, the scaffold-treated supraspinatus tendon showed regeneration of the bone-calcified fibrocartilage–fibrocartilage interface and a regrowth of tendon midsubstance (Fig. 14.7(d)). The calcified fibrocartilage and fibrocartilage layers were thicker in the repair than in the normal animals (Fig. 14.7(b) and (d)). Such cancellous bone-derived scaffolds had a number of advantages: biochemical and biomechanical properties of the mineralized end resembled those of native bone, natural materials, and intrinsic interface. Some limitations were associated with this study such as lack of mineral gradation in the graft, lack of mimicry of fiber organization at the tendon site, low number of animals used, no quantitative data on the biochemical and biomechanical properties at the interface, and the use of only an acute-injury model.

14.4.3 Synthetic hydroxyapatite nanocomposites

Insufficient bone anchoring is a major limitation of synthetic grafts for orthopedic interface tissue repair. Incorporation of hydroxyapatite is one strategy to improve the integration between the bone and grafts. It has been shown that nanocomposites containing osteoconductive components such as hydroxyapatite are critical in promoting tendon healing in a bone tunnel due to enriched bone ingrowth. Synthetic hydroxyapatite nanocomposites can be prepared in different forms such as hydrogels, cements, solid fibrous materials, and screws.

14.4.3.1 Hydroxyapatite–hydrogel composites

Ishikawa et al. (2001) evaluated the effect of injection of collagen gel mixed with hydroxyapatite powder to the interface between the Achilles tendon graft and the bone

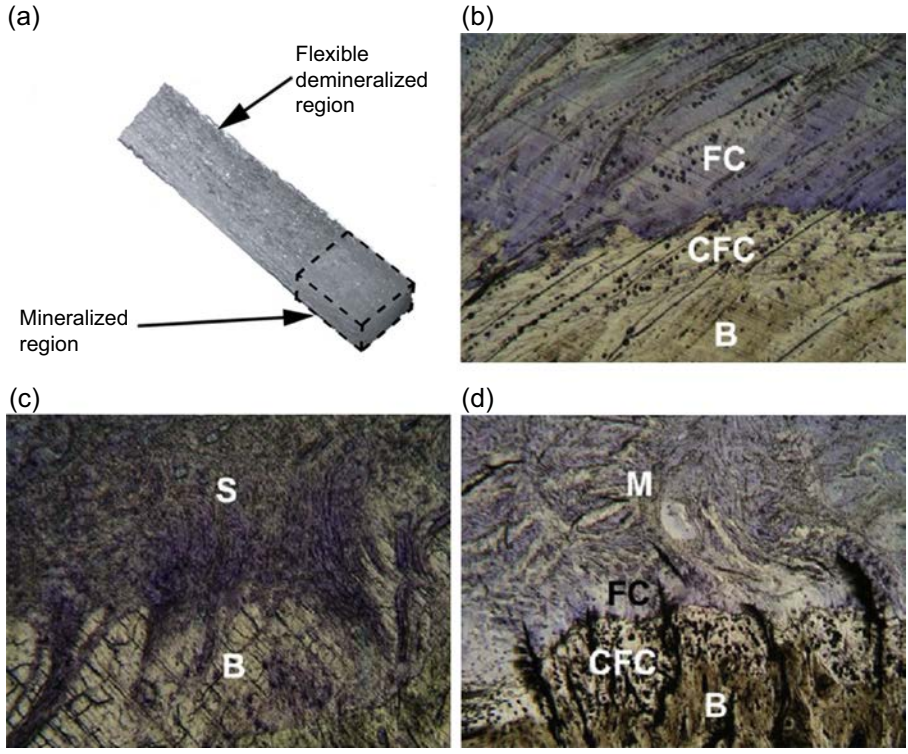

Figure 14.7 Hydroxyapatite nanocomposites for tendon-to-bone insertion repair. (a) partially demineralized cancellous bone scaffold. (b–d) MacNeal's tetrachrome staining of histological sections of the supraspinatus tendons in sheep. (b) Normal tendon. (c) Control (Standard repair: the remaining tendon portions were reconnected by suturing with a #2 Tevdek locking-loop pattern and attached to the enthesis using a bone tunnel). (d) Scaffold. S in (c): scar tissue. *FC*, fibrocartilage; *CFC*, calcified fibrocartilage; *M*, a regrowth of tendon midsubstance; *B*, Bone.
Adapted from Dickerson, D.A., Misk, T.N., Sickle, D.C.V., Breur, G.J., Nauma, E.A., 2013. In vitro and in vivo evaluation of orthopedic interface repair using a tissue scaffold with a continuous hard tissue-soft tissue transition. Journal of Orthopaedic Surgery and Research 8, 18. http://dx.doi.org/10.1186/1749-799X-8-18.

tunnel in the femoral condyle of rabbits. The grafted tendon with injection of collagen–hydroxyapatite composites was in direct contact with regenerated new bone and Sharpey-like collagen fibers arising from the grafted tendon penetrated new bone at week 4 after surgery. In contrast, in the control group (injection of saline), fibrous tissue appeared between new bone and the grafted tendon. Not until week 16 after surgery did they observe penetrating fibers from the grafted tendon into the new bone. This study highlighted the histological observations at the interface. The mechanical function of tendon-to-bone insertion after repair was not examined. In a separate study, Paxton et al. (2009) incorporated hydroxyapatite into a poly(ethylene glycol) diacrylate (PEGDA) hydrogel for making a tissue interface to engineer intact

ligaments. However, this work only showed in vitro cell attachment and characterization of mechanical properties.

14.4.3.2 Hydroxyapatite cement

Calcium phosphate cement has also been applied to enhance bone–tendon integration in the reconstruction of ACL. Tien et al. (2004) investigated the augmentation of healing at the tendon–bone interface using calcium phosphate cement (mixing equimolar $Ca_4(PO_4)_2O$ and $CaHPO_4$ in a 1 M phosphate-containing solution) as filler between the graft and bone during ACL reconstruction in a rabbit model. Early, diffuse and massive bone ingrowth was seen for calcium phosphate cement group. The control group (without using calcium phosphate cement) only showed a thin layer of new bone. The mean maximal tensile strength for calcium phosphate cement group (6.505 ± 1.333 N and 11.491 ± 2.865 N) was much higher than that of the control group (2.048 ± 0.950 N and 5.452 ± 3.955 N) at weeks 1 and 2 after surgery. These results demonstrated that calcium phosphate cement was capable of reinforcing the integration of the tendon graft to bone and enhancing the healing of tendon–bone interface. In another study, Huangfu and Zhao (2007) examined the effect of injectable tricalcium phosphate on tendon–bone healing in ACL reconstruction in a dog model. Tricalcium phosphate was used to fill those tunnel parts not filled by the graft. Filling with tricalcium phosphate resulted in earlier presence of Sharpey fibers, fibrocartilage and calcified cartilage at the tendon–bone interface and faster tendon–bone healing relative to the control (without filling of tricalcium phosphate). For the similar reason, Wen et al. (2009) investigated the osteoconductivity and bioresorption of brushite calcium phosphate cement in bone–tendon interface healing after ACL reconstruction in a rabbit model. Brushite calcium phosphate cement implanted between grafted tendon and bone tunnel resulted in the increase of the peritendon bone volume and promoted bone growth into the healing interface. The ultimate strength and stiffness of the graft–tunnel complexes was higher than that of the control at week 6 after surgery.

To further promote new bone formation at the tendon–bone interface, Ma et al. (2007) examined the synthetic calcium phosphate matrix (CPM, Etex Corp, Cambridge, Massachusetts) as a carrier for delivery of rhBMP-2 to the periphery of each tunnel surrounding the tendon graft during ACL reconstruction. It was found that rhBMP-2 showed a strong, positive dose-dependent effect on osteointegration at the tendon–bone interface. There was no bone resorption after bone formation in the tendon–bone interface using the calcium phosphate matrix as a carrier, which contrasts the use of a collagen sponge for delivering BMP-2 to the bone tunnel (Rodeo et al., 1999). Pan et al. (2011) compared the effect of injectable calcium phosphate cement and fibrin sealant combined with BMP on osteointegration between the tendon graft and bone after ACL reconstruction. Calcium phosphate cement composites showed a more prolonged osteogenic effect than that of the fibrin sealant composite. However, the slow degradation of calcium phosphate cement may inhibit new bone formation at the tendon–bone interface. To eliminate this problem, they developed synthetic calcium phosphate cement combined with recombined bone xenograft granules in their subsequent work (Pan et al., 2013). Compared with injectable calcium phosphate

cement alone, injectable calcium phosphate cement combined with recombined bone xenograft containing 3 mg BMPs significantly enhanced tendon-to-bone healing. This synthetic composite resulted in a much higher maximum load to failure than injectable calcium phosphate cement alone at week 24 after surgery.

Alternatively, strontium was incorporated to the calcium phosphate cement to further enhance new bone formation at the tendon–bone interface. Kuang et al. (2013) investigated the effect of strontium-enriched calcium phosphate cement (Sr-CPC; mixture of tetracalcium phosphate, dicalcium phosphate anhydrous, strontium hydrogen phosphate, citric acid, and polyvinylpyrrolidone K-30) on acceleration of tendon healing in the bone tunnel in a rabbit model of ACL reconstruction. The graft–bone interface was completely filled with new bone in the Sr-CPC treatment group at week 6 after surgery, whereas fibrovascular tissue was seen in the control group (without Sr-CPC treatment). The interface was remodeled into a normal ACL-bone-like insertion at week 24 in the Sr-CPC treatment group, indicating coating of Sr-CPC on tendon allograft was attributed to faster tendon healing in the tunnel. However, their study did not answer the question: was the accelerated healing solely due to the effect of strontium within the tested material? To answer this question, they further compared the effect of Sr-CPC and CPC treatment on tendon–bone interface healing (Kuang et al., 2014). Sharpey fibers appeared at week 6 and a graft–fibrocartilage–bone junction was noticed at week 12 after surgery in Sr-CPC treatment group. The Sharpey fibers were not formed until weeks 9–12 after surgery in the CPC-treatment group. Interestingly, a direct enthesis was noted in both treatment groups. The tendon graft healing in the Sr-CPC group occurred 3 weeks faster than in the CPC group. No significant difference was observed between these two groups at week 24 after surgery. These results suggested that the use of strontium in a CPC system indeed accelerated the healing rate of tendon–bone interface at the early stage.

14.4.3.3 Hydroxyapatite–fiber composites

To mimic the composition in the different regions at the orthopedic interface, Spalazzi et al. (2006b) first designed a multiphasic nanofiber scaffold inspired from native tendon-to-bone interface with distinct yet continuous noncalcified and calcified matrix regions. Based on a similar idea, their subsequent studies reported the production of biphasic nanofiber scaffolds and their performance on tendon-to-bone repair in both rodent and ovine rotator-cuff injury models (Qu et al., 2014). The histology results indicated the formation of a fibrocartilage-like matrix in both phases, and calcified fibrocartilage formed merely on the hydroxyapatite-containing phase (Fig. 14.9). Biphasic scaffold treatment resulted in the regeneration of an organized interface; however, tendon treated by PLGA nanofiber scaffolds or hydroxyapatite-incorporated PLGA nanofiber scaffolds only did not (Fig. 14.8). The mechanical functions of repaired rotator cuff were unknown for different treatment groups. It is worth mentioning that the scaffold was placed between the tendon and bone to form a “sandwich” in the animal model used in these studies instead of inserting it into a bone tunnel (Spalazzi et al., 2006a, 2008; Moffat et al., 2009; Zhang et al., 2012). Based on a similar principle, biphasic scaffolds were also used for the regeneration of alveolar

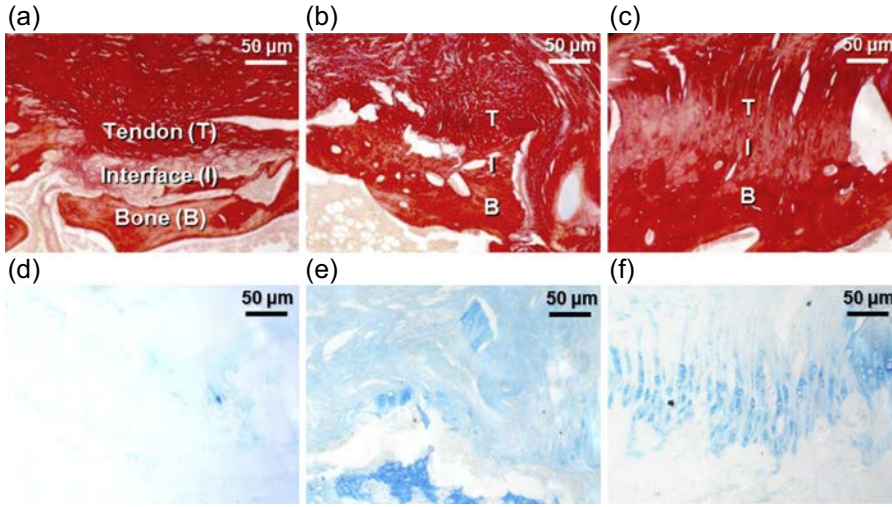

Figure 14.8 Tendon-to-bone insertion treated with (a, d) PLGA nanofiber scaffolds, (b, e) hydroxyapatite-incorporated PLGA nanofiber scaffolds, and (c, f) biphasic nanofiber scaffolds. (a–c): Picro-sirius red staining. (d–f): Alcian blue staining. Disorganized scar tissue was seen after treatment with PLGA nanofiber scaffolds or hydroxyapatite-incorporated PLGA nanofiber scaffolds. The treatment with biphasic nanofiber scaffolds resulted in the tendon–bone integration via an organized bilayer fibrocartilage zone.
Adapted from Qu, D., Mosher, C.Z., Boushell, M.K., Lu, H.H., 2014. Engineering complex orthopaedic tissues via strategic biomimicry. Annals of Biomedical Engineering 43 (3), 697–717. http://dx.doi.org/10.1007/s10439-014-1190-6, with permission from Springer.

bone/periodontal ligament complex (Vaquette et al., 2012; Dan et al., 2014; Costa et al., 2014).

Synthetic approaches have also been attempted to develop hydroxyapatite nanocomposites for recapitulating the unique composition of natural connection between tendon and bone in hopes of tricking the body to regenerate the tendon-to-bone interface. In a collaborative study, Xia group and Thomopoulos group developed an approach to fabricate nanofiber scaffolds with gradations in mineral content that are soft and pliable (tendon-like) at one end but denser and stiff (bone-like) at the other end (Li et al., 2009). The scaffold was generated by dripping 10 times as concentrated as simulated body fluid into a glass vial in which a nanofiber membrane was placed at a tilted angle. The obtained scaffolds with graded mineral content can mimic the composition at the tendon-to-bone insertion site, resulting in improved mechanical properties (eg, stiffness and strain) and preosteoblast attachment (Lipner et al., 2014). Their subsequent studies aimed to improve the mechanical properties of nanofibers by decreasing the grain size and increasing the thickness of mineral coatings (Liu et al., 2011; Kolluru et al., 2013; Lipner et al., 2014). Their most recent work demonstrated that nanofiber scaffolds with mineral gradients can control the osteogenic differentiation of adipose-derived stem cells spatially. Cells with positive proliferating cell nuclear antigen showed a negative correlation with the mineral content; cells with

positive osteogenetic markers (eg, alkaline phosphatase [ALP], runt-related transcription factor 2 [RUNX2], and osteocalcin) showed a positive correlation with the mineral content (Liu et al., 2014).

The mineral coatings in the aforementioned studies could potentially enhance mechanical properties. The mineral coating and polymeric nanofibers represented two different phases: inorganic and organic. Xie et al. (2013b) developed a novel approach to bridge these two different phases by forming a polydopamine layer (an adhesive material) between these two phases before and/or during the mineralization of electrospun fibers. They demonstrated control of morphology, grain size and thickness of minerals deposited on the surface of electrospun nanofibers. The mineral-coated electrospun fibers showed much higher stiffness, ultimate tensile strength and toughness compared to the unmodified fibers. This mineralization method can be readily extended to fabricate nanofiber scaffolds with graded mineral concentrations for use in orthopedic interface repair. In their recent studies, they also demonstrated the generation of nanofiber scaffolds with dual gradations in both mineral content and nanofiber organization (Xie et al., 2013a, 2014). Their preliminary in vivo study demonstrated the feasibility of implantation of such scaffolds at the tendon-to-bone insertion site in a rat rotator-cuff acute-injury model by inserting the mineralized end into a bone tunnel and suturing the unmineralized end to the tendon similar to the implantation of mineralized-tendon autografts in ACL reconstruction (Xie et al., 2014; Ma et al., 2013).

For the purpose of orthopedic applications in tendon repair, nanofiber scaffolds with mineral gradients were also developed in different approaches. Samavedi et al. (2011) fabricated graded fiber meshes by co-electrospinning nanohydroxyapatite–polycaprolactone and poly(ester urethane) elastomer solutions from offset spinnerets along the length of a rotating mandrel. Further treatment with five times as concentrated as simulated body fluid resulted in mineral decorated nanofiber meshes with mineral gradient. They also examined the response of bone marrow mesenchymal stem cells to both types of scaffolds (Samavedi et al., 2012). The presence of minerals in both types of scaffolds enhanced the expression of BMP-2 and osteopontin messenger RNA (mRNA) but inhibited the expression of ALP mRNA. This study also confirmed that nanofiber scaffolds with mineral gradient can spatially control the osteogenic differentiation of bone marrow mesenchymal stem cells.

However, ideal artificial grafts for tendon repair should not only enhance the integration between graft and bone but also mimic mechanical functions of the tendon–bone interface. In a recent study, to replace bone–patellar tendon–bone autografts, Chung et al. (2014) developed a biodegradable tricomponent graft consisting of porous poly(1,8-octanediol-co-citric acid)–hydroxyapatite nanocomposites (POC-HA) and poly(L-lactide) (PLLA) braids (Fig. 14.9), which was capable of not only enhancing osteointegration but also exhibiting similar mechanical properties of native tendon.

14.4.4 Hydroxyapatite–screw composites

Other than generating artificial grafts for orthopedic interface repair, hydroxyapatite has been incorporated to the screws as an osteoconductive component used for fixation

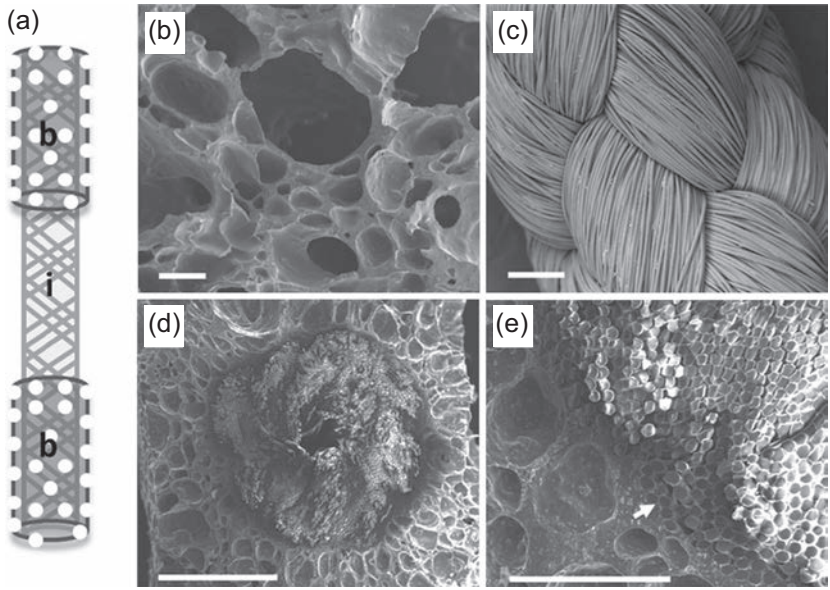

Figure 14.9 Tricomponent graft for tendon repair. (a) Schematic illustrating the graft with POC-HA bone-like part and the intraarticular PLLA braided part. (b) SEM images of porous POC-HA bone like part; (c) PLLA braid; (d) cross-section of PLLA braids embedded in the POC-HA; and (e) high magnification of bone-like ends (integration at the interface indicated by *white arrow*). Scar bars = 300 μm in (b, c, e) and 1 mm (d). Adapted from Chung, E.J., Sugimoto, M.J., Koh, J.L., Ameer, G.A., 2014. A biodegradable tri-component graft for anterior cruciate ligament reconstruction. Journal of Tissue Engineering and Regenerative Medicine. http://dx.doi.org/10.1002/term.1966, with permission from John Wiley & Sons, Inc.

of soft to hard tissue. Johnston et al. (2011) evaluated the resorption and remodeling of hydroxyapatite–poly-L-lactic acid composite screws (a commercial product from Stryker, Mahwah, New Jersey) that were used to fix tendon grafts at the femur and tibia during ACL reconstruction in patients. The hydroxyapatite–poly-L-lactic acid composite screws were slowly resorbed over time and the majority was completely resorbed between 3 and 4 years after surgery. Computed tomography (CT) scans confirmed osteoconductivity and remodeling. There were no tunnel widening, sclerosis, cysts, or inflammatory changes observed. The functional recovery from repaired orthopedic interface was not fully characterized. In a different study, Lu et al. (2009) examined the effect of BIORCI screws (Smith & Nephew) composed of poly-L-lactide coated with a hydroxyapatite mineral layer that was designed to release an engineered peptide (linkBMP-2) on the tendon–bone healing in an ovine model. They found that linkBMP-2 can be bound to the surface of a hydroxyapatite-coated PLLA screw and released from the screw in a sustained way. In addition, the linkBMP-2-bound screws showed great improvement of the histological scores at early stage of tendon–bone healing. However, no significant differences were observed with regard to the failure pattern and mechanical properties between the linkBMP-2-coated and uncoated groups.

14.5 Conclusions and perspectives

Although hydroxyapatite nanocomposites have demonstrated potential in improvement in osteointegration and strengthening of the graft–bone interface, the use of hydroxyapatite nanocomposites for tendon repair is in its infancy. Some studies have examined the efficacy of hydroxyapatite nanocomposites in tendon/ligament repair in both small and large animal models. However, most of the studies are still in the proof-of-concept stage. Very few studies have investigated the performance of hydroxyapatite nanocomposites in orthopedic interface repair in humans.

In this chapter we highlight typical examples of hydroxyapatite nanocomposites without considering other factors for tendon repair. Continued efforts need to be devoted to the development of hydroxyapatite nanocomposite grafts with multiple gradients that can mimic the composition, fiber organization and mechanical functions of native tendon-to-bone insertion. To fully regenerate orthopedic-interface tissue and restore function, other approaches should be investigated with hydroxyapatite nanocomposites including incorporation of drugs (eg, alendronate), and signaling molecules (BMP-2, BMP-12, TGF-β and Sr^{2+}), gene therapy (eg, PDGF, EGF, IGF, and BMP-2 genes), cell therapy (eg, bone marrow stem cells, adipose-derived stem cells and muscle-derived stem cells) and physical stimulations (eg, mechanical load, ultrasound, and electrical stimulation) (Thomopoulos et al., 2007; Chamberlain et al., 2014; Kuang et al., 2013, 2014; Huard et al., 2003; Hettrich et al., 2014; Hu et al., 2014). Current synthetic tendon grafts are limited to two-dimensional patches; future directions should be also devoted to the development of three-dimensional (3D) scaffolds for tendon repair as tendon thickness varies and may be up to 8 mm thick. Fig. 14.10 shows a perspective on 3D tissue constructs composed of multiple gradations and seeded stem cells for tendon-to-bone insertion repair. In addition, few synthetic grafts can match the mechanical properties of native tendon-to-bone insertion (eg, tendon, a soft tissue with a Young's modulus of 200 MPa, and bone, a hard tissue with a Young's modulus of 20 GPa). Future efforts should be made to develop hydroxyapatite nanocomposites that can resemble the mechanical function of the natural tendon–bone interface.

Further detailed information regarding the use of hydroxyapatite nanocomposites for orthopedic-interface tissue regeneration can be traced from the following research groups: Thomopoulos group at Washington University in St. Louis, Xia group at Georgia Institute of Technology, Lu group at Colombia University, and Sakane group at University of Tsukuba. These groups have demonstrated the potential of hydroxyapatite nanocomposites for tendon-to-bone insertion repair. It is worth mentioning that the Sakane group has started random trials for testing the calcium phosphate-hybridized tendon graft on ACL reconstruction in patients and demonstrated the promising results. Also, the Lu group has used biphasic nanofiber scaffolds to repair the infraspinatus tendon to bone using the double-row suture bridge technique in a large animal model (sheep), demonstrating the clinical translation potential of biphasic scaffolds for integrative rotator-cuff repair (Zhang et al., 2014). In addition, there are already commercially available products of hydroxyapatite composites—PLLA–hydroxyapatite composite screws (BIOSURE) produced by Smith & Nephew

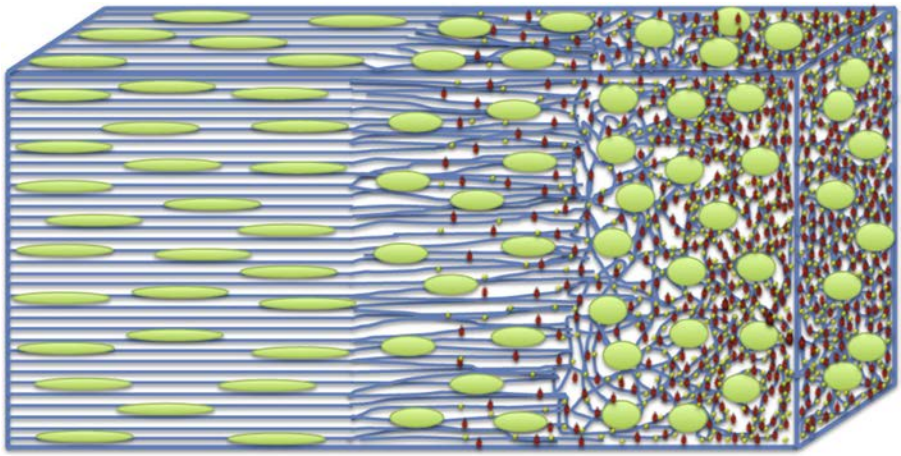

Figure 14.10 Future perspectives on the design of hydroxyapatite nanocomposites for tendon-to-bone insertion repair. 3D tissue constructs composed of multiple gradations including mineral content (red color), fiber organization (light blue), and bioactive substances (yellow color) and seeded stem cells (light green). Bioactive substances can be incorporated to either the minerals or the scaffold for enhancing interfacial tissue regeneration. The seeded stem cells are expected to differentiate into tendon fibroblasts at tendon site, chondrocytes at the cartilage site, and osteoblasts at the bone site. The thickness for the tissue construct should match the thickness of native tendon ranging from 7 to 8 mm.

(Memphis, Tennessee) to promote bone–tendon–bone graft fixation. Available from: http://www.smith-nephew.com/professional/products/sports-medicine1/knee-repair/biosure-ha-interference-screw/(accessed 30.12.14.).

Acknowledgments

This work was supported from startup funds from University of Nebraska Medical Center and National Institute of Health (grant number 1R15 AR063901-01).

References

Atesok, K., Fu, F.H., Wolf, M.R., Ochi, M., Jazrawi, L.M., Doral, M.N., Lubowitz, J.H., Rodeo, S.A., 2014. Augmentation of tendon-to-bone healing. The Journal of Bone and Joint Surgery. American Volume 96, 513–521. http://dx.doi.org/10.2106/JBJS.M.00009.

Aurora, A.J., Iannotti, J.P., Derwin, K., 2007. Commercially available extracellular matrix materials for rotator cuff repairs: state of the art and future trends. Journal of Shoulder and Elbow Surgery 16, S171–S178. http://dx.doi.org/10.1016/j.jse.2007.03.008.

Chamberlain, C.S., Lee, J.S., Leiferman, E.M., Maassen, N.X., Baer, G.S., Vanderby, R., Murphy, W., 2014. Effects of BMP-12 releasing sutures on Achilles tendon healing. Tissue Engineering Part A 21 (5–6), 916–927. http://dx.doi.org/10.1089/ten.tea.2014.0001.

Chung, E.J., Sugimoto, M.J., Koh, J.L., Ameer, G.A., 2014. A biodegradable tri-component graft for anterior cruciate ligament reconstruction. Journal of Tissue Engineering and Regenerative Medicine. http://dx.doi.org/10.1002/term.1966.

Costa, P.F., Vaquette, C., Zhang, Q., Reis, R.L., Ivanovski, S., Hutmacher, D.W., 2014. Advanced tissue engineering scaffold design for regeneration of the complex hierarchical periodontal structure. Journal of Clinical Periodontology 41, 283–294. http://dx.doi.org/10.1111/jcpe.12214.

Cummins, C.A., Murrell, G.A.C., 2003. Model of failure for rotator cuff repair with suture anchors identified at revision surgery. Journal of Shoulder and Elbow Surgery 12, 128–133. http://dx.doi.org/10.1067/mse.2003.21.

Dan, H., Vaquette, C., Fisher, A.G., Hamlet, S.M., Xia, Y., Hutmacher, D.W., Ivanovski, S., 2014. The influence of cellular source on periodontal regeneration using calcium phosphate coated polycaprolactone scaffold supported cell sheets. Biomaterials 35, 113–122. http://dx.doi.org/10.1016/j.biomaterials.2013.09.074.

Dickerson, D.A., Misk, T.N., Sickle, D.C.V., Breur, G.J., Nauma, E.A., 2013. In vitro and in vivo evaluation of orthopedic interface repair using a tissue scaffold with a continuous hard tissue-soft tissue transition. Journal of Orthopaedic Surgery and Research 8, 18. http://dx.doi.org/10.1186/1749-799X-8-18.

Evans, S., Shaginaw, J., Bartolozzi, A., 2014. ACL reconstruction– it's all about timing. International Journal of Sports Physical Therapy 9 (2), 268–273.

Galatz, L., Ball, C.M., Teefey, S.A., Middleton, W.D., Yamaguchi, K., 2004. The outcome and repair integrity of completely arthroscopically repaired large and massive rotator cuff tears. The Journal of Bone and Joint Surgery. American Volume 86 (2), 219–224.

Genin, G.M., Kent, A., Birman, V., Wopenka, B., Pasteris, J.D., Marquez, P.J., Thomopoulos, S., 2009. Functional grading of mineral and collagen in the attachment of tendon to bone. Biophysical Journal 97, 976–985. http://dx.doi.org/10.1016/j.bpj.2009.05.043.

Hettrich, C.M., Gasinu, S., Beamer, B.S., Stasiak, M., Fox, A., Birmingham, P., Ying, O., Deng, X.H., Rodeo, S.A., 2014. The effect of mechanical load on tendon-to-bone healing in a rat model. American Journal of Sports Medicine 42 (5), 1233–1241. http://dx.doi.org/10.1177/0363546514526138.

Hu, J., Qu, J., Xu, D., Zhang, T., Qin, L., Lu, H., 2014. Combined application of low-intensity pulsed ultrasound and functional electrical stimulation accelerates bone-tendon junction healing in a rabbit model. Journal of Orthopaedic Research 32 (2), 204–209. http://dx.doi.org/10.1002/jor.22505.

Huangfu, X., Zhao, J., 2007. Tendon-bone healing enhancement using injectable tricalcium phosphate in a dog anterior cruciate ligament reconstruction model. Arthroscopy 23 (5), 455–462. http://dx.doi.org/10.1016/j.arthro.2006.12.031.

Huard, J., Li, Y., Peng, H., Fu, F.H., 2003. Gene therapy and tissue engineering for sports medicine. The Journal of Gene Medicine 5, 93–108. http://dx.doi.org/10.1002/jgm.344.

Ishikawa, H., Koshino, T., Takeuchi, R., Saito, T., 2001. Effects of collagen gel mixed with hydroxyapatite powder on interface between newly formed bone and grafted Achilles tendon in rabbit femoral bone tunnel. Biomaterials 22, 1689–1694. http://dx.doi.org/10.1016/S0142-9612(00)00331-8.

Johnston, M., Morse, A., Arrington, J., Pliner, M., Gasser, S., 2011. Resorption and remodeling of hydroxyapatite-poly-L-lactic acid composite anterior cruciate ligament interference screws. Arthroscopy 27 (12), 1671–1678. http://dx.doi.org/10.1016/j.arthro.2011.06.036.

Kolluru, P.C., Lipner, J., Liu, W., Xia, Y., Thomopoulos, S., Genin, G.M., Chasiotis, I., 2013. Strong and tough mineralized PLGA nanofibers for tendon-to-bone scaffolds. Acta Biomaterialia 9 (12), 9442–9450. http://dx.doi.org/10.1016/j.actbio.2013.07.042.

Kovacevic, D., Fox, A.J., Bedi, A., Ying, L., Deng, X.H., Warren, R.F., Rodeo, S.A., 2011. Calcium-phosphate matrix with or without TGF-β3 improves tendon-bone healing after rotator cuff repair. American Journal of Sports Medicine 39 (4), 811–819. http://dx.doi.org/10.1177/0363546511399378.

Kuang, G.M., Yau, M.P., Lu, W.W., Chiu, K.Y., 2013. Use of a strontium-enriched calcium phosphate cement in accelerating the healing of soft-tissue tendon graft within the bone tunnel in a rabbit model of anterior cruciate ligament reconstruction. The Bone & Joint Journal 95-B (7), 923–928. http://dx.doi.org/10.1302/0301-620X.95B7.30748.

Kuang, G.M., Yau, W.P., Chiu, K.Y., 2014. Local application of strontium in a calcium phosphate cement system accelerates healing of soft tissue grafts in anterior cruciate ligament reconstruction: experiment using a rabbit model. American Journal of Sports Medicine 42 (12), 2996–3002. http://dx.doi.org/10.1177/0363546514549536.

Li, X., Xie, J., Lipner, J., Yuan, X., Thomopoulos, S., Xia, Y., 2009. Nanofiber scaffolds with gradations in mineral content for mimicking the tendon-to-bone insertion site. Nano Letters 9 (7), 2763–2768. http://dx.doi.org/10.1021/nl901582f.

Lipner, J., Liu, W., Liu, Y., Boyle, J., Genin, G.M., Xia, Y., Thomopoulos, S., 2014. The mechanics of PLGA nanofiber scaffolds with biomimetic gradients in mineral for tendon-to-bone repair. Journal of the Mechanical Behavior of Biomedical Materials 40C, 59–68. http://dx.doi.org/10.1016/j.jmbbm.2014.08.002.

Liu, W., Yeh, Y.C., Lipner, J., Xie, J., Sung, H.W., Thomopoulos, S., Xia, Y., 2011. Enhancing the stiffness of electrospun nanofiber scaffolds with a controlled surface coating and mineralization. Langmuir 27 (15), 9088–9093. http://dx.doi.org/10.1021/la2018105.

Liu, W., Lipner, J., Xie, J., Manning, C.N., Thomopoulos, S., Xia, Y., 2014. Nanofiber scaffolds with gradients in mineral content for spatial control of oseteogenesis. ACS Applied Materials & Interfaces 6 (4), 2842–2849. http://dx.doi.org/10.1021/am405418g.

Lu, H.H., Thomopoulos, S., 2013. Functional attachment of soft tissues to bone: development, healing, and tissue engineering. Annual Review of Biomedical Engineering 15, 201–226. http://dx.doi.org/10.1146/annurev-bioeng-071910-124656.

Lu, Y., Markel, M.D., Nemke, B., Lee, J.S., Graf, B.K., Murphy, W.L., 2009. Influence of hydroxyapatite-coated and growth factor-releasing interference screws on tendon-bone healing in an ovine model. Arthroscopy 25 (12), 1427–1434.e1. http://dx.doi.org/10.1016/j.arthro.2009.06.008.

Lui, P.P.Y., Zhang, P., Chan, K.M., Qin, L., 2010. Biology and augmentation of tendon-bone insertion repair. Journal of Orthopaedic Surgery and Research 5, 59. http://dx.doi.org/10.1186/1749-799X-5-59.

Ma, C.B., Kawamura, S., Deng, X., Ying, L., Schneidkraut, J., Hays, P., Rodeo, S.A., 2007. Bone morphogenetic proteins-signaling plays a role in tendon-to-bone healing a study of rhBMP-2 and noggin. American Journal of Sports Medicine 35 (4), 597–604. http://dx.doi.org/10.1177/0363546506296312.

Ma, B., Xie, J., Jiang, J., Shuler, F.D., Bartlett, D.E., 2013. Rational design of nanofiber scaffolds for orthopedic tissue repair and regeneration. Nanomedicine (London) 8 (9), 1459–1481. http://dx.doi.org/10.2217/nnm.13.132.

Maganaris, C.N., Paul, J.P., 1999. In vivo human tendon mechanical properties. The Journal of Physiology 521, 307–313. http://dx.doi.org/10.1111/j.1469-7793.1999.00307.x.

Moffat, K.L., Sun, W.H.S., Pena, P.E., Chahine, N.O., Doty, S.B., Ateshian, G.A., Hung, C.T., Lu, H.H., 2008. Characterization of the structure-function relationship at the ligament-to-bone interface. Proceedings of the National Academy of Sciences of the United States of America 105 (23), 7947–7952. http://dx.doi.org/10.1073/pnas.0712150105.

Moffat, K.L., Wang, I.N.E., Rodeo, S.A., Lu, H.H., 2009. Orthopaedic interface tissue engineering for the biological fixation of soft tissue grafts. Clinics in Sports Medicine 28 (1), 157–176. http://dx.doi.org/10.1016/j.csm.2008.08.006.

Mutsuzaki, H., Sakane, M., 2011. Calcium phosphate-hybridized tendon graft to enhance tendon-bone healing two years after ACL reconstruction in goats. Sports Medicine, Arthroscopy, Rehabilitation, Therapy & Technology 3 (1), 31. http://dx.doi.org/10.1186/1758-2555-3-31.

Mutsuzaki, H., Sakane, M., Nakajima, H., Ito, A., Hattori, S., Miyanaga, Y., Ochiai, N., Tanaka, J., 2004. Calcium-phosphate-hybridized tendon directly promotes regeneration of tendon-bone insertion. Journal of Biomedical Materials Research Part A 70 (2), 319–327. http://dx.doi.org/10.1002/jbm.a.30084.

Mutsuzaki, H., Sakane, M., Hattori, S., Kobayashi, H., Ochiai, N., 2009. Firm anchoring between a calcium phosphate-hybridized tendon and bone for anterior cruciate ligament reconstruction in a goat model. Biomedical Materials 4 (4), 045013. http://dx.doi.org/10.1088/1748-6041/4/4/045013.

Mutsuzaki, H., Sakane, M., Fujie, H., Hattori, S., Kobayashi, H., Ochiai, N., 2011. Effect of calcium phosphate-hybridized tendon graft on biomechanical behavior in anterior cruciate ligament reconstruction in a goat model: novel technique for improving tendon-bone healing. American Journal of Sports Medicine 39 (5), 1059–1066. http://dx.doi.org/10.1177/0363546510390427.

Mutsuzaki, H., Kanamori, A., Ikeda, K., Hioki, S., Kinugasa, T., Sakane, M., 2012a. Effect of calcium phosphate-hybridized tendon graft in anterior cruciate ligament reconstruction: a randomized controlled trial. American Journal of Sports Medicine 40 (8), 1772–1780. http://dx.doi.org/10.1177/0363546512449618.

Mutsuzaki, H., Sakane, M., Nakajima, H., Ochiai, N., 2012b. Calcium phosphate-hybridised tendon graft to reduce bone-tunnel enlargement after ACL reconstruction in goats. Knee 19 (4), 455–460. http://dx.doi.org/10.1016/j.knee.2011.03.008.

Pan, W., Wei, Y., Zhou, L., Li, D., 2011. Comparative in vivo study of injectable biomaterials combined with BMP for enhancing tendon graft osetointegration for anterior cruciate ligament reconstruction. Journal of Orthopaedic Research 29 (7), 1015–1021. http://dx.doi.org/10.1002/jor.21351.

Pan, W., Li, D., Wei, Y., Hu, Y., Zhou, L., 2013. Tendon-to-bone healing using an injectable calcium phosphate cement combined with bone xenograft/BMP composite. Biomaterials 34 (38), 9926–9936. http://dx.doi.org/10.1016/j.biomaterials.2013.09.018.

Paxton, J.Z., Donnelly, K., Keatch, R.P., Barr, K., 2009. Engineering the bone-ligament interface using polyethylene glycol diacrylate incorporated with hydroxyapatite. Tissue Engineering Part A 15 (6), 1201–1209. http://dx.doi.org/10.1089/ten.tea.2008.0105.

Price, P.A., Toroian, D., Eun, J., 2009. Mineralization by inhibitor exclusion: the calcification of collagen with fetuin. Journal of Biological Chemistry 284, 17092–17101. http://dx.doi.org/10.1074/jbc.M109.007013.

Qu, J., Thoreson, A.R., Chen, Q., An, K.N., Amadio, P.C., Zhao, C., 2013. Tendon gradient mineralization for tendon to bone interface integration. Journal of Orthopaedic Research 31, 1713–1719. http://dx.doi.org/10.1002/jor.22412.

Qu, D., Mosher, C.Z., Boushell, M.K., Lu, H.H., 2014. Engineering complex orthopaedic tissues via strategic biomimicry. Annals of Biomedical Engineering 43 (3), 697–717. http://dx.doi.org/10.1007/s10439-014-1190-6.

Rho, J.Y., Kuhn-Spearing, L., Zioupos, P., 1998. Mechanical properties and the hierarchical structure of bone. Medical Engineering & Physics 20, 92–102. http://dx.doi.org/10.1016/S1350-4533(98)00007-1.

Riley, G., 2004. The pathogenesis of tendiopathy. a molecular perspective. Rheumatology (Oxford) 43, 131–142. http://dx.doi.org/10.1093/rheumatology/keg448.

Rodeo, S.A., Arnoczky, S.P., Torzilli, P.A., Hidaka, C., Warren, R.F., 1993. Tendon-healing in a bone tunnel. A biomechanical and histological study in the dog. The Journal of Bone and Joint Surgery. American Volume 75 (12), 1795–1803.

Rodeo, S.A., Suzuki, K., Deng, X.H., Wozney, J.M., Warren, R.F., 1999. Use of recombinant human bone morphogenetic protein-2 to enhance tendon healing in a bone tunnel. American Journal of Sports Medicine 27, 476–488.

Samavedi, S., Olsen Horton, C., Guelcher, S.A., Goldstein, A.S., Whittington, A.R., 2011. Fabrication of a model continuously graded co-electrospun mesh for regeneration of the ligament-bone interface. Acta Biomaterialia 7, 4131–4138. http://dx.doi.org/10.1016/j.actbio.2011.07.008.

Samavedi, S., Guelcher, S.A., Goldstein, A.S., Whittington, A.R., 2012. Response of bone marrow stromal cells to graded co-electrospun scaffolds and its implications for engineering the ligament-bone interface. Biomaterials 33, 7727–7735. http://dx.doi.org/10.1016/j.biomaterials.2012.07.008.

Schwartz, A.G., Pasteris, J.D., Genin, G.M., Daulton, T.L., Thomopoulos, S., 2012. Mineral distributions at the developing tendon enthesis. PLoS One 7 (11), e48630. http://dx.doi.org/10.1371/journal.pone.0048630.

Shih, Y.R.V., Hwang, Y.S., Phadke, A., Kang, H., Hwang, N.S., Caro, E.J., Nguyen, S., Siu, M., Theodorakis, E.A., Gianneschi, N.C., Vecchio, K.S., Chien, S., Lee, O.K., Varghese, S., 2014. Calcium phosphate-bearing matrices induce osteogenic differentiation of stem cells through adenosine signaling. Proceedings of the National Academy of Sciences of the United States of America 111 (3), 990–995. http://dx.doi.org/10.1073/pnas.1321717111.

Spalazzi, J.P., Dagher, E., Doty, S.B., Guo, X.E., Rodeo, S.A., Lu, H.H., 2006a. In vivo evaluation of a tri-phasic composite scaffold for anterior cruciate ligament-to-bone integration. Conference Proceedings: Annual International Conference of the IEEE Engineering in Medicine and Biology Society 1, 525–528. http://dx.doi.org/10.1109/IEMBS.2006.259296.

Spalazzi, J.P., Dotym, S.B., Moffat, K.L., Levine, W.N., Lu, H.H., 2006b. Development of controlled matrix heterogeneity on a triphasic scaffold for orthopedic interface tissue engineering. Tissue Engineering 12, 3497–3508. http://dx.doi.org/10.1089/ten.2006.12.3497.

Spalazzi, J.P., Dagher, E., Doty, S.B., Guo, X.E., Rodeo, S.A., Lu, H.H., 2008. In vivo evaluation of a multiphased scaffolds designed for orthopaedic interface tissue engineering and soft tissue-to-bone integration. Journal of Biomedical Materials Research Part A 86, 1–12. http://dx.doi.org/10.1002/jbm.a.32073.

Thomopoulos, S., Hattersley, G., Rosen, V., Mertens, M., Galatz, L., Williams, G.R., Soslowsky, L.J., 2002. The localized expression of extracellular matrix components in healing tendon insertion sites: an *in situ* hybridization study. Journal of Orthopaedic Research 20 (3), 454–463. http://dx.doi.org/10.1016/S0736-0266(01)00144-9.

Thomopoulos, S., Williams, G.R., Gimbel, J.A., Favata, M., Soslowsky, L.J., 2003a. Variation of biomechanical, structural, and compositional properties along the tendon to bone insertion site. Journal of Orthopaedic Research 21, 413–419. http://dx.doi.org/10.1016/S0736-0266(03)0057-3.

Thomopoulos, S., Williams, G.R., Soslowsky, L.J., 2003b. Tendon to bone healing: differences in biomechanical, structural, and compositional properties due to a range of activity levels. Journal of Biomechanical Engineering 125, 106–113. http://dx.doi.org/10.1115/1.1536660.

Thomopoulos, S., Marquez, J.P., Weinberger, B., Birman, V., Genin, G.M., 2006. Collagen fiber orientation at the tendon to bone insertion and its influence on stress concentrations. Journal of Biomechanics 39, 1842–1851. http://dx.doi.org/10.1016/j.jbiomech.2005.05.021.

Thomopoulos, S., Matsuzaki, H., Zaegel, M., Gelberman, R.H., Silva, M.J., 2007. Alendronate prevents bone loss and improves tendon-to-bone repair strength in a canine model. Journal of Orthopaedic Research 25, 473–479. http://dx.doi.org/10.1002/jor.20293.

Thomopoulos, S., Zampiakis, E., Das, R., Silva, M.J., Gerlberman, R.H., 2008. The effect of muscle loading on flexor tendon-to-bone healing in a canine mode. Journal of Orthopaedic Research 26, 1611–1617. http://dx.doi.org/10.1002/jor.20689.

Thomopoulos, S., Genin, G.M., Galatz, L.M., 2010. The development and morphogenesis of the tendon-to-bone insertion what development can teach us about healing. Journal of Musculoskeletal & Neuronal Interactions 10 (1), 35–45.

Thomopoulos, S., 2011. The role of mechanobiology in the attachment of tendon to bone. IBMS BoneKEy 8, 271–285. http://dx.doi.org/10.1138/20110515.

Tien, Y.C., Chih, T.T., Lin, J.H.C., Ju, C.P., Lin, S.D., 2004. Augmentation of tendon-bone healing by the use of calcium-phosphate cement. The Journal of Bone and Joint Surgery. British Volume 86, 1072–1076. http://dx.doi.org/10.1302/0301-620X.86B7.14578.

Vaquette, C., Fan, W., Xia, Y., Hamlet, S., Hutmacher, D.W., Ivanovski, S., 2012. A biphasic scaffold design combined with cell sheet technology for simultaneous regeneration of alveolar bone/periodontal ligament complex. Biomaterials 33, 5560–5573. http://dx.doi.org/10.1016/j.biomaterials.2012.04.038.

Vitale, M.A., Vitale, M.G., Zivin, J.G., Braman, J.P., Bigliani, L.U., Flatow, E.L., 2007. Rotator cuff repair: an analysis of utility scores and cost-effectiveness. Journal of Shoulder and Elbow Surgery 16, 181–187. http://dx.doi.org/10.1016/j.jse.2006.06.013.

Weiler, A., Hoffmann, R.F., Bail, H.J., Rehm, O., Sudkamp, N.P., 2002. Tendon healing in a bone tunnel. Part II: histological analysis after biodegradable interference fit fixation in a model of anterior cruciate ligament reconstruction in sheep. Arthroscopy 18 (2), 124–135. http://dx.doi.org/10.1053/jars.2002.30657.

Wen, C.Y., Qin, L., Lee, K.M., Chan, K.M., 2009. The use of brushite calcium phosphate cement for enhancement of bone tendon integration in an anterior cruciate ligament reconstruction rabbit model. Journal of Biomedical Materials Research Part B: Applied Biomaterials 89 (2), 466–474. http://dx.doi.org/10.1002/jbm.b.31236.

Wen, L., Wang, Y., Wang, H., Kong, L., Zhang, L., Chen, X., Ding, Y., 2012. L-type calcium channels play a crucial role in the proliferation and osteogenic differentiation of bone marrow mesenchymal stem cells. Biochemical and Biophysical Research 424 (3), 439–445. http://dx.doi.org/10.1016/j.bbrc.2012.06.128.

Wopenka, B., Kent, A., Pasteris, J.D., Yoon, Y., Thomopoulos, S., 2008. The tendon-to-bone transition of the rotator cuff: a preliminary Raman spectroscopic study documenting the gradual mineralization across the insertion in rat tissue samples. Applied Spectroscopy 62 (12), 1285–1294. http://dx.doi.org/10.1366/000370208786822179.

Xie, J., Ma, B., Michael, P.L., Shuler, F.D., 2013a. Fabrication of nanofiber scaffolds with gradations in fiber organization and their potential applications. Macromolecular Bioscience 12 (10), 1336–1341. http://dx.doi.org/10.1002/mabi.201200115.

Xie, J., Zhong, S., Ma, B., Shuler, F.D., Lim, C.T., 2013b. Controlled biomineralization of electrospun poly(ε-caprolactone) fibers to enhance their mechanical properties. Acta Biomaterialia 9 (3), 5698–5707. http://dx.doi.org/10.1016/j.actbio.2012.10.042.

Xie, J., Ma, B., Shuler, F.D., 2014. Biomimetic nanofiber scaffolds for tendon-to-bone insertion repair. Advanced Materials Research 875-877, 331–334. http://dx.doi.org/10.4028/www.scientific.net/AMR.875-877.331.

Yamaguchi, K., Ditsios, K., Middleton, W.D., Hildebolt, C.F., Galatz, L.M., Teefey, S.A., 2006. The demographic and morphological features of rotator cuff disease. A comparison of asymptomatic and symptomatic shoulders. The Journal of Bone and Joint Surgery. American Volume 88 (8), 1699–1704. http://dx.doi.org/10.2106/JBJS.E.00835.

Yang, P.J., Temenoff, J.S., 2009. Engineering orthopedic tissue interfaces. Tissue Engineering Part B 15, 127–141. http://dx.doi.org/10.1089/ten.teb.2008.0371.

Zhang, X., Bogdanowics, D., Erisken, C., Lee, N.M., Lu, H.H., 2012. Biomimetic scaffold design for functional and integrative tendon repair. Journal of Shoulder and Elbow Surgery 21, 266–277. http://dx.doi.org/10.1016/j.jse.2011.11.016.

Zhang, X., Caldwell, J.M., Easley, J.T., Hackett, E., Doty, S., Levine, W.N., 2014. In vivo evaluation of a biomimetic biphasic scaffold in sheep. In: ORS 2014 Annual Meeting. Post No: 0113.

Zhao, S., Peng, L., Xie, G., Li, D., Zhao, J., Ning, C., 2014. Effect of the interposition of calcium phosphate materials on tendon-bone healing during repair of chronic rotator cuff tear. American Journal of Sports Medicine 42 (8), 1920–1929. http://dx.doi.org/10.1177/0363546514532781.

Ceramic–polymer nanocomposites for bone-tissue regeneration

15

P. Palmero
Politecnico di Torino, Department of Applied Science and Technology, Corso Duca degli Abruzzi 24, Torino, Italy

15.1 Introduction

This chapter reviews biomedical grade ceramic–polymer nanocomposites, focussing on their impact and recent trends in the field of bone grafting and bone-tissue regeneration.

Although autogenous and allogeneic bone grafts have been used for a long time in bone therapies, there is still a donor shortage and infection risk. As an alternative, synthetic inert biomaterials have been developed and clinically used as bone grafts, but most of them differ substantially from natural bone either compositionally or structurally. Therefore, they have a limited survivability, approximately 15 years, depending upon clinical uses. Bioactive materials are most promising, as they better mimic the natural bone-tissue biological behaviour. However, they have mechanical limitations, which limit their use in load-bearing applications. Musculoskeletal tissue reconstruction is the ultimate objective in orthopaedic surgery, which can be achieved by developing new tissue-engineering scaffolds, characterized by a superior ability to adapt in the biological environment and that would encourage local and systemic biological functions.

The design of an ideal bone graft that emulates bone's own structure and behaviour is still challenging. Owing to the composition and structural similarity to natural bone, most of the current investigations focus on nanocomposites, and particularly on the hydroxyapatite–collagen system.

This chapter first briefly reviews the characteristics of living bone (composition, architecture, mechanical and biological properties), as given in Section 15.2. These qualitative and quantitative parameters provide, in fact, adequate insights of superior biomimetic scaffolds, designed not only for replacing diseased or damaged bone tissue, but also for regenerating it (Section 15.3). After a short review on ceramics and biodegradable polymers (Section 15.4), the rational and strategy for developing tissue-engineering nanocomposites-based scaffolds are discussed in Section 15.5. Finally, this chapter addresses the state of the art of the most-investigated ceramic–polymer nanocomposites (Section 15.6) highlighting their advances in the bone-tissue regeneration field and providing suggestions for future research and development.

Nanocomposites for Musculoskeletal Tissue Regeneration. http://dx.doi.org/10.1016/B978-1-78242-452-9.00015-7

15.2 Bone as a natural ceramic–polymer nanocomposite

Bone tissue is an amazing and true biological nanocomposite. In fact, the most characteristic component of bone tissue is the mineralized extracellular matrix (ECM), containing both organic and inorganic phases: type I collagen and a specific type of calcium phosphate mineral called hydroxyapatite, $Ca_{10}(PO_4)_6(OH)_2$, hereafter referred to as HA. As later detailed, the bone architecture is organized in a complex hierarchical structure, ranging from the macro- to the nanoscale.

ECM provides mechanical support and serves as reservoir of minerals, particularly calcium and phosphate. Bone is a key example of a dynamic tissue, because it has a unique capability of self-regenerating and self-remodelling to certain extents.

The overall composition of bone is given in Table 15.1 [1–3], although we should keep in mind that the composition can vary slightly from species to species and from bone to bone [1].

All bones consist of a basic dual structure: an external layer, named cortical bone, which covers the bone: it is smooth, continuous and dense (approximately 1.85 g/cm^3). In the interior, cancellous bone is porous (with an open, honeycomb structure) with an average porosity of 75% to 95% and an average density of 0.3 g/cm^3 [4]. The main physical and mechanical properties of cortical and cancellous bone are summarized in Table 15.2 [1–6]. As described below, the cortical bone has an anisotropic structure [7] and hence anisotropic mechanical properties: for this reason, Table 15.2 collects values determined under both longitudinal and transverse directions of the applied load.

As shown in the scheme of Fig. 15.1, cortical bone, comprising 80% of the bone mass, consists of closely packed osteons, which consist on a central canal (named osteonic or Haversian canal), surrounded by concentric rings (lamellae) of matrix [6,7]. Between the rings of the matrix, the bone cells (osteocytes, see Table 15.3) are located in spaces called lacunae. The long axes of the osteons are roughly parallel to the long axis of the bone. The lamellae consist of parallel collagen

Table 15.1 Bone composition [1–3]

Component	wt%
Hydroxyapatite	60–70
Collagen	10–20
Water	9–20
Non-collagenous proteins (osteocalcin, osteonectin, osteopontin, thrombospondin, morphogenetic proteins, sialoprotein, serum proteins)	3–5
Carbonate	~4
Sodium	~0.7
Magnesium	~0.5
Other inorganic ions (Cl^-, F^-, K^+ Sr^{2+}, Pb^{2+}, Zn^{2+}, Cu^{2+}, Fe^{2+})	Traces
Other organic material (polysaccharides, lipids, cytokines)	Traces
Primary bone cells: osteoblasts, osteocytes, osteoclasts	/

Table 15.2 Physical and mechanical properties of bone [1–6]

Properties	Cortical bone longitudinal direction	Cortical bone transversal direction	Cancellous bone
Compressive Young's modulus (GPa)	17–20	6–13	0.1–5
Tensile strength (MPa)	79–151	51–56	10–20
Compressive strength (MPa)	170–193	133	7–10
Yield strength in compression (MPa)	131–224	106–131	21.3
Fracture toughness (MPa√m)	2–12	2–12	0.1

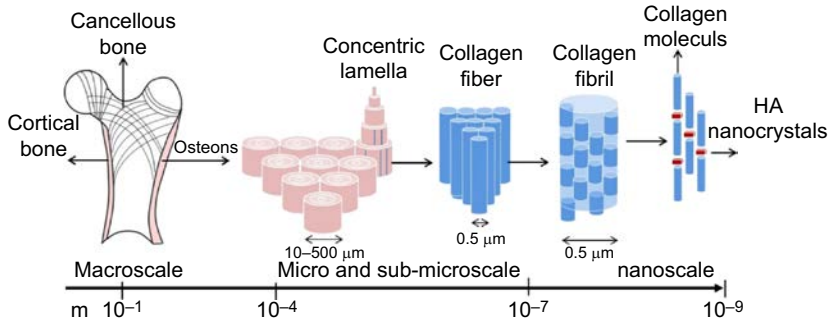

Figure 15.1 Scheme of the hierarchical structure of the bone, from macro- to nano-assembly [7].

Table 15.3 Bone cell types and respective functions [1,6,8]

Cell type	Origin	Function
Osteoblasts	MSCs	Production and secretion of organic and inorganic bone ECM, known as the *osteoid*
Osteocytes	Osteoblasts	Calcification of the osteoid matrix Maintenance of bone Mechanosensor cells of the bone
Osteoclasts	Haematopoietic	Bone resorption

fibrils, in which the fibril direction alternates in the successive, concentric layer. The collagen fibrils are themselves bundles of type I collagen and small amounts of type V collagen molecules. The specific binding points of the molecules in the fibrils act as nucleation sites for the bone mineral crystals. The HA crystals, which appear in the form of plates or needles, are about 40–60 nm long, 20 nm wide, and 1.5–5 nm thick [2,3,5].

Cancellous bone accounts for roughly 20% of the total mass of the skeleton. It exhibits a quite isotropic cellular structure, made by interconnected network of plates (trabeculae). Such network provides a low-density, open-cell structure, whereas a single trabecula gives high-density, virtually closed cells [2].

Fig. 15.1 clearly shows the hierarchical structure of the bone, from macro- to nano-level. At the macro-level, the different structure between compact and cancellous bone is well evident. Osteons and trabeculae compose the bone at the microstructural level, whereas the mineralized collagen fibrils constitute the nanostructured-bone building blocks [1,3].

The biomechanical properties of bone critically depend on this hierarchical structure. The macro-scale organization of osteons and Haversian canals provides long bones with their characteristic mechanical anisotropy. The microscale porosity in bone is ideal for cell migration and vascularization, whereas the nano-scale features act as a cell and mineral binding architecture [5].

Beside inorganic and organic components, the bone tissue is also associated with different kinds of cells. The cellular components are the essential factors for activation and control of bone metabolism. There are three types of bone cells, the function of which is summarized in Table 15.3 [1,6,8]: osteoblasts, osteocytes and osteoclasts. All of them have defined tasks and are essential for maintenance of a healthy bone tissue. *Osteoblasts* are responsible for the formation of new bone. They synthesize and secrete collagen type I, glycoproteins, cytokines and growth factors into a region of unmineralized matrix (*osteoid*) between the cell body and the mineralized matrix [5]. This substrate is essential for later mineralization of HA and other crystals. In fact, osteoblasts induce the precipitation of calcium salts and phosphorus from the blood: these minerals bond with the newly formed osteoid and mineralize the bone tissue [1]. *Osteocytes* are matured cells derived from osteoblasts that are responsible for the maintenance of bone [1]. They are transporting agents of minerals between bone and blood. *Osteoclasts* primary function is to secrete acids and proteolytic enzymes, which erode bone ECM under the influence of chemical cues [9,10].

The process of production and resorption of ECM by osteoblasts and osteoclasts plays an important role in bone remodelling, in which old bone is continuously replaced by new tissue. Bone remodelling is driven and regulated by hormones (ie, parathyroid hormone, calcitrol, glucocorticoids, sex hormones, etc.) and growth factors (ie, IGF, prostaglandins, TGF-βs, BMPs, etc.) in complicated biochemical cascades [6].

15.3 Requirements for scaffolds in bone-tissue engineering

The evolution of bone graft biomaterials can be categorized into four different generations (Fig. 15.2) [1,11].

The first-generation bone grafts are metals and alloys (stainless steel, titanium alloys, etc. [1]) which have excellent mechanical properties but are neither bioresorbable nor bioactive. Their lifetime is limited and hence need to be removed and replaced

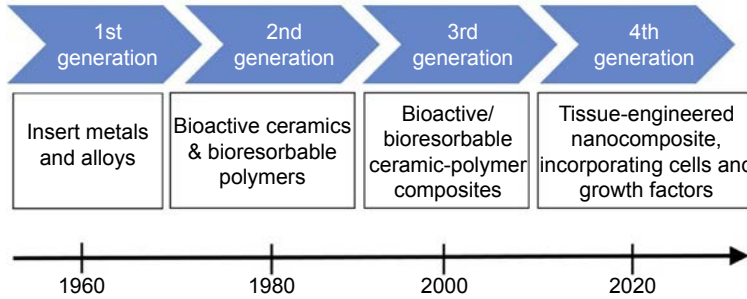

Figure 15.2 Evolution of biomaterials in bone grafting [1,11].

surgically. The second-generation bone grafts include bioactive ceramics and bioresorbable polymers [1] (HA, bioactive glass (BG), tricalcium phosphate (TCP), collagen, poly(lactic acid-co-glycolic acid) (PLGA)). Polymeric scaffolds lack bioactivity and sufficient mechanical properties, whereas ceramic scaffolds are too brittle to be used for load-bearing applications. The third-generation bone grafts are made up of composite materials which combine the strength, stiffness and osteoconductivity of ceramics with the flexibility, toughness and resorbability of polymers. Examples are HA–PE, HA–collagen, HA–PLLA [1]. The fourth-generation bone grafts are polymer–ceramic composite and nanocomposites, often incorporating osteogenic cells, growth factors or bone morphogenetic proteins (BMPs), used alone or in combination [12], thus to serve for effective tissue regeneration.

Scaffolds for bone-tissue engineering must fulfil some primary functions:

1. Biocompatibility: scaffolds should be well integrated in the host's tissue without any immune response or toxic effects;
2. Load-bearing properties: the mechanical properties of an ideal bone scaffold should match host bone properties (Table 15.2) and guarantee proper load transfer. In addition, the scaffold must provide sufficient initial mechanical support to substitute for the mechanical function until the tissue-engineered transplant is fully remodelled by the host tissue [13,14];
3. Suitable architecture for vascularization and bone ingrowth: the scaffold microstructure must ensure cell migration as well as attachment and differentiation at the pore surfaces. Moreover, for easy migration of cells within the scaffolds, the pores must be large enough. Porosities higher than 80% with pore sizes in the range 100–500 μm are suitable for bone-tissue regeneration [15,16]. Small pores (in the range 2–5 μm) are important too: when located at the walls of the scaffold, they are helpful for fibrovascular colonization and nutrient transportation. Thus, they improve the biological performance of the porous scaffold and promote the favourable bioresorption of the material [17];
4. Osteoconductive and osteoinductive properties: an ideal bone scaffold should allow the bone cells to adhere, proliferate and form ECM on its surface and pores (osteoconductive). The scaffold should also be able to induce new bone formation through biomolecular signalling and recruiting progenitor cells, a property known as osteoinduction [14];
5. Bioresorbability: the scaffold should be able to degradate with time in vivo, preferably at a controlled resorption rate and eventually creating space for the new bone tissue to grow [14];
6. Drug delivery: the scaffold should be able to deliver bioactive molecules or drugs in a controlled manner, thus to accelerate healing and prevent pathology.

According to such requirements, the fabrication of an ideal scaffold for bone-tissue regeneration requires three major factors: *cells*, *signals* and proper *biomaterials*.

Cells have been used in bone-tissue engineering for seeding in bone scaffolds before implantation. Numerous cell sources have been investigated, such as embryonic stem cells, bone marrow stromal cells and muscle-derived stem cells [18]. Bone marrow stromal cells are frequently used; they consist of haematopoietic stem cells and mesenchymal stem cells, which can differentiate into various types of cells including osteoblasts. It was demonstrated that culture-expanded bone marrow cells can heal a segmental bone defect after re-implantation [19,20] and can give rise to osteogenic tissue in a variety of animal species [21–23]. Clinical studies by Connolly [24] and recently by Quarto et al. [25] illustrate the potential for autologous bone marrow stromal cells (with a porous bioceramic scaffold) in the treatment of large bone defects, by exploiting injectable bone-marrow preparations.

Signals, such as media additives and chemical cues, are used to guide bone cells differentiation and proliferation. Chemical additives, such as dexamethasone (DEX) and β-glycerophosphate, are often added to the cell cultures to promote differentiation of bone marrow stem cells into osteoblasts [18]. Chemical cues, such as growth factors, are also used to enhance bone growth within the scaffold. They promote and/or prevent cell adhesion, proliferation, migration and differentiation by up-regulating or down-regulating the synthesis of proteins, growth factors and receptors. These molecules are essential for tissue formation. In concert with osteoprogenitor and osteoblast populations, growth factors are strongly implicated in osteogenesis. Major players in the skeletal tissue engineering are members of the TGF-β superfamily, notably the BMPs [19]. Despite clear evidence for a role of BMPs in bone development, the identification of the optimal mix of BMPs, dosage, release dynamics and suitable carrier is still a challenging open point [19]. In general, a deeper understanding of how the growth factors interact with each other and with the cells, what is their effect, which intracellular pathways are triggered by them and how they can be activated or inactivated is necessary for further developing a tissue-engineered bone.

Biomaterials must be properly selected because their physical, mechanical and biological properties will determine, to a great extent, the properties of the tissue-engineering scaffold. In Section 15.4, the main characteristics of monolithic biomaterials, precisely ceramics and polymers, are depicted, whereas in Section 15.5 the potential of ceramic–polymer nanocomposites in bone-tissue regeneration is illustrated.

15.4 Materials for bone-tissue regeneration: ceramics and polymers

The selection of the most appropriate material to produce a scaffold is a very important step towards the construction of a tissue-engineered product. Most of the time, the material properties will determine the properties of the scaffold itself. Up to now, several materials such as metals, ceramics and polymers from both natural and synthetic origins have been proposed. However, metals and most of the ceramics are not

biodegradable, which leaves the researcher's choice reduced to a small number of ceramics and to biodegradable polymers, as illustrated in the following.

15.4.1 Ceramics

Ceramics have been widely used in biomedical engineering and bone substitution/regeneration fields [26]. Upon implantation, certain ceramics, bioactive glasses (BGs) and glass ceramics undergo surface modification, with time-dependent modification kinetics. The surface forms a biologically active hydroxy carbonate apatite (HCA) layer, which is chemically and structurally equivalent to the mineral phase in bone and provides the necessary bonding interface with living tissue [27].

However, these materials have some major drawbacks. They are brittle and present a low mechanical stability, which prevent their use in the regeneration of large bone defects [8]. Furthermore, due to in vivo osteoclastic activity, their degradation/dissolution rates are difficult to predict. Too-fast degradation will compromise the mechanical stability of the scaffold, which is low by itself. At the same time, a quick degradation would dramatically increase the extracellular concentrations of Ca and P, leading to cellular death [28].

The characteristics of the main bioceramics for bone-tissue regeneration are synthetically reported in the following. In Table 15.4, their main mechanical properties and major clinical uses are collected.

15.4.1.1 Calcium phosphates

The most common types of calcium phosphate (CP) materials investigated for synthetic bone scaffolds are: HA, $Ca_{10}(PO_4)_6(OH)_2$, α- or β-TCP, $Ca_3(PO_4)_2$, biphasic calcium phosphates (BCP, consisting of HA–TCP mixtures) and multiphasic bioglasses.

Due to their close chemical and crystal resemblance to bone mineral, CPs have an excellent biocompatibility [27]. CPs possess osteoconductive properties, but they do not show osteoinductivity [1,5]. Many in vivo and in vitro studies demonstrated that CPs, regardless of the form (bulk, coating, powder, or porous) and phase (crystalline or amorphous), always support the cells attachment, proliferation, and differentiation [13]. In addition, it was found that silicon can play a role in bone mineralization and gene activation. In vitro studies have demonstrated that the incorporation of small amounts of silicon within the HA lattice significantly improves HA solubility and rate of bone apposition, as well as the proliferation of human osteoblasts [29,30]. In vivo studies have shown that bone ingrowth into Si-substituted HA granules was higher than in pure HA [31]. Therefore, the research is increasingly focussing on the substitution of silicon for calcium in synthetic HA.

Mechanical properties of synthetic CPs (Table 15.4) are highly dependent on their crystallinity, grain size, porosity and composition. In general, the mechanical properties of synthetic CPs decrease with increasing amorphous phase, microporosity, and grain size. High crystallinity, low porosity, and small grain size result in higher stiffness, compressive and tensile strength as well as higher fracture toughness [13].

Crystalline CPs have long degradation time in vivo, typically on the order of months or even years [13]. The degradation follows a dissolution–re-precipitation mechanism

Table 15.4 Mechanical properties and clinical applications of ceramics for bone-tissue regeneration

Ceramic	Compressive strength (MPa)	Bending strength (MPa)	Elastic modulus (GPa)	Fracture toughness (MPa √m)	H_V (GPa)	Clinical application	References
HA	400–900	115–200	114	0.7–1.2	5.9	Bone regeneration, non-loading sites, bone void filler (cements, granules, coatings)	[1,2,65–67]
45S5 BG	~500	40–60	30–50	0.5–1.0	5.75	Middle ear device, tooth root replacement, periodontal treatment, maxilla-facial reconstruction, bone defect filler	[13,50,68]
A/W GC	1080	215	118	2.0	6.7	Vertebrae prosthesis, iliac crest prosthesis, bone defect filler	[50,52,55]
Dehydrated CS	20–30	4–6	/	/	/	Bone filler and bone repair material; drug/growth factor delivery vehicle	[69]

in contact with biological fluids [32]. Ionic transfer occurs from the solid phase to the aqueous liquid via surface hydration of calcium, inorganic phosphate species and possible impurities like carbonates, fluorides or chlorides present in the biomaterial [5]. Under physiological conditions, this dissolution process is highly dependent on the nature of the CP substrate and its thermodynamic stability. It is recognized that the dissolution rate decreases in the following order [33]:

$$\text{Amorphous HA} >> \alpha\text{-TCP} >> \beta\text{-TCP} >> \text{crystalline HA}$$

The slowest degradation rate of crystalline HA, as compared to the other CPs, motivated the development of BCPs (ie, HA–TCP mixtures) and bioglasses with tunable (to some degree) degradation rates [34].

Concerning the use of CP-based scaffolds in regenerative medicine, it was demonstrated that cylindrical synthetic porous HA implants (pore sizes of 400 to 600 μm and 80% porosity) were able to heal femoral defects in rats [35]. Porous particles of HA (average pore size 150 μm, porosity 70%) and coral-derived HA blocks (average pore size 230 μm, porosity 66%) were used for the delivery of BMP-2 in a rat ectopic model, inducing direct osteogenesis [36]. BCP with 50% porosity and 100–150 μm pore sizes have been shown to heal femoral defects in dogs [37].

15.4.1.2 Bioactive glasses

Silica-based BGs are a group of surface-reactive glass–ceramic (GC) biomaterials, first prepared by Hench et al. in 1969 [38]. BGs possess excellent biocompatibility, the ability to bond with bone and other tissues and stimulatory effects on bone cell function [39–41] which explain their successful application as bone-substitute material for non-load-bearing applications in orthopaedic and dental surgery [41,42].

The bonding ability of BG is due to the chemical reactivity of the BG through interfacial and cell-mediated reactions in which silicon bonds are broken and a CP-rich layer is formed on the top of the glass, which crystallizes to HCA [13].

The basic constituents of most BGs are SiO_2, Na_2O, CaO, and P_2O_5. The classical 45S5 BG composition, universally known as Bioglass®, contains 45% SiO_2, 24.5% Na_2O, 24.4% CaO and 6% P_2O_5, as weight percent [13]. Depending on the BG specific composition, the bioactivity, osteoconductivity and bioresorbability can be easily tuned [13]. Rapid bonding to bone occurs for silica level in the range 42–53%, whereas glasses with 54 to 60% of silica require 2–4 weeks for bonding. Finally, when glasses contain more than 60% of silica, there is no direct bonding between BG and bone [43]. Hench defined two classes of bioactive materials (A and B) on the ground of the rate of bone regeneration and repair. Class A materials are those that lead to both osteoconduction (the growth of bone along the bone–implant interface) and osteoproduction, as a result of the rapid reactions on the implant surface [44,45]. Class B materials, instead, allow osteoconduction, but no osteoproduction [46]. Thus, as the structure and chemistry of glasses can be controlled at a molecular level, it is possible to design glasses with biological properties specific for particular applications in bone-tissue engineering.

Bioglass® implants with pores ranging from 100 to 600 μm induced ectopic bone formation in dogs [47]. Silica–calcium phosphate scaffolds with different porosities

(51, 47 and 43% generated by decreasing the silica content) and a broad distribution of pore sizes (10–300 mm) helped to regenerate bone in femoral defects in rabbits [48].

The bioactivity of BGs is facilitated by their amorphous structure, because this property decreases with the increase in crystallinity [49]. On the other hand, the amorphous structure of BGs impairs the mechanical strength of the material and lowers its fracture toughness (Table 15.4), especially in a porous form, thus limiting their use in load-bearing applications.

15.4.1.3 Glass ceramics

To overcome the limitations of the BGs, GC materials have been developed. The process involves the heat treatment of a base glass to induce controlled crystallization and to convert it into a glass–crystal mixture. The heat treatment results in the nucleation and growth of various kinds of crystalline phases with fine sizes. The resultant GC can display superior properties as compared to the base glass and to the sintered ceramics. Some biomedical grade GCs have been commercialized under trade names, such as Dicor® (mica GC), Ceravital® (apatite–devitraite GC) and Bioverit® (mica–apatite GC) [50].

Amongst GCs, increasing interest focuses on those containing apatite [$Ca_{10}(PO_4)_6(O,F_2)$] and wollastonite [$CaO{\cdot}SiO_2$] as predominant crystalline phases in the $MgO–CaO–SiO_2$ system. A particular GC system, referred to as apatite–wollastonite glass–ceramic (A/W GC), was discovered by Kokubo et al. in 1982 [51–53]. This material is very attractive owing to its biological ability to spontaneously bond to living bone (in a short period) and to keep high mechanical properties (such as toughness and strength) for a long period in a body environment [53]. The apatite phase is responsible for the spontaneous bonding to natural bone, whereas the wollastonite phase prevents straight propagation of cracks and induces a reinforcing effect [54,55]. For these exceptional properties, A/W GC is increasingly used in the replacement of natural bone [51,52].

15.4.1.4 Calcium sulphate

Calcium sulphate hemihydrate ($CaSO_4{\cdot}0.5H_2O$), (CS), known as plaster of Paris, has been used for over a 100 years in a variety of pharmaceutical, dental, and orthopaedic applications.

CS is well-known bone filler, with proven biological advantages: biodegradability, biocompatibility and osteoconductivity. CS pellets have been used as bone void fillers as early as 1892 [56]. In addition, it has been used as a binder for HA–ceramic particles in partially resorbable composite cements [57] and as a growth factor release agent [58,59]. When mixed with water, CS powder is converted into a calcium sulphate dihydrate ($CaSO_4{\cdot}2H_2O$) paste, which is regarded as one of the most successful bone cements, due to its ability to undergo in situ setting after filling the defects, without any inflammatory response [60,61].

CS is not simple space filler that allows bone to heal passively, but a soluble material that has bioactive properties and stimulates bone formation. Recent studies evidenced, in fact, an increased angiogenesis in defects filled with CS, as compared with those filled with autograft [55,56,59].

CS shows, however, some major drawbacks. The first concern is related to CS purity, as it can derive from many different natural sources. Impurities found in CS comprise a list of naturally occurring carbonates and silicates, besides other metal traces [55]. Biomedical grade materials must be assayed for these contaminants.

The second, most significant criticism of CS when used as a bone graft material is the high dissolution rate. CS degrades completely by 4 to 7 weeks, and its degradation is often much faster than the growth of the new bone [62,63]. CS pellets were seen to collapse within days after their implantation, failing to provide sufficient support for the newly forming bone. Several approaches have been used to reduce the degradation rate of CS. One approach involves the addition of HA particles to CS: the formation of a calcium phosphate surface layer was effective in delaying the degradation. Nevertheless, although the degradation rate decreased, the compressive strength of the modified CS pellets decreased as well. A second approach involves the addition of small amounts of poly-L-lactic acid (PLLA) to CS. The granular composite showed a half-life of 68 days in simulated body fluid at 37°C, whereas neat CS granules had a half-life of only 9 days under the same conditions. Currently, a medical grade calcium sulphate impregnated with tobramycin is commercially available (Osteoset; Wright Medical Technology, Arlington, Tennessee, USA) [64].

15.4.2 Polymers

Polymers are widely used for the fabrication of scaffolds in tissue-engineering applications. Many types of biodegradable polymeric materials have been already used in this field. They can be classified as follows [17]:

- *natural*-based polymers (ie, obtained from natural sources, either animal or vegetal), including polysaccharides (examples: starch, alginate, chitin/chitosan, hyaluronic acid derivatives) or proteins (soy, collagen, fibrin gels, silk);
- *synthetic* polymers, such as poly(lactic acid) (PLA, PLLA, PDLLA), poly(glycolic acid) (PGA), poly(3-caprolactone) (PCL), poly(hydroxyl butyrate) (PHB).

Natural polymers offer numerous advantages for tissue-engineering scaffolds, owing to their biocompatibility, inherent biodegradability and potential bioactivity. Collagen porous matrices healed tibia defects in rats [70], whereas a benzyl ester derivative of hyaluronic acid (with 80% to 90% porosity and pores ranging from 100 to 600 μm) was used for the delivery of BMP-2 in vitro and osteogenic differentiation of the murine pluripotent cell line C3H10T1/2 [71].

Generally, the biodegradation of natural polymers involves the cleavage of bonds through an enzymatic mechanism, leading to polymer erosion. For this reason, natural polymers are classified as enzymatically degradable materials, to distinguish them from hydrolytically degradable synthetic polymers, in which hydrolysis induces debonding [72].

Natural polymers have some major drawbacks: poor mechanical properties and high degradation rates. In addition, many of them have a limited availability, and hence a high cost [8,17]. For these reasons, natural polymers are often used in composites or submitted to chemical modification by cross-linking, to increase the mechanical

properties and reduce the degradation rate. However, these structural modifications may reduce the biocompatibility and even induce cytotoxic effects [73].

Synthetic polymers offer some advantages as compared to natural ones: the relatively good mechanical strength and the possibility to modulate the degradation rate to a certain extent. In addition, the versatility of chemically synthesized polymers enables the fabrication of scaffolds with different features (forms, porosities and pore sizes, mechanical properties) to match tissue-specific applications. The major drawbacks are the hydrophobic surfaces and lack of cell-recognition signals.

The resorption process of biopolymers is classified according to their erosion mechanism [74]. Bulk erosion is induced by rapid diffusion of water into the polymer structure, leading to hydrolysis. The subsequent mass loss occurs throughout the bulk of the material. In surface erosion, the mass loss occurs at the water–implant interface: the implant is thus resorbed from its outer surface towards the centre, while maintaining its bulk integrity.

In general, polymers of the poly(α-hydroxy acids) group undergo bulk degradation. The molecular weight of the polymer starts to decrease upon placement in an aqueous media. When molecular chains are reduced to a certain small size, they can freely diffuse out of the polymer matrix [75]. The mass loss is accompanied by the release of acidic by-products. In vivo, massive release of such acidic by-products results in inflammatory reactions, a serious clinical drawback well documented in literature [76–78]. Therefore, it is important that the scaffold–cell construct is constantly exposed to sufficient quantities of neutral culture media, especially during the period when the mass loss of the polymer matrix occurs [79].

To have tunable degradation properties, poly(ethylene glycol)-terephthalate–co-poly(butylene terephthalate) (PEGT–PBT) polymer has recently been studied for bone and cartilage regeneration. These polyether-ester multiblock copolymers belong to a class of materials known as thermoplastic elastomers, which exhibit good physical properties (like elasticity, toughness and strength [5]), which are essential for reconstructing load-bearing tissues. By varying the molecular weight of the starting PEG segments and the weight ratio of PEGT and PBT blocks, it is possible to tailor their biodegradation rate [80]. Being polyether-esters, degradation occurs in aqueous media by hydrolysis and oxidation, the rate of which varies from very low (high PBT contents) to medium and high (larger contents of PEGT and longer PEG segments).

The physical and mechanical properties, as well as major clinical applications of natural and synthetic polymers, are collected in Table 15.5.

15.5 Nanocomposites for bone-tissue regeneration: properties and processing

15.5.1 Why composite-based scaffolds for bone-tissue regeneration?

There is an increasing interest towards the development of composite materials for tissue-engineering scaffolds. The physical and mechanical properties of the constituent materials can be combined, thus to more closely match the mechanical and

Table 15.5 Physical–mechanical properties and major clinical applications of biodegradable polymers for bone-tissue engineering

Polymer	Tensile modulus (GPa)	Degradation mechanism and time (months)	Clinical application	References
PLA	1.5–2.7	Hydrolytic/Bulk erosion 12–18	Orthopaedic surgery Oral and maxillofacial surgery	[17,79,81]
PDLLA	1.9–2.4	Hydrolytic/Bulk erosion 12–16	Oral and maxillofacial surgery Orthopaedic surgery	[2,79,81,82]
PLLA	1.2–3.0	Hydrolytic/Bulk erosion >24	Orthopaedic surgery, Oral and maxillofacial surgery	[2,79–82]
PGA	5–7	Hydrolytic/Bulk erosion 3–4	Orthopaedic surgery	[17,79,81]
PLGA 50/50	1.4–2.8	Hydrolytic/Bulk erosion 3–6	Suture periodontal surgery Drug delivery	[17,79,81]
PCL	0.4–0.6	Hydrolytic/Bulk and surface erosion 24–36	Drug delivery Bone and cartilage tissue engineering	[17,79,81]
PPF	2–3	Hydrolytic/Bulk erosion >24	Orthopaedic implants, Foam coatings, drug delivery	[17,79–82]
Collagen	0.002–0.2	Enzymatic	Hard and soft tissue repair Drug delivery	[5,79,81,83]
Chitosan	0.007	Enzymatic	Soft tissue repair	[5,79,81,84]
Alginate	0.85	Enzymatic	Soft tissue repair	[5,79,81]
Silk	5–17	Enzymatic	Sutures Drug delivery	[79,81,85,86]

physiological demands of the host tissue. For instance, the strength and elastic modulus can be modulated in the composites, making them closer to natural bone, which is a composite itself (see Section 15.2).

The main advantages shown by ceramic–polymeric composites as compared to monolithic materials are here summarized:

- *Increased mechanical properties.* Bioceramics and glasses are characterized by flaw sensitivity and inherent brittleness. Conversely, polymers lack of mechanical strength and stiffness to meet the mechanical demands in surgery and in the physiologic environment. The combination of polymers and inorganic phases leads to composite materials with improved mechanical properties, minimizing their shortcomings. However, to achieve optimal properties in the composites, attention should be paid to the selection of both polymer matrix and ceramic filler. When selecting a polymer amongst different grades, its average molecular weight should be taken into consideration, because it affects the melting/crystallization behaviour, the viscosity at the processing temperatures, the mechanical properties and degradation behaviour. In general, the highest average molecular weight, amongst different grades, should be used for bone-tissue substitution purposes, to better match the strength and stiffness of the host tissue. At the same time, the processability of the polymer and hence of the composite has to be taken into consideration. A too high viscosity at the elevated processing temperature is not desired, as it can induce defects in the final composites. Concerning the ceramic filler, a number of factors can affect the composite properties, such as: (1) reinforcement shape, size and size distribution; (2) reinforcement properties and volume percentage; (3) distribution of the reinforcement in the matrix and (4) reinforcement–matrix interfacial state. By carefully controlling these features, the mechanical and biological performance of bioactive composites can be tailored, thus to meet various clinical requirements. The role of reinforcement size and morphology on the composite mechanical behaviour is briefly discussed in Section 15.5.2;
- *Increased bioactivity in the polymer matrix.* Probably, the most important driving force behind the development of polymer–bioactive ceramic composite scaffolds for bone-tissue regeneration is the need for conferring bioactive behaviour to the polymer matrix. This goal is achieved by mixing or coating the polymer with the bioactive phase. Up to a certain extent, it is possible to tailor the degree of bioactivity by controlling the volume fraction, the size, the morphology and arrangement of the bioactive fillers [27,87]. It has been shown that for HA-reinforced high-density polyethylene (HDPE) composite, the critical HA volume percentage is around 20%, above which bone apposition could occur on composite implant [88]. In general, by increasing the filler volume fraction and the surface area-to-volume ratio of inclusions, the bioactivity increases as well. For this reason, in some applications the incorporation of fibres instead of particles is favoured [88];
- *Tailored degradation behaviour.* The addition of a bioactive phase to a bioresorbable polymer can alter, positively, the polymer degradation behaviour. In fact, bioactive phases allow a rapid exchange of protons in water for alkali in the glass or ceramic. This provides a pH buffering effect at the polymer surface, thus reducing the acidic degradation of the polymer. At the same time, the addition of bioactive ceramic fillers reduces the inflammatory reactions generated by polymer biodegradation [71]. In fact, the basic degradation of CPs or BGs could buffer the acidic by-products of polymers, thus avoiding the formation of an unsafe environment for cells, due to very low pH values. With composites, it seems possible to design scaffolds having ideal degradation and resorption kinetics: this means allowing cells to proliferate and secrete their own ECM, while the scaffolds gradually vanish, leaving space for new cell and tissue growth. The physical support provided by the three-dimensional (3D) scaffold should be maintained until the engineered tissue has sufficient mechanical integrity to support itself.

15.5.2 Why nanocomposites for bone-tissue regeneration?

Nanomaterials are often reported to possess superior properties over their microscale counterpart. Moreover, natural bone is a typical example of a nanocomposite material (see Section 15.2). Therefore, the design of a bone graft in the form of nanocomposite is perceived beneficial over monolithic and microcomposite materials. The main advantages presented by ceramic–polymer nanocomposites for regenerative medicine, as compared to conventional ones, are listed below:

- *Increased mechanical properties.* The mechanical properties of particulate–polymer composites depend strongly on the particle size, particle–matrix interface adhesion and particle loading. In particular, the particle size has a key effect on these mechanical properties. For instance, it was proven that replacing microscale silica by its nanoscale counterpart allows increasing both Young's modulus and yield strength [89]. The tensile strength also increases by decreasing the ceramic particle size [90]: smaller particles have a higher total surface area for a given particle loading. This indicates that the strength increases with increasing surface area of the filled particles through a more efficient stress transfer mechanism [90]. In some cases, the reinforcing nanoparticles may have an irregular (platy or acicular) shape. For instance, wet-synthesized HA nanoparticles typically have a needle-like morphology, with elongated primary particles of about 10 to 20 nm width and 50 to 200 nm length [29]. Such irregular shape is often preferred to the spherical one, because it allows a more effective interlock with the polymer during high-temperature composite processing and thus stronger polymer–filler interfaces. On the other hand, spherical shape and smooth surfaces do not provide such a locking mechanism, favouring particle debonding from the polymer matrix under tensile or flexural stress [88];
- *Increased biological functions.* Nanostructured composite materials exhibit unique surface properties (such as surface topography, surface chemistry, surface wettability and surface energy) due to their significantly increased surface area and surface roughness as compared to conventional materials [91]. Nanostructured materials, having cell-favourable surface properties, may promote greater amounts of specific protein interactions – thus stimulating in a most efficient way the new bone growth – than conventional materials [91–93]. It was also demonstrated that nanosized surface structures provide important cues to regulate cell orientation and morphology [92]. Furthermore, the incorporation of nano-CP particles promoted or directed the osteogenic differentiation of cells. Several studies reported that nanotopography can stimulate MSC differentiation, even in absence of osteogenic supplements [92]. Webster et al. [93,94] showed that nanocrystalline HA promotes osteoblast cell adhesion, differentiation, proliferation, osteointegration and deposition of calcium containing minerals on its surface better than microcrystalline HA, thus enhancing the formation of new bone tissue within a shorter period. Kikuchi et al. [95] demonstrated a greater osteoconduction in nanoHA–collagen nanocomposites as compared to conventional bone graft. The benefit of nanostructured ceramic particles was also demonstrated by in vivo investigations: nanocrystalline HA accelerated new bone formation on tantalum scaffolds (implanted in rats) when used as an osteoconductive coating if compared to uncoated or conventional micron-size HA-coated tantalum [91]. Fig. 15.3 reproduces a schematic illustration comparing the bone-growth mechanism on the surface of nanostructured and conventional materials [91]. The bioactive surfaces of nanomaterials mimic those of natural bones: they promote greater amounts of protein adsorption and efficiently stimulate more new bone formation than conventional materials.

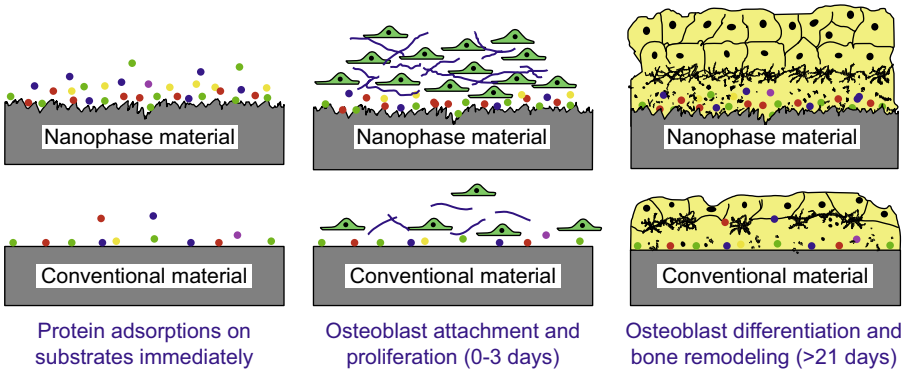

Figure 15.3 Schematic illustration of the mechanism by which nanomaterials may be superior to conventional materials for bone regeneration.
Reprinted from L. Zhang, T.J. Webster, Nanotechnology and nanomaterials: promises for improved tissue regeneration, Nano Today. 4 (2008) 66–80, with permission.

15.5.3 Processing of nanocomposites for bone-tissue regeneration

Ceramic–polymer nanocomposites are generally processed through three different methods: (1) conventional mixing; (2) self-assembly approach and (3) tissue-engineering approach.

- *Conventional mixing method* consists in blending a heterogeneous mixture of polymeric and ceramic components, leading to composites with tailor-made properties. Although the direct mixing of nanoscale components is feasible, controlling their size and structure is quite difficult. Particularly, controlling the homogeneity and uniformity of the second phases is a complex task. Due to their high surface area, nanoparticles have an intrinsic tendency to agglomerate, making difficult to yield high filler content in the polymer matrix. Aggregates of nanoparticles in composites are responsible for local stress concentration, internal cracks and worse mechanical properties [88]. To break particle agglomerates or aggregates, specially designed processing equipment is often required. Such equipment produces shear forces able to overcome particle adhesion forces during composite melt-processing, thus reducing particle agglomerates and achieving a uniform distribution of primary particles within the polymer matrix [88]. A second issue concerns the formation of weak polymer–nanofiller interface bonding: owing to the lack of strong interfaces, nanocomposites often present poor mechanical properties. To increase the interfacial strength, the ceramic nanoparticles can be surface-grafted with the polymer and further blended. For instance, various methods have been tried to modify the surface of HA particles: silane coupling agents, poly acids, polyethylene glycol, isocyanate and dodecyl alcohol were tested [88]. This approach implies the reaction of the coupling agent with the surface hydroxyl groups of the HA particles, with the aim of improving the affinity of the particle surface to the polymer matrix. Type I collagen was also immobilized on the surface of HA by covalent bonding and physical adsorption.
- *Self-assembly approach.* This method involves the nucleation and growth of nano-HA crystallites on self-assembling collagen fibres. The method exploits the ability of the negatively charged carboxylate groups of collagen to bind the calcium ions of HA. The mineralization

process is initiated by the presence of $PO4^{3-}$ ions, provided by H_3PO_4 aqueous solution, dispersed in the slightly acidic collagen gel (1 wt%) and dropped into a basic suspension containing $Ca(OH)_2$, $MgCl_2$ and $Si(CH_3COO)_4$ in simulated body fluid kept at 37°C [96]. Basic pH conditions allow the formation of collagen fibrils, which act as templates for subsequent mineralization. Upon decrease of the pH value (<8), nearly amorphous HA forms on the fibrils, while they are assembling into fibres. As the pH approaches neutral values, two distinct processes compete, involving the same binding chemical groups on the fibre surface: the organization of collagen fibres into a 3D network and contemporary HA nucleation [97]. Furthermore, is it possible to customize the extent and morphology of the final hybrid composite porosity (usually ranging between 80% and 85%) by freeze-drying processes [97]. The self-assembly and growth processes lead to composites exhibiting pseudo-plastic behaviour, similar to bone tissue, and mechanical properties close to the values found for trabecular bone at the same porosity content [98].

- *Tissue-engineering approach.* Although nanocomposites show good performance in many bone defects, some of them fail to stimulate several complex biological functions, particularly osteogenesis. Because only living bone cells ultimately generate new bone tissue, a unique approach is to develop nanocomposites through tissue engineering that are cell-responsive upon implantation. The prime concept of tissue engineering is to isolate a small biopsy of specific cells from a patient, to allow them to culture on the scaffold, to transplant the cell-engineered scaffold into the defective site of the patient's body and to guide or direct new tissue formation into the scaffold, which should degradate over time. As already described in Section 15.3, some key factors have to be considered for the success of bone-tissue engineering. They are cells, scaffold and cell–matrix (scaffold) interaction. The scaffold, an artificial ECM, plays a pivotal role in accommodating the cells. These cells then undergo proliferation, migration, and differentiation, leading to the formation of a specific tissue while secreting the ECM that is required for tissue regeneration. Furthermore, scaffold surface modification, using protein adsorption or plasma treatment, is able to provide more cues to cell attachment and response [99,100]. The immobilization of these proteins should not only promote cell adhesion and proliferation, but also increase wettability of hydrophobic polymers. Immobilizing these growth factors on the scaffold surface might significantly shorten the bone-healing process and reduce patient recovery time. However, the incorporation of biomolecules does not allow extreme temperature ranges (>70°C) or extremely aggressive chemical conditions during processing, being challenging to the scaffold-fabrication process. Another related challenge is a deeper understanding of the local impact of growth factors on the cell and tissue systems, including long-term effects [27].

15.6 Ceramic–polymer nanocomposites for tissue regeneration: state of the art and possible applications

Currently, there is abundant literature on the use of nanocomposites systems comprising nanoscale ceramics and biodegradable polymers as bone substitutes. The purpose of this section is to focus specifically on the most advanced nanostructured materials and systems (ie, the last generation of scaffolds, according to the scheme of Fig. 15.2), developed for bone regeneration and healing functions. When possible, the role of

nanostructured ceramic fillers as compared to conventional micronic ones will here be highlighted.

15.6.1 Calcium phosphate–polymer nanocomposites

Natural or synthetic HA has been intensively used in pure ceramic scaffolds as well as in polymer–ceramic composite systems. In fact, due to calcium phosphate osteoconductive properties, HA, TCP and BCP can be used as a scaffold matrix for bone-tissue engineering. However, these ceramic phases do not possess osteoinductive ability and their biodegradability is relatively slow, particularly in the case of crystalline HA (see Section 15.4.1). To overcome these drawbacks, biodegradable polymers added with osteogenic potential cells are used to make new biocomposite materials. Some of the tissue-engineered CP–polymer nanocomposite scaffolds are briefly described in the following sections, showing that both natural and synthetic polymers can be used to this aim.

15.6.1.1 Nanocomposites based on natural polymers

HA–collagen nanocomposites have gained much recognition as bone grafts not only due to their composition and structural similarity with natural bone, but also because of their unique functional properties (such as large surface area) and superior mechanical strength than their single-phase constituents [1]. Collagen is the most abundant polymer in bone tissue. By incorporating collagen into composites, it provides more cell-recognition sites and accelerates biomaterial degradation rate, thus allowing fast replacement by new bone [101]. Type I collagen–nano-HA composites are very efficient in inducing rapid mineralization by cells, even in the absence of osteogenic supplement in culture medium [101], highlighting their pivotal role in bone reconstructive or regenerative surgery. Commercial products based on CPs–natural polymer materials are already available on the market. Their composition and recommended use are displayed in Table 15.6 [11], underlying the widespread use of HA–collagen nanocomposites in osseous and maxillofacial reconstructive surgery.

Du et al. [101] developed a *HA–collagen* nanocomposite that mimics the natural bone both in composition and microstructure. The nanocomposite was obtained by aqueous precipitation of HA on type I collagen sheets, commercially sold as haemostatic sponge (porous matrix consisting of interconnected collagenous fibrils and membranes). The composite sheets were pre-soaked with culture medium (bone fragment explants), coiled and incubated for up to 21 days. This system clearly showed osteoinductive activity. The interconnecting porous structure of the composite provided a large surface area for cell attachment and sufficient space for nutrient transportation. Spindle-shaped cells migrating out of bone fragments continuously proliferated and migrated throughout the network of the coil. Cells within the composite eventually acquired a tri-dimensional polygonal shape and new bone matrix was synthesized at the interface of bone fragments and the composite.

Tampieri et al. [98,102] developed *HA–collagen*-based osteochondral scaffolds, organized in different integrated layers. This scaffold well mimics both articular

Table 15.6 Commercially available natural polymer–ceramic composites

Product	Polymer	Ceramic	Recommended use
Collagraft® (*Zimmer/NeuColl*)	Type I (bovine) collagen	HA, TCP	Acute long bone fractures and traumatic osseous defects
Collapat II® (*BioMet Inc.*)	Type I (calf skin) collagen	HA	Aseptic enclosed metaphyseal bone defects
FormaGraft® (*Maxigen Biotech Inc.*)	Type I collagen	HA, TCP	Bone-void filler
Integra Mozaik™ (*Integra OrthoBiologics*)	Type I collagen (20%)	TCP (80%)	Bone-void filler
Vitoss® or Vitoss® bioactive (*Orthovita*)	Collagen (20%)	β-TCP (80%) or β-TCP (70%)–BG (10%)	Bone-void filler, spinal and trauma surgery
Mastergraft® matrix (*Medtronic*)	Type I (bovine) collagen	BCP	Bone-void filler
CopiOs® (*Zimmer*)	Type I (bovine) collagen	CP, BCP	Bone-void filler
Biostite® (*Vebas*)	Type I (equinine) collagen, chondroitin-6-sulphate	HA	Filling of peridontal defects, pre-prosthetic osseous reconstruction, maxillofacial reconstructive surgery
Bio-Oss Collagen® (*Geistlich Biomaterials*)	(Porcine) collagen (10%)	HA	Filling of periodontal defects, alveolar ridge reconstruction
TricOs T® (*Baxter*)	Fibrin	BCP	Bone-void filler
CycLos® (*Mathys Orthopaedics Ltd.*)	Sodium hyaluronate	β-TCP	Bone-void filler
Cerasorb® (*Curasan Regenerative medicine*)	Collagen	β-TCP	Filling, bridging, reconstruction and bone fusion
Healos® (*Depuy Spine*)	Type I collagen	Nano-HA coating	Bone-void filler, spinal surgery
RegenOss® (*JRI Orthopaedics*)	Type I collagen fibres	Mg-rich, nano-HA	Long bone fractures, revision hip arthroplasty to fill acetabular defects and spinal fusion
NanOss® bioactive 3D (*Pioneer surgical*)	Collagen	Nano-HA	Bone-void filler

Reprinted from R.Y. Basha, S.T.S. Kumar, M. Doble, Design of biocomposite materials for bone tissue regeneration. Mater. Sci. Eng. C, vol. 57, pp. 452–463 (in press) http://dx.doi.org/10.1016/j.msec.2015.07.016, with permission.

cartilage and subchondral bone and can differentially support formation of such tissues. The graded scaffold, characterized by both morphological and mineralization gradients, was made by three different layers: a lower layer, composed by mineralized collagen (HA–collagen: 70/30 wt%) mimicking the subchondral bone; an intermediate layer, similar to the lower one but with a lower content of mineral phase (HA–collagen: 40/60 wt%) and resembling the tidemark; an upper layer, made by hyaluronic acid-charged collagen, mimicking the cartilaginous region. The layers were stacked and freeze-dried to obtain an integrated monolithic composite. In Fig. 15.4, an environmental scanning electron microscope (ESEM) image of the graded composite is displayed [102]. The rationale to fabricate a tri-layered scaffold instead of a bilayer one is based on the consideration that gradual changes in the mechanical features of the layers could reduce the mismatch of properties (ie, different stiffness of the differently mineralized fibres) at the interface and thus increase the composite stability. The different layers allow to induce, selectively, bone or cartilage tissues in-growth. In fact, culture of the graded material for 2 weeks after loading with articular chondrocytes yielded cartilaginous tissue formation only in the upper layer, because in the subchondral lower-bone layer only a fibrous tissue was developed. This demonstrated that the artificial cartilaginous layer of the composite scaffold was permissive to human articular chondrocyte differentiation and cartilaginous matrix deposition. On the other hand, ectopic implantation in nude mice of the graded

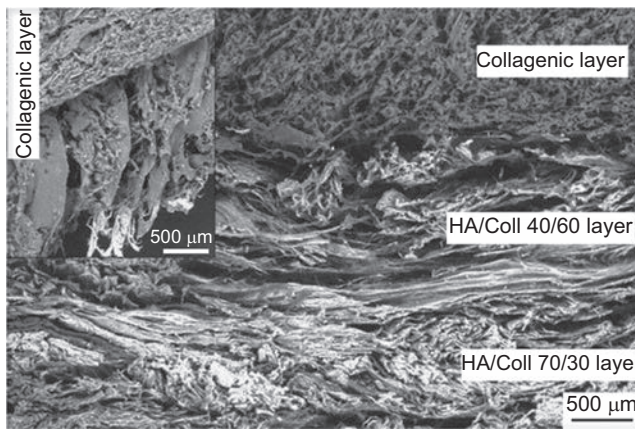

Figure 15.4 ESEM micrograph of graded HA–collagen nanocomposite scaffold for osteochondral regeneration. Three different layers are distinguishable due to the different content of mineral phase: the upper layer (cartilaginous, collagenic only), the intermediate layer (made by a 40 wt% HA–60 wt% collagen nanocomposite) and the lower-bone layer (made by 70 wt% HA–30 wt% collagen nanocomposite). The inset shows a columnar-like structure, due to the propagation of planar ice front during the freeze-dry process used to consolidate the graded material.
Reprinted from A. Tampieri, M. Sandri, E. Landi, D. Pressato, S. Francioli, Q. Quarto, I. Martin, Design of graded biomimetic osteochondral composite scaffolds, Biomaterials, 29 (2008) 3539–3546, with permission.

scaffold, after loading with bone marrow stromal cells, resulted in bone formation only in the lower mineralized layer, but not in the cartilaginous region.

Itoh et al. [103] prepared *HA–type I collagen* nanocomposite, were the nano-HA crystals were aligned along the collagen molecules. The authors investigated the biocompatibility, the osteoconductive activity and efficacy of the scaffold as a carrier of recombinant human bone morphogenetic proteins (rhBMPs). After immersion of the composite material in rhBMP-2 solution at different concentrations (0, 200, 400 μg/mL), samples were grafted in radii and ulnae in beagle dogs. As a control, three unfilled holes were left in one radius and ulna. Results support the idea that HA–collagen composite has a high osteoconductive activity and is able to induce bone-remodelling units. When the implants were grafted at weight-bearing sites, the highest rhBMP-2 concentration (400 μg/mL) was useful to shorten the time necessary for bone union.

Li et al. [104] developed a bioactive scaffold based on *nano-HA–collagen–PLLA* composite, added with a synthetic BMP-2-related peptide, designed as P24 and corresponding to residues of the knuckle epitope of BMP-2. A 5 mm diameter cranial bone defect was created in the calvariae of 30 rats and randomly implanted with three groups of composites: group A (nano-HA–collagen–PLLA composite), group B (P24–nano-HA–collagen–PLLA composite) and group C (rhBMP-2–nano-HA–collagen–PLLA composite). The P24–nano-HA–collagen–PLLA implants significantly stimulated bone growth, similarly to the rhBMP-2–nano-HA–collagen–PLLA ones, thereby confirming the enhanced bone-healing rate of these compounds compared with the unseeded nano-HA–collagen–PLLA scaffold material.

HA–chitosan scaffolds were developed as well [105]. High- and medium-molecular-weight (MW) chitosan scaffolds with 0.5, 1 and 2 wt% of nano-HA were fabricated by freezing and lyophilization. The nanocomposites were characterized by a highly porous structure and the pore size (~50–120 μm) was in a similar range for the scaffolds with different content of nano-HA. The addition of nano-HA to chitosan improved cell attachment, proliferation and spreading if compared to the reference neat polymer. In addition, after 28 days in physiological condition, nanocomposites showed about 10% lower degree of degradation in comparison to pure chitosan scaffold.

Zhao et al. [106] fabricated two types of biomimetic composite materials, *chitosan–gelatin* and *HA–chitosan–gelatin*, with the aim of investigating the effect of HA on MSC adhesion and 3D-construct development. The authors demonstrated enhanced protein and calcium ion adsorption properties for the HA-filled polymer, which improved initial cell adhesion and long-term growth, favouring osteogenic differentiation upon induction. A series of *HA–alginate* composite scaffolds was prepared by phase separation [107]. HA was incorporated into the alginate gel solution, at different alginate/HA weight ratios: 100/0, 75/25 and 50/50. The addition of HA positively affected the mechanical properties, as the compressive strength increased by increasing the HA content. In addition, it was possible to tailor the scaffold dissolution rate, by controlling the type and concentration of a cross-linking agent. Rat osteosarcoma and osteoblastic cells (UMR106) were cultured for 9 days on pure alginate and composite scaffolds. Both 75/25 and 50/50 scaffolds displayed

better cell attachment than the pure polymer scaffold, probably due to the friendly environment provided by HA for the cell attachments.

Sadat-Shojai et al. [108] prepared *HA–gelatin* hybrid hydrogels. Different cell types were encapsulated in the resulting composites, with the aim of preparing cell-laden constructs. According to the results, HA significantly improved the stiffness of gelatin hydrogels, while they maintained their structural integrity and swelling ratio. In addition, although the bare hydrogel (control) was completely inert in terms of bioactivity, incubation in simulated body fluid induced a homogeneous, 3D mineralization throughout the nanocomposites. Finally, encapsulated cells readily elongated, proliferated and formed a 3D interconnected network with neighbouring cells in the nanocomposite, suggesting a potential use of the developed composite for 3D cellular growth.

Yang et al. [109] prepared a biodegradable and biocompatible *β-TCP–gelatin* nanocomposite, in which the natural gelatin was cross-linked with small amount of glutaraldehyde. The gelatin molecules, as well as calcium and phosphorus ions, were gradually released from the composite, stimulating the proliferation and differentiation of osteoblasts. When BMPs were incorporated within the structure, the scaffold showed osteoconductivity as well as osteoinductivity properties. After 3 weeks, samples with and without BMP-4 showed similar alkaline phosphate activity; however, by the fourth week, it significantly increased in the case of BMP-added composite. In addition, greater numbers of attached cells and richer matrix deposits were found in the BMP-seeded samples. These findings suggest the possible use of this material as bone-substitute and bone-defect repair material.

Huang et al. [110] developed osteoinductive *nano-HA–silk* composite scaffolds, by adding HA–silk core–shell nanoparticles to a silk matrix. The HA–silk nanoparticles were directly dispersed in silk solution to form a uniform silk–HA blend, which gave rise to porous scaffolds after a freeze-drying process. HA nanoparticles (at varying contents up to 40%) were uniformly distributed in the silk matrix, improving the scaffold compressive modulus. Rat bone MSCs (rBMSCs) were cultured in these scaffolds. Increasing contents of HA–silk core–shell nanoparticles in the scaffolds improved the growth and osteogenic capability of rBMSCs in the absence of osteogenic growth factors and significantly increased the calcium and type I collagen deposition. In addition, compared to silk–HA composite scaffolds containing HA aggregates, the scaffolds loaded with HA–silk nanoparticles showed remarkably higher stiffness and better osteogenic property at the same HA content, implying a preferable microenvironment for rBMSCs.

15.6.1.2 Nanocomposites based on synthetic polymers

Xue et al. [111] developed a three-dimensional *nano-HA–PLGA* scaffold by a thermally induced phase separation technique, to investigate its potential application in cartilage tissue-engineering. A neat PLGA scaffold was used as a control. MSCs were seeded in both scaffolds. After 12-days culture, it was shown that the viability and proliferation of MSCs in PLGA–HA scaffolds were significantly superior to neat PLGA during in vitro culture. Through in vivo study, the efficacy of this scaffold combining

with MSCs for repairing articular osteochondral defects was evaluated in a rat model. Osteochondral defects in rats knees were left untreated, or treated with PLGA–HA–MSC composites or with PLGA–MSC composites. Twelve weeks after operation, histological examination revealed that the defects in the PLGA–HA–MSC-treated group were filled with smooth and hyaline-like cartilage, showing that this nanocomposite allows a satisfying osteochondral repair.

Li et al. [112] compared the role of surface or bulk HA particles on the osteoinduction ability of *nano-HA–PLGA* nanocomposite scaffolds. MSCs were seeded on HA-coated PLGA scaffolds as well as on a PLGA-containing HA scaffold, which were then cultured in a medium-containing *Escherichia coli*-derived recombinant human BMP-2 (ErhBMP-2). ErhBMP-2 induced new bone formation in rat calvarial defects, which was enhanced in HA-coated PLGA scaffold than in the HA-containing one, owing to the largely exposed HA particles on the pore walls of the coated scaffolds. Therefore, the surface-coated scaffold renders a more favourable niche for osteoblastic differentiation of BMSCs in ErhBMP-2-containing medium and an effective carrier for ErhBMP-2 for bone regeneration.

Cheng et al. [113,114] developed composite scaffolds made of *TCP–PLGA* by a low-temperature rapid prototyping technique, as shown in Fig. 15.5. The scaffold incorporated either endogenous bone morphogenetic protein-2 (BMP-2)

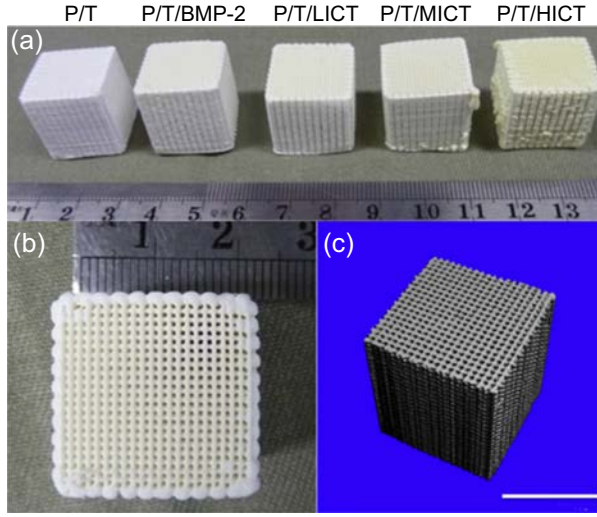

Figure 15.5 Macroscopic images of the fabricated PLGA–TCP composite scaffolds incorporating ICT and/or BMP-2.
Reprinted from S.-H. Chen, X.-L. Wang, X.-H. Xie, L.-Z. Zheng, D. Yao, D.P. Wang, et al., Comparative study on osteogenic potential of a composite scaffold incorporating either endogenous bone morphogenetic protein-2 or exogenous phytomolecule icaritin: an in vitro efficacy study. Acta Biomater 8, (2012) 3128–3137, with permission. P/T = PLGA–TCP; P/T/BMP-2 = PLGA–TCP–BMP-2; P/T/LICT = PLGA–TCP–Low ICT concentration; P/T/MICT = PLGA–TCP–Medium ICT concentration; P/T/HICT = PLGA–TCP–High ICT concentration.

(PLGA–TCP–BMP-2) or phytomolecule icaritin (ICT) (PLGA–TCP–ICT), ie, a novel osteogenic exogenous growth factor. ICT was used at three different dosages: low (8 mg), medium (32 mg) and high (80 mg) content per 10 mg of TCP–PLGA. The concentration of BMP-2 was 8 mg per 10 g of PLGA–TCP. The unseeded TCP–PLGA scaffold was used as the control group. To evaluate the in vivo osteogenic and angiogenic potentials of these bioactive scaffolds with slow release of osteogenic ICT, the authors established a 12 mm ulnar bone defect model in rabbits. Results at weeks 2, 4 and 8 post-surgery showed more newly formed bone within bone defects implanted with PLGA–TCP–ICT scaffolds as compared to the control. Histological results at weeks 4 and 8 also demonstrated more newly mineralized bone in PLGA–TCP–ICT groups, with correspondingly more new vessel in-growth. In both cases, the ICT medium content provided the better results, validating this innovative bioactive scaffold as a ready product for clinical applications. On the other hand, PLGA–TCP–BMP-2 did not show osteogenic potential, owing to loss of the original bioactivity of BMP-2 during its incorporation and fabrication procedure.

Ignjatovic et al. [115] prepared hybrid *CP–PLGA* micro- and nanoparticulates, with the aim of investigating the role of CP size on the composite biological properties. To do so, particulate material having two different particle sizes were synthesized: the former with an average particle diameter between 150 and 250 μm (micron-sized particles, MPs), the latter with an average particle diameter smaller than 50 nm (nanoparticles, NPs). In the form of injectable paste, both composites were used, for reconstructing defects in osteoporotic alveolar bones. Namely, changes in reparatory functions of tissues affected by osteoporosis were examined in mice in vivo, using these two kinds of composite materials with and without autologous plasma. The best results in the regeneration and recuperation of alveolar bone were achieved after the implantation of CP–PLGA NPs mixed with autologous plasma. In fact, the presence of growth factors and chemokines, which attract cells with active role in angiogenesis and transport of osteoprogenitor cells, provide conditions for enhanced cell proliferation, differentiation and new bone formation. The use of CP–PLGA NPs induced a more pronounced osteogenesis in rats as compared to the MPs system. It was imputed to the small size of CP particles, which enables better adhesion of osteoprogenitor cells and, together with growth factors, induces vigorous cell proliferation, differentiation and osteogenesis. This work shows that CP–PLGA particulates can be successfully used for the preparation of injectable pastes for the reconstruction of small-scale bone damages.

Liao et al. [116] developed a *nano-HA–collagen–PLA* composite scaffold, having both composition and hierarchical structure close to those of natural bone. Cell culture and animal model tests showed that the composite material was bioactive. The osteoblasts were separated from the neonatal rat calvaria. Osteoblasts adhered, spread, and proliferated throughout the pores of the scaffold material within a week. A 15-mm segmental defect model in the radius of the rabbit was used to evaluate the bone-remodelling ability of the composite. Combined with 0.5 mg rhBMP-2, the material block was implanted into the defect. The segmental defect was integrated 12 weeks after surgery, and the implanted composite was partially substituted by new bone tissue. This composite scaffold is promising for the clinical repair of large bony defects according to the principles of bone-tissue engineering.

Causa et al. [117] developed three *HA–PCL* composites with different volume ratio of HA (13, 20, and 32%). Mechanical properties and structure were analysed, along with biocompatibility and osteoconductivity. The addition of HA particles led to a significant improvement in mechanical performance of the scaffold, in particular when added at 20% and 32%. In these composites, the elastic modulus and tensile strength well matched the range of human cortical bone. 3D samples were seeded with human osteoblastic cell line (SaOS-2) cells and osteoblasts from human trabecular bone (hOB) for 1 to 4 weeks. Cell viability, adhesion, proliferation, morphology and ALP release were analysed on pure PCL as well as on the HA-loaded polymer. Results showed an improvement of osteoconduction in the filled composite as compared to neat PCL, suggesting that this system is a potential candidate for bone substitution, due to its good balance between structural–mechanical properties and biological activities.

To increase the interaction between the polymer and ceramic phases, PLC-grafted nano-HA powders were used to prepare *HA–PCL* composites [118]. PCL-grafted HA nanoparticles showed excellent colloidal stability in PCL solution, which ensured a nano-level distribution of HA in the nanocomposites. In vitro biological evaluation showed that the presence of PCL-grafted HA enhanced the nanocomposite biocompatibility as compared to unmodified HA. PLC-grafted HA provided, in fact, a more favourable environment and better surfaces for protein adsorption and cell adhesion and proliferation. The higher the amount of grafted PCL, the higher the proliferation activity of the cells.

HA–unsaturated PPF nanocomposites were developed by Jayabalan et al. [119]. The biodegradable composites were fabricated by investigating three types of HA particles: (1) calcined and (2) uncalcined rod-like nanometric HA particles (length ~50–100 nm and width ~20–40 nm) and (3) spherical, commercial HA (<200 nm). Calcined HA nanoparticles enabled very good cross-linking in the polymer molecule, with a high-cross-link density in the nanocomposite, due to the lower basicity of the calcined powder, together with its rod-like morphology. This enabled improved interfacial bonding and mechanical interlocking with the polymer matrix. As a result, this composite showed improved mechanical (Young compressive modulus and compressive strength) and biological (osteointegration) performance as compared to materials containing uncalcined or spherical HA particles.

15.6.2 Bioactive glass–polymer nanocomposites

BG (such as 45S5) has been shown to offer further advances as compared to HA or, more in general, to calcium phosphates. For instance, it was reported that granules of 45S5 BG, implanted in rabbit femurs, promoted bone proliferation more rapidly than synthetic HA [33]. Furthermore, 45S5 glass is considered to be not only osteoconductive (like HA), but also osteoinductive because it supports new bone growth along the bone–implant interface as well as within the implant away from the bone–implant interface [44].

For this reason, BG-filled polymers are seen as attractive solutions for the regeneration of bone tissues, including complex tissue structure defects, such as at soft–hard tissue interfaces. Again, both natural and synthetic polymers can be used to fabricate advanced scaffolds [120], as described in the following.

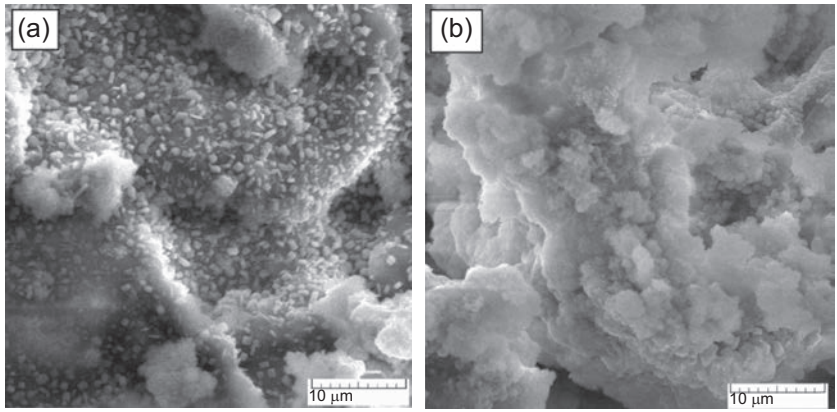

Figure 15.6 High magnification SEM micrographs of *BG–gelatin* nanocomposite scaffolds after (a) 1 day and (b) 14 days immersion in SBF.
Reprinted from M. Mozafari, M. Rabiee, M. Azami, S. Maleknia, Biomimetic formation of apatite on the surface of porous gelatin/bioactive glass nanocomposite scaffolds, Appl. Surf. Sci. 257 (2010) 1740–1749. with permission. (a) One day after immersion in SBF, small particles of apatite were created and started to grow up on the surface of scaffold samples. Furthermore, (b) after 14 days immersion in SBF, the apatite particles fully grew up and particles with plate-like structure were oriented perpendicularly to the surfaces of scaffolds and distributed over the entire surface.

Mozafari et al. [121] developed *BG–gelatin* nanocomposite scaffolds, with BG nanoparticles composition included in the ternary SiO_2–CaO–P_2O_5 system. After soaking the nanocomposites in SBF for different times (1, 3, 7, 14 days), their bioactive properties were investigated. The scaffolds showed significant enhancement in bioactivity within a few days of immersion in SBF solution, showing apatite formation at the surface of the nanocomposite samples, as shown in Fig. 15.6. In vitro experiments with osteoblast cells using human osteoblast-like cells (SaOS-2 cell line) indicated a proper penetration of the cells into the scaffold pores. The ability of the scaffolds to support cell growth was also demonstrated by the continuous increase in cell aggregation on the bioactive scaffolds while increasing the incubation time.

Peter et al. synthesized *BG–α-chitin* [122] as well as *BG–chitosan* [123] nanocomposites, in which BG–ceramic nanoparticles were synthesized by the sol–gel method. The composite porous scaffolds were prepared by using the lyophilization technique. In Fig. 15.7, SEM images of the BG–chitosan nanocomposite scaffold is depicted, showing pores in the range 150–300 μm and BG nanoparticles embedded in the polymer matrix [123]. The composite scaffolds demonstrated adequate swelling and degradation behaviour. In vitro studies, carried out by immersion in SBF solution and incubation at 37°C for 7 days, showed the deposition of apatite on the surface of the composite scaffolds, indicating the bioactive nature of the composite scaffolds. The investigation of the in vitro behaviour considering osteoblast-like cells (MG-63) indicated that cells became attached to the pore walls of the scaffolds and showed initial signs of spreading [122,123].

Verrier et al. [124] developed *BG–PDLLA* porous foams and investigated the effect of increased content of 45S5 Bioglass® (0–40 wt%) on the behaviour of MG-63

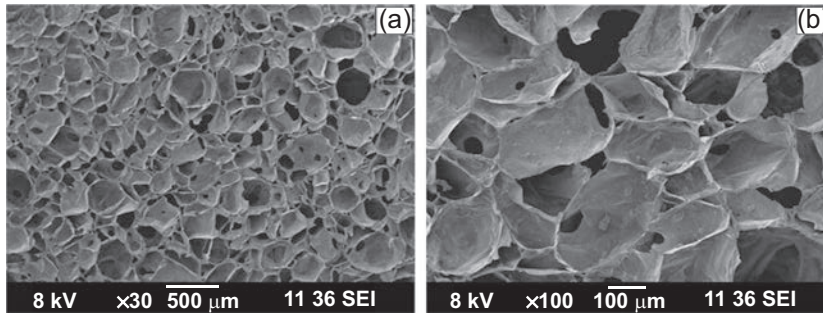

Figure 15.7 (a) SEM images, at different magnifications, of BG–chitosan nanocomposite scaffold prepared by freeze-drying technique. (b) The same composite after 7 days of biomineralization process.
Reprinted from M. Peter, N.S. Binulal, S. Soumya, S.V. Nair, T. Furuike, H. Tamura, et al., Nanocomposite scaffolds of bioactive glass ceramic nanoparticles disseminated chitosan matrix for tissue engineering applications, Carbohydr. Polym., 79 (2010) 284–289, with permission.

(human osteosarcoma cell line) and A549 cells (human lung carcinoma cell line). Two hours after cell seeding, a progressive increase of cell adhesion was observed – for both cell types – by increasing the Bioglass® content. Cell-proliferation studies performed over a period of 4 weeks showed a better aptitude of the A549 cells to proliferate on PDLLA foams containing 5 wt% Bioglass® as compared to that with 40 wt% Bioglass®. A lower proliferation rate was obtained for cells on pure PDLLA. The results confirmed for the first time the possibility for human lung epithelial type II cells to adhere and proliferate on PDLLA–Bioglass® porous scaffolds. In addition, this work provided the correct concentration of Bioglass® particles to be added to the PDLLA matrix to display such biological function.

Gerhardt et al. [125] investigated the angiogenic properties of micron-sized (μ-BG) and nano-sized (n-BG) BG particles in *BG–PDLLA* composites. Both glasses have the classical 45S5 Bioglass® composition. The μ-BG particles had an irregular shape and average particle size of 4.3 μm. The nanoparticle has a spherical morphology and diameter in the range 35–40 nm. The results of this study demonstrated the pro-angiogenic properties of μ-BG and n-BG-filled composites, both by in vitro (two-dimensional films) and in vivo (porous 3D scaffolds) investigations. On composite films containing 20 wt% μ-BG or nano-bioglass (n-BG), fibroblasts produced five times higher vascular endothelial growth factor (VEGF) than on pure PDLLA films. After 8 weeks of implantation, BG-containing scaffolds were well infiltrated with newly formed tissue and demonstrated high vascularization, with slightly higher values for the n-BG-filled composite.

The positive role of nanoscale BG particles as compared to micronic ones was also evidenced by Misra et al. [126,127]. Poly(3hydroxybutyrate), referred to as P(3HB), was added with both nanometric (~30 nm, n-BG) and micrometric (<5 μm, μ-BG) 45S5 glass particles, to produce nano- and micro-*BG–P(3HB)* composite films. Both fillers were added at three different concentrations: 10, 20 and 30 wt%.

The addition of n-BG particles had a significant reinforcing effect, as the incorporation of 10, 20 and 30 wt% of n-BG particles increased the elastic modulus of 57, 14 and 20%, respectively, as compared to the neat, unfilled polymer. On the opposite, the addition of μ-BG particles induced a decrease of elastic moduli, probably due to the poor mixing of μ-BG particles with the polymer matrix, leading to large agglomerates and, consequently, to residual porosities in the films. The addition of n-BG particles also induced the formation of a nanostructured topography on the surface of the composites, which was absent in the micronic material. The nanotopography features improved the in vitro bioactivity (HA formation), protein adsorption, wettability and led to a higher water uptake upon immersion in SBF. Furthermore, a preliminary cell proliferation study demonstrated the good cytocompatibility of the n-BG–P(3HB) composite systems [126]. In fact, cell proliferation, cell attachment, alkaline phosphatase activity and osteocalcin production, investigated by using human MG-63 osteoblast-like cells in osteogenic and non-osteogenic medium, evidenced the superiority of the n-BG–P(3HB) composite as compared to the unfilled polymer [127].

Yao et al. [128] employed 45S5 Bioglass® to develop *BG–PLGA* porous scaffolds by the following procedure. First, well-shaped microspheres were prepared by adding BG powders (30 wt%) to a PLGA solution. Then, porous scaffolds were obtained by pouring those composite microspheres (with size in the range 350–500 mm) into a Teflon mould, heated at 65°C for 1 h. The authors investigated the ability of this scaffold to promote osteogenesis of MSCs. It was shown that the porous scaffold supported MSC proliferation and promoted MSC differentiation into cells expressing the osteoblast phenotype. In fact, MSCs expressed a significantly higher level of alkaline phosphatase on the composite if compared to the neat polymer. In the presence of an exogenous inducer DEX, the alkaline phosphatase activity of PLGA–30%BG was approximately 10 times higher than on pure PLGA. These results demonstrate the potential of MSC seeding on PLGA–BG scaffold as a promising device for bone-tissue engineering, with osteoinduction signals triggered by the BG.

Lu et al. [129] showed that for *BG–PLGA* films (containing 0, 10, 25 and 50 wt% of BG), the growth, mineralization and differentiation of human osteoblast-like SaOS-2 cells, as well as the kinetics of CP-layer formation and the resulting CP chemistry were dependent on BG content. The 10 and 25 wt% BG composite supported greater osteoblast growth and differentiation compared to the 50 wt% BG composites. This suggests a threshold in the BG content that is optimal for osteoblast growth and that the interactions between PLGA and BG may modulate the kinetics of CP formation and the overall cellular response. The same *BG–PLGA system*, containing 25 wt% of BG, was used to develop a 3D porous BG [130]. The addition of BG granules to the PLGA matrix resulted in a structure with a nearly twofold increase in compressive modulus than PLGA alone. Moreover, the BG–PLGA composite was found to be a bioactive material, as it formed surface calcium phosphate deposits in SBF and in the presence of cells (human osteoblast-like SaOS-2) and serum proteins. In addition to supporting the osteoblast adhesion, growth and differentiation in vitro, the composite supported higher levels of Type I collagen synthesis than tissue culture polystyrene control.

El-Fiqi et al. [131] developed electrospun fibrous scaffolds of *BG–PCL–gelatin,* prepared by incorporating mesoporous BG nanoparticles. Namely, BG particles were loaded with osteogenic drug DEX (loaded at 63%) to elicit additional therapeutic potential. The BG-added fibre scaffolds demonstrated excellent properties, including improved mechanical tensile strength, elasticity, and hydrophilicity compared to pure biopolymer matrix. Jo et al. [132] developed a *BG–PCL* nanocomposite using BG nanofibres and compared the properties of this material with those of a composite fabricated using microscale BG particles (20 wt%). The BG nanofibres were generated using sol–gel precursors via the electrospinning process, chopped into short fibres and then incorporated into the PCL organic matrix by dissolving them in a tetrahydrofuran solvent. In vitro cell tests, carried out using the MC3T3 cell line, demonstrated enhanced biocompatibility as well as higher bioactivity of the PCL–BG nanofibre composite compared with the particulate system. In addition, the results of in vivo animal experiments using Sprague–Dawley albino rats revealed the good bone regeneration capability of the PCL–BG nanofibre composite when implanted in a calvarial bone defect, suggesting a potential use of this composite as a bone-regenerative material.

15.7 Concluding remarks

Nanocomposites combined with osteoconductive, osteoinductive factors, and/or osteogenic cells have gained much interest as a new and versatile class of biomaterial suitable for next-generation biomimetic scaffolds. The experimental examples summarized in this chapter represent some of the developments of nanocomposites designed for bone-tissue regeneration. However, further substantial research efforts are required to address some major key challenges.

The first challenge relates to bone biology: bone growth and remodelling involve a number of growth factors, the recruitment of MSCs, the action of different mature cell types (osteoblasts, osteocytes and osteoclasts) as well other factors that need further studies. A deeper understanding of how the growth factors interact with each other and with cells, what are their effects, which intracellular pathways are triggered by them and how they can be activated or inactivated is needed. The capability of improving angiogenesis within the nanocomposite graft needs further effort, because cells will not survive without an adequate blood supply. At this moment, these aspects are probably the most challenging ones to develop an artificial tissue-engineered bone.

The second aspect that needs further improvement relates to materials engineering. A new generation of biodegradable polymer–ceramic nanocomposites is currently being designed and developed, but needs further advances. A key aspect is optimizing the ceramic filler content as well as its homogeneous distribution within the polymer matrix, thus more closely matching the strength and stiffness of natural bone. Stronger interfacial bonding between the two phases is needed, especially when applications in load-bearing regions are envisaged. Tuning the bioresorbability of the composite grafts and their biomechanical properties while forming new bone is a further challenge. Besides materials

science, the scaffold processing technology also needs further improvement, even if this aspect has not been specifically addressed in this work. New rapid prototyping techniques are very promising for tissue-engineering applications. However, the development of advanced manufacturing methods towards scaffolds with enhanced mechanical properties – without influencing the porosity and interconnectivity of the architecture– with tailored surface properties and chemistry, deserves further investigation.

List of abbreviations

BCP Biphasic calcium phosphate
BG Bioactive glass
BMP Bone morphogenic protein
rhBMP Recombinant human bone morphogenetic protein
ECM Extracellular matrix
HA Hydroxyapatite, $Ca_{10}(PO_4)_6(OH)_2$
HCA Hydroxy carbonate apatite
HDPE High-density polyethylene
CP Calcium phosphate
CS Calcium sulphate
MSC Mesenchymal stem cell
PLA Poly(lactic acid)
PLLA Poly(L-lactic acid)
PDLLA Poly(D,L-lactic acid)
PGA Poly(glycolic acid)
PLGA Poly(lactic acid-co-glycolic acid)
PCL Poly(3-caprolactone)
PHB Poly(hydroxyl butyrate)
PPF Poly(propylene fumarate)
SBF Simulated body fluid
TCP Tricalcium phosphate

References

[1] R. Murugan, S. Ramakrishna, Development of nanocomposites for bone grafting, Compos. Sci. Technol. 65 (2005) 2385–2406.
[2] S. Wu, X. Liu, K.W.K. Yeung, C. Liu, X. Yang, Biomimetic porous scaffolds for bone tissue engineering, Mater. Sci. Eng. R 80 (2014) 1–36.
[3] T.M. Keaveny, E.F. Morgan, O.C. Yeh, Bone mechanics, in: M. Kuts (Ed.), Standard Handbook of Biomedical Engineering and Design (Chapter 8), The McGraw-Hill Companies, Inc., 2003.
[4] V. Karageorgiou, D. Kaplan, Porosity of 3D biomaterial scaffolds and osteogenesis, Biomaterials 26 (2005) 5474–5491.
[5] F. Barrère, T.A. Mahmood, K. de Groot, C.A. van Blitterswijk, Advanced biomaterials for skeletal tissue regeneration: instructive and smart functions, Mater. Sci. Eng. R 59 (2008) 38–71.

[6] J.R. Porter, T.T. Ruckh, K.C. Popat, Bone tissue engineering: a review in bone biomimetics and drug delivery strategies, Am. Inst. Chem. Eng. (2009) 1539–1560, http://dx.doi.org/10.1002/btpr.246.
[7] K.S. Katti, C. Gu, D.R. Katti, Biomimetics: inspiration from the structural organization of biological systems, in: J.J. Maya, T. Sabu (Eds.), Natural Polymers: Composites (Chapter 2), RSC Publishing, 2012.
[8] A.J. Salgado, O.P. Coutinho, R.L. Reis, Bone tissue engineering: state of the art and future trends, Macromol. Biosci. 4 (2004) 743–765.
[9] E.J. Mackie, Osteoblasts: novel roles in orchestration of skeletal architecture, Int. J. Biochem. Cell Biol. 35 (2003) 1301–1305.
[10] A.M. Parfitt, The cellular basis of bone remodeling: the quantum concept reexamined in light of recent advances in the cell biology of bone, Calcif. Tissue Int. 36 (Suppl. 1) (1984) S37–S45.
[11] R.Y. Basha, S.T.S. Kumar, M. Doble, Design of biocomposite materials for bone tissue regeneration, Mater. Sci. Eng. C 57 (2015) 452–463.
[12] A. Ficai, E. Andronescu, G. Voicu, D. Ficai, Advances in collagen/hydroxyapatite composite materials, in: B. Attaf (Ed.), Advances in Composite Materials for Medicine and Nanotechnology, 2011.
[13] J. Kim, S. Bhattacharyya, P. Ducheyne, Bioactive ceramics and bioactive ceramic composite-based scaffolds, in: P. Ducheyne (Ed.), Comprehensive Biomaterials, Tissue and Organ Engineering, vol. 5, Elsevier, 2011, pp. 255–267.
[14] S. Bose, M. Roy, A. Bandyopadhyay, Recent advances in bone tissue engineering scaffolds, Trends Biotechnol. 30 (10) (2012) 546–554.
[15] L. Uebersax, H. Hagenmuller, S. Hofmann, et al., Effect of scaffold design on bone morphology in vitro, Tissue Eng. 12 (2006) 3417–3429.
[16] J.D. Bobyn, R.M. Pilliar, H.U. Cameron, G.C. Weatherly, The optimum pore size for fixation of porous surfaced metal implants by the ingrowth of bone, Clin. Orthop. Relat. Res. 150 (1980) 263–270.
[17] I. Armentano, M. Dottori, E. Fortunati, S. Mattioli, J.M. Kenny, Biodegradable polymer matrix nanocomposites for tissue engineering: a review, Polym. Degrad. Stab. 95 (2010) 2126–2146.
[18] M.M. Stevens, Biomaterials for bone tissue engineering, Mater. Today 11 (5) (2008) 18–25.
[19] F.R.A.J. Rose, R.O.C. Oreffo, Breakthroughs and views. Bone tissue engineering: Hope vs. Hype, Biochem. Biophys. Res. Commun. 292 (2002) 1–7.
[20] S. Kadiyala, R.G. Young, M.A. Thiede, S.P. Bruder, Culture expanded canine mesenchymal stem cells possess osteochondrogenic potential in vivo and in vitro, Cell Transplant. 6 (1997) 125–134.
[21] B.A. Ashton, T.D. Allen, C.R. Howlett, C.C. Eaglesom, A. Hattori, M. Owen, Formation of bone and cartilage by marrow stromal cells in diffusion chambers in vivo, Clin. Orthop. Relat. Res. 151 (1980) 294–307.
[22] R. Gundle, C.J. Joyner, J.T. Triffitt, Human bone tissue formation in diffusion chamber culture in vivo by bone derived cells and marrow stromal fibroblastic cells, Bone 16 (1995) 597–601.
[23] H. Ohgushi, V.M. Goldberg, A.I. Caplan, Heterotopic osteogenesis in porous ceramics induced by marrow cells, J. Orthop. Res. 7 (1989) 568–578.
[24] J.F. Connolly, Injectable bone marrow preparations to stimulate osteogenic repair, Clin. Orthop. Relat. Res. 313 (1995) 8–18.

[25] R. Quarto, M. Mastrogiacomo, R. Cancedda, S.M. Kutepov, V. Mukhachev, A. Lavroukov, E. Kon, M. Marcacci, Repair of large bone defects with the use of autologous bone marrow stromal cells, N. Engl. J. Med. 344 (2001) 385–386.
[26] R.Z. LeGeros, Properties of osteoconductive biomaterials: calcium phosphates, Clin. Orthop. Relat. Res. 395 (2002) 81–98.
[27] K. Rezwan, Q.Z. Chen, J.J. Blaker, A.R. Boccaccini, Biodegradable and bioactive porous polymer/inorganic composite scaffolds for bone tissue engineering, Biomaterials 27 (2006) 3413–3431.
[28] C.S. Adams, K. Mansfield, R.L. Perlot, I.M. Shapiro, Matrix regulation of skeletal cell apoptosis. Role of calcium and phosphate ions, J. Biol. Chem. 276 (2001) 20316.
[29] G. Lehmann, P. Palmero, I. Cacciotti, R. Pecci, L. Campagnolo, R. Bedini, G. Siracusa, A. Bianco, A. Camaioni, L. Montanaro, Design, production and biocompatibility of nanostructured porous HAp and Si-Hap ceramics as three-dimensional scaffolds for stem cell culture and differentiation, Ceram. Silik. 54 (2010) 90–96.
[30] G. Lehmann, I. Cacciotti, P. Palmero, L. Montanaro, A. Bianco, L. Campagnolo, A. Camaioni, Differentiation of osteoblast and osteoclast precursors on pure and silicon-substituted synthesized hydroxyapatites, Biomed. Mater. 7 (5) (2012):055001.
[31] J.R. Jones, Bioactive ceramics and glasses, in: A.R. Boccaccini, J.E. Gough (Eds.), Tissue Engineering Using Ceramics and Polymers, Woodhead Publishing Limited, Cambridge, England, 2007, pp. 57–58.
[32] J.C. Le Huec, D. Clement, B. Brouillaud, N. Barthe, B. Dupuy, B. Foliguet, B. Basse-Cathalinat, Evolution of the local calcium content around irradiated beta-tricalcium phosphate ceramic implants: in vivo study in the rabbit, Biomaterials 19 (1998) 733–738.
[33] H. Oonishi, S. Kushitani, H. Iwaki, Comparative bone formation in several kinds of bioceramic granules, in: J. Wilson, L.L. Hench, D. Greenspan (Eds.), Eighth International Symposium on Ceramics in Medicine, Elsevier Science Ltd, Tokyo, Japan, 1995, pp. 137–144.
[34] S.H. Kwon, Y.K. Jun, S.H. Hong, I.S. Lee, H.E. Kim, Y.Y. Won, Calcium phosphate bioceramics with various porosities and dissolution rates, J. Am. Ceram. Soc. 85 (2002) 3129–3131.
[35] E. Damien, K. Hing, S. Saeed, P.A. Revell, A preliminary study on the enhancement of the osteointegration of a novel synthetic hydroxyapatite scaffold in vivo, J. Biomed. Mater. Res. A 66 (2003) 241–246.
[36] Y. Kuboki, H. Takita, D. Kobayashi, E. Tsuruga, M. Inoue, M. Murata, et al., BMP-induced osteogenesis on the surface of hydroxyapatite with geometrically feasible and nonfeasible structures: topology of osteogenesis, J. Biomed. Mater. Res. 39 (1998) 190–199.
[37] C. Zhang, J. Wang, H. Feng, B. Lu, Z. Song, X. Zhang, Replacement of segmental bone defects using porous bioceramic cylinders: a biomechanical and X-ray diffraction study, J. Biomed. Mater. Res. 54 (2001) 407–411.
[38] L.L. Hench, R.J. Splinter, W.C. Allen, T.K. Greenlee, Bonding mechanisms at the interface of ceramic prosthetic materials, J. Biomed. Mater. Res. 2 (1971) 117–141.
[39] A. El-Ghannam, P. Ducheyne, I.M. Shapiro, Formation of surface reaction products on bioactive glass and their effects on the expression of the osteoblastic phenotype and the deposition of mineralized extracellular matrix, Biomaterials 18 (1997) 295–303.
[40] A.J. García, P. Ducheyne, D. Boettiger, Effect of surface reaction stage on fibronectin-mediated adhesion of osteoblast-like cells to bioactive glass, J. Biomed. Mater. Res. 40 (1998) 48–56.
[41] M. Ogino, F. Ohuchi, L.L. Hench, Compositional dependence of the formation of calcium–phosphate films on bioglass, J. Biomed. Mater. Res. 14 (1980) 55–64.

[42] J. Wilson, A. Yli-Urpo, R.P. Happonen, Bioactive glasses: clinical applications, in: L.L. Hench, J. Wilson (Eds.), An Introduction to Bioceramics, World Scientific Publishing Co. Pte. Ltd, London, UK, 1993, pp. 63–73.
[43] S.M. Best, A.E. Porter, E.S. Thian, J. Huang, Bioceramics: past, present and for the future, J. Eur. Ceram. Soc. 28 (2008) 1319–1327.
[44] L.L. Hench, J.K. West, Biological applications of bioactive glasses, Life Chem. Rep. 13 (1996) 187–241.
[45] J. Wilson, S.B. Low, Bioactive ceramics for periodontal treatment: comparative studies, J. Appl. Biomater. 3 (1992) 123–129.
[46] H. Oonishi, S. Kutrshitani, E. Yasukawa, H. Iwaki, L.L. Hench, J. Wilson, E. Tsuji, T. Sugihara, Particulate bioglass compared with hydroxyapatite as a bone graft substitute, J. Clin. Orthop. Relat. Res. 334 (1997) 316–325.
[47] H. Yuan, J.D. de Bruijn, X. Zhang, C.A. van Blitterswijk, K. de Groot, Bone induction by porous glass ceramic made from Bioglass (45S5), J. Biomed. Mater. Res. 58 (2001) 270–276.
[48] A.R. El-Ghannam, Advanced bioceramic composite for bone tissue engineering: design principles and structure–bioactivity relationship, J. Biomed. Mater. Res. A 69 (2004) 490–501.
[49] M.M. Pereira, A.E. Clark, L.L. Hench, Calcium phosphate formation on sol-gel-derived bioactive glasses in vitro, J. Biomed. Mater. Res. 28 (1994) 693–698.
[50] W. Cao, L.L. Hench, Bioactive materials, Ceram. Int. 22 (1996) 493–507.
[51] T. Kitsugi, T. Yumamuro, T. Nakamura, T. Kokubo, The bonding of glass ceramics to bone, Int. Orthop. 13 (1989) 199–206.
[52] T. Yamamuro, A/W glass-ceramic: clinical applications, in: L.L. Hench, J. Wilson (Eds.), An Introduction to Bioceramics, World Scientific Publishing Co. Pte. Ltd, London, UK, 1993, pp. 89–103.
[53] T. Kokubo, M. Shigematsu, Y. Nagashima, M. Tashiro, T. Nakamura, S. Higashi, Apatite and wollastonite containing glass-ceramics for prosthetic application, Bull. Inst. Chem. Res. 60 (1982) 260–268.
[54] T. Kokubo, Bioactive glass-ceramics: properties and applications, Biomaterials 12 (1991) 155–163.
[55] T. Kokubo, S. Ito, M. Shigematsu, S. Sakka, T. Yamamuro, Mechanical properties of a new type of apatite-containing glass-ceramic for prosthetic application, J. Mater. Sci. 20 (1985) 2001–2004.
[56] J.L. Ricci, H. Alexander, P. Nadkarni, M. Hawkins, J. Turner, S. Rosenblum, L. Brezenoff, D. Deleonardis, G. Pecora, Biological mechanisms of calcium sulfate replacement by bone, in: J.E. Davies (Ed.), Bone Engineering, Em Squared Inc., Toronto, Ontario, Canada, 2000.
[57] J.R. Parsons, J.L. Ricci, H. Alexander, P.K. Bajpai, Osteoconductive composite grouts for orthopedic use, Ann. N. Y. Acad. Sci. 523 (1988) 190–207.
[58] S.F. Rosenblum, S. Frenkel, J.L. Ricci, H. Alexander, Diffusion of fibroblast growth factor from a plaster of Paris carrier, J. Appl. Biomater. 4 (1993) 67–72.
[59] S.R. Frenkel, J. Simon, H. Alexander, M. Dennis, J.L. Ricci, Osseointegration on metallic implant surfaces: effects of microgeometry and growth factor treatment, J. Biomed. Mater. Res. Appl. Biomater. 63 (2002) 706–713.
[60] Z. Huan, J. Chang, Self-setting properties and in vitro bioactivity of calcium sulfate hemihydrate-tricalcium silicate composite bone cement, Acta Biomater. 3 (2007) 952–960.
[61] W. Liu, C. Wu, W. Liu, W. Zhai, J. Chang, The effect of plaster ($CaSO_4 \cdot 1/2H_2O$) on the compressive strength, self-setting property and in vitro bioactivity of silicate-based bone cement, J. Biomed. Mater. Res. B 101 (2013) 279–286.

[62] K.N. Lewis, M.V. Thomas, D.A. Puleo, Mechanical and degradation behavior of polymer-calcium sulfate composites, J. Mater. Sci. Mater. Med. 17 (2006) 531–537.
[63] S. Borhan, S. Hesaraki, S. Ahmadzadeh-Asl, Evaluation of colloidal silica suspension as efficient additive for improving physico chemical and in vitro biological properties of calcium sulfate-based nanocomposite bone cement, J. Mater. Sci. Mater. Med. 21 (2010) 3171–3181.
[64] W.R. Moore, S.E. Graves, G.I. Bain, Synthetic bone graft substitutes, ANZ J. Surg. 71 (2001) 354–361.
[65] R. Murugan, S. Ramakrishna, Nanostructured biomaterials, in: H.S. Nalwa (Ed.), Encyclopedia of Nanoscience and Nanotechnology, vol. 7, American Scientific Publishers, California, 2004, pp. 595–613.
[66] R. Murugan, S. Ramakrishna, in: H.S. Nalwa (Ed.), Handbook of Nanostructured Biomaterials and Their Applications in Nanobiotechnology, American Scientific Publishers, California, 2005, pp. 141–168.
[67] J. Black, G.W. Hastings, Handbook of Biomaterials Properties, Chapman & Hall, London, 1998.
[68] A.K. Srivastava, R. Pyare, Characterization of ZnO substituted 45S5 bioactive glasses and glass – ceramics, J. Mater. Sci. Res. 1 (2012) 207–220.
[69] J.L. Ricci, M.J. Weiner, S. Mamidwar, H. Alexander, Calcium sulfate, in: T. Kokubo (Ed.), Bioceramics and Their Clinical Applications, Woodhead Publishing Limited, Cambridge, England, 2008, pp. 302–325.
[70] L.B. Rocha, G. Goissis, M.A. Rossi, Biocompatibility of anionic collagen matrix as scaffold for bone healing, Biomaterials 23 (2002) 449–456.
[71] H.D. Kim, R.F. Valentini, Retention and activity of BMP-2 in hyaluronic acid-based scaffolds in vitro, J. Biomed. Mater. Res. 59 (2002) 573–584.
[72] L.S. Naira, C.T. Laurencin, Biodegradable polymers as biomaterials, Prog. Polym. Sci. 32 (2007) 762–798.
[73] M.J. Van Luyn, P.B. van Wachem, L.O. Damink, P.J. Dijkstra, J. Feijen, P. Nieuwenhuis, Relations between in vitro cytotoxicity and crosslinked dermal sheep collagens, J. Biomed. Mater. Res. 26 (1992) 1091–1110.
[74] A. Göpferich, Mechanisms of polymer degradation and erosion, Biomaterials 17 (1996) 103–114.
[75] R.L. Kronenthal, Biodegradable polymers in medicine and surgery, Polym. Sci. Technol. 8 (1975) 119–137.
[76] E.J. Bergsma, W. Brujn, F.R. Rozema, R.M. Bos, G. Boering, Late tissue response to poly(L-lactide) bone plates and screws, Biomaterials 16 (1995) 25–31.
[77] O. Böstmann, E. Hirvensalo, J. MaKkinen, P. Rokkanen, Foreign body reactions to fracture fixation implants of biodegradable synthetic polymers, J. Bone Jt. Surg. B72 (1990) 592.
[78] K.E. Rehm, L. Claes, H.J. Helling, D. Hutmacher, Application of a polylactide pin. An open clinical prospective study, in: K.S. Leung, L.K. Hung, P.C. Leung (Eds.), Biodegradable Implants in Fracture Fixation, World Scientific, Hong Kong, 1994, p. 54.
[79] D.W. Hutmacher, Scaffolds in tissue engineering bone and cartilage, Biomaterials 21 (2000) 2529–2543.
[80] A.A. Deschamps, M.B. Claase, W.J. Sleijster, J.D. de Bruijn, D.W. Grijpma, J. Feijen, Design of segmented poly(ether ester) materials and structures for the tissue engineering of bone, J. Control Release 78 (1–3) (17 January 2002) 175–186.
[81] J. Gunn, M. Zhang, Polyblend nanofibers for biomedical applications: perspectives and challenges, Trends Biotechnol. 28 (2010) 189–197.
[82] M. Okamoto, B. John, Synthetic biopolymer nanocomposites for tissue engineering scaffolds, Prog. Polym. Sci. 38 (2013) 1487–1503.

[83] C.A. Grant, D.J. Brockwell, S.E. Radford, N.H. Thomson, Tuning the elastic modulus of hydrated collagen fibrils, Biophys. J. 97 (2009) 2985–2992.
[84] H.R. Le, S. Qu, R.E. Mackay, R. Rothwell, Fabrication and mechanical properties of chitosan composite membrane containing hydroxyapatite particles, J. Adv. Ceram. 1 (2012) 66–71.
[85] C. Vepari, D.L. Kaplan, Silk as a biomaterial, Prog. Polym. Sci. 32 (2007) 991–1007.
[86] G. Qin, D.L. Kaplan, Silk-based biomaterials. Biology, properties and clinical applications, in: J.O. Hollinger (Ed.), An Introduction to Biomaterials, CRC Press, Abingdon, UK, 2011, pp. 421–431.
[87] A.R. Boccaccini, V. Maquet, Bioresorbable and bioactive polymer/bioglass(R) composites with tailored pore structure for tissue engineering applications, Compos. Sci. Technol. 63 (2003) 2417–2429.
[88] M. Wang, Developing bioactive composite materials for tissue replacement, Biomaterials 24 (2003) 2133–2151.
[89] M. Sumita, T. Shizuma, K. Miyasaka, K. Ishikawa, Effect of reducible properties of temperature, rate of strain, and filler content on the tensile yield stress of nylon 6 composites filled with ultrafine particles, J. Macromol. Sci. B 22 (1983) 601–618.
[90] S.-Y. Fu, X.-Q. Feng, B. Lauke, Y.-W. Mai, Effects of particle size, particle/matrix interface adhesion and particle loading on mechanical properties of particulate–polymer composites, Compos. Part B 39 (2008) 933–961.
[91] L. Zhang, T.J. Webster, Nanotechnology and nanomaterials: promises for improved tissue regeneration, Nano Today 4 (2008) 66–80.
[92] P. Wang, L. Zhao, J. Liu, M.D. Weir, X. Zhou, H.H.K. Xu, Bone tissue engineering via nanostructured calcium phosphate materials and stem cells, Bone Res. (2014).
[93] T.J. Webster, C. Ergun, R.H. Doremus, R.W. Siegel, R. Bizios, Specific proteins mediate enhanced osteoblast adhesion on nanophase ceramics, J. Biomed. Mater. Res. 5 (2000) 475–483.
[94] T.J. Webster, R.W. Siegel, R. Bizios, Enhanced functions of osteoblasts on nanophase ceramics, Biomaterials 21 (2000) 1803–1810.
[95] M. Kikuchi, S. Itoh, S. Ichinose, K. Shinomiya, J. Tanaka, Self organization mechanism in a bone-like hydroxyapatite/collagen nanocomposite synthesized in vitro and its biological reaction in vivo, Biomaterials 22 (2001) 1705–1711.
[96] A. Tampieri, M. Sandri, E. Landi, S. Sprio, F. Valentini, A.L. Boskey, Synthetic bio-mineralization yielding HA/Collagen hybrid composite, Adv. Appl. Ceram. 107 (2008) 298–302.
[97] M. Gelinsky, B.P. Welzel, P. Simon, A. Bernhardt, U. König, Porous three-dimensional scaffolds made of mineralized collagen: preparation and properties of a biomimetic nanocomposite material for tissue engineering of bone, Chem. Eng. J. 137 (2008) 84–96.
[98] A. Tampieri, S. Sprio, M. Sandri, F. Valentini, Mimicking natural bio-mineralization processes: a new tool for osteochondral scaffold development, Trends Biotechnol. 29 (2011) 526–535.
[99] H. Shin, S. Jo, A.G. Mikos, Biomimetic materials for tissue engineering, Biomaterials 24 (2003) 4353–4364.
[100] W.S. Koegler, L.G. Griffith, Osteoblast response to PLGA tissue engineering scaffolds with PEO modified surface chemistries and demonstration of patterned cell response, Biomaterials 25 (2004) 2819–2830.
[101] C. Du, F.Z. Cui, X.D. Zhu, K. De Groot, Three-dimensional nano-HAp/collagen matrix loading with osteogenic cells in organ culture, J. Biomed. Mater. Res. 44 (1999) 407–415.
[102] A. Tampieri, M. Sandri, E. Landi, D. Pressato, S. Francioli, Q. Quarto, I. Martin, Design of graded biomimetic osteochondral composite scaffolds, Biomaterials 29 (2008) 3539–3546.

[103] S. Itoh, M. Kikuchi, K. Takakuda, Y. Koyama, H.N. Matsumoto, S. Ichinose, J. Tanaka, T. Kawauchi, K. Shinomiya, The biocompatibility and osteoconductive activity of a novel hydroxyapatite/collagen composite biomaterial, and its function as a carrier of rhBMP-2, J. Biomed. Mater. Res. 54 (2001) 445–453.
[104] J. Li, J. Hong, Q. Zheng, X. Guo, S. Lan, F. Cui, H. Pan, Z. Zou, C. Chen, Repair of rat cranial bone defects with nHAC/PLLA and BMP-2-related peptide or rhBMP-2, J. Orthop. Res. 29 (2011) 1745–1752.
[105] W.W. Thein-Han, R.D. Misra, Biomimetic chitosan-nanohydroxyapatite composite scaffolds for bone tissue engineering, Acta Biomater. 5 (2009) 1182–1197.
[106] F. Zhao, W.L. Grayson, T. Ma, B. Bunnell, W.W. Lu, Effects of hydroxyapatite in 3-D chitosan–gelatin polymer network on human mesenchymal stem cell construct development, Biomaterials 27 (2006) 1859–1867.
[107] H.-R. Lin, Y.-J. Yeh, Porous alginate/hydroxyapatite composite scaffolds for bone tissue engineering: preparation, characterization, and in vitro studies, J. Biomed. Mater. Res. Part B Appl. Biomater. 15 (2004) 52–65.
[108] M. Sadat-Shojai, M.-T. Khorasani, A. Jamshidi, 3-Dimensional cell-laden nano-hydroxyapatite/protein hydrogels for bone regeneration applications, Mater. Sci. Eng. C 49 (2015) 835–843.
[109] S.-H. Yang, C.-K. Hsu, K.-C. Wang, F.-H. Lin, Tricalcium phosphate and glutaraldehyde crosslinked gelatin incorporating bone morphogenetic protein – a viable scaffold for bone tissue engineering, J. Biomed. Mater. Res. Part B Appl. Biomater. 74 (2005) 468–475.
[110] X. Huang, S. Bai, Q. Lu, X. Liu, S. Liu, H. Zhu, Osteoinductive-nanoscaled silk/HA composite scaffolds for bone tissue engineering application, J. Biomed. Mater. Res. Part B Appl. Biomater. 17 (2014) 1–13.
[111] D. Xue, Q. Zheng, C. Zong, Q. Li, H. Li, S. Qian, B. Zhang, L. Yu, Z. Pan, Osteochondral repair using porous poly(lactide-co-glycolide)/nano-hydroxyapatite hybrid scaffolds with undifferentiated mesenchymal stem cells in a rat model, J. Biomed. Mater. Res. Part A 94 (2010) 259–270.
[112] D. Li, C. Ye, Y. Zhu, Z. Gou, C. Gao, Enhancement of osteogenesis by poly(lactide-co-glycolide) sponges loaded with surface-embedded hydroxyapatite particles and rhBMP-2, J. Biomed. Mater. Res. Part B Appl. Biomater. 100 (2012) 1003–1013.
[113] S.-H. Chen, M. Lei, X.-H. Xie, L.-Z. Zheng, D. Yao, X.-L. Wang, W. Li, Z. Zhao, A. Kong, D.-M. Xiao, D.-P. Wang, X.-H. Pan, Y.-X. Wang, L. Qi, PLGA/TCP composite scaffold incorporating bioactive phytomolecule icaritin for enhancement of bone defect repair in rabbits, Acta Biomater. 9 (2013) 6711–6722.
[114] S.-H. Chen, X.-L. Wang, X.-H. Xie, L.-Z. Zheng, D. Yao, D.P. Wang, et al., Comparative study on osteogenic potential of a composite scaffold incorporating either endogenous bone morphogenetic protein-2 or exogenous phytomolecule icaritin: an in vitro efficacy study, Acta Biomater. 8 (2012) 3128–3137.
[115] N.L. Ignjatovic, Z.R. Ajdukovic, V.P. Savic, D.P. Uskokovic, Size effect of calcium phosphate coated with poly-D,L-lactide-co-glycolide on healing processes in bone reconstruction, J. Biomed. Mater. Res. Part B Appl. Biomater. 94 (2010) 108–117.
[116] S.S. Liao, F.Z. Cui, W. Zhang, Q.L. Feng, Hierarchically biomimetic bone scaffold materials: nano-HA/collagen/PLA composite, J. Biomed. Mater. Res. Appl. Biomater 69 (2004) 158–165.
[117] F. Causa, P.A. Netti, L. Ambrosio, G. Ciapetti, N. Baldini, S. Pagani, D. Martini, A. Giunti, Poly-epsilon-caprolactone/hydroxyapatite composites for bone regeneration: in vitro characterization and human osteoblast response, J. Biomed. Mater. Res. A 76 (2006) 151–162.

[118] H.J. Lee, S.E. Kim, H.W. Choi, C.W. Kim, K.J. Kim, S.C. Lee, The effect of surface-modified nano-hydroxyapatite on biocompatibility of poly(ε-caprolactone)/hydroxyapatite nanocomposites, Eur. Polym. J. 43 (2007) 1602–1608.
[119] M. Jayabalan, K.T. Shalumon, M.K. Mitha, K. Ganesan, M. Epple, Effect of hydroxyapatite on the biodegradation and biomechanical stability of polyester nanocomposites for orthopaedic applications, Acta Biomater. 6 (2010) 763–775.
[120] E. Zeimaran, S. Pourshahrestani, I. Djordjevic, B. Pingguan-Murphy, N.A. Kadri, M.R. Towler, Bioactive glass reinforced elastomer composites for skeletal regeneration: a review, Mater. Sci. Eng. C 53 (2015) 175–188.
[121] M. Mozafari, M. Rabiee, M. Azami, S. Maleknia, Biomimetic formation of apatite on the surface of porous gelatin/bioactive glass nanocomposite scaffolds, Appl. Surf. Sci. 257 (2010) 1740–1749.
[122] M. Peter, P.T.S. Kumar, N.S. Binulal, S.V. Nair, H. Tamura, R. Jayakumar, Development of novel α-chitin/nanobioactive glass ceramic composite scaffolds for tissue engineering applications, Carbohydr. Polym. 78 (2009) 926–931.
[123] M. Peter, N.S. Binulal, S. Soumya, S.V. Nair, T. Furuike, H. Tamura, et al., Nanocomposite scaffolds of bioactive glass ceramic nanoparticles disseminated chitosan matrix for tissue engineering applications, Carbohydr. Polym. 79 (2010) 284–289.
[124] S. Verrier, J.J. Blaker, V. Maquet, L.L. Hench, A.R. Boccaccini, PDLLA/Bioglass® composites for soft-tissue and hard-tissue engineering: an in vitro cell biology assessment, Biomaterials 25 (2004) 3013–3021.
[125] L.-C. Gerhardt, K.L. Widdows, M.M. Erol, C.W. Burch, Y.A. Sanz-Herrera, I. Ochoa, R. Stämpfli, I.S. Roqan, S. Gabe, T. Ansari, A.R. Boccaccini, The pro-angiogenic properties of multi-functional bioactive glass composite scaffolds, Biomaterials 32 (2011) 4096–4108.
[126] S.K. Misra, D. Mohn, T.J. Brunner, W.J. Stark, S.E. Philip, I. Roy, V. Salih, J.C. Knowles, A.R. Boccaccini, Comparison of nanoscale and microscale bioactive glass on the properties of P(3HB)/Bioglass® composites, Biomaterials 29 (2008) 1750–1761.
[127] S.K. Misra, T. Ansari, D. Mohn, S.P. Valappil, T.J. Brunner, W.J. Stark, et al., Effect of nanoparticulate bioactive glass particles on bioactivity and cytocompatibility of poly(3-hydroxybutyrate) composites, J. Royal Soc. Interface 7 (2010) 453–465.
[128] J. Yao, S. Radin, P.S. Leboy, P. Ducheyne, The effect of bioactive glass content on synthesis and bioactivity of composite poly (lactic-co-glycolic acid)/bioactive glass substrate for tissue engineering, Biomaterials 26 (2005) 1935–1943.
[129] H.H. Lu, A. Tang, S.C. Oh, J.P. Spalazzi, K. Dionisio, Compositional effects on the formation of a calcium phosphate layer and the response of osteoblast-like cells on polymer-bioactive glass composites, Biomaterials 26 (2005) 6323–6334.
[130] H.H. Lu, S.F. El-Amin, K.D. Scott, C.T. Laurencin, Three-dimensional, bioactive, biodegradable, polymer-bioactive glass composite scaffolds with improved mechanical properties support collagen synthesis and mineralization of human osteoblast-like cells in vitro, J. Biomed. Mater. Res. A 64 (2003) 465–474.
[131] A. El-Fiqi, J.-H. Kim, H.-W. Kim, Osteoinductive fibrous scaffolds of Biopolymer/Mesoporous bioactive glass Nanocarriers with excellent bioactivity and long-term delivery of osteogenic drug, Appl. Mater. Interfaces 7 (2015) 1140–1152.
[132] J.-H. Jo, E.-J. Lee, D.-S. Shin, H.-E. Kim, H.-W. Kim, Y.-H. Koh, J.-H. Jang, *In vitro/in vivo* biocompatibility and mechanical properties of bioactive glass nanofiber and poly (ε-caprolactone) composite materials, J. Biomed. Mater. Res. B Appl. Biomater. 91 (2009) 213–220.

This page intentionally left blank

Index

'*Note*: Page numbers followed by "f" indicate figures, "t" indicate tables.'

R

S

T

This page intentionally left blank

As no one material can effectively mimic the structure of musculoskeletal tissues, scientists have looked to advanced biomaterials as substitutes. Bone and other musculoskeletal tissues naturally have a nanocomposite structure; therefore nanocomposites are ideally suited as a material for replacing and regenerating these natural tissues. In addition biological properties such as biointegration and the ability to tailor and dope the materials make them highly desirable for musculoskeletal tissue regeneration.

Nanocomposites for Musculoskeletal Tissue Regeneration provides readers with a thorough review of biocomposites and their role in musculoskeletal tissue regeneration. Part one reviews designing nanocomposites for musculoskeletal tissue regeneration. Part two looks at the properties of these important materials and polymer nanocomposites for musculoskeletal tissue regeneration. The final set of chapters cover ceramics and glass nanocomposites for bone tissue regeneration.

Dr. Huinan Liu is Assistant Professor of Bioengineering at University of California actively explore nanomaterials and nanotechnology for medical applications. Her interests lay in both fundamental mechanistic research at the interface of cell and material and applied research that targets specific disease or injury and develop more effective treatment.

ELSEVIER
WP
WOODHEAD PUBLISHING
An imprint of Elsevier • elsevier.com

ISBN 978-1-78242-452-9
9 781782 424529